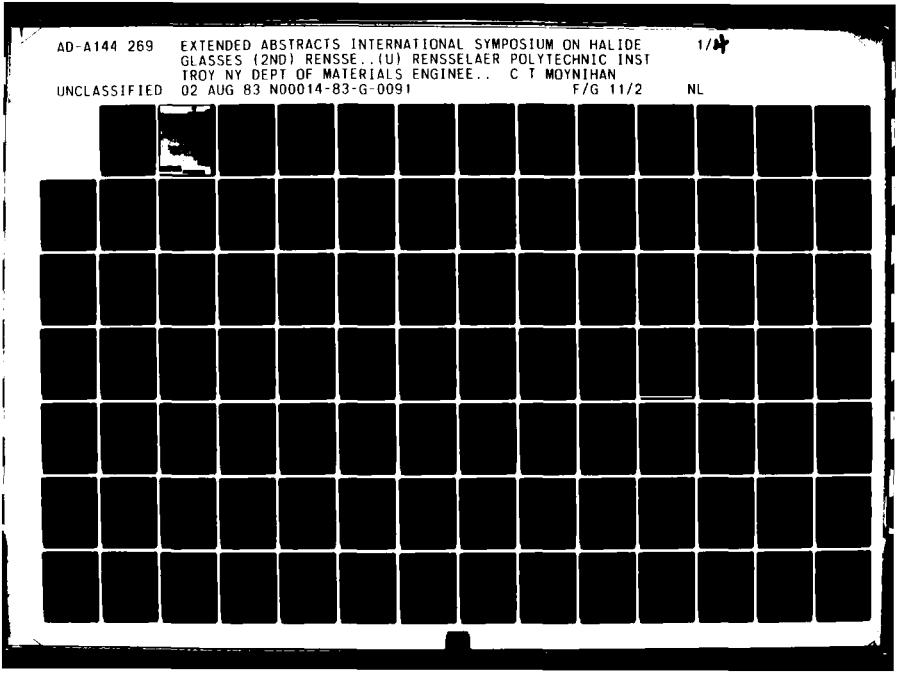
AD-A144 269 EXTENDED ABSTRACTS INTERNATIONAL SYMPOSIUM ON HALIDE 1/4
GLASSES (2ND) RENSSE..(U) RENSSELAER POLYTECHNIC INST
TROY NY DEPT OF MATERIALS ENGINEE.. C T MOYNIHAN
UNCLASSIFIED 02 AUG 83 N00014-83-G-0091 F/G 11/2 NL

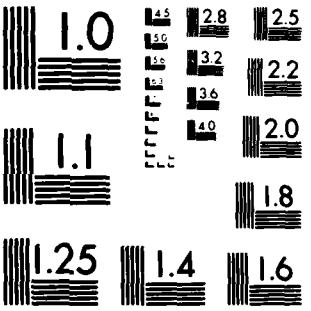

MICROCOPY RESOLUTION TEST CHART
NATIONAL BUREAU OF STANDARDS-1963-A

2-5 August 1983

Rensselaer Polytechnic Institute
Troy, New York 12181, USA

JUL 2 7

This document has been approved for public release and sale; its distribution is unlimited.

84 06 27 112

NR.039-250

ATTENDANCE LIST FOR THE 2ND INTERNATIONAL SYMPOSIUM ON HALIDE GLASSES

Ishwar D. Aggarwal
VALTEC
99 Hartwell Street
W. Boylston, MA 01583
Phone: (617) 393-7188

Rui M. Almeida
Centro de Fisica Molecular
Instituto Superior Technico
Av. Rovisco Pais, 1000 Lisboa
Portugal
Phone: 572499 ext. 213

Leonard J. Andrews
GTE Laboratories
40 Sylvan Road
Waltham, MA 02254
Phone: (617) 466-2285

C. Austen Angell
Dept. of Chemistry
Purdue University
W. Lafayette, IN 47907
Phone: (317) 494-5256

M. A. Aslami
SpecTran
Hall Road
Sturbrudge, MA 01566
Phone: (617) 347-2261

Robert M. Atkins
Bell Laboratories
600 Mountain Avenue
Murray Hill, NJ 07946
Phone: (201) 582-5120

William T. Baker
Sensors Inc.
6812 S. State Road
Saline, MI 48176
Phone: (313) 429-2100

Pranab K. Banerjee
Dept. of Electrical Engg.
University of Rhode Island
Kingston, RI 02881
Phone: (401) 792-5849

Narottam P. Bansal
Materials Engineering Dept.
Rensselear Polytechnic Institute
Troy, NY 12181
Phone: (518) 266-8051

James L. Barton
Saint Gobain Recherch
Aubervilliers
France
Phone: (1) 8349219

David G. Beck
Hughes Aircraft Co.
P.O. Box 902
E1/F102
El Segundo, CA 90245
Phone: (213) 616-9794

Bernard Bendow
The BDM Corporation
1801 Randolph Rd., SE
Albuquerque, NM 87106
Phone: (505) 848-5129

James I. Berg
Owens Corning Fiberglas
Technical Center
Granville, OH 43023
Phone: (614) 587-7630

Charles Bono
Rome Air Development Center
RADC/RBER
Griffiss AFB, NY 13441
Phone: (315) 330-2608

Mervet S. Boulos
Owens Corning Fiberglas
Technical Center
Granville, OH 43023
Phone: (614) 587-7964

Philip J. Bray
Dept. of Physics
Brown University
Providence, RI 02912
Phone: (401) 863-2587

Use Letter
14-73
A-1

Allan J. Bruce
Materials Engineering Dept.
Rensselaer Polytechnic Institute
Troy, NY 12181
PhoneL (518) 266-8048

Michael J. Burk
1629 Columbia Road, NW, #418
Washington, DC 20009
Phone: (202) 387-4246

Chandra M. Burman
Physics Dept.
SUNY-Albany
Albany, NY 12222
Phone: (518) 457-8450

Lynda E. Busse
Purdue University
Dept. of Chemistry
West Lafayette, IN 47907
Phone: (317) 494-5468

Rafael Cases
Naval Research Laboratory
(Code 6570)
Washington, DC 20375
Phone: (202) 767-3487

Ki-Ho Chung
Dept. of Chemistry
Korea Military Academy
Seoul, Korea
Phone: 972-7133

David J. Clough
Magnesium Elektron, Inc.
Flemington, NJ 08822
Phone: (201) 782-5800

Alan E. Comyns
Laporte Industries Ltd.
Moorfield Road
Widnes
Cheshire WA8 OJU
England
Phone: 051-424-5555

David J. Cronin
National Bureau of Standards
Bldg. 223, Rm. B324
Washington, DC 20234
Phone: (301) 421-2817

Margaret B. Davis
1Lt USAF
RADC/ESM
Hanscom AFB, MA 01831
Phone: (617) 861-5832

Charles DeLuca
SpecTran Corporation
Hall Road, P.O. Box 650
Sturbridge, MA 01566
Phone: (617) 347-2261

Robert P. Devaty
Naval Research Laboratory
(Code 6873)
Washington, DC 20375
Phone: (202) 767-3692

Sam DiVita
US Army Communication Electronics
Command
DRSEL-COM Rm. 1
Fiber Optics Team
Fort Monmouth, NJ 07764
Phone:

Robert H. Doremus
Materials Engineering Dept.
Rensselaer Polytechnic Institute
Troy, NY 12181
Phone: (518) 266-6373

Martin G. Drexhage
U.S. Air Force
RADC/ESM
Hanscom AFB, MA 01731
Phone: (617) 861-2211

Jean Pierre Dumas
15 Avenue Jean Martin
91-360 Villemoissan
France
Phone: (6) 904-3928

Osama H. El-Bayoumi
US Air Force
RADC/ESM
Hanscom AFB, MA 01731
Phone: (617) 861-5832

Chester F. Fisher
Naval Research Laboratory
(Code 6570)
Optical Science Division
Washington, DC 20375
Phone: (202) 767-3487

Jim W. Fleming
600 Mountain Avenue
Murray Hill, NJ 07974
Phone: (201) 582-4499

Robert C. Folweiler
GTE Laboratories, Inc.
40 Sylvan Road
Waltham, MA 02254
Phone: (617) 466-2262

Paul W. France
British Telecom Research Labs.
Martlesham Heath
Ipswich, U.K.
Phone: (44) 473-3522

David R. Gabbe
Massachusetts Institute of
Technology
77 Massachusetts Avenue
Rm. 13-3130
Cambridge, MA 02137
Phone: (617) 253-3698

John R. Gannon
Corning Glass Works
Corning, NY 14831
Phone: (607) 974-3914

David L. Gavin
Materials Engineering Dept.
Rensselaer Polytechnic Institute
Troy, NY 12181
Phone: (518) 266-8048

Robert J. Ginther
Naval Research Laboratory
Washington, DC 20375
Phone: (202) 767-3487

David L. Griscom
Naval Research Laboratory
(Code 6570)
Washington, DC 20375
Phone: (202) 767-2270

Diane E. Guenther
GTE Laboratories
40 Sylvan Road
Waltham, MA 02154
Phone: (617) 466-2270

Prabhat K. Gupta
Case Western Reserve University
Cleveland, OH 44106
Phone: (216) 368-4224

Edward Hartouni
3275 Towne Park Circle
Pomona, CA 91767
Phone: (714) 624-7285

Lowell M. Hobrock
Hughes Aircraft Co.
Bldg. E1 MS F102
2100 E. El Segundo Blvd.
El Segundo, CA 90245
Phone: (213) 616-9620

Jean Horne
STL
London Road
Harlow, Essex
England
Phone: 0279-29531

Joachim Horn
E. Merck
Frankfurter Str. 250
D-6100 Darmstadt
West Germany
Phone: 6154-722626

Cheryl A. Houser
162 Materials Research Lab.
Pennsylvania State University
University Park, PA 16823
Phone: (814) 865-1105

Kenneth A. Jackson
Bell Laboratories
Murray Hill, NJ 07974
Phone: (201) 582-4188

C. Jacobini
E.R.A. 609
Faculte des Sciences
Universite du Maine
72017 LeMans
France
Phone: (43) 247236 (412)

Raymond E. Jaeger
SpecTran Corporation
Hall Road
P.O. Box 650
Sturbridge, MA 01566
Phone: (617) 347-2261

Theresa A. Kerly
16 Parker Street
Maynard, MA 01754
Phone: (617) 897-4729

Philipp H. Klein
U.S. Naval Research Lab.
(Code 6822)
Washington, DC 20375
Phone: (202) 767-3671

Tadaaki Komatsu
One Fountain Lane
Apt. 2D-B
Searsdale, NY 10583
Phone: (914) 472-0742

Norbert J. Kreidl
1433 Canyon Road
Santa Fe, NM 87501
Phone: (505) 983-2393

William A. Lanford
Physics Dept.
SUNY Albany
Albany, NY 12222
Phone: (518) 457-8326/8450

John W-K. Lau
Dept. of Materials Science
and Engineering
University of California
Los Angeles, CA 90024
Phone: (213) 825-2451

Kenneth H. Levin
Naval Research Laboratory
(Code 6570)
Washington, DC 20375
Phone: (202) 767-2869

Susan R. Loehr
Materials Engineering Dept.
Rensselaer Polytechnic Institute
Troy, NY 12181
Phone: (518) 266-8048

Grant Lu
Naval Research Laboratory
(Code 6570)
Washington, DC 20375
Phone: (202) 767-3487

Jacques Lucas
Laboratoire de Chimie Minerale
Campus de Beaulieu University
Rennes 35042
France
Phone: (99) 354815 ext 2267

John B. MacChesney
Bell Laboratories
Murray Hill, NJ 07974
Phone: (201) 582-4722

Paul W. Mailloux
28 Mt. Vernon St.
Somerville, MA 02145
Phone: (617) 776-7616

Diane J. Martin
Air Force Weapons Laboratory
AFWL/ARAO
Kirtland AFB, NM 87117
Phone: (505) 844-0721

Steve W. Martin
133-13 Nimitz Drive
W. Lafayette, IN 47906
Phone: (317) 743-8085

James Mathew
Materials Engineering Dept.
Rensselaer Polytechnic Institute
Troy, NY 12181
Phone: (518) 266-8051

G. Maze
LeVerre Fluore
Z.I. DuChamp Martin
35230 Vern-Sur-Seiche
France
Phone: (99) 627922

Kathryn A. McCarthy
Dept. of Physics
Tufts University
Medford, MA 02155
Phone: (617) 628-5000, ext. 3517

Theresa A. McCarthy
214 Steidle Bldg.
Pennsylvania State University
University Park, PA 16801
Phone: (814) 863-2835

Bill C. McCollum
GTE Laboratories, Inc.
40 Sylvan Road
Waltham, MA 02254
Phone: (617) 466-2230

Jack Mecholsky
Organization 1845
Sandia National Laboratories
Albuquerque, NM 87185
Phone: (505) 844-0787

William J. Miniscalco
GTE Laboratories, Inc.
40 Sylvan Road
Waltham, MA 01776
Phone: (617) 466-2627

Shashanka S. Mitra
Dept. of Electrical Engineering
University of Rhode Island
Kingston, RI 02881
Phone: (401) 792-2505

Tadashi Miyashita
Ibaraki Electrical Communication Laboratory
Nippon Telegraph and Telephone Public Corporation
Tokai, Ibaraki, 319-11
Japan
(Phone) 02928-7-7510

Cornelius T. Moynihan
Materials Engineering Dept.
Rensselaer Polytechnic Institute
Troy, NY 12181
Phone: (518) 266-6125

Robert V. Mulkern
Physics Dept.
Box 1843
Brown University
Providence, RI 02912
Phone: (401) 863-3007

Suzanne R. Nagel
600 Mountain Avenue
Bell Laboratories
Murray Hill, NJ 07974
Phone: (201) 582-6623

Alana M. Nakata
Dept. of Materials Science & Engineering
University of California at Los Angeles
Los Angeles, CA 90024
Phone: (213) 8256146

George F. Neilson
Jet Propulsion Laboratory
Mail Stop 157/316
4800 Oak Grove Drive
Pasadena, CA 91109
Phone: (213) 354-6365

Masayaki Nogami
Materials Engineering Dept.
Rensselaer Polytechnic Institute
Troy, NY 12181
Phone: (518) 266-6451

Paul E. R. Nordquist
U.S. Naval Research Laboratory
(Code 6822)
Washington, DC 20375
Phone: (202) 767-3672

Chester R. Norman
Dow Chemical USA
Texas Division - 3455
Freeport, Texas 77541
Phone: (409) 238-7318

Susanne M. Opalka
Materials Engineering Dept.
Rensselaer Polytechnic Institute
Troy, NY 12181
Phone: (518) 266-8048

Carlo G. Pantano
Dept. of Materials Science & Engineering
Pennsylvania State University
University Park, PA 16802
Phone: (814) 863-2071

John Penczek
7 Sunset Terrace
Troy, NY 12180
Phone: (518) 272-9407

Norman Perazzo
Materials Engineering Dept.
Rensselaer Polytechnic Institute
Troy, NY 12181
Phone: (518) 266-8048

Donald E. Polk
U.S. Office of Naval Research
(Code 431)
800 N. Quincy Street
Arlington, VA 22217
Phone: (202) 696-4401

Marcel Poulain
University
Chemistry Laboratories
Rennes 35042
France
Phone: (99) 36-48-15 2269

Michel Poulain
University
Chemistry Laboratories
Rennes 35042
France
Phone: (99) 36-48-15 2265

Mort Robinson
Hughes Research Labs.
Malibu, CA 90265
Phone: (213) 456-6411

Herbert B. Rosenstock
Naval Research Laboratory
(Code 6510)
Washington, DC 20375
Phone: (202) 767-2225

David M. Sanders
9820 Gordon Street
Walkersville, MD 21793
Phone: (301) 921-2817

Ahmad Sarhangi
Corning Glass Works
Development Building
Sullivan Park
Corning, NY 14830
Phone: (607) 974-3355

Peter C. Schultz
Corning Glass Works
Corning, NY 14830
Phone: (607) 974-3447

John Schroeder
Physics Dept.
Rensselaer Polytechnic Institute
Troy, NY 12181
Phone: (518) 266-8408

Caroline J. Scott
Hewlett Packard
1501 Page Mill Road
Palo Alto, CA 94304
Phone: (415) 857-3057

Michael G. Scott
Standard Telecommunication
Laboratories Ltd.
Optical Waveguide Division
London Road
Harlow
Essex CM17 9NA
England
Phone: (0279) 29531 ext. 380

Angela B. Seddon
Dept. of Ceramics, Glasses and
Polymers
University of Sheffield
Northumberland Road
Sheffield S10 2TZ
England
Phone: 0742 78555

William A. Sibley
Physics Dept.
Oklahoma State University
Stillwater, OK 74078
Phone: (405) 624-6501

George H. Sigel
Naval Research Laboratory
(Code 6573)
Washington, DC 20375
Phone: (202) 767-2870

Catherine J. Simmons
Dept. of Physics - VSL
Catholic University of America
Washington, DC 20064
Phone: (202) 635-5442

Joseph H. Simmons
Dept. of Physics
Catholic University of America
Washington, DC 20064
Phone: (202) 635-5327

Gary L. Smith
Jet Propulsion Laboratory
4800 Oak Grove Drive
Mail Stop 158-110
Pasadena, CA 91109
Phone: (213) 354-3759

Kenzo Sono
Nippon Sheet Glass Co., Ltd.
1065 Edgewood Lane
Fort Lee, NJ 07024
Phone: (201) 224-7446

Martin L. Stein
Stein Associates
27 Burlington Road
Bedford, MA 01730
Phone: (617) 275-2898

John M. Stevens
SpecTran Corporation
15 Hall Road
Sturbridge, MA 01566
Phone: (617) 347-2261

Marc A. Stiller
25 Belle Avenue
Troy, NY 12181
Phone: (518) 273-2428

Michael J. Suscavage
US Air Force
RADC/ESM
Hanscom AFB, MA 01731
Phone: (617) 861-5831

Aleta A. Tesar
Pennsylvania State University
214 Steidle Building
University Park, PA 16823
Phone: (814) 863-2835

Aki Tomita
Bell Laboratories
6G327
Murray Hill, NJ 07974
Phone: (201) 582-6736

Minoru Tomozawa
Materials Engineering Dept.
Rensselaer Polytechnic Institute
Troy, NY 12181
Phone: (518) 266-6451

Danh C. Tran
Naval Research Laboratory
(Code 6570)
Washington, DC 20375
Phone: (202) 767-3487

Veneta G. Tsoukala
1312 15th Street
Troy, NY 12180
Phone: (518) 274-1195

LeGrand G. VanUitert
Bell Laboratories
Murray Hill, NJ 07974
Phone: (201) 582-3447

Charles Wilson
7 Heritage Drive
Pleasantville, NY 10570
Phone: (914) 769-2196

John A. Williams
American ACMI
300 Stillwater Avenue
Stamford, CT 06902
Phone: (203) 357-8300

Guy T. Worth
P.O. Box 613
Edgewood, NM 87015
Phone: (505) 281-1640

Adrian C. Wright
J.J. Thomson Physical Laboratory
Reading University
Whiteknights
Reading
RG6 2AF
United Kingdom
Phone: 0734-875123 ext. 388

Takashi Yamagishi
Nippon Sheet Glass Co., Ltd.
Research Laboratory
Itami City, Japan
Phone: (0727) 81-0081

S. Cherukuri
Alfred University
Alfred, NY 14802
Phone: (607) 871-2420

Barry Kinsman
BDG Chemicals Ltd.
Poole
Dorset, England

EXTENDED ABSTRACTS

SECOND INTERNATIONAL SYMPOSIUM

ON HALIDE GLASSES

Rensselaer Polytechnic Institute

Troy, NY, USA

August 2-5, 1983

In cooperation with the Glass Division of the American Ceramic Society.

PROGRAM COMMITTEE

Cornelius T. Moynihan, Chairman, Rensselaer Polytechnic Institute, Troy, NY, USA
Martin G. Drexhage, Rome Air Development Center, Hanscom AFB, MA, USA
Osama H. El-Bayoumi, Rome Air Development Center, Hanscom AFB, MA, USA
John R. Gannon, Corning Glassworks, Corning, NY, USA
Jacques Lucas, University of Rennes, Rennes, France
Marcel Poulain, University of Rennes, Rennes, France
George H. Sigel, Jr., Naval Research Laboratory, Washington, DC, USA

INDUSTRIAL AND GOVERNMENT SPONSORS

Corning Glass Works Foundation
GTE Laboratories
SpecTran Corporation
U.S. Air Force Office of Scientific Research
U.S. Office of Naval Research

INVITED AND CONTRIBUTED PAPERS

Papers are listed in alphabetical order of the names of the first authors.

Paper No.	Title and Authors
1	"A Vibrational Spectroscopy Study of the Structure of Binary Thorium Fluorohafnate Glasses" R. M. Almeida and J. D. Mackenzie
2	"Polarized Raman Spectra of Ca/Sr/Al Fluorophosphate Glasses" P. K. Banerjee, S. S. Mitra, B. Kumar and B. Bendow
3	"DSC Measurements of Crystal Growth Kinetics in Heavy Metal Fluoride Glasses" N. P. Bansal, A. J. Bruce, R. H. Doremus, and C. T. Moynihan
4	"Surface Crystallization on a Fluoride Glass" N. P. Bansal and R. H. Doremus
5	"Fundamental Optical Properties of Heavy Metal Fluoride Glasses" B. Bendow
6	"An F^{19} NMR Study of Heavy Metal Fluoride Glasses Based on ZrF_4" P. J. Bray, R. V. Mulkern, M. G. Drexhage, S. Greenbaum, and D. C. Tran
7	"DSC Study of Nucleation and Crystallization of Heavy Metal Fluoride Glasses" A. J. Bruce, C. T. Moynihan, O. H. El-Bayoumi, and M. G. Drexhage
8	"Far-IR Transmitting Cadmium Iodide Based Glasses" E. I. Cooper and C. A. Angell
9	"Multicomponent Heavy Metal Fluoride Glasses Containing MgF_2" O. H. El-Bayoumi, M. G. Drexhage, J. R. Gannon, and P. Tick
10	"Trace Impurity Analysis of Fluoride Glasses and Materials" C. F. Fisher, P. Nordquist, and D. C. Tran
11	"Mechanical Properties of Infrared Transmitting Fibers" P. W. France, S. F. Carter, J. R. Williams, and K. J. Beales

INVITED AND CONTRIBUTED PAPERS (cont.)

Paper No.	Title and Authors
12	"Raman Scattering in ZrF_4 Based Glasses" J. A. Freitas, Jr., R. P. Devaty, D. C. Tran and U. Strom
13	"Sub-Tg Aging of Heavy Metal Fluoride Glasses" D. L. Gavin, A. J. Bruce, S. Loehr, S. Opalka, C. T. Moynihan, M. G. Drexhage, and O. H. El-Bayoumi
14	"Fluoride Glasses of Uranium IV and 3d Transition Metals" J. Guery, G. Courbion, C. Jacobini, and R. DePape
15	"Surface Studies of Fluorozirconate Glasses" C. A. Houser and C. G. Pantano
16	"Preparation and Properties of Transition Metal Fluoride Glasses" C. Jacobini
17	"CALPHAD Calculation of the Effect of AlF_3 Additions on the Glass Compositions of Ternary ZrF_4-LaF_3-BaF_2 Fluorides" L. Kaufman and D. Birnie
18	"Optical Properties of Fluorophosphate Glasses" B. Kumar and R. Harris
19	"Nuclear Reaction Analysis and Rutherford Backscattering Spectrometry in the Study of the Reaction Between Fluoride Glasses and Water" W. A. Lanford, C. Burman, and R. H. Doremus
20	"Scattering Loss Contributions in Fluoride Glasses" K. H. Levin, D. C. Tran, and G. H. Sigel, Jr.
21	"Effect of Alkali Fluoride Additions on Properties of BaF_2/ThF_4 Glasses" S. Loehr, A. J. Bruce, K.-H. Chung, N. L. Perazzo, and M. G. Drexhage
22	"Characterization of Crystals in Fluorozirconate Glasses" G. Lu, C. F. Fisher, M. J. Burk, and D. C. Tran
23	"ThF_4 Based Glasses: Improvement of Viscosity and Chemical Purity by Reactive Atmosphere Processing and the Addition of Doping Fluorides" J. Lucas, D. Tregoat, and G. Fonteneau

INVITED AND CONTRIBUTED PAPERS (cont.)

Paper No.	Title and Authors
24	"ThF_4/MnF_2 Based Glasses: Recent Developments" J. Lucas, Y. LePage, and G. Fonteneau
25	"Recent Progress in Halide Glass Research at the University of Rennes" J. Lucas
26	"Halide Glasses Based on Chlorides and Bromides" J. D. Mackenzie
27	"Progress in Cadmium Halide Glasses" M. Matecki, Michel Poulain, and Marcel Poulain
28	"Large Scale Preparation of Heavy Metal Fluoride Glasses" G. Maze
29	"Fluoride Glass Optical Fibers" G. Maze
30	"Dissolution of Fluorozirconate Glasses" T. A. McCarthy and C. G. Pantano
31	"Mechanical Properties of Heavy Metal Fluoride Glasses" J. J. Mecholsky
32	"Fracture Analysis of Fluoride Glass Fibers" J. J. Mecholsky, J. Lau, J. D. Mackenzie, D. Tran, and B. Bendow
33	"Progress in Fluoride Glass Fiber Research and Development in [illegible]" T. Miyashita and [illegible]nabe
34	"Environmental Effects on the Strength of Fluoride Glass Fibers" A. Nakata, J. Lau, and J. D. Mackenzie
35	"Crystallization of ZrF_4-BaF_2-LaF_3-AlF_3 Glass" G. Neilson, G. Smith, and M. Weinberg
36	"Structure of Heavy Metal Fluoride Glasses" Marcel Poulain
37	"Mixed Halide Effect in Fluorozirconate Glasses" Marcel Poulain and J.-L. Adam

INVITED AND CONTRIBUTED PAPERS (cont.)

Paper No.	Title and Authors
38	"Early History of Heavy Metal Fluoride Glasses" Michel Poulain
39	"ThF_4 and LiF - Based Fluoride Glasses" Michel Poulain and Marcel Poulain
40	"The Structure and Properties of Pure and Nd Doped BeF_2 Based Glasses" L. D. Pye, S. C. Cherukuri, and I. Joseph
41	"Energy Transfer Between Mn(II) and Er(III) in a Gallium Lead Fluoride Glass" R. Reisfeld, E. Greenberg, C. Jacobini, R. Depape, and C. K. Jørgensen
42	"Synthesis of High Purity Starting Materials for Heavy Metal Fluoride Glasses" M. "Sunny Jim" Robinson
43	"Three Loss Mechanisms in Halide Glass Fibers" H. B. Rosenstock
44	"Thermal Conductivity of Several Halide Glasses" H. H. Sample and K. A. McCarthy
45	"Light Scattering in Fluoride Glasses" J. Schroeder
46	"Heavy Metal Fluoride Glasses as Mid-IR Laser Materials" W. Sibley and M. D. Shinn
47	"Chemical Durability Studies of Heavy Metal Fluoride Glasses" C. J. Simmons, S. Azali, and J. H. Simmons
48	"Diamond-like Carbon Coatings for Protection of Halide Glass Surfaces" M. Stein, A. Green, B. Bendow, O. H. El-Bayoumi, and M. G. Drexhage
49	"Effect of NaF Additions Upon the Mechanical Behavior of Fluorozirconate Glasses" A. Tesar, R. C. Bradt, and C. G. Pantano
50	"Preparation of Heavy Metal Fluoride Glass Optical Fibers" D. C. Tran, M. J. Burk, and G. H. Sigel, Jr.

INVITED AND CONTRIBUTED PAPERS (cont.)

Paper No.	Title and Authors
51	"Optical and Lasing Properties of Nd(III)-Doped BeF_2 Glasses" M. J. Weber, C. F. Cline, G. J. Linford, D. Milam, S. E. Stokowski, and S. M. Yarema
52	"Neutron Diffraction and Molecular Dynamics Studies of Vitreous NaF-DyF_3-BeF_2" A. C. Wright, G. Etherington, S. A. Brawer, M. J. Weber, and R. N. Sinclair
53	"Viscosity of Some Glass-Forming Bromide Melts" D. Wynne, J. Lau, and J. D. Mackenzie
54	"New Halide Glasses in the CuCl-CsBr-$PbBr_2$ System" T. Yamagishi, J. Nishii, and Y. Kaite

POSTER PAPERS

Paper No.	Title and Authors
P1	"A Potential Suitable for Calculating Absorption in Halide Glasses" H. B. Rosenstock
P2	"Vibrational Spectroscopy of Pb/Mn/Ga Fluoride Glasses" B. Bendow, P. K. Banerjee, S. S. Mitra, C. Jacobini and R. DePape
P3	"EXAFS Determination of the Coordination of Divalent Lead in PbO-$PbCl_2$ Glasses" K. J. Rao and J. Wong
P4	"Bonding and Structure of Nd^{+3} in BeF_2 Glass by XANES and EXAFS Spectroscopy" K. J. Rao and J. Wong
P5	"IR Spectroscopy Measurement of the Rate of Surface Layer Development on ZrF_4-BaF_2-LaF_3 Glass in Aqueous Solution" A. J. Bruce, S. R. Loehr, N. P. Bansal, D. Murphy, C. T. Moynihan and R. H. Doremus
P6	"Electrical Conductivity and Relaxation in ZrF_4-BaF_2-LaF_3 Glasses" N. L. Perazzo, D. L. Gavín, A. J. Bruce, S. R. Loehr and C. T. Moynihan

A VIBRATIONAL SPECTROSCOPY STUDY OF THE STRUCTURE OF BINARY THORIUM - - FLUOROHAFNATE GLASSES

Rui M. Almeida

Centro de Física Molecular
Instituto Superior Técnico
Av. Rovisco Pais, 1000 Lisboa, Portugal

and

John D. Mackenzie

Materials Science and Engineering Department
University of California
Los Angeles, CA 90024, USA

Glass samples were prepared in the HfF_4 - ThF_4 binary system, containing between 32 - 43 mol% HfF_4. Starting materials were the anhydrous fluorides and there was extensive preferential vaporization of HfF_4 during the melting procedure, due to its volatility and the absence of a modifier.
Glass transition and crystallization temperatures, measured by DTA, were ~ 200°C higher than those of glasses which contain a modifying compound such as BaF_2.
Infrared absorption spectra showed two strong high-frequency bands, characteristic of the antisymmetric stretching vibrations of fluorine atoms bridging Hf and Th cations, respectively. Polarized Raman spectra were substantially different from those of binary barium - fluorohafnate glasses. While the high - frequency band of the latter at 580 cm^{-1} decreased in intensity and shifted to ~ 620 cm^{-1}, the intermediate frequency range considerably increased its intensity and developed new features due to the presence of a large amount of Th atoms.
A vibrational assignment has been made, based on results previously obtained for HfF_4 - BaF_2 and ZrF_4 - ThF_4 glasses and on the vibrational spectra of crystalline HfF_4 and ThF_4. The results have been interpreted in terms of a

predominant six - fold coordination for Hf and eight - fold coordination for Th. A small number of seven and eight-coordinated Hf and nine - coordinated Th are also likely to occur.

The substitution of a network modifier such as BaF_2 by a network former like ThF_4 substantially increased the degree of bridging and appeared to change the structure from a predominantly one - dimensional type to a three - dimensional network.

Composition and characteristic temperatures of thorium-fluorohafnate glasses

Batch composition (mol %)			Analyzed composition (mol %)			Sample	T_g (°C)	T_{cryst} (°C)	$T_{cryst}-T_g$ (°C)
HfF_4	ThF_4	BaF_2	HfF_4	ThF_4	BaF_2				
40	60		32	68		A	501	559	58
50	50		—	—		B	504	570	66
60	40		—	—		C	—	—	—
70	30		—	—		D	502	562	60
80	20		43	57		E	500	565	65
60	20	20	—	—	—	F	—	—	—
70		30	66		34	G	308	360	52

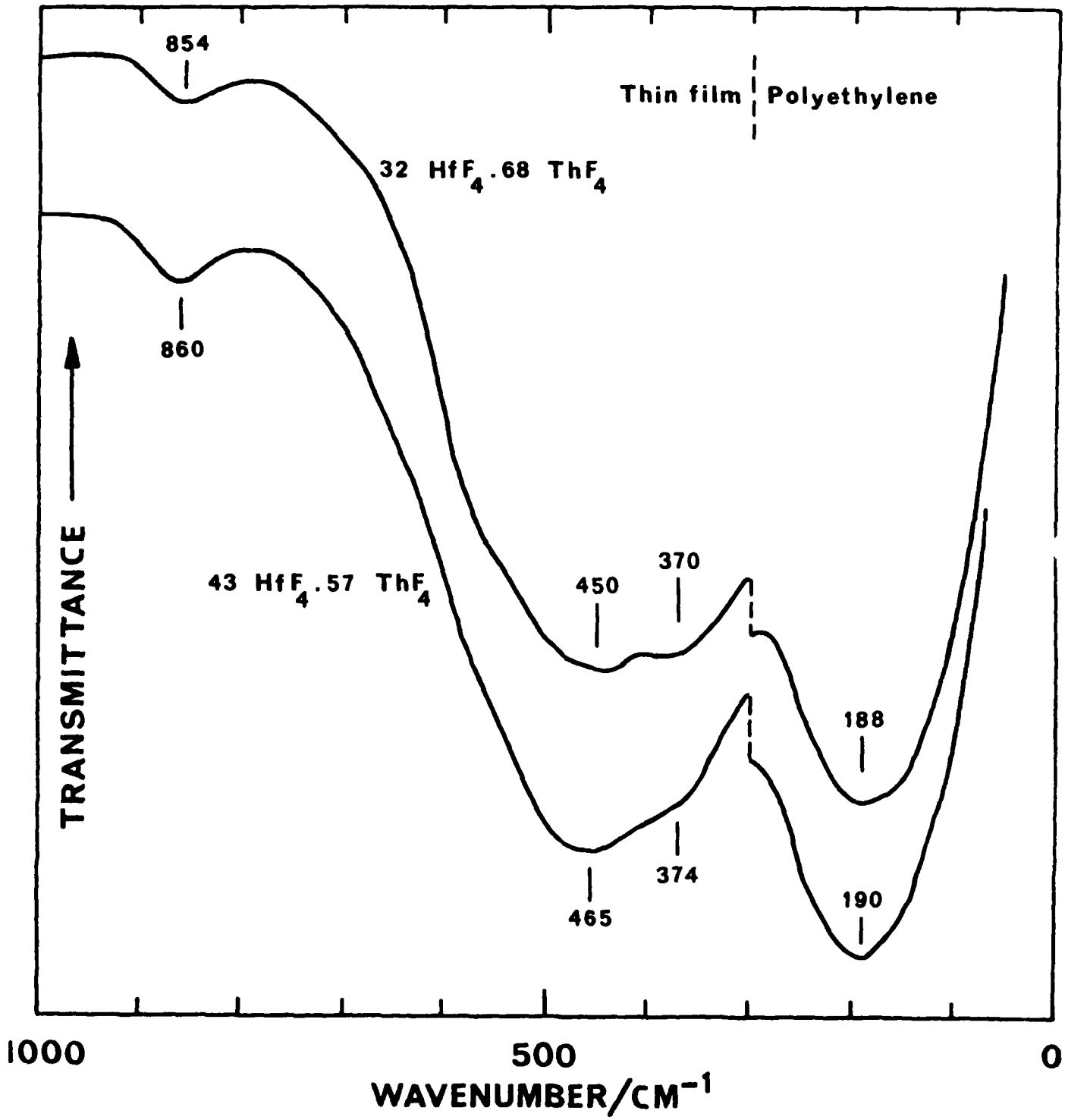
854
Thin film
Polyethylene
32 HfF4.68 ThF4
860
TRANSMITTANCE
43 HfF4.57 ThF4
450
370
188
374
465
190
1000
500
0
WAVENUMBER/CM-1

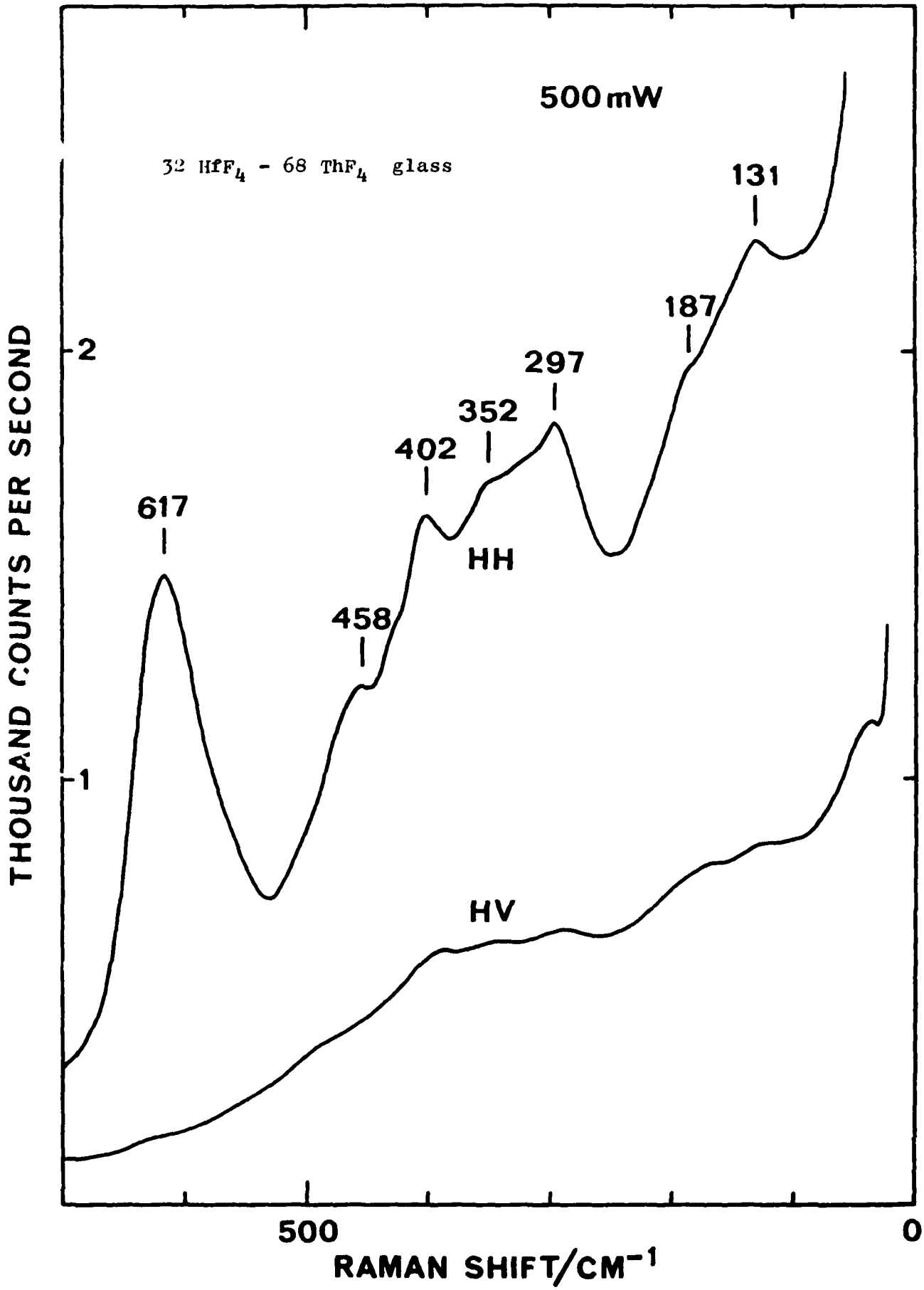
500 mW
32 HfF_4 - 68 ThF_4 glass
131
187
297
352
402
617
458
HH
HV
2
1
THOUSAND COUNTS PER SECOND
500
0
RAMAN SHIFT/CM^{-1}

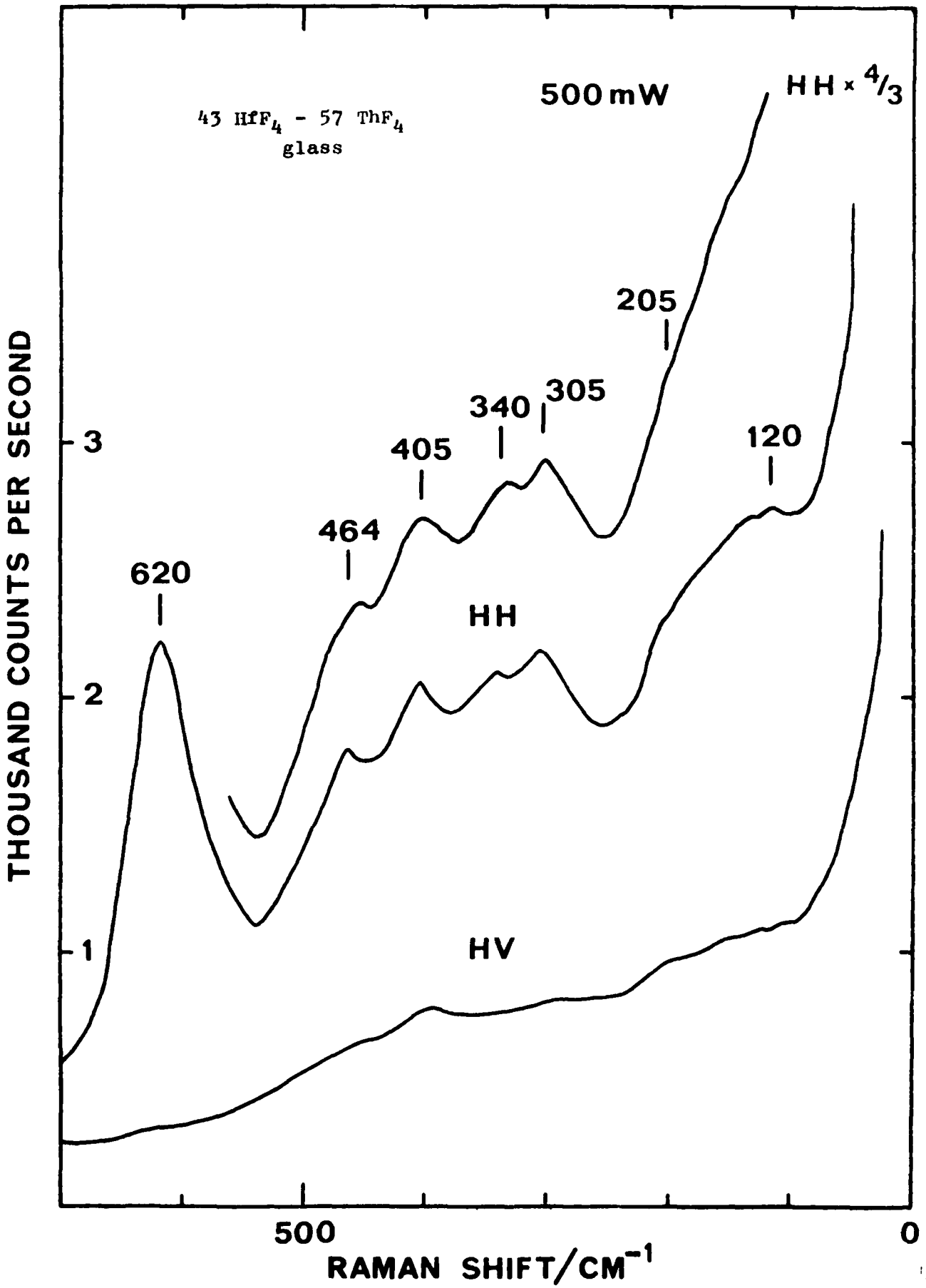
500 mW
HH × 4/3
43 HfF4 - 57 ThF4
glass
205
340
305
405
120
464
620
HH
HV
3
2
1
THOUSAND COUNTS PER SECOND
500
0
RAMAN SHIFT/CM-1

POLARIZED RAMAN SPECTRA OF Ca/Sr/Ba/Al FLUOROPHOSPHATE GLASSES

Pranab K. Banerjee and Shashanka S. Mitra
Department of Electrical Engineering
University of Rhode Island, Kingston, RI 02881

Binod Kumar
University of Dayton Research Institute, Dayton, OH 45469

Bernard Bendow
The BDM Corporation, Albuquerque, NM 87106

An investigation of the vibrational characteristics of fluorophosphate glasses was conducted using polarized Raman scattering and fundamental IR reflectivity measurements. Glasses for this study were synthesized at UDRI using analytical grade raw materials which were melted in a Pt crucible in air at 950C and then refined at 850C. Glasses were obtained by pouring the melt into graphite molds and annealing the glass at 450C for several hours. The glass compositions, consisting primarily of aluminum and alkaline earth fluorides combined with a small amount of P_2O_5, are indicated in Table 1. Polarized Raman spectra were obtained using a Spex 1400 monochrometer and argon ion laser, and reflectivity spectra were obtained using a Perkin-Elmer 983 IR spectrophotometer.

Typical results of the measurements are indicated in figures 1 through 3. Strong and highly polarized peaks were obtained in Raman (see Figure 1) in the vicinities of 525cm^{-1} and 970 - 1040cm^{-1} (double peaks), which are also manifested as deep minima in the depolarization spectrum of Figure 2. A second set of less intense polarized bands were observed in the vicinities of 730 and 1350cm^{-1}. A weakly polarized broad band, manifesting a multiplicity of fine structure, was found to span the 225 to 350cm^{-1} region.

Reflectivity spectra (see Figure 3) reveal a strong and relatively broad band centered near 630cm^{-1}, a weak and very broad band centered near 1050cm^{-1}, and a variety of broad features with complex fine structure in the 200 - 450cm^{-1} region.

The features of the observed spectra have been interpreted by comparison with either measured or calculated spectra of the individual constituents where available, in either the crystal, glass and/or gas (molecule) form. On this basis, the two intense peaks in the Raman spectrum (near 525 and 1000cm^{-1}) have been assigned to stretching vibrations between Al and F, the bands near 730 and 1350cm^{-1} to stretching vibrations between P and O, and the low frequency features (225-350cm^{-1}) to a combination of stretching vibrations between the alkaline earth atoms and F and rotational modes involving Al and F. The strong band near 630cm^{-1} in the IR reflectivity is assigned to AlF_3, the weak broad band at 1050cm^{-1} to P_2O_5, and the low frequency bands (200-350cm^{-1}) to the alkaline earth fluorides. The origin of the band near 400cm^{-1} is uncertain, but could be associated with P_2O_5, AlF_3, or a combination mode involving Al, alkaline earths and fluorine.

Based on the above observations, one concludes that the fluorophosphates investigated are comprised of two separate (but possibly interlaced) networks of P_2O_5 and AlF_3. The polarizability, and therefore the Raman cross section, associated with the fluoride constituents in the glass is larger than that for P_2O_5. Each network is comprised of well defined structural units containing two different types of bonds, which therefore display two polarized modes in Raman, while the alkaline earth ions appear to be distributed outside the main network.

TABLE 1. FLUOROPHOSPHATE GLASS COMPOSITIONS (wt%)

	FPI	FPII	FPIV	FPV
CaF_2	40	20	20	20
SrF_2	20	20	0	40
BaF_2	0	20	40	0
AlF_3	30	30	30	30
P_2O_5	10	10	10	10

Figure 1

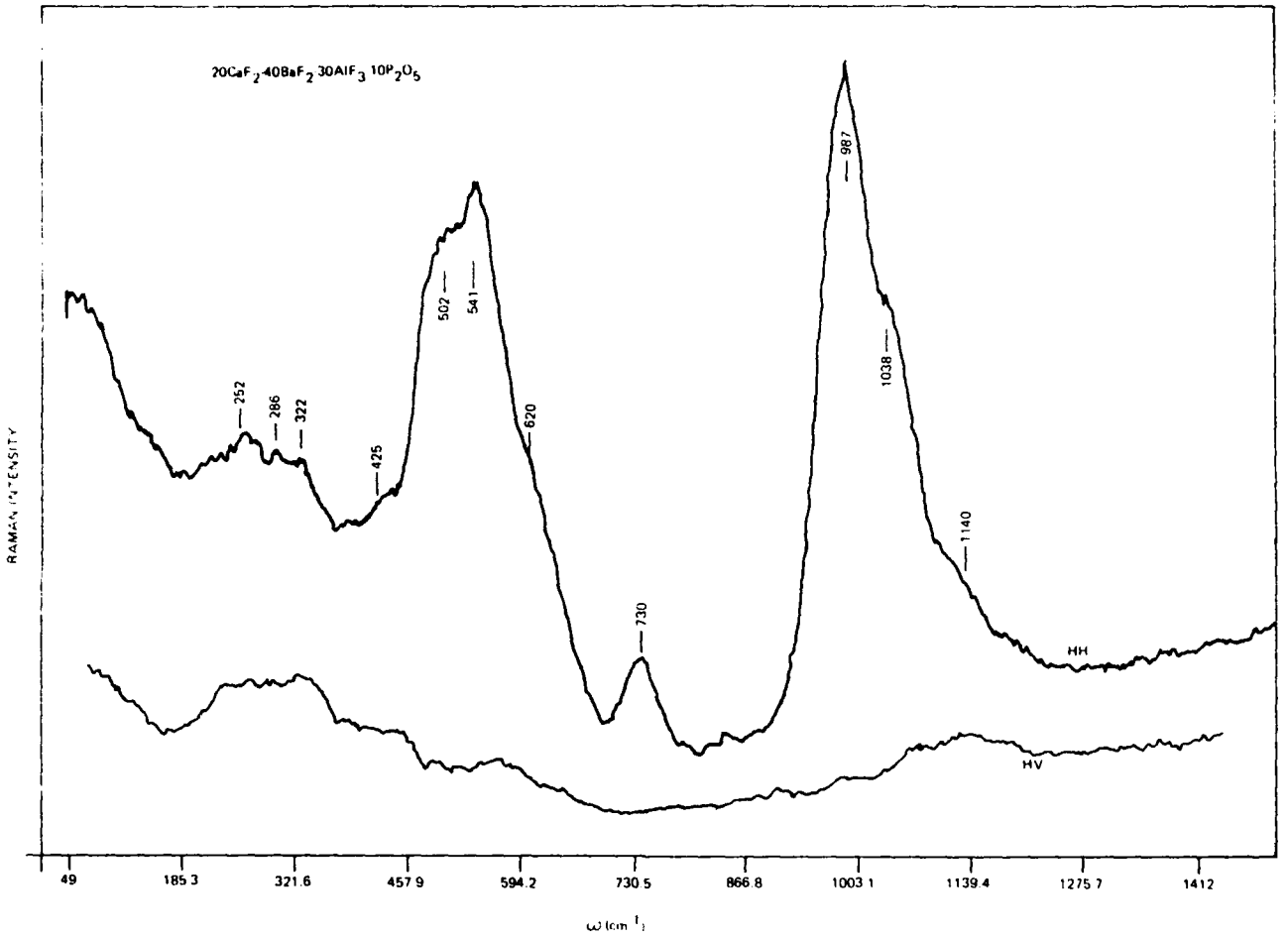
20CaF2·40BaF2·30AlF3·10P2O5
RAMAN INTENSITY
252
286
322
425
502
541
620
730
987
1038
1140
HH
HV
49
185.3
321.6
457.9
594.2
730.5
866.8
1003.1
1139.4
1275.7
1412
ω (cm⁻¹)

Figure 2

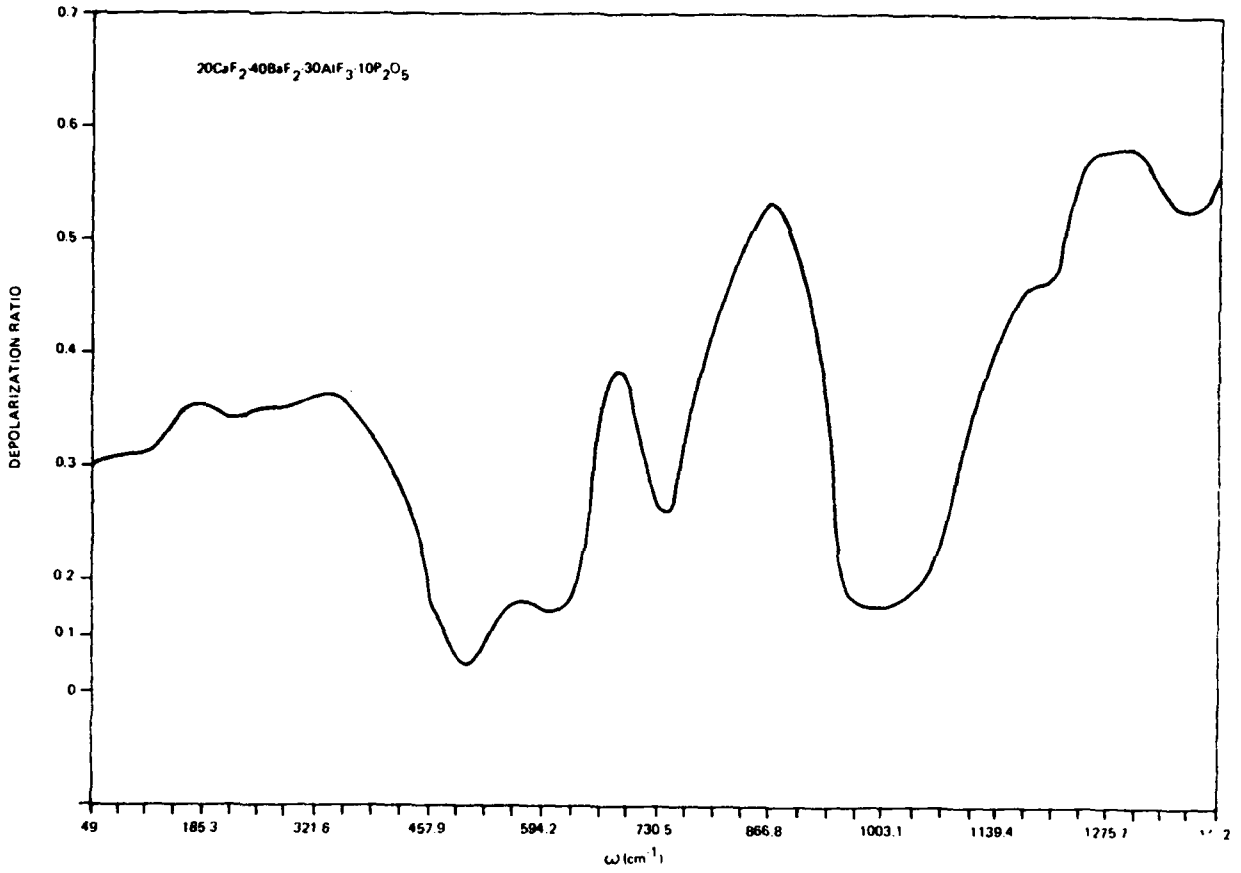

Figure 3

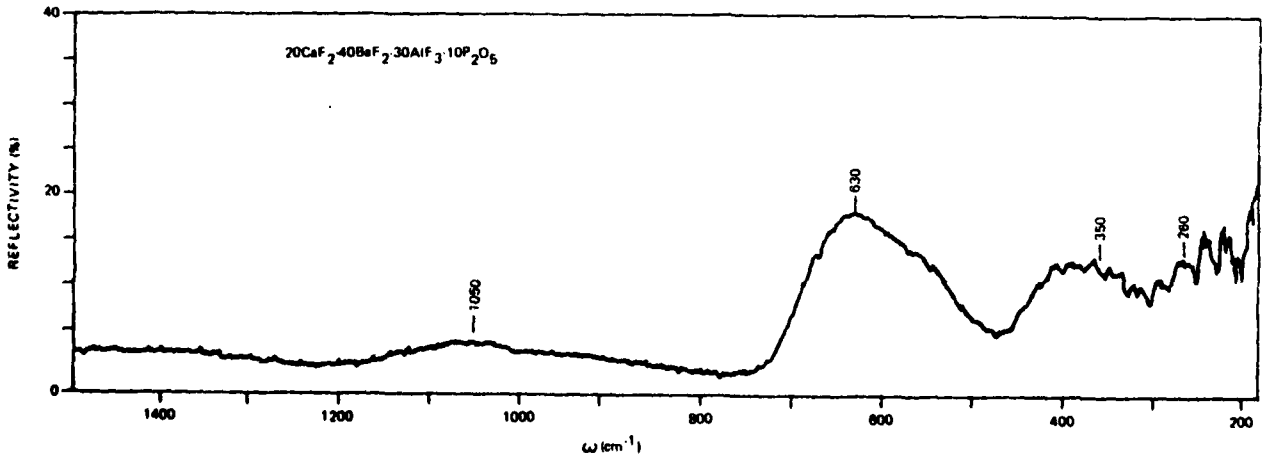

DSC MEASUREMENTS OF CRYSTAL GROWTH KINETICS IN HEAVY METAL FLUORIDE GLASSES

N.P. BANSAL*, A.J. BRUCE, R.H. DOREMUS, and C.T. MOYNIHAN
Materials Engineering Department, Rensselaer Polytechnic Institute, Troy, New York 12181, USA

Introduction

The heavy metal fluoride glasses (HMFG) are highly transparent from the UV (~0.2 microns) to the IR (~8-10 microns) and have potentially very low optical absorption in the mid-IR. These glasses are therefore strong candidate materials for optical fibers for low loss, long distance, repeaterless communication systems. An understanding of the crystallization behavior of the HMFG is important for obtaining high quality optical fibers without devitrification.

We are studying the crystallization kinetics of these fluoride glasses, and the results for a ZrF_4-BaF_2-LaF_3 glass (ZBL, Table 1) were recently reported[1,2]. It is now well established[3-5] that modifying the ZBL composition by addition of AlF_3 and/or sodium or lithium fluoride leads to glasses with improved resistance to devitrification, which in turn should be manifested by a change in the crystallization kinetic parameters. We report here results of a DSC study of the crystallization kinetics of two such modified glasses, ZBLALi and ZBLALiPb (Table 1), which are currently being used for fiber fabrication and testing at NRL[4,6,7], and a comparison with the previously reported[1] crystallization kinetics of the base ZBL glass.

Preliminary DSC scans at a 10 K/min heating rate are shown in Figure 1 for the three glasses. Each scan exhibits three thermal events; in order of increasing temperature these are an endothermic peak at Tg, a large exothermic peak due to crystallization (the primary subject of this study), and a small

exotherm due to transformation of metastable crystals to a more stable form. A crude indication of the greater stability against crystallization of the ZBLALi and ZBLALiPb glasses is the larger difference between Tg and the temperature of the crystallization exotherm compared to the ZBL glass.

Isothermal DSC Crystallization Measurements

The isothermal crystallization of a glass may be described by the Avrami law:

$$-\ell n\ (1-x) = (kt)^n \qquad (1)$$

where x is the volume fraction crystallized after time t, n the Avrami exponent which depends on the morphology of crystal growth, and k the crystallization rate constant. Taking the logarithm of Eq. (1) gives:

$$\ell n\ (-\ell n(1-x)) = n\ \ell n\ k + n\ \ell n\ t \qquad (2)$$

As explained in Ref. 1, x may be determined by DSC by rapidly heating the sample from below Tg to a temperature of interest and monitoring the exothermic crystallization peak as a function of time during subsequent isothermal DSC operation. Typical results for isothermal crystallization on the DSC are shown in Fig. 2 for ZBLALiPb glass at four temperatures; the graphical determination of x is illustrated on one of the isotherms. The values of n and k at each temperature are determined (cf. Eq. (2)) from a linear least square fit of $\ell n\ (-\ell n(1-x))$ vs. $\ell n\ t$. The average activation energy, E, and frequency factor, ν, for crystallization are then evaluated from a linear least squares fit of k as a function of T to the

Arrhenius equation:

$$\ell n\ k = \ell n\ \nu - E/RT \qquad (3)$$

These Arrhenius plots are shown in Fig. 3 for the three glasses of Table 1. The linearity of the plots indicates that Eq. (3) is a good approximation for the temperature dependence of k over the short temperature interval covered by the data for each glass. Alternatively, E may be evaluated from the slope (= -E/R) of an Arrhenius plot of $\ell n\ t_m$ vs. 1/T, where t_m is the time at the maximum in the isothermal crystallization exotherm at temperature T (cf. Fig. 2). The crystallization kinetic parameters obtained from these two treatments are given in Table 2 for the three glasses.

Nonisothermal DSC Crystallization Measurements

In the nonisothermal method the glass sample is heated from below Tg through the crystallization region at a number of heating rates α. Typical results are shown in Fig. 4. The temperature T_p of the maximum in the crystallization exotherm varies with heating rate α according to the expression[1]:

$$\ell n\ (T_p^2/\alpha) = \ell n(E/R) - \ell n\ \nu + E/R\ T_p \qquad (4)$$

Plots of $\ell n\ (T_p^2/\alpha)$ vs. $1/T_p$ are shown in Fig. 5 for the three glasses and are linear over the experimental temperature range. Values of the kinetic parameters E and ν obtained via Eq. (4) are listed in Table 2.

Discussion

Presuming that crystallization is diffusion controlled in the temperature

range of our study, the activation energies E reported in Table 2 should be the same as those for viscous flow. It is now well established[5,8] that the temperature dependence of viscosity of fluorozirconate melts is highly non-Arrhenius, i.e., E appears to be a strong function of temperature. Hence the E values of Table 2 must be considered average values for the temperature range over which crystallization was observed. Given this, there is excellent agreement for each glass between the E values measured by the isothermal and nonisothermal methods.

In an earlier study[5] it was found that "modified" fluorozirconate glasses containing AlF_3 or alkali fluoride had lower viscous flow activation energies in the glass transition region than did the "base" ZBL glass. It was suggested that this accounted for the concomittant decrease in tendency to devitrification of the "modified" glasses relative to the "base" glass, since the lower activation energies of the "modified" glasses would cause them to remain highly viscous over a larger temperature range above Tg. The results of Table 2 show that this effect persists into the actual crystallization range, viz., the E values of the "modified" ZBLALi and ZBLALiPb glasses are only about 2/3 that of the "base" ZBL glass. (As was pointed out in Ref. 5, the lower activation energies of the "modified" glasses are immediately evident in the more gradual onset of their crystallization exotherms in Fig. 1, i.e., the increase in (T_x-T_x') of the "modified" glasses relative to the "base" glass.) Hence it now appears fairly certain that a major source of the improvements in glass quality caused by addition of AlF_3 and/or alkali fluoride to ZBL compositions is due to modification of the viscosity temperature dependence of the melt. The same conclusion was reached in the study of Ref. 4, although in that study a strong effect of PbF_2 on melt viscosity temperature dependence was observed which does not appear in

the present study.

Acknowledgements

This work was supported by Contract No. N00014-83-K-0278 from the Office of Naval Research. ZBLALi and ZBLALiPb glass specimens were kindly provided by D.C. Tran and G.H. Sigel of the Naval Research Laboratory.

References

1. N.P. Bansal, R.H. Doremus, A.J. Bruce, and C.T. Moynihan, J. Am. Ceram. Soc., 66, 233 (1983).

2. N.P. Bansal and R.H. Doremus, J. Am. Ceram. Soc. (in press).

3. A. Lecoq and M. Poulain, Verres Refract., 34, 333 (1980).

4. D.C. Tran, R.J. Ginther and G.H. Sigel, Mat. Res. Bull., 17, 1177 (1982).

5. C.T. Moynihan, D.L. Gavin, K.-H. Chung, A.J. Bruce, M.G. Drexhage and O.H. El-Bayoumi, Glastech. Ber., 56, 862 (1983).

6. D.C. Tran, K.H. Levin, C.F. Fisher, M.J. Burk and G.H. Sigel, Jr., Electron. Lett., 19, 165 (1983).

7. D.C. Tran and G.H. Sigel, Jr., Paper No. 50, Extended Abstracts, 2nd International Symposium on Halide Glasses.

8. H. Hu and J.D. Mackenzie, J. Non-Cryst. Solids, 54, 241 (1983).

Table 1. Compositions (mole%) of Heavy Metal Fluoride Glasses

Glass	ZrF_4	BaF_2	LaF_3	AlF_3	LiF	PbF_2
ZBL	62.0	33.0	5.0	-	-	-
ZBLALi	50.7	20.7	5.2	3.2	20.2	-
ZBLALiPb	49.83	16.96	5.06	3.16	20.09	4.09

Table 2. Kinetic Parameters for Crystallization of Fluoride Glasses Obtained from Isothermal and Non-Isothermal DSC Studies

Glass	Isothermal				Non-isothermal	
		$\ell n\ k$ vs. $1/T$		$\ell n\ t_m$ vs. $1/T$		
	n	$\nu(s^{-1})$	E(kJ/mol)	E(kJ/mol)	$\nu(s^{-1})$	E(kJ/mol)
ZBL	3.2 ± 0.2	7×10^{21}	301	332	6.36×10^{22}	314
ZBLALi	3.3 ± 0.8	2.3×10^{14}	203	189	2.52×10^{11}	168
ZBLALiPb	2.2 ± 0.2	5.2×10^{17}	220	174	1.66×10^{14}	197

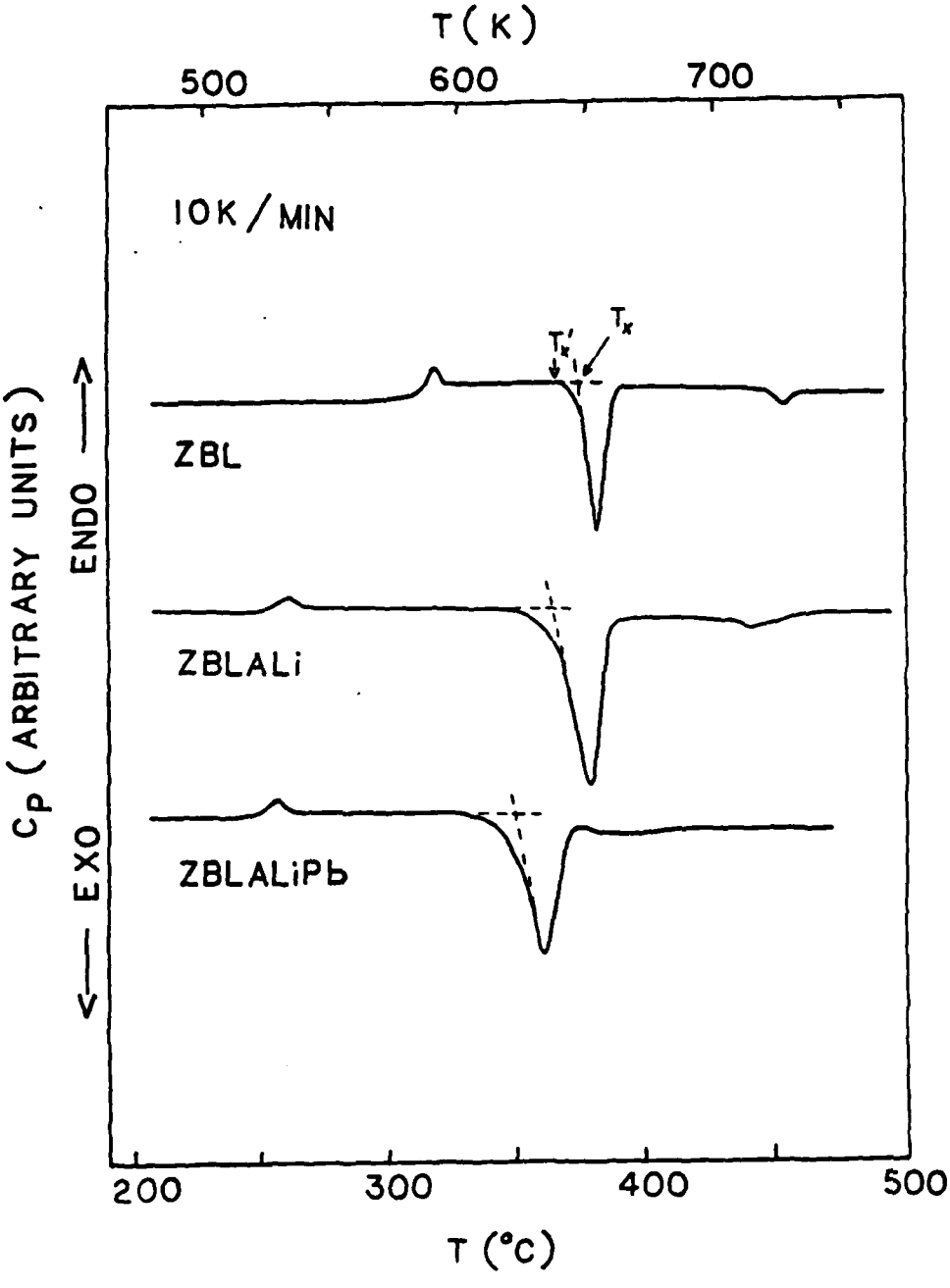

Figure 1. DSC Scans at 10 K/min heating rate of ZBL, ZBLALi and ZBLALiPb glasses.

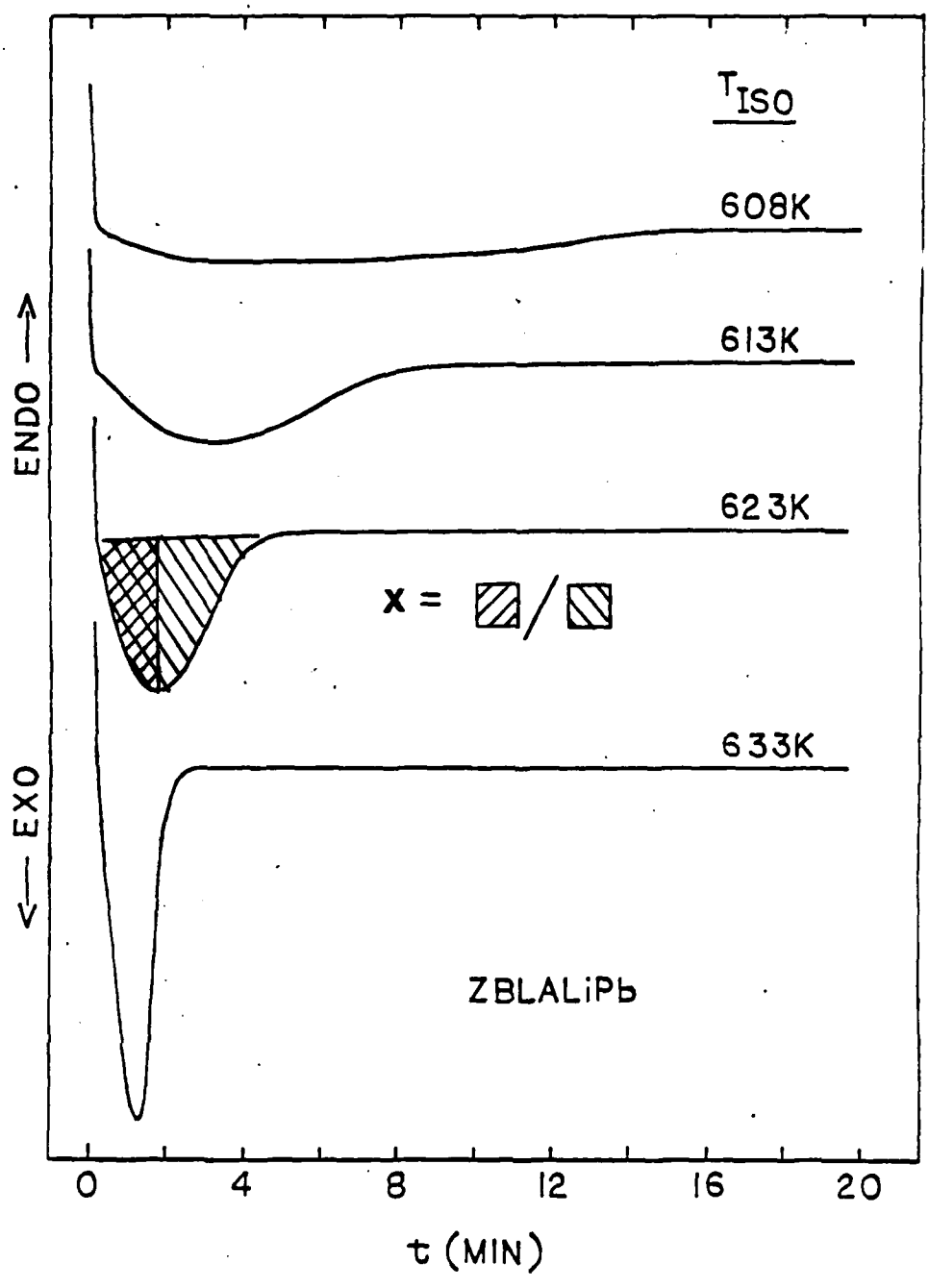

Figure 2. DSC output during isothermal crystallization of ZBLALiPb glass at four temperatures.

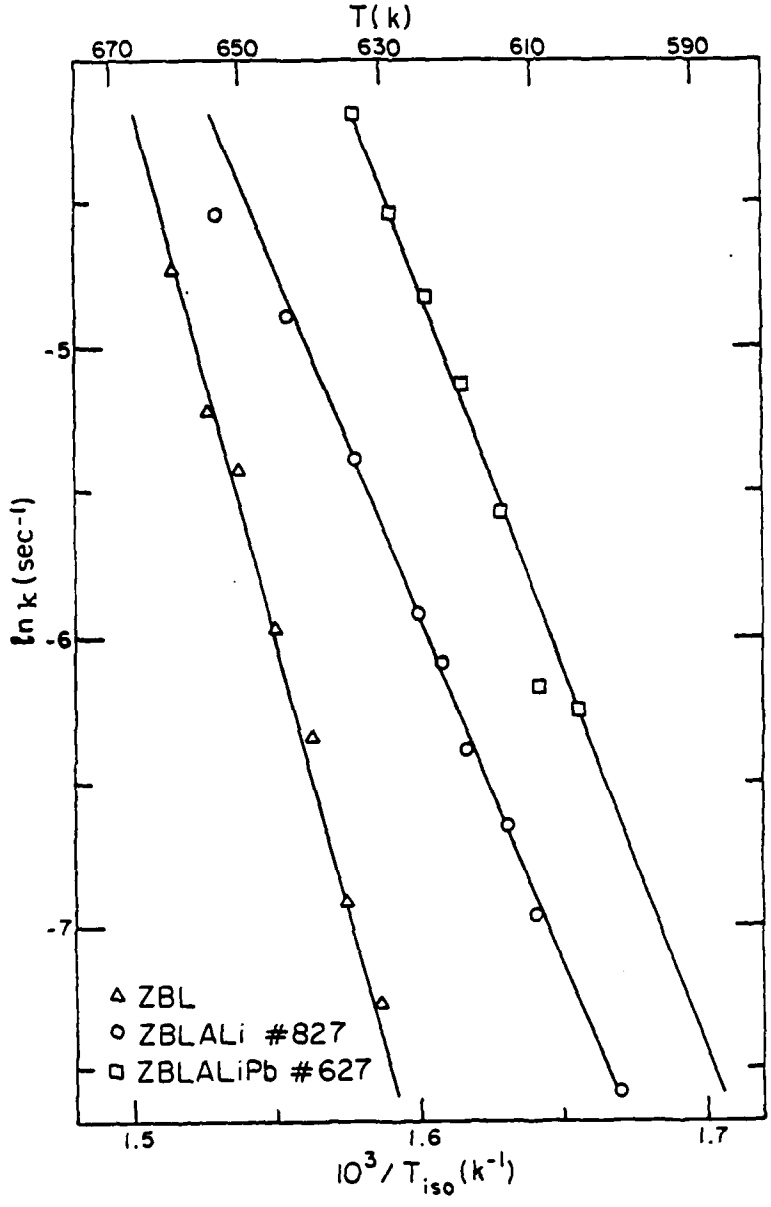

Figure 3. Arrhenius plots for crystallization rate constants obtained from isothermal DSC measurements. Lines are linear least squares fits of ℓn k vs. $10^3/T$.

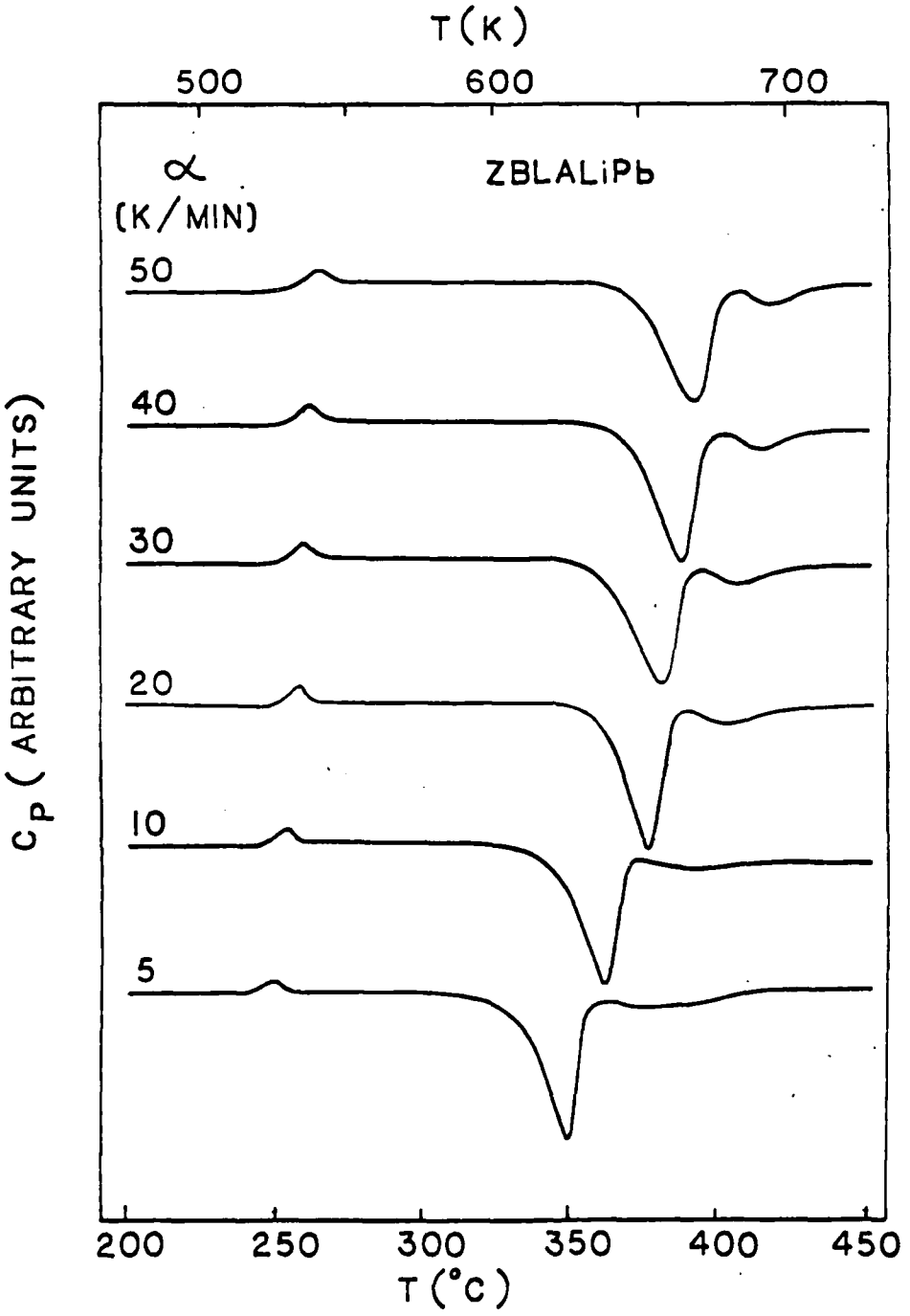

Figure 4. DSC scans at different heating rates α for ZBLALiPb glass.

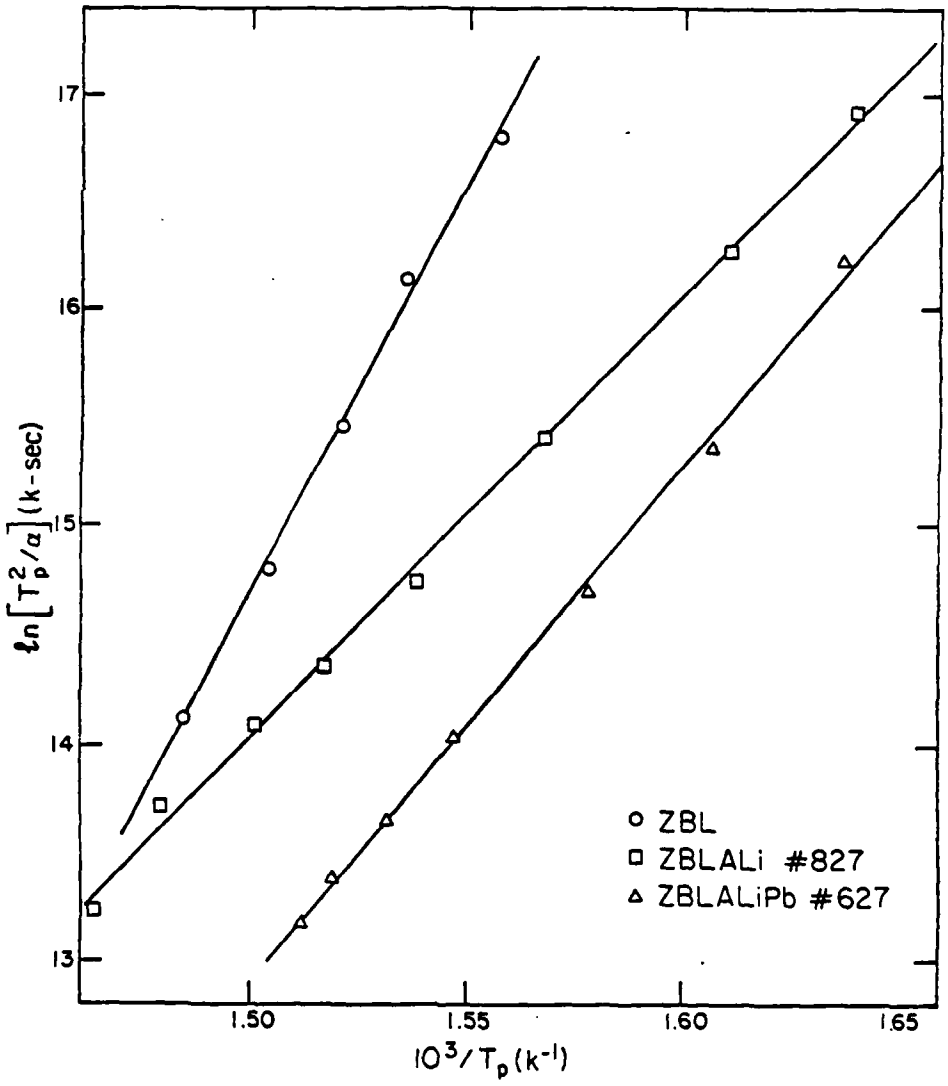

Figure 5. Plots of $\ell n(T_p^2/\alpha)$ vs. $1/T_p$ for crystallization of fluoride glasses. Lines represent least-squares fit of data.

SURFACE CRYSTALLIZATION ON FLUORIDE GLASSES

R. H. Doremus and N. P. Bansal
Rensselaer Polytechnic Institute
Materials Engineering Department
Troy, New York 12181
USA

The usefulness of fluoride glasses as optical components depends on control of surface properties. Surface crystallization can change the optical properties of the glass and destroy its mechanical integrity. Therefore we studied the crystallization of fluoride glass surfaces after they were heated, and found fine crystals that grew to a certain size, after which wrinkled regions grew out from these initial crystals.

The glass composition chosen for study was 62% ZrF_2, 33% BaF_2, 5% LaF_3, mole%. Slices of glass were cut with a diamond saw and polished with 1 μm diamond paste. Under the optical microscope the glass surface showed no scratches or other features. Samples were heated at temperatures from 322° to 390°C, after which they were observed in the optical microscope. Selected samples were observed in the scanning electron microscope after the surface was coated with gold.

As the samples were heated for successively longer times, individual small crystals grew on the surface. They seemed to be all of about the same size, suggesting that they were nucleated early in the heating cycle. There was some evidence that these crystals were associated with dark regions in crystals containing these regions.[1] Dark regions are formed when the glasses are melted in an inert atmosphere; they are not present when a small amount of chlorine is added to the inert gas.

When these crystals reached about 10 μm in size, wrinkled regions grew out from them on the glass surface. The nature of these wrinkled regions is uncertain. They could be crystals growing along the surface, or they

could result from deformation of a surface layer caused by stresses in the surface. More work is needed to determine their origin.

References

1. S. L. Callahan, M.S. Thesis, Rensselaer Polytechnic Institute, 1982.

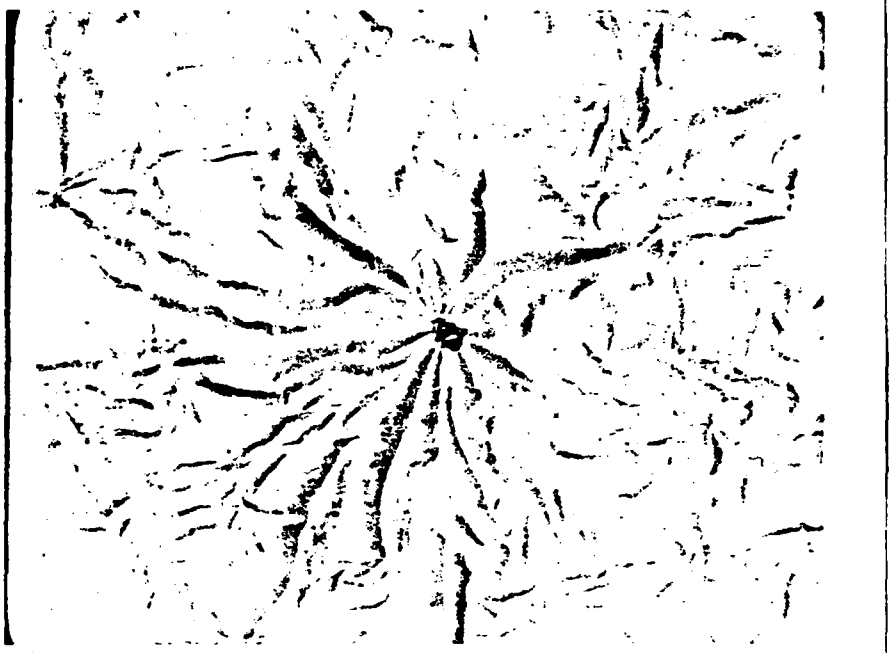

Fig. 1. Optical micrograph of surface crystals on a ZBL glass after heating for 45 min at 390°C; 250X

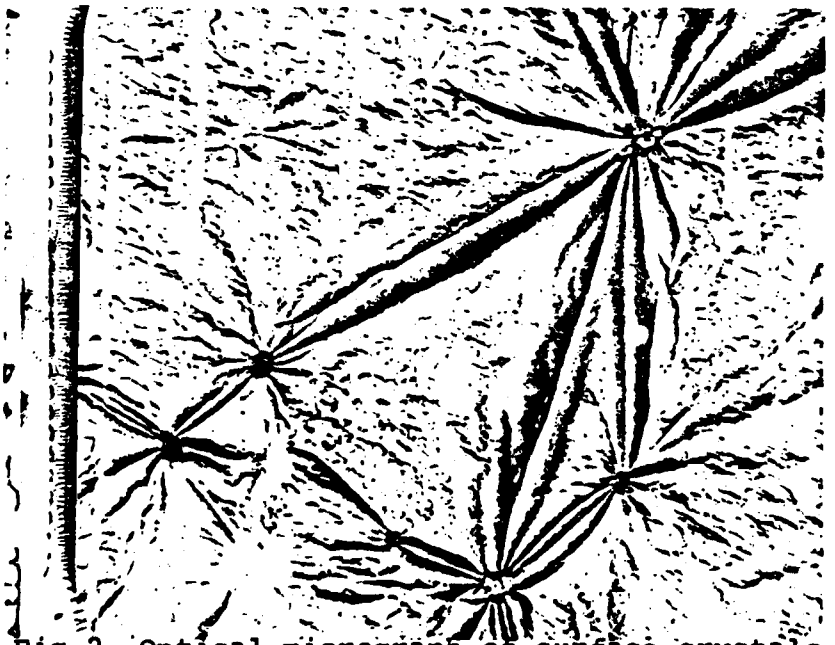

Fig.2. Optical micrograph of surface crystals on a ZBL glass after heating for 90 min at 390°C; 250X

FUNDAMENTAL OPTICAL PROPERTIES OF HEAVY METAL FLUORIDE GLASSES

Bernard Bendow
The BDM Corporation
Albuquerque, NM 87106

This paper reviews the current state of knowledge on the optical properties of heavy metal fluoride (HMF) glasses. Although far from comprehensive, considerable data is nevertheless now available for many HMF glasses, on a variety of optical properties such as: IR and UV absorption; fluorescence; fundamental IR reflectivity; Raman, Brillioun and Rayleigh scattering; refractive index, and its wavelength and temperature dependence; and photoelastic constants. These data enable evaluation of the characteristics and performance of optical components fabricated from HMF glasses, as well as providing insight into fundamental properties such as structure and bonding. The current and projected values of several key optical parameters are summarized in Table 1.

Some salient points regarding glass transparency are: HMF glasses are capable of continuous high transparency (absorption coefficient less than 0.1 cm^{-1}) from about 0.3 μm in the near-UV to 7 μm in the mid-IR. The IR edges are relatively steep and structureless, similar to those of alkaline-earth fluoride crystals, and display dependences characteristic of intrinsic multiphonon edges (see Figure 1). The longest wavelength IR edges observed to date are for Ba/Th fluoride glasses such as BaF_2-ZnF_2-YF_3-ThF_4. The UV edges are highly dependent on glass processing conditions, with near-exponential edges being observed in certain circumstances (see Figure 2). Constituents which limit the IR, visible and/or UV transparency of the glasses have been identified. For example, addition of AlF_3 has been shown to shift the IR edge to shorter wavelength (see Figure 3). Extensive studies of absorption and/or emission associated with a wide variety of impurities and/or dopants ranging from rare-earths to OH have been reported, and quantitative relations been absorption levels and concentration have been established in many cases.

The refractive index of HMF glasses vary over a relatively broad range as a function of composition, with typical values 1.48-1.49 for Ba/Th fluoride glasses and 1.50 to 1.53 for fluorozirconates. Visible and IR dispersion is low, with typical Abbe numbers in the range 65-85, and low material dispersion ($d^2n/d\lambda^2$) over a broad range of IR wavelengths (see Figure 4).

Thermal distortion associated with transmission of high energy laser light through optical elements depends on a number of parameters such as $\partial n/\partial T$ and the photoelastic constants p_{ij}, as indicated in Table 2. Recent measurements indicate values of $\partial n/\partial T$ in the range -9 to $-16(10^{-6}/C)$, and of birefringence $|p_{11}-p_{12}|$ ranging from ~0.005 to 0.13.

Other significant results include: Measurements of Rayleigh scattering displaying a λ^{-4} dependence, and scattering cross sections comparable or less than that of fused silica; measured values of total integrated scatter in the IR as low as 10^{-3}; and measured minimum losses in fibers of nearly 10dB/km.

Fundamental IR spectroscopy of HMF glasses has provided substantial insight into their bonding, structure and vibrational characteristics. For example, the spectra of flurozirconate glasses imply they possess partially ionic bonding and contain well-defined ZrF_x structural units. On the other hand, Ba/Th glasses do not appear to possess a single well-defined unit dominating the glass structure.

The observed and projected properties imply that HMF glasses are extremely promising candidates for a wide variety of applications, as indicated for high energy lasers, for example, in Table 3. Some examples: (a) Their IR edge characteristics and low Rayleigh scattering imply a minimum loss in HMF glass optical fibers as low as 10^{-3}dB/km (see Figure 5). Combined with their low material dispersion, HMF glass fibers emerge as viable candidates for ultralong repeaterless communications links. (b) Their low absorption and favorable properties for ultralow thermal distortion (see Table 4) make them highly attractive candidates for high energy laser transmissive otpics over a broad range of operating wavelengths. (c) Their multispectral transmission, low absorption and low total scatter offer promise for missile dome applications in the 2-6 μm regime. Other capabilities include narrow band absorption filters, low dispersion lenses and IR laser hosts.

Research supported in part by Naval Ocean Systems Center under Contract No. N66001-83-C-0153.

TABLE 1

OPTICAL PROPERTIES OF FLUORIDE GLASSES

	CURRENT	PROJECTED
REFRACTIVE INDEX	1.45 - 1.60	*
DISPERSION	$d^2n/d\lambda^2$ ~$5x10^{-3}$ μm^2 (IR)	*
ABSORPTION COEFFICIENT	~$2x10^{-5}$ cm^{-1} (HF) ~10^{-4} cm^{-1} (6348Å)	~$2x10^{-8}$ cm^{-1} (HF & DF) ~10^{-5} cm^{-1} (6348Å)
RAYLEIGHT SCATTERING	SIMILAR TO SiO_2	LOWER THAN SiO_2
TIS	~10^{-2} TO 10^{-3} (DF)	<10^{-3} (MID-IR)
BIREFRINGENCE	$P_{11}-P_{12}$ ~ .005	*
dn/dT	(-.9) TO (-1.5) x $10^{-5}/^oK$	*
THERMAL DISTORTION	~$1x10^{-6}/^oK$	~$1x10^{-7}/^oK$
LASER DAMAGE (BULK)	VERY GOOD* (DF)	EXCELLENT
SURFACE FINISH	VERY GOOD	EXCELLENT

*DATA IS CLASSIFIED

TABLE 2

THERMAL DISTORTION FORMULA FOR BULK ABSORPTION IN A SINGLE SLAB

STREHL RATIO $\quad SR = \frac{I}{I_o} = 1 - \Delta$

Δ IS THE DEGRADATION IN THE STREHL RATIO ($\Delta \gtrsim .2$ TO SATISFY MARECHAL's CRITERION). WITH $k = 2\pi/\lambda$,

$$\Delta = (k\Delta TL)^2 \, \delta$$

$$\delta = U(f_1 + 2f_2)^2 + Sf_2^2 \equiv U(dn/dT)_e^2$$

WHERE

$$f_1 = (\partial n/\partial T) + \alpha(n^3/2)\left[(1-\nu)p_{12} - p_{11}\right] + \alpha(1+\nu)(n-1)$$

$$f_2 = \alpha n^3(1+\nu)(p_{11} - p_{12})$$

n IS THE REFRACTIVE INDEX, ν IS POISSON'S RATIO, p_{ij}'s ARE PHOTOELASTIC CONSTANTS

TABLE 3

HEL APPLICATIONS FOR FLUORIDE GLASS

- LASER WINDOWS (HF/DF, Nd:YAG, I_2, FELs, EXCIMERS)
- BEAM EXPANDERS (FELs)
- GRATINGS (SINGLE OR MULTI-λ)
- HR/AR COATINGS FOR REFLECTIVE/TRANSMISSIVE COMPONENTS
- RUGATE COATINGS FOR EO SYSTEMS LASER HARDENING AND FOR MULTIWAVELENGTH COMPONENTS
- CORROSION RESISTANT COMPONENTS/SUBSTRATES FOR HALIDE GAS LASERS
- ULTRALOW DISTORTION LASER RODS

TABLE 4

GLASS PERFORMANCE (PHOSPHATES AND FLUORIDES)

MATERIAL	FoM(Δ) $p_{ij} = 0$	FoM(Δ) $p_{ij}=p_{ij}(SiO_2)$	$(dn/dT)_e$ $p_{ij} = 0$ $(10^{-6}/^oC)$	$(dn/dT)_e$ $p_{ij}=p_{ij}(SiO_2)$ $(10^{-6}/^oC)$
Phosphates:				
LG750	2.24		2.40	
LG760	2.20		2.15	
LG810	0.0270	4.12	0.324	2.52
LH6-8	1.30		2.17	
LH6-10	0.373	6.87	1.16	3.15
Flourides:				
ZBLA		2.26*		1.81*
HBL ($+p_{ij}$)		0.886*		1.13*
HBL ($-p_{ij}$)		7.17*		5.09*

* measured values of p_{ij} used for fluoride glasses

$\beta = 5 \times 10^{-6}$ cm^{-1}; $h = 0.1$ $W/(cm^2\text{-}^oC)$; $L = 0.5cm$; $I/I_o = 1$
$S = 0.1997$; $U = 0.06319 \rightarrow 1/e^2$ beam edge

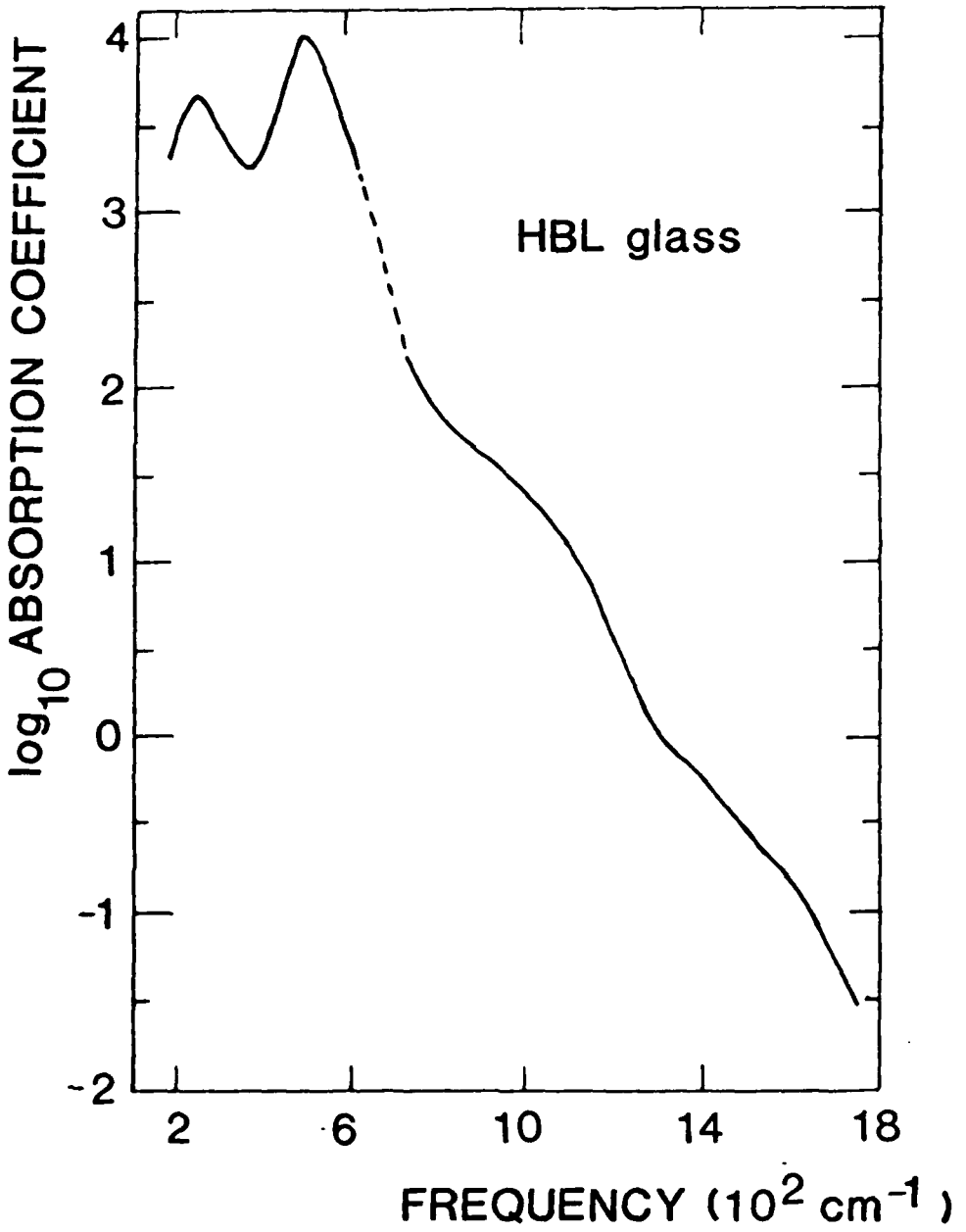
HBL glass
log10 ABSORPTION COEFFICIENT
4
3
2
1
0
-1
-2
2
6
10
14
18
FREQUENCY (10^2 cm^-1)

Figure 1

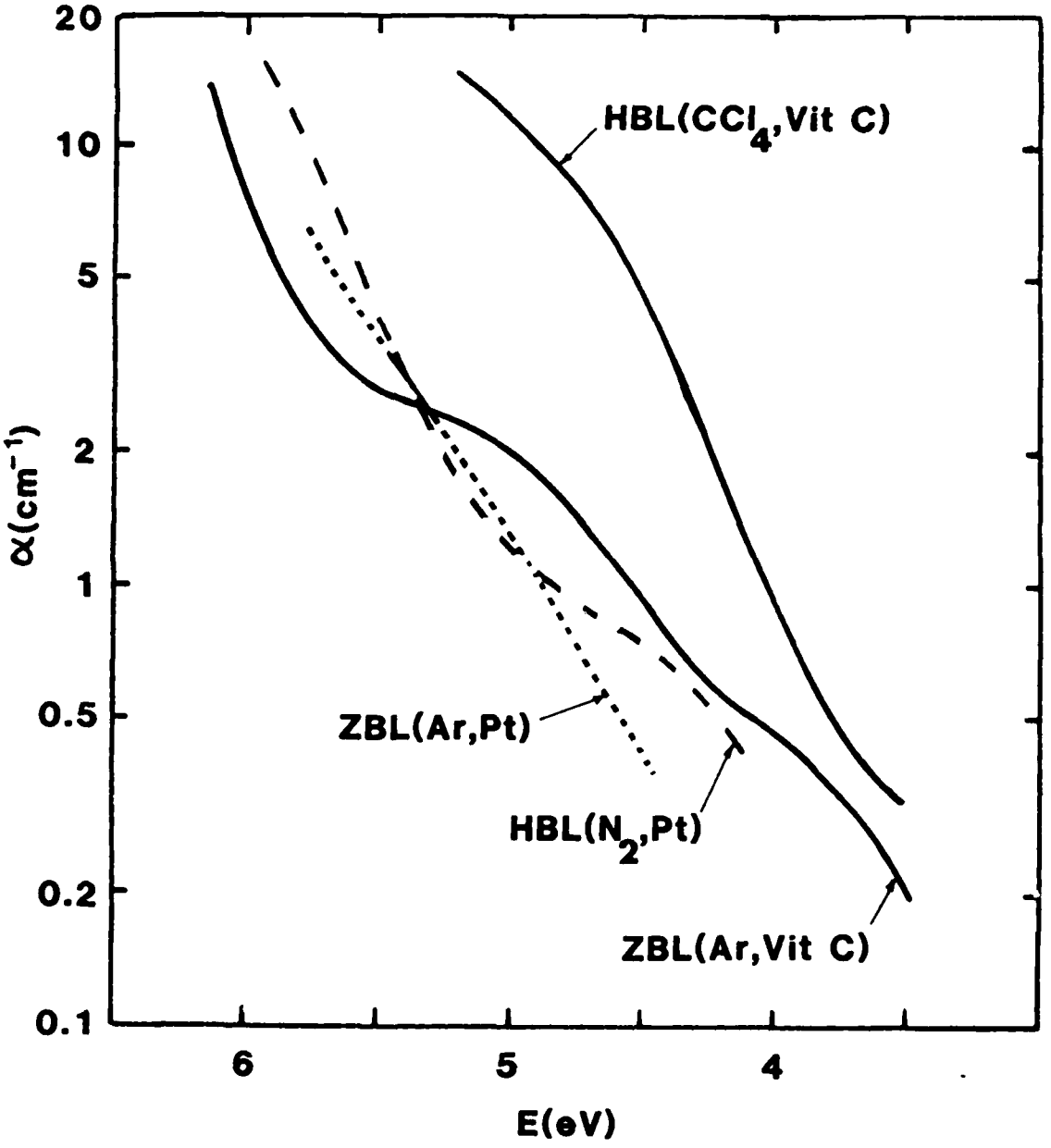
20
10
5
2
1
0.5
0.2
0.1
α(cm⁻¹)
HBL(CCl4,Vit C)
ZBL(Ar,Pt)
HBL(N2,Pt)
ZBL(Ar,Vit C)
6
5
4
E(eV)

Figure 2

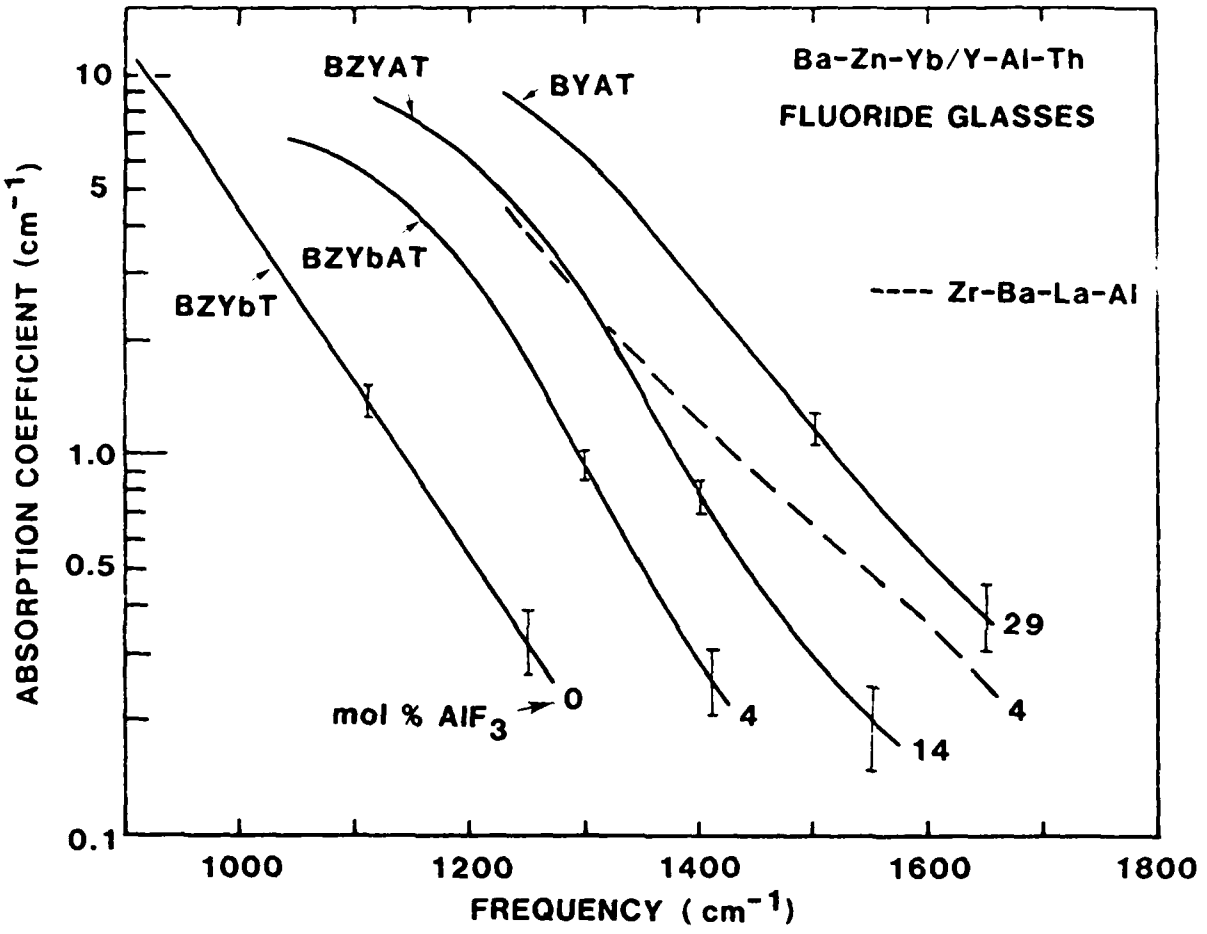
Ba-Zn-Yb/Y-Al-Th
FLUORIDE GLASSES
BZYAT
BYAT
BZYbAT
BZYbT
---- Zr-Ba-La-Al
mol % AlF3
0
4
14
29
4
ABSORPTION COEFFICIENT (cm-1)
10
5
1.0
0.5
0.1
1000
1200
1400
1600
1800
FREQUENCY (cm-1)

Figure 3

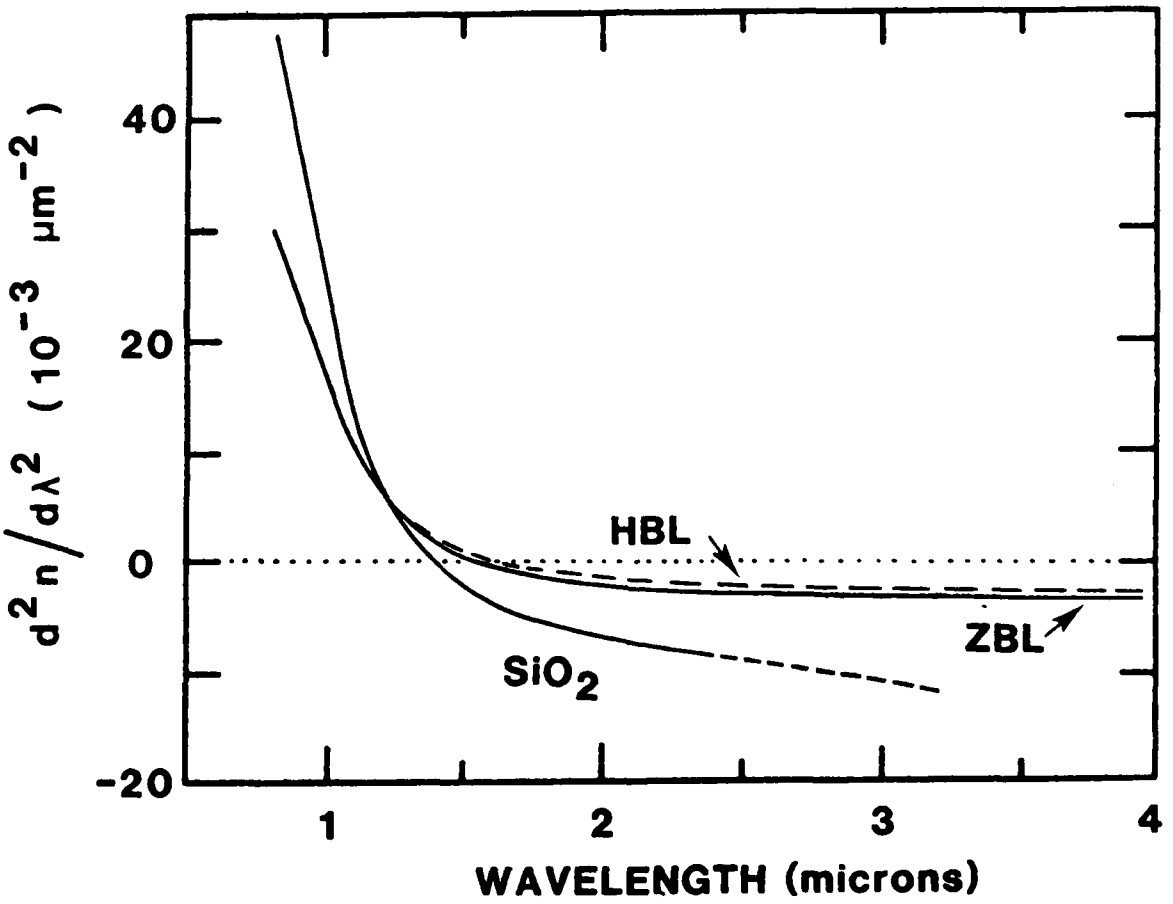
40
20
0
-20
1
2
3
4
$d^2n/d\lambda^2$ (10^{-3} μm^{-2})
WAVELENGTH (microns)
HBL
ZBL
SiO_2

Figure 4

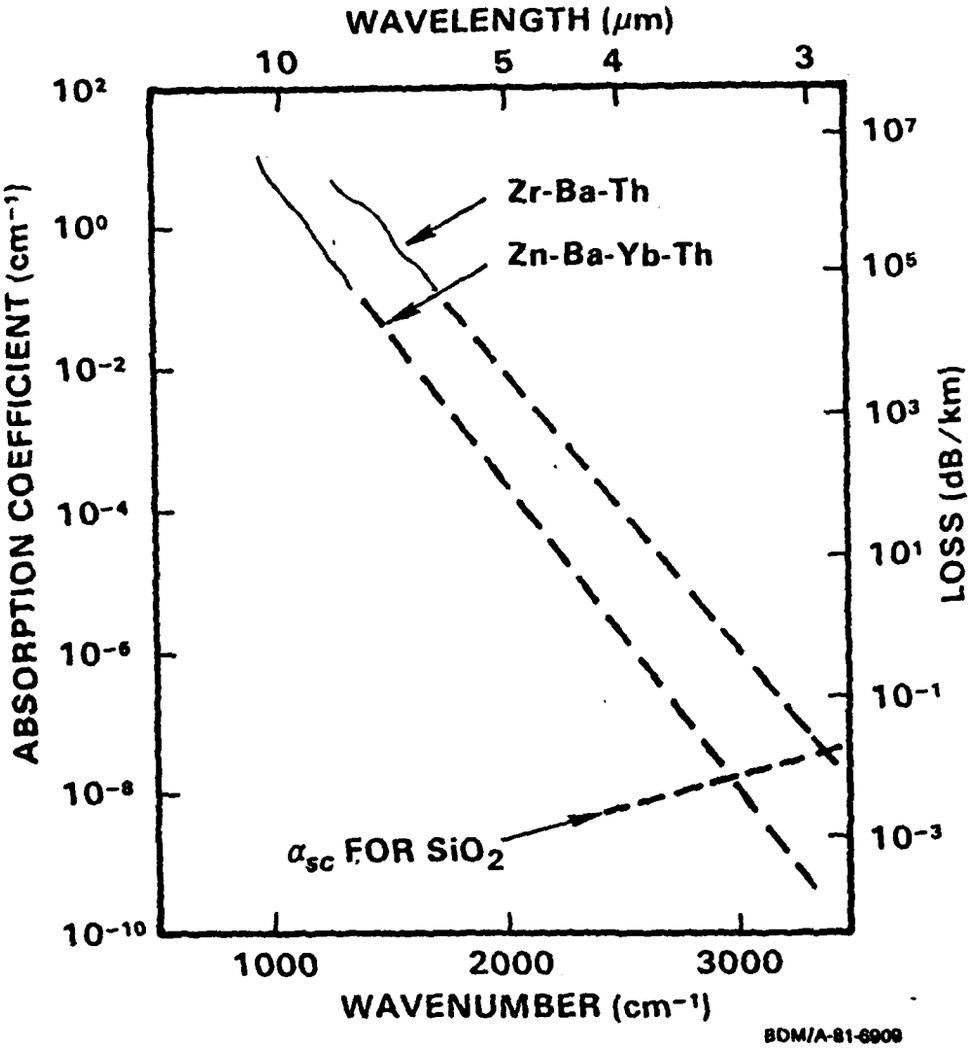
WAVELENGTH (μm)
10
5
4
3
ABSORPTION COEFFICIENT (cm⁻¹)
10²
10⁰
10⁻²
10⁻⁴
10⁻⁶
10⁻⁸
10⁻¹⁰
LOSS (dB/km)
10⁷
10⁵
10³
10¹
10⁻¹
10⁻³
Zr-Ba-Th
Zn-Ba-Yb-Th
αsc FOR SiO2
1000
2000
3000
WAVENUMBER (cm⁻¹)
BDM/A-81-6909

Figure 5

AN F^{19} NMR STUDY OF HEAVY METAL FLUORIDE GLASSES BASED ON ZrF_4

P.J. Bray and R.V. Mulkern, Brown U., Providence, RI
M.G. Drexhage, RADC, Hanscom AFB, MA
S.G. Greenbaum and D.C. Tran, Naval Research Lab., Washington, DC

Several compositions of ZrF_4 based glasses have been studied using F^{19} NMR. The spin-lattice relaxation time, T_1, of the F^{19} nucleus was measured over a wide temperature range. Figure 1 portrays a typical ln T_1 vs. 1000 /T plot for these glass systems. Activation energies, E_a, for fluorine motion were calculated from these plots through the application of the Bloembergen, Pound, and Purcell (BPP) theory. From Table 1 it may be seen that these activation energies are compositionally dependent. The addition of stabilizing agents such as LaF_3 and AlF_3 to the binary ZrF_4-BaF_2 system increased the activation energies, indicating a suppression of fluorine motion in the more stable glasses.

A marked difference in activation energy was found between NaF containing glasses (0.31 e.v./ion) and LiF co: ning glasses (0.71 e.v./ion). This difference seems to confirm the observations of Poulain and LeCoq[1] that the Na^+ and Li^+ ions play different structural roles in the vitreous network.

---

1) "Lanthanum Fluorozirconate Glasses", A. LeCoq and M. Poulain, J. Non-Cryst. Solids, 34(1979) 101-110.

Table 1

Glass	Composition mol%	E_a (e.v./ion)
ZB-2-8	$57.7ZrF_4 - 42.3BaF_2$	0.25
ZF-s-28	$63.5ZrF_4 - 29.5BaF_2 - 7LaF_3$	0.30
ZBL	$62ZrF_4 - 33BaF_2 - 5LaF_3$	0.29
ZBLA	$57ZrF_4 - 36BaF_2 - 3LaF_3 - 4AlF_3$	0.42
HBLA	$57HfF_4 - 36BaF_2 - 3LaF_3 - 4AlF_3$	0.44
ZF-698	$51ZrF_4 - 20LiF - 16BaF_2 - 5LaF_3 - 3AlF_3 - 5PbF_2$	0.71
ZF-4-20	$51ZrF_4 - 20NaF - 16BaF_2 - 5LaF_3 - 3AlF_3 - 5PbF_2$	0.31

Figure 1

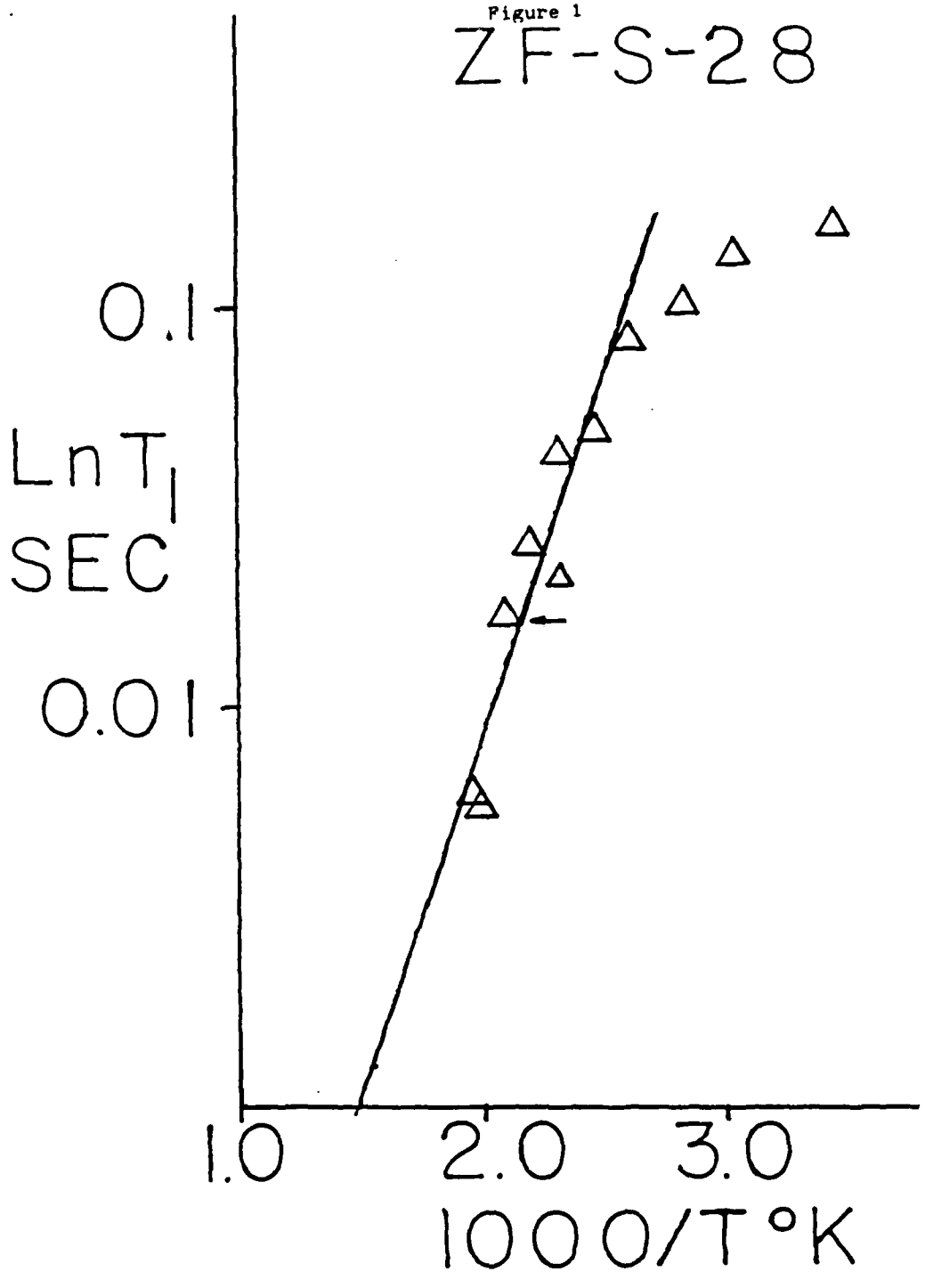

DSC STUDY OF NUCLEATION AND CRYSTALLIZATION OF HEAVY METAL FLUORIDE GLASSES

A. J. Bruce and C. T. Moynihan
Rensselaer Polytechnic Institute
Troy, New York 12181
USA

and

O. H. El-Bayoumi and M. G. Drexhage
Rome Air Development Center
Hanscom AFB, MA 01731
USA

Whether or not heavy-metal fluoride glass (HMFG) fibers will ultimately be used for ultra-low loss, long range optical communcation will depend (1) on improving the material purity and (2) minimizing glass instabilities (e.g. against crystallization, physical aging and corrosion) during the fiber production and use.

Matecki et al.[1] have suggested that all HMFG may be unstable against homogeneous nucleation at their annealing temperatures (cf. Figure 1) and that the nuclei produced on annealing fibers preforms may grow sufficiently at the drawing temperatures to produce unacceptable scattering losses in the resultant fibers.

In this study the nucleation effects produced on annealing 10 BaF_2-50 MnF_2-40 ThF_4 (BMT-1) glass (mol%) in the vicinity of the glass transition temperature ($\sim$ 600K) have been investigated using DSC.

Figure 2 shows DSC rate heating scans (10K/min) obtained for BMT-1 glass samples after annealing them for 10 hours at T_A and then cooling them rapidly (-100K/min) to 540K. The magnitude of the heat capacity change ΔC_p at the glass transition is proportional to the fraction of the sample which is amorphous; i.e., ΔC_p is smaller for a partly crystalline sample than for a completely amorphous sample. The plot of ΔC_p versus annealing temperature (Figure 3(a))

indicates that a negligible amount ($\leq$ 2%) of crystallization occurred during the 10 hour anneals of BMT-1 at temperatures at or below 610K. Relative shifts in the first crystallization exotherm X_1 (cf. Figure 2) on subsequent rate heating are therefore attributed to increases in the number of growth centers during annealing (i.e., nucleation). The same conclusion is indicated by the variation of the enthalpy change ΔH_1 for the crystallization exotherm (Fig. 3(b)).

After annealing treatments in the range 610-650K the ΔC_p values measured on subsequent rate heatings are observed to decrease with increasing annealing temperature, reaching zero by 640K. This indicates that substantial crystal growth occurs during these annealing treatments, although, at a relatively slow rate, 10 hours being required for $\sim$ 50% crystallization at 630K. Note that the high temperature exotherm X_2 in Figure 2 is unaffected by changes in annealing temperature. This exotherm is most probably due to a solid-solid transformation from a metastable polymorph initially formed on crystallization to a more stable polymorph.

In Figure 4 our interpretations are superimposed on plots of characteristic temperatures versus prior annealing temperatures. The maximum shift in the crystallization onset temperature T_{x_1} after annealing at 590K is therefore attributed to a maximum in the nucleation rate (I) at this temperature for the 10 hour annealing treatments.

In Figure 5 the location of the nucleation and growth curves deduced from the present study of BMT-1 glass are compared with those for "stable" and "unstable" glasses. It is seen that the BMT glass does indeed fall into the unstable category, although the degree of overlap between the nucleation and growth rate peaks is relatively small. Measurement of the scattering effects due to the nuclei and their subsequent growth at typical drawing temperatures remain

to be made.

Acknowledgement

Research was supported by the Rome Air Development Center under Contract Number F19628-83-C-0016.

Reference

1. M. Matecki, M. Poulain, J. Lucas, D. R. MacFarlane and C. A. Angell, Mat. Res. Bull. 18, 293 (1983).

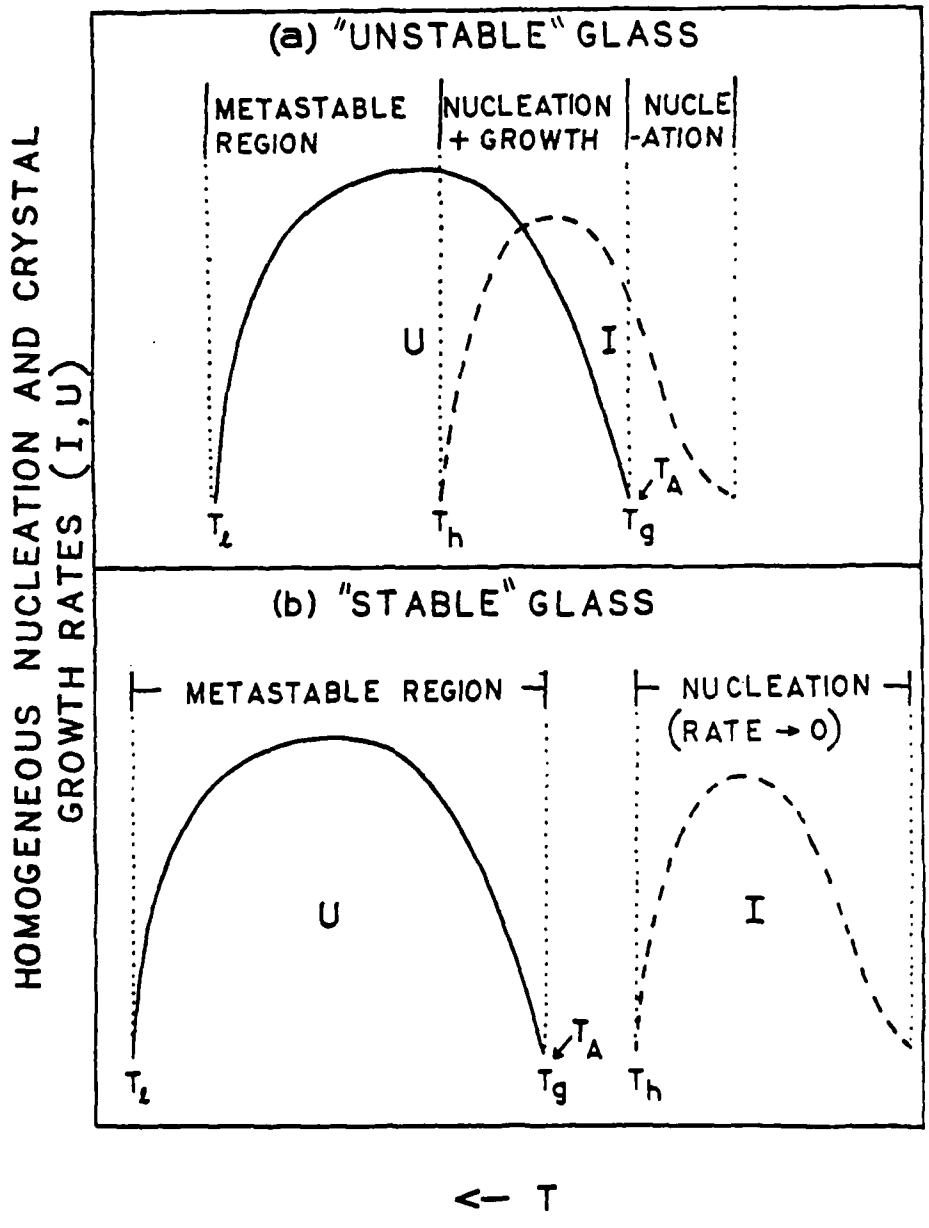

Figure 1. A schematic representation of nucleation (I) and crystal growth rates (U) for

(a) an "unstable" and
(b) a "stable" glass.

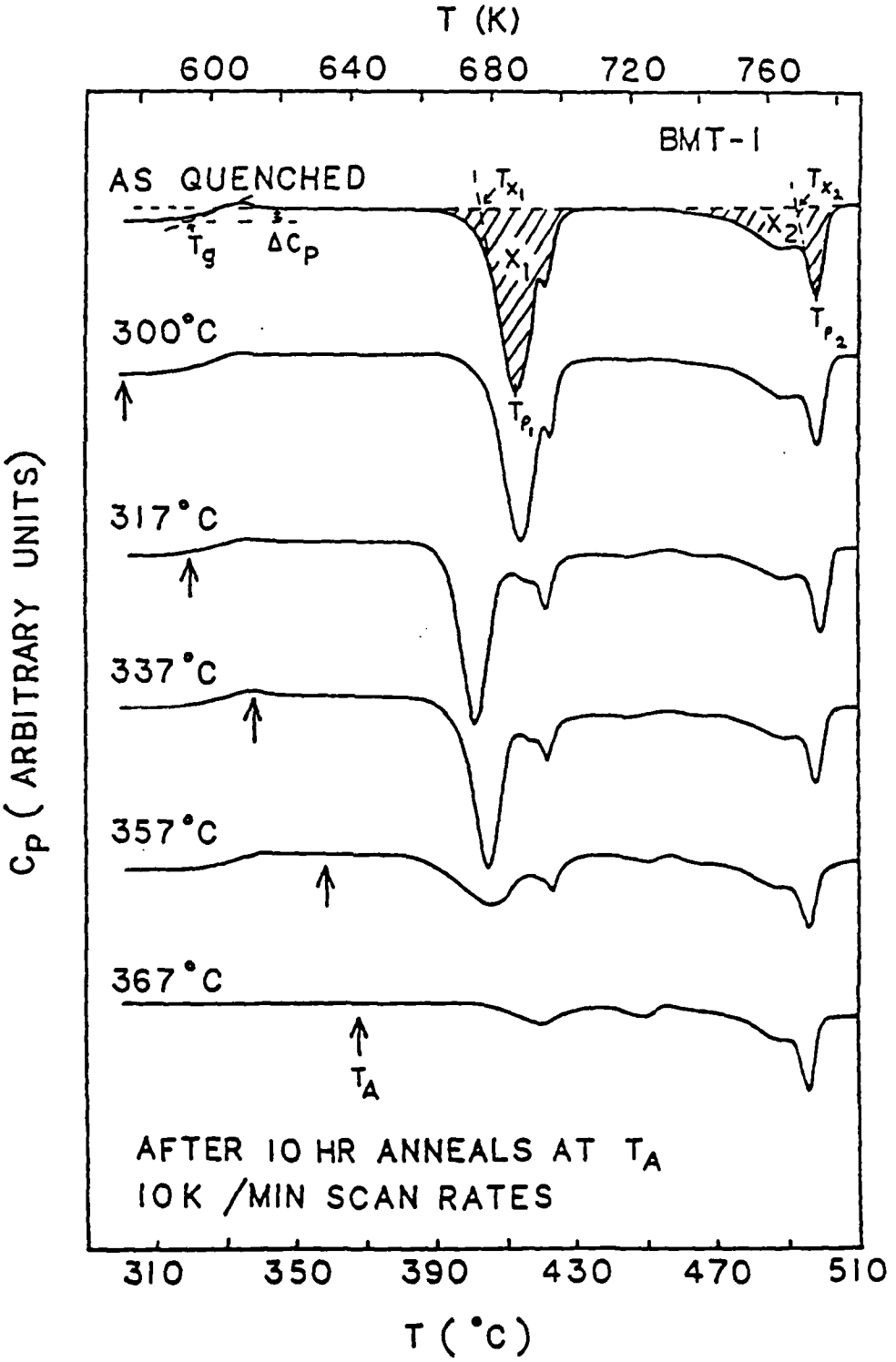

Figure 2. DSC rate heating scans (10K/min) for BMT-1 glass samples previously annealed for 10 hours at T_A and then rate cooled to 540K at 100K/min.

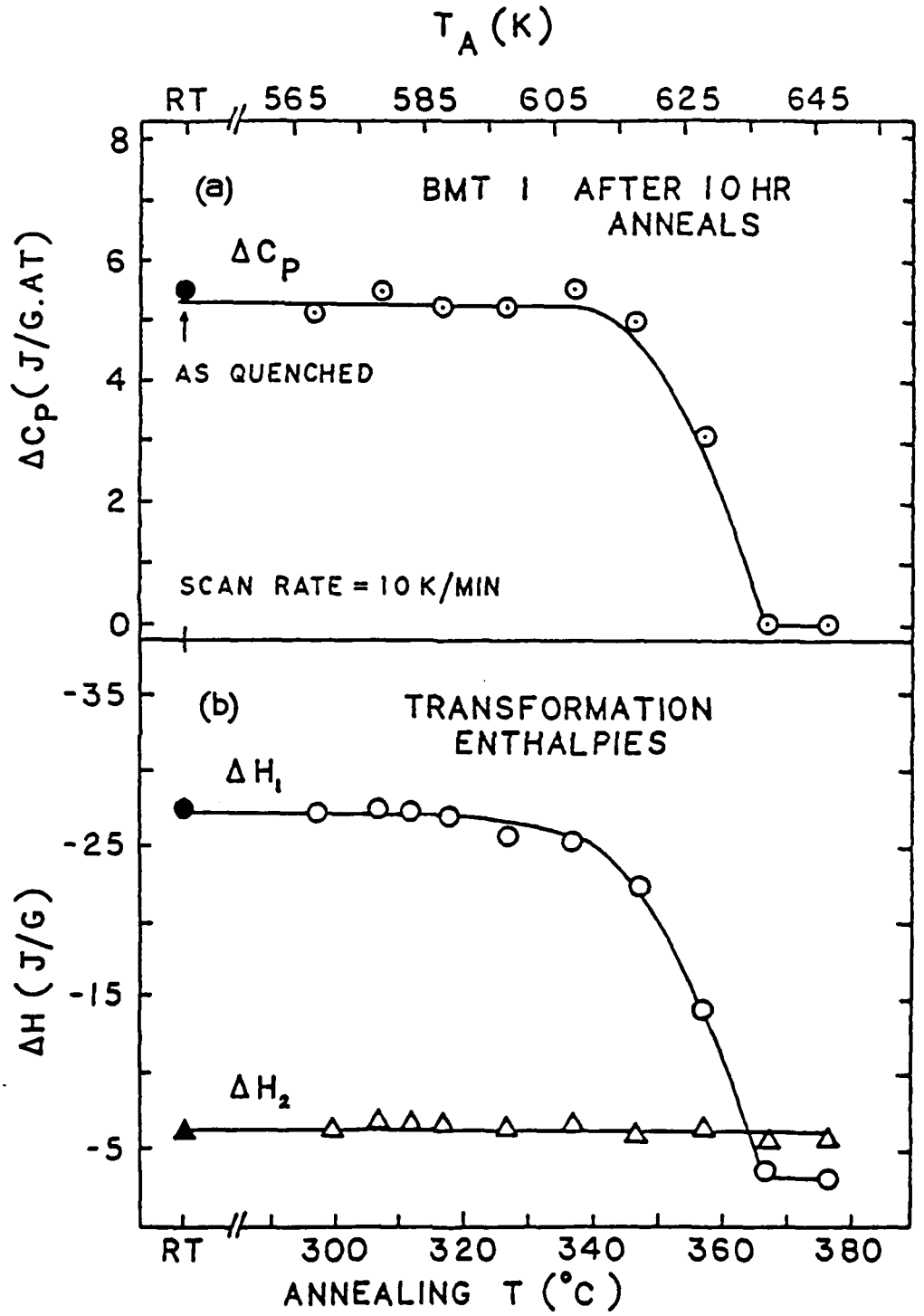

Figure 3. (a) ΔC_p and
(b) ΔH_1 and ΔH_2
values for BMT-1 glass versus annealing temperature after 10 hour anneals.

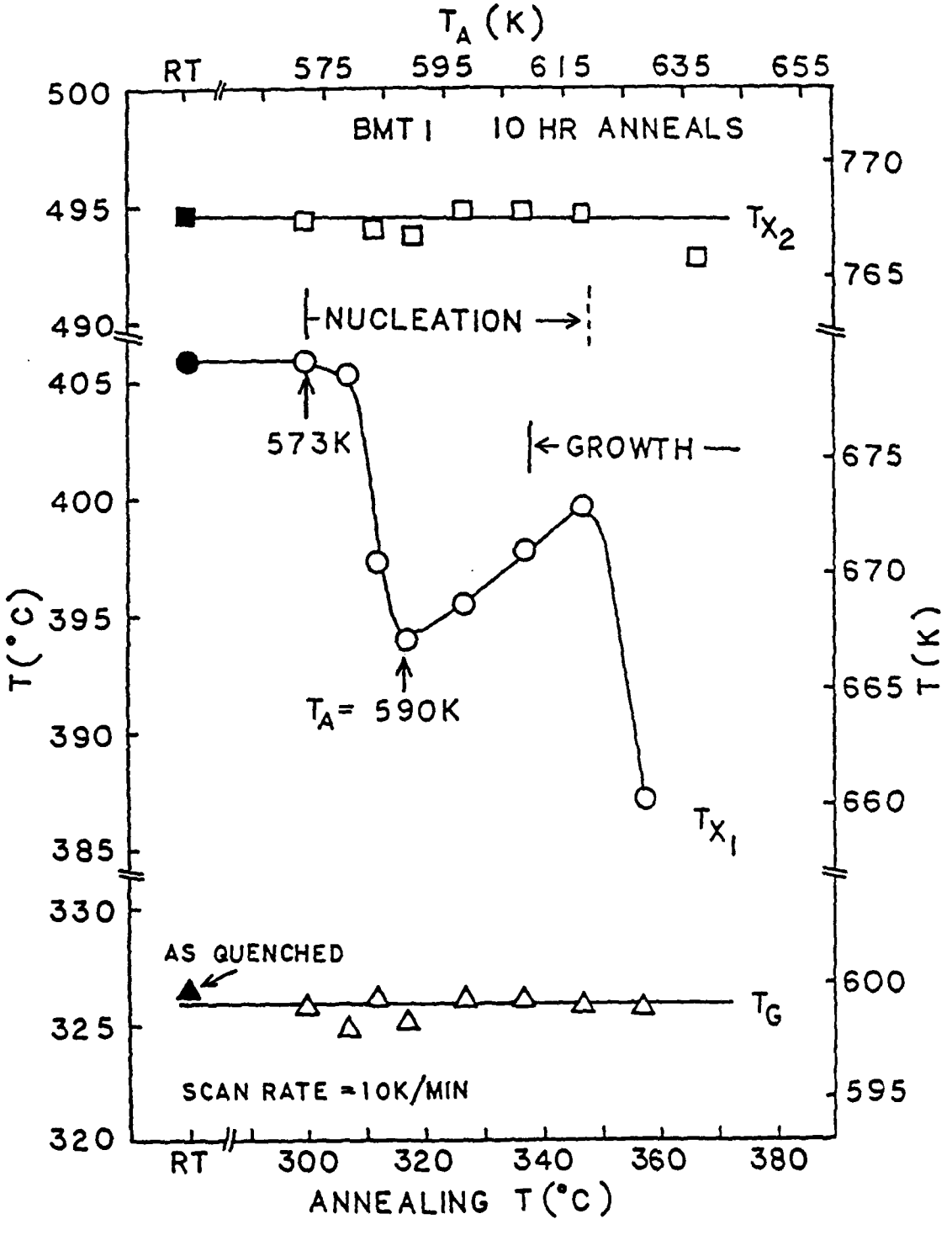

Figure 4. Characteristic temperatures for BMT-1 measured after 10 hour anneals versus annealing temperature.

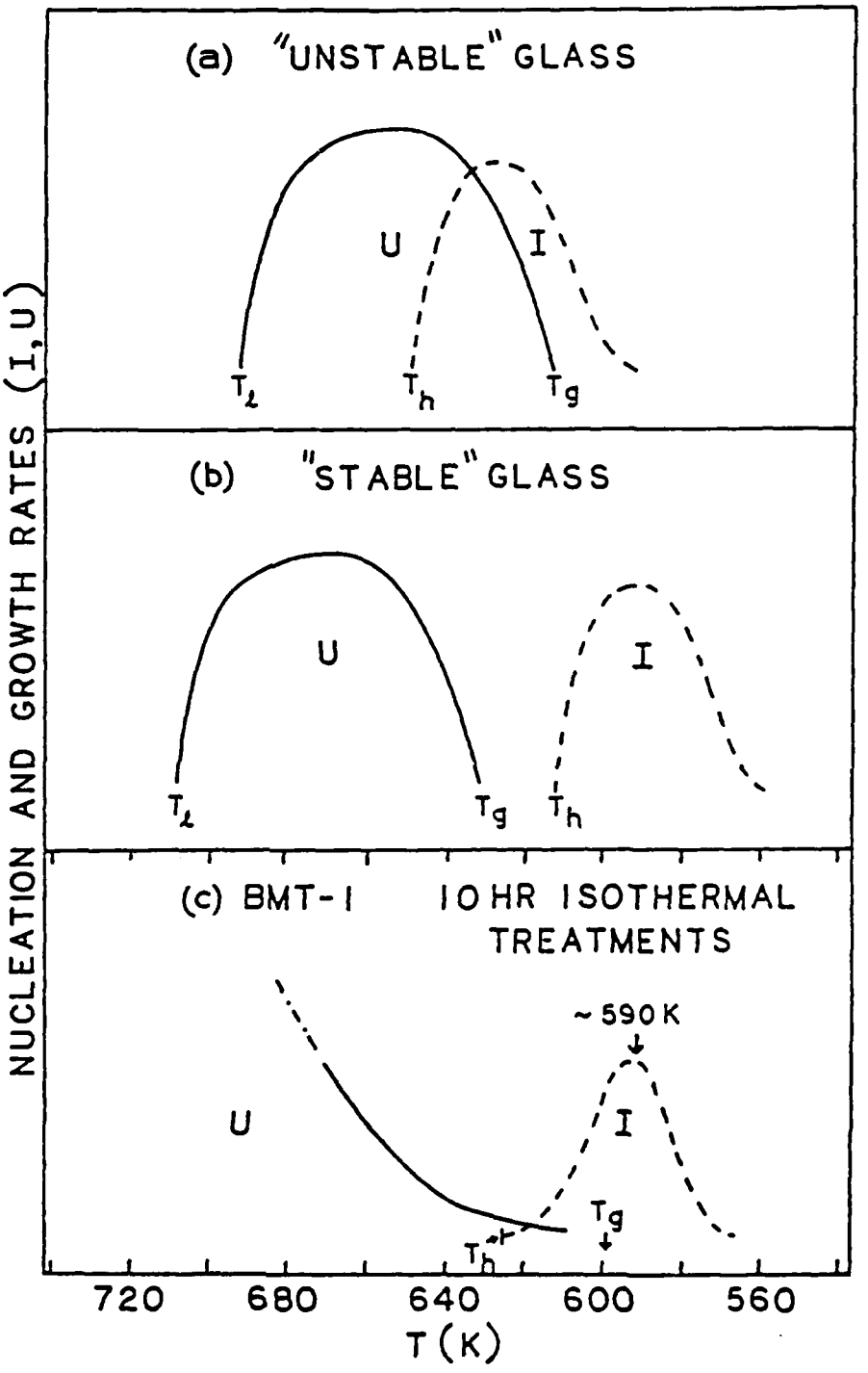

Figure 5. A comparison of the nucleation (I) and crystal growth rates (U) for

(a) an "unstable",

(b) a "stable" and

(c) BMT-1 glass (for 10 hour anneals).

FAR-IR TRANSMITTING, CADMIUM IODIDE-BASED GLASSES

E. I. Cooper and C. A. Angell

Department of Chemistry
Purdue University
West Lafayette, Indiana 47907

A new class of inorganic halide glasses is described, in which iodide is either the only or the main anion. The glass-formation progenitor is CdI_2 (usually 40-60 mol%); other components used were CsI, KI, TlI, PbI_2, the corresponding bromides, etc. The iodide glasses exhibit remarkably high far-IR-transmittance (down to ~350 cm^{-1} for 2 mm thick plates), and a much better resistance to humidity than that of known chloride glasses; however the low glass-transition temperatures (10-35°C) lead to relatively poor stability. High lead halide content "marginal" glasses of higher T_g ($\lesssim$ 63°C) and excellent moisture resistance are briefly described.

Much effort has been invested over the last several years in the investigation of fluoride glasses [1]. The possibility of glass-formation in systems of the heavier halides--chlorides, bromides and iodides--has received less attention. $ZnCl_2$ has long been known to be a glass-former [2] and has been suggested as the ultimate low-loss fiber material. However, its very high hygroscopicity makes its manipulation difficult and its use questionable, and its binary chloride solutions with "modifiers" are not glass-forming unless splat cooling or droplet techniques are used in contrast with their fluoroberyllate analogues. Recently described $BiCl_3$-based glasses are easy to form, but are also hydrogroscopic [3]. $ThCl_4$-based glasses, also recently described [4], are neither easy to form nor moisture resistant.

The insoluble halides of lead suggest themselves as possible starting points for systems free of air stability problems, but these only yield glassy phases under extreme quenching conditions [5]. Our preliminary results on glasses prepared from mixtures of lead halides with cadmium, thallium and/or alkali halides--some of which we report below--point to similar limitations.

On the other hand CdI_2, which is only moderately soluble in water (one mole per 24 of H_2O at 20°C) and forms no hydrate above 0°C, offers interesting prospects.

We have investigated, with moderate success, the possibility of forming room-temperature stable, moisture-resistant glasses, from the systems CdI_2-CsI-KI, CdI_2-CsI-TlI, and some ternary and quaternary systems containing PbI_2 additions, and report herein the results.

In general compositions in the systems of this study have glass transitions between 10°-35°. Compositions with a $T_{liquidus}$ below 220-240°C were at least marginally glass-forming; for these, $T_g/T \gtrsim 300K/500K = 0.6$, which is the approximate value at the edge of the glass-forming range in many

cases. Large samples of iodide glass could not be made, even if fourth components such as PbI_2 were introduced (although such additions may have other beneficial effects, see below). The maximum thickness (for some cases) was 2 mm. On the other hand, if both Pb^{++} and Br^- are added major increases in crystallization resistance during cooling may be obtained and thick sections stable for a few weeks at their glass transition temperatures (about room temperature) can be obtained. Furthermore, crystallization when it occurred was obviously by a heterogeneous mechanism.

The glass-forming domain in the CdI_2-CsI-KI system is shown in Figure 1; values for T_g, $T_{c,o}$ and $(T_{c,o}-T_g)$ are shown in Table 1. The last column gives a recommended criterion for glass stability against crystallization during annealing that does not necessarily indicate the difficulty of avoiding crystals during cooling.

Although CdI_2 + Tl halide solutions are not glass-forming themselves, replacing 10-16 mol% of CdI_2 by PbI_2 in the eutectic composition of Cd, Tl ▌ I, Cl and optionally making the mix $\leq$ 12 mol% in bromide, yields compositions which are almost indifferent to moderate humidity. One such sample (no. 15 in Table 1) was exposed 40 days to air and light and formed only a 10-20μ skin of crystalline material. Unfortunately, they cannot be made in large sections, in fact are "marginally glass-forming" by our classification. Even more marginal glasses in which $PbBr_2$ and PbI_2 are the major components (e.g., glass no. 21, Table 1) show no effects of exposure at all. These glasses also have higher T_g's ($\leq$ 63°C) hence high stability against devitrification under ambient conditions, and merit further work.

The absorption spectrum of a typical CdI_2 glass in the UV-Vis-IR range is compared, in Figure 3, to the spectra of some common IR transmitters. The lack of absorption bands up to ~15μm, and the high transmittance up to ~30μm speaks for itself. On the visible side, it is interesting to remark that the absorption band of TlI--only yellow as a pure compound--is pushed into the UV range, so that the glass has only a very faint brownish tint. This is probably an example of a blue shift in the $Tl^+ {}^3P_1 \rightarrow S_o$ transition caused by the transfer into a more acidic environment. The reflectivity is high as can be expected of a material of high refractive index. The far-IR spectrum of crystallized samples is practically indistinguishable from that of the glass. The all-iodide glasses should make exceptional laser hosts.

ACKNOWLEDGMENT

This work was supported by the National Science Foundation under Solid State Chemistry Grant No. DMR-8-07053AZ.

REFERENCES

[1] Poulain, M., Chanthanasinh, M. and Lucas, J., Mat. Res. Bull. 12 (1977) 151.
[2] Schultz, I., Naturwissenschaften 44 (1957) 536.
[3] Ziegler, D. C. and Angell, C. A., Appl. Opt. 21 (1982) 2096.
[4] Hu, H. and MacKenzie, J. D., J. Non-Cryst. Solids 51 (1982) 269.
[5] Tammann, G. and Elbrächter, E., Z. anorg. allg. Chem. 267 (1932) 268.

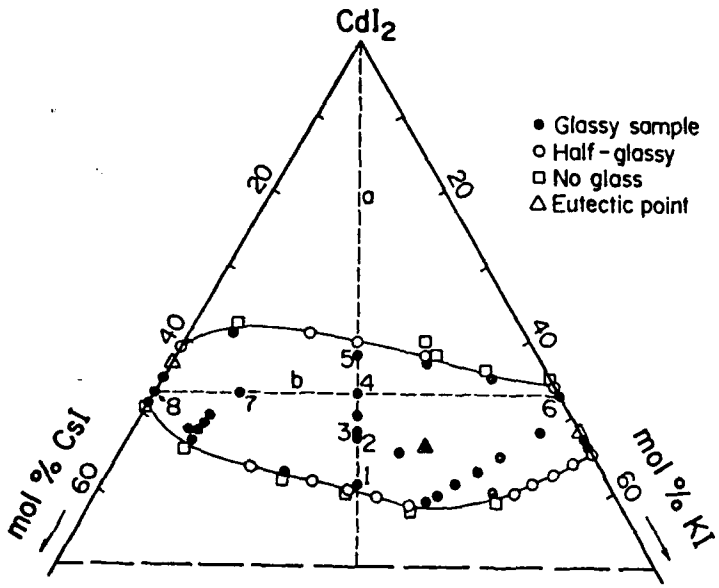

Figure 1
Glass-formation domain in the CdI_2-CsI-KI system.

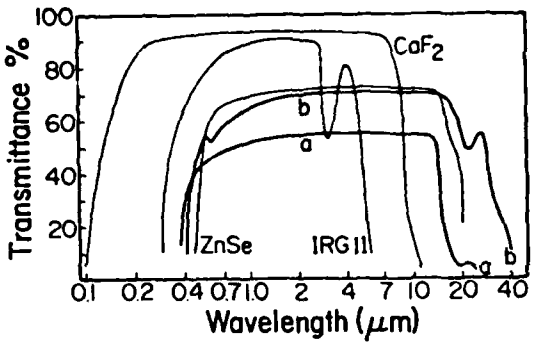

Figure 2
Transmittance of various infrared materials and glasses.

CaF_2, ZnSe, IRG11--5 mm thick

a--60$BiCl_3$: 40KCl(mol%) glass, 1.2 mm thick (ref. 8)

b--52CdI_2 : 38CsI : 10TlI(mol%) glass, 2 mm thick (this work)

Table 1. Glass transition and crystallization temperatures of selected compositions of heavy halide glasses.

No.	Cation mol%						Anion mol%			T_g[1]	$T_{c,o}$[2]	$T_{c,p}$[3]	$\frac{T_{c,o}-T_g}{T_g}$
	Bi^{3+}	Cd^{2+}	Pb^{2+}	Cs^+	K^+	Tl^+	I^-	Br^-	Cl^-				
1		41		29.5	29.5		100			11*	32	35	0.074
2		47		26.5	26.5		100			19*	35	39	0.055
3		48		26	26		100			20*	33	40	0.044
3'		48		26		26	100			19	53	59	0.116
4		53		23.5	23.5		100			14*	40	44	0.091
5		58		21	21		100			11	43	49	0.113
5'		58		21		21	100			9*	45	55	0.128
6		53			47		100			13*	24	29	0.046
7		53		37	10		100			22*	50	59	0.095
7'		52		38		10	100			21	60	65	0.133
8		53		47			100			16	46	50	0.104
9		53		47			90	10		17	50	54	0.114
10		53		47			80	20		17*	45	50	0.097
11		53		47			70	30		17*	47	50	0.103
12		48	5	47			100			29	65	70	0.119
13[4]		47.5	7	37.5		8	100			24	67	71	0.145
14		42.6	11.2	46.2			100			30	75	78	0.149
14'	same as 14, after 20 days at 22-23°									34	73	76	0.127
15		34	16			50	69	10	21	29*	46	50	0.056
16		48	6	27	19		74.5	25.5		24	97	109	0.246
16'	same as 16, after 15 days at 22-23°									24	90	100	0.222
17[5]	70				30				100	31	96	99	0.224
18[5]	70				30			12.5	87.5	24	89	98	0.219
19[5]	70				30			87.5	12.5	10	63	71	0.187
20[5]								100		9	58	64	0.174
21[6]		12	88				53	47		43	58	67	0.047
21'	same as 21, after 70 days of exposure									46*	60	72	0.044
22		17	73	10			18	82		63	98	100	0.104

Notes: (1) An asterisk next to a T_g-value indicates that crystallization starts slightly above T_g, before a complete return of the recorder pen to a straight baseline
(2) See Figure 2. (3) Temperature of the first crystallization peak.
(4) DSC-run after keeping the sample for 30 days at 22-23°.
(5) Sample exposed to air for 7 days.

MULTICOMPONENT HEAVY METAL FLUORIDE GLASSES CONTAINING MgF_2

Osama H. El-Bayoumi and Martin G. Drexhage
Solid State Sciences Division
Rome Development Center
Hanscom AFB, MA 01731

John R. Gannon and Paul Tick
Research and Development Division
Corning Glassworks
Corning, NY 14831

A large number of multicompnent heavy metal fluoride glass compositions have been developed in the last four years. Although the french scientists (e.g. Lucas, Poulain and Poulain) prepared sizable bulk glass samples and optical fibers from mixtures of the fluorides of many elements in the periodic table, the search continues for new heavy metal fluoride glasses with better physical, mechanical and optical properties. The multi-component BaF_2/ThF_4 glass exhibits a significant decrease in the 6-10 μm IR absorption coefficient relative to the fluorozirconate glass family (ZBLA). In this study we report preliminary results on glass formation in the system MgF_2/ThF_4. The optical, physical and thermal properties for selected compositions of these new glasses are discussed. The effect of ThF_4, YbF_3, AlF_3 and PbF_2 on the stability of these glasses is reported.

All glass samples prepared in the course of the study were prepared by melting 10gm batches of the mixed fluorides in vitreous carbon crucibles in an argon atmosphere. Since some elements were added as oxides, 4 to 5 times the stoichiometric amount of ammonium bifluoride was mixed with the batch to convert oxide species to fluorides. A resistance heated furnace was used to obtain temperatures of 950-1100°C which is required to insure complete melting.

The glass melts were quenched to room temperature between two brass plates. Few compositions were cast in a slot-type brass mold to obtain plates 3mm x 3cm x 3cm thick smaples. Glasses were annealed near the glass transition temperatures.

Batch compostions melted during this work are divided into three groups. Table 1 shows the compositions in the first category which contain no ThF_4 or YbF_3. Only two compositions yielded 1.0mm-thick glass sheets upon quenching. When YbF_3 was added to the batch compositions of the second group, four glass samples were obtained as shown in table 2. The best results were obtained when both YbF_3 and ThF_4 were added to the batch compositions of the third group in table 3. In this case, eight melts yielded glass samples. Furthermore, 3mm-thick glass samples were obtained by casting melts of compositions containing AlF_3 in combination with ThF_4 and YbF_3.

Table 4 shows compositions, glass transition temperatures (Tg), crystallization temperatures (Tx) and refrative indices of selected compositions. These data are compared with that of fluorozirconate and BaF_2/ThF_4 glasses. In general, Tg's of the Mg/Th glass family are similar to that of Ba/Th glasses i.e, Tg is not affected by relacing Ba by Mg. The refractive index of two glass samples of different compositions are measured and found to be similar to the ZBLA and Ba/Th glass families.

Figure 1 is the percent transmission versus wavelength of glass compositions listed in table 4. The absorption coefficients of these glasses in the 6-10 μm region are shown in figs. 2 and 3. Data for the representitive ZBLA and Ba/Th glasse are also indicated. The IR edge absorption of Mg/Th glasses containing 10 mole % AlF_3 is identical to the ZBLA glass containing only 4 mole % AlF_3. On the other hand, addition of 15 mole % AlF_3 caused the absorption edge to shift towards shorter wavelength. The substitution of MgF_2 for BaF_3 and its effect on the IR absorption is shown in Fig 3. It is clear that such substitution did not effect the absorption in the 6-10 μm region.

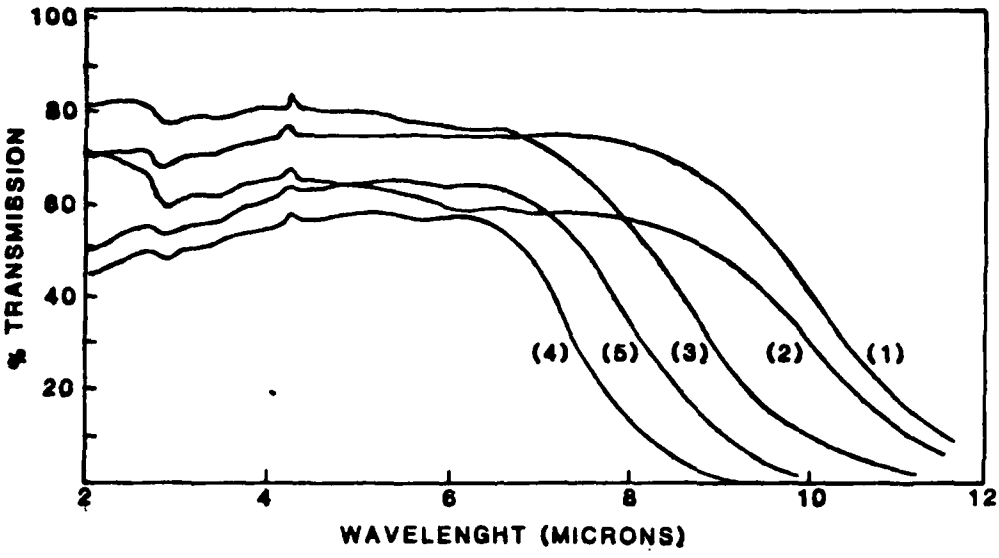

Figure 1: Transmission of Glass Compositions Listed in Table 4

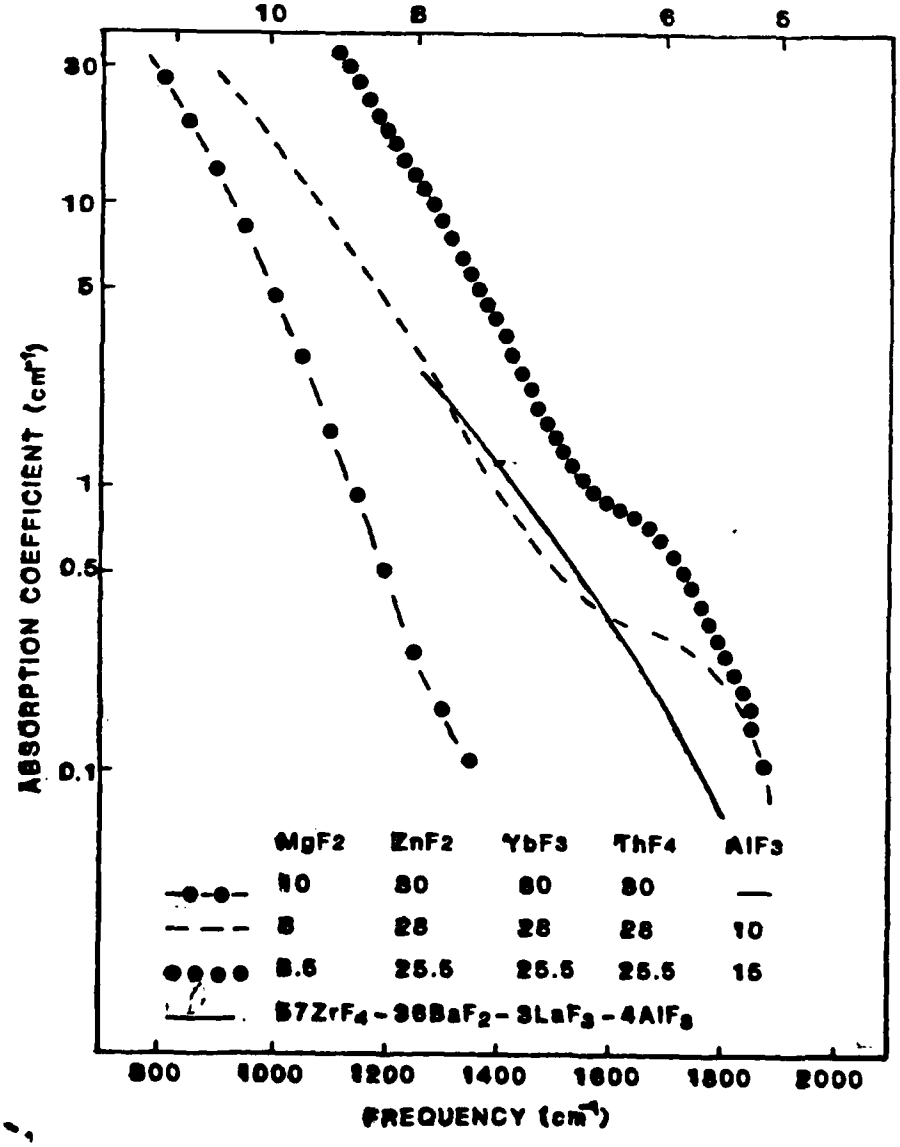

Figure 2: Effect of AlF_3 on the absorption Coefficient

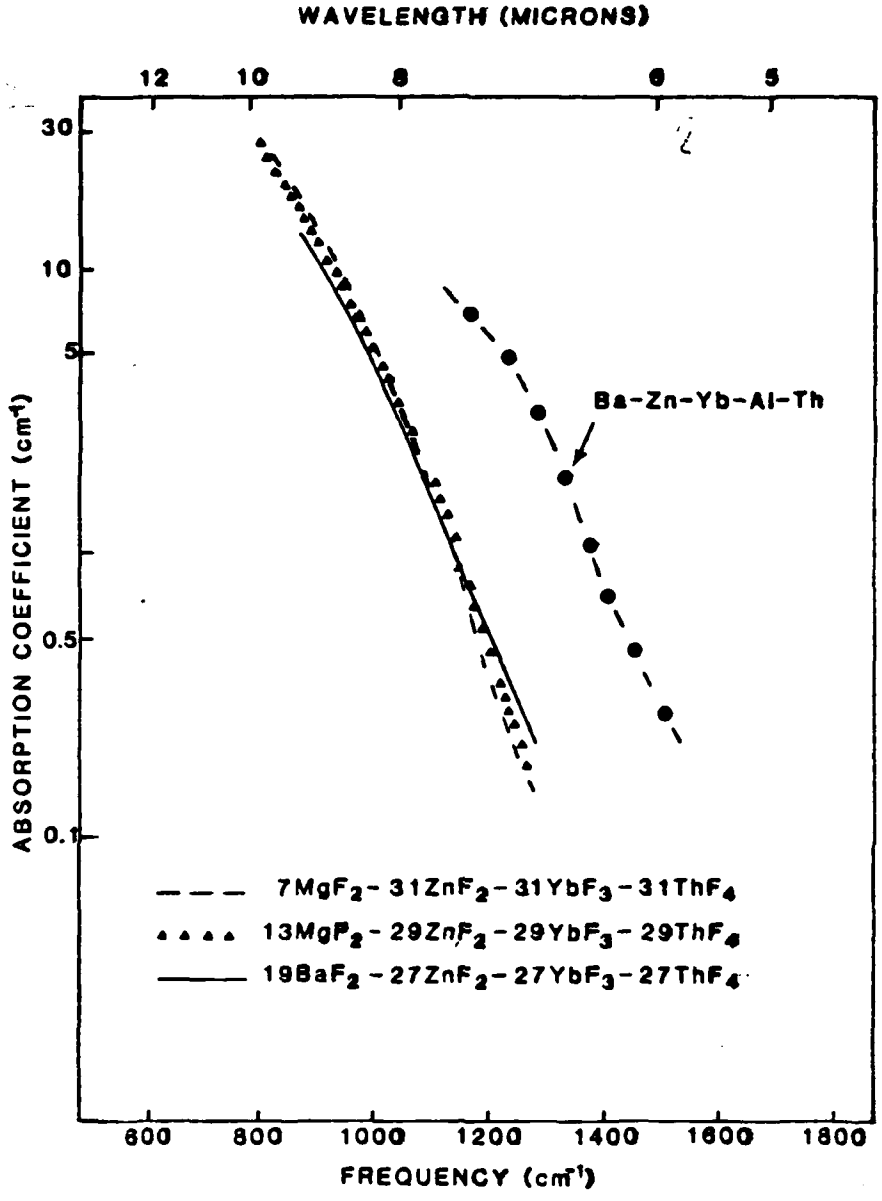

Figure 3: Effect of Substitution of Mg for Ba on the Absorption Coefficient

GLASS #	COMPOSITION (MOLE %)				STATE
	MgF_2	ZnF_2	AlF_3	PbF_2	
1	15	15	35	35	XTAL
2	20	15	30	35	XTAL
3	20	15	35	30	XTAL
4	20	20	30	30	GLASS
5	20	20	45	15	XTAL
6	20	10	40	30	GLASS
7	20	10	30	40	XTAL
8	20	10	50	20	XTAL
9	25	15	30	30	XTAL
10	25	20	25	30	XTAL
11	10	20	40	30	XTAL
12	22	12	33	33	XTAL
13	23.8	4.8	35.7	35.7	XTAL
14	25	25	35	15	XTAL

Table 1: Glass Compositions Containing no YbF_3 or ThF_4

GLASS #	COMPOSITION (MOLE %)					STATE
	MgF_2	ZnF_2	YbF_3	AlF_3	PbF_2	
1	20	10	10	30	30	GLASS
2	20	15	5	30	30	GLASS
3	19.8	19.8	11	29.7	19.7	XTAL
4	19.8	19.8	11	19.7	29.7	XTAL
5	19.8	9.8	11	29.7	29.7	XTAL
6	9.8	19.8	11	29.7	29.7	XTAL
7	18	18	10	27	27	GLASS
8	17	17	15	25.5	25.5	GLASS

Table 2: Glass Composition Containing YbF_3

GLASS #	COMPOSITION (MOLE %)					STATE
	MgF_2	ZnF_2	YbF_3	ThF_4	AlF_3	
1	19	27	27	27	—	GLASS
2	13	29	29	29	—	GLASS
3	25	25	25	25	—	GLASS
4	10	30	30	30	—	GLASS
5	7	31	31	31	—	GLASS
6	10	20	25	25	20	GLASS
7*	6	28	28	28	10	GLASS
8*	8.5	25.5	25.5	25.5	15	GLASS
9	3.4	27.2	27.2	27.2	15	XTAL

*CAST

Table 3: Glass Compositions Containing Both YbF_3 & ThF_4

GLASS #	COMPOSITION (MOLE %)						Tg °C	Tx °C	Tx-Tg °C	ND
	MgF_2	ZnF_2	YbF_3	ThF_4	AlF_3	PbF_2				
1	13	29	29	29	—	—	337	378	41	1.521
2	7	31	31	31	—	—	329	383	34	
3	6	28	28	28	10	—	345	419	74	
4*	8.5	25.5	25.5	25.5	15	—	350	414	64	1.503
5	20	10	10	—	30	30	353	393	40	
6	$57ZrF_4$-$36BaF_2$-$3LaF_2$-$4AlF_3$						310	390	80	1.516
7	$19BaF_2$-$27ZnF_2$-$27LuF_3$-$27ThF_4$						353	433	99	1.534

* CAST

Table 4: Compositions, Glass Transition (Tg), Crystallization (T_x) Temperatures and Refractive Index.

TRACE IMPURITY ANALYSIS OF FLUORIDE GLASSES AND MATERIALS

C. F. Fisher, P. Nordquist, and D. C. Tran
Naval Research Laboratory
Washington, DC 20375

A number of selected instrumental techniques applicable for the qualitative and quantitative analysis of transition and rare earth element impurities at the ppb to ppm concentration levels in raw materials and final glasses is discussed. Chemical problems associated with reagent impurities, material solution, matrix-impurity separation and impurity reconcentration are outlined. Preliminary results for analysis by D.C. plasma spectro-photometry of selected transition and rare earth elements in glasses, in raw materials from various commercial sources, and in laboratory prepared materials purified by sublimation and solution recrystallization are presented.

Transition metal impurities at the 1 ppm level in fluoride glasses have been shown to cause extrinsic absorption losses as high as 130 dB/km in the 1 to 3 μ region.[1] The presence of impurities at this concentration level in fibers is evident in the loss spectra of a recently reported fiber drawn at NRL which had an absorption loss in the same wavelength region of from 50 to 100 dB/km.[2] Future progress in reducing the total attenuation loss of fluoride glass fibers is very likely to be dependent upon the elimination of the sources of these impurities. The task of identification, quantification and elimination requires the judicious choice of a suitable analytical instrument and the development of analytical techniques capable of providing data routinely at the sub-ppm level. Of the various instruments available, DC plasma spectrometry offers a number of advantages over other methods such as ICP, atomic absorption, mass spectra and uv-visible spectrometers. Employing this analytical method, we have evaluated the purity of a number of commercial

sources of fluoride glass reagents and several in-house purified materials.

Commercial sources of ZrF_4, a major component of the NRL glass composition, ranged in impurity levels from several thousand ppm to 10 ppm. Iron was generally found at an order of magnitude greater than the concentration of Cu, Co or Ni. No commercial source having 1 ppm or less of iron was found for this material. Lanthanum oxide from two sources had iron concentrations at the 1 ppm level. Barium carbonate, lithium carbonate and aluminum oxide -- reagents from which fluorides can be readily prepared -- showed impurity levels at less than a few hundred ppm.

These data indicate that the major source of transition element impurities in fluoride glasses of the NRL composition prepared from commercially available reagents originate with the ZrF_4 component. Purification by multiple sublimations of this reagent can reduce the Fe impurity content to the 5-10 ppm level.

References

1. Ohishi, Y., Matachi, S., and Kanamori, T., Japan. J. of Applied Physics, Vol. 20, No. 11, pp. L787-L788, (1981).
2. Tran, D. C., Levin, K. H., Fisher, C. F., Burk, M. J., Sigel, G. H., Electron. Lett. 19, No. 5, pp 165-166 (1983).

MECHANICAL PROPERTIES OF INFRA-RED TRANSMITTING FIBRE

P.W.FRANCE, J.WILLIAMS, S.F.CARTER, K.J.BEALES
BRITISH TELECOM RESEARCH LABORATORIES, MARTLESHAM HEATH, IPSWICH, U.K.

1.INTRODUCTION

Although there has been a considerable amount of work published on the structure and optical properties of both fluoride and chalcogenide glasses for use in 2-5 um optical systems, to date there has been little work describing the mechanical properties. The aim of this work was to determine the intrinsic material strengths of these new materials and to characterise their fatigue properties, so that they could be compared with the more conventional oxide systems.

2. EXPERIMENTAL

2.1 Fluoride Fibres

Fluoride glasses were made up in approximately 100gm batches from mixtures of 99.5% purity fluorides. The water contents were lowered to around 300 ppb (measured on bulk samples) by bubbling with reactive gasses, and after fining the glasses were cast into gold-coated moulds. Single material preforms, 15 mm in diameter and 10 cm in length were drawn into fibre using a short hot zone furnace, flushed with dry nitrogen. The diameter was controlled to 125 + 4 um and UV-cured epoxy acrylate coatings were applied in line. In general between 200-300 m of fibre could be drawn in this way.

2.2 Chalcogenide Fibres.

Ge-As-Se glasses of 5*9's purity were prepared by vaccuum melting in sealed silica ampoules using a rocking furnace. Because of their longer working ranges and better stability these glasses were drawn into fibre using silica double crucibles, from which either single material or clad fibre could be made. Lengths up to 1.0 km were coated with either silicone resin or epoxy-acrylate and again the diameter was controlled to 125 + 4 um.

2.3 Strength Measurements.

These were made using the two point bending technique which has been described in detail elsewhere (1). The advantages of this technique are that firstly it only measures short gauge lengths and is therefore more likely to measure intrinsic material strengths and secondly it can be easily adapted to measure strength in different environments e.g. liquid nitrogen.

3 RESULTS

3.1 Strength of Fluoride Fibres

Results from a Zr-Ba-La-Al-Li (2) single material fibre are shown in fig. 1. The median ambient strength of 0.9% corresponds to a stress of 0.46 GPa (Young's Modulus was 51 GPa) or 66,000 psi. The results at -196°C were taken on uncoated fibre, since the strength of the coating at these low temperatures was greater than the fibre. The uncoated fibre was carefully handled to minimise microdamage, and in short gauge lengths gave the same median strengths under ambient conditions as the coated fibre. The median inert strength of 1.05% or 0.54 GPa was surprisingly low in view of published values of K_{1c} (3) and it is not yet clear whether this is really the intrinsic strength or the result of numerous surface flaws such as

crystallites.

The difference between the ambient and the inert strength indicates that stress corrossion was occurring in these glasses, and results in water and isopropanol indicate that OH was causing fatigue. The ratio between the ambient and the inert strengths can be used to estimate a value of N, the stress corrosion susceptibility, according to:

$$R = (B(N-1)0.42v / S_i Er) \quad . \quad . \quad . \quad (1)$$

where R is the ratio, v is the bend test velocity, r is the fibre radius, S_i is the inert strength and E is Young's Modulus. B is a material constant and was assumed to be 10^{-2}. A ratio of 0.86 predicts a value of 95 for N.

Fig. 2 shows results on a Zr-Ba-La-Al fluoride fibre which had been stored in water at room temperature under zero stress. The strength decreased rapidly with time and reduced to approximately half it's initial value after 24 hours.

3.2 Results on Chalcogenide Fibre.
Fig.3 shows results on a $Ge_{30}As_{15}Se_{55}$ fibre coated with silicone resin. Results in ambient conditions were similar to those at -196°C with a median strength of 3.8% strain. Results at higher velocities and in water also gave identical results and indicated that stress corrosion was not occurring in this fibre. The reason for this was that all fractures examined occurred from internal flaws, thought to be small bubbles about a um in diameter, and these internal flaws were possibly immune to the effects of static fatigue. Fig.4 shows results on a $Ge_{33}As_{12}Se_{55}$ fibre which also exhibited surface flaws. Because these surface flaws were now exposed to atmospheric water vapour they were subject to static fatigue, and consequently gave higher strengths when measured in liquid nitrogen. Using equation (1) the ratio between the measurements corresponds to an N of 14.

These results can be used to estimate values of inert strength in the absence of internal flaws. We would expect approximately 15% breaking strain at -196°C and correspondingly 5% at room temperature.

ACKNOWLEDGEMENTS
The authors would like to thank W. J. Duncan for useful discussions and the Director of Research, British Telecom, for permission to publish this paper.

REFERENCES
(1) P. W. France,W. J. Duncan, D. G. Smith, K. J. Beales; J.Mats.Science,18(1983)785-792.
(2) G. H. Siegel,Jr. and D. C. Tran; Proc. OFC 1983, New Orleans.
(3) J. J. Mecholsky, M. G. Drexage, O. H. El-Bayoumi, C. T. Moynihan; Proc. 1st Int. Sym. on Halide and Other Non-oxide Glasses,1983,Cambridge.

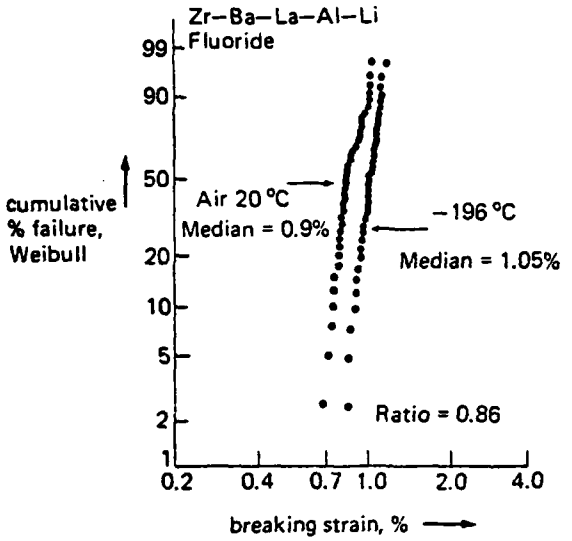

FIG. 1

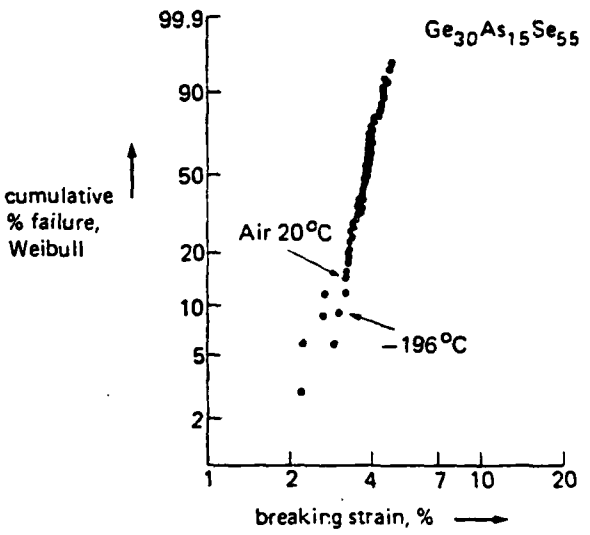

FIG. 3

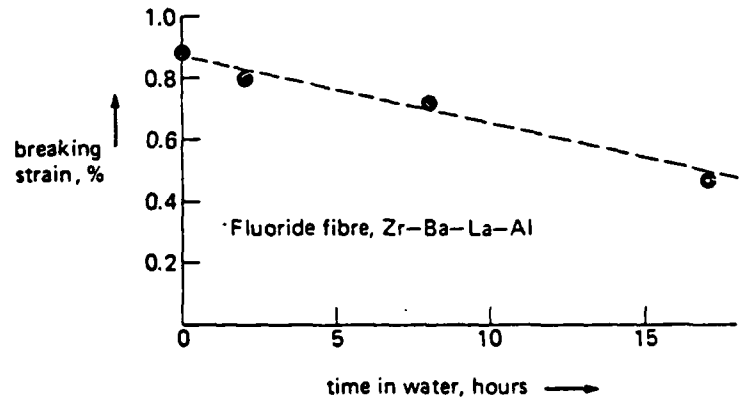

FIG. 2

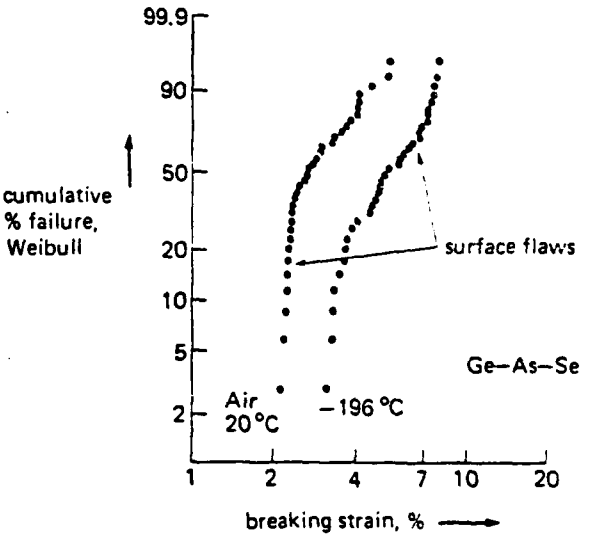

FIG. 4

SUB-T_g AGING OF HEAVY METAL FLUORIDE GLASSES

D. L. Gavin, A. J. Bruce, S. Loehr, S. Opalka and C. T. Moynihan
Rensselaer Polytechnic Institute
Troy, New York 12181
USA

M. G. Drexhage and O. H. El-Bayoumi
Rome Air Development Center
Hanscom AFB, MA 01731
USA

All glasses undergo physical aging - a slow change of properties such as refractive index, enthalpy and volume with time - due to structural relaxation well below T_g. The closer to T_g the faster the physical aging. Since the heavy metal fluoride glasses have relatively low T_g's, the question arises whether physical aging will occur to a significant extent in these materials at ambient temperature. Differential scanning calorimetry (DSC) has been used to study enthalpy relaxation during physical aging of a heavy metal fluoride glass. The glass composition studied was 58 ZrF_4-33 BaF_2-5 LaF_3-4 AlF_3 (ZBLA).

Samples of ZBLA glass were rate cooled through T_g and then annealed isothermally below T_g for various times extending up to several months. After this the heat capacity C_p was measured while reheating the glass through the transition region at 10 K/min. To determine the structural state of the glass at the start of the isothermal anneal, the sample was then rate cooled again through T_g at the initial rate and its heat capacity immediately remeasured. The change in the enthalpy as a result of sub-T_g annealing was expressed in terms of the fictive temperature. The fictive temperatures T_f of the glass before and after the isothermal anneal were calculated from the C_p data by the method of Moynihan et al.[1] and were reproducible to $\pm$ 0.5 K. The entire set of experiments is summarized in Fig. 1. Isothermal annealing of the ZBLA glass was carried out at 524 K (T_g-58 K), 472 K (T_g-110 K) and

376 K (T_g-206 K).

The DSC traces of samples annealed at 524 K (Fig. 2) show a progressive increase in the C_p "overshoot" at T_g with increasing annealing time due to the recovery of larger and larger amounts of enthalpy lost during annealing (cf. Fig. 1). For glasses cooled at 100 K/min and annealed at 472 K the enthalpy lost during annealing is recovered below T_g and a corresponding peak in C_p below T_g is observed (Fig. 3). This is a consequence of the non-linear, non-exponential relaxation process[2] and has been observed previously in organic polymer[3,4], metallic[5] and network oxide[6] glasses.

The dependence of T_f on annealing time for the anneals at 472 and 524 K are shown in Fig. 4. Note that if the glasses were to anneal completely to equilibrium, T_f would drop with time to the annealing temperature, i.e., to 472 or 524 K. Hence in the experimental annealing periods of Fig. 4 the glasses are moving only on a small amount of the way to equilibrium. At 524 K T_f initially drops rapidly with time, but after about 10 days the rate of physical aging decreases markedly. Also at 524 K the more rapidly cooled glass (100 K/min) ages initially much more rapidly than the more slowly cooled glass (10 K/min), but after several days the two glasses age at comparable rates. This is a manifestation of the highly non-linear (autocatalyzing or self-retarding) character of structural relaxation.[2,7] The same effect is observed during annealing at 472 K, although at this temperature the rate of aging is much less rapid than at 524 K.

In Fig. 5 are shown heat capacity scans for ZBLA glass initially cooled at 10 K/min and reheated immediately after cooling and after 143.3 days annealing at 376 K. The C_p scans are identical within experimental error, showing that at 376 K no relaxation occurred at all in 143.3 days.

Physical aging has been shown to occur for heavy metal fluoride glasses

well below T_g. The present results show that aging at room temperature will probably not be a problem for glasses of moderately high T_g (582 K for ZBLA) cooled at rates up to 100 K/min. However, further studies are needed to assess ambient temperature aging rates for heavy metal fluoride glasses which have experienced very rapid quenching rate (e.g., fibers) and/or have markedly lower T_g's than ZBLA glass.

Acknowledgement. This research was supported by Contract No. F19628-83-C-0016 from the Rome Air Development Center.

References

1. C. T. Moynihan, A. J. Easteal, M. A. DeBolt and J. Tucker, J. Am. Ceram. Soc., 59, 12 (1976).

2. I. M. Hodge and A. R. Berens, Macromolecules, 15, 762-770 (1982).

3. I. M. Hodge and G. S. Huvard, Macromolecules, 16, 371 (1983).

4. H. S. Chen and T. T. Wang, J. Appl. Phys., 52, 5898 (1981).

5. H. S. Chen, J. Non-Cryst. Solids, 46, 289 (1981).

6. H. S. Chen and C. R. Kurkjian, J. Am. Ceram. Soc., in press.

7. C. T. Moynihan et al., Ann. NY Acad. Sci., 279, 15 (1976).

EXPERIMENT

- Cool glass on DSC through T_g at a rate of 10 or 100 K/min
- Anneal isothermally below T_g for extended period
- Measure C_p while reheating at 10K/min
- Cool at 10 or 100 K/min and immediately measure C_p while reheating at 10 K/min
- Determine T_f for annealed glass and glass immediately after rate cool

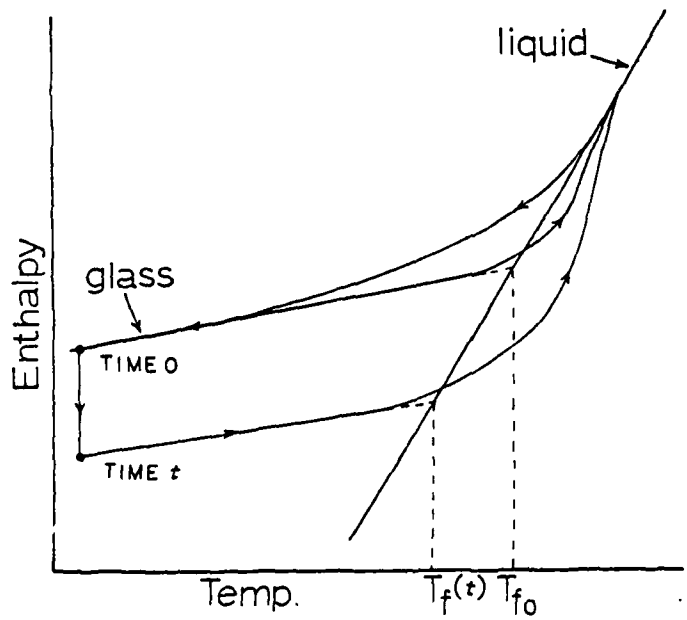

Figure 1. Outline of experimental procedure and schematic illustration of the variation of enthalpy with time and temperature and of T_f determination.

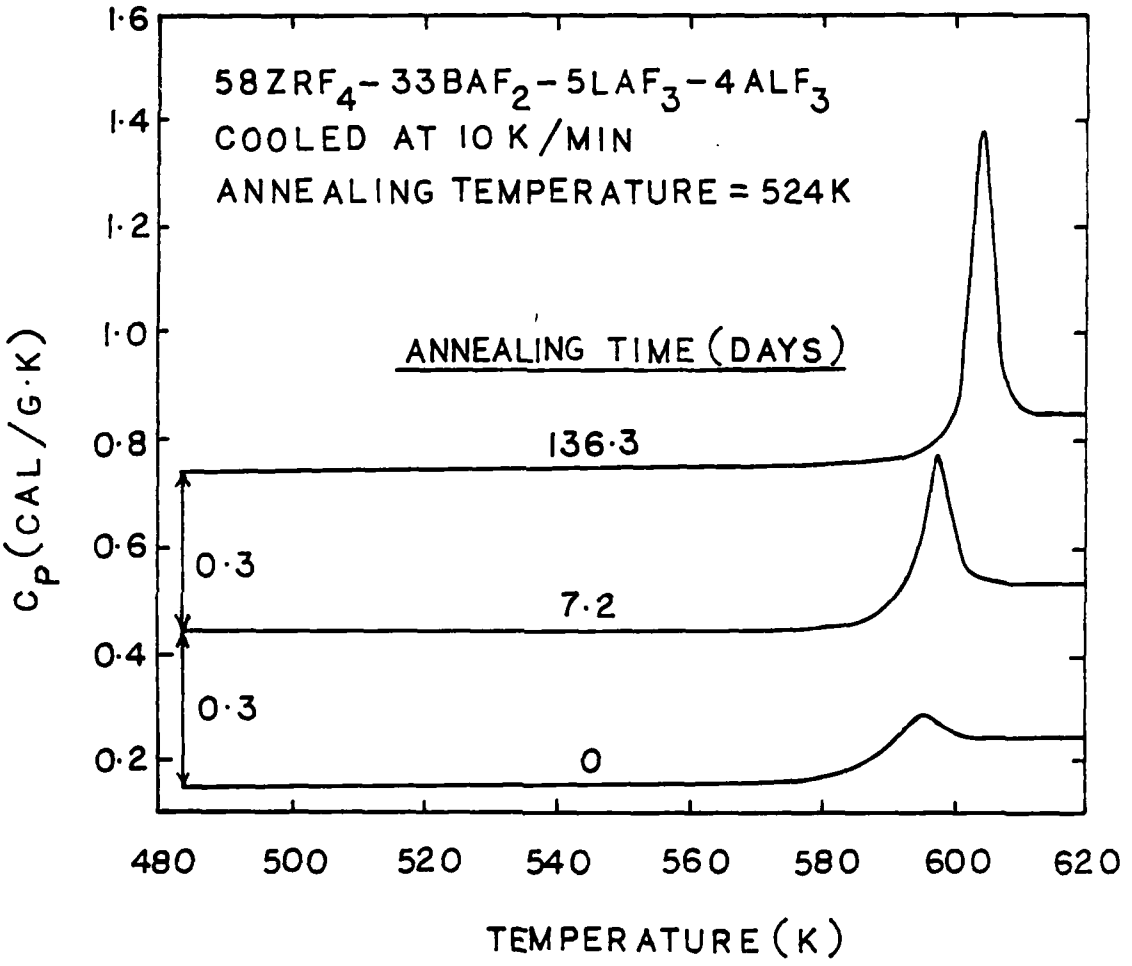

Figure 2. Specific heat of ZBLA glass measured at a heating rate of 10 K/min following a rate cool at 10 K/min and annealing at 524 K for 0 days, 7.2 days and 136.3 days. The C_p plots for the annealing times of 7.2 days and 136.3 days have been displaced upwards by 0.3 and 0.6 cal/gK respectively for clarity.

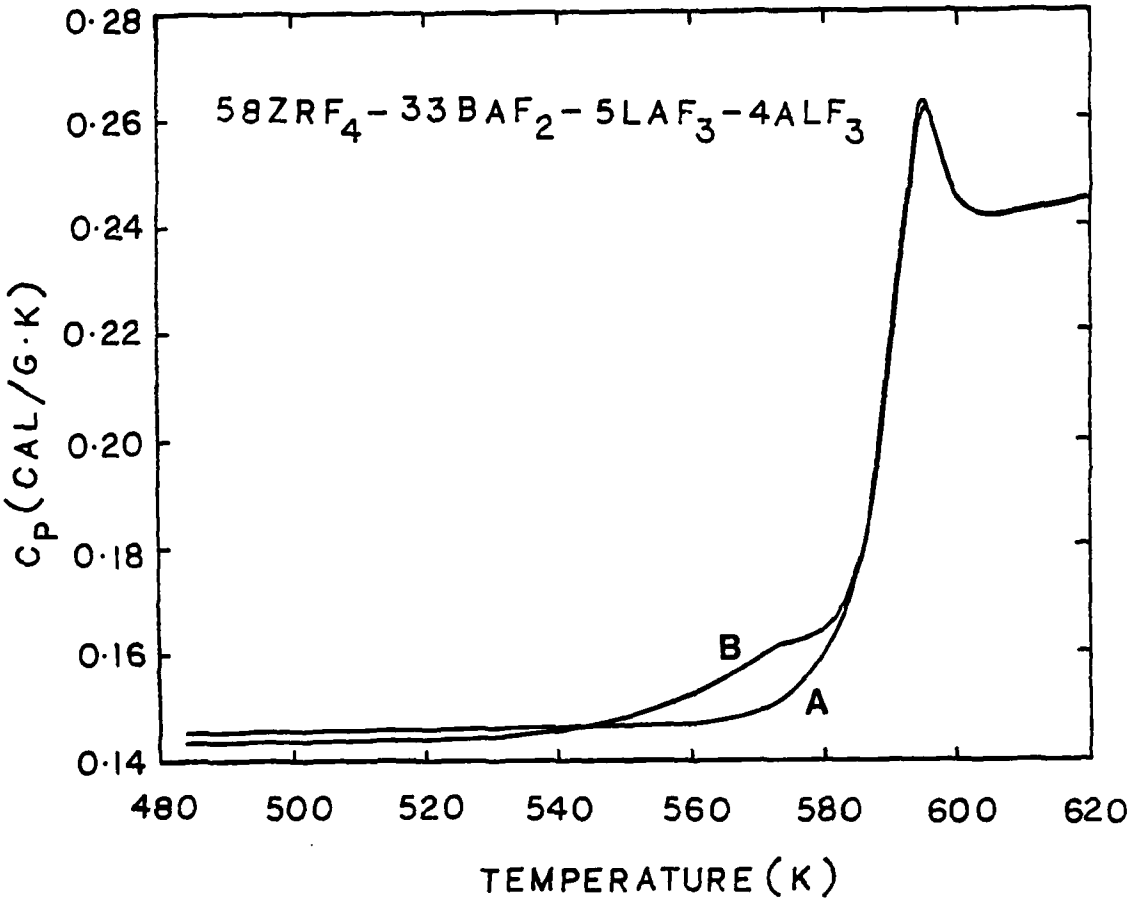

Figure 3. Specific heat of ZBLA glass measured at a heating rate of 10 K/min following a rate cool at 100 K/min and annealing at 472 K for (A) 0 days and (B) 50.5 days.

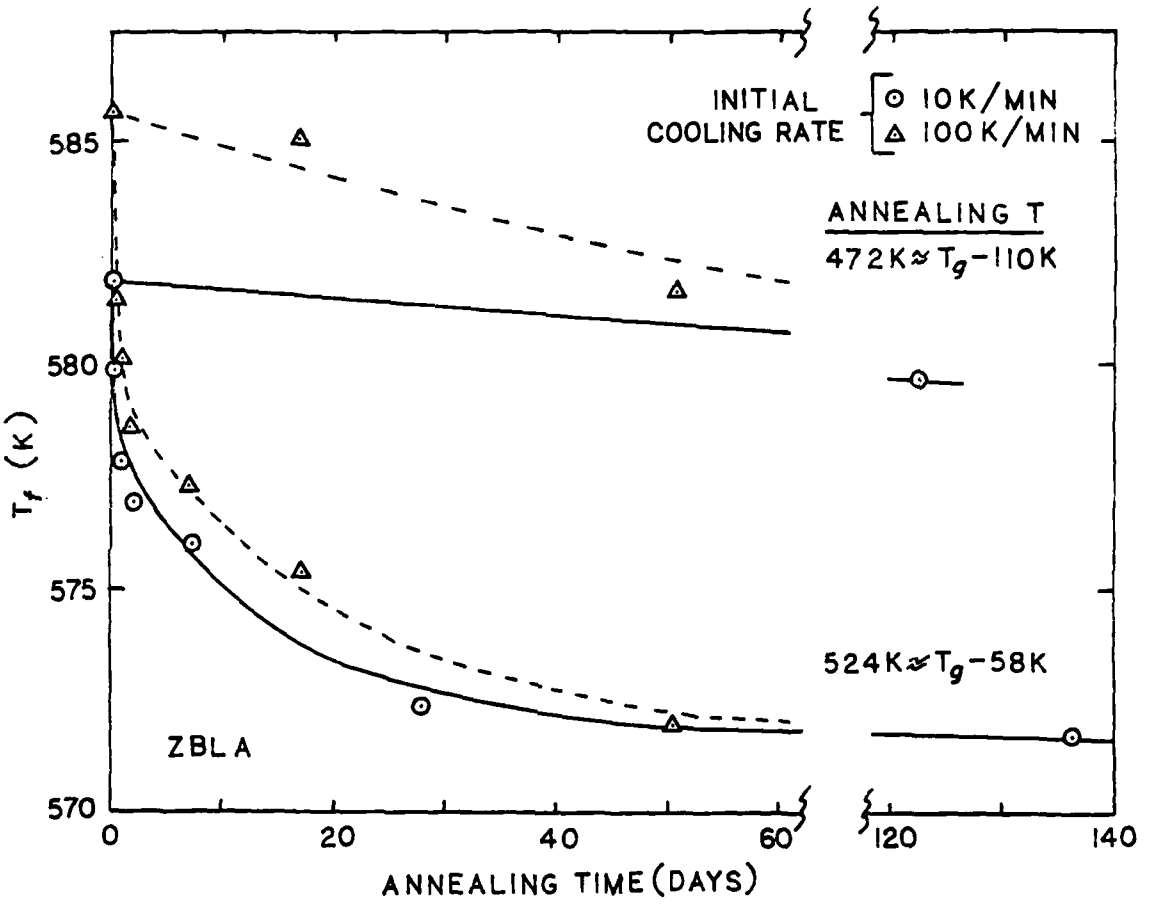

Figure 4. T_f vs. annealing time for ZBLA glass samples annealed at 524 and 472 K.

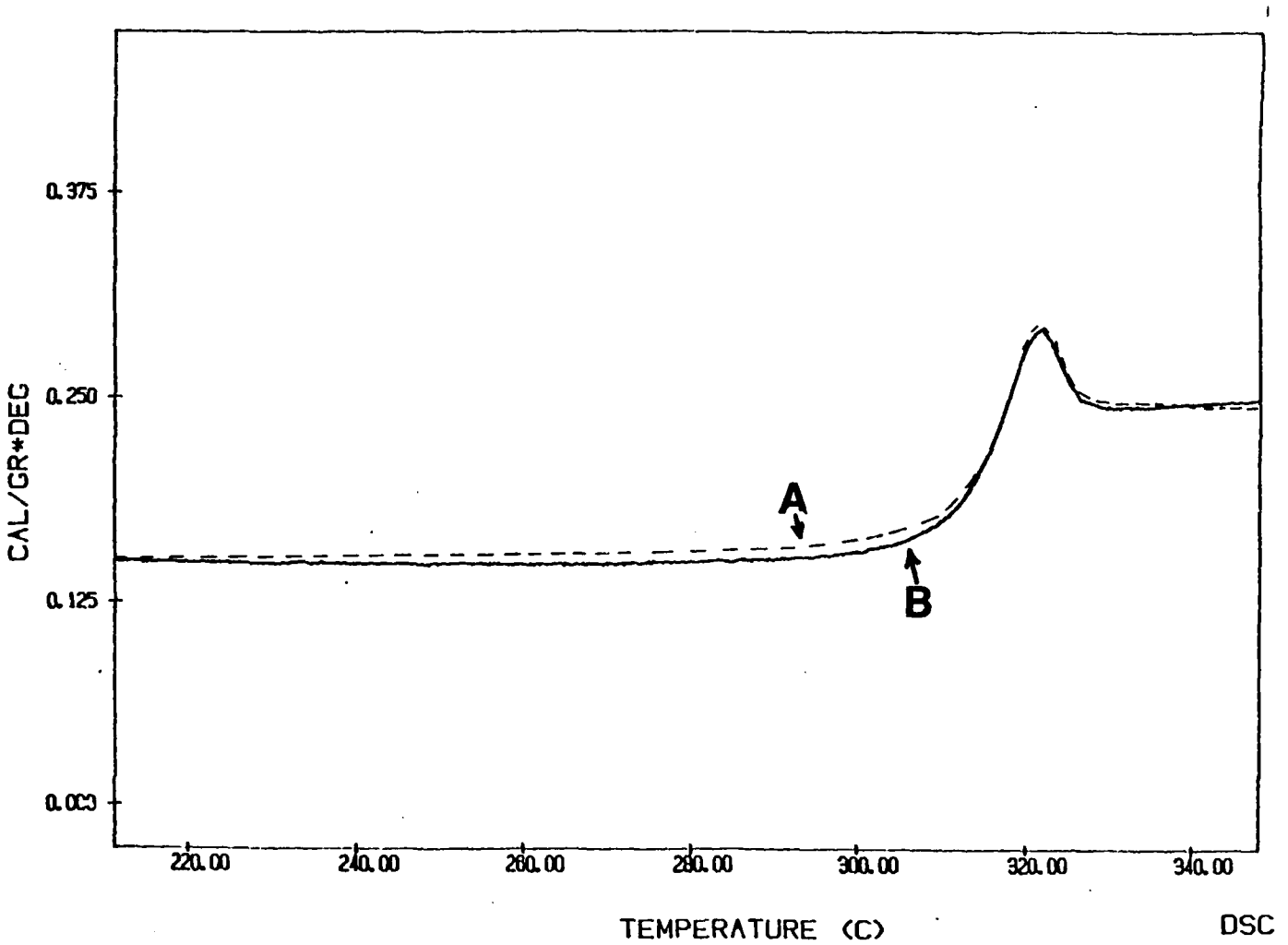

Figure 5. Specific heat of ZBLA glass measured at a heating rate of 10 K/min following a rate cool at 10 K/min and annealing at 376 K for (A) 0 days and (B) 143.3 days.

FLUORIDE GLASSES OF URANIUM IV AND 3d TRANSITION METALS

J. GUERY, G. COURBION, C. JACOBONI and R. DE PAPE

Laboratoire des Fluorures et Oxyfluorures Ioniques - ERA 609
Faculté des Sciences - Route de Laval - 72017 LE MANS Cédex

New fluoride glasses with BaF_2-M_tF_n-UF_4 formula (M_tF_n = MnF_2, ZnF_2, FeF_2, CuF_2, TiF_3, VF_3, FeF_3, GaF_3) have been prepared (1). The vitreous areas are established for M_tF_n = ZnF_2, MnF_2, FeF_3 (Figure 1). Glassy domains are centered on the pseudo binary system BaM_tF_{n+2}-UF_4. These glasses accept large variation of composition and in the case of BaF_2-FeF_3-UF_4 system, numerous fluorides can be added (till 20 % mole) leading for example to the composition : 20 BaF_2 - 20 FeF_3 - 40 UF_4 - 20 MF_n (M = Li, Na^+, K^+, Rb^+, Cs^+, Ag^+, Mg^{2+}, Ca^{2+}, Sr^{2+}, Cd^{2+}, Mn^{2+}, Fe^{2+}, Co^{2+}, Cu^{2+}, Zn^{2+}, Ti^{3+}, V^{3+}, Ga^{3+}, Y^{3+}, Ln^{3+}). BaF_2 - FeF_3 - UF_4 is a very good glassy system which allows the preparation of samples up to 20 x 8 x 5 mm^3 without any additives, on the contrary for Mn^{2+} or Zn^{2+} systems a small addition of YF_3 and AlF_3 stabilizes the glass. Table I gives the characteristics and composition of some glasses.

These glasses have good chemical stability, they can be kept up to 250°C in air without damages, 100 h chemical resistance tests in HCl or NaOH solution show that for YF_3 containing glasses as 20 YF_3 - 20 BaF_2 - 20 FeF_3 - 40 UF_4 no attack take place even in 40 % HF.

I.R. spectra show always an important optical density and an absorption band shut the transmission window near 10.7 µm. In the visible and near I.R., spectra are identical to those of figure 2a ; they are representative of U^{4+} whose transitions have been identified in comparison with U^{4+} spectra in CaF_2 or aqueous solution. Spectrum 2b concerns another lead fluoride glass containing only 0.5 % of UF_4. The similarity of both spectra shows that either as glass forming ion or as doping ion U^{4+} cannot be a sensitive optical probe for structural information.

The fundamental aim of this work concerns magnetic studies which have been performed for susceptibility by the Faraday method and for magnetization by the Foner method in the temperature range 4.2 K - 300 K. It has been found for all glasses a strong temperature dependence for susceptibility (Figure 3). For BaF_2-ZnF_2-UF_4 glasses the χ versus T variation indicates that U^{4+} are not six - but rather eight coordinated (2). Surprisedly , studies of the diamagnetic dilution of BaF_2-ZnF_2-UF_4 glasses $\frac{(1-x)}{2}$ [BaF_2 + ZnF_2] - x UF_4 or BaF_2 - 2ZnF_2 -(2-x) ThF_4-xUF_4) shows that both asymptotic Curie temperature and effective magnetic number are independent of U^{4+} composition : $|\theta p|$ ≈ 100K, nU^{4+} ≈ 3.3 μ_B. The invariability of $|\theta p|$ with U^{4+} content has not yet been observed in dilution of crys-

talline compounds (3) and is interpreted as coming from UF_8 polyedra clusters formation in the glass. For 3d paramagnetic elements containing glasses ($M_t = Mn^{2+}$, Fe^{3+}) the general trend of curves $1/\chi = f(T)$ is identical but $|\theta p|$ values are rather different ($30K \leq |\theta p| \leq 80\,K$). Magnetization measurements on Mn^{2+} or Fe^{3+} glasses (down to 2K, applied field up to 18 Koe) indicate magnetic ordering at low temperature but no remanent magnetization have been observed (IRM or TRM) at 2K. A.C. susceptibility on BaF_2-FeF_3-UF_4 shows near 1.4K a tendancy to rounded cusp characteristic of spin glass behavior (4, 5). Interpretation of magnetic behavior is more much difficult than in crystalline compounds but first, a comparison of $|\theta p|$ values can be made (assuming that $|\theta p|$ is representative of mean strenghts of the magnetic interactions between nearest neighbours). From this point of view, it may be concluded that antiferromagnetic interactions via a superexchange mechanism predominate in these glasses and antiferromagnetic interactions can be sorted out as U^{4+}-$U^{4+} \approx Fe^{3+}$ - $Fe^{3+} > Mn^{2+}$ - Mn^{2+}. On the contrary M_t-U interactions are ferromagnetic. The constancy of $|\theta p|$ value for different M^{3+} ions, compared with dependence for M^{2+} ions is consistent with more numerous M^{2+}-U^{4+} than M^{3+}-U^{4+} interactions.

From the optical and magnetic studies these glasses can be seen as clusters of UF_8 polyedra connected by 3d elements octahedra with a reticulation rate clusters -3d octahedra greater for divalent ions than for trivalent ions.

REFERENCES

1 - J. GUERY, G. COURBION, C. JACOBONI and R. DE PAPE
Materials Chemistry 7, 715-722 (1982)

2 - C.A. HUTCHINSON and G.A. CANDELA
J. Chem. Phys., 27, 707 (1957)

G.A. CANDELA, C.A. HUTCHINSON and W.B. LEWIS
J. Chem. Phys., 30, 246-250 (1959)

3 - J.K. DAWSON
J. of Chem. Soc. (London) 1185 (1952)

4 - J.P. RENARD, J.P. MIRANDAY and F. VARRET
Sol. State Com., 35, 41-44 (1980)

5 - J.P. RENARD, C. DUPAS, E. VELU, C. JACOBONI, G. FONTENEAU and J. LUCAS
Physica 108 B, 1291-1292 (1981)

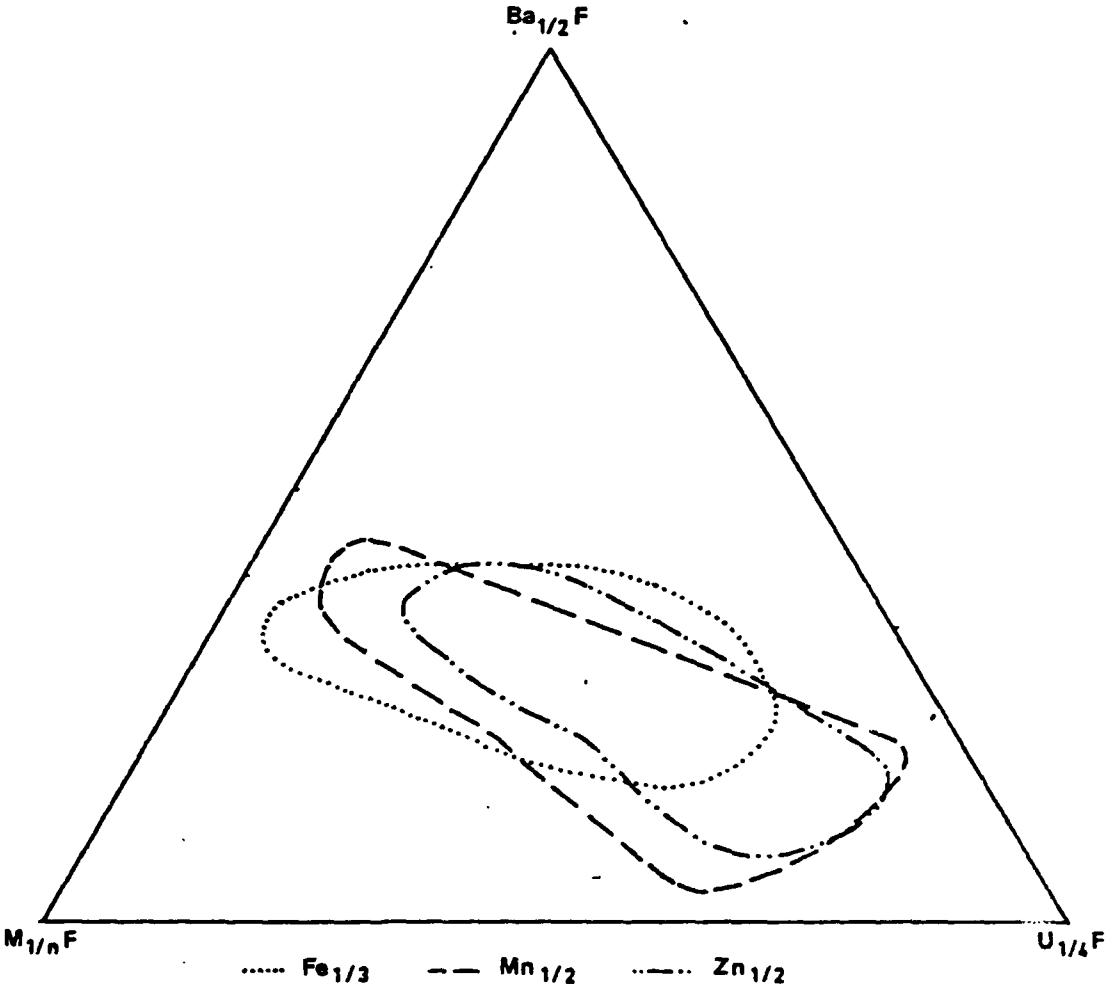

FIGURE 1

Vitreous domains in the BaF_2 - M_tF_n-UF_4 systems.

M_tF_n = MnF_2, ZnF_2, FeF_3

TABLE 1

PHYSICAL CONSTANT OF SOME URANIUM FLUORIDE GLASSES

COMPOSITION (% molaire)	Tg(°C)	Tc(°C)	Tf(°C)	ñ	υ	Cexp	$nU^{4+}(\mu_B)$	θp(K)
33 BaF_2 : 33 MnF_2 : 33 UF_4	317	362	666			1,91	3,30	-32
31 BaF_2 : 31 MnF_2 : 33 UF_4 :5 AlF_3				1,554	38			
33 BaF_2 : 33 ZnF_2 : 33 UF_4	314	353	601			1,87	3,24	-103
31 BaF_2 : 31 ZnF_2 : 33 UF_4 :5 AlF_3				1,549	43			
33 BaF_2 : 33 FeF_3 : 33 UF_4	346	432	597	1,505	20	3,83	3,01	-79

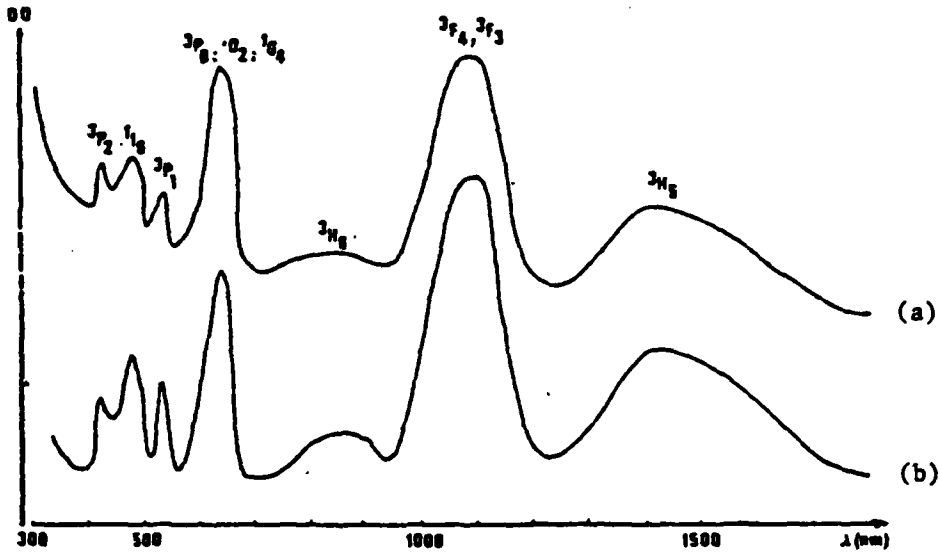

FIGURE 2

Absorption spectra : a) 40 BaF_2 - 40 ZnF_2 - 20 UF_4

b) 46 PbF_2 - 22 ZnF_2 - 30 GaF_3 - 2 LaF_3 - 1,5 AlF_3 - 0,5 UF_4

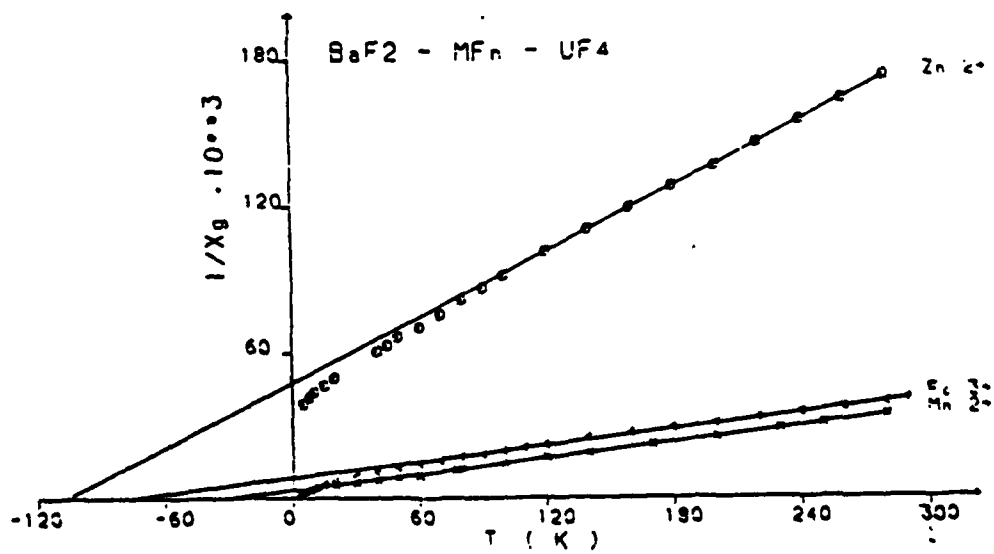

FIGURE 3

$1/\chi$ versus T for BaF_2 - M_tF_n - UF_4 glasses ; M_tF_n = MnF_2, ZnF_2, FeF_3

SURFACE STUDIES OF FLUOROZIRCONATE GLASSES

by

C. A. Houser and C. G. Pantano
Department of Materials Science and Engineering
The Pennsylvania State University
University Park, PA 16802

The effects of water on the surface of ZBLA fluorozirconate glass were studied using secondary ion mass spectrometry (SIMS) and scanning electron microscopy (SEM). Infrared spectroscopy was also used to determine the effect of the surface layers formed on the infrared transmission. Sample surfaces were prepared by several methods in order to observe the effect of surface finish on the glass durability. Samples were then exposed to a variety of aqueous solutions and to humidity.

High quality ZBLA glass was obtained from La Verre Fluore, Rennes, France. Three types of surfaces were prepared for study: fracture surfaces and ground surfaces with a final polish done with 1 μm diamond paste or a cerium oxide and water slurry.

Samples were exposed to water for times from 5 to 60 minutes in 30°C deionized water with a surface area to volume ratio of approximately 10^{-3}. Samples were also prepared at 60 and 40°C in deionized water and at 30°C in pH 2 HF solution, in pH 10 NH_4OH solution, and at 95% relative humidity.

The SIMS in-depth concentration profiles for a surface polished with diamond paste and hydrated 20 minutes in 30°C deionized water are shown in Fig. 1. The results indicate a build up of hydrogen, oxygen, and carbon in the surface layer. There is also a slight silicon peak, probably due to silicon release from the solution container. The zirconium, barium, fluorine, aluminum, and sodium profiles show a slight surface build up followed by a depleted region. At longer exposure times, the depth profiles, particularly that of carbon, show additional structure, possibly indicating the formation of several layers.

Profiles for surfaces polished with cerium oxide were similar to those for the diamond paste polished samples except that the cerium oxide samples appeared to hydrate at a lower rate. Film formation on the cerium oxide samples tended to be less uniform.

The depth of the oxygen-enriched layer increased with solution temperature as well as with exposure time. Figures 2a to 2c show the oxygen, hydrogen, and carbon depth profiles for diamond paste polished samples exposed 20 minutes to 30, 40, and 60°C deionized water. The samples were rotated at a rate of 20 revolutions per minute to minimize the formation of surface precipitates; however, rotating the samples was also found to increase the thickness of the hydrated layer. Figures 3a and 3b show the infrared transmittance spectra for the samples discussed in Fig. 2. Also shown is the spectrum for a sample polished in cerium oxide and exposed 20 minutes to 30°C deionized water.

The effects of solution pH were also investigated. Samples exposed to pH 2 HF solution showed the formation of a thick surface film over the hydrated surface, as can be seen in Fig. 4a. At pH 10, Fig. 4b, a similar sample showed almost no uptake of carbon, hydrogen, or oxygen. The sodium signal showed a slight depletion and the barium signal was reduced from the level of the unhydrated signal.

Samples placed in 95% relative humidity showed almost no hydration with narrow surface peaks of sodium and carbon.

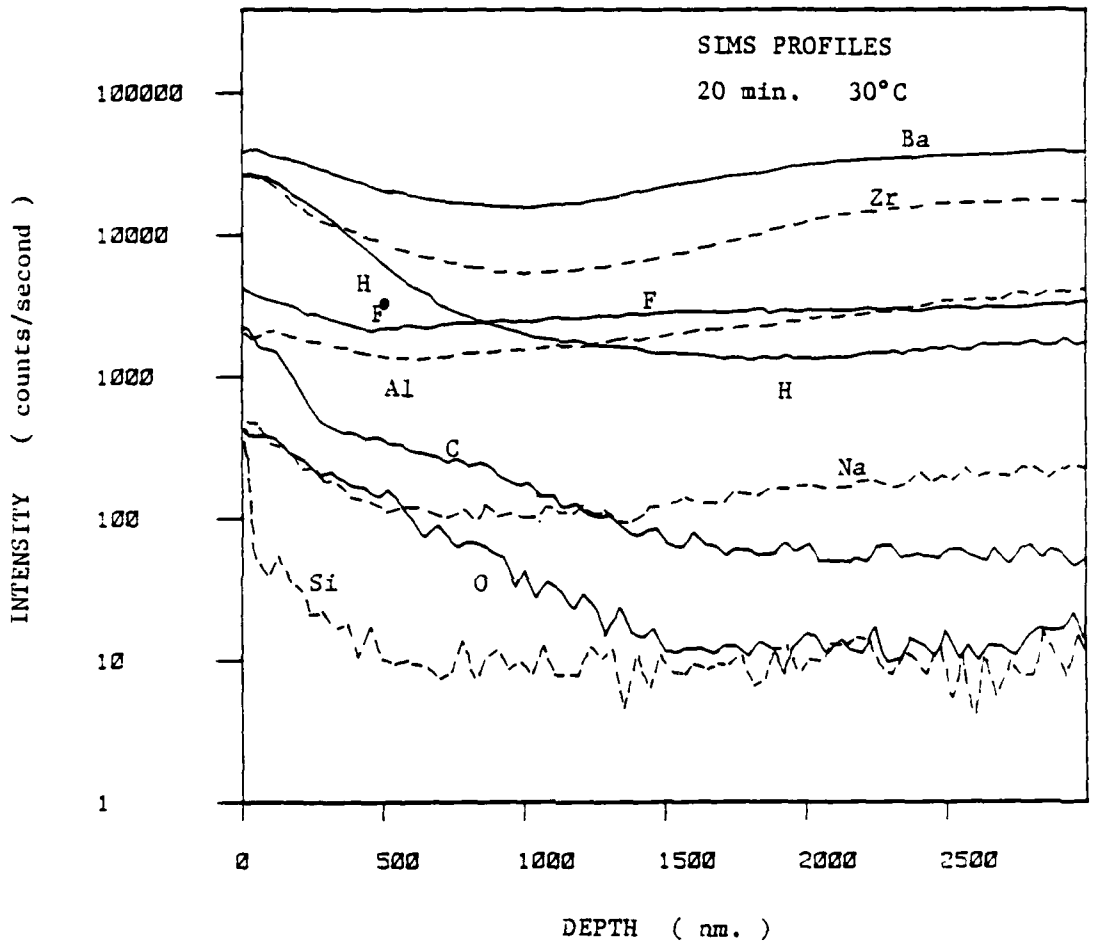

Fig. 1 ZBLA exposed to 30°C deionized water for 20 minutes. The sample was polished with 1 μm diamond paste.

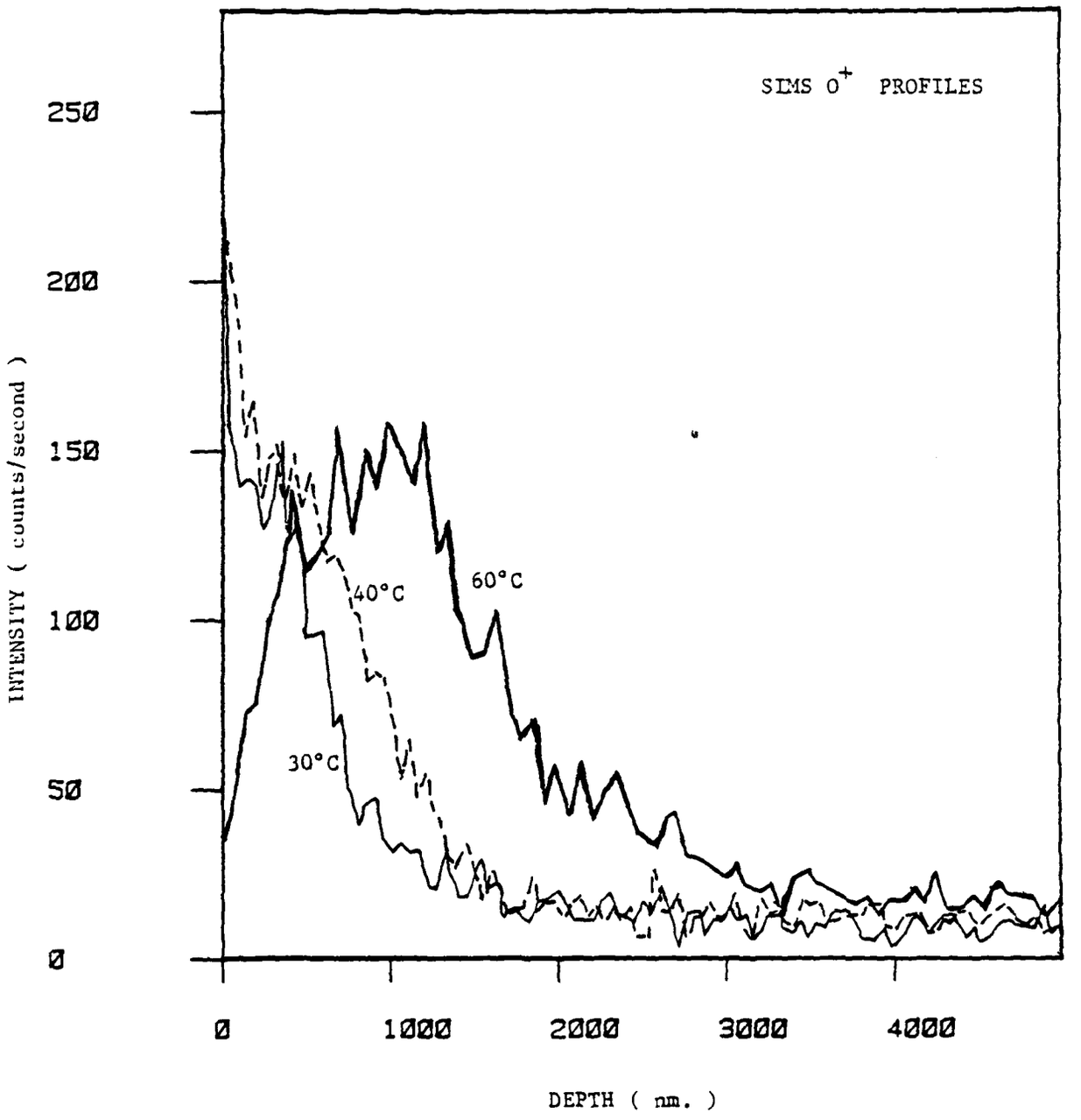

Fig. 2a SIMS depth profiles for diamond paste polished ZBLA surfaces exposed 20 minutes to 60, 40, and 30°C deionized water.

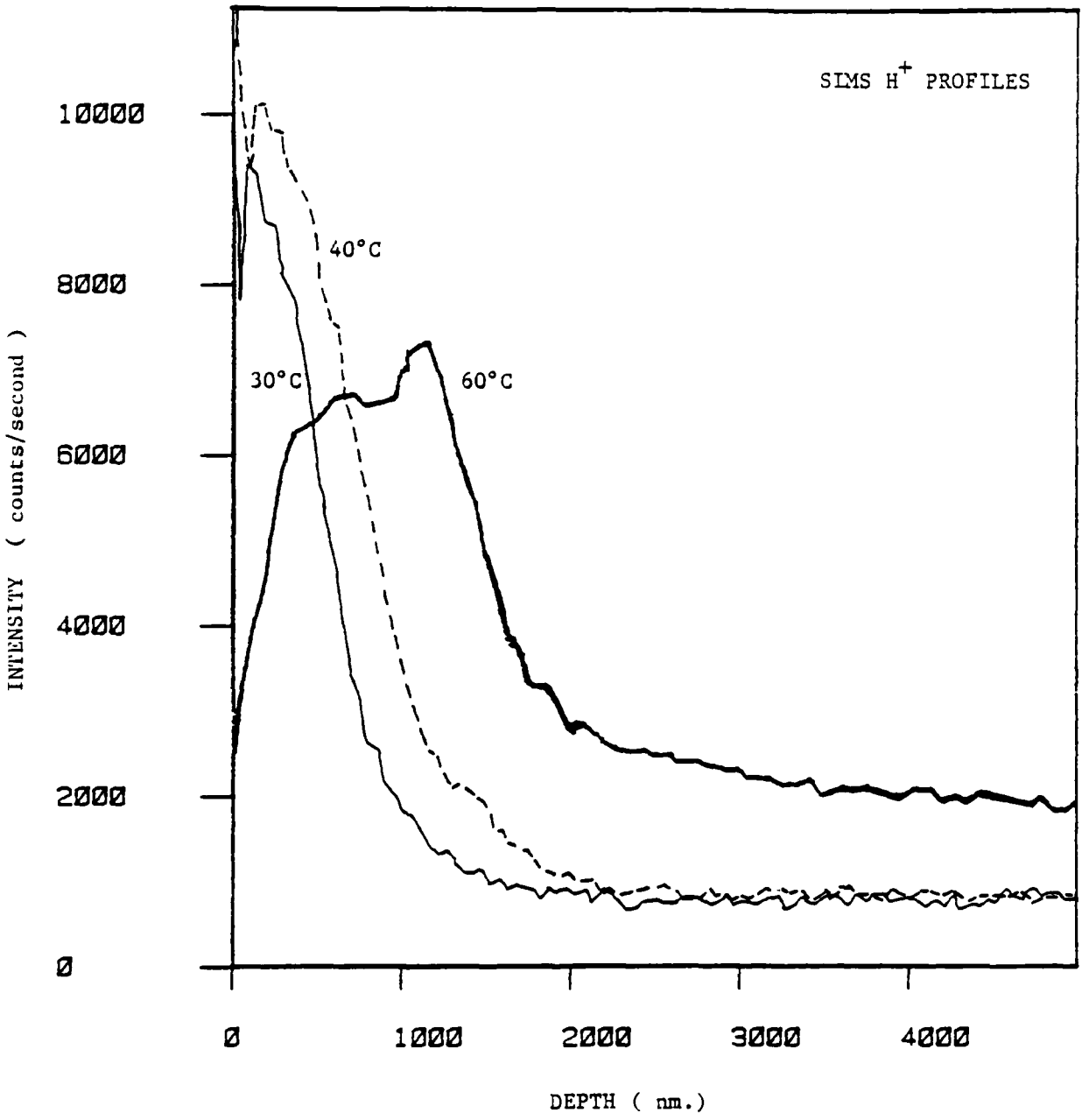

Fig. 2b Hydrogen SIMS depth profiles for diamond paste polished ZBLA surfaces exposed 20 minutes to 60, 40, and 30°C deionized water.

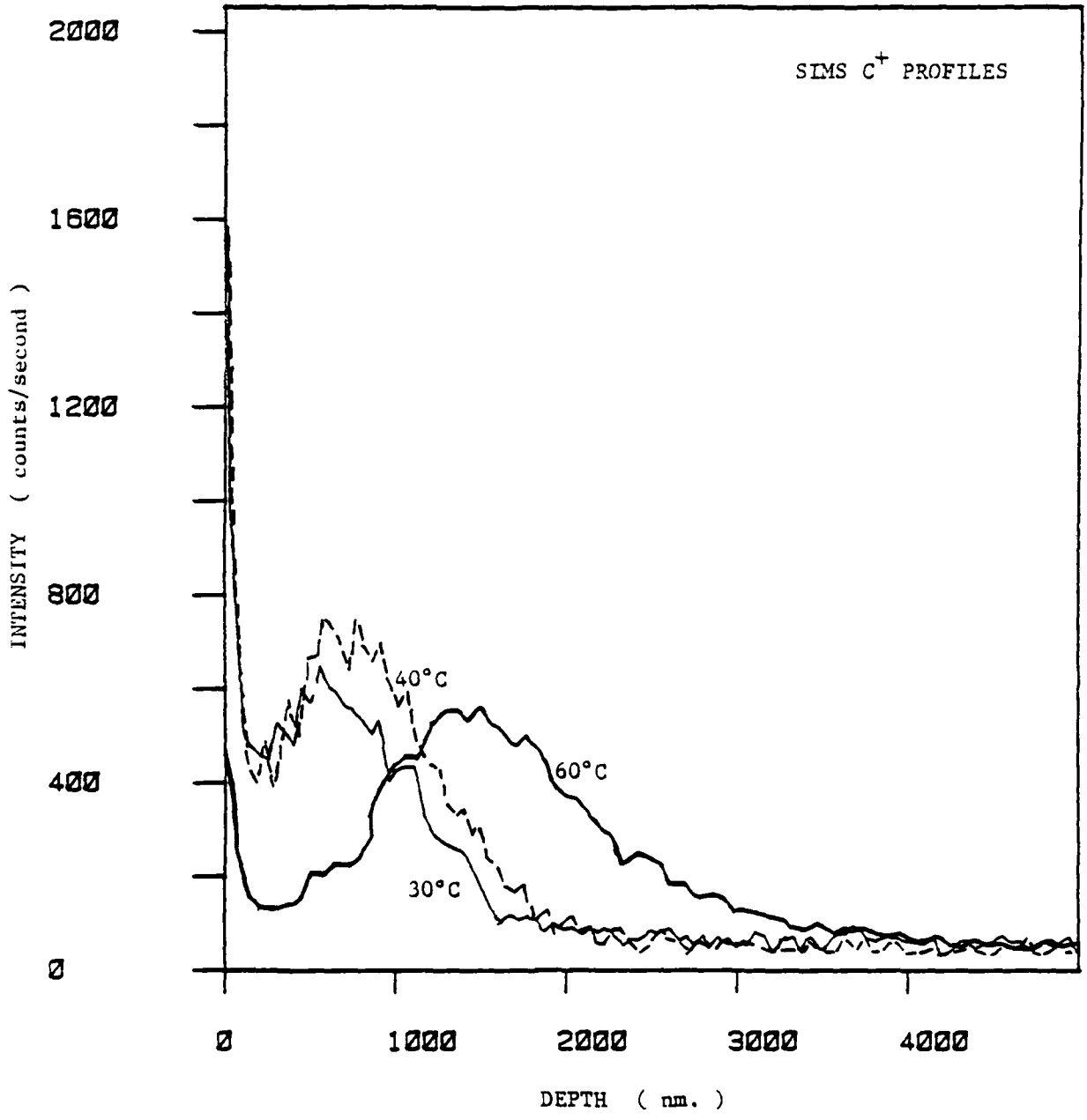

Fig. 2c Carbon SIMS depth profiles for diamond paste polished ZBLA surfaces exposed 20 minutes to 60, 40, and 30°C deionized water.

AD-A144 269 EXTENDED ABSTRACTS INTERNATIONAL SYMPOSIUM ON HALIDE GLASSES (2ND) RENSSE..(U) RENSSELAER POLYTECHNIC INST TROY NY DEPT OF MATERIALS ENGINEE.. C T MOYNIHAN

2/4

UNCLASSIFIED 02 AUG 83 N00014-83-G-0091 F/G 11/2 NL

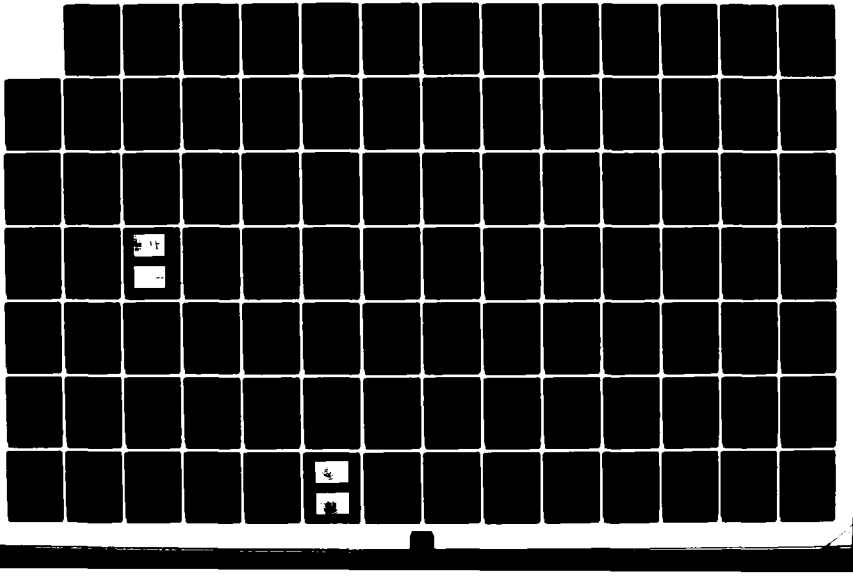

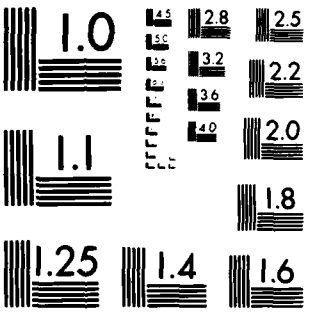

MICROCOPY RESOLUTION TEST CHART
NATIONAL BUREAU OF STANDARDS-1963-A

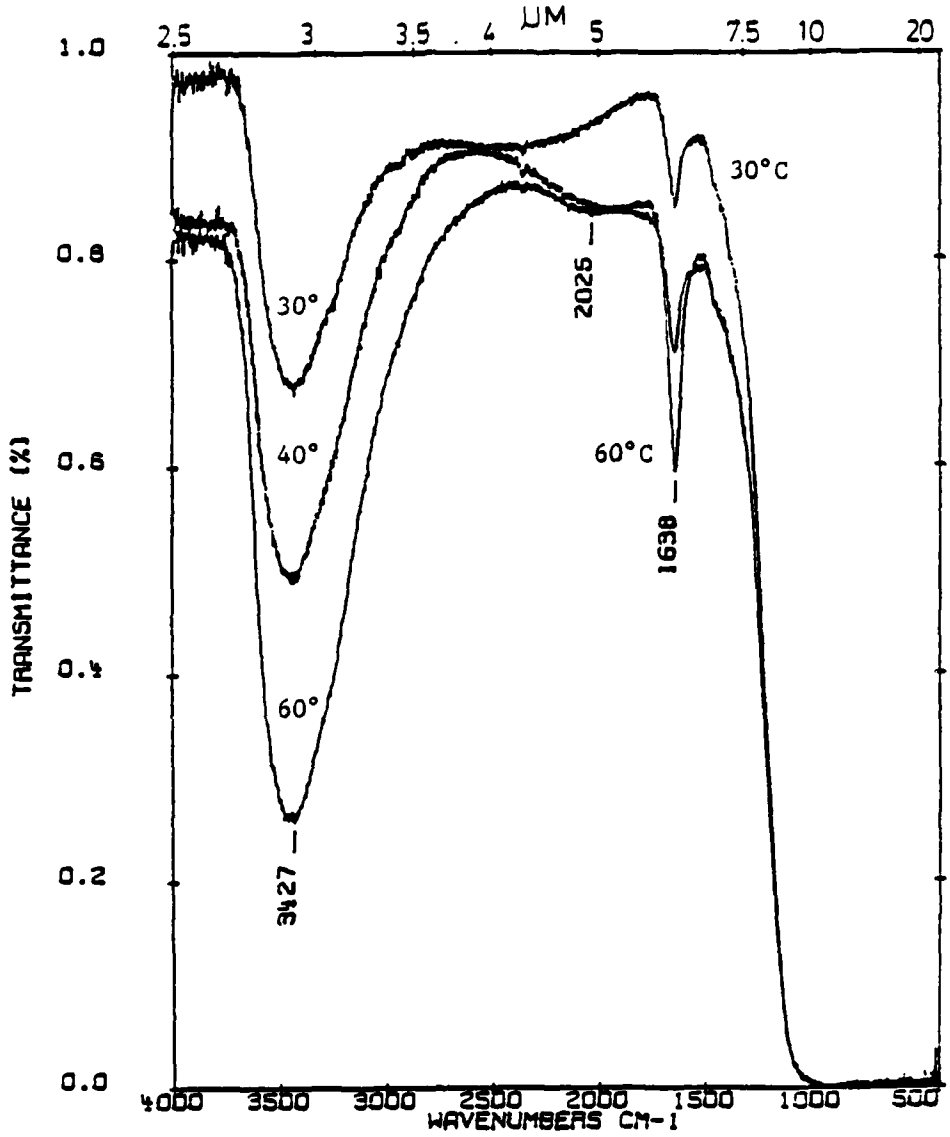

Fig. 3a IR spectra for diamond paste polished ZBLA exposed 20 minutes to 60, 40, and 30°C deionized water.

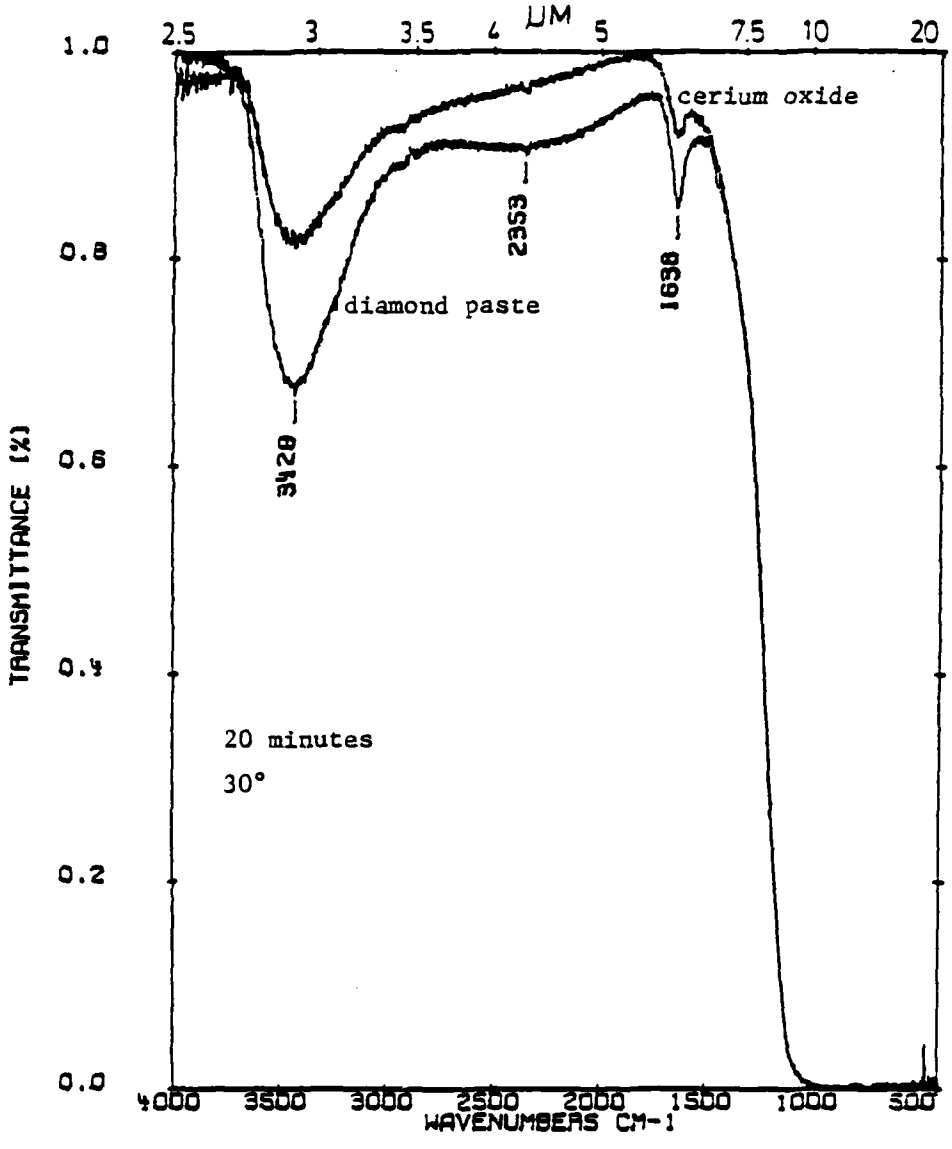

Fig. 3b IR spectra for diamond paste polished and cerium oxide polished ZBLA exposed 20 minutes to 30°C deionized water.

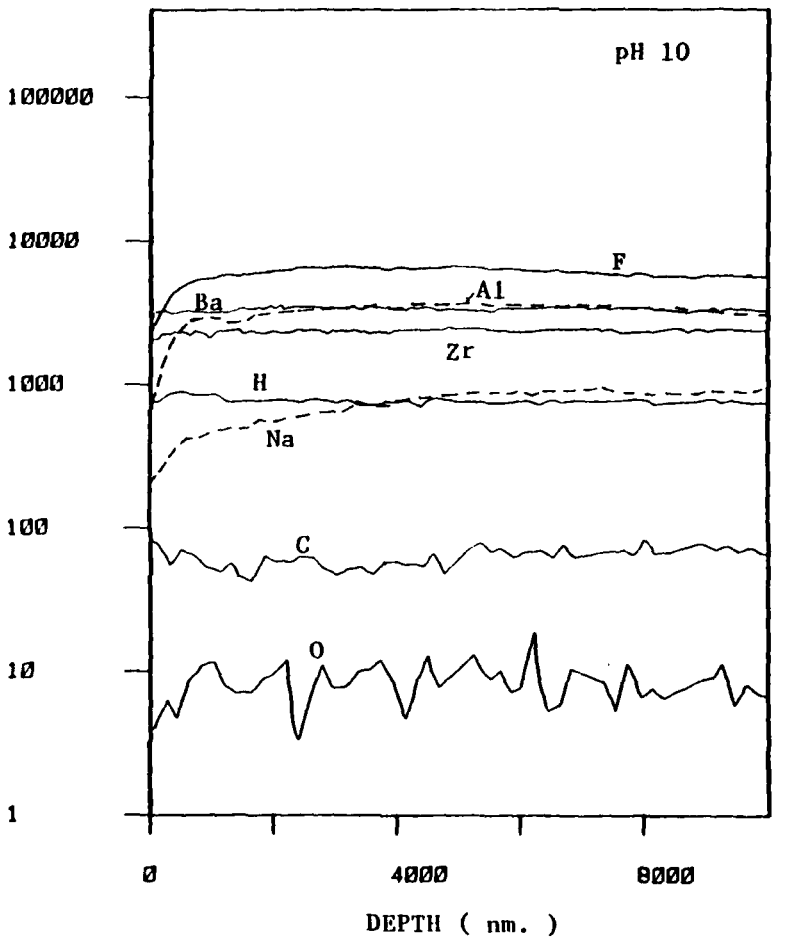

Fig. 4b SIMS depth profiles of ZBLA polished with cerium oxide and exposed to pH 10 NH_4OH solution for 10 minutes at 30°C.

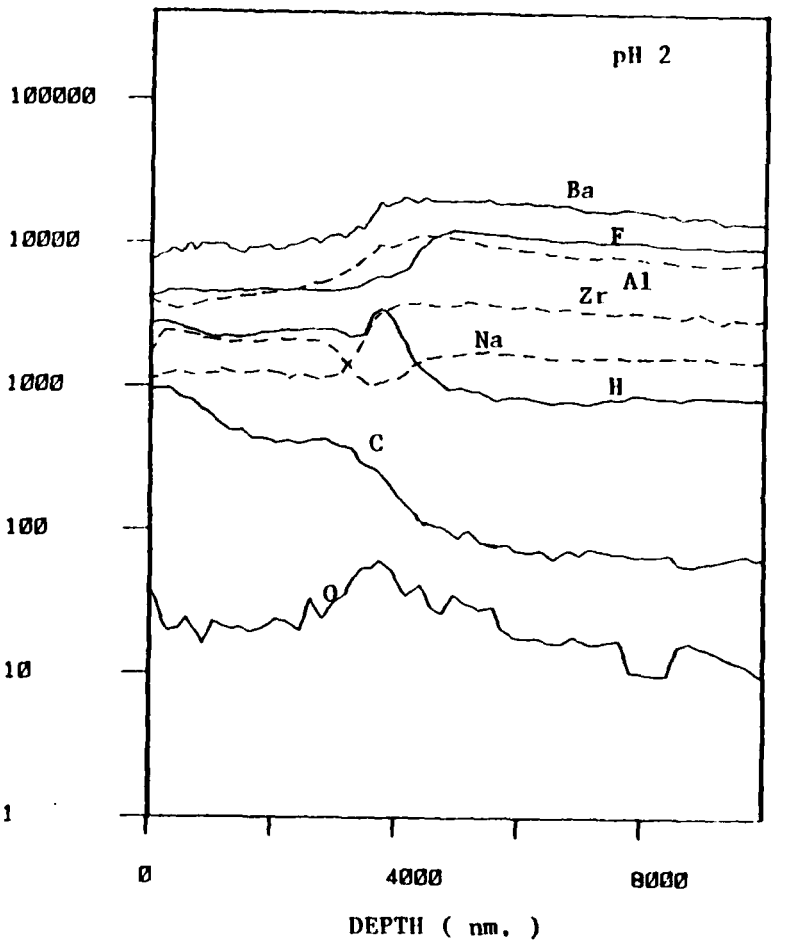

Fig. 4a SIMS depth profiles of ZBLA polished with cerium oxide and exposed to pH 2 HF solution for 10 minutes at 30°C.

PREPARATION AND PROPERTIES OF TRANSITION METAL FLUORIDE GLASSES

C. JACOBONI

Laboratoire des Fluorures et Oxyfluorures Ioniques - ERA 609
Faculté des Sciences - Route de Laval - 72017 LE MANS Cédex

Since 1978 (1, 2, 3), numerous glassy systems have been found in Le Mans involving 3d transition metals fluorides as glass progenitors :

$M^{I}F - M^{II}F_2 - M_t^{III}$ and $PbF_2 - M_t^{II}F_2 - M_t^{III}F_3$

with M^{I} = Li, Na, K, Rb ; M^{II} = Ca, Sr, Cd, Ba, Pb ;

M_t^{II} = Mn, Fe, Co, Ni, Cu, Zn and M_t^{III} = V, Cr, Fe, Ga, In.

Figure 1 shows glassy ternary diagrams, it must be noted that some of them extends towards binary systems.

Starting fluorides are, for the most part of them, prepared at the Laboratory from HF gas on dehydrated chlorides or by thermal decomposition of $(NH_4)_3M^{III}F_6$ or dehydration under HF gas of hydrated fluorides. Complete works (weighting, mixing, melting and casting) are performed in dry-boxes in line (<10 ppm H_2O) to prevent hydrolysis by atmospheric water which leads to oxydes formation at higher temperatures. The mixture of the starting fluorides in a covered platinium crucible is heated between 600-900°C and cast on a preheated (200-250°C) bronze mould. The mould temperature is kept for 30 mn then cooled to room temperature. Table I gathers some compositions with their main physical characteristics. The standart size of the samples is 8 x 8 x (20-100) mm^3. These glasses can be kept up to 200°C in air without damage but their resistance in aqueous solutions (especially acidic medium) is bad. Thermal expansion is about $\alpha = 15\ 10^{-6}$ and the hardness is $200 < H_{v100} < 300$. The glasses can be polished on dry or oiled abrasives surfaces and cleaned by trichlorethylène or chloroform.

Figure 2 shows that the transparency is excellent for PMF and PMG glasses till 7.5 µm. So, these glasses, especially PMG glasses, are potential candidats for 2 - 6 µm range. Devitrification studies have been performed and fiber realization will take place in Autumn 1983.

Another optical property concern Rare Earth luminescence extensively studied by R. REISFELD and C. K. JORGENSEN (4,5, Session VIII-3).

One of the fundamental scope provided by these glasses concern magnetic behavior. Magnetic studies for high content 3d transition metals fluorides glasses corroborate, as expected the predominance of superexchange antiferromagnetic interactions (figure 3). In the case of Mn^{2+} - Fe^{3+} (d^5 - d^5) glasses, the frustration, induced by topological disorder leads to "spin glass" behavior (figure 4). Taking advantage of this last property extensive neutron diffraction experiments have

been made on fluoride glasses "$PbMnFeF_7$" and "Pb_2MnFeF_9" to provide informations about the magnetic short range order of pairs M-M ($M = Mn^{2+} - Fe^{3+}$) (6). The magnetic correlation function shows in both glasses prevailing strong antiferromagnetic first neighbour interaction at 3.6 Å and two ferromagnetic interactions at 5.4 and 6.7 Å (Figure 5). Furthermore, the local environment of transition metal (M_t) and lead has been studied by E.X.A.F.S. (7) for some fluoride glasses in the system PbF_2-$M_t^{II}F_2$-$M_t^{III}F_3$ ($M_t^{II} = Mn^{2+}$, Zn^{2+} and $M_t^{III} = Fe^{3+}$, Ga^{3+}). According to previous visible absorption results on Ni^{2+}, Co^{2+}, V^{3+} or Cr^{3+} based glasses (2), transition metals are sixfold coordinated and M_t-F distances are very close to those known in crystallized compounds. Lead has eight to nine fluorine neighbours forming a very distorted polyhedra (Table II - Figure 6). Radial distributions, show a very weak second peak probably due to heavy atoms like Pb or Mt (F^- contribution is too weak for the second shell) but the precise nature of the second neighbours and the distances cannot be determined without ambiguity.

As shown in figure 1 the glassy domain expands on binary PbF_2-FeF_3 system and both vitreous and crystalline forms exist for 0.625 PbF_2 - 0.375 FeF_3 ($Pb_5Fe_3F_{19}$). Single crystals have been prepared and structural determination have been carried out on X Ray automatic diffractometer data. The structure is built up with two kinds of chains - α trans $(FeF_5)_n$ chains and β mixed $(PbFe_2F_{14})$ chains, both chains are elongated on $\vec{c}$ (Figure 7-8). This structure is closely related to $BaFeF_5$ one which consists of an arrangement of α and γ chains. β and γ chains are related by the substitution : $\underset{\beta}{(PbFe_2F_{14})^{6-}} + FeF_3 \rightarrow \underset{\gamma}{(Fe_3F_{15})^{6-}} + PbF_2$.

A crystallochemical analogy exists between the crystallized compounds PbF_2 β, $Pb_5Fe_3F_{19}$ and "$PbMnFeF_7$" and "Pb_2MnFeF_9" glasses in term of relatively close-packing which must leads to a similar coordination of 9 for Pb^{2+} and F^- toward large ions (as seen by EXAFS). So it seems that the stability of numerous fluoride glasses comes from the existence of a mixed packing of F^- ions and large ions ; the structural disorder is a result of the random character of the packing and of the wide diversity of the sites for the small cations. The structural unity of the PbF_2-MnF_2-FeF_3 glasses is then consistent with α [$(MnFe)F_5$] chains and intermediate (β-γ) chains connected together.

This work have been performed by the "glass group" of LE MANS (C. JACOBONI, A. LEBAIL, G. COURBION, J. GUERY, N. AURIAULT, A.M. MERCIER and R. DE PAPE) with financial support of DRET.

REFERENCES

1 - J.P. MIRANDAY, C. JACOBONI, R. DE PAPE
Revue Chimie Minérale 16, 277 (1979)

2 - J.P. MIRANDAY, C. JACOBONI, R. DE PAPE
J. of Non Cryst. Solids, 43, 393-401 (1981)

3 - C. JACOBONI, A. LE BAIL, R. DE PAPE
Glass Technology, 24, 3, 164-167 (1983)

4 - R. REISFELD, G. KATZ, N. SPECTOR, C.K. JORGENSEN, C. JACOBONI, R. DE PAPE
J. of Solid State Chem., 41, 253-261 (1982)

5 - R. REISFELD, G. KATZ, C. JACOBONI, R. DE PAPE, M.G. DREXHAGE, R.N. BROWN, C.K. JORGENSEN
J. of Solid State Chem., in press

6 - A. LE BAIL, C. JACOBONI, R. DE PAPE
J. of Solid State Chem, in press

7 - A. LE BAIL, C. JACOBONI, R. DE PAPE
J. de Physique, Colloque C9, 43, C9 - 677 (1982)

TABLE I

	T_g °C	T_c °C	T_f °C	n	υ	λ μm max	ρ g cm^{-3}
30 KF : 25 PbF_2 : 45 GaF_3	295	329	547				
30 NaF - 25 PbF_2 : 45 CrF_3	330	382	595				
30 NaF - 25 SrF_2 : 45 VF_3	311	365	650				
42 PbF_2 - 17 MnF_2 32 FeF_3 3 SrF_2 - 5 YF_3 - 2 AlF_3 (PMF 18)	251	317	520	1.627	34	7.6	5.4
36 PbF_2 - 24 MnF_2 - 35 GaF_3 5 YF_3 - 2 AlF_3 (PMG 13)	273	336	526	1.5767	40	7.9	5.6

TABLE II

EXAFS : First neighbour parameters for glasses and crystallized compounds (under parenthesis : the known χ-ray values)

Glass	Edge	R_1 (Å)	σ_1 (Å)	$N_1 \pm 1$
"$PbMnFeF_7$"	Mn	2.099	0.058	5.72
	Fe	1.924	0.047	5.93
	Pb	2.63	0.104	8.1
"Pb_2MnFeF_9"	Mn	2.108	0.058	5.35
	Fe	1.930	0.063	5.51
	Pb	2.65	0.107	8.3
α-$LiMnFeF_6$	Mn	(2.126)		(6.0)
	Fe	(1.935)		(6.0)
$Pb_5Fe_3F_{19}$	Pb	(2.71)		(8.7)

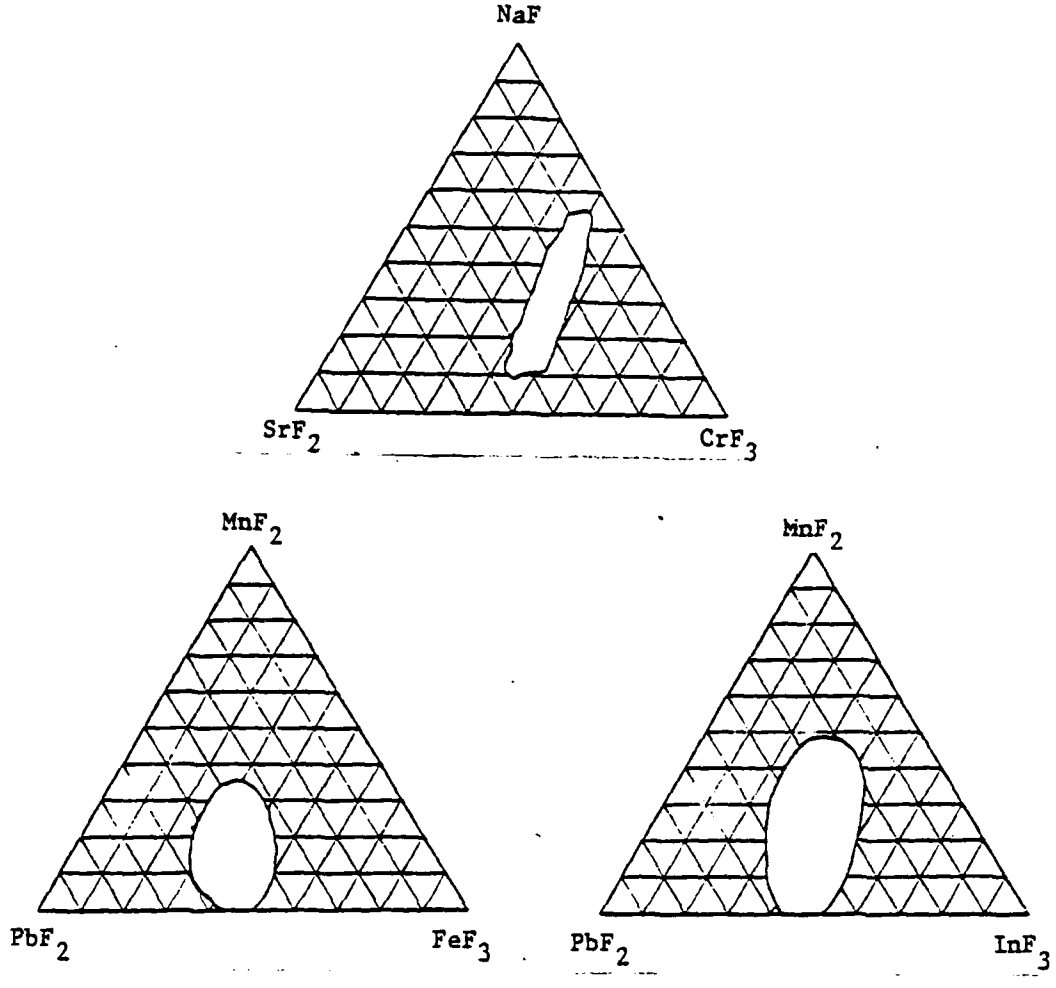

FIGURE 1

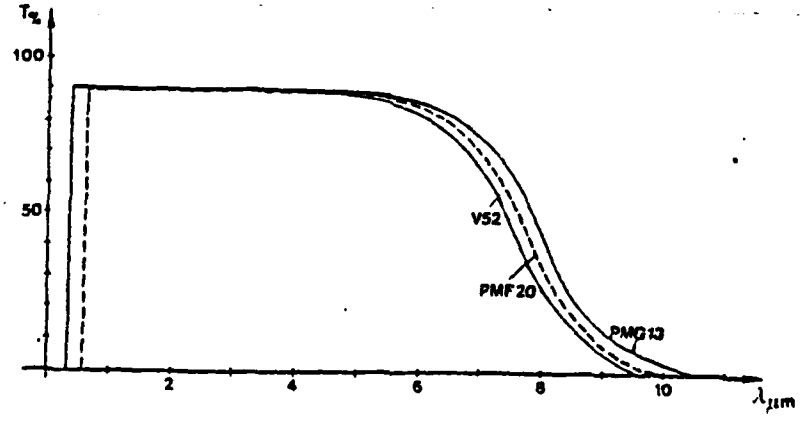

FIGURE 2

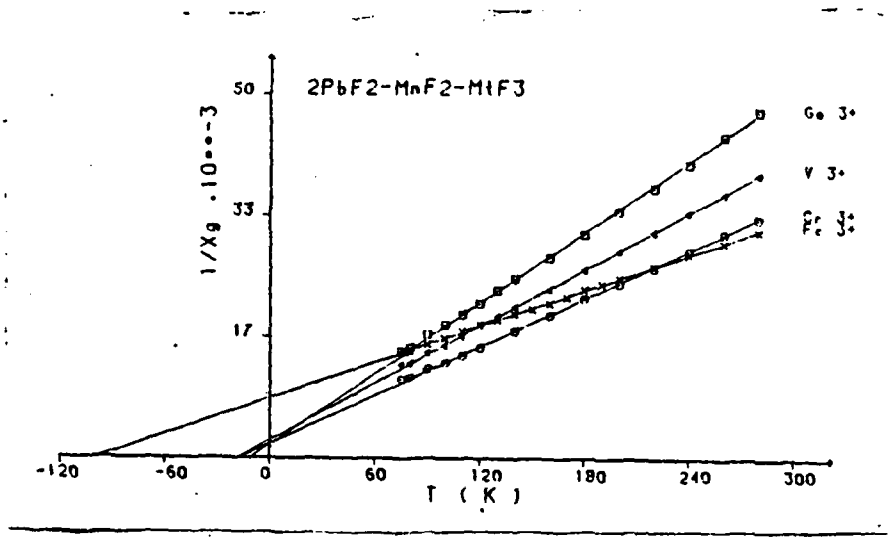

FIGURE 3

Variation of magnetic susceptibility per gram with temperature for "$PbMnM_tF_9$" glasses

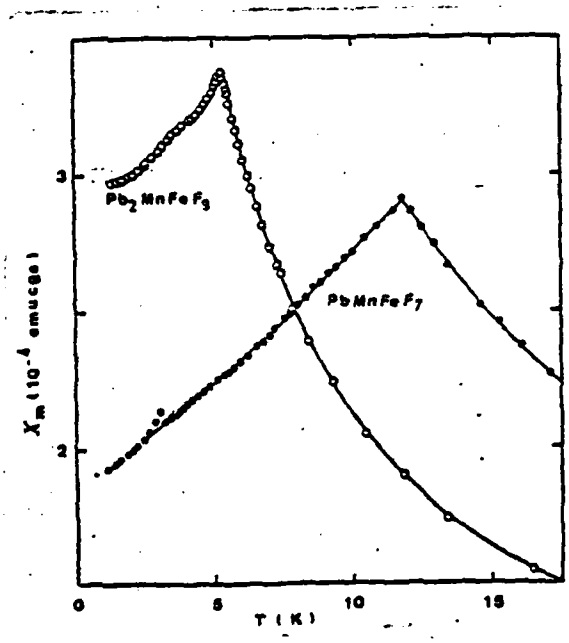

FIGURE 4

A.C. susceptibility per gram versus T of fluoride glasses "$PbMnFeF_7$" and "Pb_2MnFeF_9" (ν = 72 Hz)

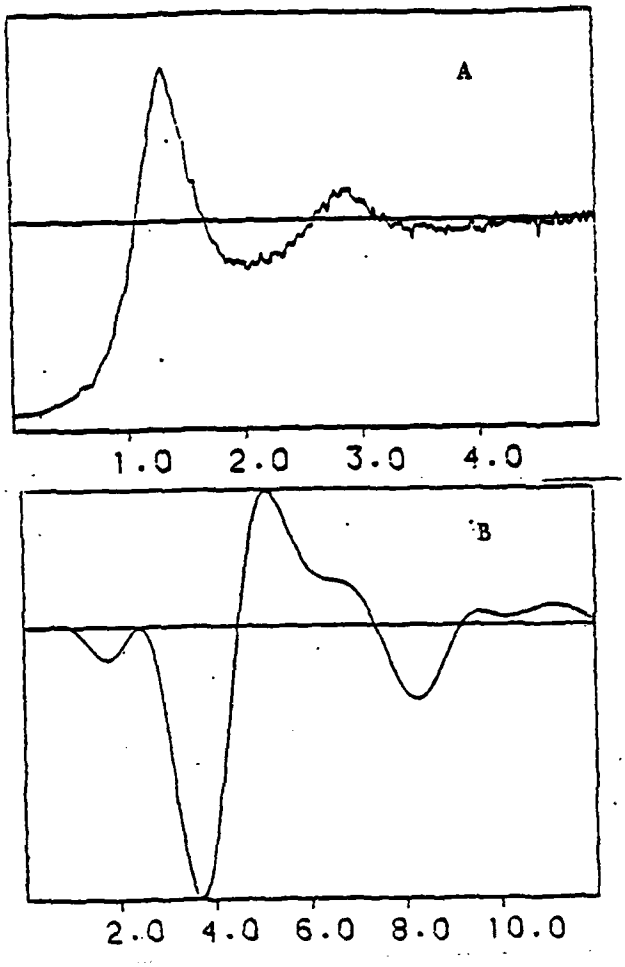

FIGURE 5

A - Difference spectra (4K - 250K)
B - Fourier Transform F(R)
} for "$PbMnFeF_7$" glass

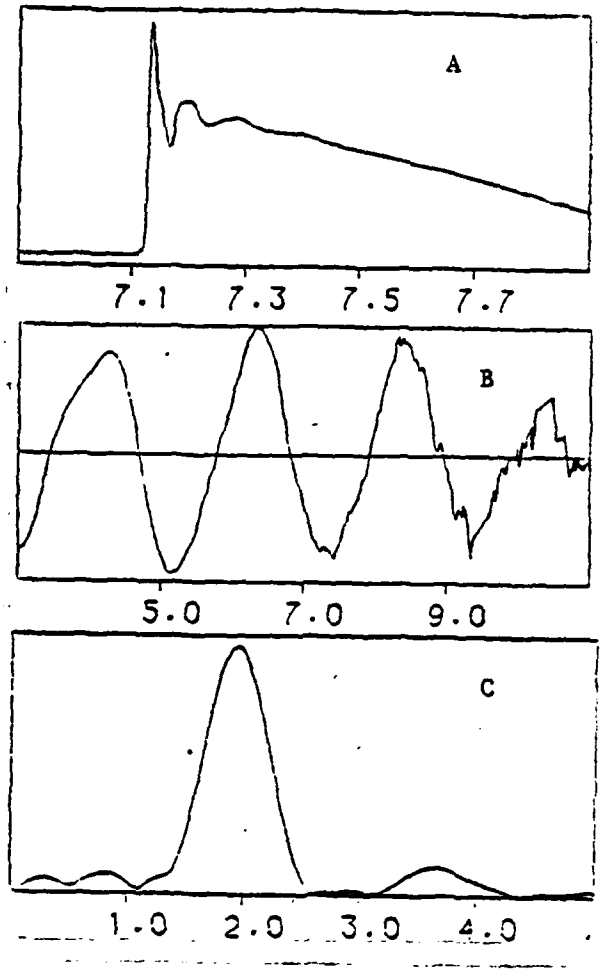

FIGURE 6

A - Absorption spectra of "$PbMnFeF_7$" on Iron K Edge (7111 eV)
B - $k^3\chi(k)$ filtered experimental spectra from A
C - Fourier Transform F(R) is having first neighbours at 1°93 Å and second neighbours at 3.5 Å.

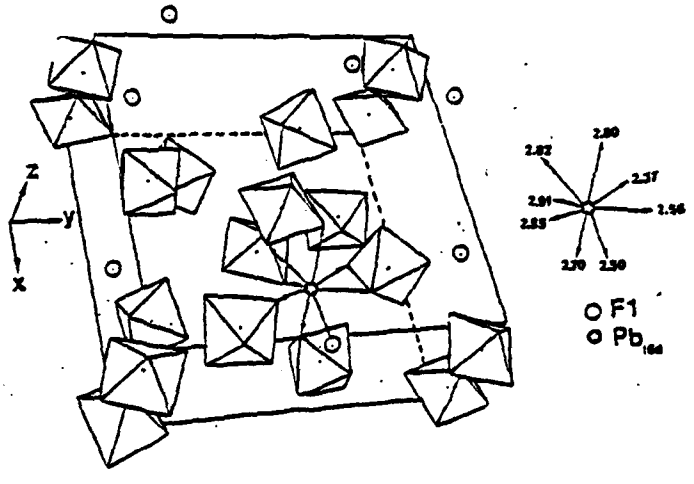

FIGURE 7

$Pb_5Fe_3F_{19}$ structure

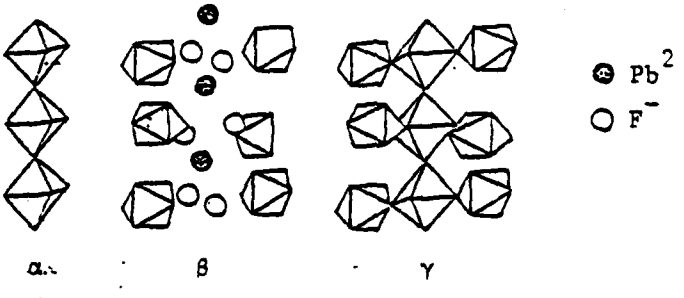

FIGURE 8

α, β, γ chains

CALPHAD CALCULATION OF THE EFFECT OF AlF_3 ADDITIONS ON THE GLASS COMPOSITIONS OF TERNARY ZrF_4 - LaF_3 - BaF_2 FLUORIDES*

by

Larry Kaufman and Dunbar Birnie

ManLabs, Inc. 21 Erie St. Cambridge, Mass. 02139 USA

The recent discovery of a new family of non-oxide glasses based on mixtures of ZrF_4 or HfF_4 with other metallic fluorides by M. Poulain and coworkers offers great potential in optical fiber, windows and source/detector application. Due to the limited phase diagram data available for the binary, ternary and multicomponent fluoride systems currently employed to synthesize these glasses most of the progress in identifying new compositions has proceeded along empirical lines. In order to remedy this situation, the CALPHAD method (1-3) for coupling phase diagram and thermochemical data has been applied to develop a data base covering metallic flourides. The objective is to permit computation of multicomponent phase diagrams which can be used to identify the composition range where the liquid is most stable. The latter offers opportunities for glass formation as demonstrated by predictions of new metallic glasses. Currently the data base covers combinations of 0.2 ZrF_4 (ZF), 0.25 LaF_3 (LF), 0.333 BaF_2 (BF), 0.333 PbF_2 (PF), 0.5 NaF (NF), 0.5 RbF (RF), 0.5 CsF (CF) and 0.5 KF (KF) which have been developed along the lines described earlier for III-VI, II-VI and SIALON systems (2-3). Figure 1 shows the calculation of isothermal sections in the LF-ZF-BF system which illustrates the range of composition in which the liquid has the greatest stability. These compositions agree well with those in which Poulain and coworkers have discovered glass formation (4,5). These calculation were presented at the symposum held in 1982 at Churchill College (6) and were recently published. The current data base has been extended to cover AlF_3 (AF=0.25AlF_3) by employing expermental data provided by Thoma (8) to evaluate AFAFLT=13389-8.368T J/g. at and LAFZF=25104 J/g. at=LZFAF, LAFBF=4184 J/g. at=LBFAF and LAFLF=20920 J/g. at=LLFAF. Utilization of these parameters along with those found previously permits calculation of the range of maximum stability of the liquid phase for ternary LF-ZF-BF glasses with additions of 4, 9 and 15 atom percent of AF. The results are displayed in Figure 2 as a function of temperature. Figure 2 also compares the calculated results for the glasses with 0 and 4 atom percent AF with the experimental finding of glass formation published by Lecoq and Poulain.

References

1. L. Kaufman, CALPHAD (1977) 1 14.
2. L. Kaufman, F. Hayes and D. Birnie, CALPHAD (1981) 5 163.
3. L. Kaufman, J. Nell, K. Taylor and F. Hayes, CALPHAD (1981) 5 185.
4. A. Lecoq and M. Poulain, J. Non-Crystalline Solids (1979) 34 101.
5. M. Poulain, M. Poulain and J. Lucas, Rev. de Chem. Mineral (1979) 16 267.
6. L. Kaufman, J. Agren, J. Nell and F. Hayes "Calculation of Ternary Glass Compositions" FIRST INTERNATIONAL SYMPOSIUM OF HALIDE GLASSES, Churchill College Cambridge, England March 1982
7. L. Kaufman, J. Agren, J. Nell and F. Hayes, CALPHAD 7, 71 (1983)
8. R.E. Thoma, Advances in Molten Salt Chemistry, J. Braunstein, G. Manator and G.P. Smith Eds. Plenum Press, N.Y. (1975) page 302
9. A. Lecoq and M. Poulain , Verres Refract. 34 333 (1980)

---

*This work has been sponsored by the Air Force Office os Scientific Research, Bolling Field, D.C. under AF4962-80-C-0020.

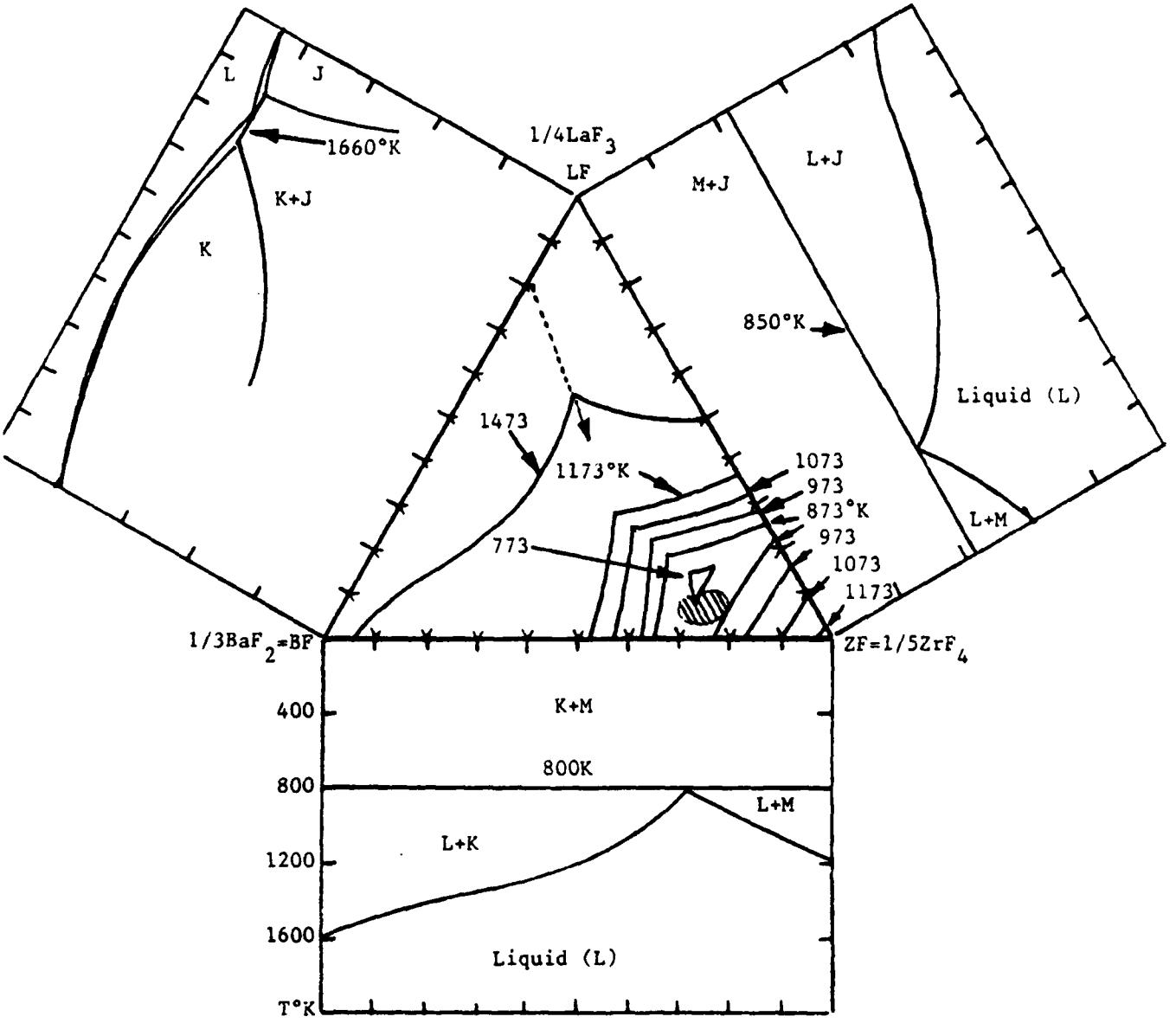

Figure 1. Calculated Edge Binary Systems and Liquidus Projections in the LF-ZF-BF Syster The hatched region in the ternary denotes the glass forming composition range established experimentally by Lecoq and Poulaine (4).

LF=0.25 LaF_3, ZF=0.20 ZrF_4, BF=0.333 BaF_2, AF=0.25 AlF_3

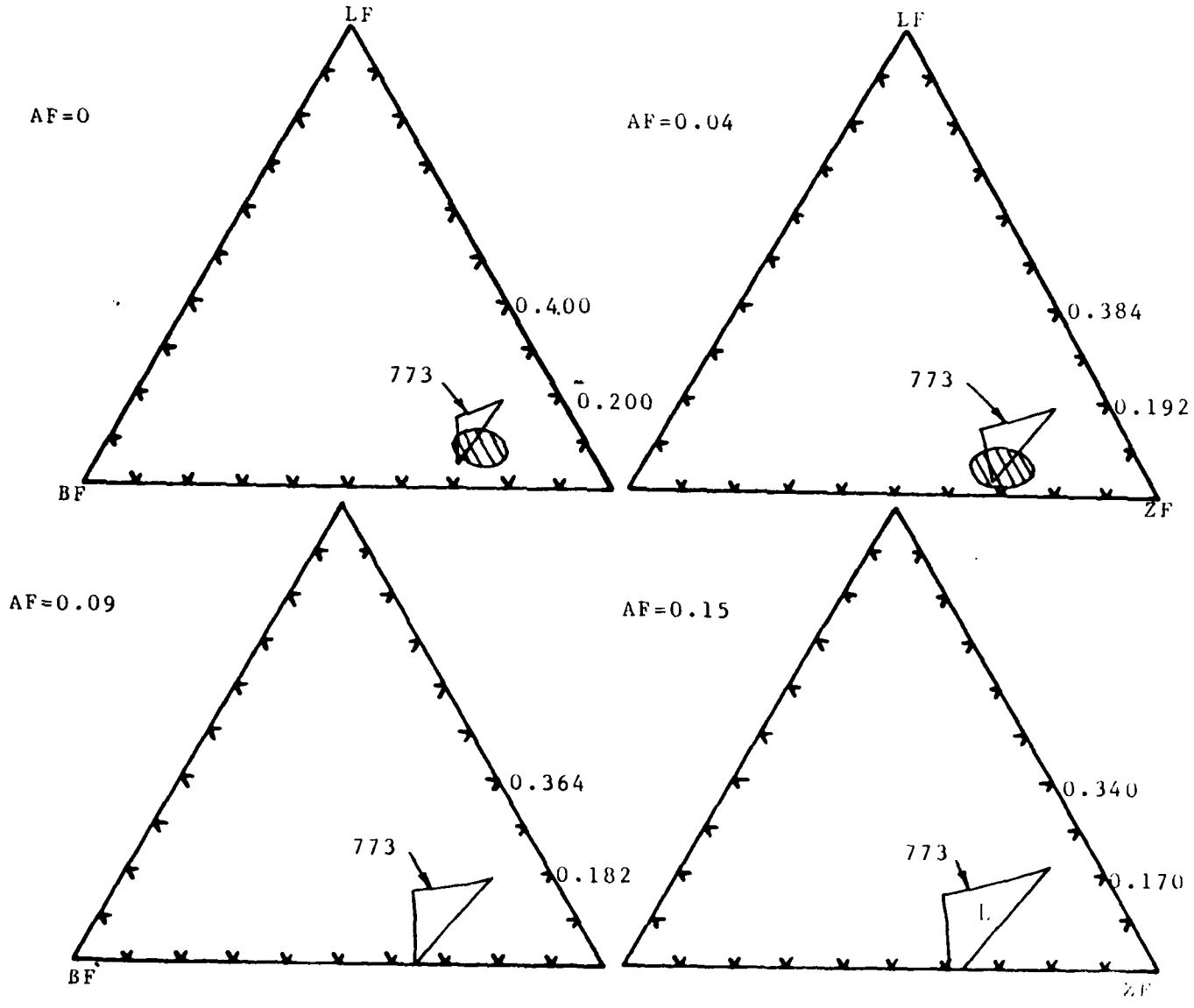

Figure 2 Calculated Range of Liquid Stability at 773°K at different Aluminum Fluoride levels compared with the observed ranges of glass formation (hatched) (9)

OPTICAL PROPERTIES OF FLUOROPHOSPHATE GLASSES

Binod Kumar and R. Harris

University of Dayton, Dayton, Ohio 45469

A study of the optical properties of fluorophosphate glasses was conducted. Glasses for this study were synthesized using analytical grade raw materials which were melted in a platinum crucible at 950°C and then refined at 850°C. Two different types of furnaces were used: (i) A normal atmosphere furnace where no attempt was made to control the melting environment and henceforth referred to as the normal atmosphere melting. (ii) A controlled atmosphere furnace where an Argon atmosphere was maintained during the melting and fining and henceforth referred to as the Argon atmosphere melting. Cast specimens ranging in thickness of 10-15mm were further annealed at 450°C for several hours before optical characterization. The glass compositions which consisted of AlF_3, RF_2 (R = alkaline earth), and P_2O_5 are presented in Table 1. Optical characterization included spectral transmission, temperature coefficient of refractive index and the absorption coefficient at 1.30 μm.

A typical transmission spectra from a specimen 8mm thick and melted under the normal atmosphere is shown in Figure 1. The spectra exhibit U.V. absorption edge, water absorption band and the first overtone of P-O stretching vibration located around 0.3 μm, 3 μm, and 4.80 μm, respectively. The intensity of the 3.0 μm absorption band was used to determine water concentration. For the glasses melted in the normal atmosphere, location of the U.V. absorption edge was related to the water concentration as shown in Figure 2. Also, the absorption coefficient (β_{eff}) at 1.30 μm was related to the water concentration.

The Argon atmosphere melted glasses exhibit greatly enhanced U.V. transmission as shown in Figure 3. It is believed that the Argon atmosphere melting significantly reduces

melt contamination thereby improving the U.V. transparency. All glasses exhibited similar characteristics. The Argon atmosphere melting, in general, reduced the water concentration in glasses but produced an insignificant effect on the visible and I.R. transmission characteristics.

Refractive indices of these glasses are in the range of 1.4421 to 1.4568. All of these glasses have negative temperature coefficient of refractive index and ranges from -0.685×10^{-5} to -1.086×10^{-5}/°C over room temperature to 90°C.

TABLE 1

Fluorophosphate Glass Compositions (wt%)

	FPI	FPII	FPIV	FPV
CaF_2	40	20	20	20
SrF_2	20	20	0	40
BaF_2	0	20	40	0
AlF_3	30	30	30	30
P_2O_3	10	10	10	10

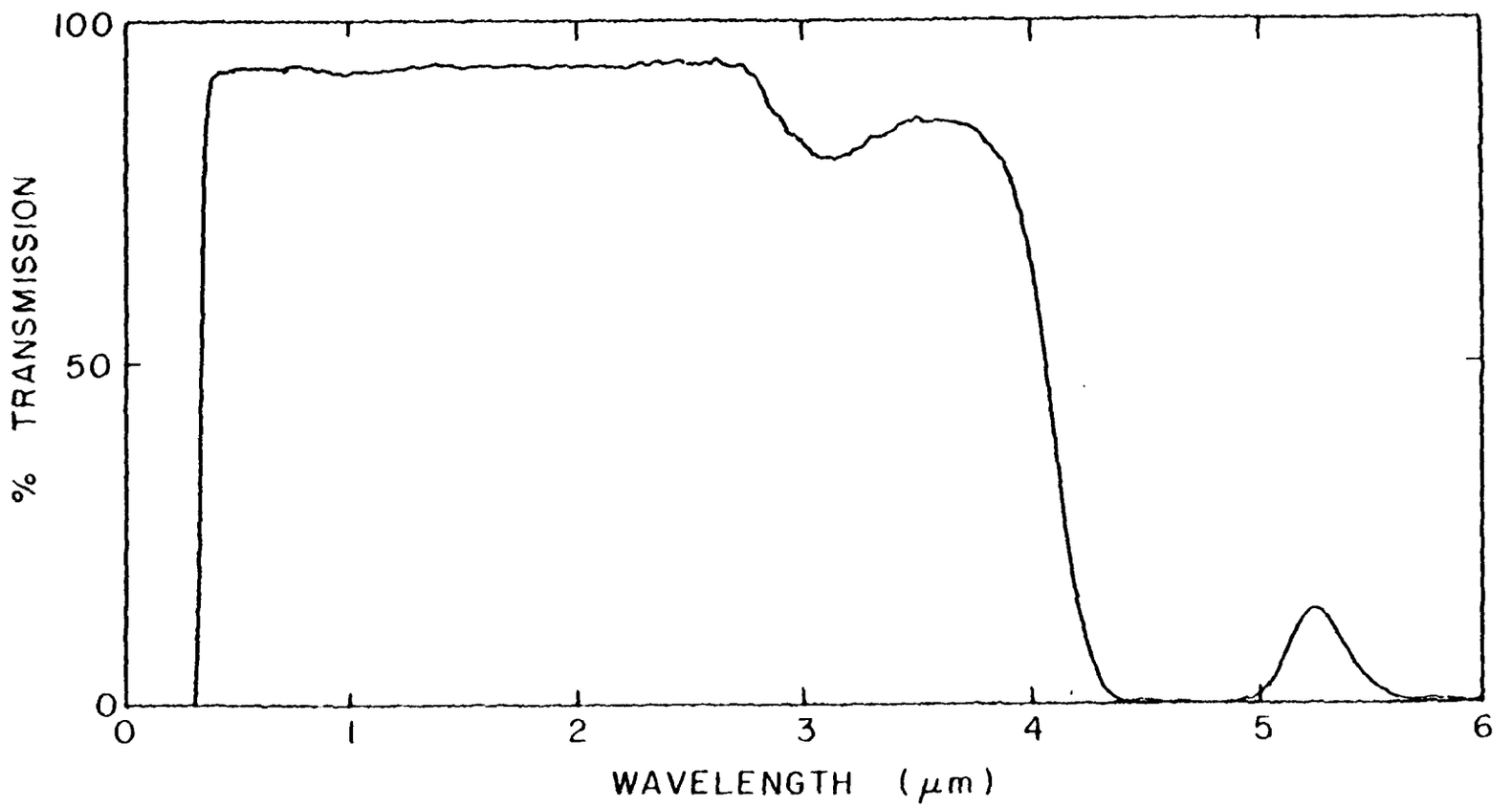

Figure 1. A Typical Transmission Spectrum from a Fluorophosphate Glass (FPV, Specimen Thickness 7.55mm).

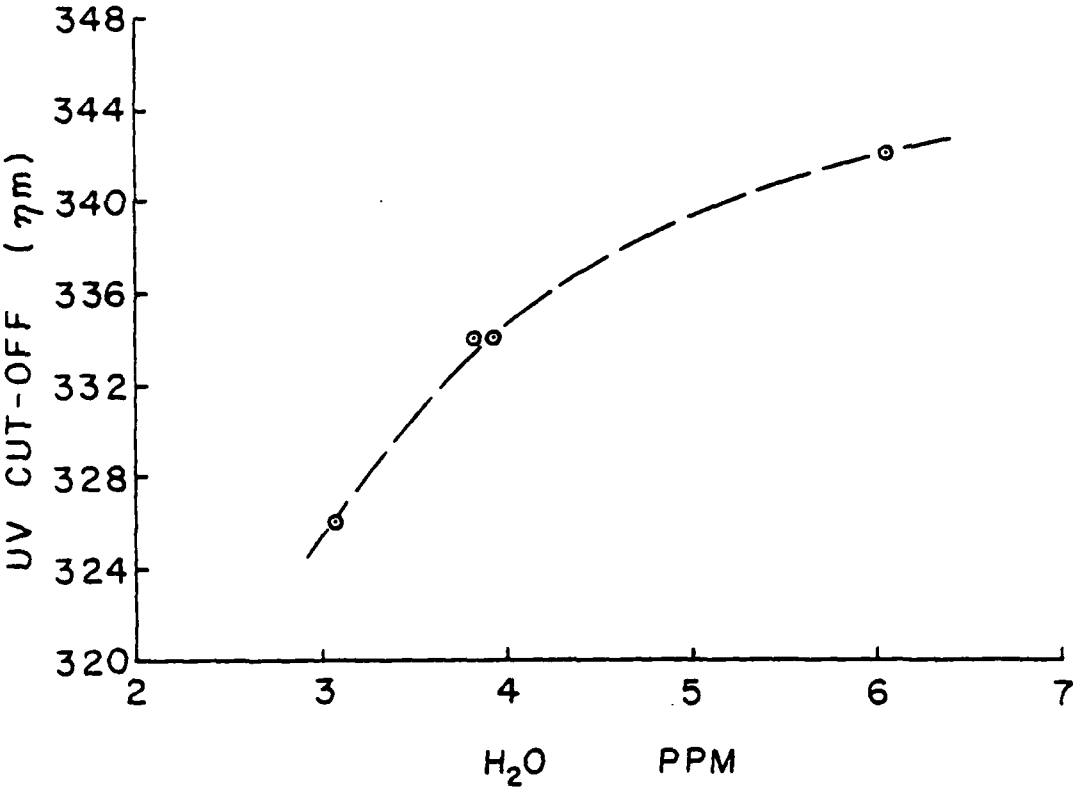

Figure 2. Effect of Water on the U.V. Absorption Edge of Fluorophosphate Glasses.

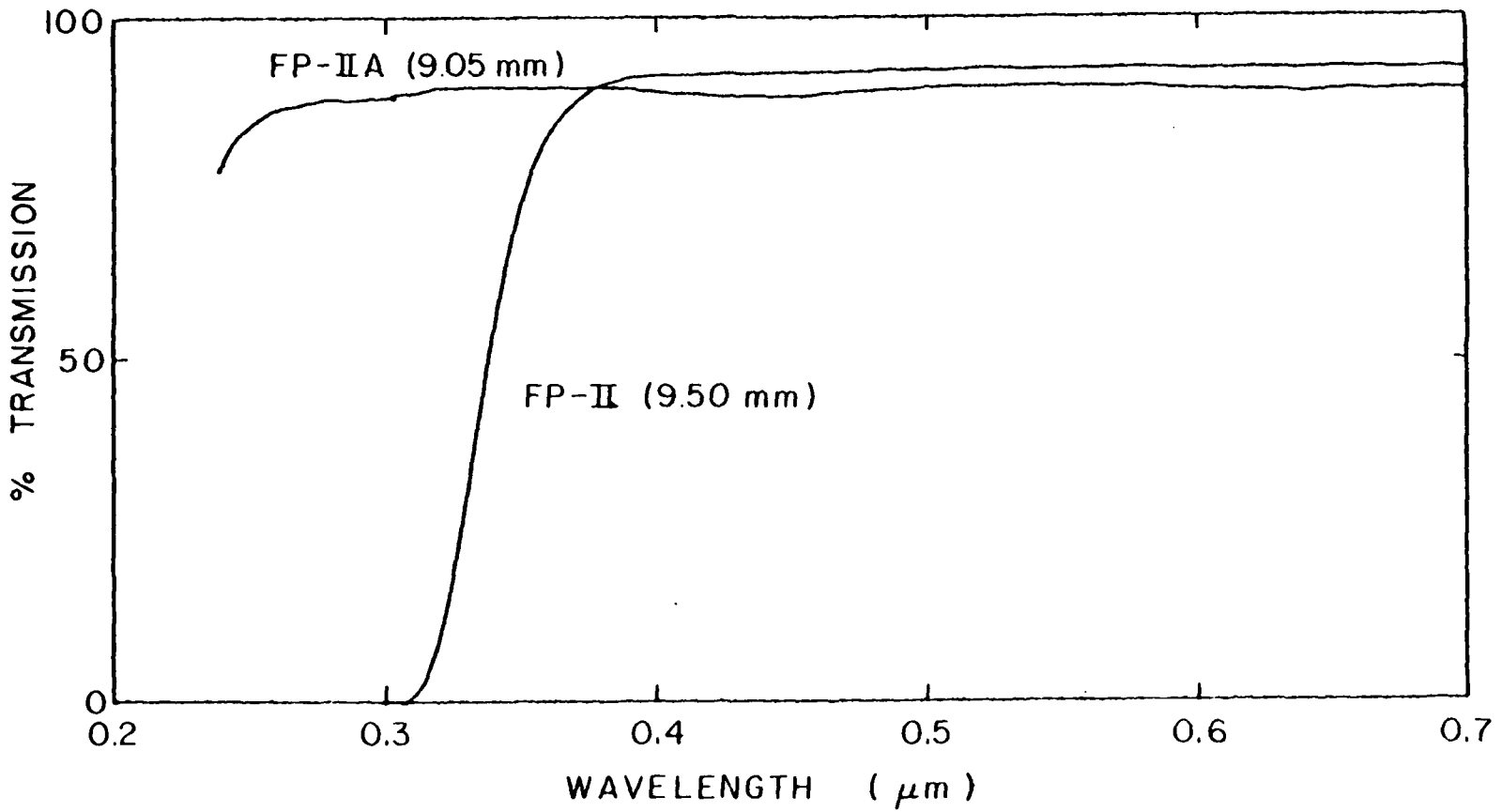

Figure 3. U.V. and Visible Transmission Spectra from Fluorophosphate Glasses Melted Under Normal and Argon Atmospheres.

NUCLEAR REACTION ANALYSIS AND RUTHERFORD BACKSCATTERING SPECTROMETRY STUDIES OF THE REACTION BETWEEN FLUORIDE GLASSES AND WATER+

W.A. Lanford and C. Burman
Department of Physics, SUNY/Albany
Albany, New York 12222

R.H. Doremus
Materials Engineering Department
Rensselaer Polytechnic Institute
Troy, New York 12181

Nuclear reaction analysis (NRA) and Rutherford Backscattering Spectrometry (RBS) have been used to determine the elemental concentration profiles near the surfaces of ZBL (62-33-5) glasses exposed to liquid water and to water vapor. The goal of this study is to quantitatively characterize the durability of this glass under various conditions and to attempt to determine the fundamental mechanisms governing these surface reactions.

Techniques such as NRA and RBS which are based on the study of changes in surface composition are in some cases complementary to and in many cases of more general utility than the more conventional methods of testing glass durability based on analysis of the solution attacking the glass. For example, in the present case, analysis of surface composition and of what goes into solution give complementary views of the reaction of this ZBL glass with liquid water, and either method might give sufficient information to answer a particular question. However, the method based on analysis of the solution can only be applied for relatively simple attacking solutions. Futhermore, it cannot be

applied at all in the technologically important case of the reaction between glass and water vapor. Unlike most silicate glasses, the reaction between this ZBL glass and water is very different depending on whether the water is liquid or vapor.

In this paper, the principles of NRA for measuring hydrogen concentration profiles and RBS for measuring heavy element profiles will be discussed and illustrated by applications to this ZBL glass and to other glasses.

These results along with ancillary x-ray fluorescence, x-ray diffraction and microscopic studies will be discussed in light of our present understanding of the reaction mechanisms. One clear observation is the important role of liquid water in preferentially removing and redepositing particular components of this glass, resulting in the "whitish" coating commonly observed by workers in this field.

One observation which may have technological importance that needs further study is that surfaces of glasses with the same bulk composition have different reaction rates apparently because of different (and unintentional) surface preparations. Such a surface modification may provide a practical means of increasing the effective durability of this glass while preserving its important optical characteristics.

+Research supported by grants from the Office of Naval Research (SUNY/Albany) and the National Science Foundation (R.P.I.)

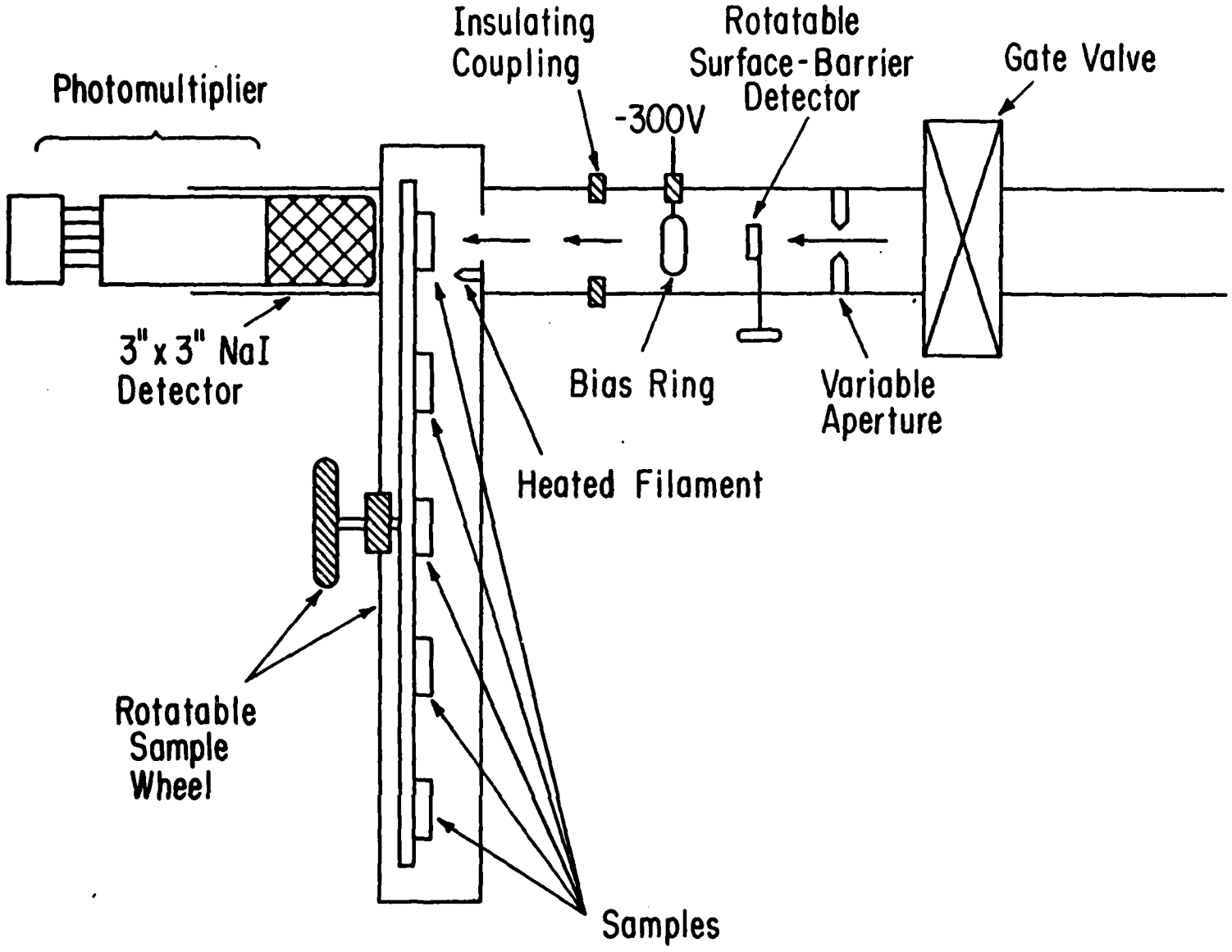
Photomultiplier
Insulating Coupling
-300V
Rotatable Surface-Barrier Detector
Gate Valve
3" x 3" NaI Detector
Bias Ring
Variable Aperture
Heated Filament
Rotatable Sample Wheel
Samples

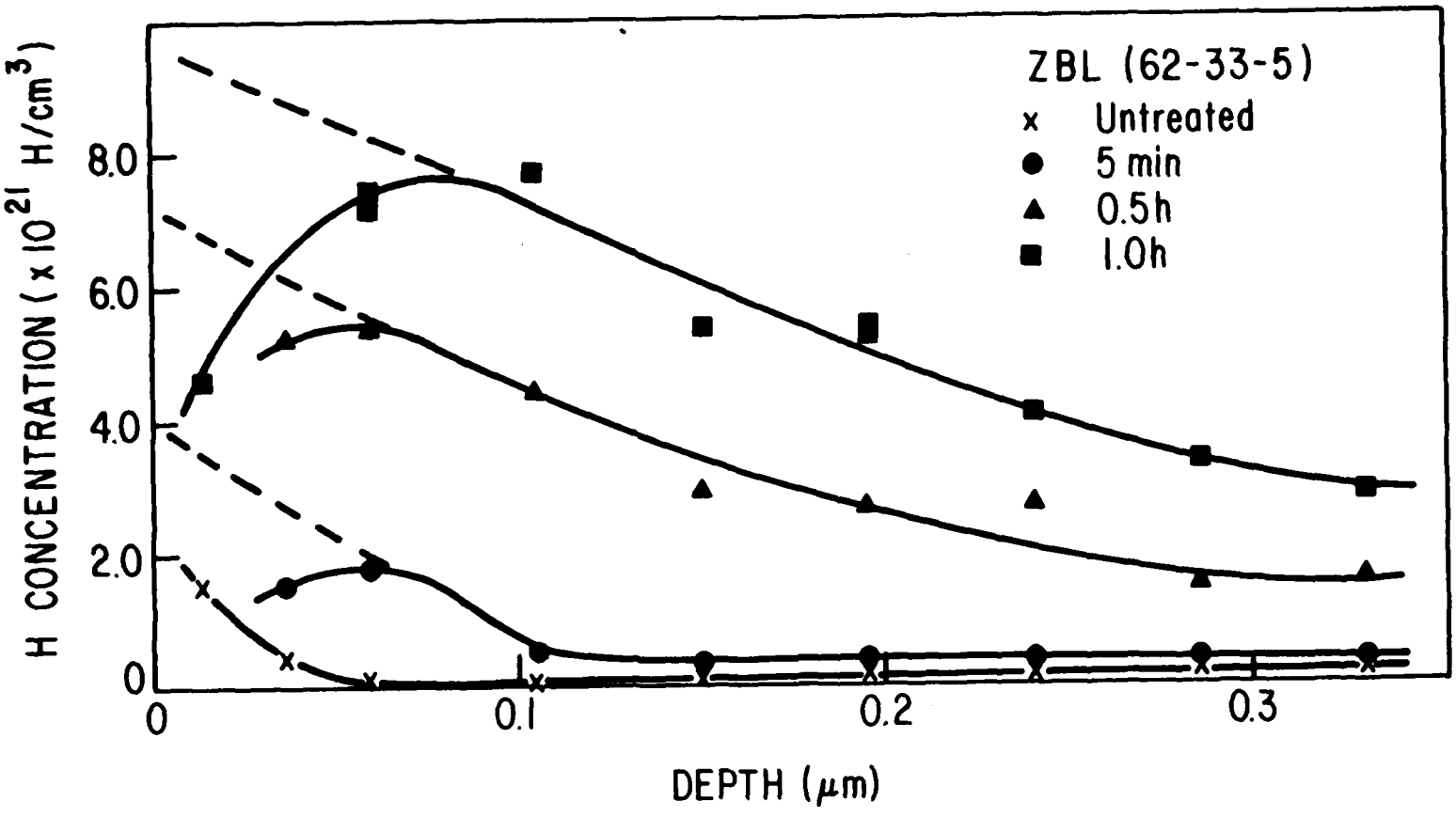
ZBL (62-33-5)
x Untreated
● 5 min
▲ 0.5h
■ 1.0h
H CONCENTRATION (x 10^21 H/cm^3)
8.0
6.0
4.0
2.0
0
0
0.1
0.2
0.3
DEPTH (μm)

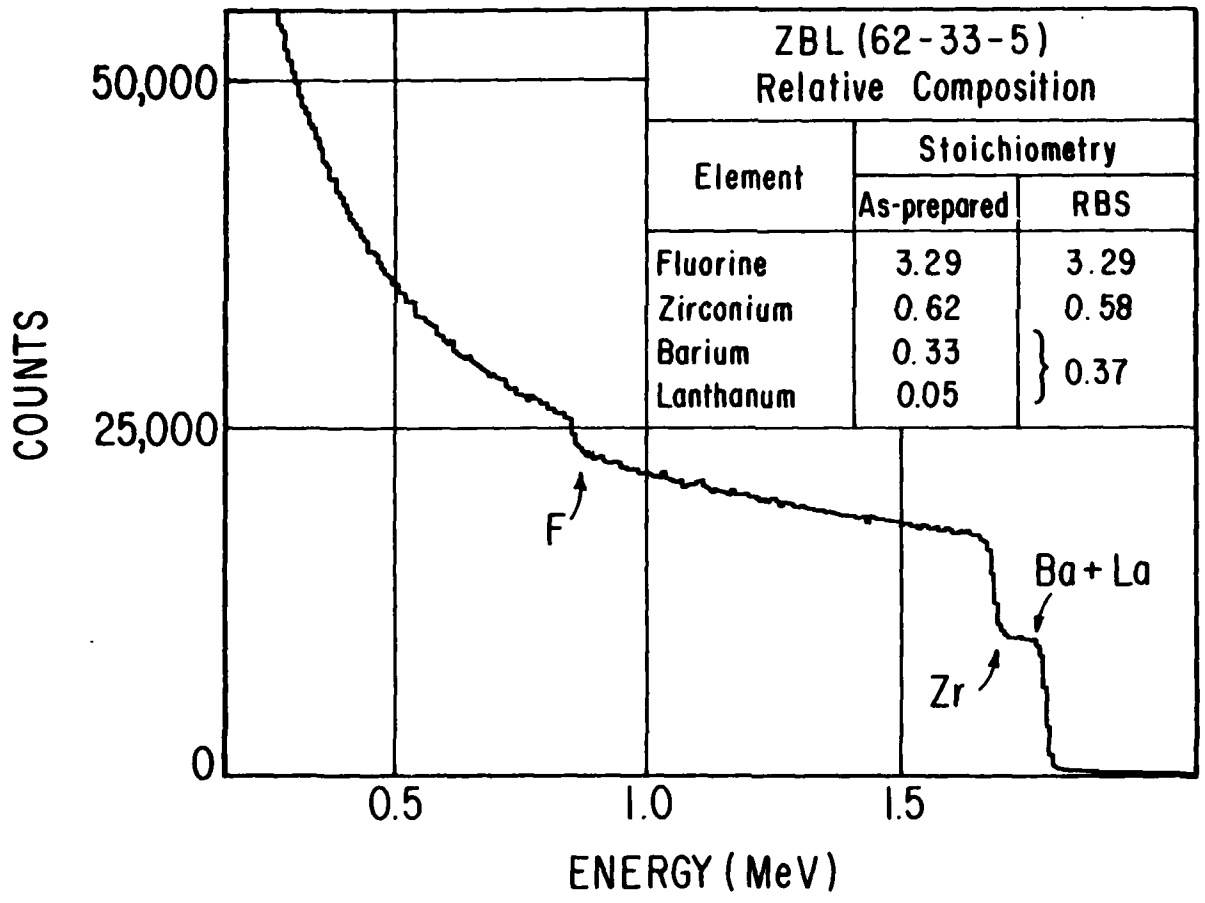
ZBL (62-33-5)
Relative Composition
Element
Stoichiometry
As-prepared
RBS
Fluorine 3.29 3.29
Zirconium 0.62 0.58
Barium 0.33 0.37
Lanthanum 0.05
50,000
25,000
0
COUNTS
F
Ba + La
Zr
0.5
1.0
1.5
ENERGY (MeV)

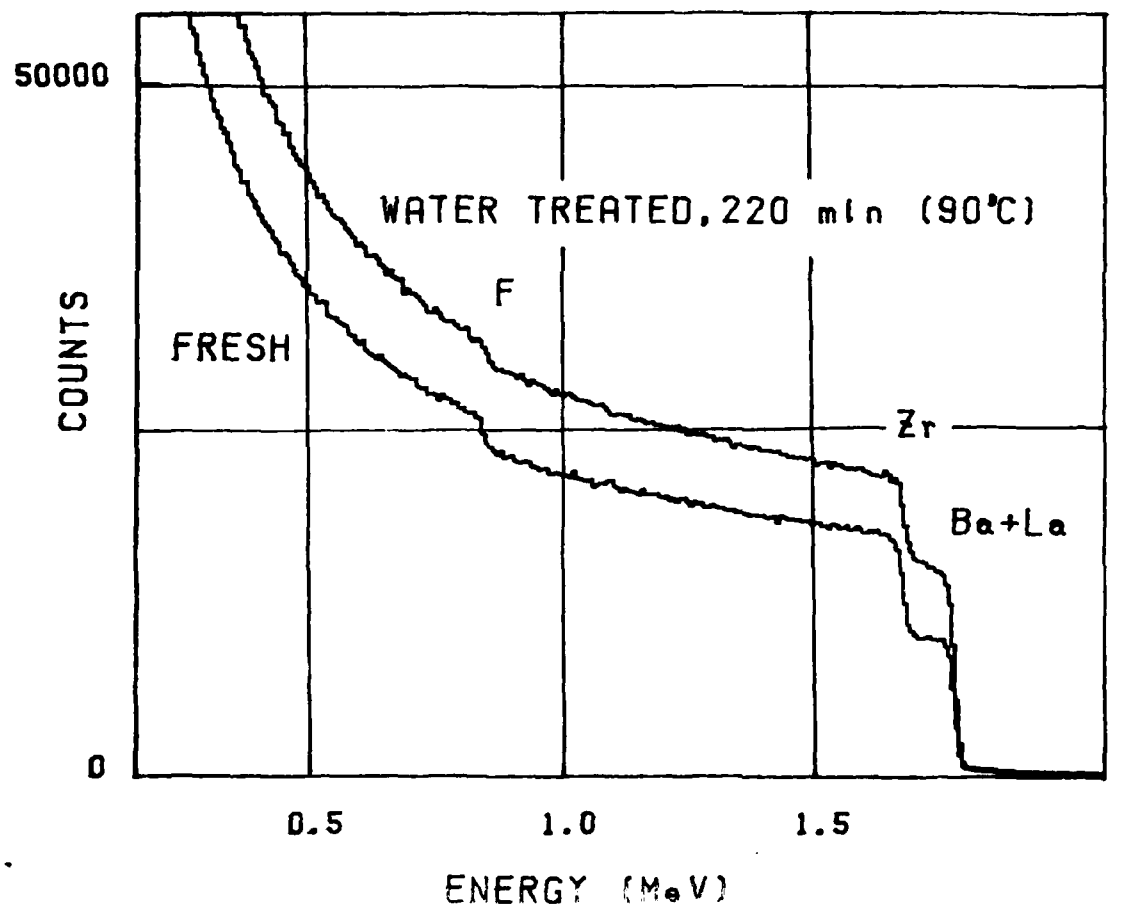
50000
0
COUNTS
WATER TREATED, 220 min (90°C)
F
FRESH
Zr
Ba+La
0.5
1.0
1.5
ENERGY (MeV)

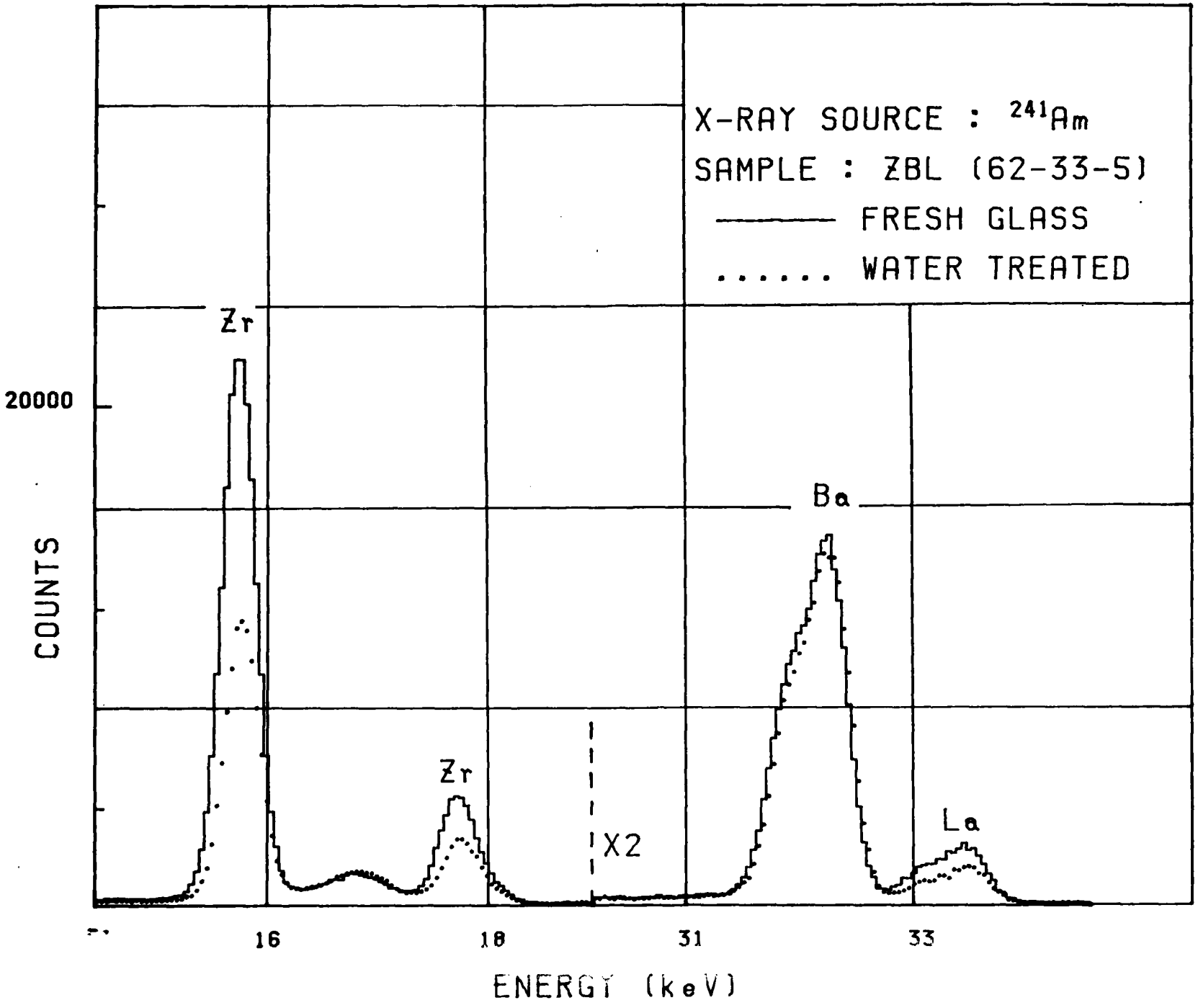
X-RAY SOURCE : ^{241}Am
SAMPLE : ZBL (62-33-5)
——— FRESH GLASS
..... WATER TREATED
Zr
Zr
Ba
La
X2
20000
COUNTS
16
18
31
33
ENERGY (keV)

SCATTERING LOSS CONTRIBUTIONS IN FLUORIDE GLASS FIBERS

K. H. Levin*, D. C. Tran and G. H. Sigel, Jr.
Naval Research Laboratory
Washington, DC 20375

A major obstacle to achieving the theoretically predicted low loss of fluoride glass fibers has been the high scattering loss. We have studied the various sources of scattering in the fibers, and determined the optimum draw conditions for fibers prepared from the ZrF_4-BaF_2-LaF_3-AlF_3-LiF and ZrF_4-BaF_2-LaF_3-AlF_3-LiF-PbF_2 glass systems. One major source of scattering is the growth of microcrystallites due to improper temperature control during fiber drawing. The scattering loss has been measured for a number of fibers having different draw parameters. Slight variations in the optimum drawing temperature have resulted in scattering losses ranging from a few hundred to thousands of dB/km. Other sources of scattering loss include undissolved materials, diameter fluctuations, water impurity, and poor quality starting preforms.

We have used optical microscopy to identify some of the scattering centers in the fibers. The fiber with the lowest loss showed only a few defects each less than 1 micron in diameter. The high loss fibers, on the other hand, showed many defects from 10-20 microns in diameter. These defects were mainly undissolved microcrystallites.

The spectral dependence of the scattering loss was measured for both the high loss and low loss fibers. The scattering losses for the high loss fibers were either wavelength independent or else varied only slightly with wavelength, due to the large size of the scattering centers. The low loss

*Sachs/Freeman Associates, Inc.
Bowie, MD 20715

fiber exhibited a scattering loss which varied as λ^{-4}, typical of Rayleigh scattering. The extrapolated Rayleigh scattering loss for this fiber was .01 dB/km at 4 microns. However, this fiber also showed a wavelength independent offset loss of 5 dB/km. In order to determine the origin of this offset, the scattering loss was measured as a function of mode number. The higher order modes, which propagate mainly along the core-clad interface, showed a much higher scattering loss than the low order modes, which propagate along the center of the fiber core. In addition, when the launch N.A. was increased from .1 to .2, the Rayleigh scattering component remained the same, but the offset increased from 5 to 30 dB/km. These results indicate that the offset is due to defects in the core-clad interface, which are probably from scratches on the mechanically polished preform. The scattering from the fiber core is Rayleigh and of a low value due to the small size of the defects observed.

In summary, the sources of scattering loss were investigated in a variety of fluoride glass fibers, with comparisons made between high and low loss fibers. The results indicate a substantial surface scattering contribution for the lowest loss fluoropolymer clad fiber. We believe that with improved surface preparation, the scattering losses in fluoride glass fibers can be reduced to intrinsic levels with the use of proper glass processing and fiber drawing conditions.

HIGH-ORDER MODE SCATTERING LOSS

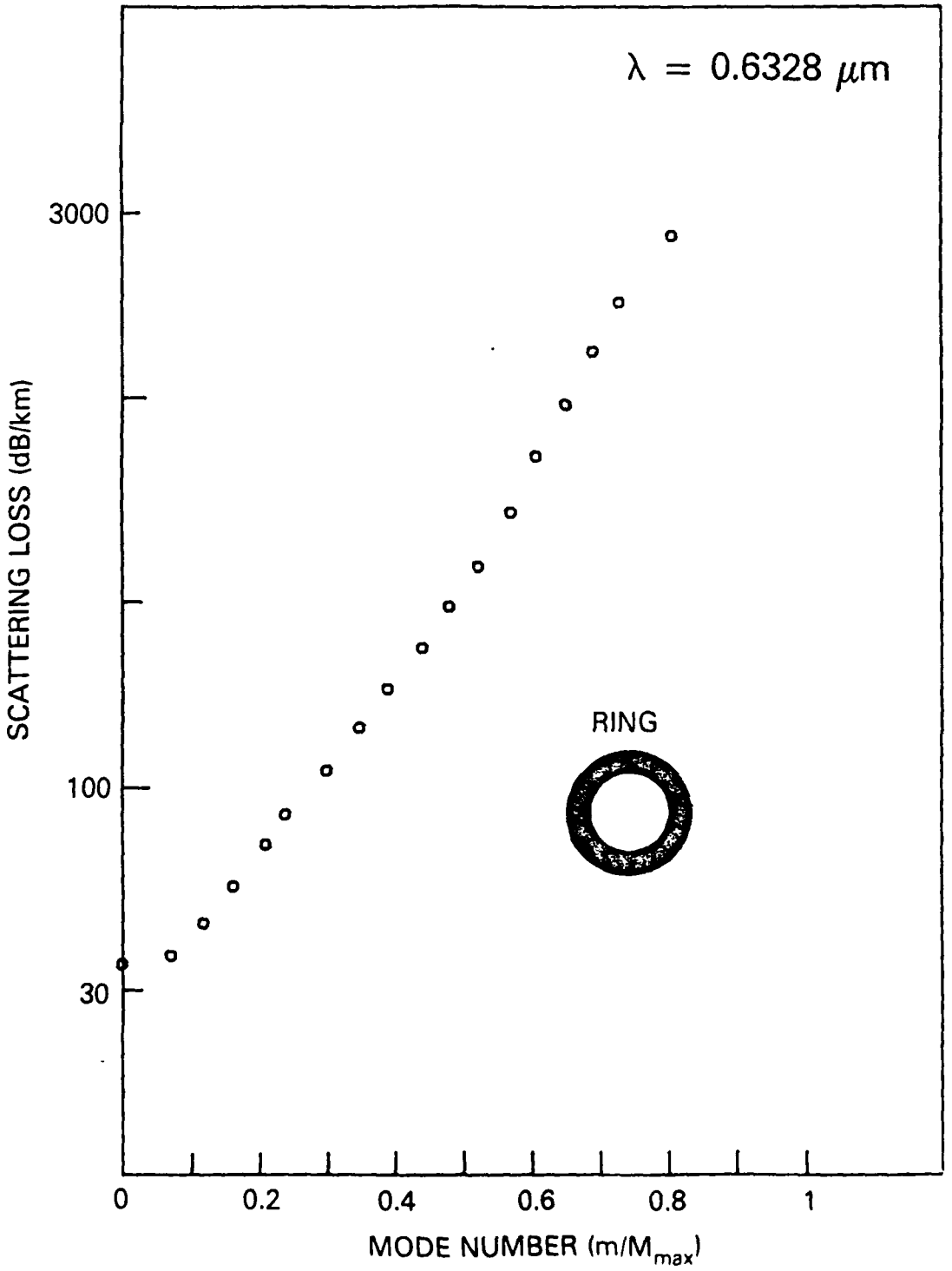

FIBER SCATTERING LOSS vs. DRAW TEMPERATURE

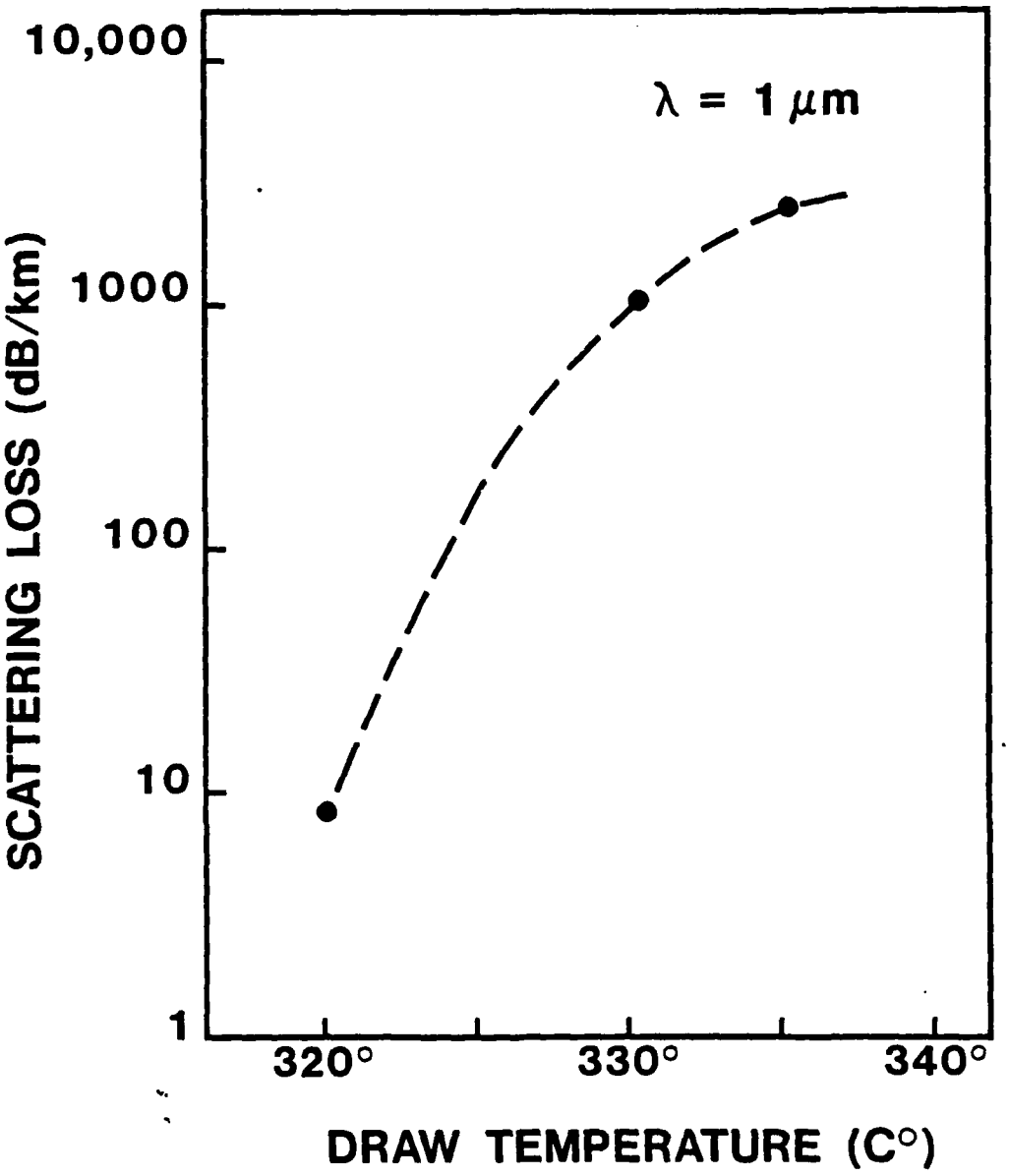

FLOURIDE GLASS FIBER SCATTERING LOSS SPECTRUM

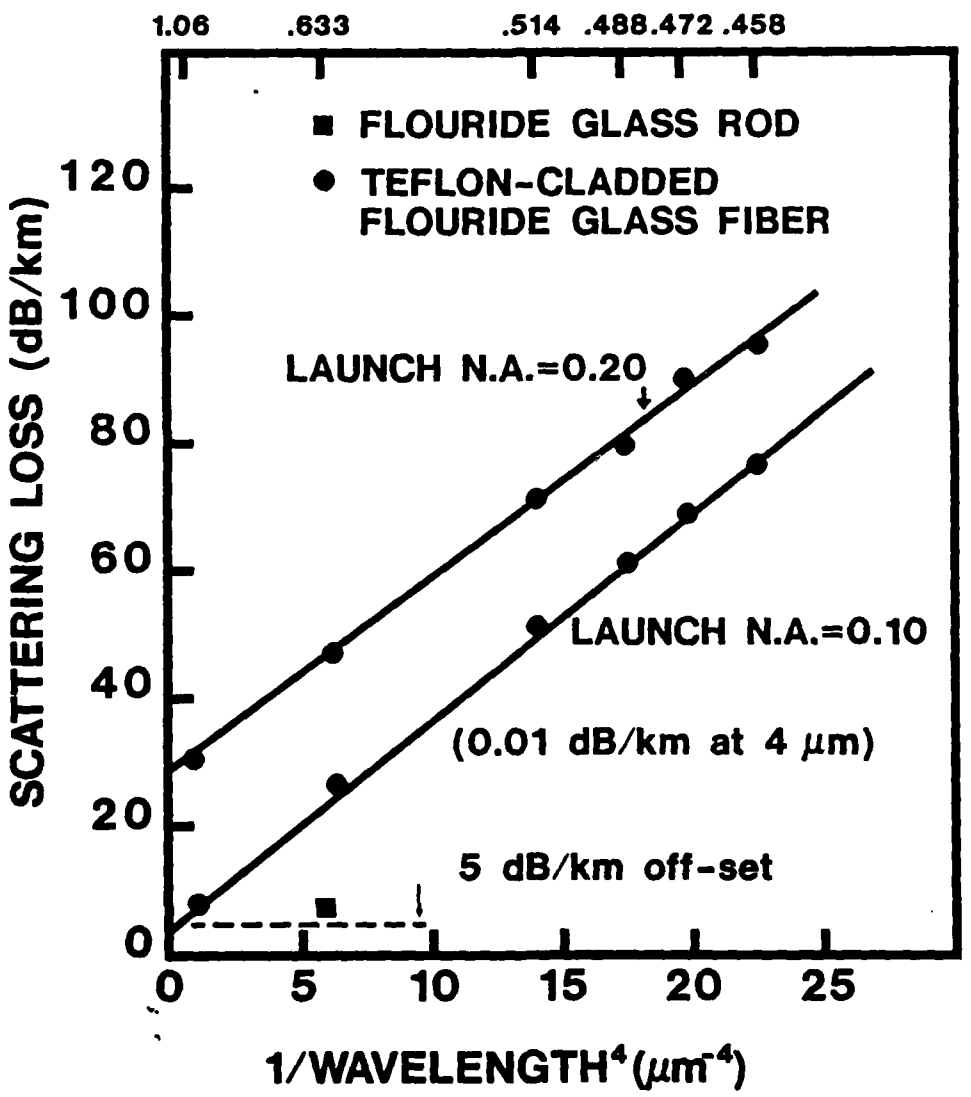

EFFECT OF ALKALI FLUORIDE ADDITIONS ON OPTICAL PROPERTIES OF BaF_2/ThF_2 GLASSES

S. R. Loehr, A. J. Bruce, K.-H. Chung, N. L. Perazzo and C. T. Moynihan
Rensselaer Polytechnic Institute, Troy, New York 12181
USA

and

M. G. Drexhage, RADC, Hanscom AFB, MA 01731
USA

Starting with four compositions of BaF_2-ZnF_2-YbF_3-ThF_4 glass, alkali fluorides (LiF, NaF and KF) were substituted, separately and in mixtures up to 15% mol% at the expense of BaF_2. Fluoride starting materials from Cerac/Pure and Fisher were mixed with an excess of ammonium bifluoride to reduce oxide and hydroxyl impurities. The glasses were prepared in vitreous carbon crucibles and taken to approximately 1250K to insure complete melting. Reactive atmosphere processing (RAP) of 3.5% Cl_2/N_2 was used during the latter stages of fusion to further reduce hydroxyl and oxide impurities. The glasses were quenched between copper plates and annealed near their glass transition temperatures. Glass samples from a fraction of a millimeter to several millimeters thick were obtained; the thickness was dependent upon the glass forming ability of the particular composition.

Samples were polished using silicon carbide paper (180 to 600 grit) and lapping oil to obtain smooth, parallel faces for infrared spectroscopy. A final polish was made with 5 micron alumina powder in water or ethylene glycol. The samples were ultrasonically cleaned in methanol and hexane to minimize surface contaiminants. Spectra were obtained on a Perkin Elmer 983 infrared spectrophotometer (Figure 1) and absorption coefficients α were calculated by using Beer's Law.

A semi-logarithmic plot of α vs. $\bar{\nu}$ for 19 BaF_2-27 ZnF_2-27 YbF_3-27 ThF_4 base glass, as well as plots for those substituted with varying types and amounts of alkali fluorides are shown in Figure 2. The addition of LiF shifts the

multiphonon edge to higher frequencies, while the addition of NaF or KF has little effect on the absorption edge. This is consistent with the previously published, semi-empirical rules of Moynihan et al. for multicomponent ZrF_4- and HfF_4-containing glasses which states that monovalent cation fluorides no lighter than NaF contribute negligibly to the IR edge absorption.

Glass transition and crystallization temperatures, T_g and T_x (cf. Fig. 3), were measured on a Perkin Elmer DSC-4 differential scanning calorimeter at a 10K/min heating rate. These values are listed in Table 1 for a typical base glass and its alkali fluoride substituted variants. The difference, T_x-T_g, is a rough measure of the glass forming ability, i.e., of resistance to devitrification. The (T_x-T_g) values in Table 1 indicate that replacement of 5 mol% BaF_2 by 5 mol% NaF or NaF/LiF slightly improves the glass forming ability of the base glass, while 5 mol% KF reduces it markedly. Figures 4A and 4B show plots of (T_x-T_g) vs. alkali fluoride content for the four base compositions studied here as well as for the corresponding alkali fluoride substituted compositions. The 19 BaF_2-27 ZnF_2-27 YbF_3-27 ThF_4 and 15 BaF_2-28.33 ZnF_2-28.33 YbF_3-28.33 ThF_4 compositions appear to be the most stable glasses on the basis of the (T_x-T_g) values. On the other hand, the 25 BaF_2-25 ZnF_2-25 YbF_3-25 ThF_4 glass is a poor glass former and improvements in glass forming ability result from addition of any alkali fluoride.

In general the addition of NaF or LiF gives slight improvements in the glass forming ability, while the addition of KF increases the tendency of the glass to devitrify.

Overall, NaF containing glasses appear to be the best choice for alkali substituted BaF_2-ZnF_2-YbF_3-ThF_4 glasses. NaF contributes negligibly to the multiphonon absorption edge and somewhat enhances glass forming ability.

Acknowledgement:

Research supported by Rome Air Development Center under Contract No. F19628-83-C-0016.

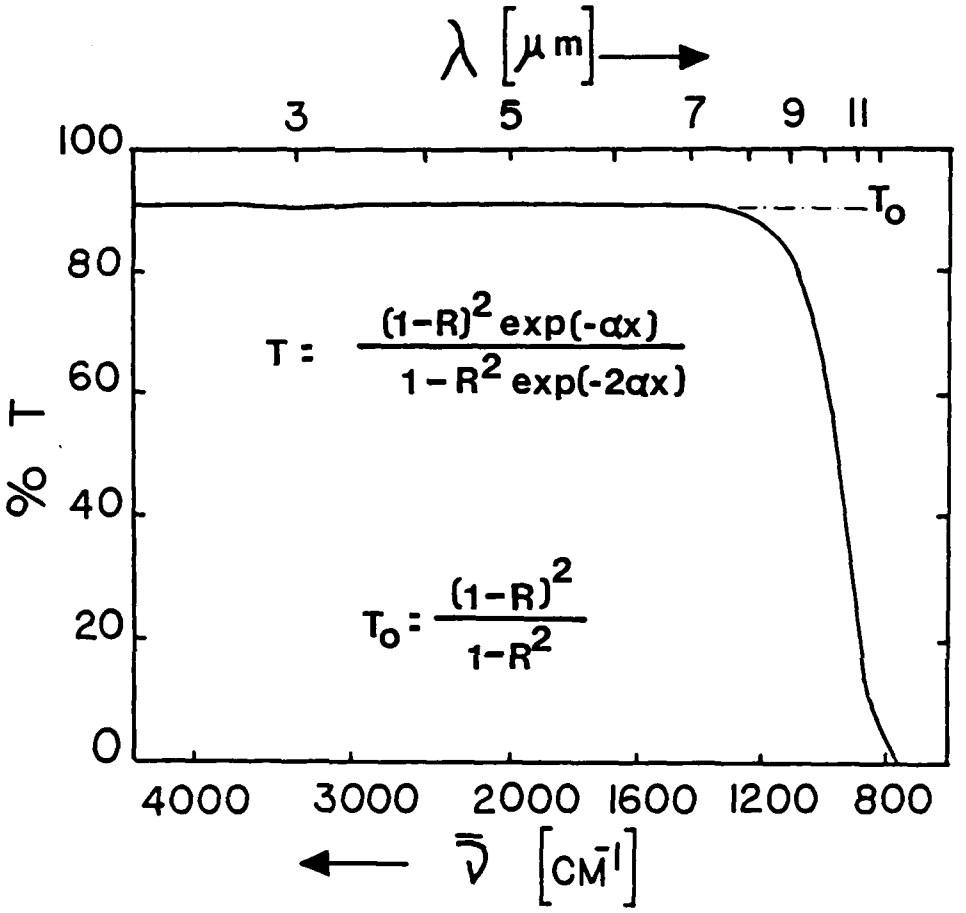

Figure 1 IR spectrum of $20BaF_2$-$25ZnF_2$-$25YbF_3$-$25ThF_4$-5NaF glass

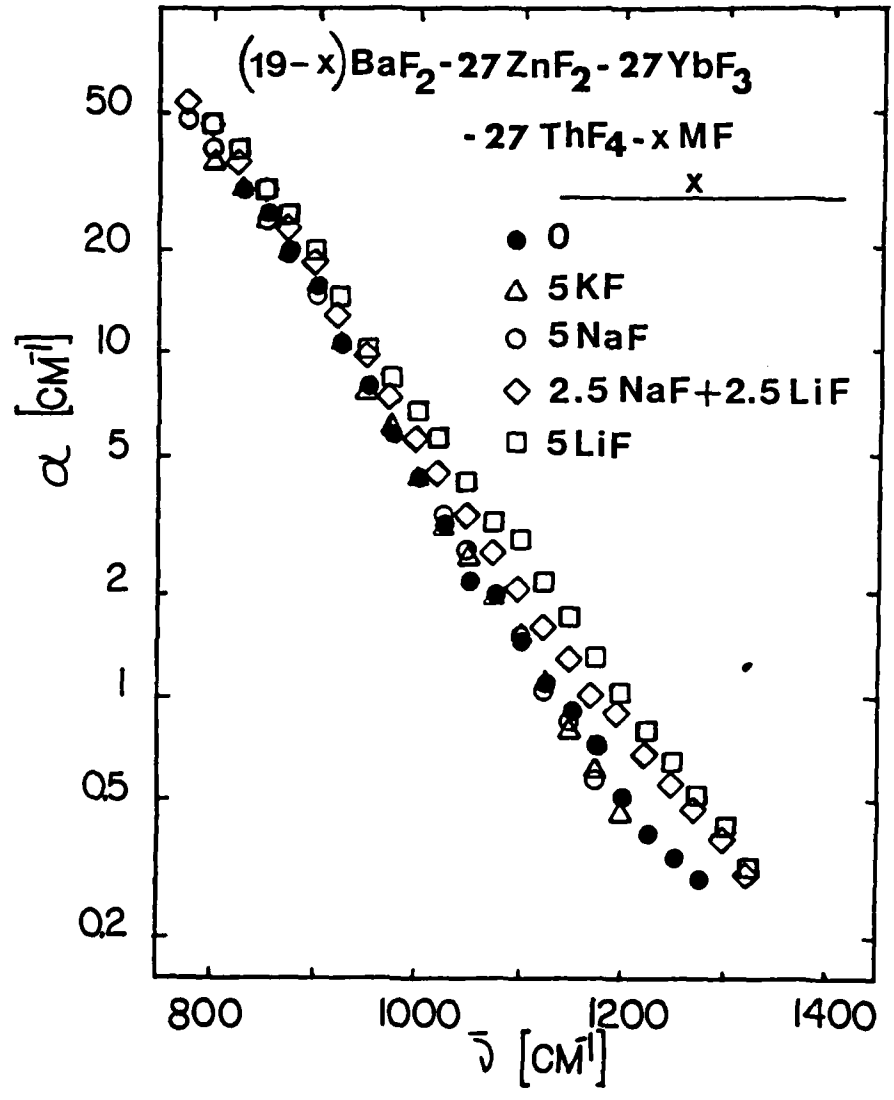

Figure 2 Absorption coefficient vs. frequency for alkali substitution in $19BaF_2$-$27ZnF_2$-$27YbF_3$-$27ThF_4$ glass

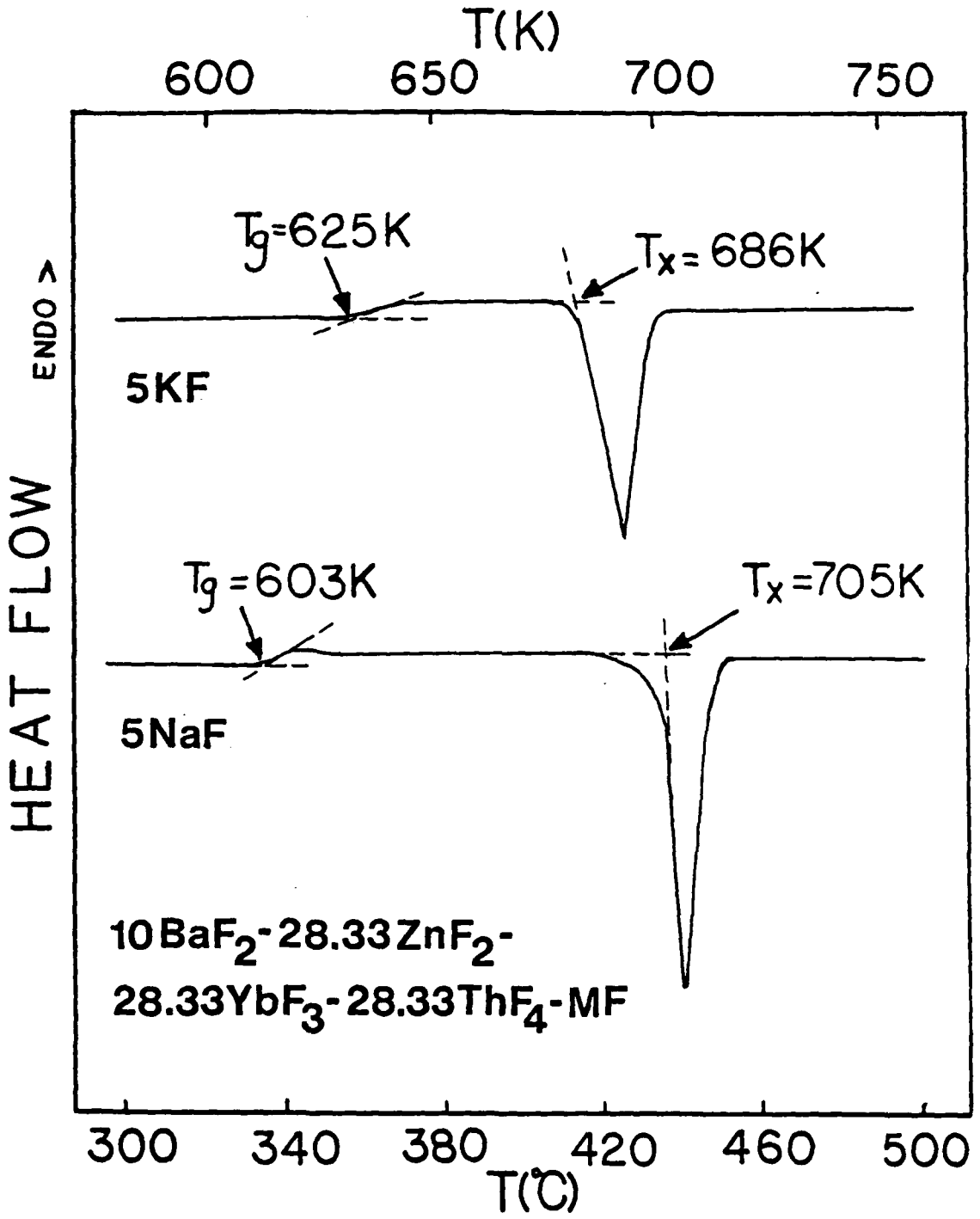

Figure 3 DSC traces for KF and NaF substitutions in 15BaF_2-28.33ZnF_2-28.33YbF_3-28.33ThF_4 glass, 10K/min scan rate

Sample #	Composition (mol%)					T_g	T_x	T_x-T_g (K)
	BaF_2	ZnF_2	YbF_3	ThF_4	MF			
6-4-83	19	27	27	27		622	719	97
24-3-82	14	27	27	27	5 LiF	601	699	98
1-4-82	14	27	27	27	2.5 LiF 2.5 NaF	602	708	106
4-3-82	14	27	27	27	5 NaF	613	717	104
1-6-83	14	27	27	27	5 KF	631	682	51
29-4-83	14	27	27	27	5 FLiNaK*	607	700	93
9-3-82	9	27	27	27	10 NaF	603	694	91

* 46.5 LiF-11.5 NaF-42 KF

Table 1 T_g, T_x, and T_x-T_g for alkali fluoride substitution in $19BaF_2$-$27ZnF_2$-$27YbF_3$-$27ThF_4$ glass

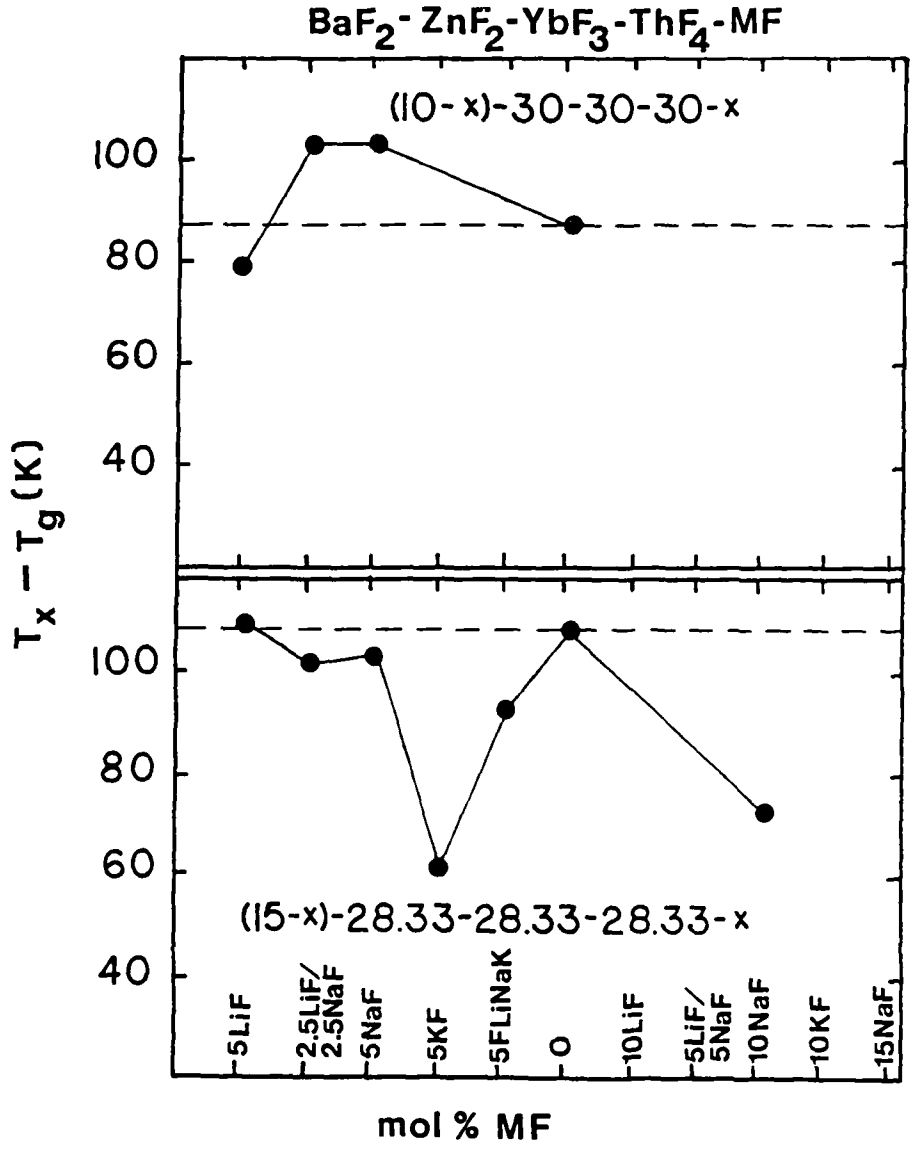

Figure 4A Effect of alkali fluoride substitutions on T_x-T_g for BaF_2-ZnF_2-YbF_3-ThF_4 glasses 10-30-30-30 and 15-28.33-28.33-28.33 mol%

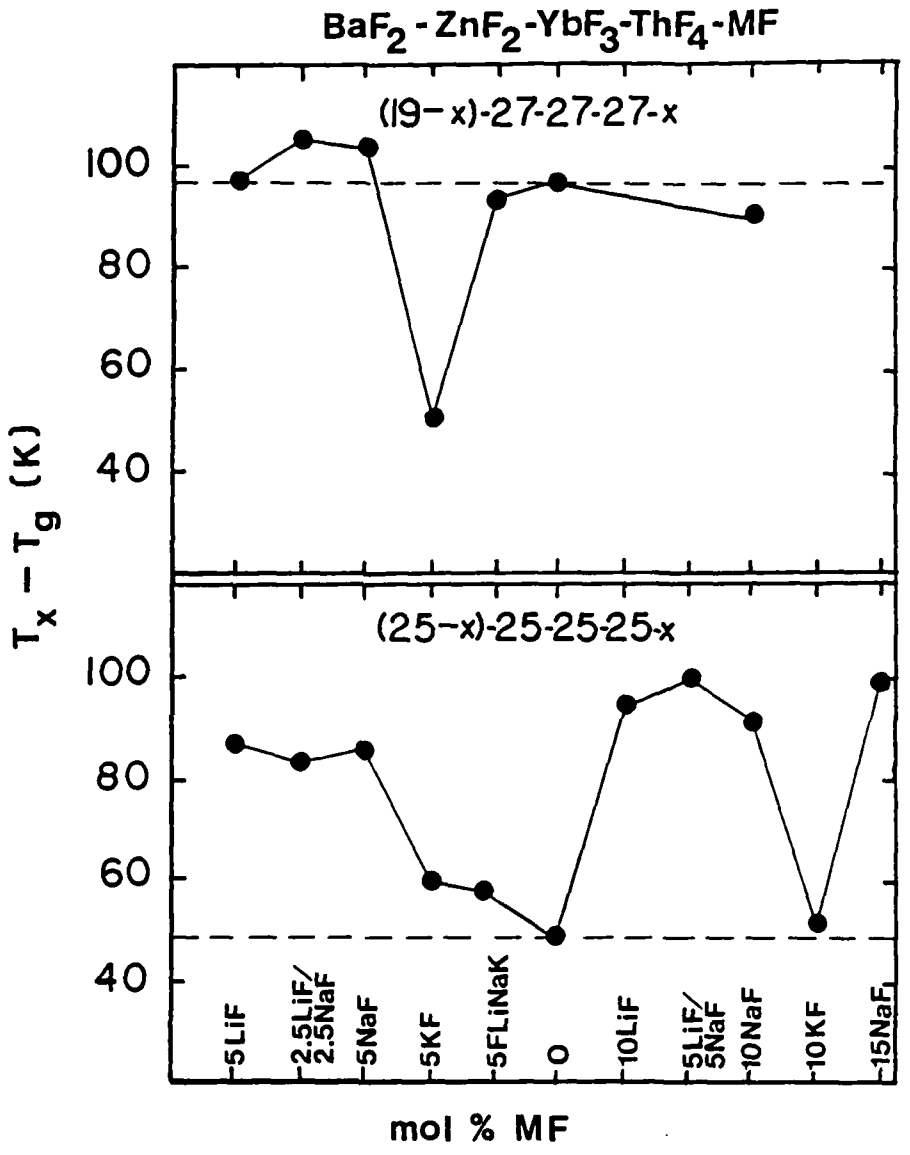

Figure 4B Effect of alkali fluoride substitutions on T_x-T_g for BaF_2-ZnF_2-YbF_3-ThF_4 glasses 19-27-27-27 and 25-25-25-25 mol%

CHARACTERIZATION OF CRYSTALS IN FLUOROZIRCONATE GLASSES

G. Lu, C. F. Fisher, M. J. Burk and D. C. Tran
Naval Research Laboratory
Washington, D.C. 20375

Extrinsic scattering due to the formation of crystallites is one of the factors which has prevented the theoretically predicted minimum loss from being attained in fluoride optical fibers. It is important to characterize these crystallites so that the processing parameters can be modified to avoid devitrification. For optical fiber research, it is more important to identify the first crystals which appear in the glass, rather than to simply characterize the final crystallization products in a mostly or totally crystallized sample. Even extemely low levels of crystallization such as $V_c < 10^{-10}$, where V_c is the volume fraction crystallized, cannot be tolerated in ultra-low loss optical fibers.

In this study, the degree of crystallization of the ZrF_4-BaF-LiF-AlF_3-LaF_3 glass composition ranged from $V_c \simeq 10^{-6}$ to less than 10^{-10}. The crystallites were analyzed by optical microscopy, micro X-ray diffraction, and SEM. Optical microscopy with transmitted polarized light was found to be the most useful technique for rapid characterization of the degree of crystallization and identification of the crystal habit. The electron image mode from the SEM was not found to be useful for such a low degree of crystallization. Without careful preparation, there was virtually no chance that a crystal could be found on the surface of the sample.

The analysis of fluorescent X-rays from the SEM was also found to be of limited value since lithium could not be detected, the lanthanum peaks were usually masked by the barium peaks, and the aluminum peak was partially masked by the large zirconium peak. Micro X-ray diffraction was found to be the most useful technique for identifying the crystalline phase. Particles as small as a few microns could be analyzed in a specially prepared X-ray diffractometer.

Many different crystallization products were observed to form from the same glass composition, depending on the processing conditions. Several of the common ones were analyzed in more detail. The cubic particle in Figure 1 was identified by micro X-ray diffraction as AlF_3, while the hexagonal platelet in Figure 2 was identified as LaF_3. The results are also consistent with SEM/EDAX analyses on isolated crystals and with birefringences reported in the literature.

Although many different crystals were observed over the course of the investigation, there were usually only one or two morphologies present in a given sample. These well-formed crystals grew during quenching and were not undissolved batch. Such monitoring of the crystallization products can show whether the high-temperature melting process has been sufficient to dissolve all crystals and whether the quenching rate is sufficiently high to prevent significant recrystallization.

The scattering coefficient of these crystals was calculated for a wavelength of 4 microns. It was assumed that the crystals were

spherical in shape. For relative refractive indices of m = 0.9 or m = 1.1, it was found that the scattering coefficient increased as r^2 (where r is the radius) over the range of particle sizes r = 0.5 microns to r = 5 microns. For small particles, the scattering coefficient was relatively independent of refractive index. For larger particles, the scattering coefficient increased dramatically when $m < 0.9$ or $m > 1.1$.

This study has found optical microscopy to be the most powerful tool in characterizing the state of crystallization of a glass suitable for optical fibers. With this knowledge of the crystallite size, number and morphology, the processing conditions can be modified to minimize crystallization.

Figure 1 Cubic crystal identified as AlF_3

Figure 2 Hexagonal platelet identified as LaF_3

ThF_4 BASED GLASSES : IMPROVEMENT OF VISCOSITY AND CHEMICAL PURITY BY REACTIVE ATMOSPHERE PROCESSING AND THE ADDITION OF DOPING FLUORIDES

J. Lucas, D. Tregoat, A. El Houari, G. Fonteneau

Laboratoire de Chimie Minérale, Université de Rennes,
Campus de Beaulieu, Avenue du Général Leclerc, 35042 Rennes Cédex
(France)

Hydroxyl groups and oxide impurities in heavy metal / ThF_4/BaF_2 fluoride glasses exhibit absorption bands in the mid I.R. region near 2.9 µm (OH^-) and in the 8-9 µm region (M-O bond). Reactive atmosphere processing (R.A.P.), which has been proved by ROBINSON to be efficient for fluorozirconate glasses, has been extended to purify ThF_4-BaF_2 glasses. These materials, which have a large optical window 0,2 → 8 µm, show a great tendency to devitrification so that fast quenching is required. The transformation of oxide in sulfide has been successfully obtained in using carbon disulfide CS_2 as gas phase reactant. The study of the reaction on different samples, with the optimized composition $Ba_{15}Th_{28,3}Yb_{28,3}Zn_{28,3}$ is described in the present study.

Glass melts, contained in a vitreous carbon crucible have been submitted, in a closed silica apparatus, to CS_2 atmosphere by bubbling N_2 gas in liquid CS_2. Fast quenching is obtained in diving the silica container in liquid air and using a large flow of helium previously cooled. Homogen vitreous samples are thus obtained as discs of 4 cm diameter and 2-8 mm thick. The OH^- bands are completly removed and the I.R. edge is shifted to higher wavelengths.

Total oxygen content has been measured by tritium activation method. Before RAP, for a sample prepared in an open air crucible, using the oxide-ammonium fluoride preparation technic, the O content is 1000 ppm. After a 30 minutes RAP treatment, it decreases to 200 ppm.

To improve the synthesis and handling of ThF_4 glasses some doping effects have been investigated. Although beneficial for glass formation, the addition of aluminium has a deleterious effect on the I.R. transparency range by the formation of a strong Al-F bond. Replacement of Al^{3+} by isoelectronic but heavier In^{3+} has a good effect on the preparation condition without modifying the I.R. edge. The adding of indium decreases the T_G, increases slightly cristallisations T_C and specially decreases the melting temperature. Thus yttrium containing glasses which are more difficult to elaborate than ytterbium materials can be stabilized and samples of several centimeters in diameter and 5-6 mm thick have been prepared.

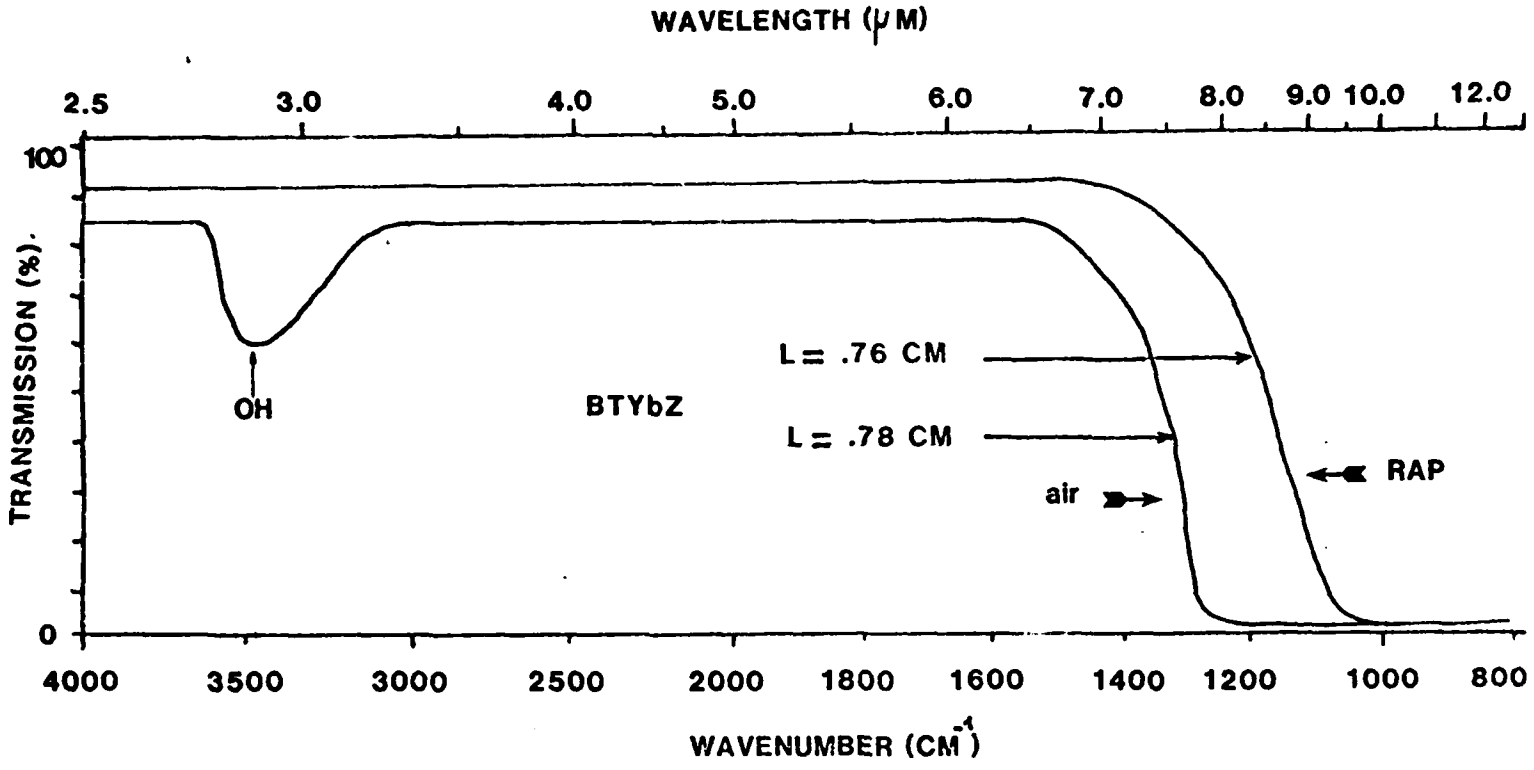
WAVELENGTH (μM)
2.5
3.0
4.0
5.0
6.0
7.0
8.0
9.0
10.0
12.0
100
0
TRANSMISSION (%)
OH
BTYbZ
L = .76 CM
L = .78 CM
air
RAP
4000
3500
3000
2500
2000
1800
1600
1400
1200
1000
800
WAVENUMBER (CM-1)

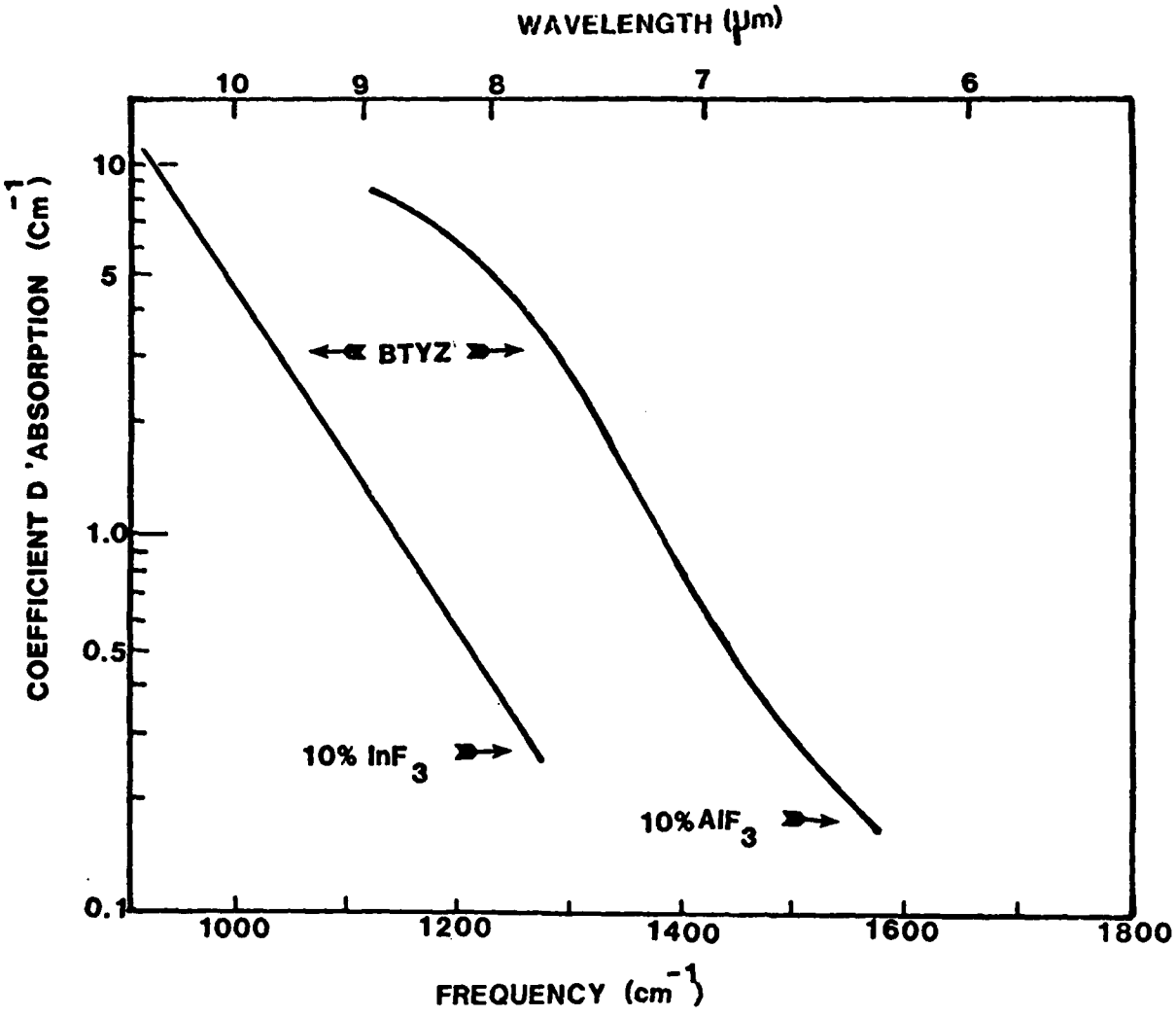
WAVELENGTH (μm)
10
9
8
7
6
COEFFICIENT D 'ABSORPTION (Cm-1)
10
5
1.0
0.5
0.1
BTYZ
10% InF3
10% AlF3
1000
1200
1400
1600
1800
FREQUENCY (cm-1)

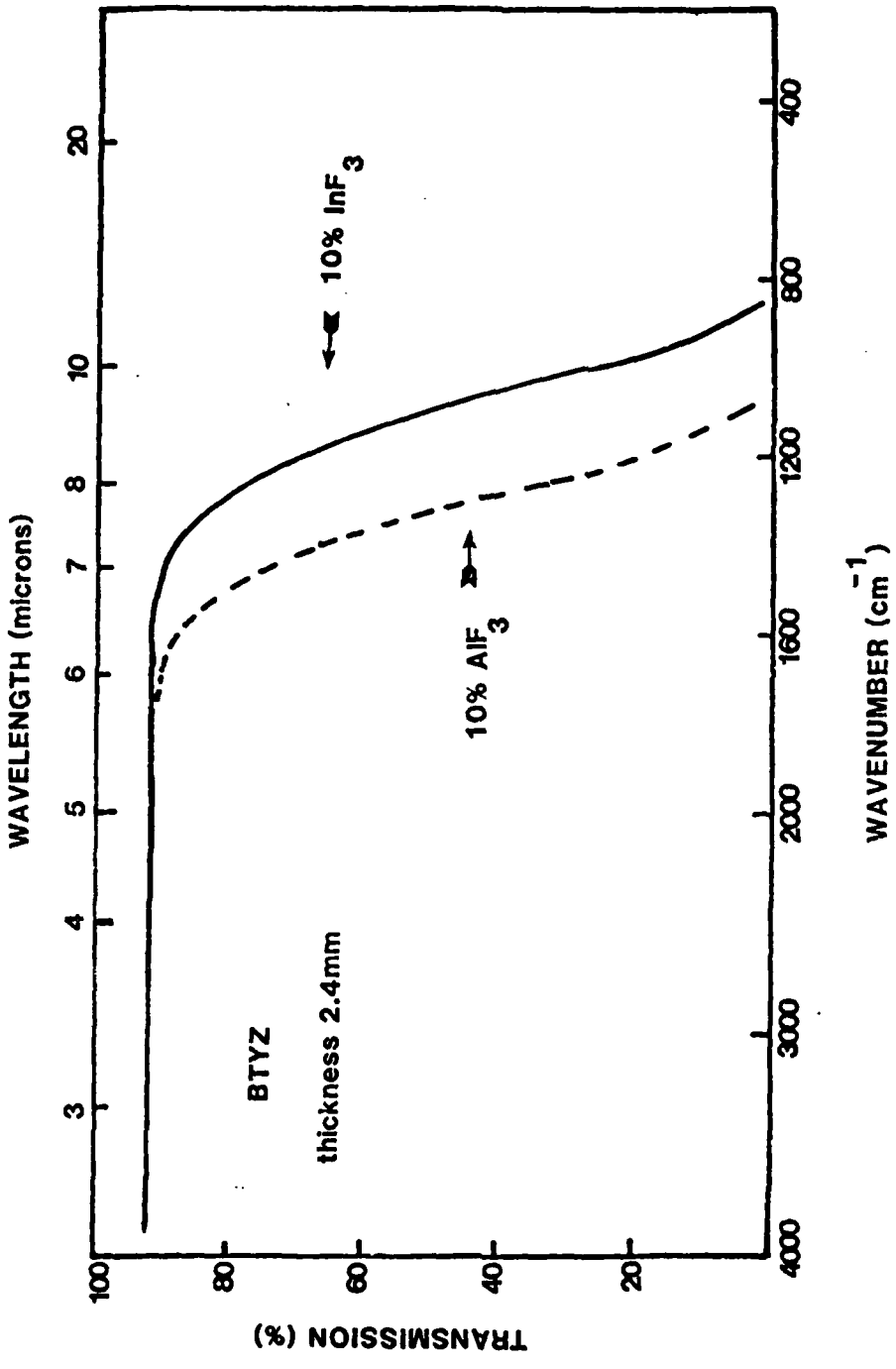
WAVELENGTH (microns)
3
4
5
6
7
8
10
20
10% InF_3
10% AlF_3
BTYZ
thickness 2.4mm
100
80
60
40
20
TRANSMISSION (%)
4000
3000
2000
1600
1200
800
400
WAVENUMBER (cm^{-1})

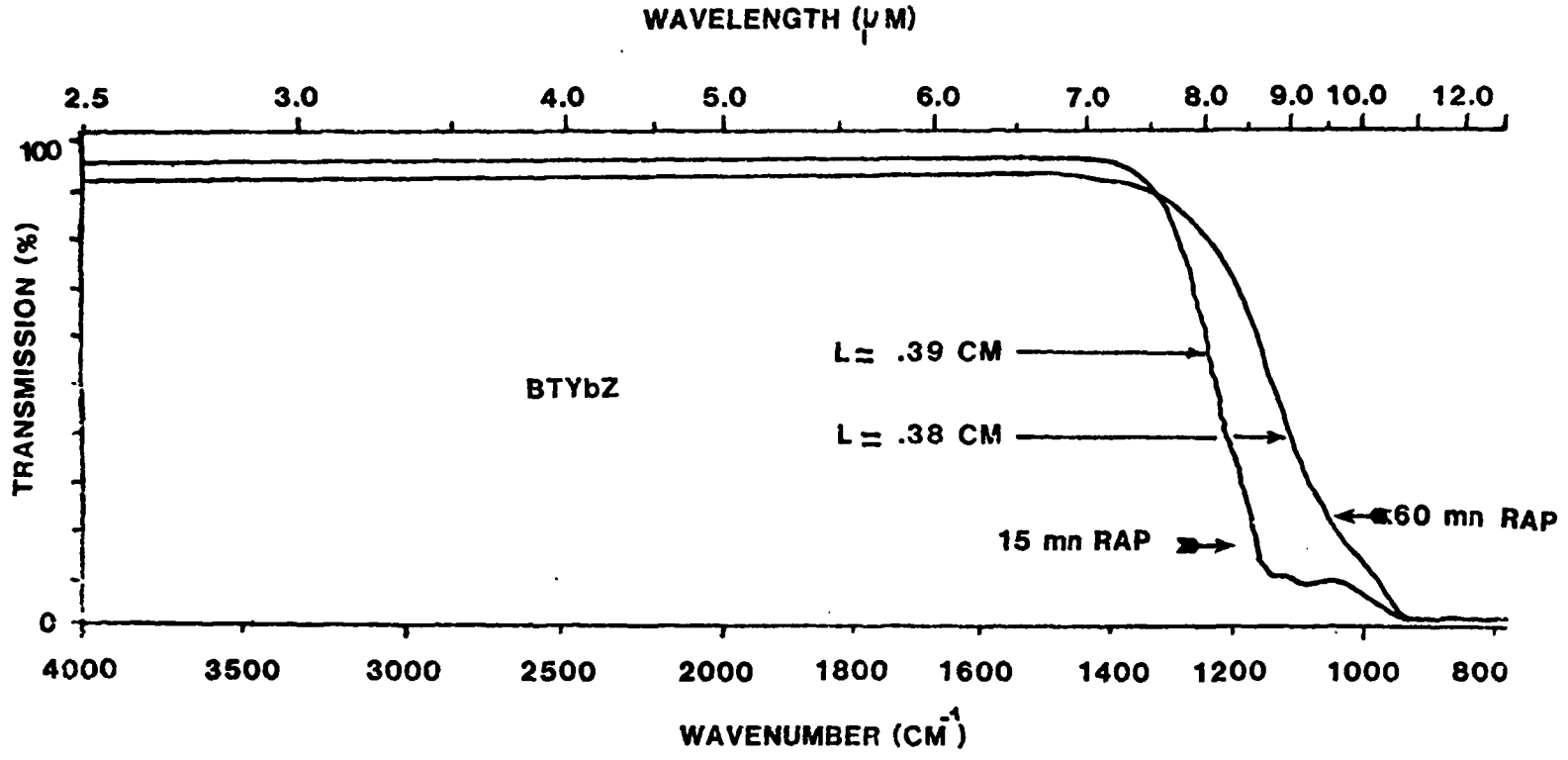
WAVELENGTH (μM)
2.5
3.0
4.0
5.0
6.0
7.0
8.0
9.0
10.0
12.0
100
TRANSMISSION (%)
0
BTYbZ
L = .39 CM
L = .38 CM
60 mn RAP
15 mn RAP
4000
3500
3000
2500
2000
1800
1600
1400
1200
1000
800
WAVENUMBER (CM-1)

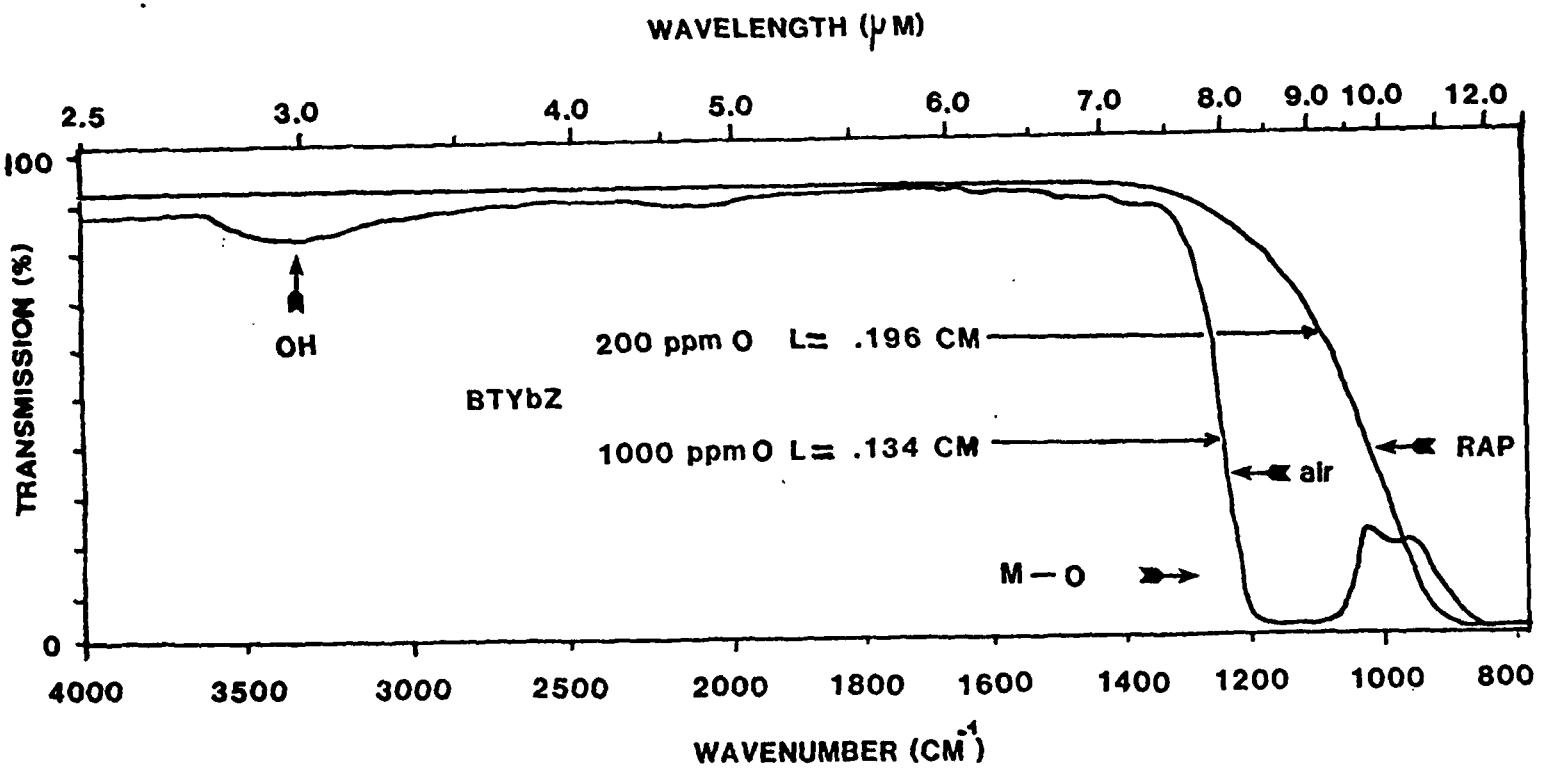
WAVELENGTH (μM)
2.5
3.0
4.0
5.0
6.0
7.0
8.0
9.0
10.0
12.0
100
0
TRANSMISSION (%)
OH
200 ppm O L= .196 CM
BTYbZ
1000 ppm O L= .134 CM
air
RAP
M—O
4000
3500
3000
2500
2000
1800
1600
1400
1200
1000
800
WAVENUMBER (CM-1)

ThF_4/MnF_2 BASED GLASSES : RECENT DEVELOPMENTS

J. Lucas, Y. Le Page, G. Fonteneau

Laboratoire de Chimie Minérale D, Associé au C.N.R.S. n° 254
Université de Rennes-Beaulieu, Avenue du Général Leclerc
35042 RENNES CEDEX (France)

Glass formation is observed in the ternary system ThF_4-MnF_2-YbF_3. Because of the high rate of crystallization of these glassy materials, only small samples can be prepared by rapid quenching. Apparently, they contain only network formers and no network modifier element. In order to stabilize the manganese (II)-thorium based glasses, the quaternary system BaF_2-ThF_4-MnF_2-YbF_3 has been investigated. In the basic ternary system ThMnYb, the composition (mole %) 40 % ThF_4-30 % MnF_2-30 % YbF_3 (BTMYb-1) exhibits the lowest crystallisation rate. A D.S.C. analysis (heating rate : 5° C/mn) gives the following typical temperatures : T_g = 346° C, T_c = 396° C and T_f = 670° C.

Systematic studies have been carried out by adding barium fluoride to the previous ternary system. In order to rationalize the research of the glasses having the lowest tendency to devitrify, the selected compositions (40 % ThF_4-30 % MnF_2-30 % $YbF_3)_{1-x}(BaF_2)_x$ have been analyzed by D.S.C. The largest difference ΔT between T_g and T_c is obtained when 10 to 12.5 % BaF_2 is used. For the composition 12.5 % BaF_2-35 % ThF_4-26.25 % MnF_2-26.25 % YbF_3 (BTMYb-4), T_g = 358° C, T_c = 441° C and T_f = 637° C, so that samples of 8 mm thick are available.

Data concerning thermal expansion, refractive index are given. The study of the chemical durability of the BTMYb glasses in a fluorine atmosphere, indicates a partial oxidation of Mn(II) in violet Mn(III). Optical spectra (U.V., visible, near I.R.) show the typical absorption bands due to Mn^{2+} and Yb^{3+} ions.

The I.R. edge for a 4 mm thick sample lies in the 7-8 μm region. Absorption coefficients in the 7-10 μm region are reported. Extrinsic absorption losses are often due to hydroxyl groups (2.9 μm) and sometimes metal-oxygen vibrations shift the I.R. edge to shorter wavelengths. Using a reactive atmospheric processing, the OH^- band can be completely removed. In these heavy metals fluoride glasses, the substitution of YbF_3 by LuF_3 or YF_3 gives a continuous optical window. Unfortunately YF_3 only permits thin samples (1 mm) to be synthesized.

Vitreous domain in the ternary system

$ThF_4 - MnF_2 - YbF_3$

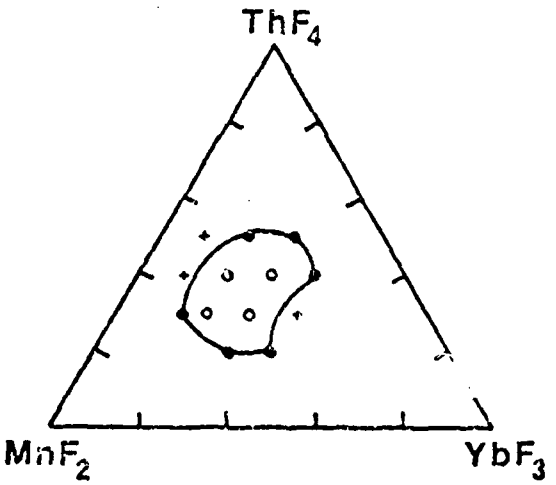

o Glass

⊙ Glass + Crystals

\+ Crystals

Quaternary system BaF_2 - ThF_4 - MnF_2 - YbF_3

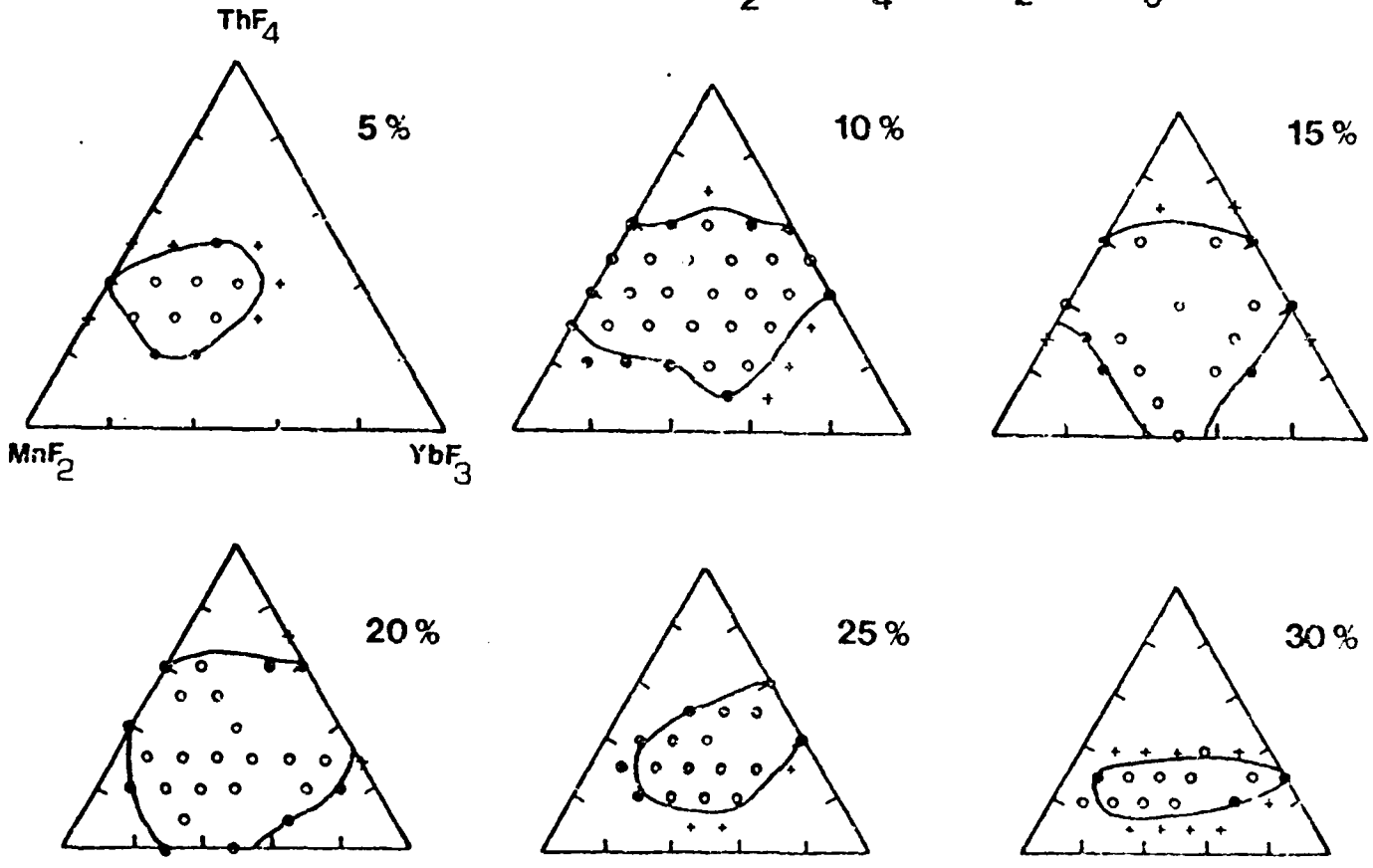

Vitreous areas in the sections corresponding to 5%,10%,15%,20%,25%,30% of BaF_2

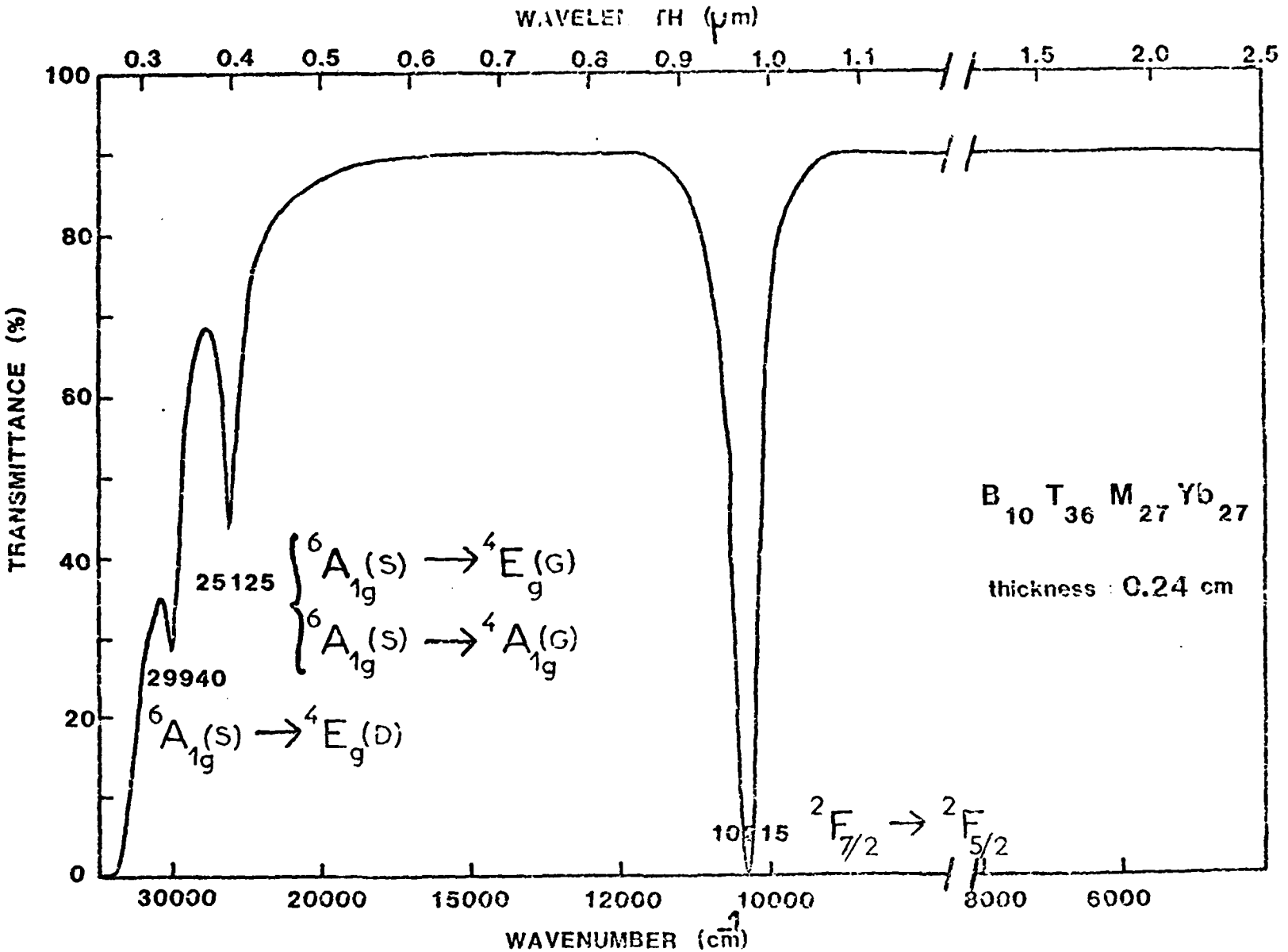
WAVELENGTH (μm)
0.3
0.4
0.5
0.6
0.7
0.8
0.9
1.0
1.1
1.5
2.0
2.5
100
80
60
40
20
0
TRANSMITTANCE (%)
25125
$^6A_{1g}(S) \rightarrow {}^4E_g(G)$
$^6A_{1g}(S) \rightarrow {}^4A_{1g}(G)$
29940
$^6A_{1g}(S) \rightarrow {}^4E_g(D)$
10315
$^2F_{7/2} \rightarrow {}^2F_{5/2}$
$B_{10}T_{36}M_{27}Yb_{27}$
thickness : 0.24 cm
30000
20000
15000
12000
10000
8000
6000
WAVENUMBER (cm^{-1})

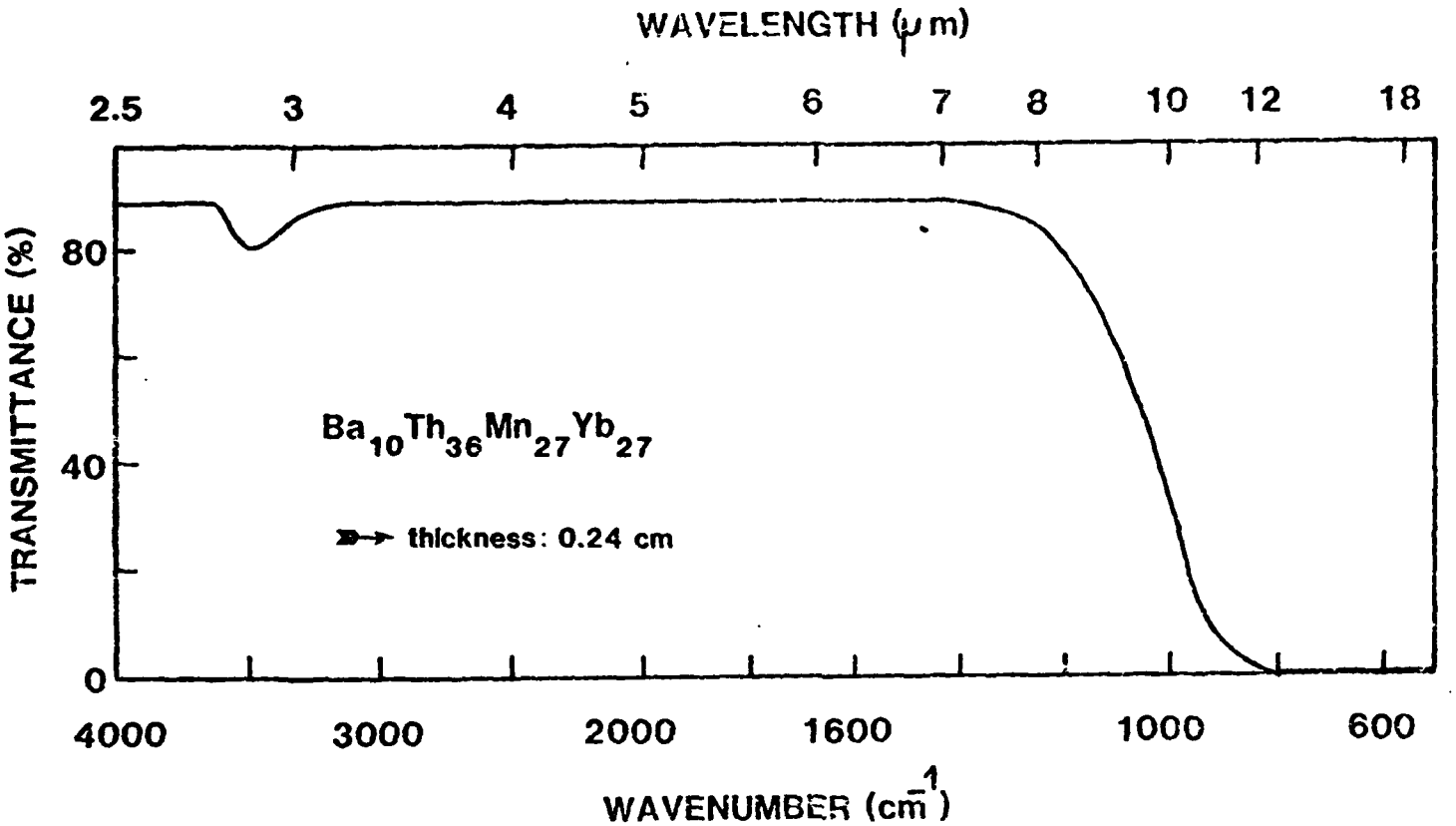
WAVELENGTH (μm)
2.5
3
4
5
6
7
8
10
12
18
TRANSMITTANCE (%)
80
40
0
$Ba_{10}Th_{36}Mn_{27}Yb_{27}$
thickness: 0.24 cm
4000
3000
2000
1600
1000
600
WAVENUMBER (cm^{-1})

RECENT PROGRESS IN HALIDE GLASS RESEARCH AT THE UNIVERSITY OF RENNES

Jacques LUCAS, University of Rennes (France)

The main activity of the group is devoted to the research of new glass forming compositions, improvement of the quality of ZrF_4-based or ThF_4-based fluoride glasses. Most of the significant results will be presented in others papers and will be here only briefly summarized. They concern for example :

1) the study of new ThF_4-based glasses
2) the effect of InF_3 addition on properties of ThF_4 glasses
3) the oxygen purification of those glasses by a CS_2 R.A.P. treatment in relation with the I.R. transmission in the 7-8μ région
4) the doping of fluoride glasses by uranyl ions UO_2^{2+} for luminescent solar concentrators
5) the synthesis and characterization of new cadmium halide glasses.

Therefore most of the attention in this presentation will be focussed on the proposition of a structural model for the simple fluorozirconate glasses isolated in the binary system ZrF_4-BaF_2. X-Ray scattering studies of those glasses and more specifically on the composition 2 ZrF_4 - 1 BaF_2 will be presented.

Radial electron distribution has been obtained and gives important and significant informations on the anion-cation vectors in the 2-3 Å région. For instance, the Zr-F distance is centered at 2,1 Å, the coordination number of F around Zr^{4+} is 7,5, two Ba-F vectors at 2,66 and 3,19 Å respectively indicate that Ba^{2+} has two kinds of neighbors bridging and non-bridging.

In the cation-cation region, a small peak at 3,6 Å could be attributed to a short Zr-Zr distances through a F-F bridge as very recently mentioned in the α high temperature form of α ZrF_4 The strong peak at 4.06 Å is attributed to the major Zr-Zr vectors indicating that the Zr-F-Zr angle is not flat but closed to 150°.

All those experimental results will be compared with the data of the four crystalline materials used as reference α and β $BaZrF_6$ and α and β ZrF_4. In view of the atomic distances, angles, coordination number, a structural model for fluorozirconate glasses will be presented. A model extended to the most complicated ternary glass ZrF_4-BaF_2-LaF_3 will be discussed in view of spectroscopical results using the rare earth ions as local probe.

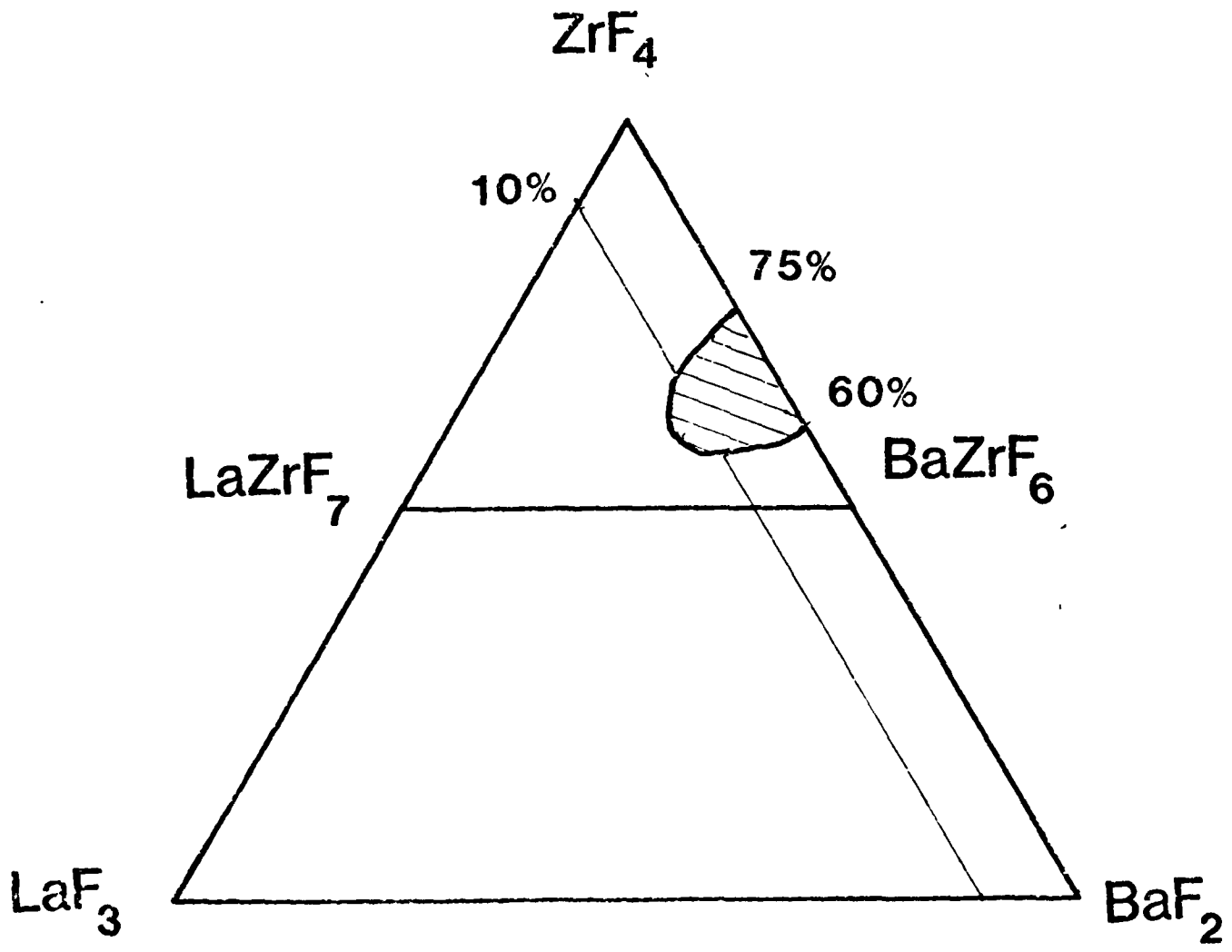
ZrF4
10%
75%
60%
LaZrF7
BaZrF6
LaF3
BaF2

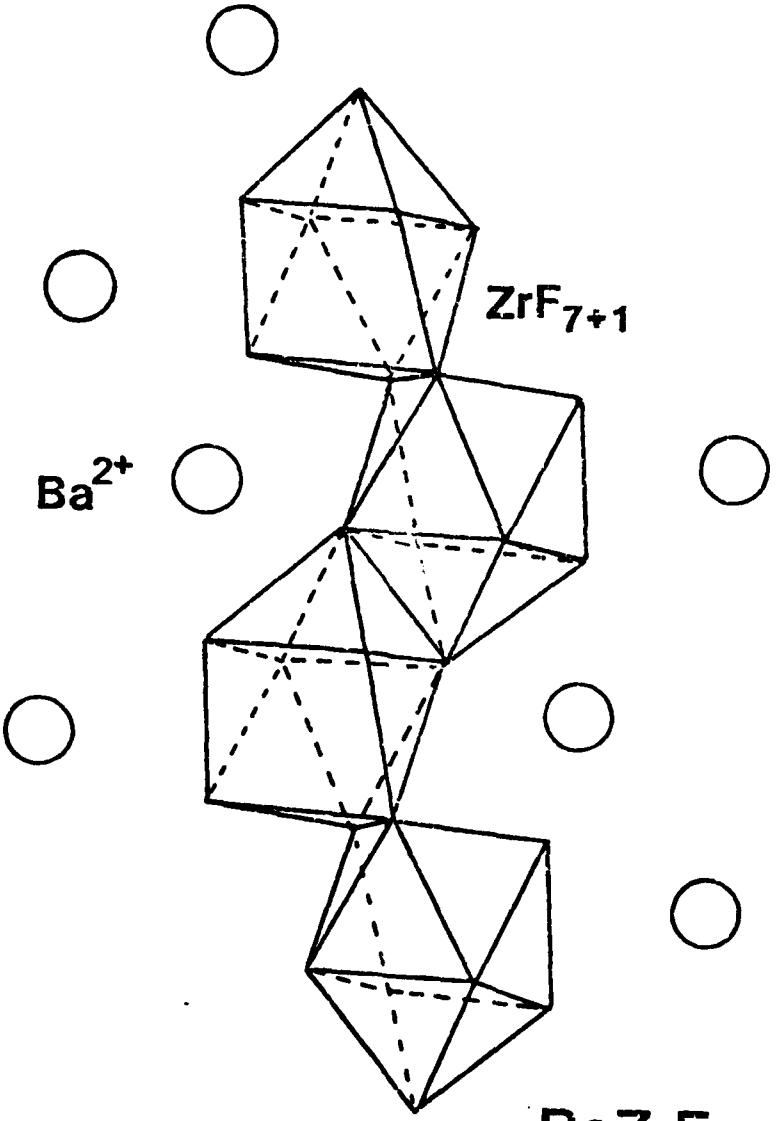

$BaZrF_6$ α

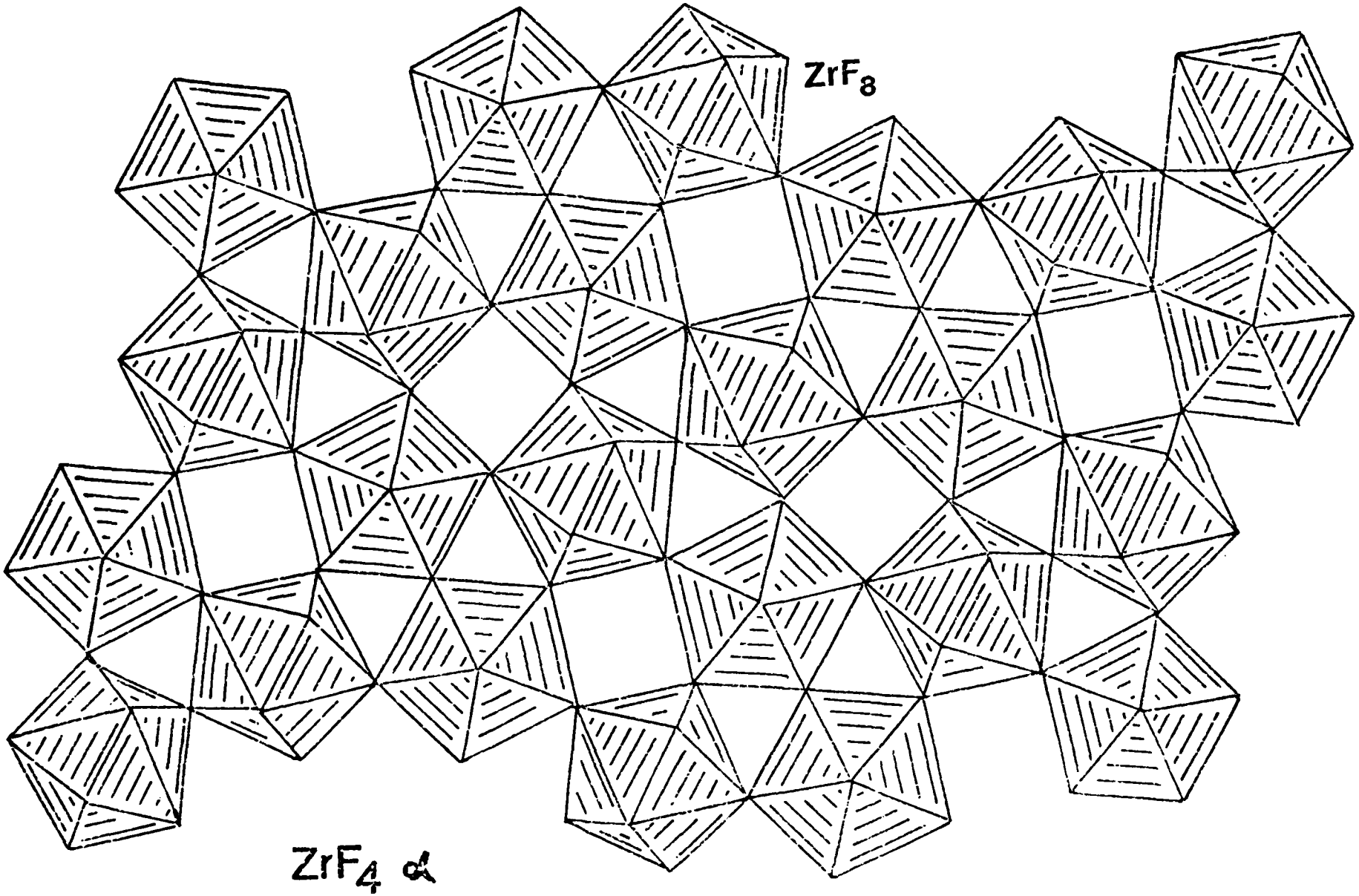

ZrF_4 α

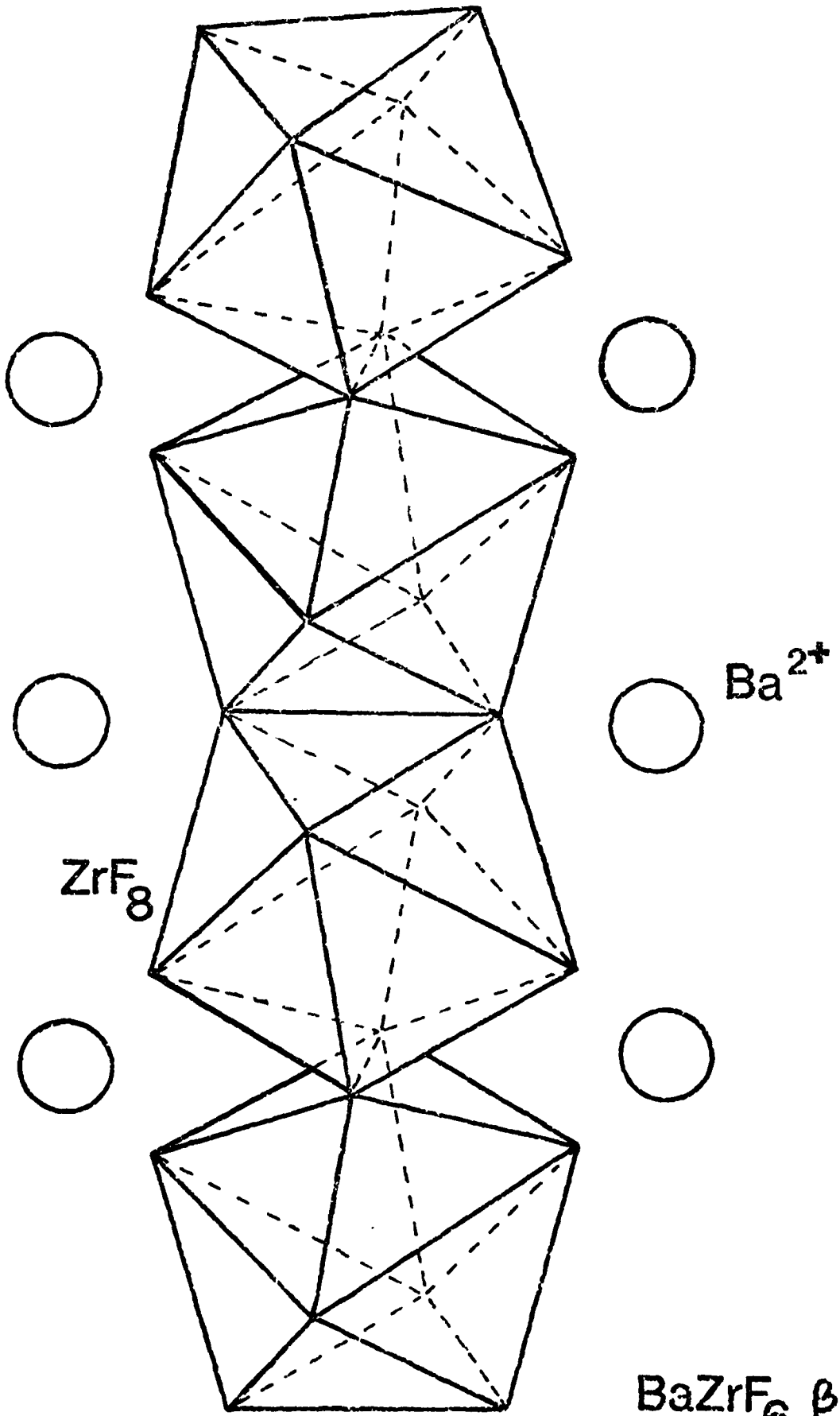
Ba^{2+}
ZrF_8
$BaZrF_6$ β

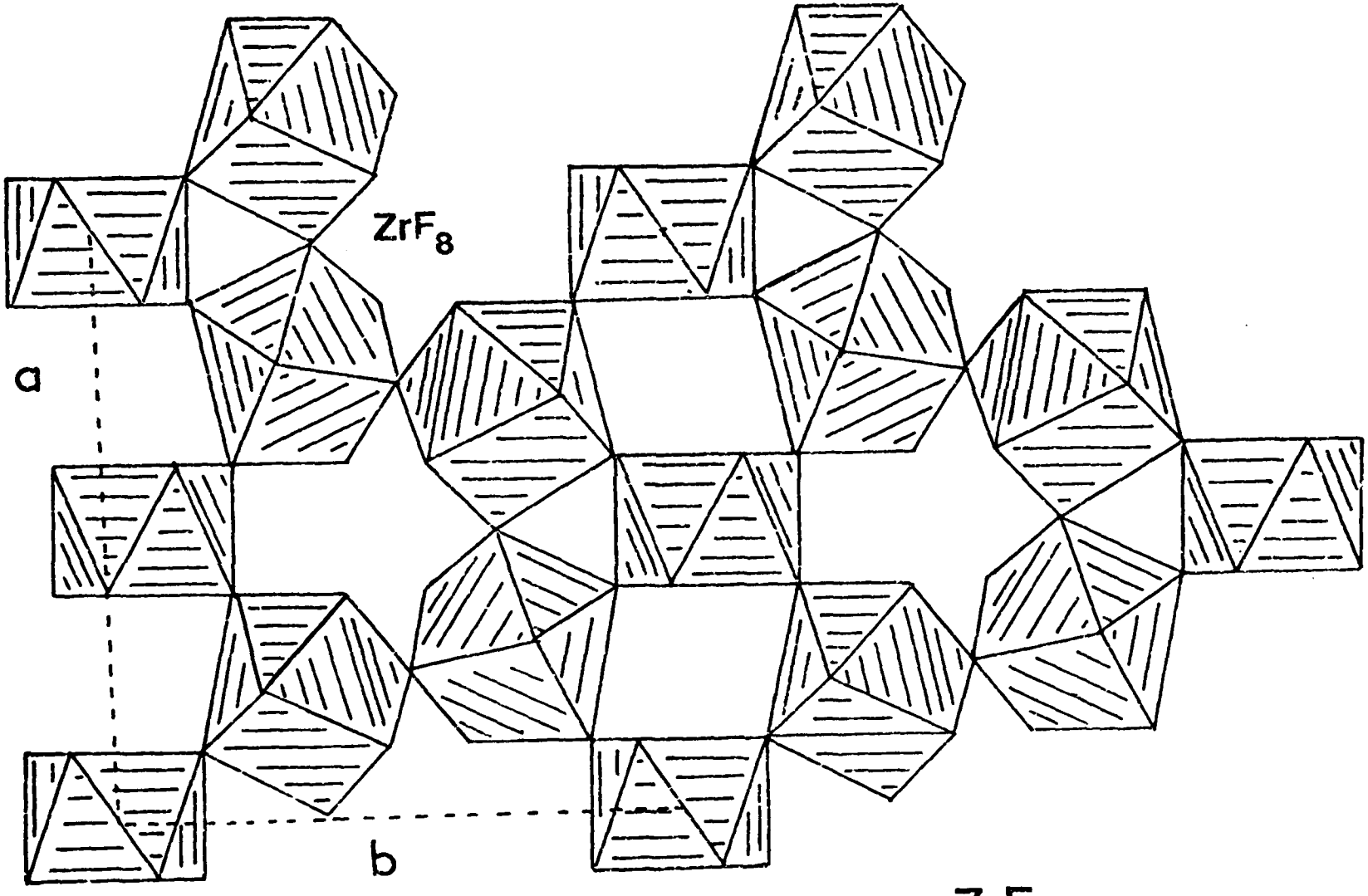

ZrF_4 β

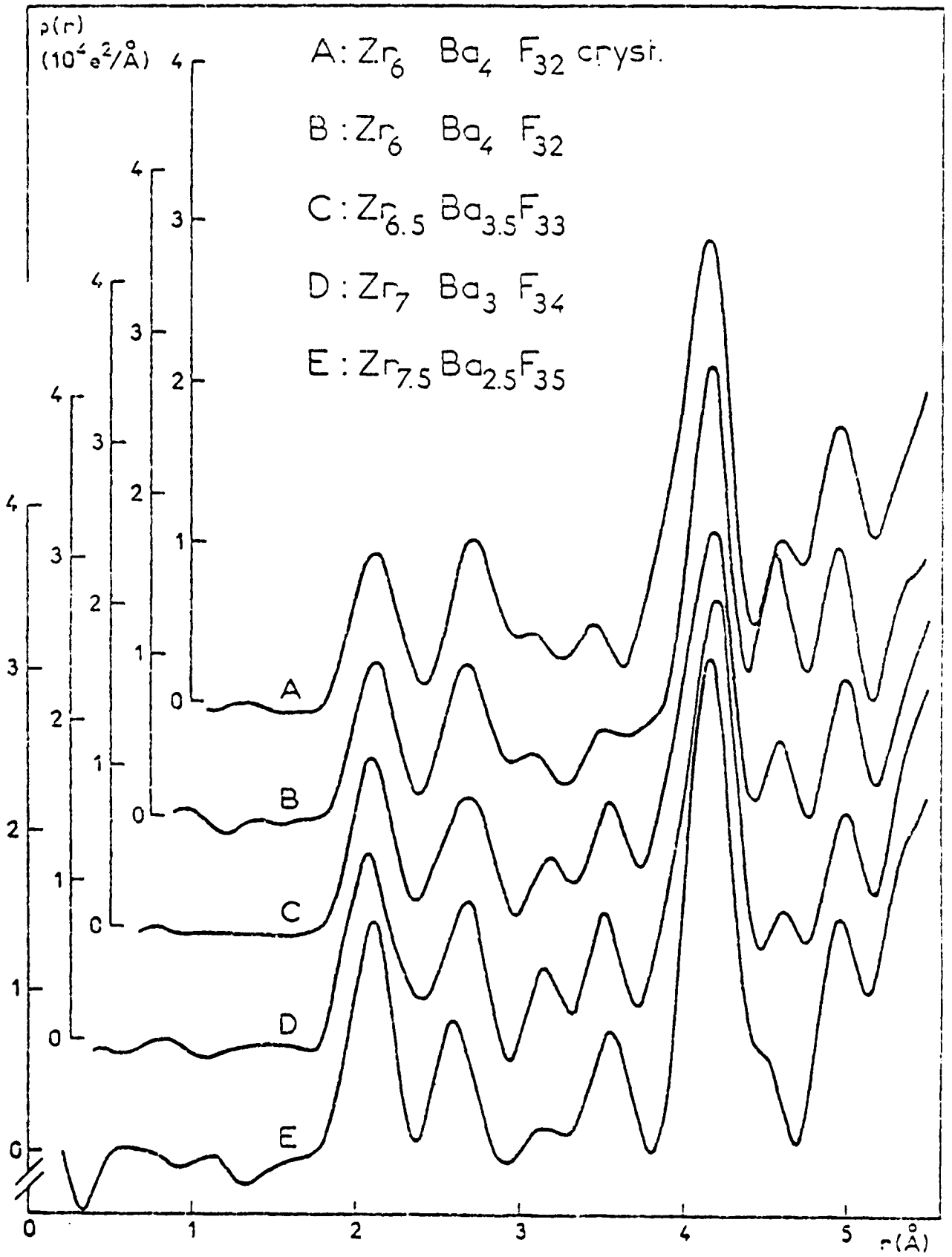
p(r)
(10⁴e²/Å)
A: Zr6 Ba4 F32 cryst.
B: Zr6 Ba4 F32
C: Zr6.5 Ba3.5 F33
D: Zr7 Ba3 F34
E: Zr7.5 Ba2.5 F35
A
B
C
D
E
0
1
2
3
4
5
r(Å)

STRUCTURE OF THE GLASSES $BaZr_2F_{10}$

X-RAY SCATTERING RESULTS

PEAK 1 → Zr-F INTERACTION → 2.1 Å

→ COORDINATION NUMBER AROUND Zr^{4+} → CN = 7.5

PEAK 2, 3 → Ba-F INTERACTIONS TWO TYPES PROBABLY WITH F_B AND F_{NB}

- $Ba\text{-}F_{LONG}$ → 3.20
- $Ba\text{-}F_{SHORT}$ → 2.66

PEAK 4 → Zr-Zr SHORT DISTANCES SMALL %

- Zr-Zr → 3.60

PEAK 5 → STRONG INTERACTIONS Zr-Zr → 4.20

SMALL DEVIATIONS OF Zr-F-Zr → 180°

AVERAGE VALUE Zr $\overset{\alpha}{\frown}$ Zr → 155°

PEAK 6 → Ba-Zr → 4.5

PEAK 7 → Ba-Ba → 4.9

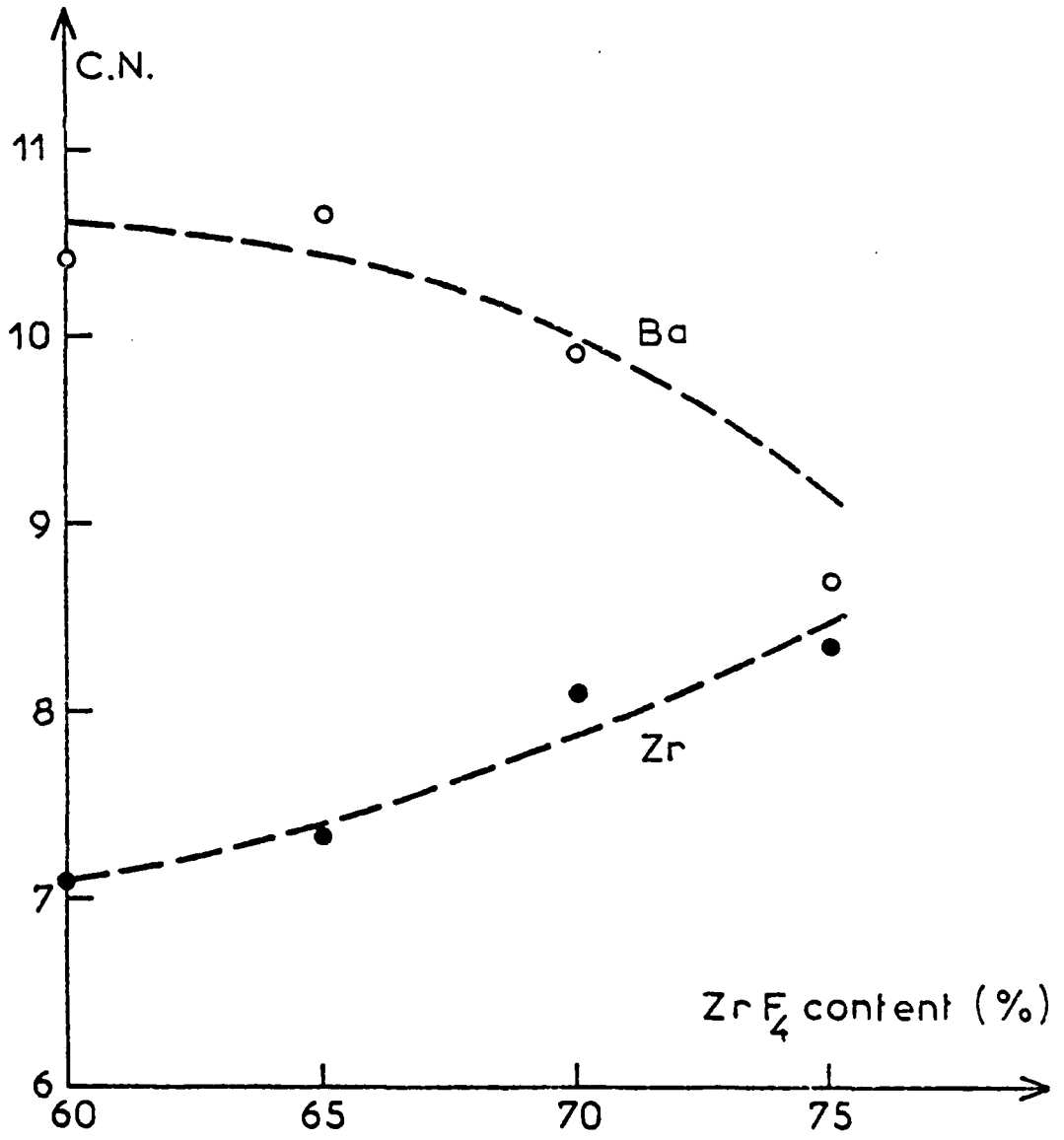
C.N.
11
10
9
8
7
6
Ba
Zr
ZrF4 content (%)
60
65
70
75

STRUCTURE OF THE GLASS $BaZr_2F_{10}$

$BaF_2, 2\ ZrF_4$

$BaZr_2F_{10}$: $Ba_{0,5}[ZrF_5]$ → 3_D COVALENT NETWORK

Ba^{2+} MODIFIER ION

AVERAGE COORDINATION NUMBER FOR Zr^{4+} CN = 7.5

3_D NETWORK BUILT UP BY THE ASSOCIATION OF :

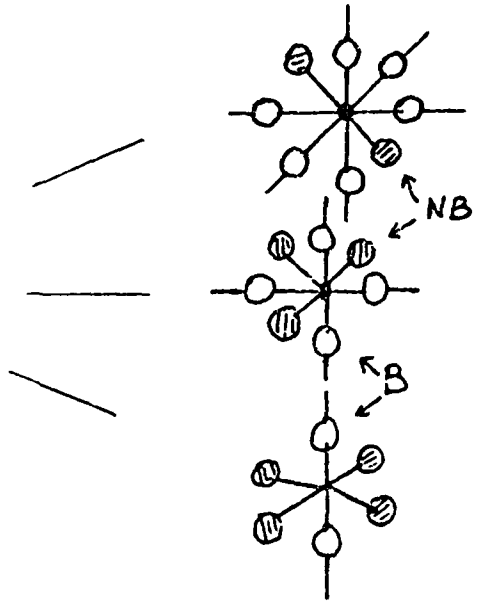

- ZrF_8 POLYHEDRA WITH 6 F_B, 2 F_{NB}

  $ZrF_{B\ 6/2}F_{NB\ 2}$ → ZrF_5

- ZrF_7 POLYHEDRA WITH 4 F_B, 3 F_{NB}

  $ZrF_{B\ 4/2}F_{NB\ 3}$ → ZrF_5

- ZrF_6 POLYHEDRA WITH 2 F_B, 4 F_{NB}

  $ZrF_{B\ 2/2}F_{NB\ 4}$ → ZrF_5

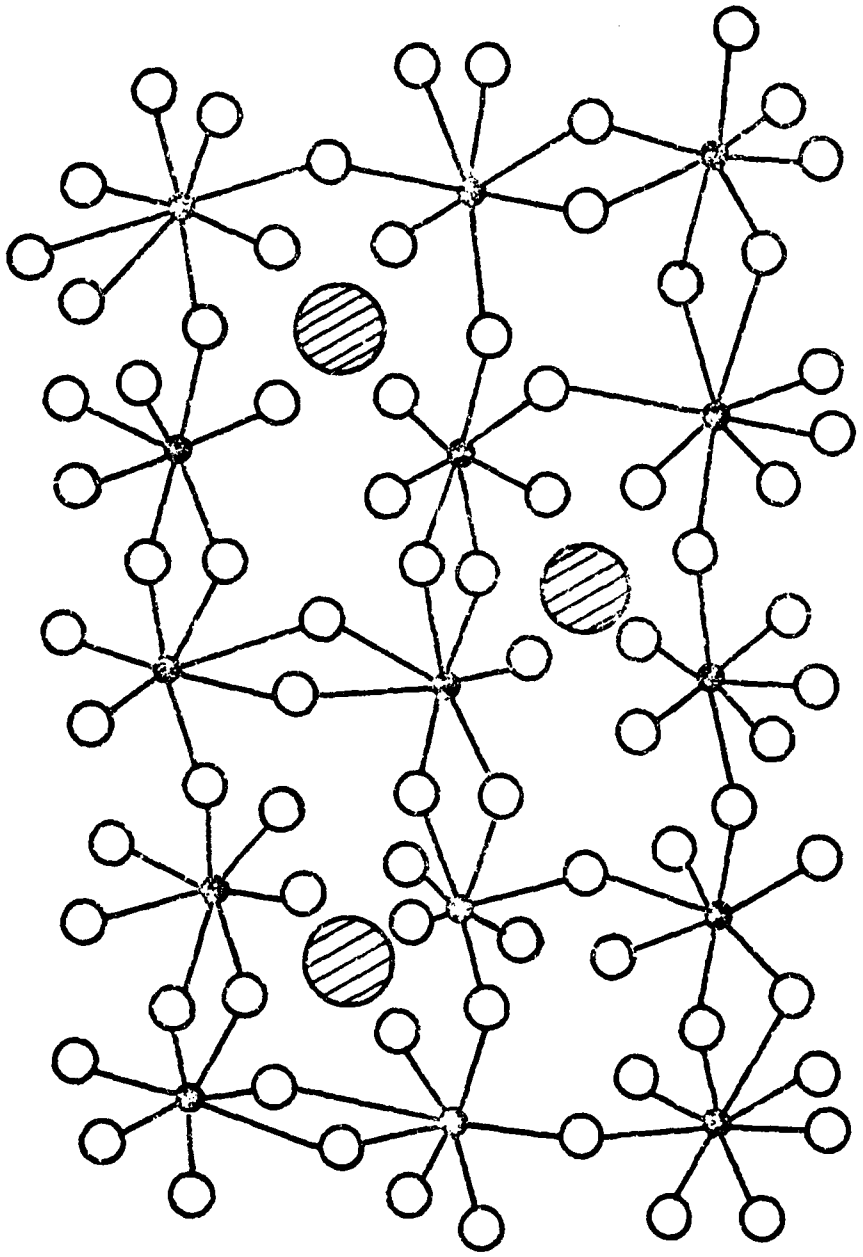
Zr
F
Ba

Halide Glasses Based on Chlorides, Bromides and Iodides*

by J.D. Mackenzie

Department of Materials Science and Engineering

University of California, Los Angeles

Extended Abstract

for

Second International Symposium on Halide Glasses

August 2-5, 1983

Rensselaer Polytechnic Institute

Troy, New York

* This work is being supported by the Directorate of Chemical and Atmospheric Sciences, Air Force Office of Scientific Research

There is relatively little information on glasses based on chlorides, bromides, iodides and their mixtures. On the other hand, fluoride glasses have been widely studied in the past few years because of their potential practical importance and their interesting scientific features. This paper is a review of what is currently known about the chloride, bromide and iodide glasses and an evaluation of their potential.

Most of the known halide glasses containing no fluorine are shown in Table 1. Glasses based on $ThCl_4$-NaCl-KCl are transparent to 20μ. The AgI-AgBr-based glasses are photochromic. It is thus natural to inquire if other halide glasses of potential usefulness can be prepared. Theoretical predictions of glass-forming tendency can be made through a number of approaches. Thus the magnitude of the ratio of single-bond energies to melting temperatures (Rawson, 1956) or the ratio of cationic to anionic field strengths (Poulain, 1981) can be used as a guide. Assuming ideal behavior, such treatments can be applied to polycomponent systems. Table 2 shown some systems which are glass-forming. The values of E_{AV}/T_l and P_i are all within the predicted ranges of glass formation. It would appear that these two approaches are fairly good tools for prediction.

The viscosities of the melts of systems shown in Table 2 are all much lower than those of oxide glass-forming systems. The glass transition temperatures are all lower than 200°C. In the absence of phase diagrams, it is not possible to predict T_g values. In general, however, it appears unlikely that glasses with T_g higher than those of the fluoride glasses can be prepared. No chemical durability data exist on the glasses in question. Again, assuming ideality, predictions can be made via the known solubility in

water data of halides. Here too, the information on potential glass-forming systems is very limited. Some solubility data of interest are shown in Table 3. Chemical durability would appear to be a key problem in the development of these halide glasses. With the exception of $ZnCl_2$, no structural information is available. The question of coordination of cations, when two or more different halogens are present in a glass, will be an interesting structural problem for future studies.

Table 1

KNOWN NON-FLUORIDE HALIDE GLASSES

$ZnCl_2$

$ZnCl_2$-KI

$BiCl_3$-KCl

$ThCl_4$-KCl

$ThCl_4$-NaCl

$ThCl_4$-KCl-NaCl

$CdCl_2$-$BaCl_2$

$CdCl_2$-$BaCl_2$-NaCl

$BiBr_3$-TlCl-$PbCl_2$

CdI_2-KI

CdI_2-KI-CsI

$CdCl_2$-AgCl-$PbCl_2$

CsBr-AgBr-$PbBr_2$

AgI-AgBr-$PbBr_2$-CsBr-$CdBr_2$

Table 2

HALIDE GLASSES AND PREDICTED
GLASS FORMING TENDENCIES

System	$\frac{E_{Av}}{T_l}$	P_i
$ZnCl_2$	0.086	6.0
$ZnBr_2$	0.062	6.5
$ZnBr_2$-KCl (55-45)	0.080	4.2
$ZnBr_2$-KBr (55-45)	0.058	4.2
$ZnBr_2$-KI (55-45)	0.084	4.3
$ZnBr_2$-TlCl (55-45)	0.075	4.1
$ZnBr_2$-TlBr (55-45)	0.073	4.2
$ZnBr_2$-KBr-TlI (55-35-10)	0.079	4.2
$ZnBr_2$-KBr-KI-TlBr (55-25-10-10)	0.079	4.2

NOTE: $P_i = \chi_i F_i$ (2.5 to 10)

$E_{AV} = \Sigma E_i v_i \chi_i / \Sigma v_i \chi_i$

(> 0.05)

Table 3

Some Insoluble Halides at 20°C In Water

	I^-	Br^-	Cl^-	F^-
Ag	3×10^{-7}	8×10^{-6}	2×10^{-4}	196
Pb	0.07	0.9	1.0	0.06
Bi	i	d	d	i
Cr^{3+}		i	i	i
Hg^{2+}	0.01	0.6	7	
Tl	6×10^{-4}	0.05	0.3	80
Th	s	s	s	i
Zr	d	d	s	1.4
Al	d	s	70	0.6

PROGRESS IN CADMIUM HALIDE GLASSES

Marc MATECKI, Michel POULAIN and Marcel POULAIN

Université de Rennes - Campus de Beaulieu
Laboratoire de Chimie Minérale D, Laboratoire Associé au C.N.R.S. n° 254, Avenue du Général Leclerc - 35042 Rennes Cédex (France)

INTRODUCTION

Various examples of the glass forming ability of ZnF_2 were recently described (1-3) while that of $ZnCl_2$ is well known (4). This paper is centered upon systems including cadmium which is isoelectronic with zinc and therefore is likely to show some glass forming ability. The main interest of such research lies in the improvement of I.R. transmission and also in increasing the water resistance of chlorine containing phases.

1. GLASS FORMING SYSTEMS

1.1. Fluoride glasses

By classical synthesis methods, quenched glasses have been obtained in the CdF_2-ZnF_2-BaF_2 and CdF_2-MnF_2-BaF_2 ternary systems. Binary glasses $(Cd_{0.5}Ba_{0.5})F_2$ have been synthesized. As shown in figure 1, the glass forming area is large, but the crystallization rate at cooling is always high. Therefore, only thin samples may be prepared.

1.2. Chloride glasses

Cadmium chloride may acts as a glass progenitor : this is demonstrated by the occurrence of quenched glasses in the $CdCl_2$-$BaCl_2$-NaCl or KCl ternary systems (figure 2). Binary glasses

(Cd, Ba)Cl_2 are also observed. Although vitreous materials may be prepared at room atmosphere, better results are obtained using a dry glove box. These chloride glasses are much less sensitive to moisture than $ZnCl_2$ glasses.

1.3. Mixed halide glasses

Glass formation seems to be rather common in many polyhalide systems including cadmium halides such as $CdCl_2$-CdF_2-BaF_2, $CdCl_2$-CdF_2-$BaCl_2$, $CdCl_2$-CdF_2-KI or KBr (figure 3). When using pure starting materials, samples of 5 mm in thickness may be obtained. The stability versus atmospheric moisture increases with the fluorine content. Typical glass compositions are reported in table I.

2. PHYSICAL PROPERTIES

The characteristic temperatures were measured by D.S.C. (DU PONT 1090 thermal analyser). For fluoride glasses, the values are similar to that of fluorozirconate glasses while the average value of T_G is 180° C and that of T_M around 400° C for chloride and mixed halide glasses (table II).

The I.R. multiphonon absorption edge is shifted beyond 10 microns for thin samples, as shown in figure 4. The influence of impurities such as phosphates and sulfates on I.R. transmission is drastic : less than 100 ppm of SO_4^{2-} result in a strong absorption band at 9 µm, and, for thick samples, the acceptable lever of S or P is likely below 1 ppm. Figure 5 shows the I.R. transmission curve of a purified cadmium polyhalide glass (as expected, the multiphonon absorption edge lies between that of fluoride and that of chloride glasses).

In most cases, a residual OH band at 3 µm is observed. As for fluoride glasses, it may be removed by a convenient processing.

3. DISCUSSION

From a structural point of view, cadmium halide glasses show some similarities with zinc halide glasses by the anion to cation ratio and by the electronic structure. However, Cd^{2+} ionic radius (0.95 Å) is closer to that of Bi^{3+} (1.03 Å) which has also a d^{10} electronic configuration. Further structural investigations would be helpful to determine the actual coordinations, although an octahedral arrangement seems to be probable for Bi and Cd in chlorine containing glasses. The simplest structural model for these glasses is that of a random packing of anions in which cations are randomly inserted.

Potential applications of cadmium polyhalide glasses may be foreseen both for I.R. bulk components and I.R. optical fibres. The values of T_G are high enough to allow most uses. The decrease of the absorption coefficient with the wavelength suggests that the minimum value of the absorption losses is very low insofar as Rayleigh scattering is not too important (figure 6).

REFERENCES

1. J.P. MIRANDAY, C. JACOBONI and R. DE PAPE - J. Non-Cryst. Solids 43, 393 (1981)
2. G. FONTENEAU, F. LAHAIE and J. LUCAS - Mat. Res. Bull. 15, 1143 (1980)
3. M. MATECKI, M. POULAIN and M. POULAIN - Mat. Res. Bull. 16, 749 (1981)
4. H. RAWSON - Inorganic Glass Forming Systems, Academic Press, New-York (1967).

TABLE 1

Cadmium halide glass compositions (in mole %)

	CdF_2	$CdCl_2$	BaF_2	ZnF_2	ThF_4	$BaCl_2$	NaCl	KCl	KRb	KI
FCB 0	50		50							
FCBZ 3	40		40	20						
FCBZ 6	20		40	40						
FCBT	47		47		6					
CCBK 1		50				40		10		
CCBN 1		50				40	10			
CCB 0		50				50				
XCB 4	40	30	30							
XCB 5	65	2				33				
XCB 0	65					35				
WCK 2	20	30							50	
QCK 2	20	40								40

TABLE 2

Characteristic temperatures of cadmium halide glasses

	T_G	T_C	T_M
FCB 0	325	380	625
FCBZ 3	283	345	643
FCBT	354	406	589
CCBK 1	180	232	363
CCBN 1	170	212	366
CCB 0	179	224	448
XCB 4	182	216	443
XCB 5	184	203	455
WCK 2	114	164	314
QCK 2	104	117	278

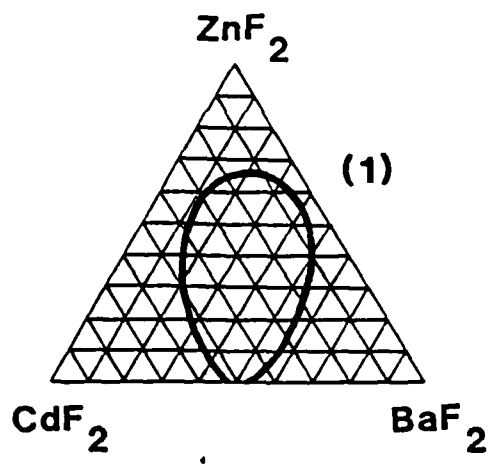

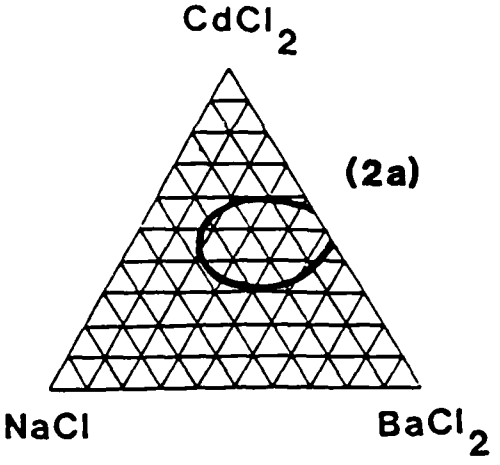

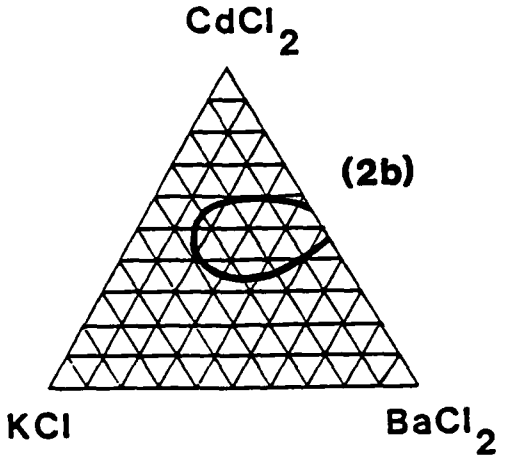

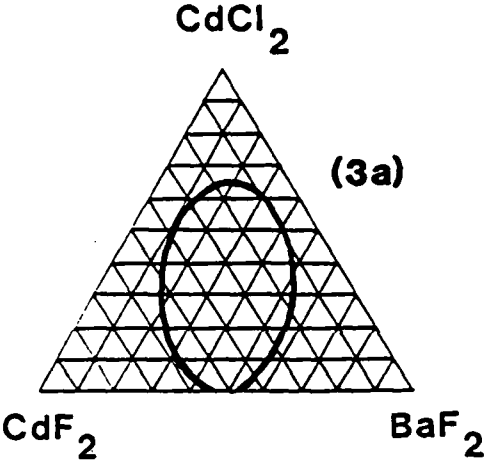

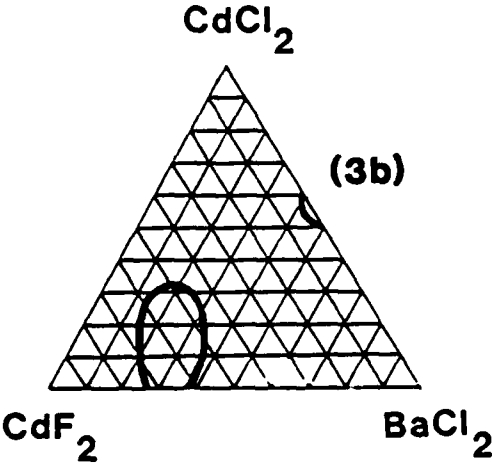

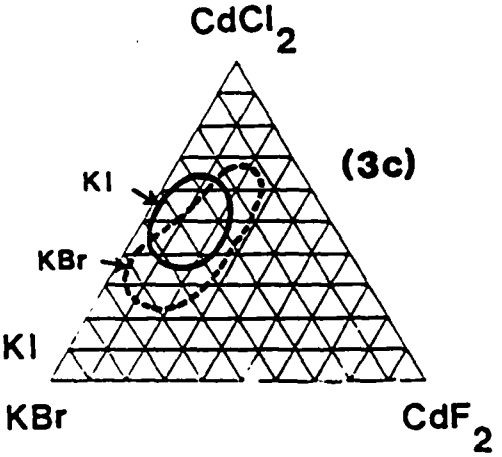

Figures 1, 2, 3

Vitreous areas in cadmium halide systems : 1. fluorides ; 2. chlorides ; 3. mixed halides.

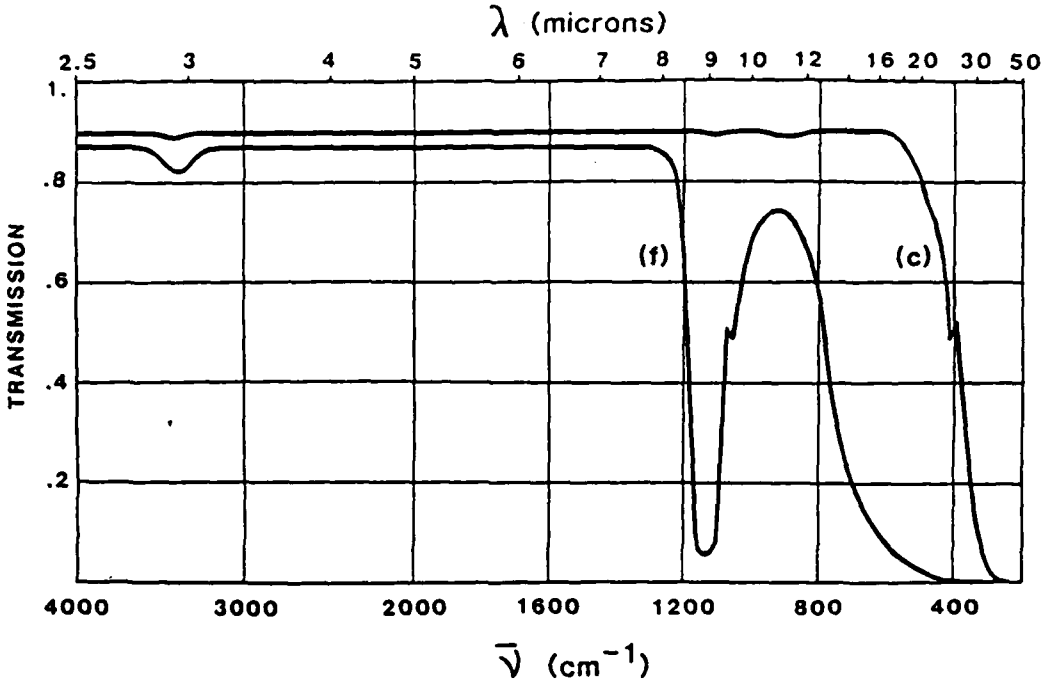

Figure 4

Infrared transmission of two thin glass samples : FCBZ-6 *and* CCBK-1. *Average thickness* : 0.4 *mm*

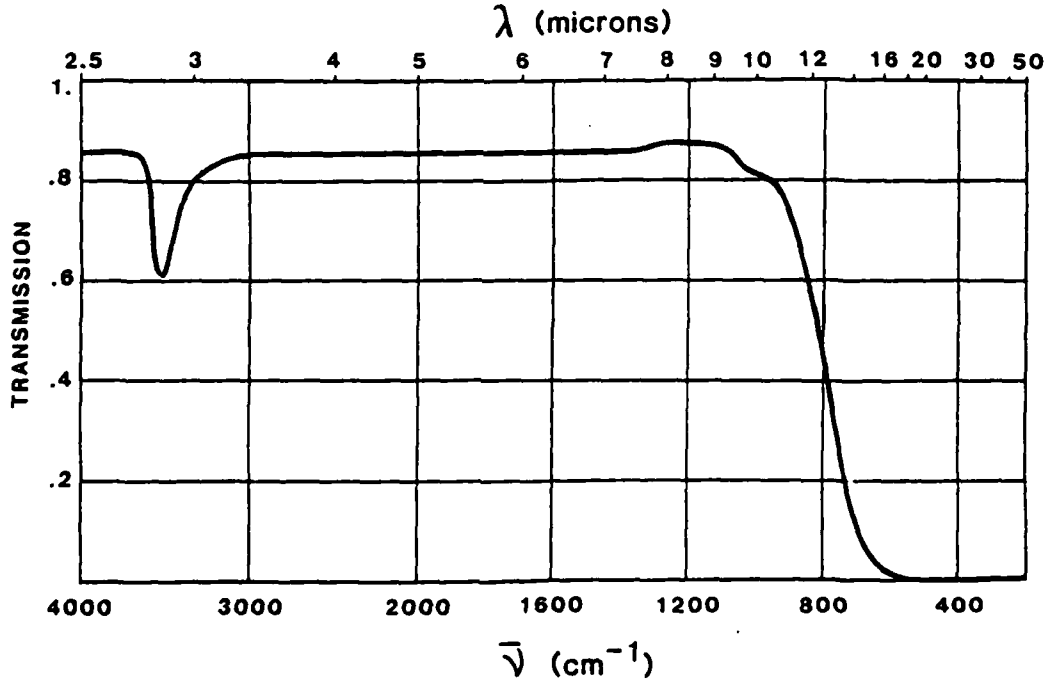

Figure 5

Infrared transmission of a cadmium polyhalide glass XCB-5 : $Cd_{0.67}Ba_{0.33}Cl_{0.7}F_{1.3}$

Sample thickness : 1.3 *mm*

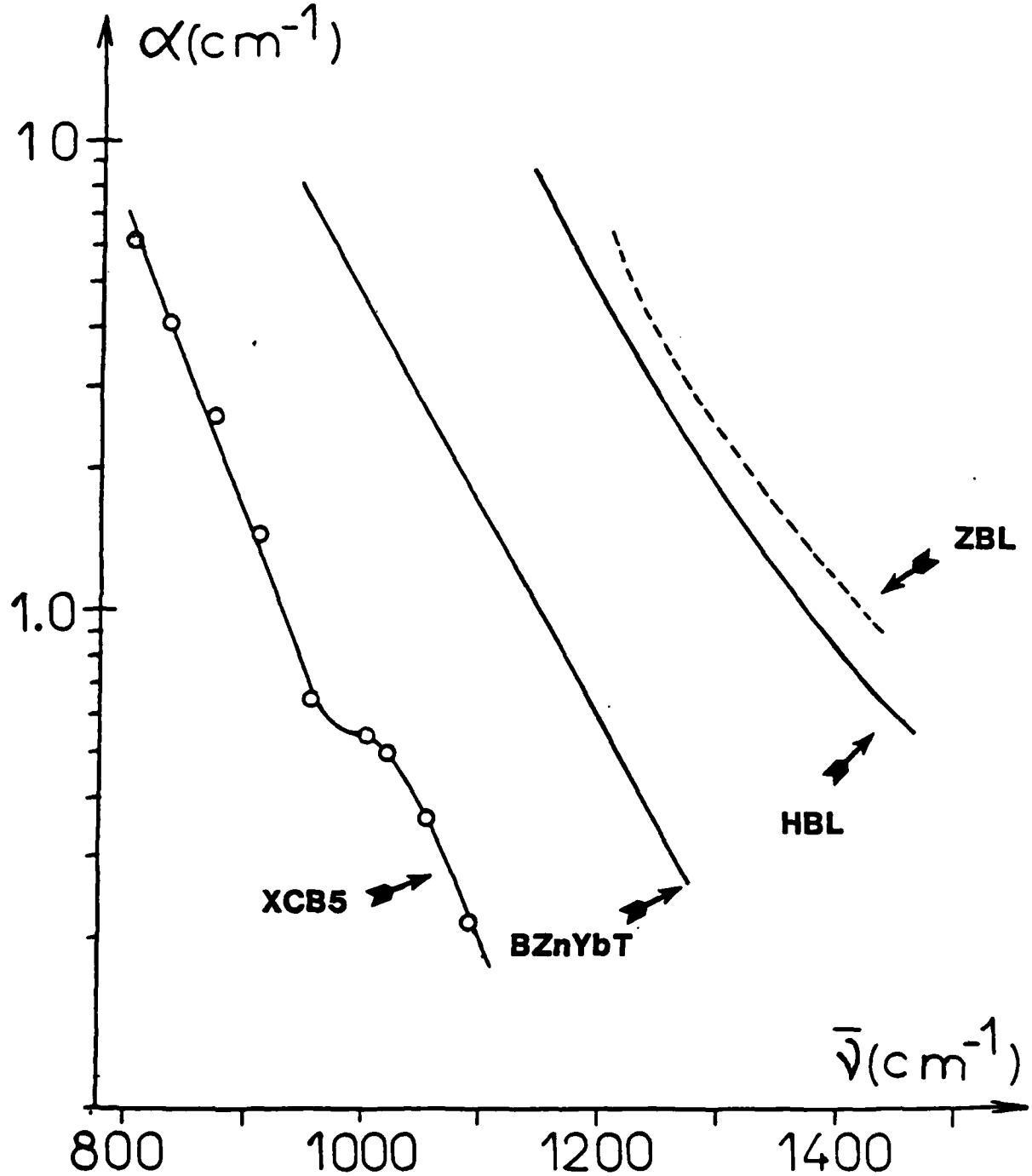

Figure 6

Absorption coefficient α versus frequency ν for different halide glasses

LARGE SCALE PREPARATION OF HEAVY METAL FLUORIDE GLASSES

Gwenaël MAZE

Le Verre Fluoré, Z.I. du Champ Martin
VERN/SEICHE, 35230 SAINT ERBLON (France)

INTRODUCTION

Speaking of heavy metal fluoride glasses, what can be qualified as a large scale preparation ? As an example, a small window 25,4 mm in diameter and 3 mm thick weights 7 g. Taking in account the losses at polishing and a serious coefficient of security, 20 g of glass will be necessary to get a single window. The manufacturing of 10,000 windows will require 200 kg, provided that there is a market for such quantities of windows or other fluoride glass components. With the same quantity of glass, it should be possible to do 50 large optical windows 300 mm in diameter and 15 mm thick.

If we cast a glance at optical fibers, we can calculate that to obtain 250 m of optical fibers, 140 µm in diameter, one must start with 100 g of glass, taking in account the losses at polishing, at the ends of the preform and a large coefficient of security. One kilometer of optical fibers will require 400 g of glass.

One can imagine that a major factor has to be taken in account by the fluoride glass manufacturer : that is the specifications of the glass. Glass preparation for optical fibers drawing or high power laser windows and lenses require high

purity starting materials and, sometimes, in a first step, the purification of some of them. The time requested for these operations, the cost of the raw materials and special equipement necessary to produce 1 kg of such glass are far above the cost of the glass devoted to standard I.R. components

In this paper, we shall describe some of the techniques which are suitable to produce some thousands kg of fluoride glasses of optical quality and discuss some of their advantages and limits.

PREPARATION TECHNIQUES

A simple way to manufacture fluoride glasses is to melt an adequate mixture of fluorides and pour it in a mold. Here are two stable glass compositions

ZrF_4	57	BaF_2	34	LaF_3	5	AlF_3	4
AlF_3	28,75	YF_3	28,75	ThF_4	22,5	BaF_2	20

Another way consists to start from oxides and fluorides mixed with ammonium hydrogeno difluoride in order to convert oxides in fluorides. The main reactions which are assumed to occur during the fluorination stage are :

$$2\ ZrO_2 + 7\ NH_4FHF \rightarrow 2\ (NH_4)_3ZrF_4 + NH_3\uparrow + 4\ H_2O\uparrow \quad (1)$$

$$(NH_4)_3ZrF_4 \rightarrow ZrF_4 + 3\ NH_4F\uparrow$$

One of the most critical problems in fluoride glass preparation is its reaction with water. Fluorides react with water according to reactions which can be resumed by :

$$\text{Fluorides} + H_2O \rightleftarrows \text{Oxyfluorides} + HF\uparrow$$

These compounds are not much soluble in the glass. One can succeed to dissolve them at high temperature if their concentration remains at a low level. These compounds affect dramatically the refractive index of the glass as can be shown in figures 1 and 2. When the concentration of oxyfluorides is too

high, it is impossible to obtain a glass : the batch crystallizes.

MANUFACTURING DEVICES

The fluoride glass manufacturer must be aware that to obtain 1 l of glass (i.e. 4,5 kg), he has to start from a volume of 6 l of fluoride powders or 10 l of the mixture of oxides, fluorides and NH_4FHF. The volume of the powders is reduced of an half during the fluorination step and drops down at melting.

1. Open system (fig. 3)

A simple and relatively low cost device is made of a crucible (vitreous carbon, platinium or gold) of the suitable volume and a resistance heating furnace. Apart from the cost, its main advantage lies in the possibility of making, in a single casting, a volume of glass equal to 2/3 of the crucible volume. This system actually gives the possibility to add powders as their level drops down.

This advantage has his backside : the open system makes easier the exchanges between the inside of the crucible and the outside atmosphere. They are all the more important since the level of the molten glass in the crucible is higher (figure 4).

2. Controlled atmosphere system (figure 5)

In this system, the crucible is placed in a vessel made of glass or silica, through which is blowed a current of gas, and heated by an induction or a resistance heating furnace.

This king of device eliminates the pollution due to atmospheric aqueous vapor. On another side, the volume of glass

which can be melted in a single casting does not exceed in most cases 1/10 of the crucible volume. By this method, the preparation of 900 g of glass requires a 2 l crucible. With the same crucible, it can be done 6 kg of glass in the open system.

3. Continuous manufacturing system (figure 6).

It is made of a crucible, with a tiny opening at its bottom, which is continuously fed by the upside. An adequate adjustment of the thermal profile of the furnace gives rise to a continuous flow of droplets of glass through the bottom aperture.

The advantage of this system is the possibility to use a tiny crucible to prepare large quantities of glass. On the other hand, the feeding apparatus gives rise to contaminations which do not exist in the previous systems.

FINING

According to the needs, the glass can be fined, immediately after the fluorides have melted, or stocked to be fined later. In both cases, fining is a critical step of the preparation process. Among the phenomena which occur during fining, we shall retain :

- the oxidation of low oxidized compounds
- evacuation of gas dissolved into the glass
- removing of OH ions
- homogeneization of the melt
- dissolution of the less soluble compounds.

In order to achieve a satisfactory result, the glassmaker has at his disposal the following means : heating treatment, mechanical agitation, controlled atmosphere processing -neutral or reactive (figures 7 and 8), chemical addings Each family of glass, each composition, even each preparation requires a particular fining process.

Let us consider one of the problems the fluoride glass manufacturer faces everyday - OH^- ion removing. It can be achieved when conjugating heating treatment and controlled atmosphere processing. For most of zirconium based fluoride glasses, the OH absorption band can be reduced to less than 1 % of the transmission level. with an accurate thermal process conducted under neutral atmosphere

These fining techniques have already some intrinsic limits which arise from the fundamental properties of the glass and the fining conditions :

- evacuation of remaining gases can be done only at very high temperature and this is paid by a degradation of the glass with the departure of sublimated ZrF_4 ;

- the OH removing process can be schematically represented as follows :

$$XFOH \rightleftharpoons XO + HF$$

Remove an OH^- ion leads to fix an oxygen atom and, therefore, increase the metal-oxygen bonds into the glass

- dissoluting of insoluble compounds can be obtained, for an example, by small amounts of phosphates. The price of this fining is the strong absorption band of the phosphate and its overtones.

CASTING

A simple manner to extract the glass from the crucible is to pour it in a metallic or graphite mold. During pouring, the glass is exposed to atmosheric humidity. The hydrolysis reaction takes place to the larger an extend the greater the glass surface exposed by unit of time.

The glass poured out licks the inner surface of the crucible, carries away the compounds condensated during the glassmaking process and contributes to pollute the casting with insoluble elements which are nothing more than cristallizing agents.

The extent of these phenomena is naturally linked to the casting temperature. At high temperature, fluoride glasses exhibit two phases : a liquid and a gaseous one. The last acts as a protecting atmosphere which effect is to catch aqueous vapor. At high temperature also the condensed compounds will be carried away more easily with the risk to obtain a non-hydrolyzed but highly cristallized glass.

On the other hand, when pouring is made at low temperature, the first glass congeals in the inner surface of the crucible making a protecting film for the following glass. As a counterpart, there is no gaseous phase upon the liquid glass surface which is exposed to hydrolysis with atmospheric aqueous vapor.

All these disadvantages can be avoided when extracting the bulk glass from the crucible. It is easy to do when the crucible is conically shaped. The best results are obtained with platinium-gold alloys which do not damp the glass.

CONCLUSION

Large scale preparation techniques of heavy fluoride glasses have been developed for optical applications. It involves four steps :

1. preparation of the raw materials (purification and fluorination
2. melting
3. fining
4. casting.

According to the product specifications, the fluoride glass manufacturer will choose for each step in the manufacturing process the appropriate technique.

Once the glass has been prepared, then starts another story : the manufacturing of optical components : windows, lenses, prisms, beamsplitters ... and optical fibers.

(1) Verres fluorés, Recueil de publications du L.A. 254
Université de Rennes I, 1981

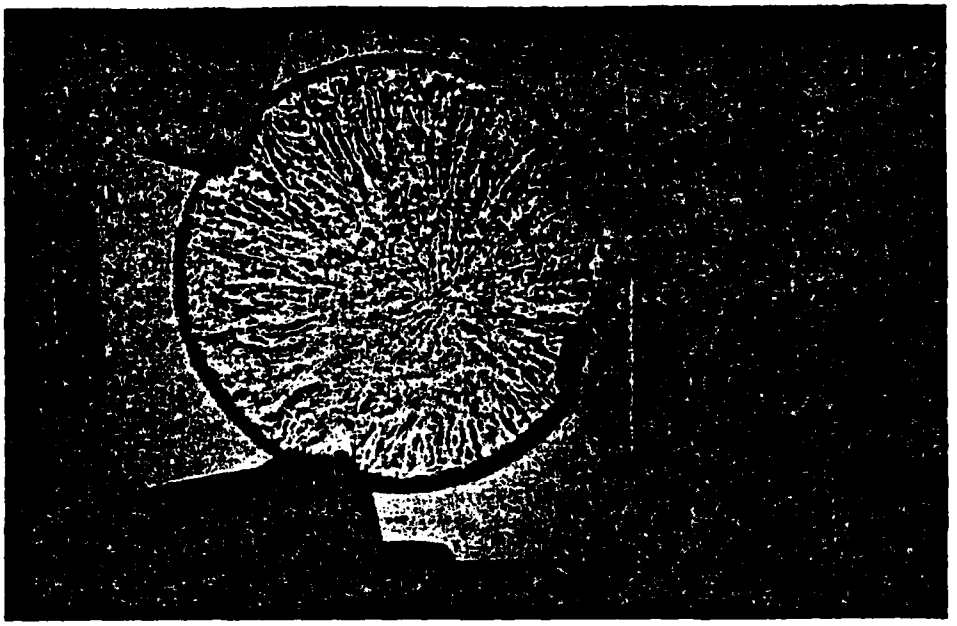

Fig. 1

Shadow of a glass with a large amount of oxyfluorides

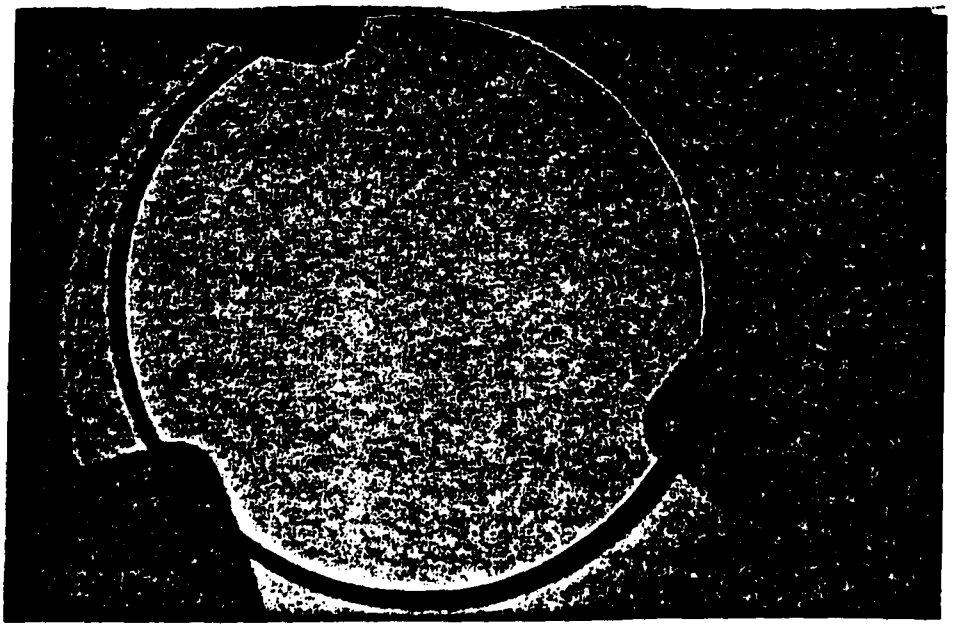

Fig. 2

Shadow of a good optical glass

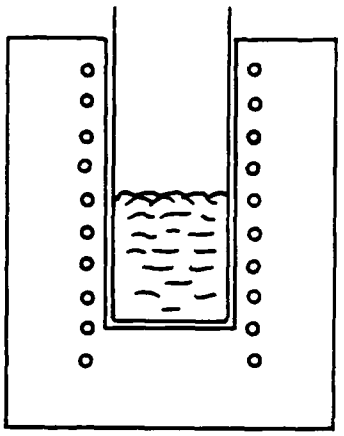

Fig. 3

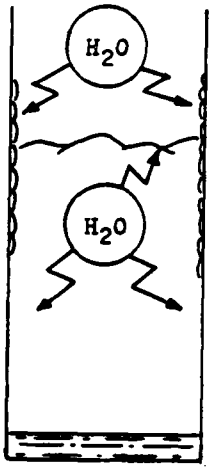

Fig. 4

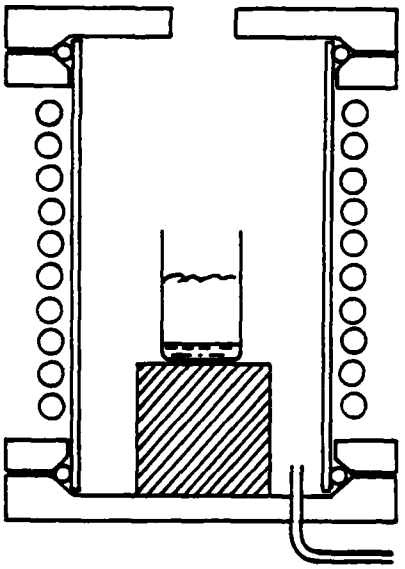

Fig. 5

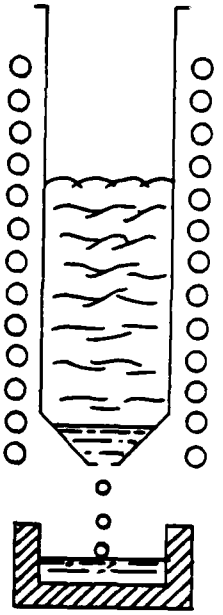

Fig. 6

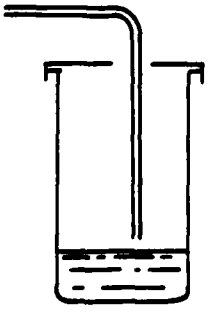

Fig.7

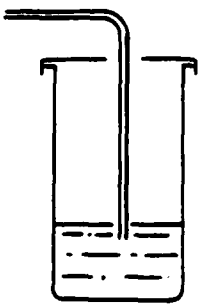

Fig. 8

FLUORIDE GLASS OPTICAL FIBRES

Gwenael MAZE, Vincent CARDIN, Marcel POULAIN
LE VERRE FLUORE
Z.I. du Champ Martin, Vern/Seiche, France

This paper is devoted to the drawing conditions of different fluoride glasses and the ways to achieve large numerical apertures.

Fibre drawing

Four glasses have been chosen according to their thermal properties. Their drawing temperatures ranges from 325 to 540 °C. A zirconium-free glass in the diagram AlF_3-YF_3-ThF_4-BaF_2 diagram offers an exceptional chemical resistance. Their compositions and main properties are given in tables I and II.

These glasses have been prepared with a mixture of oxides and fluorides with ammonium hydrogeno difluoride, heated under neutral atmosphere. The glass has been fined under anhydrous atmosphere.

Pro analysis products were used as starting materials. The Fe content of the glass has been estimated to 12 ppm, the Cu and Ni content 4 ppm.

Rods have been obtained by pouring the glass in a brass mold heated at a temperature next to T_g. The preforms have been obtained according to the method described by HAUSSONNE & al. Rods and preforms diameters were between 8 and 20 mm, their lenght between 5 and 30 cm.

The drawing of the fibres have been made using a hot gas or resistance heating furnace. The drawing speed was kept between 5 and 50 m/min, according to the expected fibre diameter (50 to 200 µm). Step index fibres have been coated with an UV curable resin.

Spectral loss measurements have been made by the cut-back method, using a system composed of an halogen, or blackbody source

a grating monochromator which spectral range lies from 0.5 to 5 µm, a PbS or an InSb detector. The light is focused at the entry of the monochromator, the fibre and the detector by a set of fluoride glass lenses, respectively 55, 25 4 and 9.5 mm in diameter. The signal modulated at 250 hz is detected by a lock-in amplifier. Second order spectrum of the grating monochromator are filtered by a set of 4 long pass filters (Fig. 1)

Numerical aperture

A step index fibre is obtained when starting from two glasses, with refractive index n_1 and n_2. The numerical aperture of the fibre determines the angle of the entry cone :

$$NA = \sqrt{n_1^2 - n_2^2} = n \sin \theta$$

In order to encrease the amount of energy injected in the fibre it is sometimes necessary to encrease θ. This is done by enlarging the difference between n_1 and n_2.

Starting from a multicomponent glass it is possible to obtain a core or a cladding glass by substitution of two elements of the glassy composition. The cladding glass is obtained by encreasing the molar concentration of the less polarizing element. Inversely the core glass is obtained by encreasing the content of the most polarizing element.

This method makes possible to achieve small values of NA. The limitations arises from the small extent of stable glassy areas in multicomponent fluoride glasses. In Fig.2 is represented the glassy area in the diagram ZrF_4-BaF_2-YF_3-AlF_3. The aluminium content lies from 0 to 14 %. But stable glasses can be obtained only between 4 and 8 % of AlF_3. In Fig.3 is plotted the refractive index vs % molar fraction of ZrF_4 and AlF_3. Te greatest numerical aperture corresponding to these limits is 0.12.

Another possibility consist to dope a very stable glass, used as cladding, with a highly polarizing element, PbF_2, for instance, to obtain the core glass. In this case, also, the margin is narrow if we wan to keep a good stability to the core glass.

Starting from two distinc glasses with very different refractive index, a third way consist to adjust their chemical, thermal and mechanical properties in order to get compatible core and cladding. Some glasses cristallise very quickly when they are doped with a very tiny amount of ZnF_2. The association of such a glass with

another containing ZnF_2 will probably lead to a cristallised interface.

Adjustment of thermal expansion and fibre drawing temperature can be done by adjustment of the concentration of the components, mainly alcaline and earth-alcaline elements which have a marked tendency to encrease the thermal expansion of the glass.

Using this method it is possible to obtain stable and compatible glasses,for both core and cladding, with a large numerical aperture. Table III gives an example of a core and cladding glass with a numerical aperture of 0.2.

Conclusion

Various fluoride glasses have been drawn into fibres at temperatures ranging from 325 to 540 °C and a method have been studied in order to obtain large numerical apertures in zirconium based fluoride glass optical fibres.

TABLE I

	ZrF_4	BaF_2	LaF_3	ThF_4	AlF_3	NaF	LiF	CaF_2	PbF_2	YF_3
V 18	53	22	4,2	7,7	0,6	3,4	6,9	0,4	1,8	
ZiBaLaAl	57	34	5		4					
ZiBalNa	52	24			4	20				
AlYThoBa		20		22,5	28,75					28,75

TABLE II

	n_d	d	T_g	T_c	T_d	T_m	$\alpha\ 10^{-6}\ K^{-1}$
V 18	1,527	4,54	282	408	380	490	165
ZiBaLaAl	1,519	4,54	320	392	390	510	168
ZiBalNa	1,498	4,36	257	325	325	493	201
AlYThoBa	1,487	5,10	446	554	540	710	147

TABLE III

	ZrF_4	BaF_2	LaF_3	AlF_3	PbF_2	NaF	YF_3	n_d
Core	60	30	3,5	2,5	4			1,525
Cladding	56	28	3,5	5		4,5	3	1,511

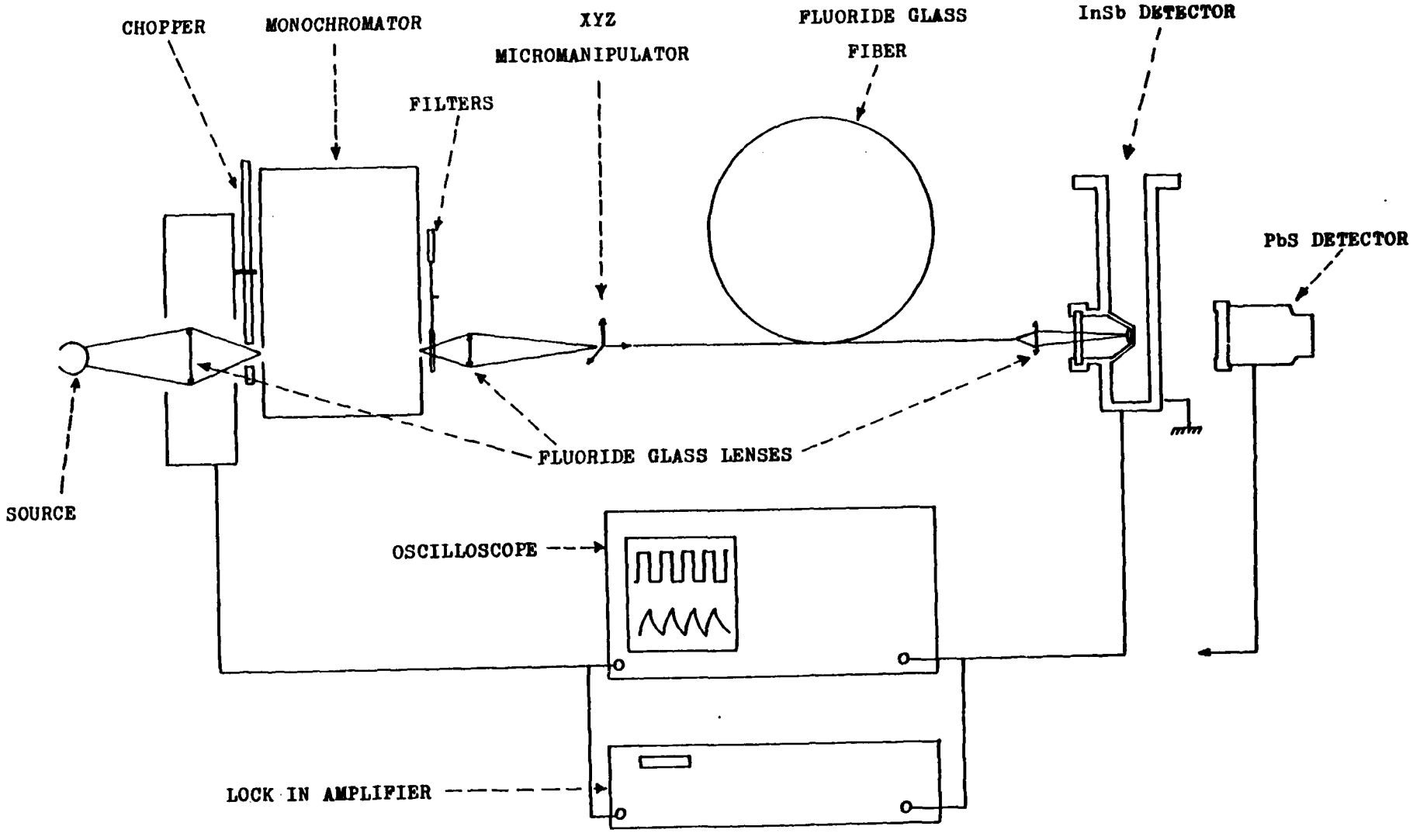
CHOPPER
MONOCHROMATOR
XYZ
MICROMANIPULATOR
FILTERS
FLUORIDE GLASS
FIBER
InSb DETECTOR
PbS DETECTOR
FLUORIDE GLASS LENSES
SOURCE
OSCILLOSCOPE
LOCK IN AMPLIFIER

Fig. 1

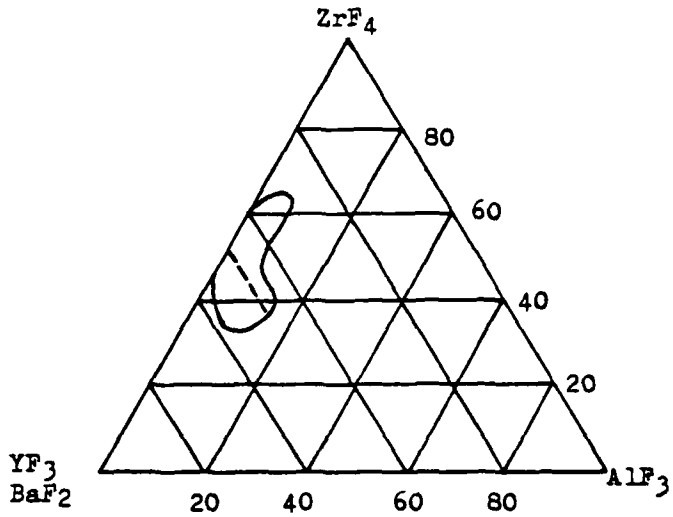
ZrF4
80
60
40
20
YF3
BaF2
20
40
60
80
AlF3

Fig. 2

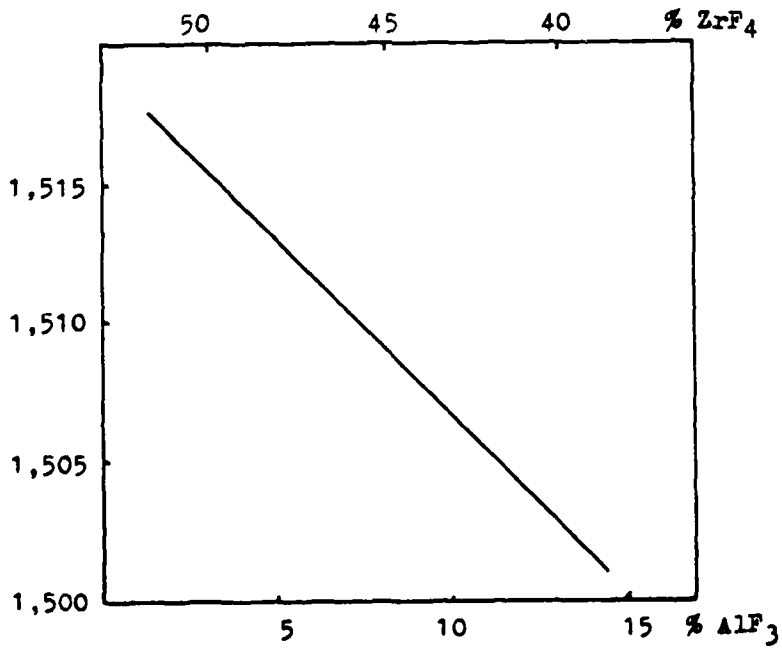
50
45
40
% ZrF4
1,515
1,510
1,505
1,500
5
10
15
% AlF3

Fig. 3

Extended Abstract

DISSOLUTION OF FLUOROZIRCONATE GLASSES

by

T.A. McCarthy and C.G. Pantano
Department of Materials Science and Engineering
The Pennsylvania State University
University Park, PA 16802

Fluoride glasses are finding applications in fields where traditional oxide glasses cannot be used. One of the limiting factors in the development of these glasses is their poor chemical durability. Therefore, it is advantageous to understand the mechanism of dissolution of fluorozirconate glasses.

The kinetics and pH dependence of dissolution have been investigated. A ZBLA glass of composition $0.57ZrF_4 \cdot 0.36BaF_2 \cdot 0.03LaF_3 \cdot 0.04AlF_3$ was examined. The dissolution rates were measured in solutions of constant pH= 2,4,6,8 and 10. The high pH solutions were made with ammonium hydroxide and de-ionized water. The lower pH solutions were maintained with HF acid. The corrosion solutions were analyzed periodically for the ions of interest.

During leaching in low and intermediate pH solutions, there is an initial preferential release of fluorine into the solution. Later, however, the solution reaches a composition whose cation to fluorine ratio is stoichiometric with the glass. This is illustrated in Figure 1. For a corrosion solution of pH= 2, the dissolution of the glass is nearly congruent. In de-ionized water, the glass dissolves nearly congruently; the deviation from congruent dissolution is due to the slower release of La into the solution as shown by the solution analysis data. At pH= 10, the glass is relatively insoluble. Although the pH decreases from an initial value of 10 to 8.5, no detectable Al, Zr or La concentrations are found in the solution. Small amounts of Ba and F are leached from the glass at high pH.

AD-A144 269 EXTENDED ABSTRACTS INTERNATIONAL SYMPOSIUM ON HALIDE GLASSES (2ND) RENSSE..(U) RENSSELAER POLYTECHNIC INST TROY NY DEPT OF MATERIALS ENGINEE.. C T MOYNIHAN 3/4

UNCLASSIFIED 02 AUG 83 N00014-83-G-0091 F/G 11/2 NL

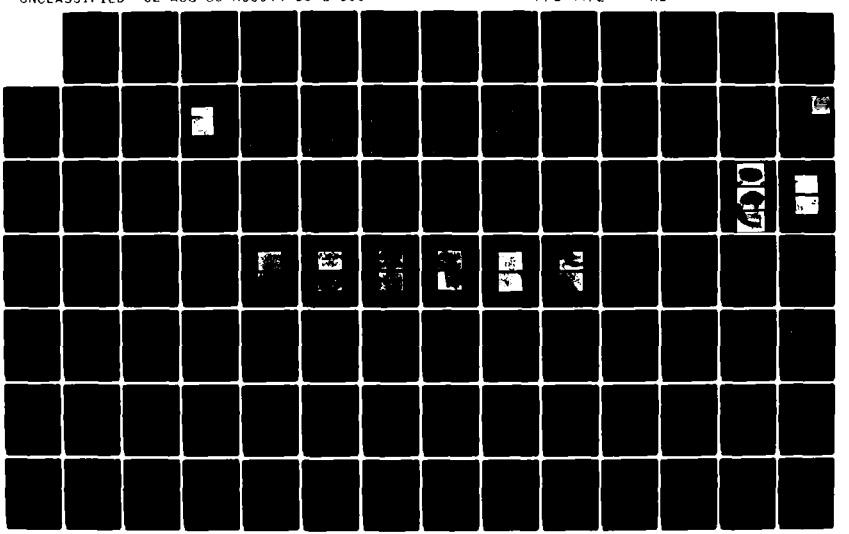

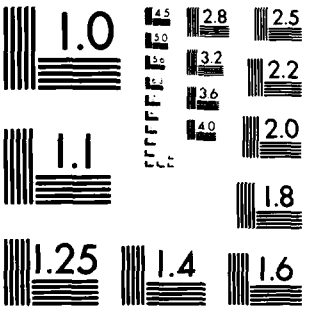

MICROCOPY RESOLUTION TEST CHART
NATIONAL BUREAU OF STANDARDS 1963-A

A decrease in pH is observed during leaching of a ZBLA glass regardless of the initial pH of the solution. This suggests an exchange between the hydroxyl species in solution and fluoride species in the glass. Yet at high pH where the hydroxyl ion concentration is high, little or no dissolution is observed. At low pH the glass dissolves at a high rate. Very often, the crushed glass specimens are transformed into a hydrated crystalline material. It is implied that these hydrates, which form either on the glass surface or as a precipitate in the solution, are insoluble at high pH and soluble at low pH.

The dissolution reaction can be represented as:

$$H_2O + F^- \text{ (glass)} \longrightarrow HF + OH^- \text{ (glass)}.$$

Since the pH decreases as hydroxyls are consumed in the reaction, it is desirable to determine dissolution kinetics at constant pH. Constant pH measurements enable the determination of the reaction rate and reaction order according to the relation:

$$\frac{dC}{dT} = \frac{SA}{V}\left\{k_{\text{dissolution}} a_{H^+}^{\ n} - k_{\text{precipitation}}\right\}$$

where C is the concentration, SA and V are the surface area and volume of the glass and a_{H^+} is the activity of the H^+ ion. The pH by definition is the $\log\{a_{H^+}\}$. The $k_{\text{precipitation}}$ term can be eliminated by considering only short time dissolution.

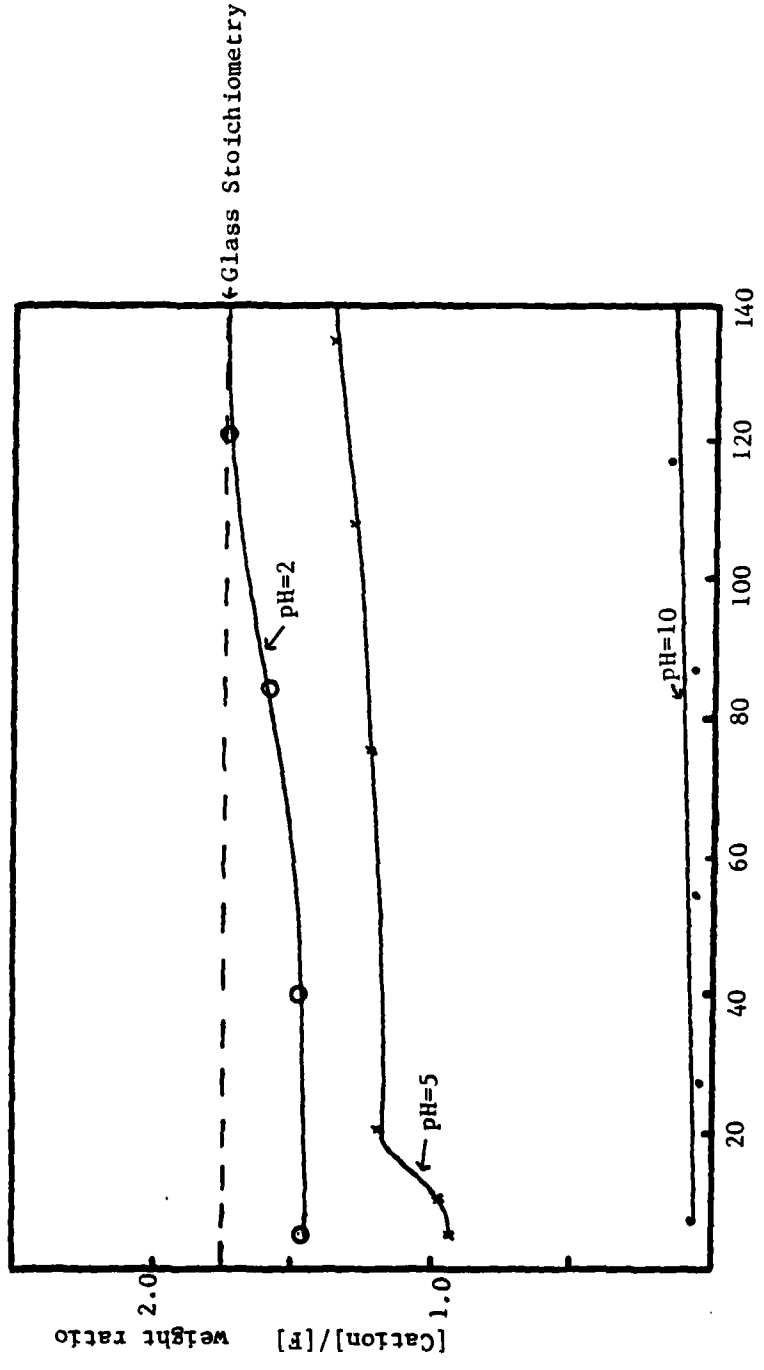

Figure 1: The [cation]/[F] weight ratio in the corrosion solution versus time in minutes for various pH solutions at 60 degrees c.

Mechanical Properties of Heavy Metal Fluoride Glasses

J. J. Mecholsky
Sandia National Laboratories
Albuquerque, N. M. 87185

We measured the microhardness, density, modulii of elasticity, Poisson's ratio, stress corrosion susceptibility, fracture strength and toughness of fluoride based glasses. A systematic change in composition of heavy metal fluoride glasses containing yttrium or ytterbium demonstrated that compositions can be optimized for mechanical properties. These glasses are mechanically superior to fluorozirconates and fluorohalfnates. The toughness in fluoride based glasses ranges from 0.2 to 0.5 $MPam^{1/2}$. The elastic modulus and (Vickers) hardness varied between 5.5 to 7.5 x 10^4 MPa and 200 - 350 Kg/mm^2 , respectively. At this time it is not clear what combinations of structural changes will result in improved mechanical properties. Some generalities can be made in the context of these limited experiments. Additions of aluminum to the basic fluorohalfnates (HBL, HBLA) and fluorozirconates (ZBL, ZBLA) tended to increase slightly the hardness and toughness. Increased barium in barium-thorium-zinc-ytterbium glasses tended to increase the hardness, modulus, and toughness.

In general, the silicate based glasses have higher elastic modulii, hardness and toughness than the fluorides. However, silicates are not suitable for applications requiring mid-infrared transparency. Most fluoride based glasses are mechanically superior to the simpler compounds of the infrared transmitting chalcogenide glasses (i.e., S, Se, As_2S_3 and As_2Se_3).

The stress corrosion susceptibility (n) was measured by the identation technique, delayed failure of flexure bars and stressing rate (between 0.1 - 20 MPa/s) fracture of fibers. A high n value indicates resistance to stress corrosion.

The fluoride glasses tested seemed to fall in two categories; the first had an $n \approx 10$ to 12, the second exhibited little or no slow crack growth. The glasses that had no OH^- band as indicated by infrared spectroscopy exhibited no slow crack growth by the indentation technique. There were some compositions with varying amounts of OH^- also exhibiting no crack growth. Other fluoride glasses, both with and without aluminum, exhibited growth of the indentation cracks, however, there did not seem to be any correlation with OH^- content. Delayed failure of flexure bars indicated the same type of "n" behavior for presumably similar compositions of the ZBLA and HBLA glasses. This indicates that the fluorides are sensitive to minor chemical variations with regard to their stress corrosion susceptibility. Thus, there is hope to find compositions that are resistant to slow crack growth due to stress corrosion.

There was no effect of stressing rate on the fracture stress of alkali-fluorozirconate fibers. This implies little or no susceptibility to stress corrosion. However, it could also mean that the degradation that occurs, does so relatively rapidly after exposure to air and reaches a steady state corrosion rate. It is important to understand the interaction of corrosion and stress corrosion in these glasses before long term lifetime predictions are made. Future experiments will have to control the atmosphere after fabrication and before testing.

Projections for the potential strength of infrared transmitting fluoride based glass fibers are promising. The ultimate, theoretical strength can be estimated from the fracture toughness value (~ 0.5 MPa $m^{1/2}$) to be approaching 10,000 MPa. Coatings for protecting the fiber from moisture have to be developed to obviate the stress corrosion potential. In fiber production, attention to the purity and protection of the preform or melt is the key to mechanically superior fibers. However, in order to understand and predict the mechanical behavior of these glasses, it will be necessary to combine the results of structural determinations, corrosion measurements, optical measurements, and fracture analyses.

MANY RESEARCHERS CONTRIBUTED TO THIS WORK

M.G. DREXHAGE & O.H. EL-BAYOUMI	RADC
A.J. BRUCE & C.T. MOYNIHAN	RPI
J. LUCAS & M. POULAIN	U. OF RENNES
B. BENDOW	BDM CORP.
D.C. TRAN	NRL
J. LAU & J.D. MACKENZIE	UCLA

NOMENCLATURE

GLASS SYSTEM	PRINCIPAL CONSTITUENTS	DESIGNATION
FLUOROZIRCONATES & FLUOROHALFNATES	$\begin{Bmatrix} ZrF_4 \\ HfF_4 \end{Bmatrix}$ BaF_2 LaF_3 $\begin{Bmatrix} AlF_3 \end{Bmatrix}$	ZBL, ZBLA HBL, HBLA
Ba/Th FLUORIDES	BaF_2 ZnF_2 $\begin{Bmatrix} YF_3 \\ YbF_3 \end{Bmatrix}$ ThF_4	BZYT BZYbT

COMPOSITION AFFECTS PROPERTIES

	Fracture Toughness (MPa $m^{1/2}$)		
	Water	Air	Oil
18B 29Z 29Yb 29T	0.26 ± .01	0.27 ± .01	0.31 ± .01
10B 30Z 30Yb 30T	0.26 ± .01	0.28 ± .01	0.30 ± .02
15B 28Z 28Yb 28T	0.31 ± .01	0.32 ± .01	0.36 ± .01

B = BaF_2; Z = ZnF_2; Yb = YbF_3; T = ThF_4

ADDITION OF BaF_2 TENDS TO INCREASE TOUGHNESS

Composition	Fracture Toughness (MPa $m^{1/2}$)		
	Water	Air	Oil
13B 29Z 39Y 29T	0.26 ± .01	0.28 ± .01	0.27 ± .02
10B 30Z 30Y 30T	0.29 ± .01	0.29 ± .01	0.31 ± .01
17.5B 28Z 28Y 28T	0.26 ± .01	0.28 ± .01	0.33 ± .01
15B 28Z 28Y 28T		0.34 ± .01	0.32 ± .01
20B 27Z 27Y 27T	0.30 ± .01	0.33 ± .02	0.38 ± .01

B = BaF_2
Z = ZnF_2
Y = YF_3
T = ThF_4

MODEST IMPROVEMENTS ARE POSSIBLE WITH COMPOSITION CHANGES

	Fracture Toughness ($MPa\ m^{1/2}$)	Hardness (kg/mm^2)	Elastic Modulus ($MPa \times 10^4$)
ZBL	0.25 ± 0.05	288 ± 3	
ZBLA	0.31 ± 0.08	267 ± 4	5.5
BZYbT	0.32 ± .01	276 ± 5	7.0
BZYT	0.33 ± .02	290 ± 2	6.7

ZBL = $62ZrF\ 33BaF_2\ 5LaF$

ZBLA = $57ZrF\ 36BaF_2\ 3LaF\ 4AlF$

BZYbT = $15BaF_2\ 28.3ZnF_2\ 28.3\ YbF_3\ 28.3ThF_4$

BZYT = $20BaF_2\ 26.7ZnF_2\ 26.7YF_3\ 26.7\ ThF_4$

PROJECTIONS FOR IMPROVEMENT ARE PROMISING

PROPERTY	CONDITION	VALUE
Stress Corrosion Susceptibility, n	Chemical treatments or Coatings	99
Fracture Toughness	Bulk (Composition)	0.5 MPa $m^{1/2}$
Strength (maximum)	Fibers	9700 MPa

CONCLUSIONS ARE BASED ON OPTIMISTIC VIEWPOINT

I. Mechanical Properties can be optimized &predicted
- cooperative research is the key to understanding.

II. Surface has to be protected from moisture

III. Prospects look promising

K_{Ic} ➡ 0.6 $MPam^{1/2}$
S_{th} ➡ 10,000 MPa
n ➡ 99

Fracture Analysis of Fluoride Glass Fibers

J. J. Mecholsky, Sandia National Laboratories, Albuquerque, NM
J. Lau and J. D. Mackenzie, U. of California, Los Angeles, CA
D. Tran, Naval Research Laboratory, Washington, DC
B. Bendow, BDM Corporation, Albuquerque, NM

Alkali-fluorozirconate glass fibers were broken in tension, in air (25-50%rh) at room temperature. The purpose was to compare the failure characteristics with those in chalcogenide- and silicate-based fibers. Examination of the fracture surfaces of the fluoride fibers suggest that all failures originated at the surface (Figure 1). The fracture stress, σ, ranged from ~30 - 580 MPa depending on the size of the critical crack, c. The well known characteristic fracture features known as mirror, mist, hackle and crack branching were observed on these fibers. These features help in determining the source of failure and fracture stress. The mirror constants ($\sigma r_j^{1/2}$) where r_j is the radius from the origin of fracture to the beginning of the mist (j = 1), hackle (j = 2) or crack branching (j = 3) region, were determined to be M_1 = 1.6 + 0.4 MPa $m^{1/2}$, M_2 = 1.7 $\pm$ 0.5 MPa$^{1/2}$ and M_3 = 1.8 $\pm$ 0.5 MPa $m^{1/2}$. These values should be considered preliminary data and only used for estimates of fracture stress. Much more data are needed before these constants are established with certainty. Recall that we assume that $\sigma r_j^{1/2} = M_j$. Although this relationship is valid for silica fibers, evidence suggests that it may not be valid for chalcogenide based fibers. More fracture data are needed on bulk fluoride glasses in order to extend the σ-r_j relationship over an order of magnitude in stress for fluoride based glass.

The fracture toughness, or resistance to rapid crack propogation, may also be estimated from the size of the fracture initiating crack, c, and the fracture stress, σ : $K_{IC} = 1.24 \sigma \sqrt{c}$, where K_{IC} is the critical stress intensity factor (or fracture toughness), from which we obtain K_{IC} ~0.5 MPa $m^{1/2}$. This is slightly higher than we obtained for bulk glasses ($\approx$0.35 MPa $m^{1/2}$). There are several possible reasons for the difference. (1) Residual (compressive) stress could be present on the surface of the fiber in which case the actual tensile fracture stress would be lower and thus K_{IC} would be lower. (2) Errors in the measurement of the critical crack sizes (~1μm) on the fibers could result in higher K_{IC} values. (3) The composition differences between the fiber and bulk glasses could make a difference in K_{IC}. At this time it is impossible to determine which is the correct reason for the difference or whether they all are correct reasons. We think that the toughness in bulk and fiber should be close in value. We can estimate the theoretical strength of fluoride glass from K_{IC} :

$$\sigma_{th} = \frac{K_{IC}(\text{Fluoride})}{K_{IC}(\text{Silica})} \times \sigma_{th}\ \text{Silica} \approx 9700\ \text{MPa}$$

A comparison of fluoride glass mechanical properties with those of chalcogenides and silicates are given in Table I.

Stressing rate tests of teflon coated fluoride fibers showed that the fracture stress (~ 60 MPa) was approximately constant for a stressing rate between 0.1 - 12 MPa/s. This does not necessarily mean that there is no stress corrosion, but rather that all the moisture effect that occurs, will occur in the first few days. Initial strengths in air measured right after manufacture were ~140 MPa. These fibers were then stress rate tested ~1 month after manufacture and were exposed to moisture during that time. Long term tests are needed to evaluate the stress corrosion degradation of fluoride fibers with coatings. As with silica fibers, water or moisture will eventually degrade the fiber strength even with a good organic coating. Metal or ceramic coatings may be able to protect the surface for long times just as with silica based fibers and should be investigated.

Table I

FRACTURE CHARACTERISTICS OF FIBERS

	Fluoride	Chalcogenide	Silica
K_{IC} ($MPam^{1/2}$)*	0.5 ± .1	.25 ± .03	.72 ± 0.1
σ (MPa) **	400	200	580
σ_{th} (MPa) +	10×10^3	5×10^3	14×10^3

$K_{IC} = 1.24\ \sigma\sqrt{c}$

** is compared at the same crack size (~1μm)

+ Theoretical strength based on fracture toughness values

FRACTURE ANALYSIS OF FLUORIDE GLASS FIBERS

Provides Research & Troubleshooting Tools

J.J. Mecholsky	SNLA
J. Lau & J.D. Mackenzie	UCLA
D.C. Tran	NRL
B. Bendow	BDM Corp.

Figure 1 - Alkali-Fluorozirconate Fiber Fracture Surface.

Origin of fracture shown by arrow.

OUTLINE CONCENTRATES ON STRENGTH AND TOUGHNESS

I. Production & Testing Procedures

II. Fractographic Analysis Of Fibers

III. Stressing Rate Effect on Fracture

IV. Comments , Conclusions & Predictions

FLUORIDE FIBERS APPROACH SILICA IN MECHANICAL PROPERTIES

	Fluoride	Chalcogenide	Silica
K_{Ic} ($MPam^{1/2}$)	0.5	0.25	0.72
S_{avg} (MPa)	400	200	580
S_{th} (MPa)	10,000	5000	14,000

FIBERS AND BULK VALUES COMPARE

	K_{Ic} (MPa $m^{1/2}$)	σ (MPa)	n
Fibers	0.5 (air)	70 to 600	?
Bulk	0.4 (air)	20 to 350	10 to 50

OBSERVATIONS ARE PRELIMINARY TO CONCLUSIONS

I. Moisture Affects Strength (immediately?)

II. Strength Values Related to K_{Ic}

III. Fractography Provides "Free" Information

- provides S_f , C $\longleftrightarrow$ K_{Ic}

PREDICTIONS FOR FIBER FUTURE

ARE BASED ON OPTIMISTIC VIEW & DATA

I. Theoretical Strength Approaches 10,000 MPa

II. "Practical" Strengths $\approx$ 3800 MPa

III. Stress Corrosion Can Be Controlled

CONCLUSIONS

I. Fiber Must Be Protected From Moisture

II. I.R. Fibers Can Be Mechanically Strong

III. Fractography Is Useful For Diagnosis

PROGRESS IN FLUORIDE GLASS FIBER RESEARCH AND DEVELOPMENT IN JAPAN

T. MIYASHITA AND T. MANABE
IBARAKI ELECTRICAL COMMUNICATION LABORATORY
NIPPON TELEGRAPH AND TELEPHONE PUBLIC CORPORATION
TOKAI, IBARAKI 319-11, JAPAN

1. Introduction

This paper reviews the current status of fluoride glass optical fiber development in Japan. Aiming at the attainment of ultra-low loss fibers, fluorozirconate glass systems have been most extensively investigated. Glass composition, material purification, fiber fabrication and optical properties are presented.

2. Fiber Glass Composition

Table 1 lists the typical glass compositions investigated for optical fibers. The most important criterion in the selection of a composition is that it forms a sufficiently stable glass. The compositions listed in Table 1 feature high glass formability, though they are required to be improved for fabrication of homogeneous long fibers.

3. Material Purification

Starting materials are commercially available fluorides of 99.99 percent purity. All these reagents are purified prior to the glass melting(3). Both vapor- and liquid-phase processes could be applicable to purification, and, however, the former seems to be more useful for the present purpose. ZrF_4 and AlF_3 are purified by sublimation in an inert atmosphere of low pressure. On the other hand, BaF_2 and GdF_3 are purified by sublimating out impurity fluorides. Such sublimation is found to be considerably effective in reducing transition metal impurities(Table 2).

4. Fiber fabrication

Figure 1 shows the working process for cladded fiber fabrication. The purified materials are weighed and mixed. Core and cladding mixtures are treated with $NH_4F.HF$ at 400 °C for 0.5 h and melted at 900 °C for 2 h in separate gold crucibles. Fiber preforms are obtained by a built-in casting method, specially developed for fluoride glass fiber, which is shown schematically in Fig.2. The preform obtained is jacketed in a Teflon-FEP tube and heated zonally by an electric furnace at a temperature around

350-400 °C. The fiber is wound onto a plstic bobbin at a 20 m/min. drawing speed. Fig.3 shows an interference microscope photograph of a multi-mode fiber cross section. Single-mode fiber is also fabricated. Teflon-FEP cladded fibers are prepared by glass core - Teflon FEP tube technique.

5. Optical Properties

The optical loss spectra are measured in 0.7 - 5.0 μm wavelength range. The measurements are usually made with 20 - 100 m long fibers. Fig.4-a and 4-b show transmission loss spectra for ZrF_4-BaF_2-GdF_3-AlF_3 and ZrF_4-BaF_2-LaF_3-NaF-AlF_3 glass fibers, respectively(4,5). Optical attenuation consists of absorption and scattering. The large peak at 2.9 um is assigned to the OH fundamental stretching vibration. The broad band in 0.7 - 2.5 μm wavelength range is assigned to impurity absorption by extrinsic transition metals such as Fe^{+2} and Cu^{+2}, as is shown in Fig. 4-a. The increase in the longer wavelength region than 3.6 um is due to glass matrix vibrational absorption.

Imperfections such as bubble, micro-crystal and phase separation produce rather wavelength-independent scattering loss, which is observed in 1.0 - 2.5 μm wavelength range in Fig. 4-b. Up to now, the minimum loss of 8.5 dB/km is obtained at 2.1 μm for ZrF_4-BaF_2-GdF_3-AlF_3 glass fiber(4).

Material dispersion characteristics are also investigated. The fluoride glasses exhibits zero material dispersion at 1.5 - 1.7 μm and a gentle slope for the dispersion curve.

Other characteristics such as mechanical strength and chemical durability will be discussed.

References

(1) K. Ohsawa, T. Shibata, K. Nakamura and M. Kimura, 1st intl. sympo. halide and other noneoxide glasses, Cambridge,23-26 March 1982.

(2) S. Mitachi, T. Miyashita and T. Kanamori, Electron. Lett., V.17, No.17, p591, 1981

(3) S. Mitachi, Y. Ohishi and T. Miyashita, J. lightwave Tech., V. LT-1, No.1, 1983.

(4) S. Mitachi, Y. Ohishi and T. Miyashita, presented at IOOC'83, Tokyo, 27-30 June 1983.

(5) T. Shibata, K. ohsawa, K. Takahashi M. Kimura and M. Masuda, to be published.

Table 1 Typical fluoride glass compositions for optical fiber (1, 2)

core	61.0 ZrF_4 - 32.0 BaF_2 - 3.9 GdF_3 - 3.1 AlF_3	
cladding	59.5 " - 31.2 " - 3.8 " - 5.5 "	(mol %)
core	58.0 ZrF_4 - 15.0 BaF_2 - 6.0 LaF_3 - 21.0 NaF - 4.0 AlF_3	
cladding	Teflon - FEP	(molar ratio)

Table 2 Estimated concentration of metal impurities in drawn fibers

	Fe^{+2}	Cu^{+2}	Ni^{+2}	Cr^{+2}
	(ppm)			
fiber with raw materials	0.79	0.81	0.10	0.18
fiber with purifed materials	0.42	0.10	0.16	0.14

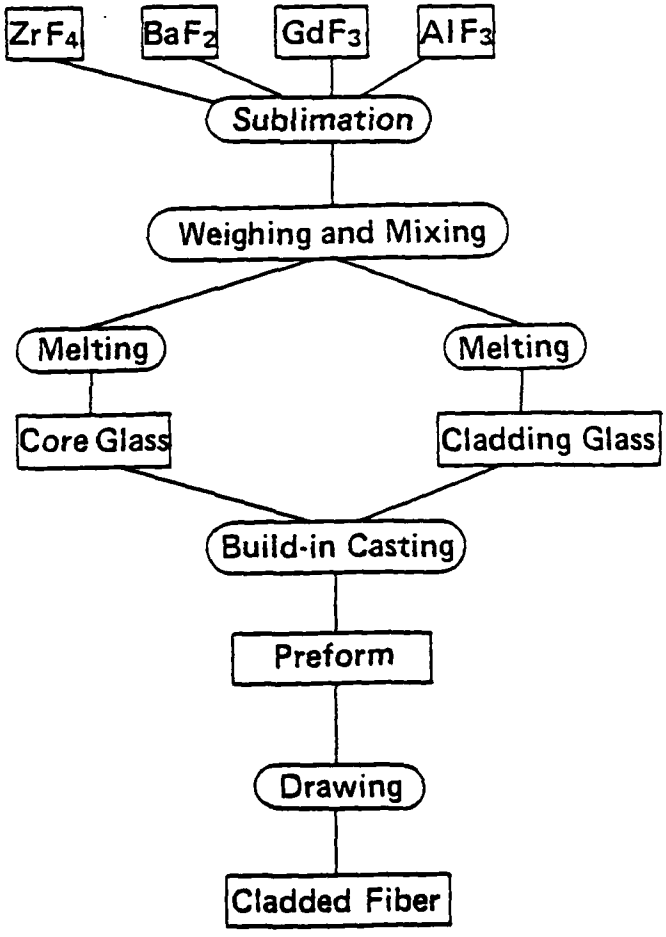

Fig.1 Fluoride glass fiber fabrication process

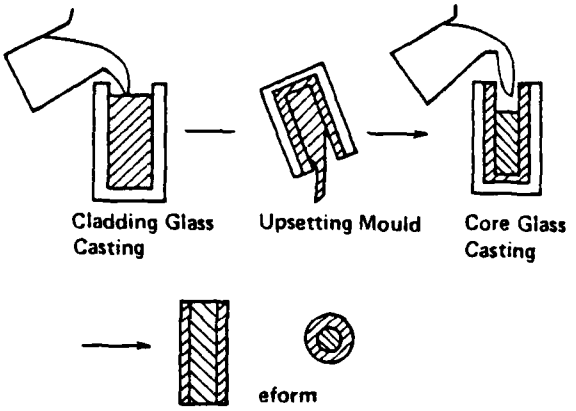

Fig. 2 Preform preparation by casting the core into the cladding.

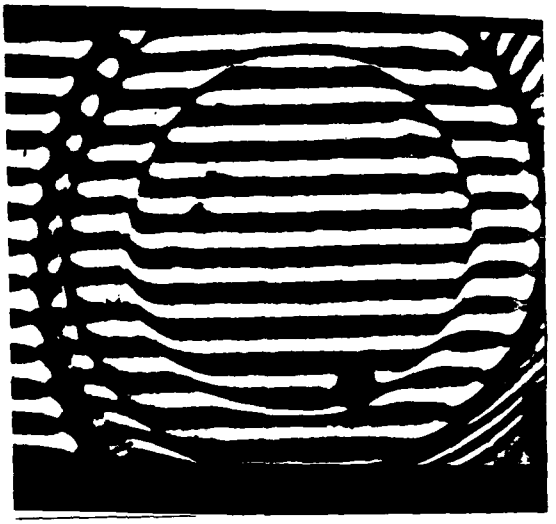

Fig. 3 Interference microscope photograph of fiber cross-section

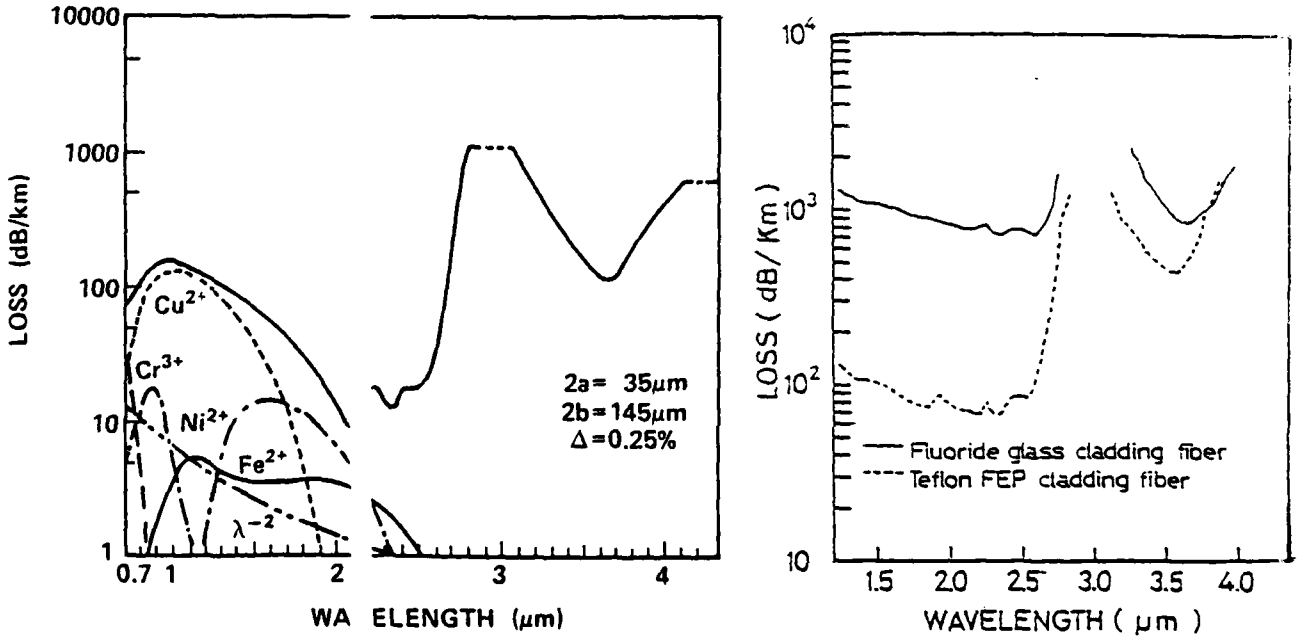

a) (b)

Fig. 4 Transmission loss spectra for fluoride glass fibers
a) ZrF_4-BaF_2-GdF_3-AlF_3 system
b) ZrF_4-BaF_2-LaF_3-NaF-AlF_3 system

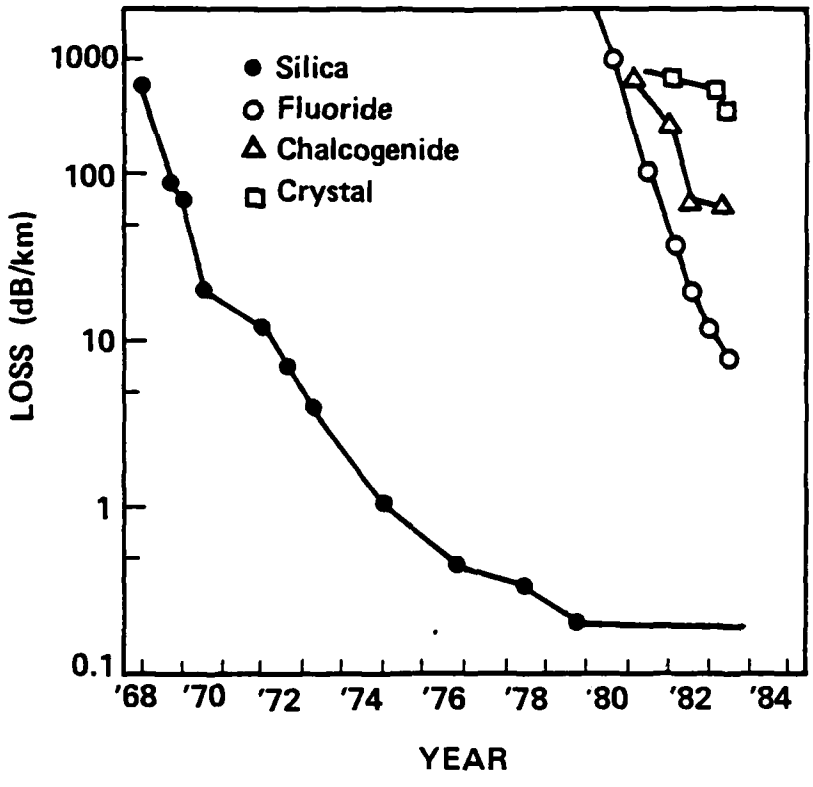

Fig.5 REDUCTION OF OPTICAL FIBER LOSSES

ENVIRONMENTAL EFFECTS ON THE STRENGTH OF FLUORIDE GLASS FIBERS*

by

Alana M. Nakata, John Lau and John D. Mackenzie

Department of Materials Science and Engineering

University of California, Los Angeles

Extended Abstract

for

Second International Symposium on Halide Glasses

August 2-5, 1983

Rensselaer Polytechnic Institute

Troy, New York

* This work is being supported by the Directorate of Chemical and Atmospheric Sciences, Air Force Office of Scientific Research.

Extended Abstract

It is well-known that moisture can adversely affect the strength of oxide glasses. It is also known that fluorozirconate glasses are, in general, less chemically durable than silicate glasses. Thus it appears that the surface of fluoride glass fibers must be adequately protected from the ambient atmosphere for long term applications. Teflon FEP has been considered as a possible protective cladding for fluorozirconate glass fibers. This paper is concerned with the effect of a humid atmosphere on the tensile strength of one type of fluorozirconate glass fiber.

Fluoride glass fiber of about 100-170 μm in diameter and cladded by Teflon FEP were drawn by a preform method. One lot of such fiber was stored in a dry-box with less than 10ppm H_2O. Another lot was stored in 100% humidity atmosphere at room temperature for periods up to two weeks. Figure 1 is a comparison of the average strengths of these fibers. The maximum strengths of freshly drawn fiber of about 150 μm diameter were as high as 100,000 p.s.i. These values compare favorably with those of some silicate fiber of the same diameter. There is no doubt that the strengths of fluoride glass fibers decreased significantly in the wet atmosphere. Apparently, Teflon FEP is not an effective protecting material. Table 1 shows that water can permeate fairly rapidly through Teflon FEP and that a monolayer of water can be formed on the fiber in less than 5 minutes. Scanning electron micrographs were obtained on stripped fibers and confirmed that deterioration of the glass surface had occurred.

Water Permeability of Teflon FEP Resin

Calculations were based on the use of a 135 μm diameter fluoride fiber with a 25.4 μm teflon cladding thickness.

Area of water molecule	~0.44 $\AA^2$ (4.4×10^{-21} m^2)
Surface area of 1 meter length of fiber	4.2×10^{-4} m^2
Number of water molecules required to form monolayer on the surface of the fluoride fiber	~9.5×10^{16} molecules (2.9×10^{-6} grams)
Permeability constant* of Teflon FEP resin at 23°C	1.4 g/ m^2/ 24hrs (9.7×10^{-4} g/ m^2/ min)
Rate of permeation of water vapor through 25.4 μm teflon cladding	6.9×10^{-7} g/ min
Time to form monolayer on fluoride fiber surface	~4.2 minutes

*Journal of Teflon, 11(1), 8(1970).

TABLE 1

Strength vs. Time

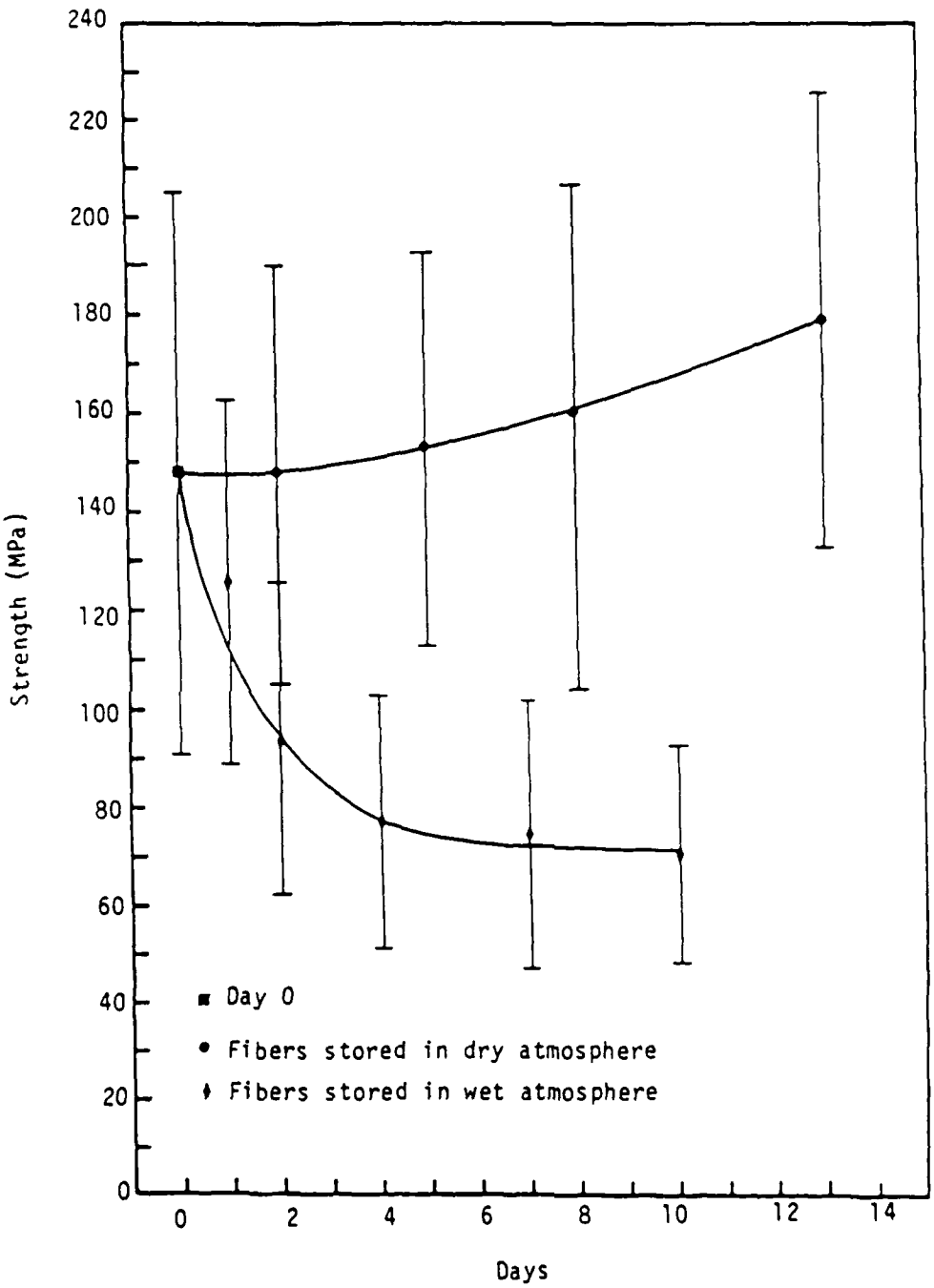

FIGURE 1

CRYSTALLIZATION OF $ZrF4_4$-BaF_2-LaF_3-AlF_3 GLASS

G. F. Neilson, G. L. Smith and M. C. Weinberg

Jet Propulsion Laboratory
Applied Mechanics Division
California Institute of Technology
4800 Oak Grove Drive
Pasadena, California 91109

ABSTRACT

Fluoride glasses based upon ZrF_4 and HfF_4 exhibit excellent optical transmission behavior from the near-UV to the mid-IR region, and they are attractive candidates for fiber optic materials. However the usefulness of such fluoride glasses for this application may be limited by their short working range and their tendency to readily crystallize or at least develop small crystallites during glass formation. Hence, detailed crystallization studies of these glasses would be useful to help surmount such difficulties.

In a previous study we examined the isothermal crystallization behavior at 370°C of a ZBLA glass having the nominal composition in mole percent of $57ZrF_4$-$36BaF_2$-$3LaF_3$-$4AlF_3$. Herein we report the results of a more extensive study of crystal nucleation and growth in glasses of this same nominal composition. In particular, the nature of the crystallization behavior and the crystal products formed in this ZBLA glass at lower temperatures as a function of the initial glass condition will be discussed. The principle experimental tools employed in this study include powder x-ray diffraction (XRD), scanning electron microscopy (SEM), optical microscopy (OM), differential thermal calorimetry (DTA) and electron microprobe analysis.

The measurements were made on heat-treated cubes cut from two glass bars (1 and 2) formed and quenched under only slightly differing conditions. For glass 1 on which DTA measurements were made, Tg was approximately 285°C, and crystallization peaks were noted at about 360° and 390°. For both glasses heat treatments were done as a function of time at temperatures of 320°, 355° and 370°C. Cubes having pristine surfaces, cut surfaces or ground surfaces were heat treated to determine if surface condition affects surface crystallization behavior. XRD analysis was done on entire and ground heat-treated cubes to identify and determine relative amounts of crystal species forming internally and/or at the surface. Internal and surface morphological detail and variation were measured on ground and polished specimens with both OM and SEM. In this manner, an estimate of nucleation frequency and crystal growth rate could be made of crystallites observed to be forming internally and randomly within these glasses at the two lower temperatures studied.

The morphological structure of the internally forming crystallites was observed to be temperature dependent, but always very different from the crystal morphology of the crystallization products which formed at the surface and grew inwards. By XRD analysis only two crystal species were found to form at 320° and 355°. One crystal phase was positively identified as β-barium fluorozirconate (β-$BaZrF_6$). This phase was tentatively determined to be the crystal phase forming and growing from the glass surfaces. The other crystal species was also identified from its XRD pattern as the low temperature α modification of this composition (α-$BaZrF_6$), whose crystallites form internally within the glasses, perhaps by a homogeneous nucleation mechanism. The initial internal crystallite concentration and rate of crystallization were both found to be much larger in glass 2 than in the similarly prepared glass 1, which is interpreted as support for the above tentative conclusion.

CRYSTALLIZATION OF ZrF_4 - BaF_2 - LaF_3 - AlF_3 GLASS*

G. F. NEILSON
G. L. SMITH
M. C. WEINBERG

JET PROPULSION LABORATORY
CALIFORNIA INSTITUTE OF TECHNOLOGY
PASADENA, CALIFORNIA

*THIS STUDY WAS SPONSORED BY THE OFFICE OF SPACE SCIENCE AND APPLICATIONS OF THE NATIONAL AERONAUTICS AND SPACE ADMINISTRATION (NASA-OSSA).

OBJECTIVES OF STUDY

1. STUDY MORPHOLOGICAL DETAILS OF CRYSTALLIZATION PRODUCTS AND DETERMINE NATURE OF CRYSTALLINE PHASES FORMED AT DIFFERENT TEMPERATURES DURING ISOTHERMAL HEAT TREATMENTS OF ZBLA GLASS.

2. STUDY CRYSTALLIZATION PROCESSES AT THESE TEMPERATURES WITH RESPECT TO BOTH SURFACE AND INTERNAL CRYSTAL DEVELOPMENT.

3. OBTAIN CRYSTALLITE NUCLEATION AND GROWTH RATE INFORMATION.

4. DETERMINE EFFECT OF GLASS SURFACE CONDITION ON SUBSEQUENT CRYSTALLIZATION BEHAVIOR.

PREPARATION OF GLASSES 1 AND 2

1. THEORETICAL COMPOSITION (WEIGHT PERCENT) -

   56.8 ZrF_4 - 37.6 BaF_2 - 3.5 LaF_3 - 2.0 AlF_3.

2. BATCH AMOUNT (GLASS 1 AND 2)

   50g + 5.6g $NH_4F \cdot HF$.

3. MELTING CONDITIONS (GLASS 1 AND 2) - UNDER DRY N_2 + CCl_4 ATMOSPHERE, HEATED FROM RT TO 850°C IN 130 MIN. PLUS 30 MIN. AT 850°C.

4. COOLING TIME AFTER POURING -

   GLASS 1 - 60 SEC.
   GLASS 2 - 90 SEC.

5. SLAB WEIGHT / DIMENSIONS

   GLASS 1 - 45.6g / 5.0 X 3.7 X 0.63 CM
   GLASS 2 - 46.7g / 5.0 X 3.7 X 0.64 CM

6. COLOR OF GLASS -

   GLASS 1 - YELLOW
   GLASS 2 - COLORLESS

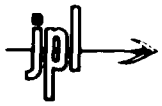

METHODS OF APPROACH

1. 57 ZrF_4 - 36 BaF_2 - 3LaF_3 - 4AlF_3 GLASS BARS CUT INTO ONE cm CUBES WITH OPTIONAL SURFACE TREATMENT.

2. CUBES HEAT TREATED FOR VARIOUS TIMES TO PROMOTE ONLY PARTIAL CRYSTALLIZATION AT TEMPERATURES OF 320°C, 355°C AND 370°C.

3. INTERIORS AND SURFACES OF HEAT TREATED CUBES STUDIED BY MEANS OF OPTICAL MICROSCOPY AND POWDER X-RAY DIFFRACTION.

4. QUANTITATIVE CRYSTAL NUCLEATION AND GROWTH RATE DETERMINATIONS MADE ON INDIVIDUAL GLASS CUBES GIVEN SUCCESSIVE HEAT TREATMENTS BETWEEN MEASUREMENTS.

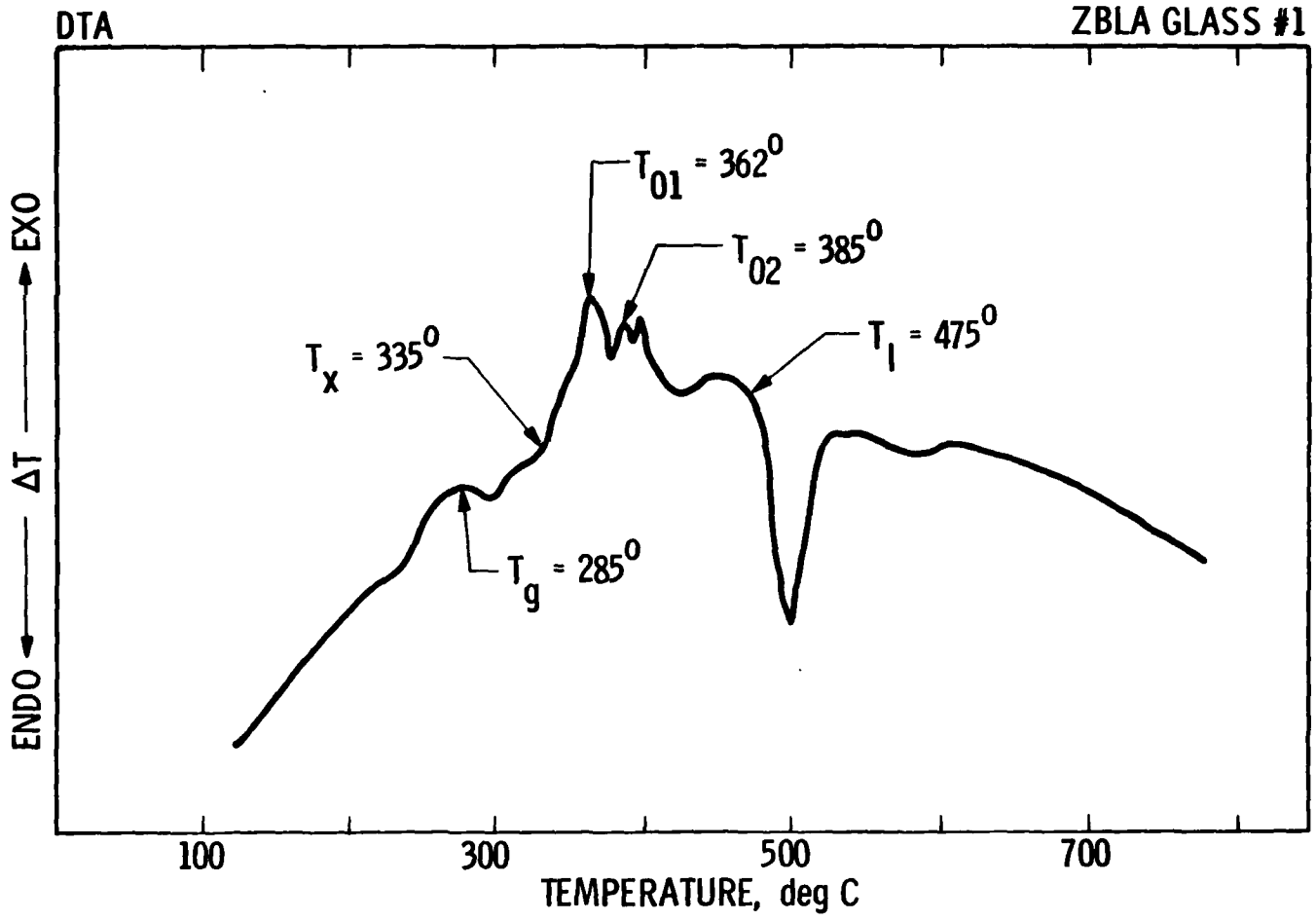
DTA
ZBLA GLASS #1
$T_{01} = 362^0$
$T_{02} = 385^0$
$T_x = 335^0$
$T_l = 475^0$
$T_g = 285^0$
ENDO ← ΔT → EXO
100
300
500
700
TEMPERATURE, deg C

GLASS #1

NO HEAT TREAT

GLASS #1

355°C - 15 MIN

GLASS #2

355°C - 15 MIN

GLASS #1

GLASS #2

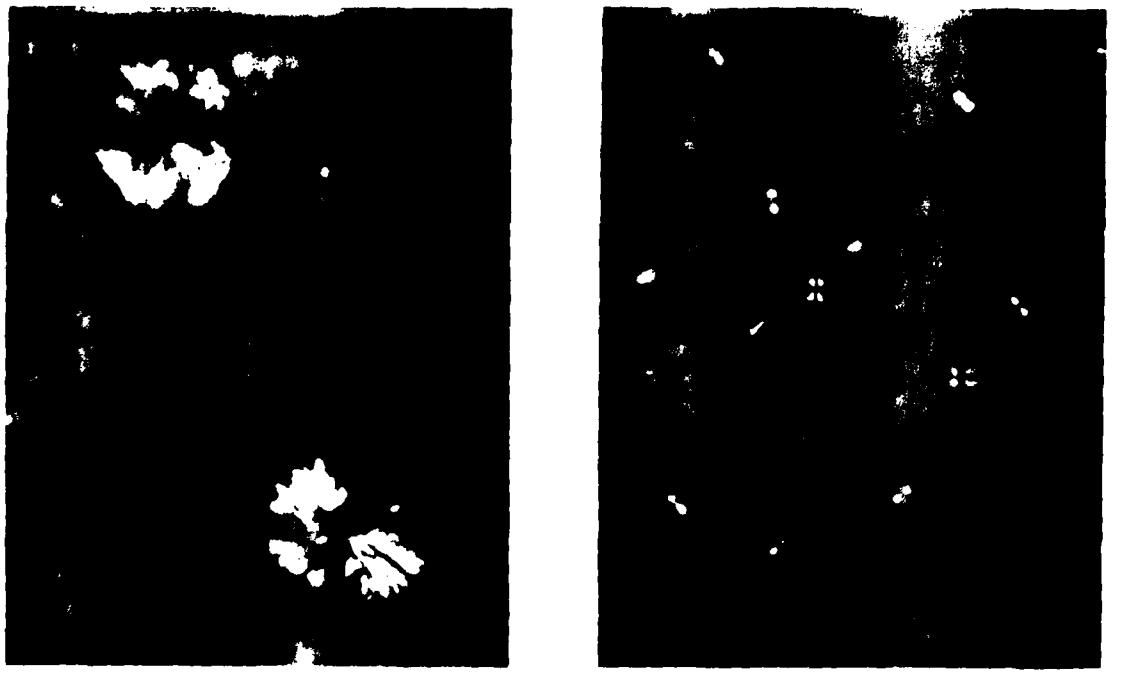

NO HEAT TREAT

MAG = 240 X

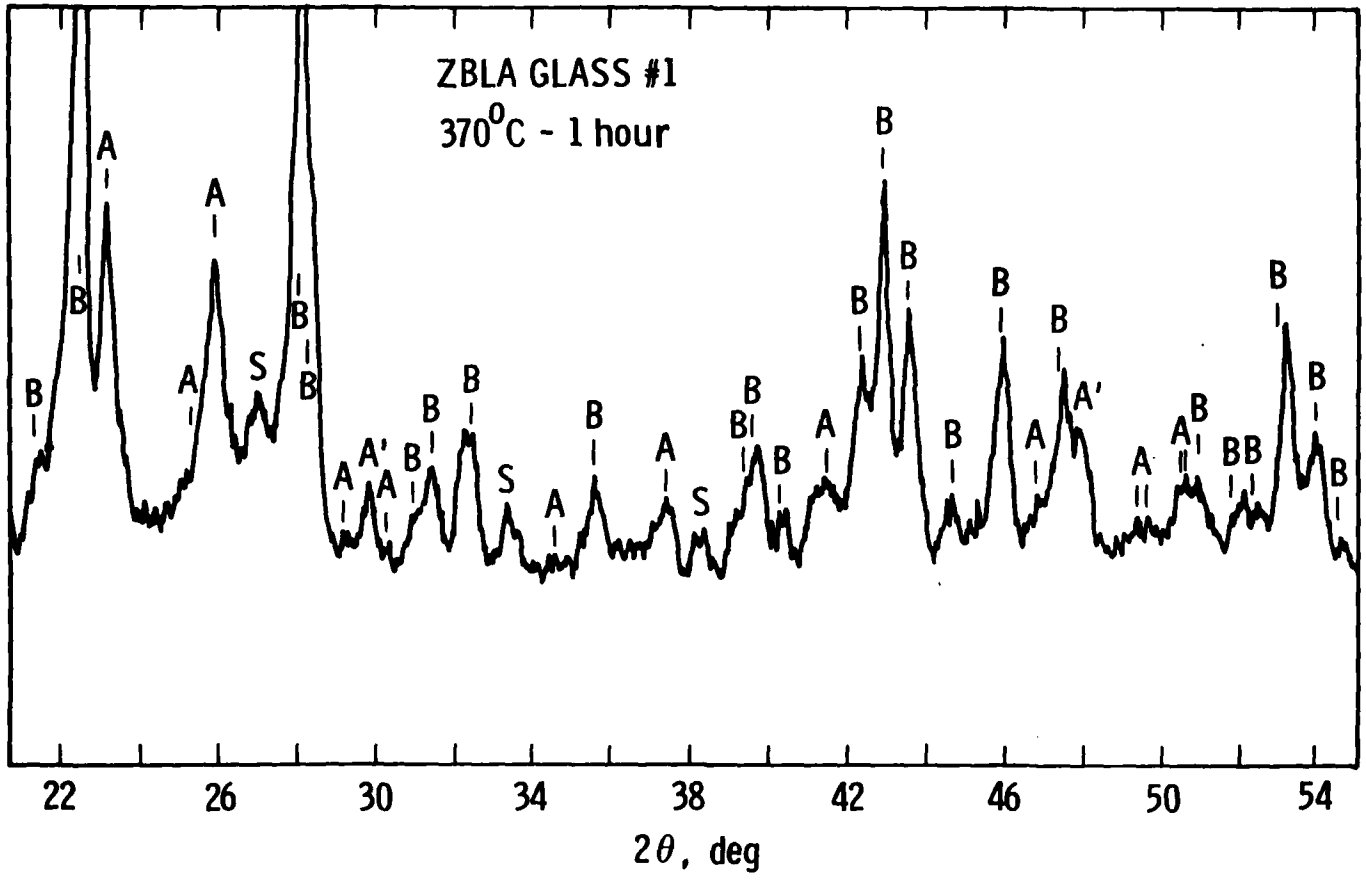
ZBLA GLASS #1
370°C - 1 hour
22
26
30
34
38
42
46
50
54
2θ, deg

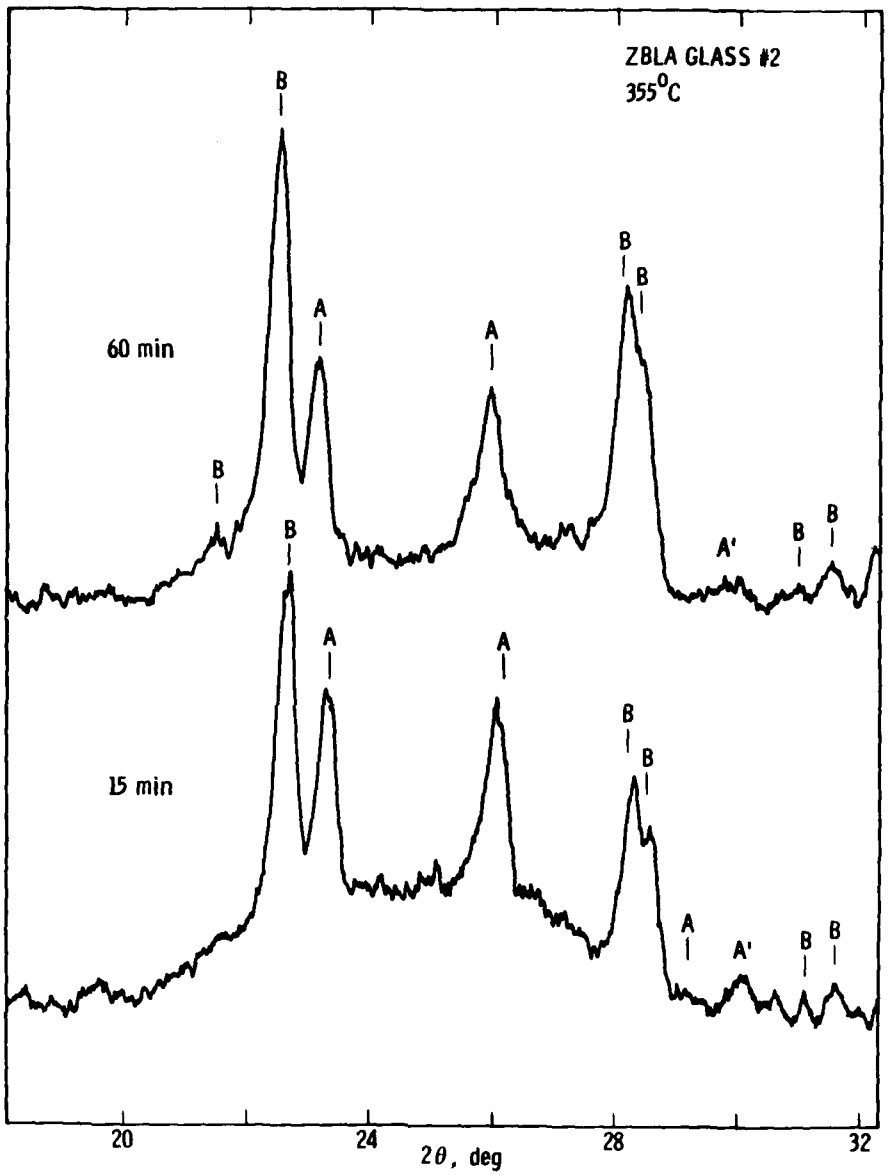
ZBLA GLASS #2
355°C
60 min
15 min
B
A
A'
20
24
28
32
2θ, deg

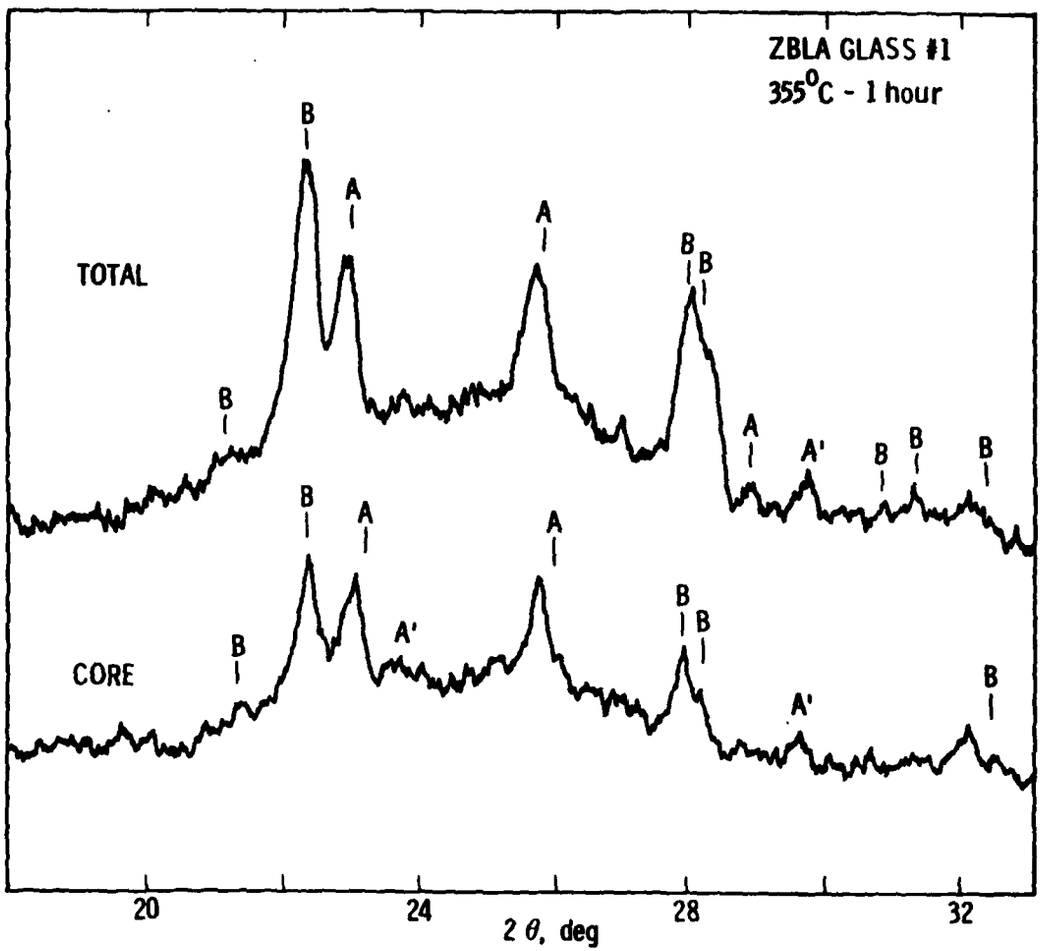
ZBLA GLASS #1
355°C - 1 hour
TOTAL
CORE
B
A
A'
20
24
28
32
2 θ, deg

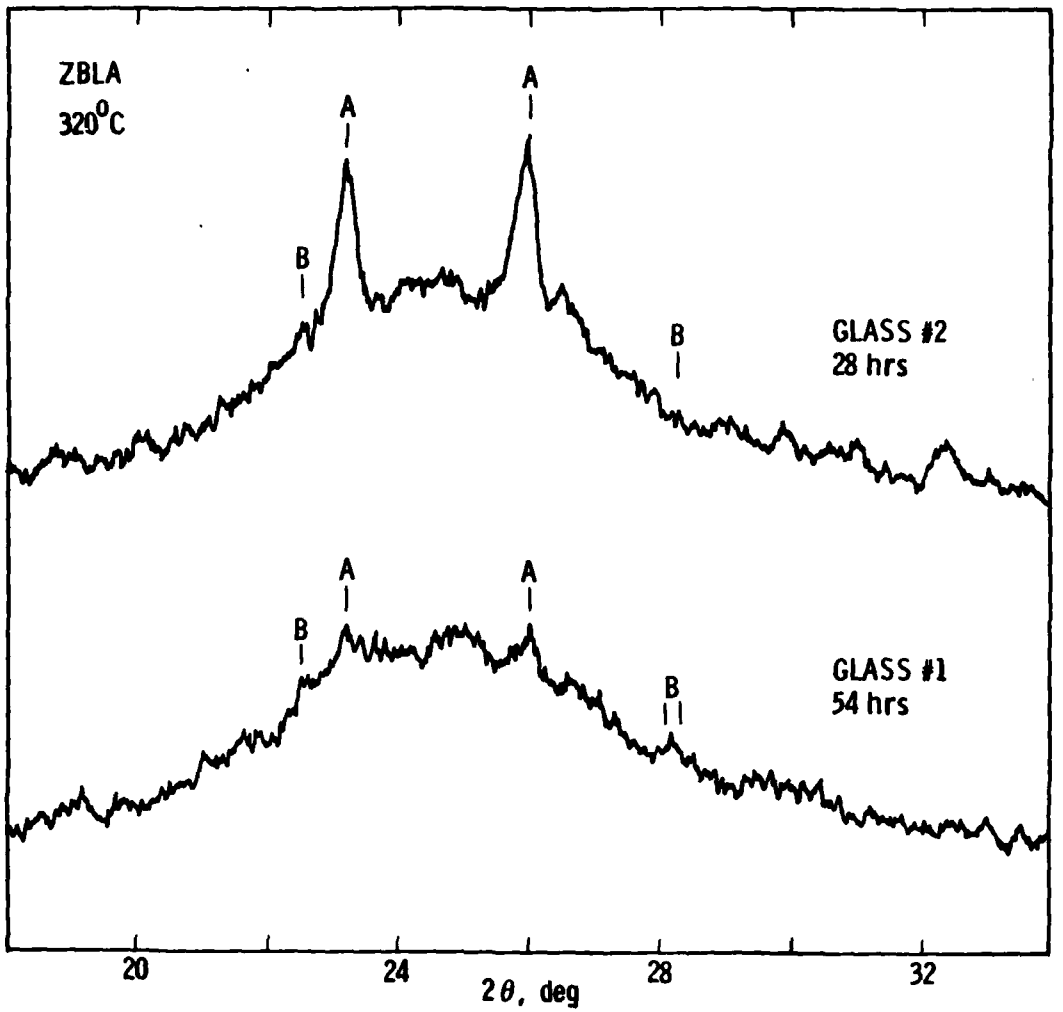
ZBLA
320°C
A
A
B
B
GLASS #2
28 hrs
A
A
B
B
GLASS #1
54 hrs
20
24
28
32
2θ, deg

GLASS #1

MAG = 43 X

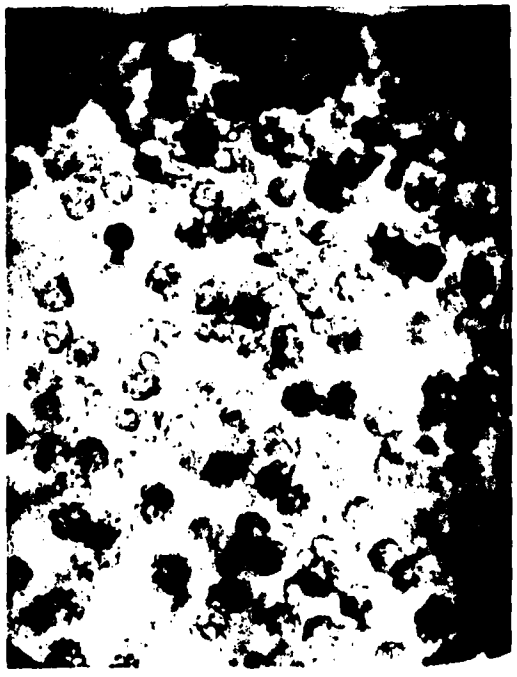

54 HOURS

320°C

112 HOURS

GLASS #1

MAG = 102 X

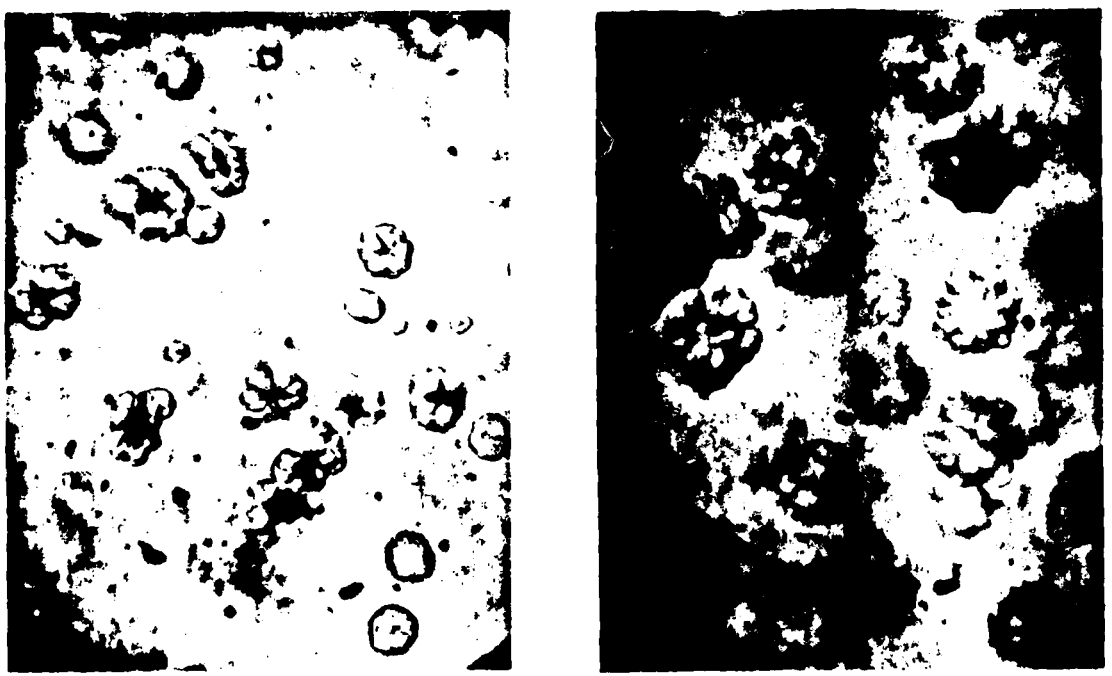

54 HOURS

320°C

112 HOURS

GLASS # 1 MAG = 240 X

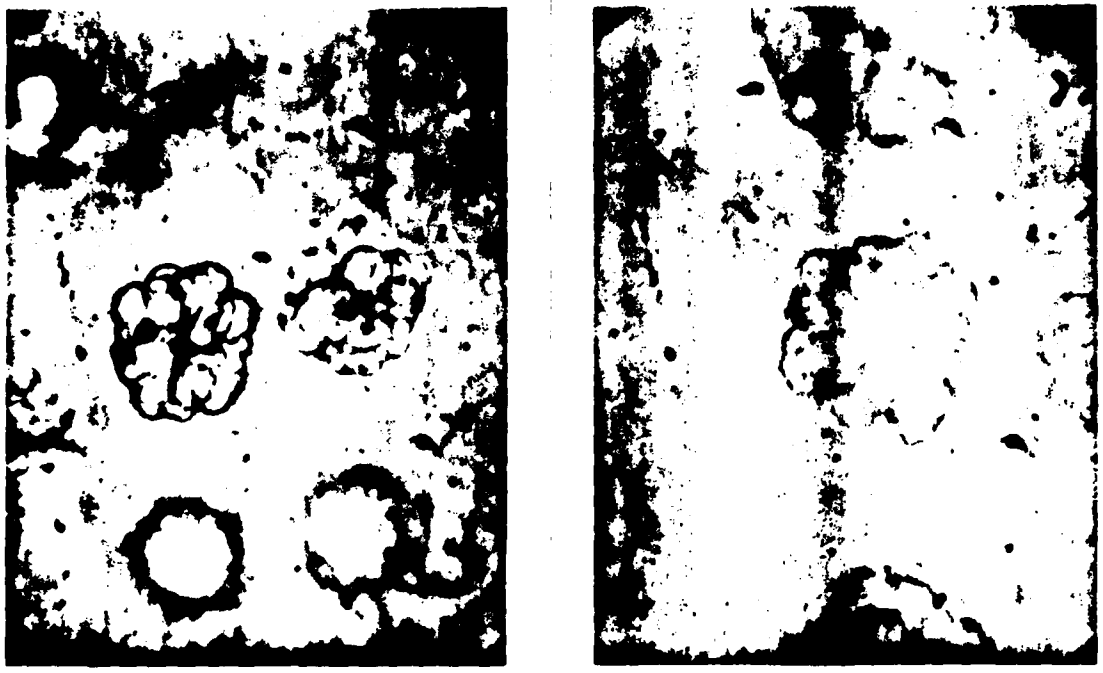

54 HOURS 320°C 112 HOURS

GLASS #2

MAG = 102 X

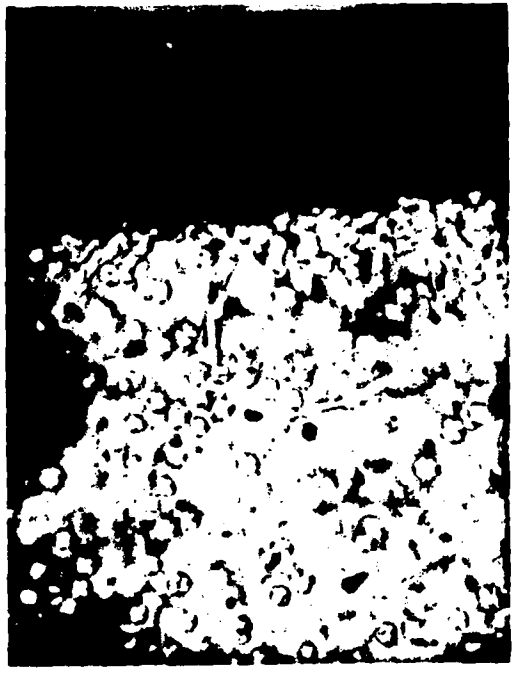

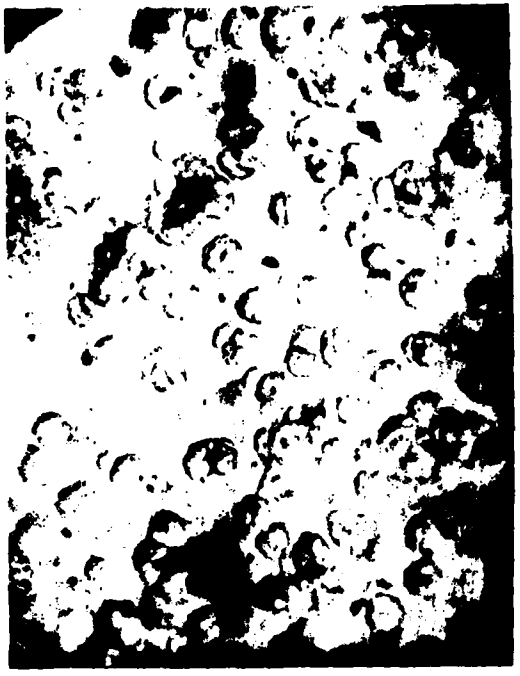

8 HOURS

320 C

28 HOURS

GLASS # 1

$355^{o}C$ - 15 MIN

MAG = 43 X

MAG = 240 X

GLASS #1

355°C - 15 MIN

MAG = 43 X

MAG = 600 X

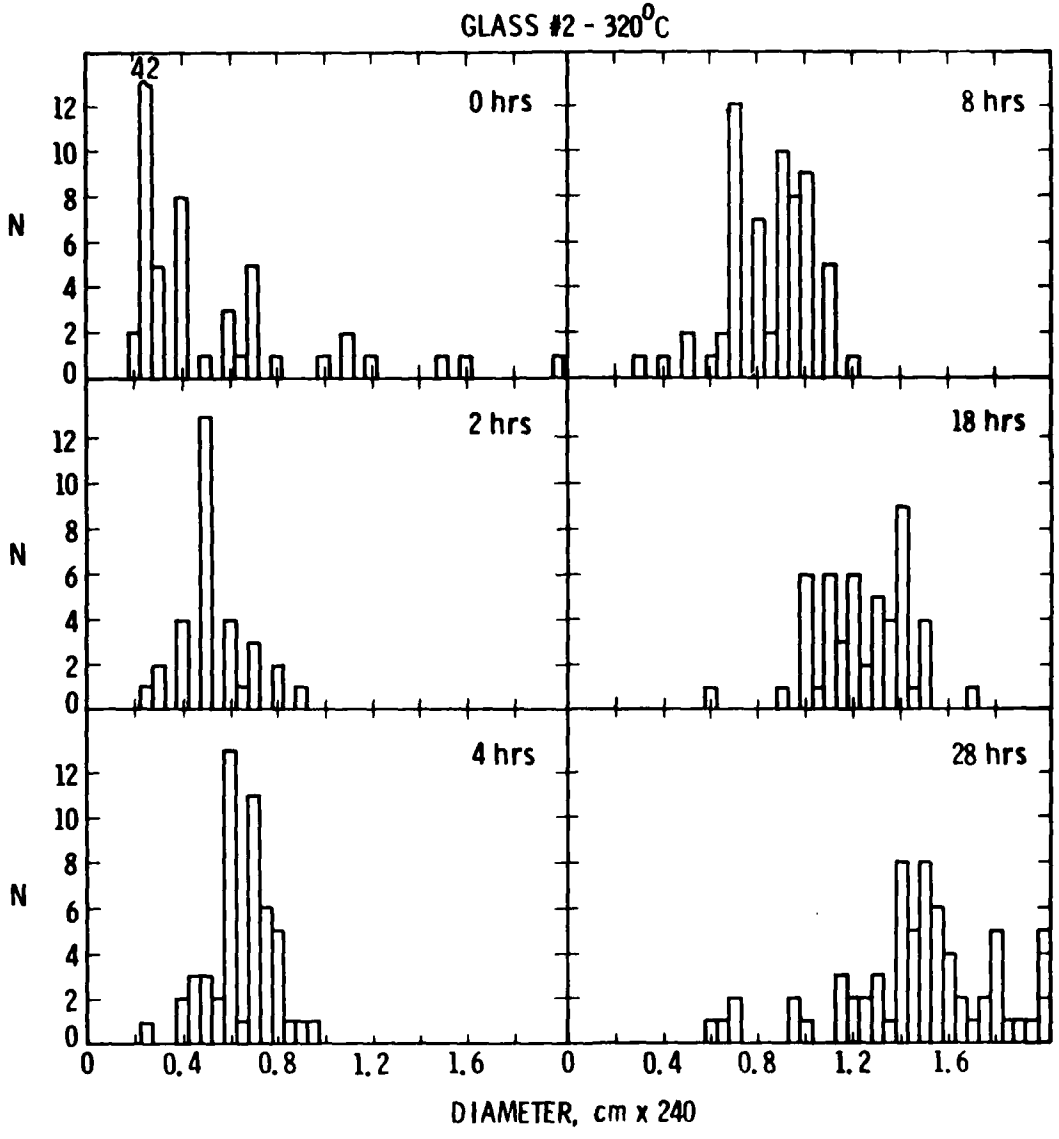
GLASS #2 - 320°C
42
0 hrs
8 hrs
2 hrs
18 hrs
4 hrs
28 hrs
N
0
2
4
6
8
10
12
0
0.4
0.8
1.2
1.6
DIAMETER, cm x 240

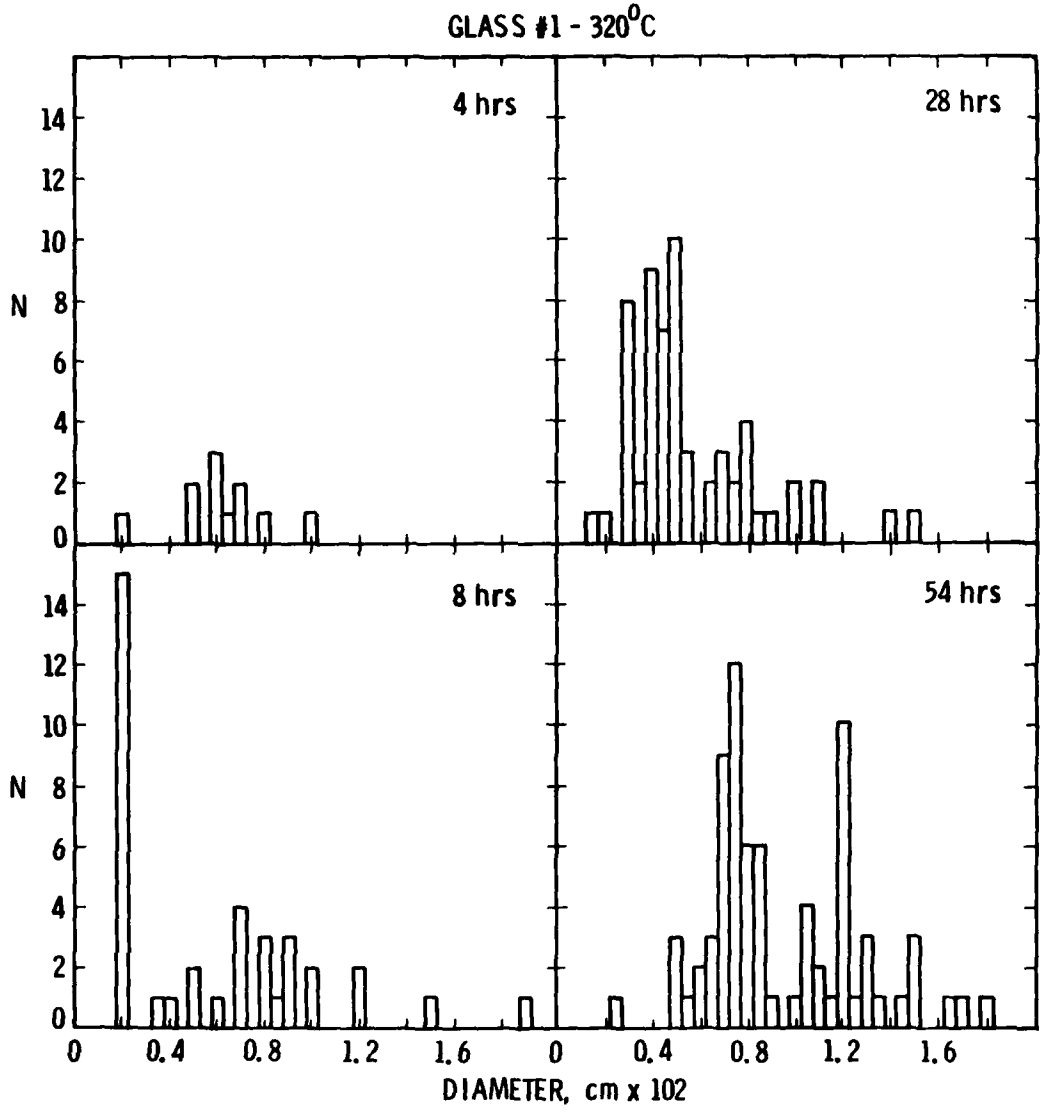
GLASS #1 - 320°C
4 hrs
28 hrs
8 hrs
54 hrs
N
0
2
4
6
8
10
12
14
0
0.4
0.8
1.2
1.6
DIAMETER, cm x 102

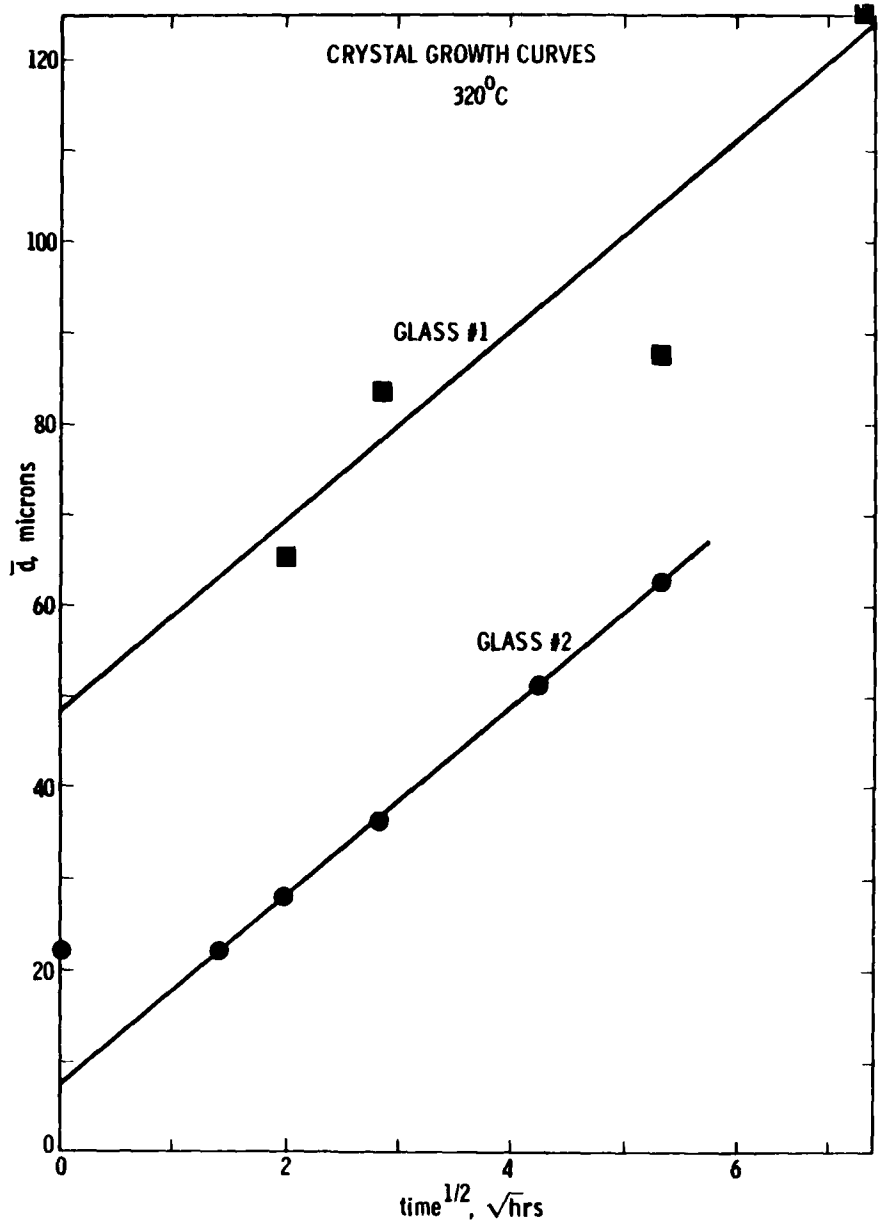
CRYSTAL GROWTH CURVES
320°C
GLASS #1
GLASS #2
$\bar{d}$, microns
time$^{1/2}$, $\sqrt{\text{hrs}}$
0
20
40
60
80
100
120
0
2
4
6

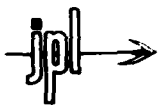

CRYSTALLIZATION RESULTS

TIME-320°C (HOURS)	CRYSTAL VOLUME FRACTION GLASS#1	GLASS #2
2	———	.0051
4	.0074	.015
8	.018	.026
18	———	.058
28	.010	.11
54	.035	———
T_g (°C)	285	285
$T_x - T_g$ (°C)	50	45

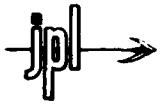

RESULTS

1. CRYSTALLIZATION TENDENCY OF ZBLA GLASS EXTREMELY SENSITIVE TO DETAILS OF GLASS PREPARATION PROCEDURE.

2. SURFACE CRYSTALLIZATION BEHAVIOR NOT SENSITIVE TO CONDITION OF SURFACE.

3. AT ALL TEMPERATURES STUDIED, SAME TWO MAJOR CRYSTALLINE PHASES OBSERVED TO DEVELOP, PLUS ADDITIONAL MINOR PHASE AT 370°C. RATIO OF AMOUNT OF B TO A PHASES INCREASES WITH INCREASING TEMPERATURE.

4. CONTINUOUS INTERNAL CRYSTAL NUCLEATION DURING ISOTHERMAL HEAT TREATMENTS OCCURS IN GLASSES. MORPHOLOGICAL DETAILS OF GROWING CRYSTALLITES ARE TEMPERATURE DEPENDENT.

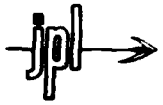

CONCLUSIONS

1. INTERNAL CRYSTAL NUCLEATION OCCURS ON A VERY SHORT TIME SCALE AND OVER A RANGE OF TEMPERATURE DURING THE INITIAL GLASS QUENCH.

2. PHASE FORMED BY SURFACE CRYSTALLIZATION IS PREDOMINANTLY β - $BaZrF_6$. ACICULAR OR WORM-LIKE GROWTH OF THIS PHASE FROM THE SURFACE TO THE GLASS INTERIOR OCCURS.

3. CONTINUOUS INTERNAL NUCLEATION OF CRYSTALLITES HAVING α - $BaZrF_6$ STRUCTURE OCCURS. GROWTH OF THESE CRYSTALLITES IS DIFFUSION CONTROLLED.

4. THE INTERNAL CRYSTALLITE CONCENTRATION MAY HAVE A BIMODAL PARTICLE SIZE DISTRIBUTION WHOSE SHAPE CHANGES DURING HEAT TREATMENT. THIS REFLECTS NUCLEATION AND GROWTH AT DIFFERENT TEMPERATURES.

STRUCTURE OF HEAVY METAL FLUORIDE GLASSES

Marcel POULAIN

Université de Rennes, Campus de Beaulieu
Chimie Minérale B, L.A. C.N.R.S. n° 254
Avenue du Général Leclerc - 35042 RENNES CEDEX (France)

INTRODUCTION

The description of glass structures is dominated by the Zachariasen's concepts. In their previous form, they have accounted for most existing glasses. However, the occurence of numerous new vitreous systems -polymers, metal glasses, halide glasses- makes necessary more general formulation of the atomic arrangement in glass (1).

The first condition for glass formation is that the nucleation and crystal growth processes are frustrated during the cooling of the melt (2). Unfortunately, this essential kinetical condition does not result in obvious structural requirements because the mechanisms of ordering and the intermediate states between crystal and glass are not well understood. Therefore, one must keep as a starting basis the Zachariasen's original statement : glass and crystal energy must be comparable although it has been demonstrated that this condition is not sufficient (2).

1. BASIC STRUCTURAL INFORMATIONS

The understanding of glass structures may be achieved by the analysis of convenient physical date (X-rays, neutrons, EXAFS..., spectroscopic measurements). Following Zachariasen, it may be postulated that the interatomic forces in crystal and glass are the same. Therefore, one may expect the same coordi-

nation polyhedra, bond lengths and ionic radii. Indeed, until now, all structural informations agree with this postulate. The usual coordination numbers and bond lengths of the cations entering fluoride glass compositions are given in table 1. As not all atoms are equivalent in glass, deviations from these values may be observed for a few of them as an exception to the general rule. For example, while diffraction studies indicate that the zirconium coordination is around 8, it is conceivable that some Zr % atoms are 6-fold coordinated and lower fractions 5- or even 4-fold coordinated.

Other structural informations arise from computer simulations (3). The chemical formula also gives a relationship between the coordination numbers. A general equation may be written :

$$|y| = |x_i| \; |L_{ij}| \; |\omega_j|$$

where y is the number of anions in the chemical formula M_xF_y

$|x_i|$ is the line matrix $|1xn|$ of the cationic fractions

$|\omega_j|$ is the column matrix of the anionic weights (the inverse of the anion coordination number)

$|L_{ij}|$ is a rectangular matrix characteristic of the structure. Each element L_{ij} is equal to the number of anions from the j^{th} anionic site surrounding the i^{th} cationic site

This equation may be used for crystalline as well as for vitreous structure

2. THE NETWORK MODEL

If we consider any solid, it is possible to locate the cations, then to define the coordination polyhedra with the anions -or alternatively the Voronoi's polyhedra-, and finally to observe the way these polyhedra are linked together. The network model therefore applied for crystals as well as for glasses and various examples may be given (4) : NaCl, NiAs, NbO, ZnO, TiO_2, ReO_3...

The network model is suitable when one type of cation is preponderant, or when the binding energy of the network is higher than that of the other structural elements. For example, the binary glasses ZrF_4-ThF_4 may be described as a random network of ZrF_7, ZrF_8, ThF_8, ThF_9 polyhedra sharing vertices. Binary ZrF_4-BaF_2 glasses consist of Ba^{++} ions trapped into the interstices of the network constructed by the association of the ZrF_8 and ZrF_7 polyhedra.

However, in various systems it becomes more difficult to decide which cations are into the network (vitrifiers") or outside ("modifiers"). Li^+ and Na^+ ions are usually labeled modifiers although their coordination polyhedra are similar to those of Al^{3+}, Zr^{4+} and Th^{4+}. A geometric criterion is therefore difficult to define -in fluoride glasses, the network unit is not constant : tetrahedron, octahedron, dodecahedron-

Another problem arises when the network represents a lower part of the total energy than the rest of the structure. This is the case of the ZnF_2-SrF_2, CdF_2-BaF_2, ThF_3-LiF binary glasses : the single bond strengths Zn-F and Cd-F are lower than Sr-F and Ba-F (5). Finally, the network model would suggest that the glass forming ability decreases with the network connectivity : the polymeric character is lowered and the melt viscosity decreased. In fact, the incorporation of chlorides or phosphates often results in more stable glasses.

In conclusion, the network model cannot be used so extensively for fluoride glasses as for SiO_2-based glasses.

3. THE IONIC MODEL

An alternative structural model for fluoride glasses is that of the random packing of fluorine anions in which cations are inserted into sites corresponding to their usual crystal-chemistry. In order to be non periodic this random packing must not be closed packed and the average F to F coordination is therefore lower than 12. As diffraction studies show that the coordination numbers of Ba^{++} and Pb^{++} are

around 10, one may suggest that this random packing includes both F^- anions and Ba^{++} and/or Pb^{++} cations which is consisten with the important part acted by barium in most fluoride glasses.

If we consider, as an example, the binary glass $Zr_{0.65}Ba_{0.35}F_{3.33}$, the glass structure results from the disordered insertion of zirconium in the packing of F^- and Ba^{2+} ions. The lack of ordering results both from the random structure of the packing and from the excess of available sites for Zr -the number of host sites being proportional to the anion to cation ratio. The above topologic equation shows that the average coordination number (CN) of fluorine is 2.5 (versus cations) assuming C.N. of 7.35 for Zr and 10.7 for Ba (6). Simple electrostatic rules indicate that the interionic distance between higher charge cations is maximized . For a 3-fold coordinated fluorine, this results in a larger value of the Zr-F-Zr angle by comparison to the Zr-F-Ba angle, in agreement with the X-ray scattering studies (150° and 105°).

The observed fluorine concentration expressed as the number of F^- ion.g per cm^3 may be deduced from simple density measurements. It is nearly constant and varies between 80 and 100.10^{-3} ion.g cm^{-3} for most fluoride glasses. The variations depend on cation sizes, and mainly on the smaller one. This high compactness is directly related to the minimization of the coulombic energy and is therefore accounted for by the ionic model.

CONCLUSION

The description of glass structure as a random ionic packing offers several advantages. It may include tetrahedral glasses and suggests some relationships with metal glasses. It accounts for glass formation in complex systems such as polyhalides, oxyhalides, fluorophosphates or ionic salts. Finally, it makes conceivable the occurence of glasses in unexpected system.

REFERENCES

1. A.R. Cooper - J. Non-Cryst. Solids 49, 1 (1982)
2. D.R. Uhlmann - J. Am. Ceram. Soc. 66, 95 (1983)
3. C.A. Angell - First symposium on halide glasses, Cambridge, march 1982
4. A.F. Wells - Structural inorganic Chemistry, Clarendon Press, Oxford (1975)
5. C.M. Baldwin and J.D. Mackenzie - J. Am. Ceram. Soc. 62, 573 (1979)
6. R. Coupé, D. Loüer, J. Lucas and A. Léonard - Ceram. J. in the press (1983)

MIXED HALIDE EFFECT IN FLUOROZIRCONATE GLASSES

Marcel POULAIN and Jean-Luc ADAM

Université de Rennes - Campus de Beaulieu
Laboratoire de Chimie Minérale D, Laboratoire Associé au C.N.R.S. n° 254, Avenue du Général Leclerc - 35042 RENNES CEDEX (France)

INTRODUCTION

Early experiments showed that fairly large amounts of chlorine (1) or heavier halides (2) could be incorporated in fluorozirconate glasses. However, no systematic investigation has been carried out on the resulting changes of the glass forming ability and the physical properties. This paper focuses on the variation of the optical transmission range in relation with the chlorine content in chloro-fluoride glasses.

1. BIHALIDE GLASSES IN THE SYSTEMS ZrF_4-BaF_2-NaCl-LaF_3 AND ThF_4

The incorporation of NaCl was carried out into the standard fluorozirconate glasses ZBL and ZBT.

ZBT	0.575 ZrF_4	0.338 BaF_2	0.087 ThF_4
ZBL	0,62 ZrF_4	0,30 BaF_2	0.08 LaF_3

Linear composition rules were defined :

a) $0.575(1-x)\ ZrF_4$ $0.338(1-x)\ BaF_2$ $0.087(1-x)\ ThF_4$ x NaCl
b) $(0.62-0.5x)\ ZrF_4$ $(0.30-0.4x)\ BaF_2$ $(0.08-0.1x)\ LaF_3$ x NaCl

Later on, these glasses will be referred to as XZBTN and XZBLN glasses. Sodium chloride was droped directly into the melt using a long open platinum crucible. As some volatilization of $ZrCl_4$ may occur, the synthesis time was kept as constant as possible. Chemical

analysis showed that up to 10 % of Cl may be lost. However, systematic controls were not carried out and the compositions given here are those of the batch.

For $0 < x < 0.3$, sample may be obtained by pouring the melt into a preheated mould. When $x > 0.4$, quenching is required to obtain glass. In this way, up to 60 % in mole of NaCl could be incorporated. The limits of the glass forming area has been determined at 30 % in mole of NaCl in the ZrF_4-BaF_2-LaF_3-NaCl quaternary system (figure 1). By comparison with the basic Zr-Ba-La system, NaCl incorporation helps glass formation and results in ternary glasses ZrF_4-BaF_2-NaCl.

These glasses are yellow coloured, stable at room atmosphere and more sensitive to moisture than chlorine-free glasses. When increasing the NaCl content, refractive index increases, density decreases and the characteristic temperatures T_G and T_M are lowered (figures 2 - 4).

2. SPECTROSCOPIC STUDIES

- U.V. absorption edge

The incorporation of NaCl results in a marked shift of the U.V. absorption edge as shown in figure 5. This is related to the chlorine content : when removing chlorine from the melt -for example by heating the melt at 750° C for 30 mn in open atmosphere- the U.V. absorption is reduced and the yellow colour disappears. It is suggested that chlorine ions could induce the formation of coloured centres.

- I.R. multiphonon absorption edge

A shitf of the I.R. multiphonon absorption edge is observed when the NaCl content increases (figure 6). Extrinsic absorption arises at 1625 cm^{-1} (surface H_2O) and 1325 cm^{-1} (over-

tune of M-O vibrations). It appears that NaCl enhances the fixation of molecular water at glass surface. Consequently, sample alterations occur in a wet atmosphere when NaCl-content is higher than 15 %. The shift of the multiphonon absorption edge may be related to the decrease of the Zr and F concentration in the vitreous matrix. Assuming this hypothesis, the theoretical absorption may be computed. It is still higher than the experimental value (figure 7). From the lines of figure 7, the extrapolated values of the attenuation coefficient at 2000 cm^{-1} are 60 dB/km for the theoretical value and 13 dB/km for the experimental one. This result appears as the mixed halide effect. It may be pointed out that chlorine incorporation changes the coupling between the elementary vibrators Zr-F. As a result, the halfheight bandwidth of the fundamental absorption peak at 480 cm^{-1} is reduced and consequently the multiphonon absorption edge shifted toward longer wavelength. By comparison with a study in the Zr-Ba-La-F-Cl system carried out by R.M. Almeida and J.D. Mackenzie (3), a small shift of the average frequency of the Zr-anion vibration may be also taken into account.

CONCLUSION

The characterization and the confirmation of the mixed effect on infrared transmission have to be carried out in other systems to provide a set of observations sufficient for a good understanding. This effect may result in a best I.R. transmission of the polyhalide glasses than expected from the monohalide glass characteristics

REFERENCES

1. M. CHANTHANASINH, M. POULAIN - Unpublished results (1975)
2. M. POULAIN - European Applied Research. Report Nuclear Sci. and Tech. 3, n° 5, 1005 (1981)
3. R.M. ALMEIDA, J.D. MACKENZIE - J. Non-Cryst. Solids 51, 187 (1982)

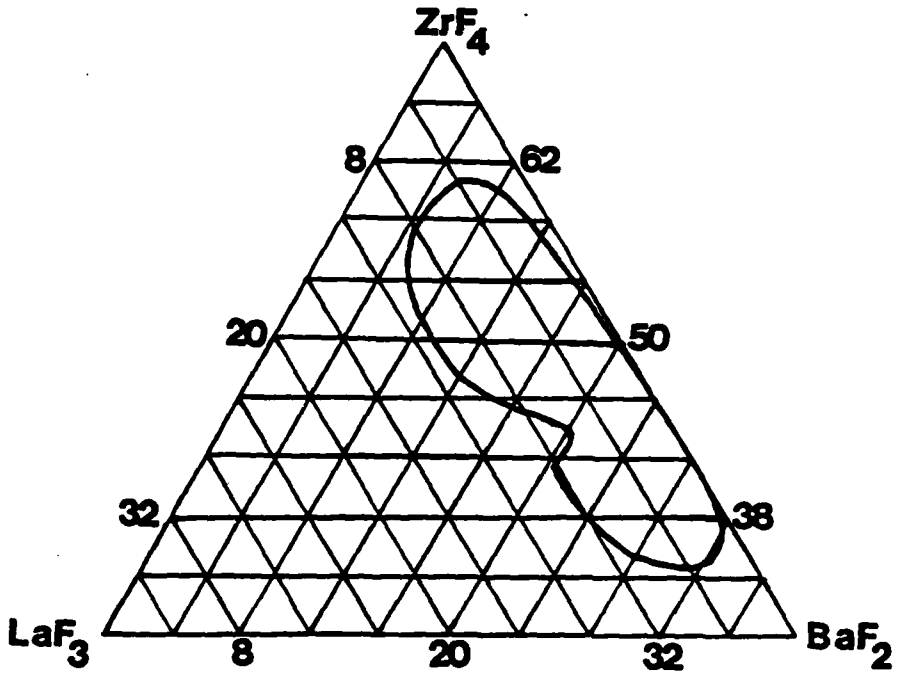

Figure 1

Glass forming area in the ZrF_4-BaF_2-LaF_3-NaCl quaternary system at a constant 30 % NaCl content

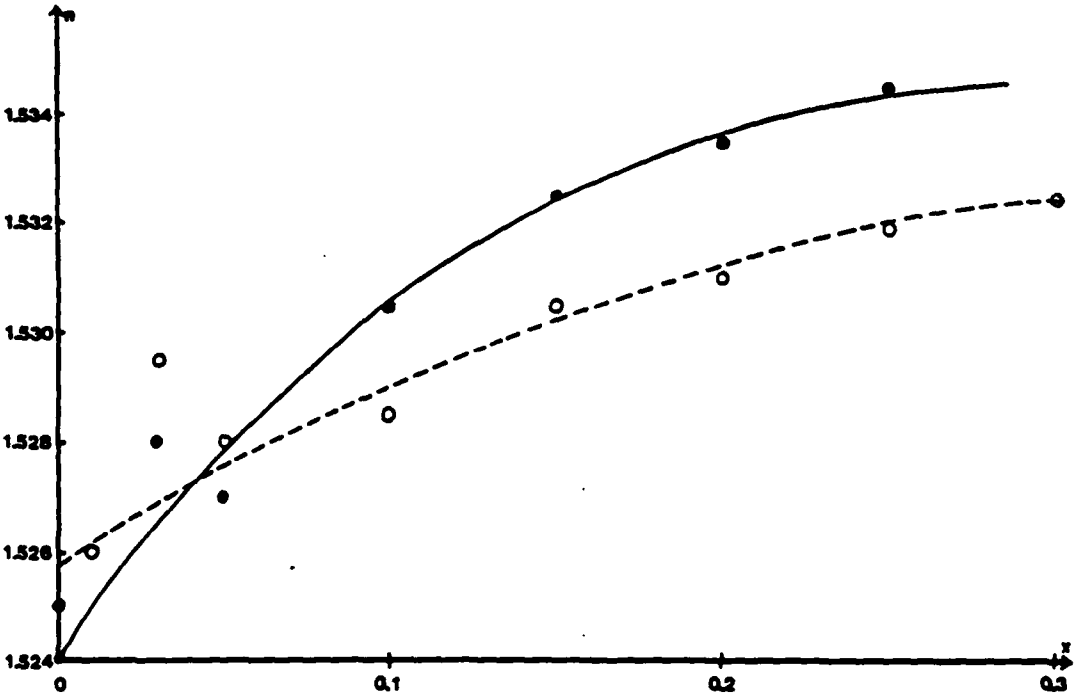

Figure 2

Evolution of the refractive index n_D of XZBTN (____) and XZBLN (---) glasses versus the NaCl content x.

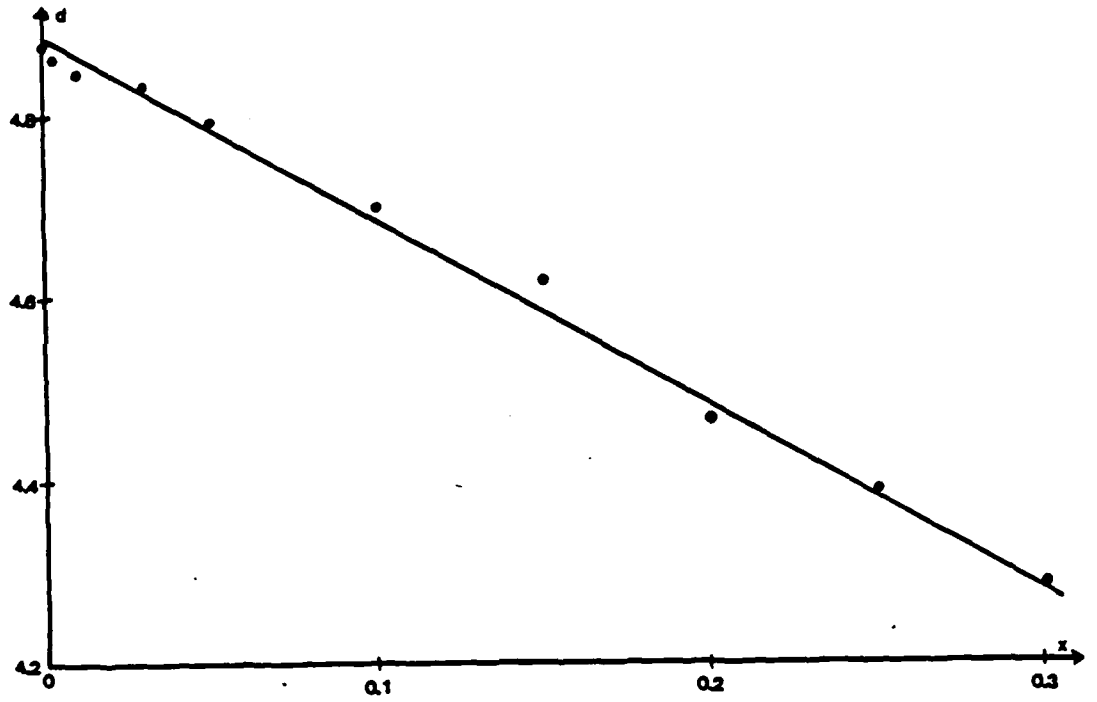

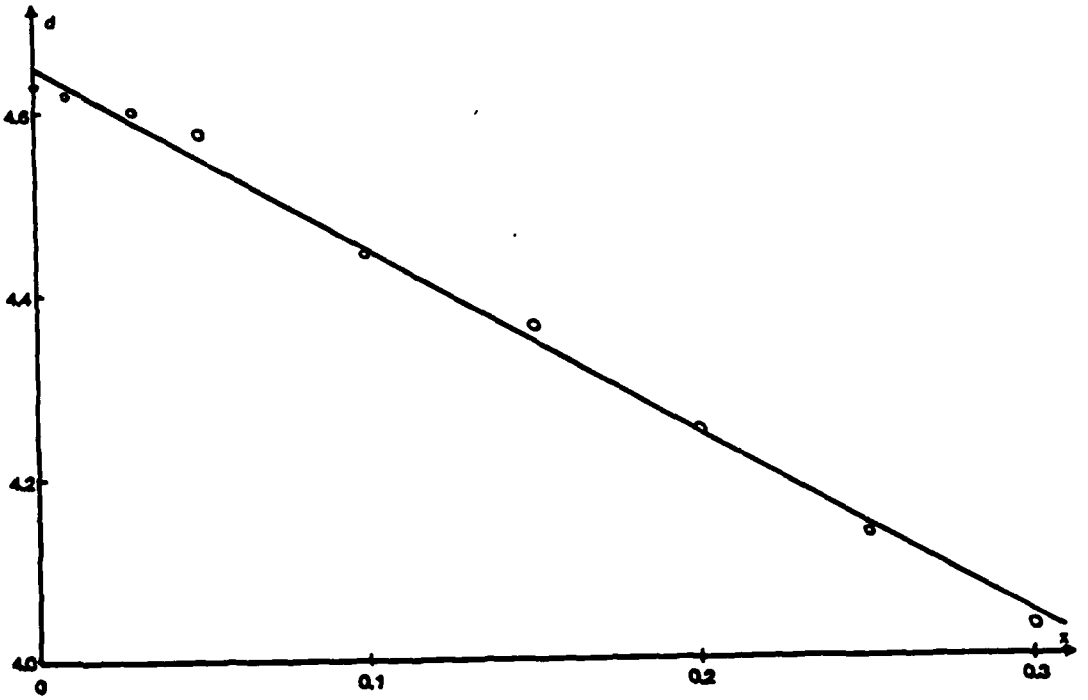

Figure 3

Evolution of the density of XZBTN (a) and XZBLN (b) glasses versus the NaCl content x.

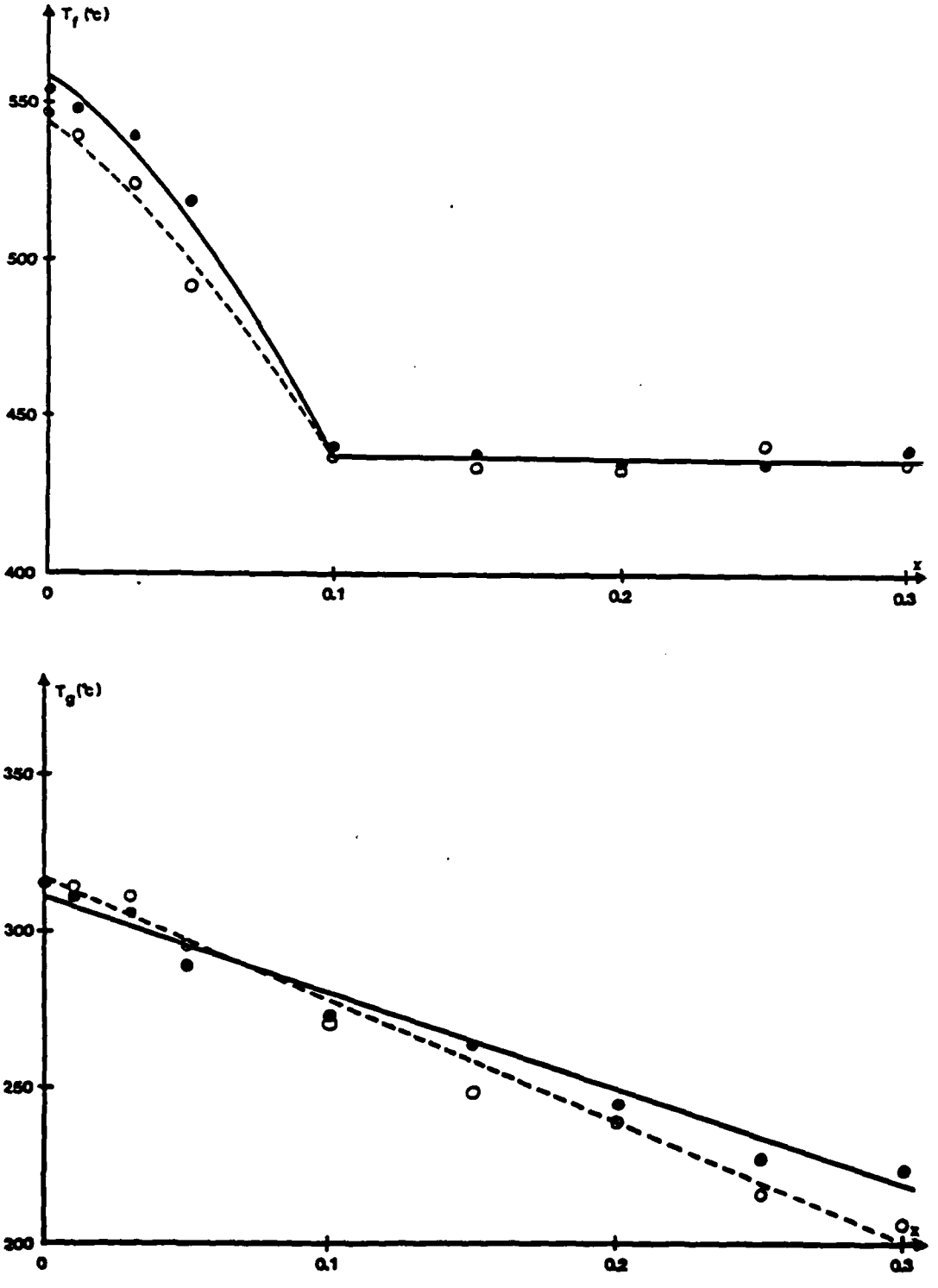

Figure 4

Evolution of the temperature of glassy transition T_G and melting T_F versus the NaCl content for the XZBLN (----) and XZBTN (____) glasses.

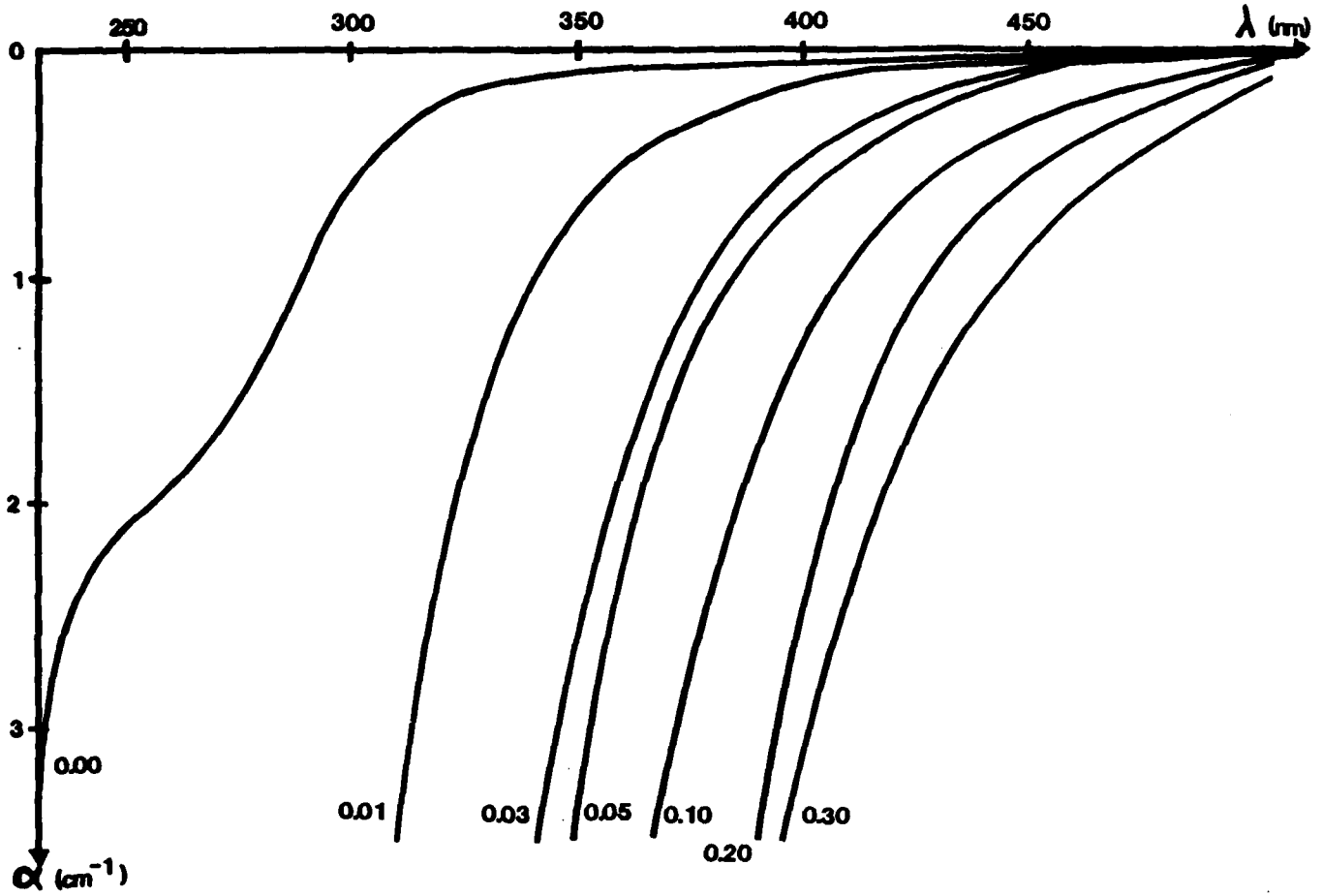

Figure 5

U.V. absorption edge of the XZBLN glass as a function of the molar content of NaCl.

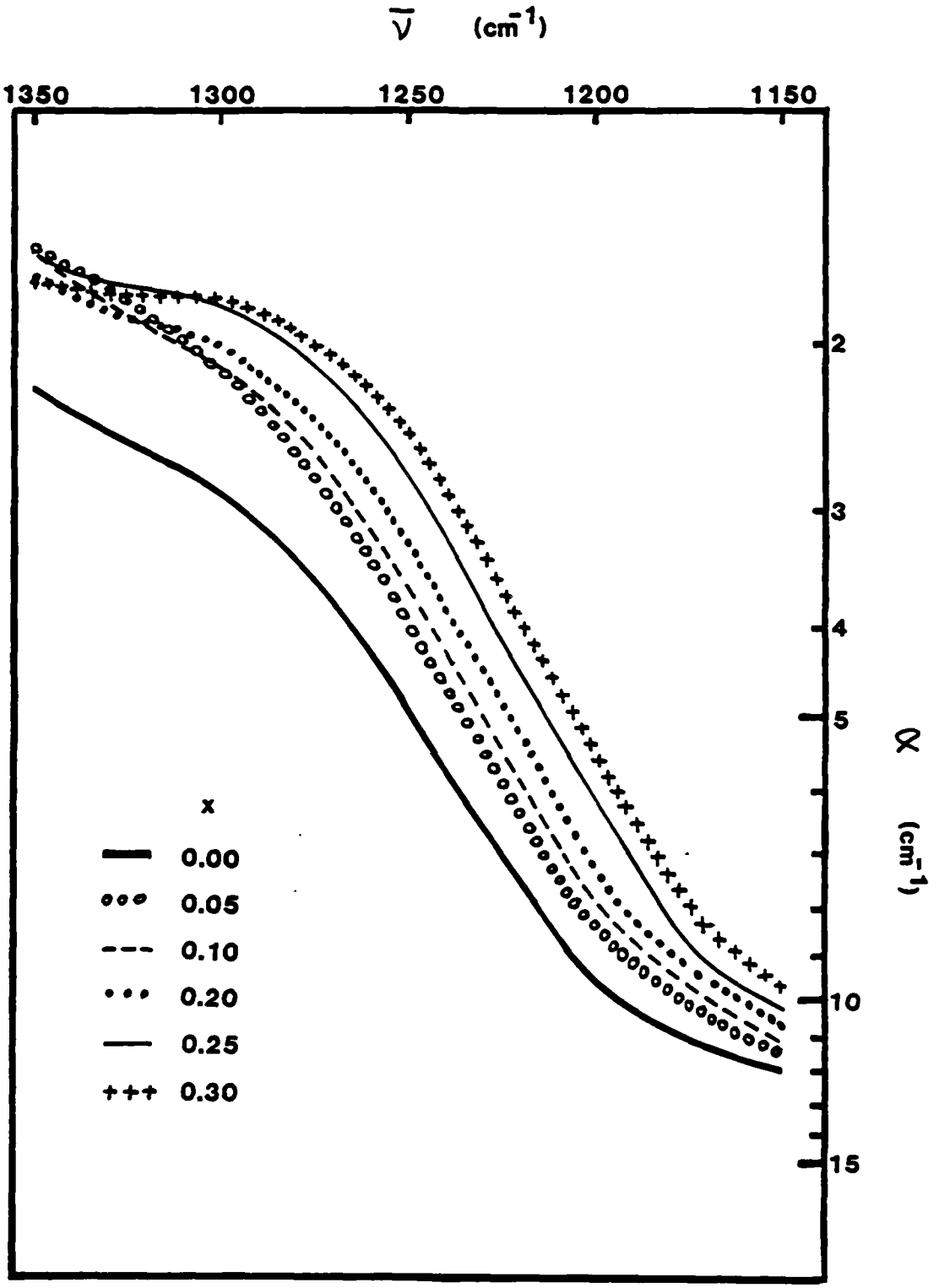

Figure 6

I.R. multiphonon absorption edge of the XZBTN glass as a function of the molar content of NaCl.

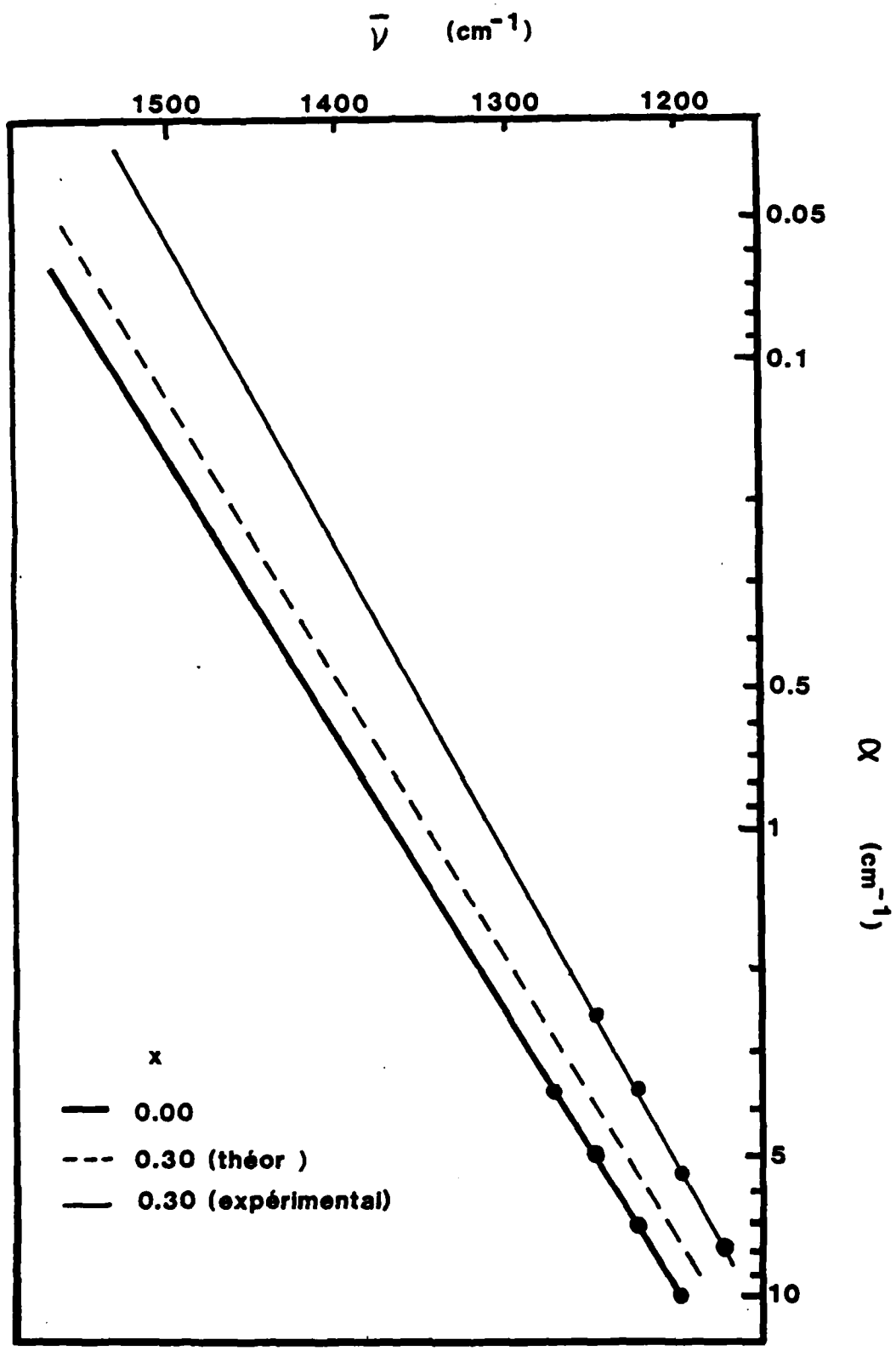

Figure 7

Intrinsic multiphonon absorption edge for the 30 % NaCl-substituted ZBT glass (___) compared with pure ZBT (___) and with the theoretical prediction (---)

EARLY HISTORY OF HEAVY METAL FLUORIDE GLASSES

By Michel POULAIN

Université de Rennes - Campus de Beaulieu
Laboratoire de Chimie Minérale D - Laboratoire Associé au C.N.R.S. n° 254 - Avenue du Général Leclerc - 35042 RENNES CEDEX (France)

The discovery of fluorozirconate glasses was one of those where luck must be taken into account. The first glass pieces we found into a sealed tube were the result of a preparation which missed its aim. For the years 1972-1974, we have been working on crystallized compounds $LnZrF_7$ and we determined the structure of one of them, $SmZrF_7$. Considering this structure, we thought is would be possible to put into it one more cation to fill up a cage appearing in the model. To reach this result, we coupled two combinations : $ZrF_4 + NdF_3$ and $ZrF_4 + BaF_2 + NaF$, Following the scheme :

$$LnF_3 + ZrF_4 \rightarrow LnZrF_7$$
$$LnZrF_7 + (M, M')ZrF_7 \rightarrow LnMM'Zr_2F_{14}$$

with M = Ba and M' = Na

$$NdF_3 + BaF_2 + NaF + 2\ ZrF_4 \rightarrow \text{purple glass} + NdF_3$$

Finally $BaF_2 + NaF + 2\ ZrF_4 \rightarrow$ colourless glass

We heated a sealed tube up to 900° C and after we droped it into cool water. A X-Ray diffraction diagram revealed an amorphous structure which was a failure from a crystallographic point of view. After a rather long reflection, we followed out our study of ternary system ZrF_4-BaF_2-NaF.

The use of sealed tubes was not convenient to glass technics. We improved our process by using platinum crucible. For us, this method was usual because we transform oxides into fluorides in platinum crucible. Mixture of fluorides and oxides

with ammonium fluoride was put into crucible and heated slowly in a first time. When smokes had disappeared, we heated up to fusion and poured the bath on a metal piece. This method allowed us to perform more preparations and to get samples in brass moulds.

Other systems were prospected (figure 1) on the basis of similar chemical properties or structural analogy. They provided the best compositions of fluorozirconate glasses we know. This work run over several years, then a problem was coming up : "Is it possible to get fluoride glasses without zirconium ?". The answer was we consider as our second stage : glass without zirconium.

We had observed the presence of BaF_2 in most mixture and beneficial part of ThF_4, YF_3 and AlF_3. Our test was carried out on the quaternary system Ba-Al-Th-Y-F... (BATY). Then, we prepared glasses without one of the constituents Ba, Th or Y. We reached more complicated preparations (figure 2). Study was extended to other systems without zirconium using elements in the same columns as Zr, Y or Al in the periodic table. This explorer work provided good samples on qualitative results. Here, we can point out some ternary systems : Sc-Y-Ba or In-Ba-Y or Ti-Ba-Na and glasses with alkali fluorides Th, Li, Ba or Th, Li, Na, K (figure).

A rather short time was devoted to fluorophosphate glasses with $NaPO_3$, LiF, CaF_2, AlF_3. Their interest is poor and their properties not special. Nevertheless, when molar percentage of $NaPO_3$ is weak, these glasses are moisture resistant.

With fluorozirconate glasses, we thought there was a limit in I.R. transparency. To go further in I.R. range, we tride to find glasses without fluorine. The first tests uses only chlorine compounds. Best results came from the ternary system : $CdCl_2$ $BaCl_2$-NaCl. Samples were thin and got only after quenching the melt. The track was good and interesting results were found by M. Matecki by using mixed halide compositions. This study is only at the beginning.

For illustrating our method, we give an example of short quaternary study. Starting from ternary Th, Li, Ba, we com-

plete a quaternary by associating ZrF_4. A glassy volume from Zr = 0 % to Zr = 60 % is continuous and gives good samples.

In conclusion, discovery of new glasses requires a little amount of luck, some fancy and also stubborness. With these rules, new glasses will surely appear in the future.

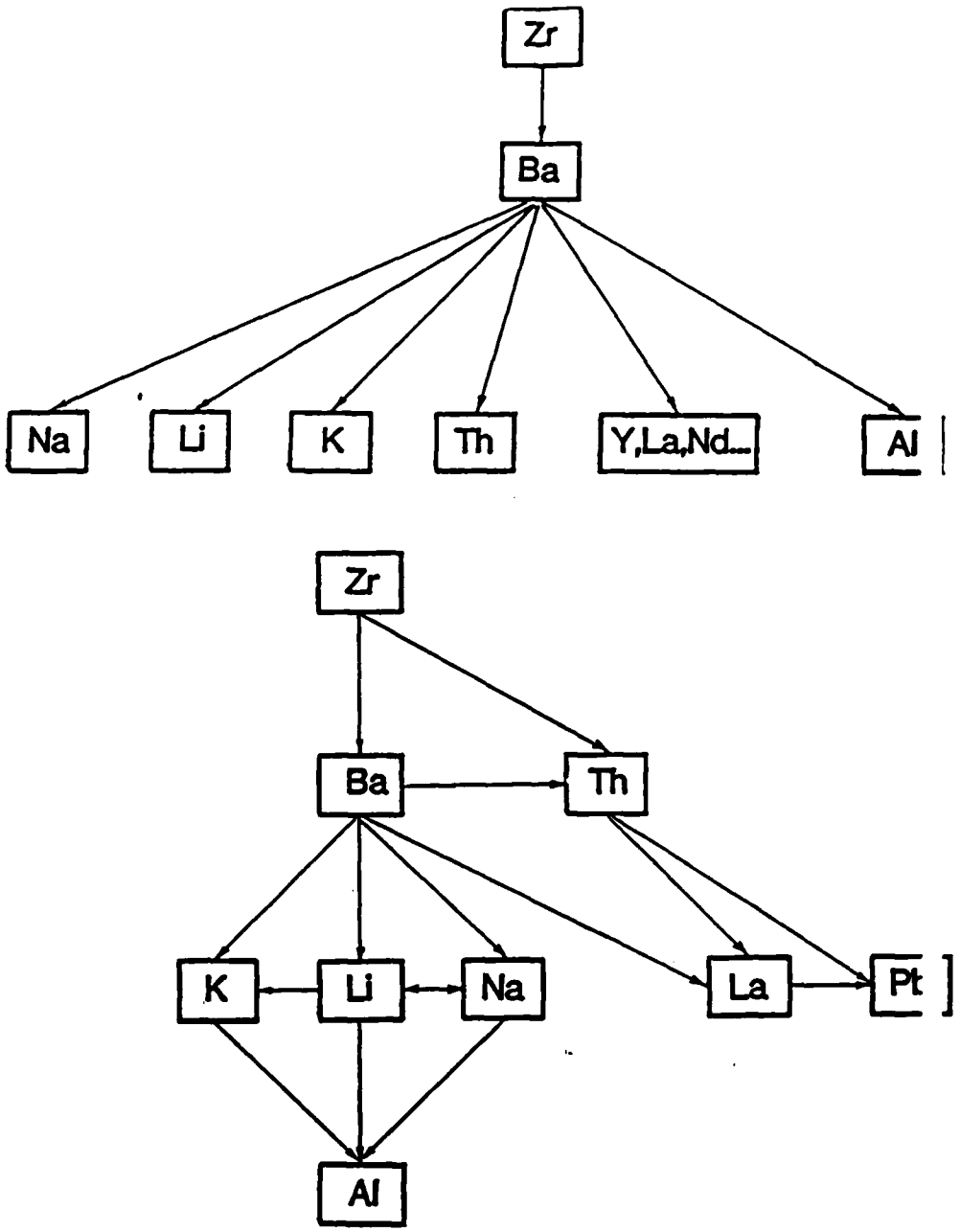

Figure 1

Cation combinations in fluorozirconate glass systems

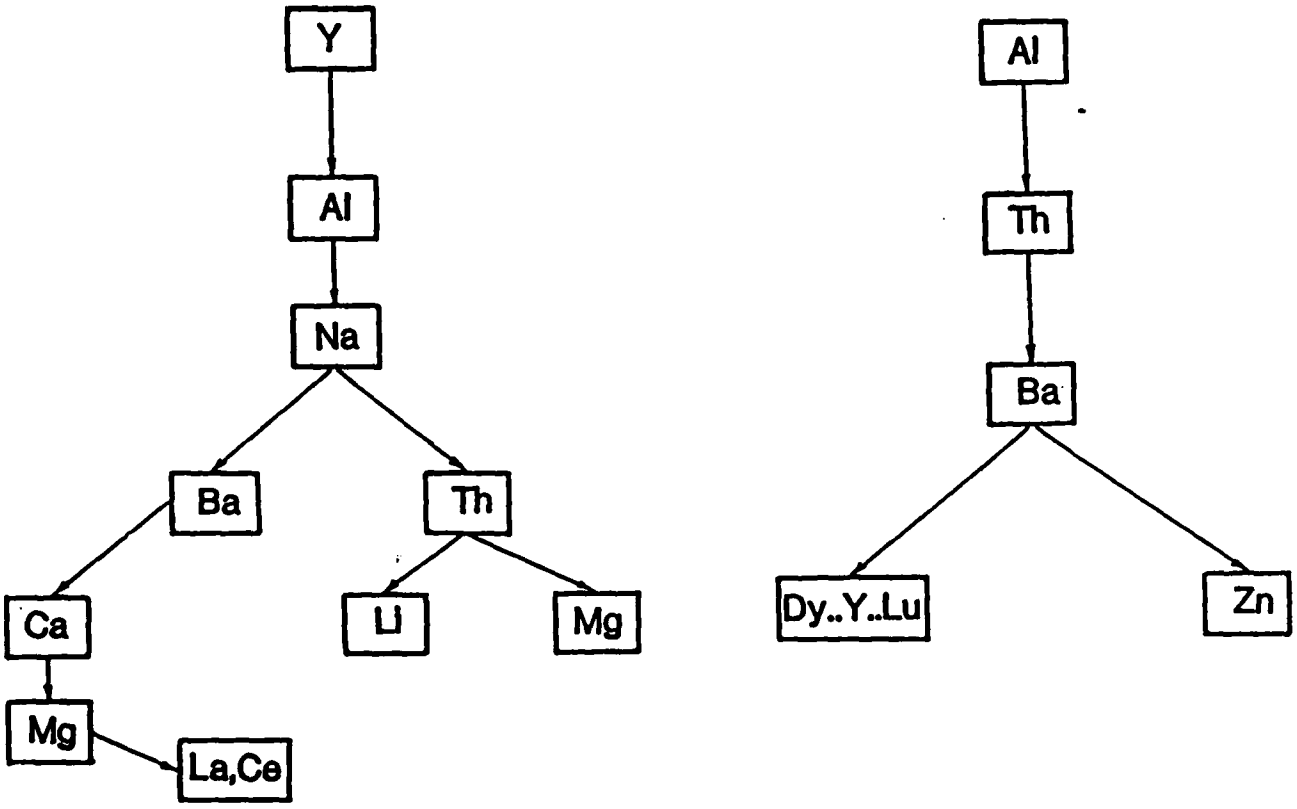

Figure 2

Cation combinations in fluoroaluminate glasses systems

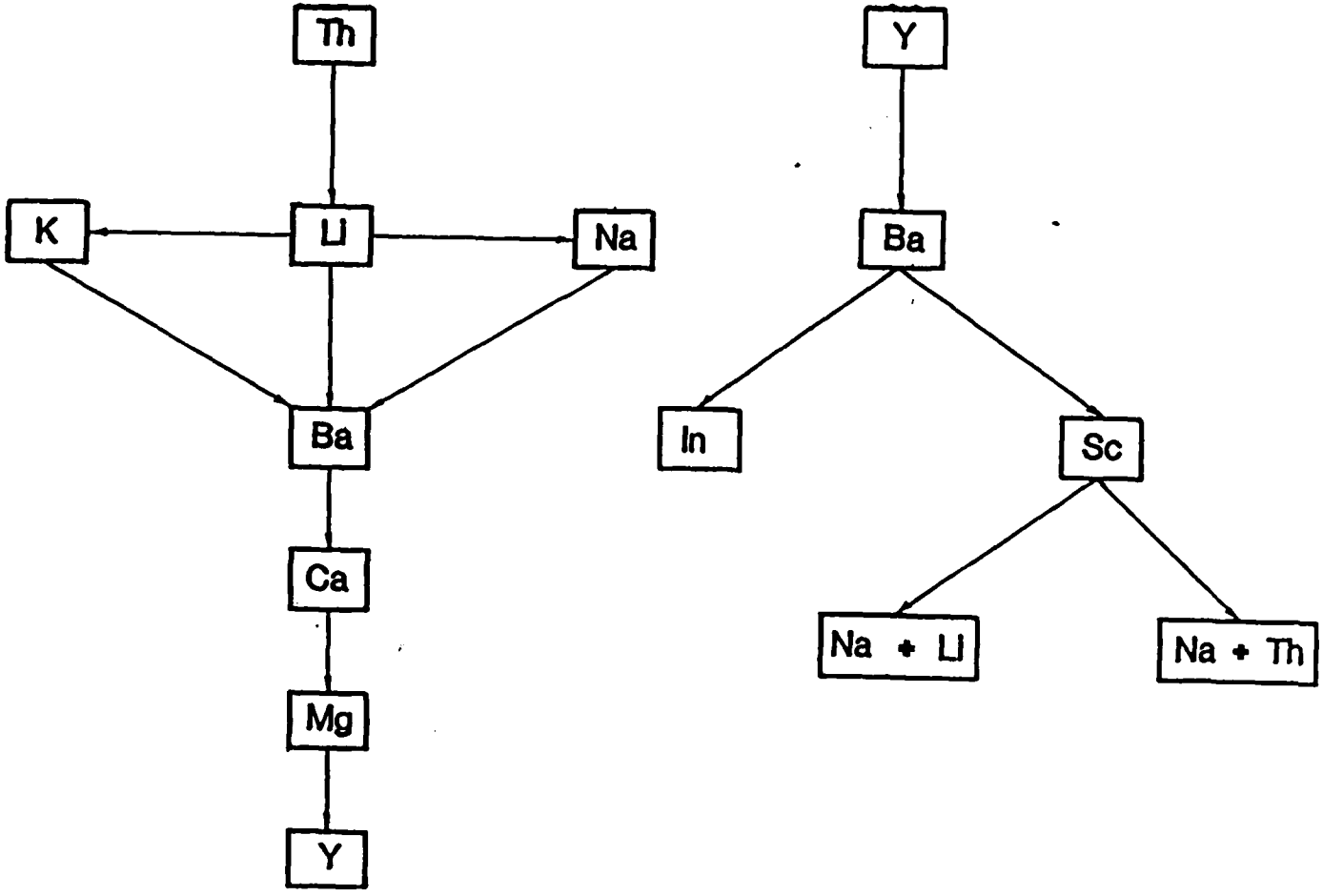

Figure 3

Cation combinations in fluoride glass systems free of classical vitrifier (Zr, Hf, Al, Zn).

ThF_4 AND LiF-BASED FLUORIDE GLASSES

Michel POULAIN and Marcel POULAIN

Université de Rennes - Campus de Beaulieu
Laboratoire de Chimie Minérale D, Laboratoire Associé au C.N.R.S. n° 254, Avenue du Général Leclerc, 35042 Rennes Cédex (France)

INTRODUCTION

The first stable fluorozirconate glasses included thorium fluoride (1) and since that time numerous fluoride glass systems including ThF_4 have been investigated (2 - 5). In most cases, ThF_4 was associated with other vitrifying fluorides such as AlF_3 or ZnF_2. This paper is centered upon combinations of ThF_4 with alkali and earth alkali fluorides.

1. THE TERNARY SYSTEM ThF_4-LiF-BaF_2

Glass formation was studied using an experimental procedure which has been described elsewhere (2). Thorium was introduced as ThO_2 with an excess of NH_4HF_2 as fluorinating reagent. The limits of the glass forming area are shown in the figure 1. A central composition is $Th_{0.3}Li_{0.6}Ba_{0.1}F_2$ and a binary glass $Th_{0.3}Li_{0.7}F_{1.9}$ is observed. With convenient starting materials, sample of 3 mm in thickness may be prepared in the ternary range.

2. OTHER GLASS FORMING SYSTEMS

Various experiments were carried out in systems excluding BaF_2, such as ThF_4-NaF-LiF, ThF_4-LiF-KF and the quater-

nary ThF_4-LiF-NaF-KF. The results are shown in figures 2 and 3. Most glasses can be prepared only by fast cooling between two metallic plates. Full lines indicate the most stable compositions.

Other fluorides were included in the glass in order to help glass formation, as reported in table I. Despite the high alkali content , glass samples are stable at room atmosphere and the Th-Li-Ba glass (TLB-3) does not display any surface change or significant weight loss after 24 hours in water at 20° C.

3. GLASS PROPERTIES

Characteristic temperatures were measured by differential scanning calorimetry (D.S.C. DU PONT 1090). Glass transition usually occurs between 200 and 250° C, and melting around 500° C. Several values of density and refractive index were measured (table II).

The infrared transmission of a ternary glass TLB-3 is shown in figure 4. The position of the multiphonon absorption edge is intermediate between that of fluoroaluminate and that of fluorozirconate glasses, in agreement with the prediction of C.T. Moynihan and M.G. Drexhage (6). A classical OH-band is observed at 3 µm. The U.V. transmission is improved by comparison with fluorozirconate glasses. Depending on the thickness and the material purity (Fe, Cr...), some transmission below 200 nm must be observed.

4. DISCUSSION

At first glance, glass formation in ThF_4-based systems seems to be logical, as thorium shows numerous chemical similarities with zirconium and hafnium, which are good fluoride vitrifiers. However, the molar composition ranges differ substantially, and until now, the most stable glasses have not included more than 30 % ThF_4. Thereofre, a description based on the clas-

sical network model implies numerous discontinuities in the tridimensional development of the thorium-based network. For example, in $(Th_{0.3}Ba_{0.1}Li_{0.6})F_2$ glass, the average number of unshared corners is 5.33 if we assume an 8-fold coordination of Th, and 4.33 with a coordination number of 9. For lower concentrations in Th, such as in $Th_{0.2}Li_{0.4}Na_{0.4}F_{1.6}$ glass, there is a good probability of the occurrence of discrete units ThF_8 or ThF_9. Therefore, it seems more convenient to use an ionic model as the basis for description of these glasses, as suggested previously. The anion array causes a non periodic packing, in which the cations are randomly inserted at sites corresponding to their usual crystal-chemistry. In this way, these fluoride glasses show some similarities with metallic glasses, which are described as random packing of hard or soft spheres. Alkali fluoride glasses have also been reported in ZnF_2-MF systems at only 10 - 20 % ZnF_2 (7) and, like some ThF_4-MF glasses, they may be considered as resulting from the disordering of the NaCl-type structure.

From a structural point of view, the incorporation of ThF_4 in glass composition leads to an increase of the anion to cation ration which is a condition for constructing an aperiodic structure. Moreover, according to the well known "confusion principle", the mixing of cations displaying different ionic charges and radii makes the atomic rearrangements more difficult and frustrates a crystalline structure. This probably results from the relatively favourable electrostatic energy of the disordered ionic configurations.

The recent discovery of $ThCl_4$-based glasses (8) suggests that mixed halide glasses could be synthesized from numerous systems which include thorium, in the same was as chlorine may be included in fairly large amounts in ZrF_4-based glasses (9).

REFERENCES

1. M. POULAIN, M. POULAIN, J. LUCAS and P. BRUN - Mat. Res. Bull. 10, 243 (1975)
2. M. POULAIN and J. LUCAS - Verres Réfract. 32, 4, 505 (1978)

3. M. MATECKI, M. POULAIN, M. POULAIN and J. LUCAS - Mat. Res. Bull. 13, 1039 (1978)
4. G. FONTENEAU, F. LAHAIE and J. LUCAS - Mat. Res. Bull. 15, 1143 (1980)
5. M. POULAIN, M. POULAIN and M. MATECKI - Mat. Res. Bull. 16, 555 (1981)
6. C.T. MOYNIHAN, M.G. DREXHAGE, B. BENDOW, M. SALEH-BOULOS, K.P. QUINLAN, K.H. CHUNG and E. GBOJI - Mat. Res. Bull. 16, 25 (1981)
7. C. WIEKER, W. WIEKER and E. THILO - Silikatechnik 17, 341 (1966)
8. H. HUE and J.D. MACKENZIE - J. Non-Cryst. Solids 51, 269 (1982)
9. R.M. ALMEIDA and J.D. MACKENZIE - J. Non-Cryst. Solids 51, 187 (1982)

TABLE I

Glass compositions (in mole %)

Ref.	ThF_4	LiF	NaF	KF	BaF_2	CaF_2	MgF_2	YF_3
TN0	20		80					
TL0	30	70						
TLN2	20	40	40					
TLK2	20	40		40				
TLB3	30	60			10			
TLNK2	20	30	40	10				
TLN*1	30	50	7		7	3	3	
TLN*2	30	50	10		7	3		
TLN*3	30	45	10	3	7	1	1	3
TLNB1	20	36	36		8			
TLNB2	20	34	38		8			
TLN*6	20	30	30	10	7	3		
TL*4	30	60			5	2	1	2

TABLE II

Glass characteristics

Ref.	T_G	T_C	T_M	n_D	d
TN0	242	333	564		
TL0	249	284	538		
TLN2	200	277	513		
TLK2	295	332	490		
TLB3	256	310	560	1.4945	5.29
TLNK2	173	197	505	1.425	3.78
TLN*1	248	327	518	1.483	5.32
TLN*2	250	329	503	1.4895	5.35
TLN*3	261	348	504	1.4895	5.30
TL*4	262	341	526	1.493	5.38
TLN*6	209	235	465	1.442	4.59
TLNB2	210	233	510	1.442	4.68
TLNB1	213	246	500	1.445	4.75

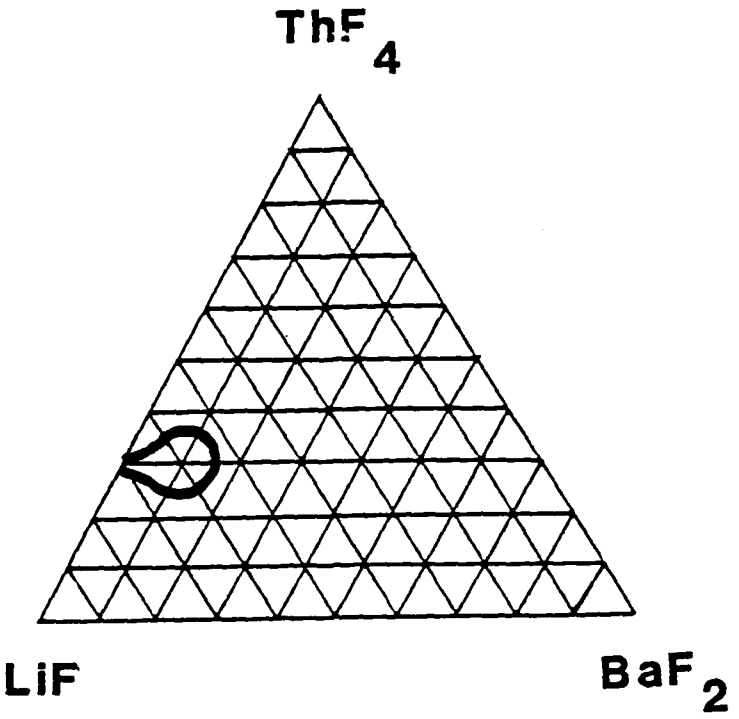

Figure 1

Glass forming area in the ThF_4-LiF-BaF_2 ternary system

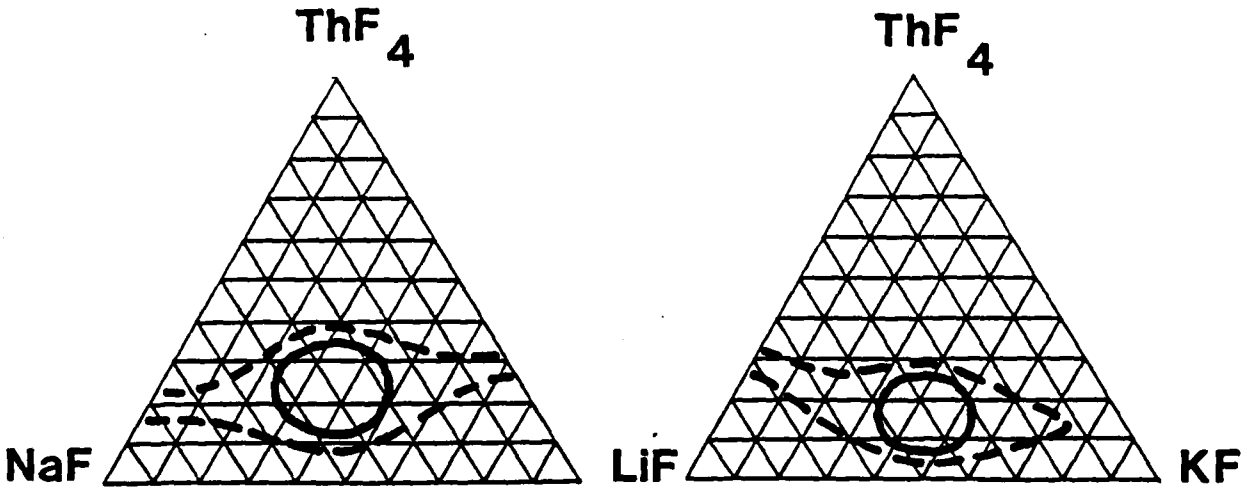

Figure 2

Glass forming areas in the ThF_4-LiF-NaF and ThF_4-LiF-KF ternary systems

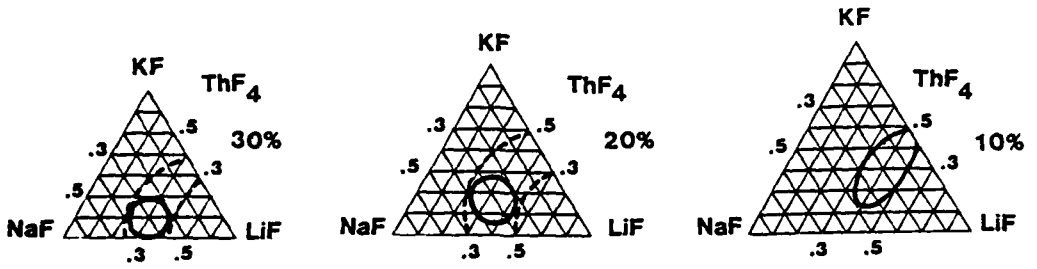

Figure 3

Vitreous area in the ThF_4-LiF-NaF-KF quaternary system at 10 %, 20 % and 30 % of ThF_4

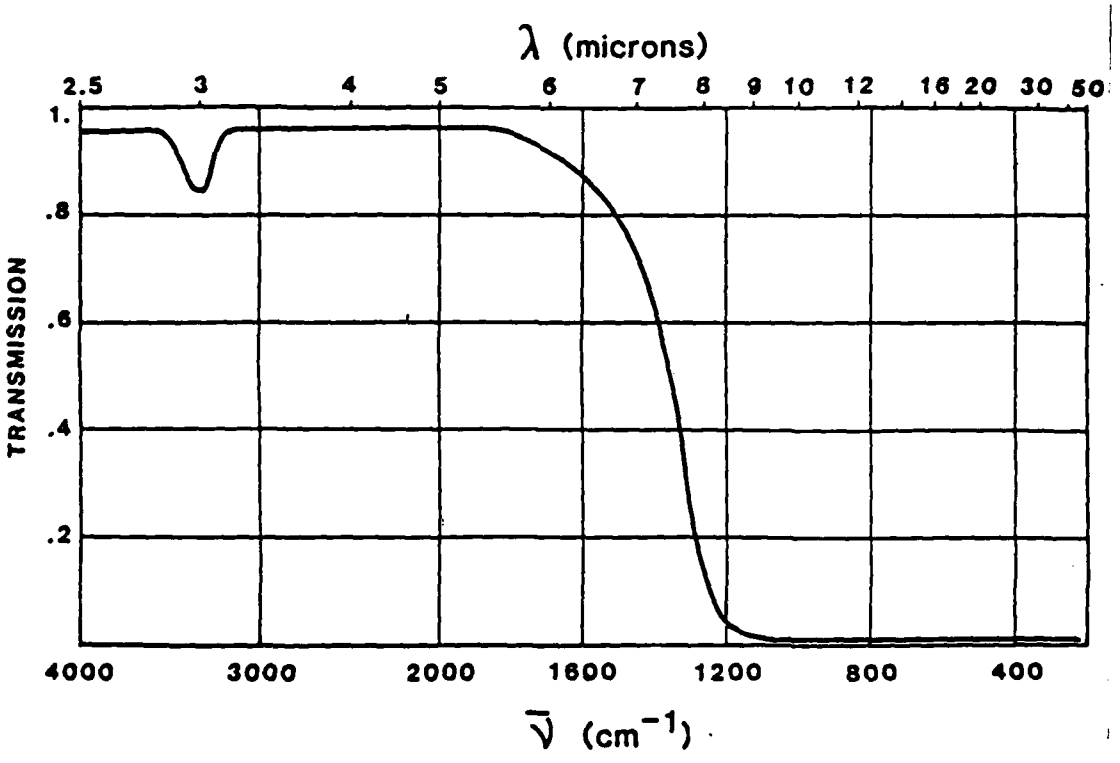

Figure 4

Infrared transmission of a TLB-3 glass. Sample thickness : 2.4 mm

Magneto-Optic Effect in Pure and Nd Doped BeF_2 Based Glasses

L.D. Pye, S.C. Cherukuri and I. Joseph

N.Y.S. College of Ceramics at Alfred University,

Alfred, NY 14802.

EXTENDED ABSTRACT

Magnetic field induced circular birefringence is called Faraday rotation. It is essentially a linear magneto-optic effect in which the off-diagonal elements of the dielectric tensor are affected resulting in optical activity of an isotropic medium[1]. The angle of rotation of linearly polarized light wave is given by the following equation[2]:

$$\Theta = VLH.s$$

where L is the length of the medium in meters, H is the applied magnetic field in teslas, s is a unit vector in the direction of propagation and Θ is the angle of rotation in radians. V is a constant of proportionality which is known as the Verdet constant and is expressed in the units of radians/tesla.meter. By convention, V is considered to be positive for diamagnetic rotation and negative for paramagnetic rotation.

In this work, Faraday effect was studied for a pure BeF_2 glass (sample: B815) and also a mixed fluoride glass containing BeF_2, AlF_3, KF and CaF_2 with varying concentrations of NDF_3

(B415, B416 and B419). Compositions of these glasses are shown in Table I. An excellent review of the preparation, properties and applications of these glasses was given by Cline and Weber[3].

Table I. Compositions of the glasses used in this work*

Glass	BeF_2	AlF_3	KF	CaF_2	NdF_3
B815	100	-	-	-	-
B415	47	10	27	16	-
B416	47	10	27	15	1
B419	47	10	27	13	3

* values in mole%

The Verdet constant of the pure BeF_2 glass was found to be 2.01 radians/tesla.meter, which is probably the lowest or one of the lowest of all diamagnetic Verdet constants of both oxide and non-oxide glasses. The variation of the Verdet constant with the concentration of NdF_3 in the mixed fluoride glass is shown in Fig. 1. It is evident from Fig. 1 that very little concentration of NdF_3 (1.8 mol% or 5.06×10^{20} ions/cc of Nd) is needed for the paramagnetic contribution to nullify the diamagnetic

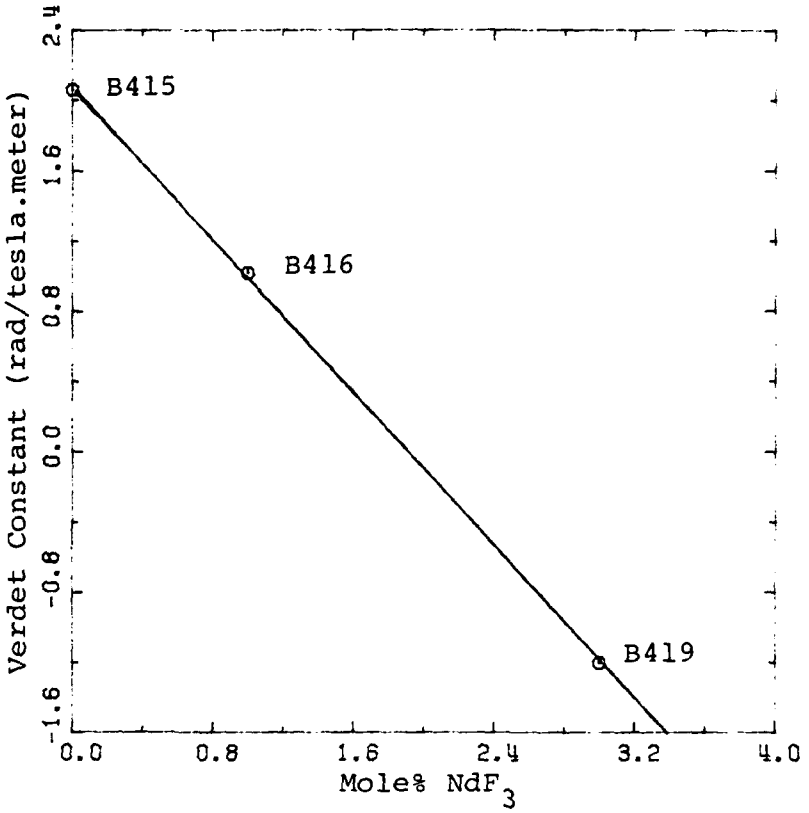

Figure 1. Variation of the Verdet constant with NdF_3 concentration at 632.8 nm.

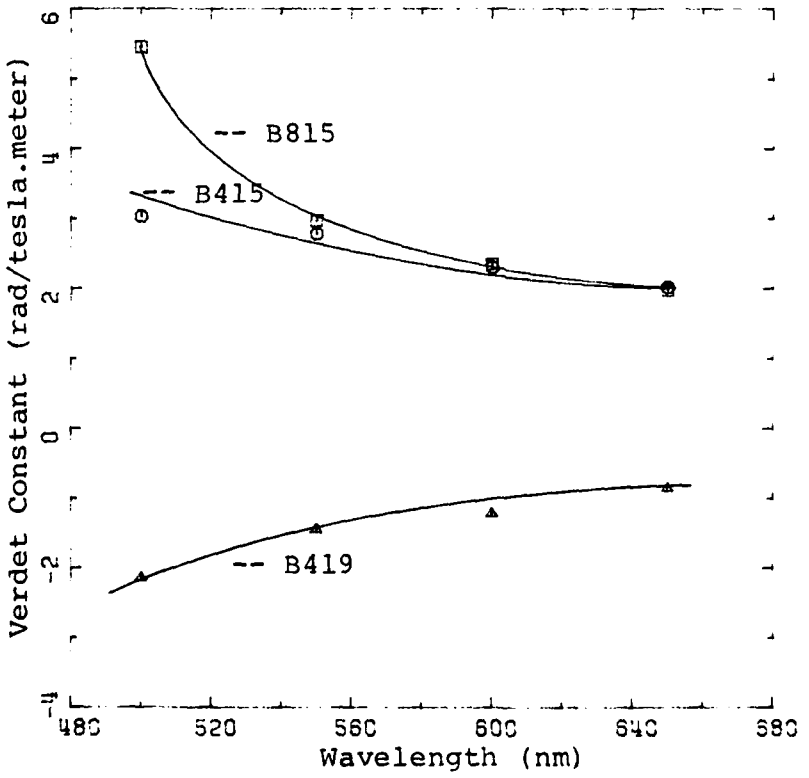

Figure 2. Wavelength dispersion of the Verdet constant.

rotation leading to a zero-rotation glass. Several compositions of such zero-rotation glasses were reported earlier by Cherukuri and Pye in germanate[4] and fluoride[5] glass systems.

Wavelength variation of the Verdet constant for these glasses is shown in Fig. 2. It is noticed from Fig. 2 that pure BeF_2 glass has a stronger wavelength dependence than B415 or B419 glasses.

References:

1) A. Nussbaum and R.A. Phillips, Contemporary Optics for Scientists and Engineers, Prentice-Hall, NY, pp370-416 (1975)

2) E. Hecht and A. Zazac, Optics, Addison-Wesley Inc., Reading, Mass., pp261-262 (1976).

3) C.F. Cline and M.J. Weber, "Beryllium Fluoride Optical Glasses: Preparation and Properties," Wiss.Ztschr.Friedrich-Schiller-Univ.Jena,Math.-Nat.R., 28.Jg.(1979)

4) S.C. Cherukuri, L.D. Pye, "Faraday Rotation of Rare Earth Alkali Germanate Glasses," Proc. Rare Earths in Modern Science and Technology, Vol 3, (1982) 465, Plenum, NY.

5) L.D. Pye et al, "The Faraday Effect in Some Non-crystalline Fluorides," J. Non. Cry. Solids, (1983).

Energy Transfer between Manganese(II) and Erbium(III) in a Gallium Lead Fluoride Glass

R.REISFELD and E.GREENBERG,
Department of Inorganic and Analytical Chemistry,
Hebrew University,Jerusalem,Israel 91905,
C.JACOBONI and R.DE PAPE,
Laboratoire des Fluorures et Oxyfluorures Ioniques,
Université du Maine,F-72017 Le Mans Cedex,France,
and C.K.JØRGENSEN,
Département de Chimie minérale,analytique et appliquée,
Université de Genève,CH 1211 Geneva 4,Switzerland.

The luminescence yields of both the lowest quartet state of $3d^5$ Mn(II) and the fourth and fifth excited J-levels $^4F_{9/2}$ and $^4S_{3/2}$ (emitting at 550 nm) of $4f^{11}$Er(III) are unusually high in fluoride glasses(corresponding to only weak competition by non-radiative de-excitation).The decay is not exponential,but the mean life-time 0.06 ms of $^4S_{3/2}$ is decreased to 0.01 ms in presence of Mn(II), providing a broader emission at 630 nm.$^4F_{9/2}$ emitting at 668 nm (life-time 0.08 ms shortened by Mn to 0.025 ms) is below the lowest Stokes threshold of any Mn(II) site,but can be efficiently fed by the long-lived quartet(1.4 ms without erbium present) with the result that 668 nm emission of a mixed sample has a short-lived,intense component(much weaker by 370 nm excitation in the absence of manganese) and a weak,long-lived emission paid back by Mn(II) storing the energy. Other results of mutual energy transfer and cascading-down are observed by excitation below 400 nm,and the probability of mutual energy transfer theoretically evaluated.

FIG.1.Absorption spectrum due to manganese(II) in the glass C with molar composition 36 PbF_2:24 MnF_2:35 GaF_3:5 $Al(PO_3)_3$:2 LaF_3 measured at 25°C.

FIG.2.Excitation spectra of manganese(II) emission at 626 nm. Curve(a): glass C.Curve(b): glass D where the 2 mole% LaF_3 of C is replaced by ErF_3.Measured at 27°C.

FIG.3.Fluorescence spectra of various glasses.Curve(a): Glass C excited at the Mn(II) peak at 395 nm.Curve(b): Glass F excited at the Er(III) peak at 370 nm.Curve(c): Glass D excited at the Mn(II) peak at 395 nm. Curve(d): Glass D excited at the Er(III) peak at 370 nm.Curve(e): Glass D excited at the Mn(II) peak at 480 nm.The sensitivity used for curves (c),(d) and (e) are all 10 times higher than the sensitivity used for curves (a) and (b).Measured at 27°C.

FIG.4.Absorption spectra due to erbium(III).Curve(a): Glass D measured against the erbium-free glass C as reference,with the intention of compensating the absorption due to manganese.Dashed curve(b): Glass F containing no manganese.Measured at 25°C.

FIG.5.Excitation spectra of erbium(III) emission in the manganese-free glass F.The full curve(a) is monitored for fluorescence at 543 nm.The dashed curve(b) is monitored at 666 nm,using 20 times higher sensitivity than for curve(a).Measured at 27°C.

FIG.6.Major radiative(thick vertical arrows for strong fluorescence) and non-radiative(wavy arrows) processes in a fluoride glass doped with Er(III) alone(to the left) or both Er(III) and Mn(II)(to the right). The symbols of atomic spectra indicate J-levels of the $4f^{11}$ system erbium(III) and the terms ^6S and ^4G of $3d^5$ manganese(II).The group-theoretical symbols $^4\Gamma$ indicate quartet states belonging to Mn(II) on (probably inequivalent) sites of undetermined point-group symmetry. Energy transfer (e.t.) shown as stipled slopes.

FIG.7.Emission spectra of Mn(II) and Er(III) in glass D under (a): excitation at 395 nm,(b):excitation at 463 nm,and (c):excitation at 520 nm.

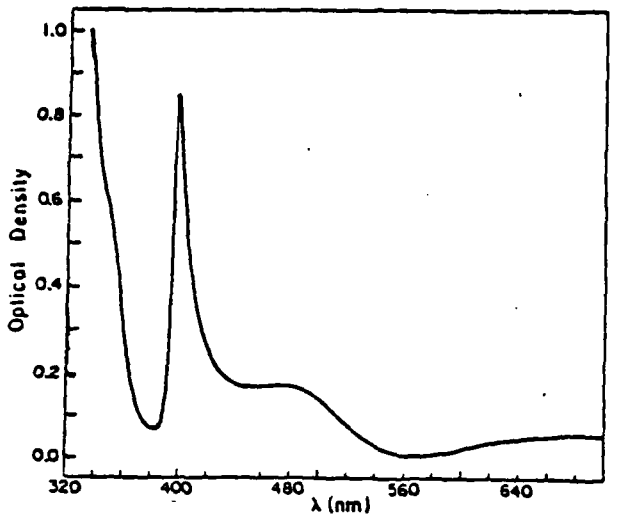

FIG. 1

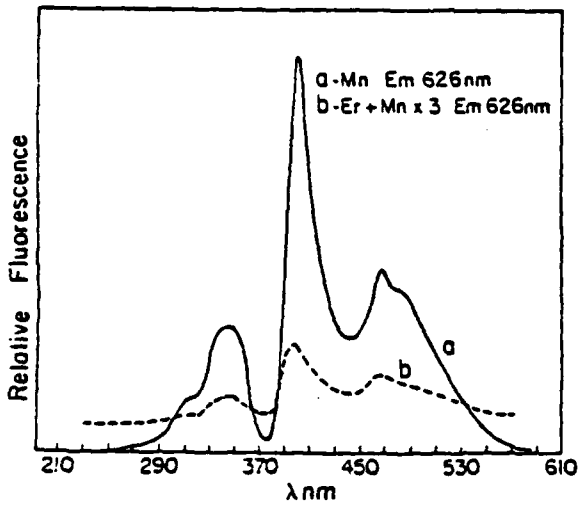

FIG. 2

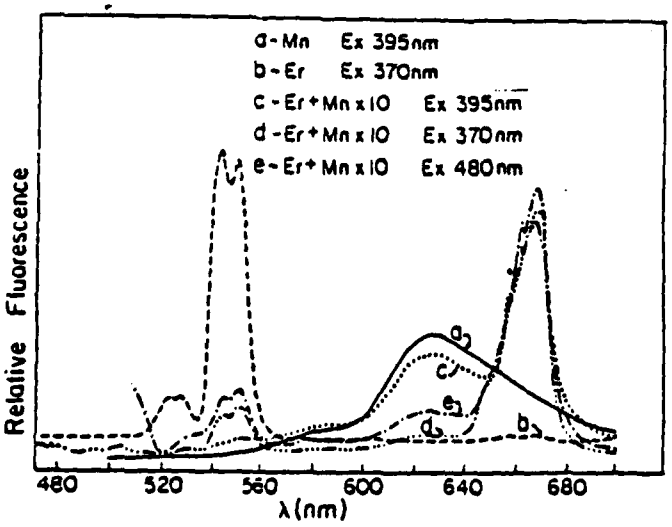

FIG. 3

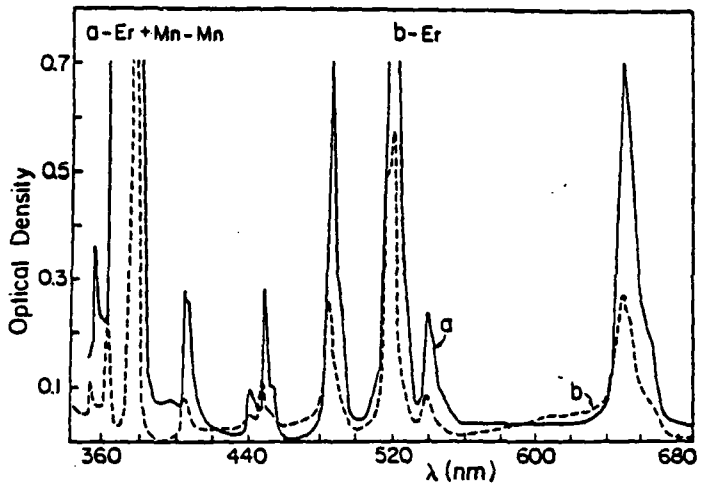
a-Er+Mn-Mn
b-Er
0.7
0.5
0.3
0.1
Optical Density
a
b
360
440
520
600
680
λ (nm)

FIG. 4

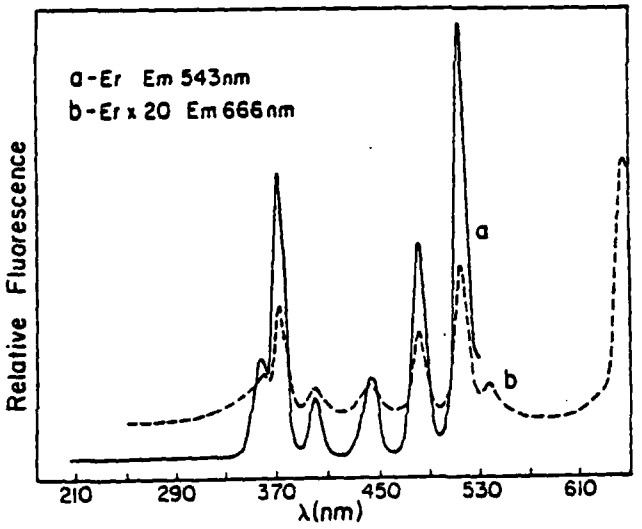
a-Er Em 543nm
b-Er x 20 Em 666nm
Relative Fluorescence
a
b
210
290
370
450
530
610
λ(nm)

FIG. 5

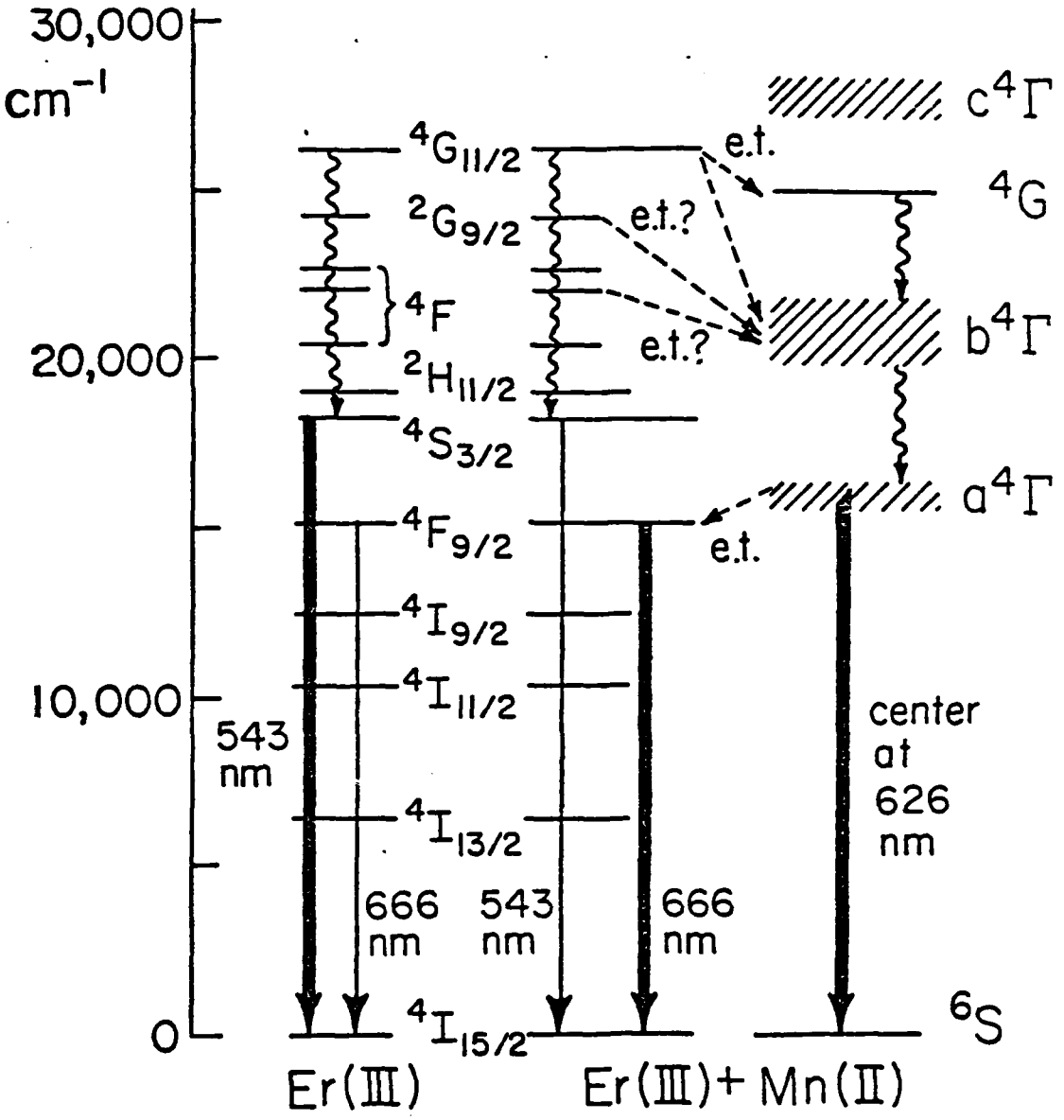
30,000
cm⁻¹
20,000
10,000
0
c⁴Γ
⁴G
b⁴Γ
a⁴Γ
⁴G11/2
²G9/2
⁴F
²H11/2
⁴S3/2
⁴F9/2
⁴I9/2
⁴I11/2
⁴I13/2
⁴I15/2
⁶S
e.t.
e.t.?
e.t.?
e.t.
543 nm
666 nm
543 nm
666 nm
center at 626 nm
Er(III)
Er(III)+ Mn(II)

FIG. 6

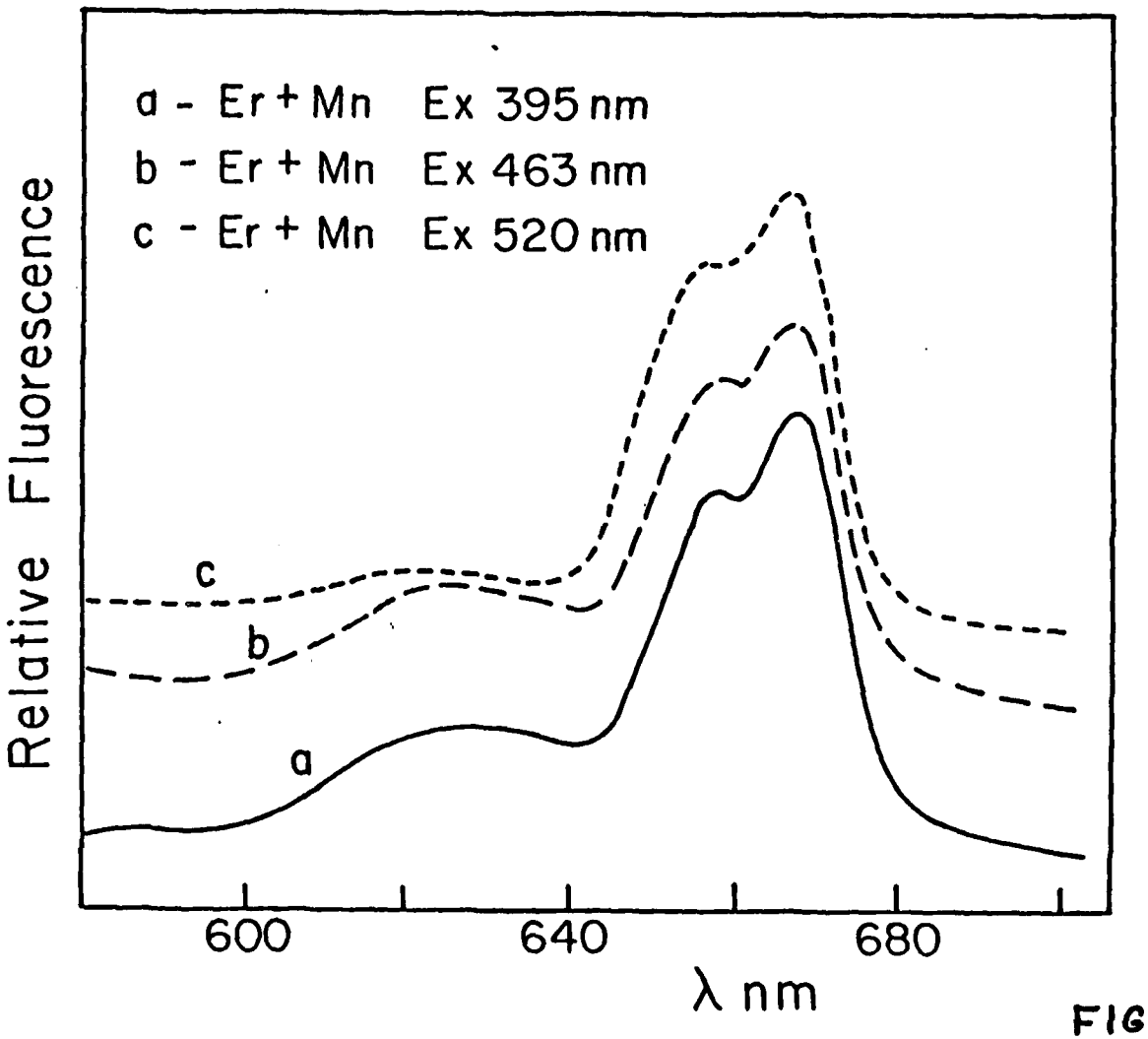
a - Er + Mn Ex 395 nm
b - Er + Mn Ex 463 nm
c - Er + Mn Ex 520 nm
Relative Fluorescence
c
b
a
600
640
680
λ nm

FIG. 7

SYNTHESIS OF HIGH PURITY STARTING MATERIALS FOR HEAVY METAL FLUORIDE GLASSES[+]

M. Robinson

Hughes Research Laboratories
Malibu, California 90265, USA

A problem common to all fluoride materials is their inherent lack of high purity, especially with regard to the anion. For the preparation of low loss optic fibers and highly transparent IR optical components, a high overall purity of all glass components is a prerequisite. Purification methods are being studied to significantly reduce anion, cation and carbon type impurities typically present in ZrF_4 and HfF_4 based glasses. Recently, Mitachi and Miyashita[1] reported perhaps the lowest measured loss (21 db/km at 2.55 um) thus far achieved from a ZrF_4:BaF_2:GdF_3:AlF_3 (ZBGA) glass. From their data, one sees that large losses result from residual impurities such as OH^- and ions of Fe, Cu, and Ni.

This paper describes the purification techniques of selected glass components specifically in relation to the removal of oxyanion impurities (OH^-, $O^=$ and $OF^{\equiv}$) and transition ions such as Fe^{3+}. Carbon impurities are effectively removed by heating individual starting materials (oxides or fluorides) in a dry oxygen atmosphere at 1000°C. The reactive atmosphere process for the preparation

---

[+]This work is sponsored in part by the Naval Research Laboratories as Contract N00014-83-C-2097.

[1]S. Mitachi and T. Miyashita, Elect. Lett., 18, 170 (1982).

of OH^- free BaF_2 and LaF_3 utilizing $HF_{(g)}$ and $CF_{4(g)}$ is described. Figure 1 shows the IR transmission spectrum of Bridgman grown BaF_2 single crystals. Crystals were grown in either He-HF atmosphere or a He-HF-CF_4 atmosphere. Absorption bands in the IR from undefined impurities are not readily removed by processing and growth of BaF_2 at its melting point (1350°C) in HF/He as shown in Fig. 1a. However, a prolonged HF soak at 1550°C greatly reduces all of the indicated absorption peaks. The soaking period is reduced if the secondary RAP gas CF_4 is used. Figure 1b gives the spectrum of a BaF_2 crystal grown in an atmosphere consisting of HF, He, and CF_4.

The results of an impurity analysis on ZrF_4 derived from reactive atmosphere sublimation will be given, and the sublimation process described and evaluated. Table 1 gives some preliminary analytical results for Fe in various ZrF_4 specimens, and vitreous carbon.

Table 1

IRON ANALYSIS - ZrF_4

	Fe (PPM)	Method
BDH (as received, special grade)	4	ZAA
BDH (sublimed in HF)	1.5	ZAA
BDH (sublimation residue)	1900	ESA
CERAC (99.5% purity)	320	ESA
CERAC (99.5% purity - sublimed in HF)	<100*	ESA
CERAC (99.5% purity - sublimation residue)	11000	ESA
Vitreous carbon crucible	10	ZAA

ZAA = Zeeman Atomic Absorption

ESA = Emission Spectrographic Analysis

* 100 PPM is the limit of detectability for Fe in ZrF_4 by ESA

AD-A144 269 EXTENDED ABSTRACTS INTERNATIONAL SYMPOSIUM ON HALIDE GLASSES (2ND) RENSSE..(U) RENSSELAER POLYTECHNIC INST TROY NY DEPT OF MATERIALS ENGINEE.. C T MOYNIHAN 4/4

UNCLASSIFIED 02 AUG 83 N00014-83-G-0091 F/G 11/2 NL

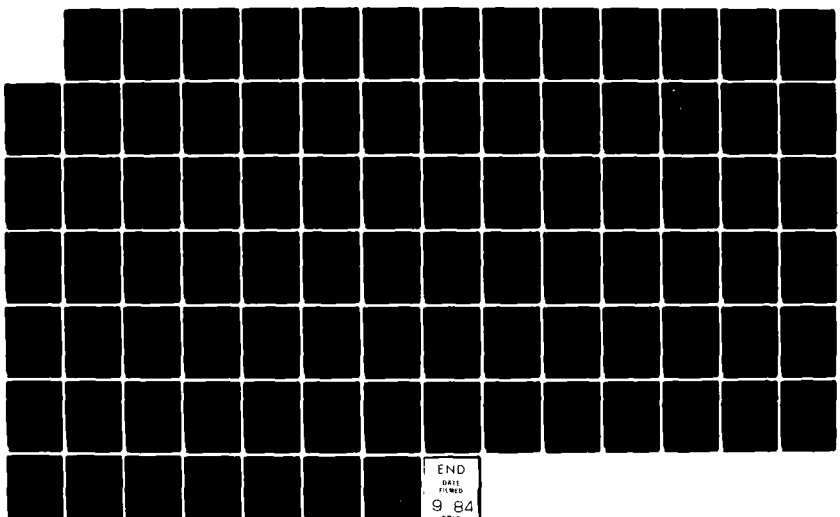

END
DATE FILMED
9 84
DTIC

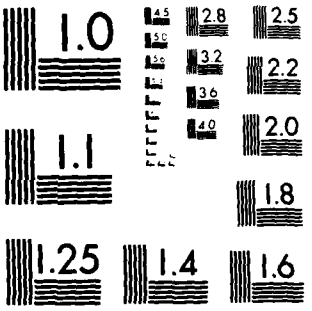

MICROCOPY RESOLUTION TEST CHART
NATIONAL BUREAU OF STANDARDS-1963-A

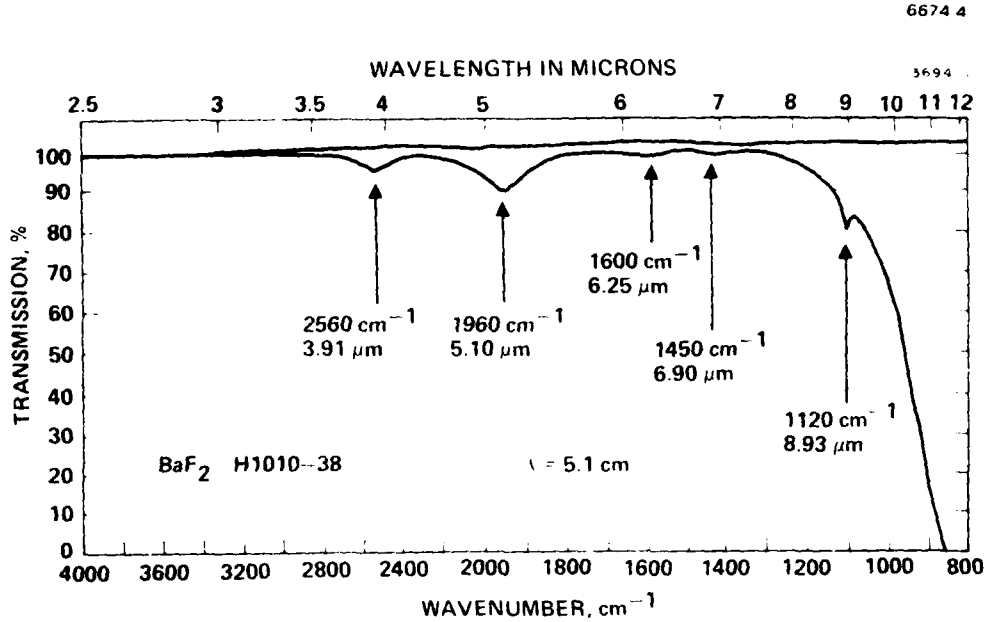

(a) BaF_2 Crystal Growth in HF/He

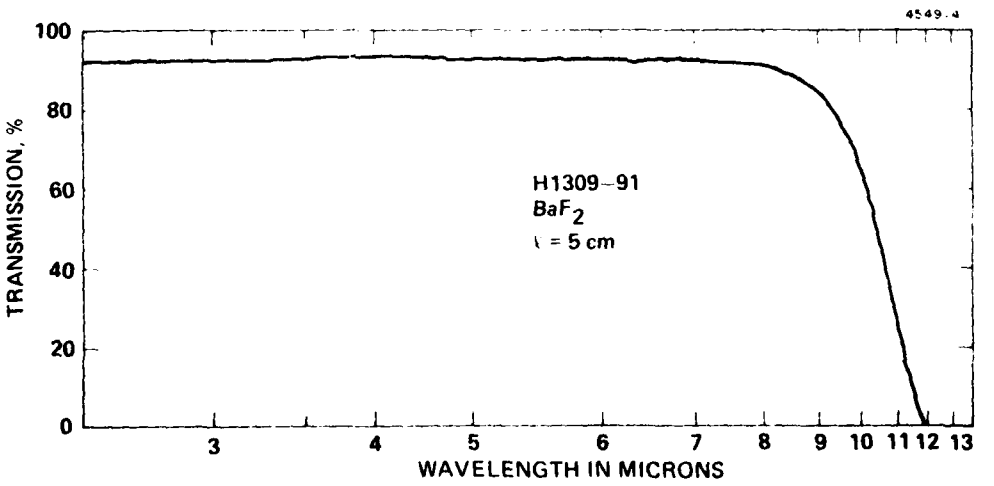

(b) Crystal Grown From Same Starting Material Using (HF, CF_4)/He

FIGURE 1. INFRARED SPECTRA OF BaF_2 CRYSTALS

THREE LOSS MECHANISMS IN HALIDE GLASS FIBERS

Herbert B. Rosenstock*
Naval Research Laboratory
Washington, DC 20375

As scattering[1] and absorption[2] of halide glasses are reduced, other optical effects limiting communication distance in fibers should be considered. The index of refraction n, and hence the propagation velocity varies with frequency ν,

$$n(\nu) = n_0 + n' \Delta\nu + \frac{1}{2} n'' (\Delta\nu)^2 + \ldots$$

(where $\Delta\nu = \nu - \nu_0$ and ' denotes derivative); this causes pulse spread for at least three different reasons: (a) frequency spread may be present in the original light source,[3,4] it is caused by (b) chopping "monochromatic" light into pulses initially[4] and (c) can arise later from frequency shifts due to Raman effect.[5]

(a) Two frequencies ν_0 and ν that start at the same time, will, according to (1), arrive at point L at times $L\, n'\Delta\nu/c$ apart; the (theoretically) simple solution is the use of a spectrally pure source (small $\Delta\nu$).

(b) This possibility disappears if short pulses, which introduce a broad spectrum of frequencies, are used for modulation. We have studied this effect for different pulse shapes, obtaining explicit results for square as well as Gaussian pulses. The main result is a quadratic dependence $L = a\tau^2$ of the attainable propagation distance L on the initial pulse width τ; for the few halide glasses or which $n(\nu)$ data exist, an initial pulsewidth of 1 nanosecond leads to substantial spread within several thousand km. The dependence of pulse spread on n"[3,6] and n'[4,7] about which divergent statements appear in the literature, is analyzed.

(c) By contrast, stimulated Raman effect can be discussed in terms of two lengths, $L_a = A/g\ P$ and $L_s = c\ \tau/n_o\ n'\ \Delta\nu$, where A, g, P, c, and $\Delta\nu$ are, respectively, cross-sectional area, Raman gain coefficient, beam power, speed of light, and the Raman frequency shift. L_a is then the distance required for amplification to take place, while L_s is the distance in which the shifted frequency separates from the pulse, thus eliminating further amplification. The effect cannot occur if the latter is smaller. L_s again depends on the pulse width, though linearly. Thus, contrary to the trend in effect (b), this one can be eliminated by reducing the pulse width.

1. D.C. Tran, G.H. Sigel, Jr., K.H. Levin, R.J. Ginther, Electron. Lett. 18, 1046 (1982).
2. M. Drexhage, B. Bendow, R.B. Brown, P.K. Banerjee, H.S. Lipson, G. Fonteneau, J. Lucas, C.T. Moynihan, Appl. Optics 21, 971 (1982).
3. D. Gloge, A.J. Marcatili, D. Marcuse, S.D. Personick, Ch. 4 in "Optical Fiber Communications," S.E. Miller and A.G. Chynoweth, eds. (Academic Press, New York, 1979).
4. D. Marcuse, Appl. Optics 19, 1653 (1980).
5. R.H. Stolen, Ch. 5 in Ref. 3.
6. J.E. Midwinter, "Optical Fibers for Transmission," (Wiley, New York, 1979), p. 78.
7. T. Okoshi, "Optical Fibers," (Academic Press, New York), p. 73.

* Sachs Freeman Associates, Bowie, Md.

Thermal Conductivity of Some Halide Glasses

H.H. Sample and Kathryn A. McCarthy*

Physics Department, Tufts University, Medford, MA

The thermal conductivities of three fluorozirconate glasses[1] have been measured in the 1.5-100 K temperature range. The measurements were carried out utilizing the steady-state method, in a cryostat previously described[2]. To our knowledge the only other such measurements on fluoride glasses is that of Guckelsberger and Lasjaunias[3] on vitreous BeF_2.

The thermal conductivities K(T) for the three glass specimens are shown in Fig. 1, along with the compositions (mole %) of the samples. These glasses exhibit the typical temperature dependence[4] of K(T) for amorphous materials: with increasing temperature, the thermal conductivity increases until at temperatures (~ 10 K) a "plateau" region is reached; at somewhat higher temperatures (~ 40 K) the thermal conductivity again increases slowly with temperature. It should be noted that in the temperature range 1.5 K to the onset of the plateau, the thermal conductivity does not appear to be a function of chemical composition, as expected. In the plateau region, the ZBLAN glass has a slightly lower conductivity than do the other two glasses. A universally accepted explanation of the plateau region does not yet exist, although the tunneling sites models[5] extended by Zaitlin and Anderson[6] give reasonable fits for the silicate glasses. It is expected that the plateau region in the fluorozirconate glasses can also be fitted by this model.

---

*The authors acknowledge support received from the Tufts University Faculty Research Fund.

1. The authors are grateful to D.C. Tran and G.H. Sigel, Jr., of the Naval Research Laboratory, and to M.G. Drexhage of RADC for providing the fluoride glass samples.

2. R.A. Kashnow and K.A. McCarthy, J. Phys. Chem. Solids 30, 813 (1969); M. Jirmanus, K.A. McCarthy, H.H. Sample and J. Bulman (unpublished).

3. K. Guckelsberger and J.C. Lasjaunais, Comptes Rendus Hebd. Sean. Acad. Sci. 270, 1427 (1970). The K vs T of BeF_2 exhibits a slight shoulder, but not a distinct plateau. See, A.J. Leadbetter, A.P. Jeapes, C.G. Waterfield and R. Maynard, J. Physique 38, 95 (1977).

4. See, for example, R. Berman, Thermal Conduction in Solids, (Clarendon Press, Oxford, 1976), Chapter 9, and A.C. Anderson: in Amorphous Solids, ed. by W.A. Phillips (Springer-Verlag, Berlin, 1981), Chapter 5.

5. P.W. Anderson, B.I. Halperin, and C.M. Varma, Phil. Mag. 25, 1(1972); W.A. Phillips, J. Low Temp. Phys. 7, 351 (1972).

6. M.P. Zaitlin and A.C. Anderson, Phys. Rev. B12, 4475 (1975) and Phys. Stat. Sol.(b) 71, 323 (1975). See also, D.P. Jones, N. Thomas, and W.A. Phillips, in Phonon Scattering in Condensed Matter: ed. H.J. Maris (Plenum, New York, 1980)p. 49 for the effect of Rayleigh scattering.

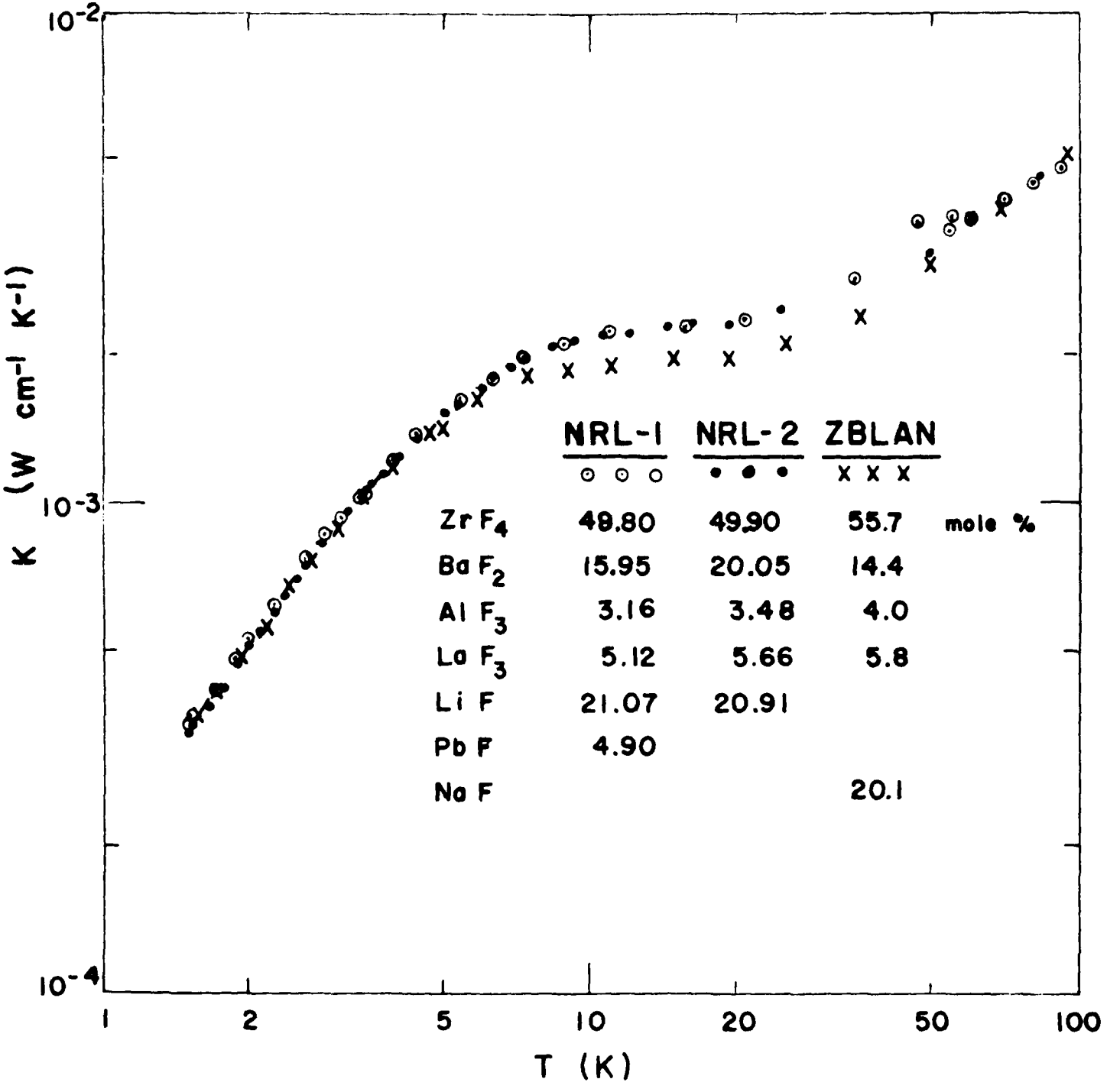
10^{-2}
10^{-3}
10^{-4}
K (W cm^{-1} K^{-1})
1
2
5
10
20
50
100
T (K)
NRL-1
NRL-2
ZBLAN
Zr F$_4$ 49.80 49.90 55.7 mole %
Ba F$_2$ 15.95 20.05 14.4
Al F$_3$ 3.16 3.48 4.0
La F$_3$ 5.12 5.66 5.8
Li F 21.07 20.91
Pb F 4.90
Na F 20.1

Light Scattering in Fluoride Glasses*

John Schroeder
Department of Physics
Rensselaer Polytechnic Institute
Troy, N.Y. 12181

INTRODUCTION

Heavy metal fluoride glasses are a recently synthesized class of non-oxide amorphous materials whose molecular structure, morphology and optical behavior is at variance from the more common and conventional oxide based glasses.(1) The compositional flexibility of these heavy metal fluoride glasses is such that glasses with a broad range of optical transmission, refractive index and magneto-optic characteristics can be produced.

Considerable work has been devoted recently in the preparation and characterization of these multicomponent heavy metal fluoride glasses, especially fluorozirconates(2) and fluorohafnates(3) where the network formers are ZrF_4 and HfF_4, respectively, with modifiers being BaF_2 and fluorides of rare earths, group-III elements or alkalies. These glasses exhibit high transparency over a frequency range spanning the mid IR to the near UV. This property alone makes them possible candidates for a wide variety of applications ranging from laser windows, infra-red transmitting windows to infra-red fiber optics.

Attenuation of light in a glass is brought about by several mechanisms. Fortunately, the different mechanisms may be isolated since they are not of equal magnitude at the same wavelength of the exciting light. Rayleigh scattering seems to dominate below 2000 nm.

*This work is supported by A.F. Contract No. F19628-83-C-0016 from Rome Air Development Center (AFSC), Hanscom AFB, Mass.

At longer wavelengths, absorption features, for example those of the OH ion dominate, and beyond 5000 nm multi-phonon absorption is many orders of magnitude larger than the Rayleigh scattering or the OH^- absorption. Hence, it is most important to understand the basic Rayleigh scattering behavior of a glass if we wish to make predictions about its attenuation up to about 6000 nm and be able to reduce the scattering losses such that a fluoride glass could be employed as a suitable material for fiber optic applications in the near infra-red regime.

THEORETICAL BACKGROUND

Rayleigh scattering in dense disordered materials is brought about due to microscopic fluctuations in the dielectric susceptibility about its equilibrium value. Consequently, the intensity of the scattered light is given by $I(\theta) \propto \langle \Delta \varepsilon_k^2 \rangle$ where $\langle \Delta \varepsilon_k^2 \rangle$ is the k-th component of the mean square fluctuations of the dielectric constant.

For a binary component glass or quasi-binary glass it follows that[4,5]

$$\langle \Delta \varepsilon_k^2 \rangle \propto \left(\frac{\partial \varepsilon}{\partial \rho}\right)_{T,c}^2 \langle \Delta \rho_k^2 \rangle + \left(\frac{\partial \varepsilon}{\partial c}\right)^2 \langle \Delta c_k^2 \rangle$$

where the entire scattering problem can be described by four quantities; namely, the mean square fluctuations of density and concentration, and the gradients of the dielectric susceptibility with respect to density and also concentration. Hence, the above equation shows that the scattering can be minimized if any of these components can be reduced or made to approach zero.

The nature of $\langle \Delta \rho_u^2 \rangle$ and $\langle \Delta c_K^2 \rangle$ will be discussed in light of certain thermodynamic models based on possible structural models of these new fluoride glasses.

METHOD OF MEASUREMENT

In this letter we report the results of investigations concerning Rayleigh-Brillouin scattering in these heavy metal fluoride glasses, in order to provide detailed information about scattering losses and also to provide for the first time measurements of the elastooptic and elastic properties of these materials.

The methods employed to obtain the Rayleigh-Brillouin spectra of the heavy metal fluoride glasses are laser excitation (Argon-ion) operating at 488 nm coupled to a multi-pass high contrast Fabry-Perot interferometer with a photon counting detection system and associated data handling electronics. A comprehensive schematic of this equipment will be found in Figure 1. The glass samples employed for these measurements were prepared at our laboratories utilizing techniques described elsewhere.(1) The primary quantities that are measured in this study are the Landau-Placzek ratio (a normalized Rayleigh intensity), the Brillouin intensities and the shift of the Brillouin lines.

RESULTS AND DISCUSSION

Table I summarizes the constituents of the seventeen fluoride glass samples used in this study and identifies each glass. Table IIa shows the results of the scattering loss measurements made at 488 nm, in terms of the Landau-Placzek ratio, for the

heavy metal fluoride glasses. The Landau-Placzek ratio of SiO_2 is also given for comparison purposes. One should note that some of the fluoride glasses show a scattering loss that is about equal or even less than the pure SiO_2 sample. For some of the fluoride glass samples the scattering loss in dB/km is also given.

Table IIb and Table IIc summarize the elastic properties of some of the fluoride glass samples. In addition Table IIb contains some Verdet constants calculated from Faraday rotation measurements at two wavelengths. Table IIc gives Poisson's ratio for several of the fluoride glass samples and the measured value of Poisson's ratio of ~ 0.25 indicates that these glasses have a much more elastic structure (softer lattice) than the pure SiO_2 sample. The sound velocities also give an indication that in the fluoride glasses we are dealing with a less rigid lattice than in a typical silicate glass. The elastic constants of the fluoride glasses are of comparable size to the SiO_2 sample C_{11} and that is primarily caused by the much greater densities of the fluoride compared to the silicate glass.

The Pockels' elastooptic coefficients are summarized in Figure 2. Here the P_{12} of the fluoride glasses show at most a linear dependence with refractive index. This is in contrast to a binary sodium-silicate glass that shows a higher order functional dependence of P_{12} on refractive index. P_{44} changes extremely slowly as the refractive index changes, again atypical when compared with a silicate glass.[6]

CONCLUSION

1. Successfully measured the intensity and spectral distribution of the various heavy metal fluoride glasses.

2. Some of the heavy metal fluoride glasses exhibit less Rayleigh scattering than the best SiO_2 glass.

3. The relatively low value of the transverse Brillouin shifts for the fluoride glasses are due to the higher coordination number of this material compared to oxide glasses. The high coordination number inhibits transverse vibrations in fluorides that normally dominate the elastic behavior of tetrahedrally coordinated glasses.

4. Multiple scattering is the predominant extrinsic scattering mechanism.

5. On the basis of λ^{-4} scaling, some heavy metal fluoride glasses with low Rayleigh scattering losses are prime optical wave guide material for the near infra-red regime.

REFERENCES

(1) M. G. Drexhage et al. Advances in Ceramics, Vol. II: Physics of Fiber Optics. B. Bendow and S. Mitra, editors. Amer. Cer. Soc., Columbus, Ohio, 1981, p. 57-73.

(2) B. Bendow et al. J. Appl. Phys. 52, 1460 (1981).

(3) B. Bendow et al. Sol. State Comm. 37, 485 (1981).

(4) J. Schroeder et al. J. Amer. Cer. Soc. 56, 510 (1973).

(5) J. Schroeder, Treatise on Material Science and Technology, Vol. 12, Edit. by M. Tomozawa and R. H. Doremus. Academic Press, N.Y., 1977, pp. 157-222.

(6) J. Schroeder, J. Non-Crystalline Solids 40, 549 (1980).

The contributions to this work of M. Fox-Bilmont, B. G. Pazol, V. Tsoukala, M. G. Drexhage, and O. El-Bayoumi are gratefully acknowledged.

TABLE I

Selected Heavy-metal Fluoride Glass Compositions in Mole %

Glass #	ZrF_4	BaF_2	LaF_3	AlF_3	HfF_4	PrF_4	HoF_3	EuF_3	NaF
ZBLA-139	57	36	3	4	-	-	-	-	-
ZBLA-129	57	36	3	4	-	-	-	-	-
HBLA-153	-	36	3	4	57	-	-	-	-
HBLA-148	-	36	3	4	57	-	-	-	-
ZBLA-131	57	34	3	4	-	2	-	-	-
ZBLAH-144	57	34	3	4	-	-	2	-	-
ZBLAEu-147	57	34	3	4	-	-	-	2	-
HBLAP-286	-	34	3	4	57	2	-	-	-
HBLAH-287	-	34	3	4	57	-	2	-	-
HBLAEu-240	-	34	3	4	57	-	-	2	-
ZBLAN-428	55.7	14.4	5.8	4	-	-	-	-	20.1

Glass #	BaF_2	NaF	AlF_3	HoF_3	ZuF_2	LaF_3	ThF_4	YbF_3	MnF_2	$D_{..3}$
BZLT-268	19	-	-	-	27	27	27	-	-	-
BZYbT-265	19	-	-	-	27	-	27	27	-	-
BMDNT-357	9.5	5	-	-	-	-	38	-	38	9.5
BMAYT-384	8.5	-	5	-	-	-	34	10	42.5	-
BMHT-335	10	-	-	8	-	-	40	-	42.0	-
BMYT-382	9	-	-	-	-	-	36	10	45.0	-

TABLE IIa

Landau-Placzek Ratio and Scattering Attenuation Coefficients for Heavy Metal Fluoride Glasses at 488 nm and at 300°K

Glass #	Landau-Placzek Ratio	Scattering Loss (dB/km)
ZBLA-139	22.1	4.00
ZBLA-129	838.0	195
HBLA-153	26.7	10.94
HBLA-148	78.8	33.00
ZBLAP-131	201	-
ZBLAH-144	341	-
ZBLAEu-147	36.4	8.00
HBLAP-286	2112	-
HBLAH-287	2059	-
HBLAEu-240	543	-
ZBLAN-428	16.9	-
BZLT-268	549	87.6
BZYbT-265	1276	-
BMDNT-357	44.5	13.5
BMAYT-384	147	12.4
BMHT-335	11690	-
BMYT-382	1098	-
SiO_2	21.9	11.6

TABLE IIb

Longitudinal Sound Velocity, Elastic Constant (C_{11}) and the Verdet Constants for Some Selected Heavy Metal Fluoride Glasses

Glass #	V_L(m/s)	C_{11}(GPa)	Verdet Constant (min/cmG) (442 nm)	(632.8 nm)
ZBLA-139	4026	74.7	0.0137	0.0073
ZBLA-129	4231	82.5	0.0161	0.0071
HBLA-153	3615	76.9	0.0145	0.0059
BHLA-148	3680	79.6	0.0134	0.0098
ZBLAEu-147	4218	82.0	0.0146	0.0061
BZLT-268	3707	88.6	0.0302	0.0114
BMDNT-357	4090	107.9	-0.0519	-0.0143
BMAYT-384	4175	112.4	0.0048	0.0121

TABLE IIc

Sound Velocities (Longitudinal and Transverse) Elastic Constants (C_{11},C_{44}) and Poisson's Ratio (σ) of Some Selected Heavy Metal Fluoride Glasses and SiO_2

Glass #	V_L(m/s)	V_T(m/s)	C_{11}(GPa)	C_{44}(GPa)	σ
ZBLA-139	4026	2333	74.7	25.1	0.250
ZBLAEu-147	4218	2384	82.0	26.2	0.265
Fluorozirconate*	3980	-	76.1	23.2	0.279
SiO_2	5944.2	3748.7	79.0	30.97	0.166

*$58ZrF_4 \cdot 34BaF_2 \cdot 8ThF_4$ (Ultrasonic Data)
From: M.P. Brassington et al.
Mat. Res. Bull. 16, 613 (1981)

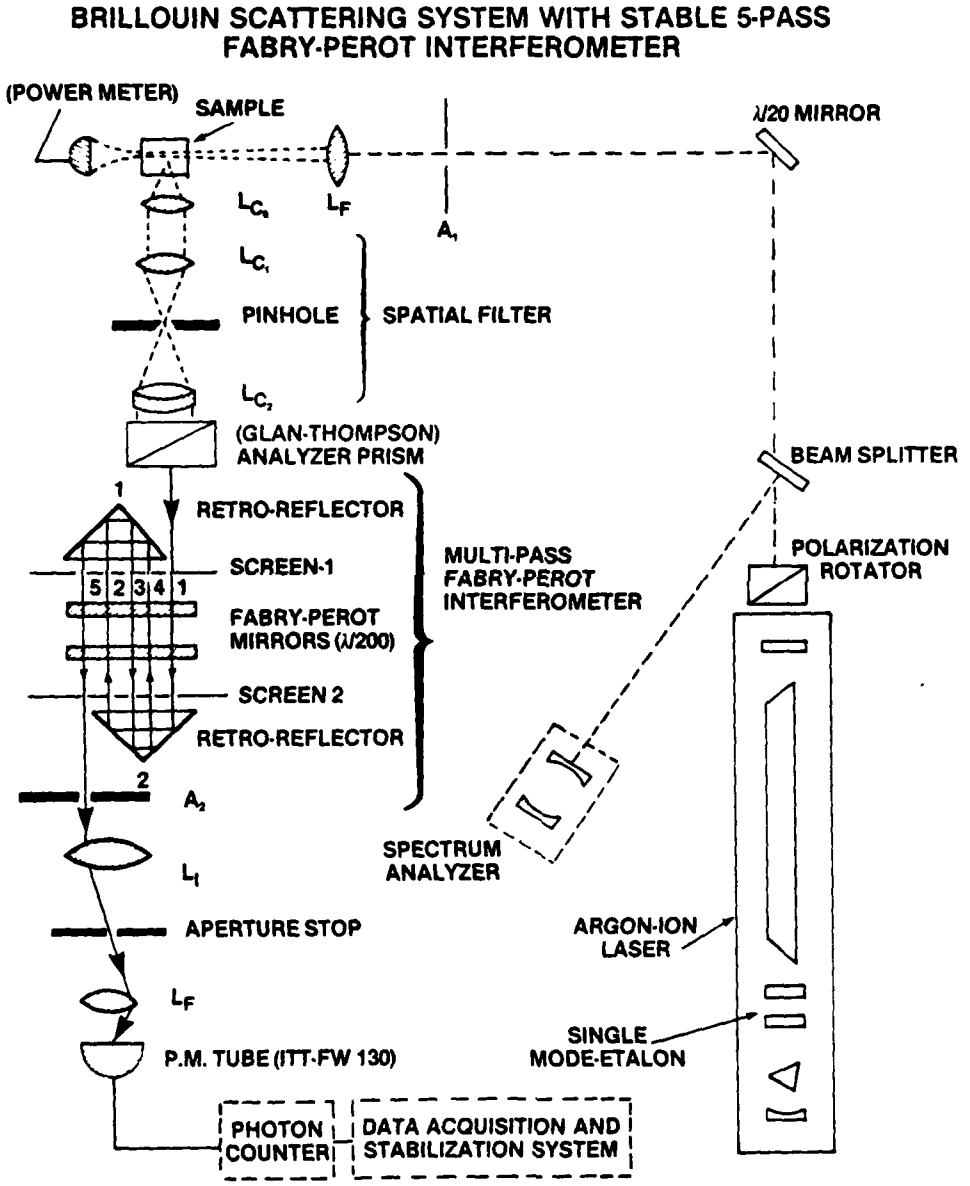

FIGURE 1. Schematic of Rayleigh-Brillouin Scattering Apparatus.

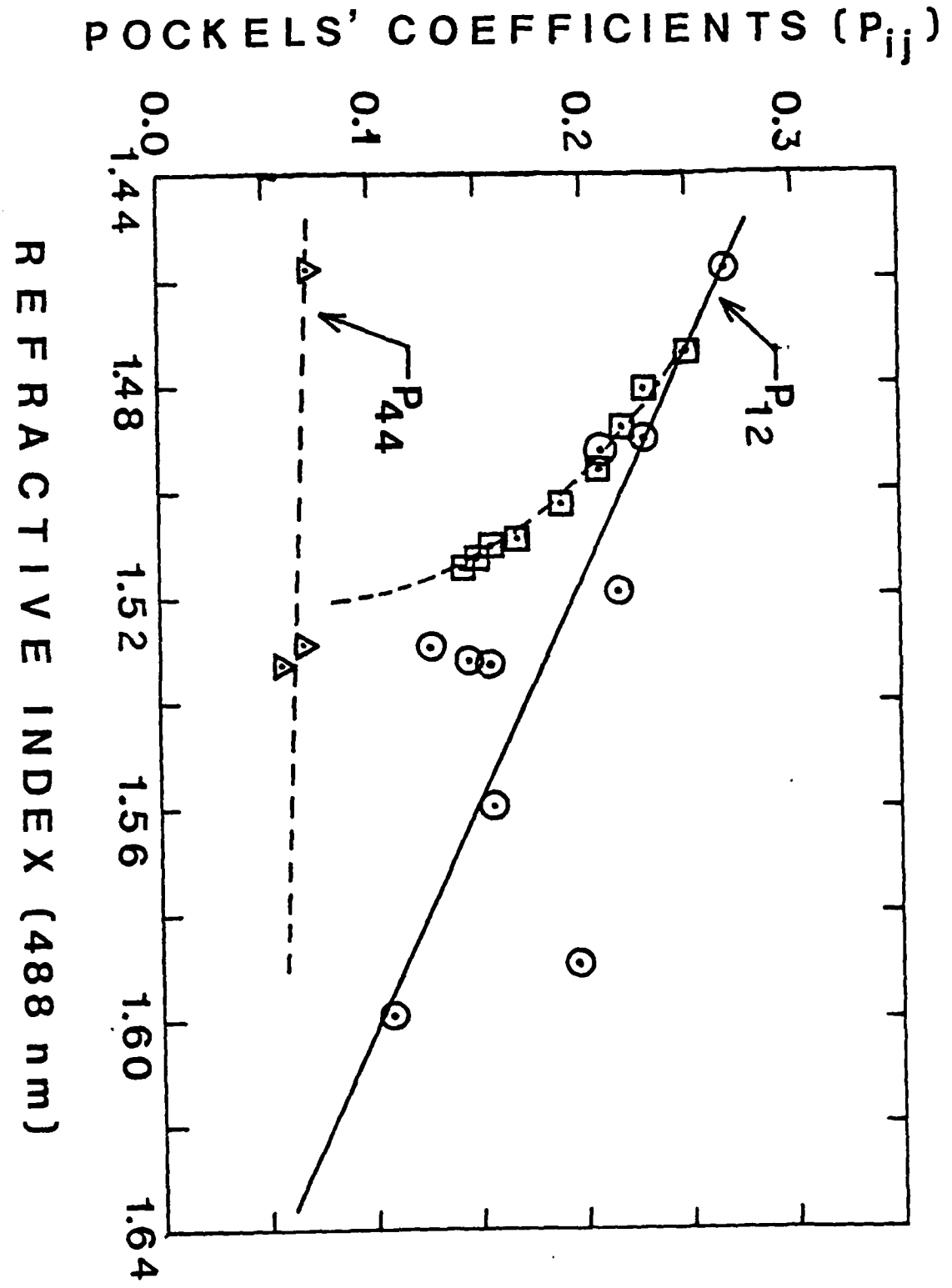

FIGURE 2. Pockels' elastooptic coefficients versus refractive index for heavy metal fluoride glasses (⊙, △) and a binary $Na_2O{\cdot}SiO_2$ glass (⊡).

HEAVY METAL FLUORIDE GLASSES AS MID- IR LASER MATERIALS

W. A. Sibley and M. D. Shinn
Oklahoma State University
Stillwater, Oklahoma

This paper concerns the optical absorption, emission and excitation spectra for Erbium and Holmium ions in fluorozirconate glass. Fluorozirconate glass is a heavy metal fluoride glass which is highly transparent from .3 to 6.0 microns. It is relatively easy to prepare and can be doped with rare earth fluorides or 3d transition metal fluorides without the need of charge compensation. There are a number of promising potential applications of this material in the laser and optical fiber communication industries. The optical properties of rare earth ions such as Er^{3+} and Ho^{3+} have been extensively studied. [1-7] [1]The purpose of this paper is to present data on the optical properties of Er^{3+} and Ho^{3+} ions in fluorozirconate glass. Broad band excitation is employed which means the observed optical properties are the sum of the transitions of the individual ions in the various sites within the glass. Special consideration will be given the radiative and non-radiative rates of transitions. Judd[1] and Ofelt[2] have shown that by using simplifying assumptions the probabilities of forced electric dipole transitions can be expressed as the sum of a small number of phenomenological parameters. These parameters can be determined by a best fit of calculated and observed oscillator strengths and can then be used to find the electric dipole contribution to the total spontaneous emission probabilities. Numerous authors [4-6] have found in the past that this approach is effective for determining the probability of non-radiative transitions. This probability can in turn be used to evaluate the usefulness of the heavy metal glass as a host for possible laser use. The Judd-Ofelt theory has been used extensively to predict radiative rates of transitions for rare earth ions in crystals, glasses or solutions. We investigate the reliability of the Judd-Ofelt predictions by extensive temperature dependent lifetime measurements. Room temperature lifetime measurements are found to be representative of the radiative rate only when the number of phonons required for the non-radiative transition is ten or greater. This investigation uses measurements of low temperature lifetimes to confirm the predictions of Judd-Ofelt theory for Er^{3+} ions. The differences between the calculated and measured rates are within the accuracy of the predicted rates or can be accounted for by multiphonon emission. The low temperature value of the multiphonon emission rate and the temperature dependence can be described by the configuration coordinate model of Huang and Rhys. This model predicts essentially the same values as those found with the often used single phonon model. The agreement is best at the higher temperatures. The method developed by Flaherty and DiBartolo[7] for the determination of radiative and non-radiative rates of Er^{3+} and MnF_2 was used and found to agree with the Judd-Ofelt predicted rates within the accuracy of the methods. The Flaherty-DiBartolo method was found to be highly sensitive to the accuracy of the data used. It can only be

applied with confidence or adjacent emitting states. These conditions limit its applicability. Our results indicate the optical properties for Er^{3+} and Ho^{3+} doped fluorozirconate glasses are similar to those for Er^{3+} doped crystals. The emission lifetimes are close to single expenditial even under broad band excitation. The absorption and emission bands are relatively narrow when compared to similar bands in oxide glasses. The observed multiphonon emission rates are lower than the rates observed in germinate or tellurite glass. If time permits, the radiation damage aspects of the fluorozirconate glasses will also be discussed.

1. B.R. Judd, Phys. Rev. 127, 750 (1962).

2. G.S. Ofelt, J. Chem. Phys. 37, 511 (1962).

3. G.H. Dieke, Spectra and Energy Levels of Rare-Earth Ions in Crystals (Interscience, New York, 1968).

4. M.J. Weber, Phys. Rev. 157, 231 and 262 (1967) and Phys. Rev. B8, 47 (1973).

5. W.F. Krupke, Phys. Rev. 145, 325 (1966).

6. R. Reisfeld, G. Katz, N. Spector, C.K. Jorgensen, C. Jacoboni and R. DePape, J. Solid State Chem. 41, 253 (1982).

7. J.M. Flaherty and R. DiBartolo, J. Lumin 8, 51 (1973).

CHEMICAL DURABILITY STUDIES OF HEAVY METAL FLUORIDE GLASSES

by

Catherine J. Simmons, Saied Azali and Joseph H. Simmons

Catholic University of America

Washington, D. C. 20064

This presentation covers several studies related to the chemical durability (ie. corrosion resistance) of a variety of fluoride glasses, shown in Table 1.

Table 1: **COMPOSITION (mole %)**

GROUP I

	ZrF_4	BaF_2	LaF_3	AlF_3	LiF	NaF	PbF_2	Source
ZBL	62	33	5	.....	.....	.....	.....	R.P.I.
ZBLA	58	33	5	4	.....	.....	.....	
ZBLAN	54.0	15.0	6.0	4.0	.....	21.0	.....	
ZBLAL	51.8	20.0	5.3	3.3	19.6	.....	.....	N.R.L.
ZBLALP-1	50.2	19.3	5.1	3.1	18.9	.....	3.4	
ZBLALP-2	50.4	15.5	4.9	3.1	20.2	.....	4.9	

GROUP II

	BaF_2	ZnF_2	LuF_3	YbF_3	ThF_4	NaF	Source
BZLT	19	27	27	.....	27	.....	R.A.D.C.
BZYbT	19	27	.....	27	27	.....	R.P.I.
BZYbTN	10	27	.....	27	27	9	

I. Resistance to Aqueous Attack:

A. Composition Study

All glasses were immersed in deionized water at 25 C to determine their leach rates as a function of time. Chemical analyses of the leaching solutions showed that, within each family of glasses, the leach rates observed were virtually identical, regardless of variations in composition. However, the results show a distinct difference between the Zr/Hf based glasses and those based on Th-Ba, with the latter exhibiting an improvement in leach resistance of 50-100 times. (See Figs. 1 and 2 for leach data of individual components of BZYbT and BZYbTN glasses, Fig. 3 for leach data of individual components of ZBLAL, and Fig. 4 for a general comparison between the 2 families of halide glasses with well-known silicate glasses.) Whereas the Zr/Hf glasses had developed a thick, hydrated surface layer, overlayed by a crystalline crust, and were quite opaque after 5 days of exposure, the Th-Ba glasses appeared to have suffered much less damage and were still fairly transparent. The thickness of these crusts was determined by SEM to be > 150 μm for the Group I glasses and $\sim$ 2-3 μm for the Group II glasses. This ratio is in good agreement with the leach rate data (Table 2).

Weight loss was measured for all samples and, when compared with solution analysis, proved to be up to 15% too low in estimating the leach rates due to hydration during leaching.

B. pH Effects

One composition (ZBLAL) was selected for study in a variety of solutions at different pH values. Results show an increase in leach rate of approximately 10 times at pH 2 as compared with deionized water at pH 5.7. In more alkaline solutions (pH 10-11) the Zr leach rate drops due to the formation of insoluble hydroxides and, although the other components continue to leach, the rate decreases sharply with time. This appears to be caused by the formation of a protective $Zr(OH)_4$ barrier on the surface.

C. Powdered-vs-Bulk Samples

Two samples of ZBLAL glass, one powdered and one in the form of a polished rectangular parallelpiped, were leached to determine the validity of powder test results. The surface areas were calculated to be identical initially. Leach rates were comparable for the first 4 hours. However, this was followed by a steady decline in powder sample rates as the surface area decreased. At the end of 4 days, the leach rates for the powder samples were 1/10 those of the bulk sample. The results of this study strongly suggest that powder samples should be used only for very short term testing (ie. < 4hrs.) when leaching non-durable glasses such as these.

II. Humidity Effects:

Infrared transmittance spectra were obtained from a ZBLAL polished sample before, midway through, and after exposure to 100% relative humidity at 80 C for 7 days. Care was taken to maintain the sample at the same temperature in order to avoid condensation of water vapor. There was no visible damage to the

glass over the period of the test, and the IR spectra only showed a loss in transmittance of ~5% centered at 2.85 μm due to OH^- presence.

III. SEM Surface Studies:

The surface topography of leached samples was examined by scanning electron microscopy. Once again, samples within Group I or II were very similar to one another in the extent of attack and type of surfaces formed. Group II (Th-Ba) glasses were found to be far less damaged by aqueous leaching. Elements contained in the crystal deposits on the surfaces were identified by x-ray analysis using a wavelength dispersive spectrometer and are listed in Table 2.

Table 2: Summary of Observations in Composition Study

Type	Leach Rate g/cm^2 day	Sample Surface	Crust Thickness	Crystals Identified
Group I	10^{-2}	Opaque	150 μm	Zr, Ba, La
Group II	10^{-4}	Frosted	3 μm	Ba, Yb, Th

Acknowledgements:

The authors would like to thank the following for providing samples for this study: Professor C. T. Moynihan and Drs. A. J. Bruce and D. L. Gavin, Rensselaer Polytechnic Institute; Dr. D. C. Tran, Naval Research Laboratory; and Drs. O. H. El Bayoumi and M. G. Drexhage, Rome Air Development Center. In addition we would like to thank Mr. V. Rogers, Vitreous State Laboratory, Catholic University, for the chemical analysis. This work was supported in part by the Office of Naval Research under contract N0014-83-K-0276.

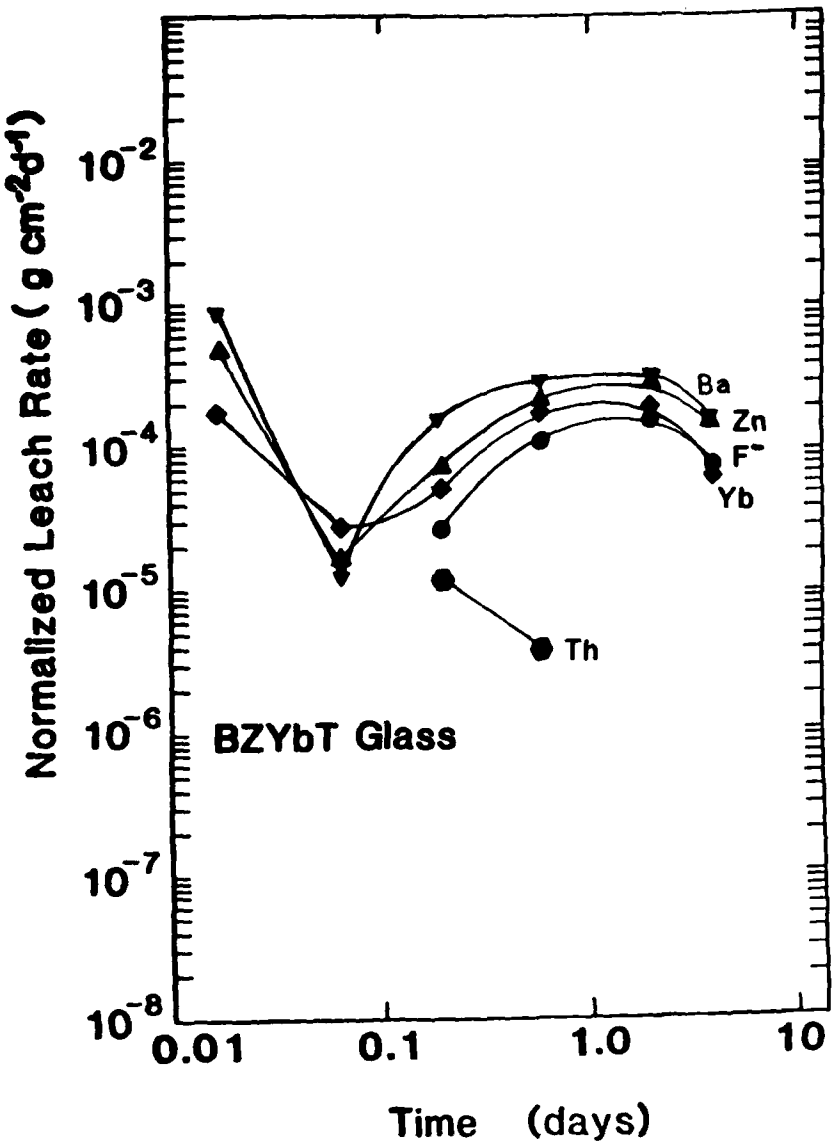

Fig.1: Leach rates, normalized to composition, show nearly congruent dissolution except for Th, which was found in high concentration in the crystalline crust.

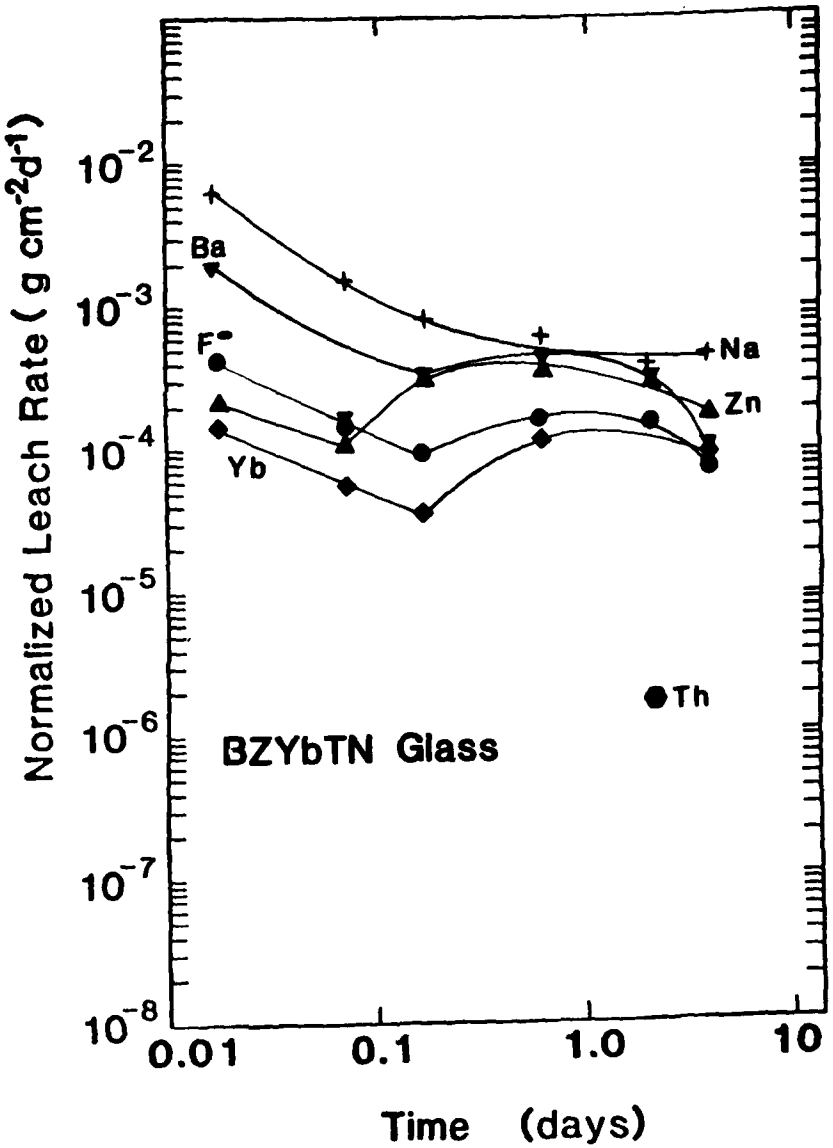

Fig.2: Addition of Na accelerates Ba and Zn dissolution slightly.

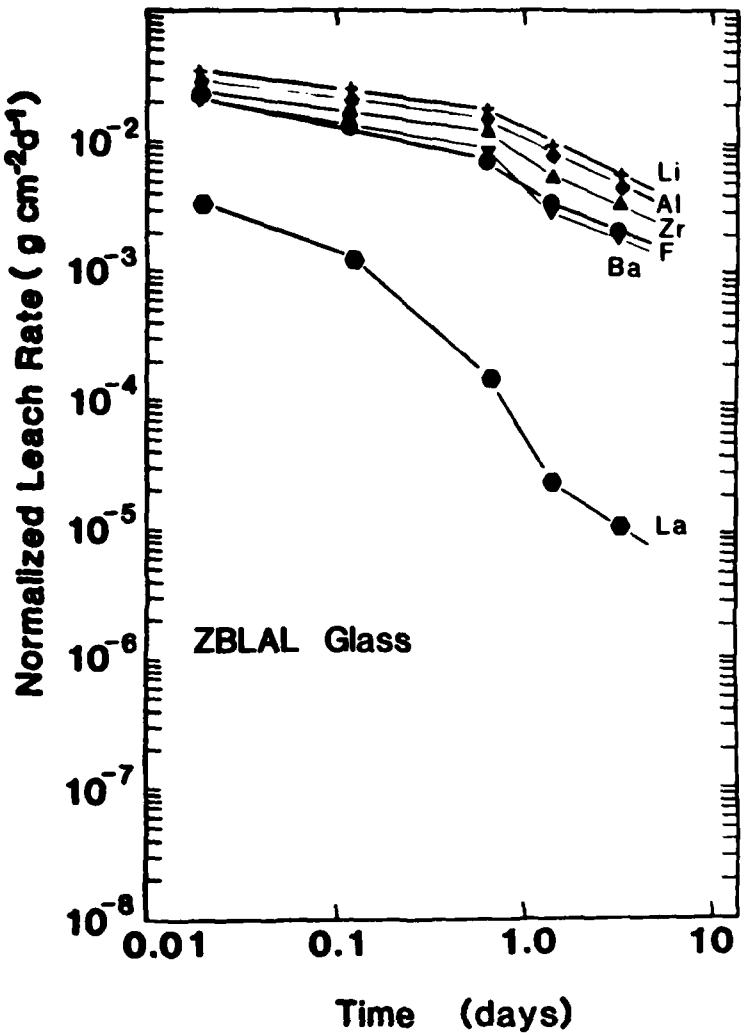

Fig.3: Typical of all Group I compositions, this shows nearly congruent leaching except for La which deposits in the crust.

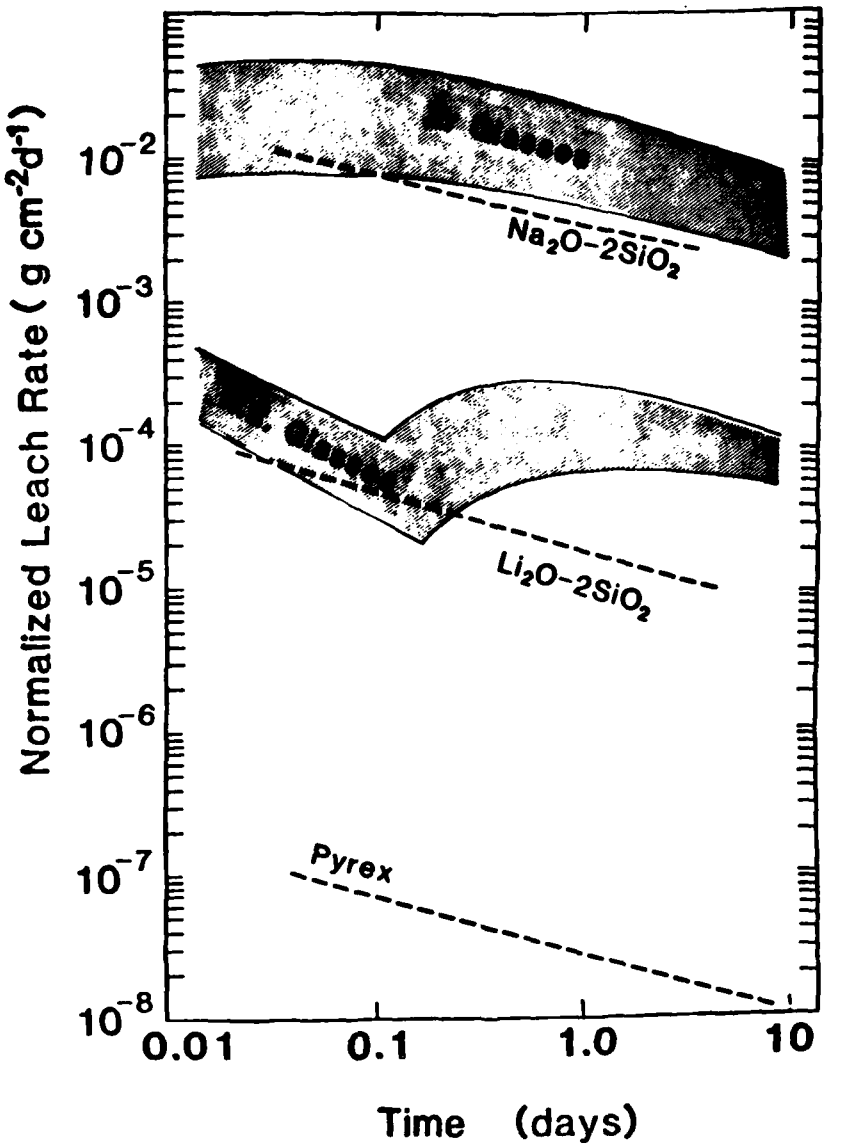

Fig.4: Leach rate comparison of Group I (Zr Glasses) and Group II (R.E. Glasses) with some well known silicate glasses.

DIAMOND-LIKE CARBON COATINGS FOR PROTECTION OF HALIDE GLASS SURFACES

Martin L. Stein
Stein Associates, 27 Burlington Rd, Bedford, MA 01730
&
SpecTran Corporation, Hall Road, Sturbridge, MA 01566

Arold Green
Naval Weapons Center, China Lake, CA 93555

Bernard Bendow
The BDM Corporation 1801 Randolph St. SE, Albuquerque, NM 87106

Osama El-Bayoumi & Martin G. Drexhage
Solid State Sciences Division, Rome Air Development Center
Hanscom AFB, MA 01731

This report describes the feasibility of using Diamond-Like Carbon (DLC) coatings for protection of halide glass surfaces.

Recent advances in fluoride glasses and processing technology have indicated that these materials are suitable for a wide variety of optical applications requiring low distortion and low loss. While the projected optical characteristics of fluoride glasses are outstanding, and their intrinsic strength and hardness is acceptable, the surface of the glass is subject to corrosion which may compromise the suitability of the glass for many applications. The susceptibility to corrosion has been observed by many groups, and several reports have been released describing the attack of fluoride glass surfaces in aqueous environments.

Corrosion has been reported to occur in fluoride glass fibers and can produce significant reductions in strength over relatively short time periods in air. The attack in water is expected to be much more severe, based on the data of Simmons et al and Fjeldy. Thus the prospects for exploiting the outstanding potential of fluoride glass optical fibers depends on an effective means of protecting the surface of the glass from attack.

Diamond-Like Carbon films have been deposited sucessfully for almost two decades and have been studied intensively as protective hermetic coatings for sensitive optical surfaces for the last few years, primarily for high power lasers. However, due to the variability of the deposition techniques and methods used for evaluation, the suitability of DLC for protection of halide glasses, chalcogenide glasses, and crystalline materials is unknown.

DLC is typically formed by ion processes such as plasma or ion beam deposition on suitable substrates (Fig. 1). Attempts at carbon film deposition by atomic or molecular techniques which do not incorporate charged particles have typically not produced films with "diamond-like" properties. Consequently, it appears that film nucleation and growth processes are dependent upon the kinetic energies provided by incoming ions. Films posessing diamond-like properties are produced with simultaneous ion bombardment energies ranging from 40 to 100 eV.

The transmission spectrum of Diamond-Like Carbon (Fig. 2.) illustrates the potential for broadband optical windows. Besides suitable optical properties, primary requirements for a protective coating are that it serve as a moisture barrier and provide a chemically inert, hardened environmental surface. Properties of DLC that have been reported by the authors and others are summarized in Fig (3). As noted, many properties are a function of the deposition process and are related to the bombarding ion energies.

While deposition on covalent substrates has resulted in films with good adhesion, problems had arisen when coating ionic substrates such as alkaline earth fluorides. A technique has been developed which produces continuous adherent films on ZBLA Fluoride glasses and Calcium Fluoride. This approach has resulted in high adhesion coatings 100 to 1000 A thick with good optical properties. The technique involves modifiying the incoming ion energy so as to produce a carbon concentration gradient between substrate and coating. The depth profile is controlled to produce a concentration gradient approximately 100 Angstroms thick as predicted by atomic scattering theory and as measured by ESCA and Auger spectroscopy. These measurements also indicated that the Carbon film was relatively pure. A gradually decreasing trace of oxygen was observed towards the substrate, at which point an increase in oxygen, possibly indicative of the prior surface, was observed.

The compositional and structural alteration of the zone between coating and substrate may be regarded as an ion modified surface in which factors such as radiation damage, sputtering, and implantation also take part in surface formation as shown in Fig 4. Future work will involve studying the chemical bonding characteristics, structure, and stochiometry of this zone which we plan to correlate with the desired physical and optical properties for the intended applications and materials. An effective coating of this type may find application for several optical components such as high power laser windows, domes, canopies and other optical elements where broad band hardened surfaces are required. DLC coatings have been deposited on-line on silcate fibers and have sucessfully demonstrated improved hermeticity. It is anticipated that application of these techniques can be applied to Halide glasses as well.

References:

1. C.J. Simmons, H. Sutter, J.H. Simmons, and D.C. Tran,"Aqueous Corrosion Studies of a Fluorozirconate Glass," Mat. Res. Bull., 17, 1203-1210 (1982).

2. M.G. Drexhage, O.H. El-Bayoumi, and C.T. Moynihan, "Progress in Heavy Metal Fluoride Glass for Infrared Fibers", Society of Photo-Optical Inttrumentation Engineers (SPIE), Proceedings, Vol 320, Advances in IR Fibers II, p.27(1982).

3. M.L. Stein and S. Aisenberg, "High Energy Ion Deposited Carbon Films", Proceedings of the Workshop on Diamond-Like Carbon Coatings", Albuquerque, NM, B. Bendow, ed., pp. 78-99 (1982).

4. M.L. Stein, S. Aisenberg, J.M. Stevens, "Ion Plasma Deposition of Hermetic Coatings for Optical Fibers", Physics of Fiber Optics, Vol II, B. Bendow, ed., The American Ceramic Society, Columbus OH, 1981; pp 124-133.

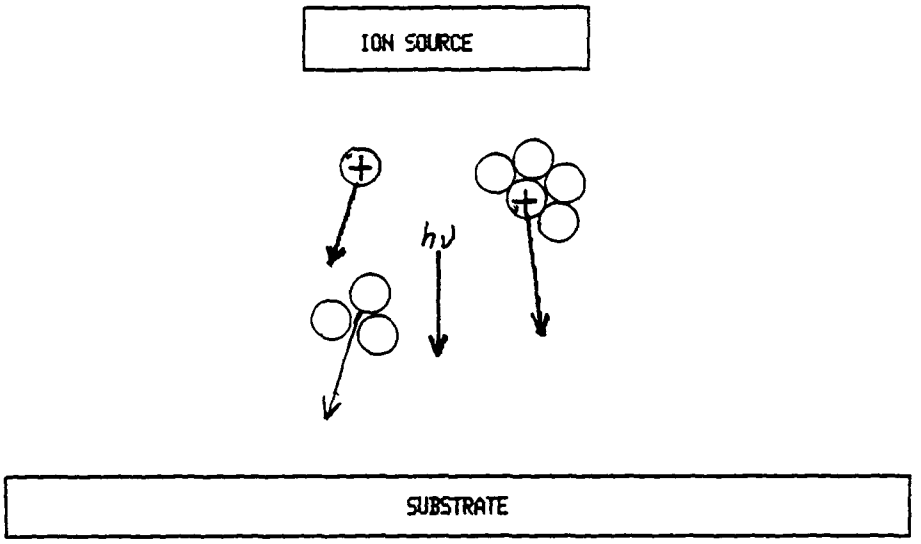

FIGURE 1. THE ION DEPOSITION PROCESS

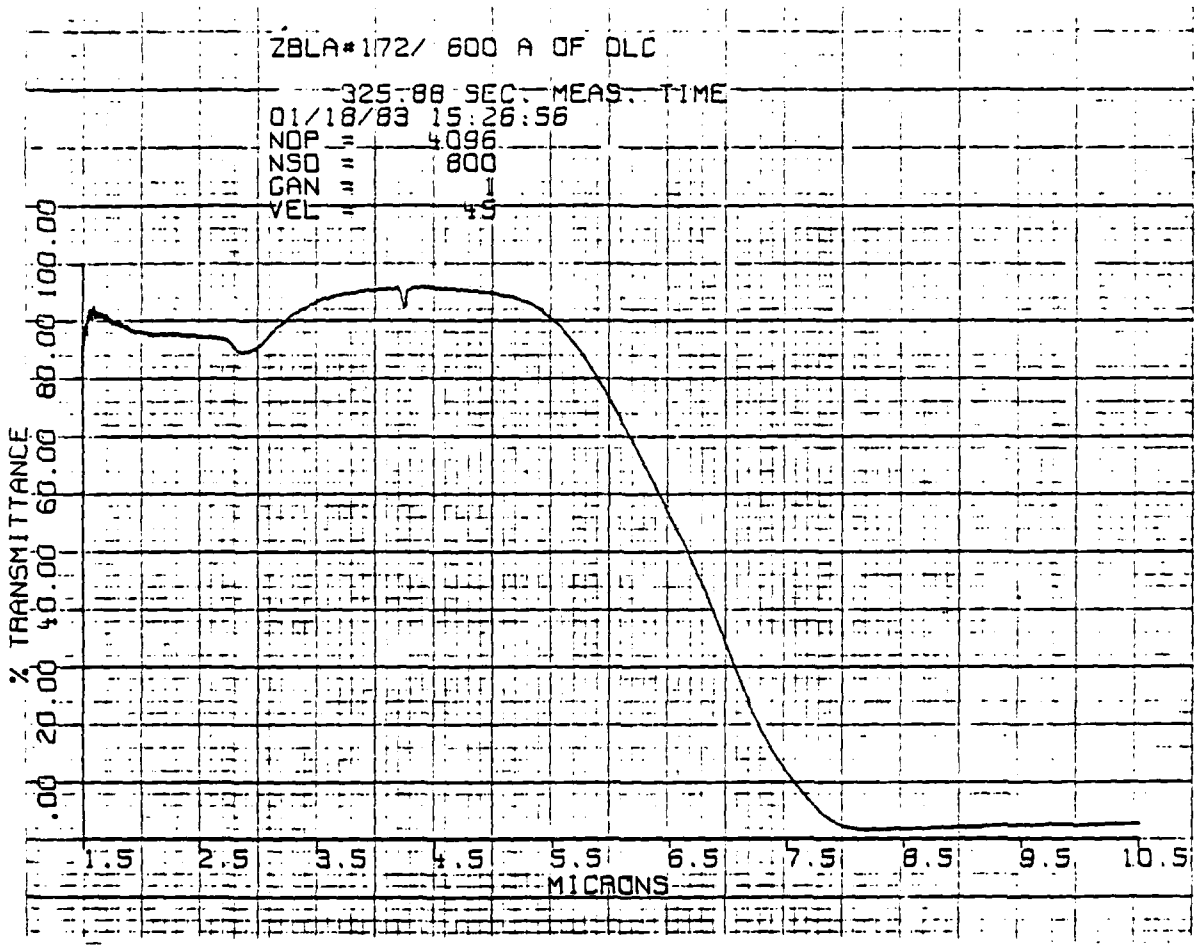

FIGURE 2. TRANSMISSION SPECTRA OF DLC ON ZBLA GLASS

* Optically Transparent - Low absorption from 0.3 to 30 microns.
* Electrically Insulating - $> 10^{12}$ Ohm-cm bulk resistivity.
* Chemically Inert - Has not been observed to change properties when exposed to acids, bases, or organic solvents.
* Low Optical Scatter - Primarily a function of cleanliness of the deposition process.
* Hardness - 1800 to 2000 Knoop Hardness
* Refractive Index - Varies between 1.8 and 2.3 dependent on process.
* Composition - Primarily Carbon with 1% to 20 % Hydrogen incorporated
* Structure - Amorphous to polycrystalline, function of process
* Density - 2.0 to 2.36 g/cc, function of process.

FIGURE (3) PROPERTIES OF DIAMOND-LIKE CARBON

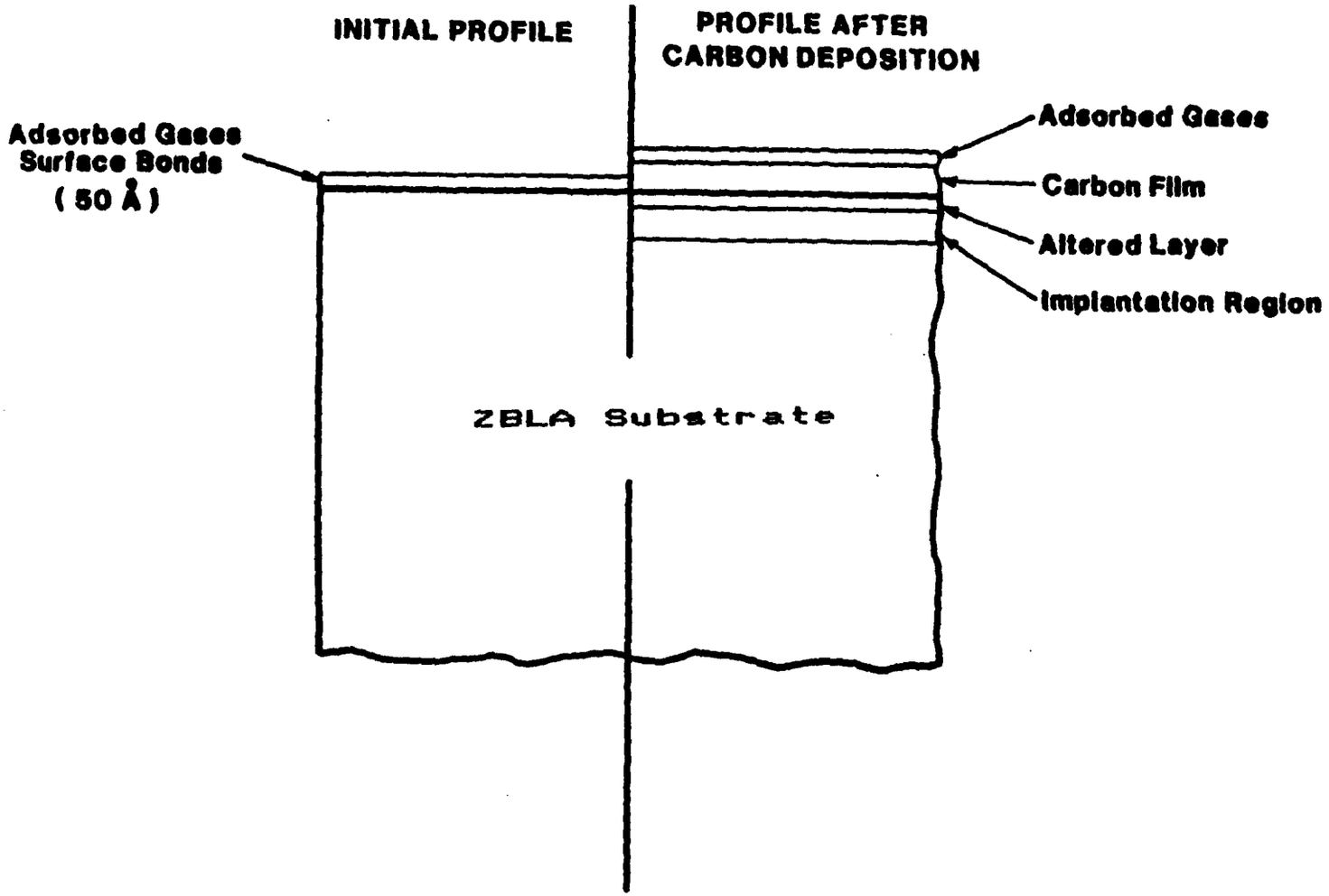

FIGURE 4. SURFACE MODIFICATION AND COATING OF ZBLA GLASS

Effects of NaF Upon the Mechanical Properties of Fluorozirconate Glasses

A. Tesar, R.C. Bradt and C.G. Pantano
Department of Materials Science and Engineering
The Pennsylvania State University
University Park, PA 16802

There has been a considerable interest in the development of fluorozirconate glasses over the past few years. Preliminary indications are that the fracture toughnesses of these glasses are low and that the glasses are very reactive in the presence of aqueous environments. Thus, it is to be expected that these glasses may be very susceptible to stress corrosion phenomena. Obviously, these properties will limit the utilization of fluoride glasses in optical and fibre optic applications.

So far, there has not been any detailed nor systematic study of the fracture and stress corrosion behavior of any fluoride glasses. Most of the measurements reported to date were carried out on a few selected compositions. The specimens available for the studies have been small, and therefore, only a limited number of mechanical properties could be evaluated.

The primary objective of this study has been to establish the influence of bulk composition, and systematic changes in structure, upon the elastic constants, fracture toughness and the stress corrosion susceptibility. A series of glasses have been prepared in the system $.56ZrF_4 \cdot (.34-X)BaF_2 \cdot .06LaF_3 \cdot .04AlF_3$ XRF where R = Li, Na, K or Cs, although here, only the glasses with XRF=0, .05NaF, .10NaF, and .15NaF are reported and discussed. While the addition of NaF is shown to reduce the infrared frequency cut-off, it considerably improves the glass-forming and fibre-forming characteristics of the glass. And in a sense, the NaF substitutions represent a structural probe. Thus, the results should provide insight to those material characteristics which control the mechanical properties.

The fracture mechanics techniques which can provide the most useful and relevant information about the mechanical response of fluoride glasses require relatively large, homogeneous and stress-free specimens for study. Clearly, the preparation of these specimens was a project in itself. In any event, large glass specimens which are visibly homogeneous and clear have been prepared for each of these compositions. The batch consisted of anhydrous fluorides for all constituents except zirconium which was introduced as a high-purity oxide and converted to ZrF_4 with ammonium bifluoride. The batch was melted under a controlled atmosphere of N_2 and CCl_4 and then cast into slabs on a brass mold. The plates were annealed at temperatures determined by differential scanning calorimetry. The elastic moduli were measured by the resonance frequency technique. The fracture toughness and stress corrosion susceptibilities were deduced from the flexural strengths of test bars containing controlled microflaws. The physical properties were obtained using standard test methods.

Table 1 presents some of the properties measured for the compositional series of glasses. In addition, the corresponding properties for a commercially available glass, whose composition approximates the glass with X=0, is also included. It can be seen that the range of infrared transmission is degraded by the sodium fluoride substitutions. However, utilizing the parameter (T_x-T_g), it is apparent that the glass forming ability is enhanced by the sodium fluoride substitutions. In general, these property trends verify the compositional variations introduced in the glass batch. Nonetheless, the composition of the glasses is being evaluated independently with wet chemical and spectroscopic techniques.

Table 2 presents the mechanical properties measured for these glasses as well as some other multicomponent fluoride glasses. As has been previously reported by others, the Young's elastic modulus is about 60 GPa. This value is comparable to many silicate glasses and does not represent any special result. The hardness is not

very substantial, suggesting that these glasses may be particularly susceptible to surface damage. There is not much of a trend in hardness with NaF additions, perhaps indicating that the hardnesses of these glasses cannot be changed very substantially without some dramatic departure from the base compositional system studied here. The fracture toughness does not present a dramatic compositional change, either, but is rather consistent at about 0.33 MPa $m^{-\frac{1}{2}}$ typical of most other reports on fluoride glasses. Fracture toughnesses between 0.3 and 0.4 MPa $m^{-\frac{1}{2}}$ are typical of many chain-like structure glasses such as the chalcogenides and phosphates. Since MacKenzie and co-workers have suggested that these fluoride glasses consist of chain structures, low fracture toughnesses are exactly what should be expected. Only radical compositional and structural changes should be expected to improve the fracture toughnesses of these fluoride glasses, which are low by comparison with most silicate glasses. Strengths of fluoride glasses may be expected to be correspondingly lower too, if surface flaw conditions are comparable to those of silicates.

The slow crack growth parameters, or N-values, for these glasses were all negative. This is very unusual and indicates that the flaws are blunting or healing during the stressing rate/strength tests and the specimens are actually becoming stronger for slower stressing rates. This is exactly the opposite to the process of slow crack growth weakening observed for most silicate glasses. It is, however, comparable to the strengthening observed when viscous glassy silicates blunt cracks in refractories at elevated temperatures. Details of these crack tip dissolution strengthening processes in glasses have not been worked-out in total, but certainly relate directly to the original Charles-Hillig concepts. The manifestation of the strengthening effect in these fluoride glasses almost certainly relates to their very high reactivity in aqueous environments.

Table 1. Properties of glasses in the system $.56ZrF_4 \cdot (.34-x)BaF_2 \cdot .06LaF_3 \cdot .04AlF_3 \cdot xNaF$

	ρ(gm/cm^3)	T_g(C)	T_x(C)	α(x10^{-6}/C)	n	ν cut-off (μm)
0 NaF	4.82	312	396	12.7	1.523	7.7
.05 NaF	4.7273	293	385	14.6	1.518	7.5
.10 NaF	4.6412	284	383	16.4	1.510	7.43
.15 NaF	4.5880	276	373	17.1	1.506	7.38
Le Verre Fluore (≅0 NaF)	4.7417	304	389	-	1.522	-

ρ = density

T_g = glass transition temperature

T_x = crystallization temperature

α = thermal expansion coefficient

n = refractive index

ν cut-off = infrared transmission limit

Table 2. Mechanical properties of glasses in the system $.56ZrF_4 \cdot (.34-x)BaF_2 \cdot .06LaF_3 \cdot .04AlF_3 \cdot xNaF$

	E(GPa)	G(GPa)	K(GPa)	ν	H_v (kg/mm^2)	K_{Ic} ($MPa/m^{\frac{1}{2}}$)	N
0 NaF	60.2	24.0	40.8	.25	209	.34±.02	- 2.33
.05 NaF	56.7	22.7	37.8	.25	223	.32±.04	- 2.24
.10 NaF	58.3	23.8	35.3	.23	221	.34±.02	- 2.23
.15 NaF	62.4	26.7	31.5	.17	233	.29±.03	- 2.26
Le Verre Fluore	54.1	20.9	-	.29	209	.26±.1	-
$60ZrF_4/32BaF_2/4GdF_3/4AlF_3$*	53.1	20.5	-	.20	-	.30±.01	-
$27BaF_2/27CaF_2/5YF_3/4AlF_3$*	63.8	24.6	-	.30	-	.38±.01	-

* Courtesy of Nippon Telegraph and Telephone

E = Young's elastic modulus

G = Shear modulus

K = Bulk modulus

ν = Poisson's ratio

H_v = Vicker's microhardness

K_{Ic} = Fracture toughness

N = Slow crack-growth parameter

PREPARATION OF HEAVY METAL FLUORIDE GLASS OPTICAL FIBERS (A New Approach)

D. C. Tran, M. J. Burk and G. H. Sigel, Jr.
Naval Research Laboratory
Washington, DC 20375

A vapor phase approach, termed reactive vapor transport process (RVT), was investigated for the fabrication of fluoride glass optical fibers. The refractive index profiles, obtained from preforms prepared via the novel technique, indicate that both multimode graded-index and monomode fluoride glass fiber waveguides can be readily prepared.

The only method for making fluoride glass fibers known to date is to cast the fluoride glass melts.[1-3] The casting process appears to be limited to step-index fibers. In addition, careful examination of our cast preforms of substantial lengths (> 6 in) generally revealed density variations in the core and microcrystallites at the core-clad interface. These scattering defects have resulted in wavelength-independent fiber losses ranging from 5 dB/km[4] to several hundred dB/km. To avoid casting the melts, a reactive vapor or mixture of vapors originated from low vapor pressure metal halides or from halogenated gases, were carried inside a fluoride glass tube. With proper control of processing parameters such as temperature, time, and reactive vapor concentration, substantial amounts of chlorine, bromine, or iodine ions were exchanged and incorporated into the fluoride glass structure, thus raising the refractive index and forming a core region. A cross-section of a fluoride glass tube preform is shown in Fig. 1.

The difference in refractive indices $\Delta n = [n_i - n(b)]$ is plotted against b in Fig. 2, where n_i represents the measured index at the inner wall of the tube and b is the overall tube wall thickness. The parabolic index profile suggests a diffusion controlled process. The index difference of Fig. 2

corresponds to a N.A. of only 0.045. However, in separate RVT experiments, it was demonstrated that N.A. > 0.1 and c (core wall thickness of Fig. 1) > 3 cm can be achieved. Optical characteriation of the core glass revealed a slight shift of the IR edge toward longer wavelengths, an appearance of two IR reflectivity bands at around 549 cm^{-1} and 478 cm^{-1}, and a substantial decrease in the OH absorption band with respect to the cladding glass. All of these are attributed to the presence of Cℓ, Br, or I in the core glass structure. There was no microcrystals present at the core-clad interface.

In summary, a new fluoride glass fiber manufacturing process using reactive vapors was developed to suppress the extrinsic scattering loss generally observed in our substantially long cast preforms. In addition, the new approach allows (1) the modeling of the refractive index profile by varying the processing conditions, (2) the preparation of fluoride glass preforms having a very small core, (3) the prevention of OH contamination since reactive vapors are used, and (4) the prevention of contamination from dirt particles since it is an inside process.

Acknowledgments

The authors are grateful to Dr. P. Klein and Mr. C. Fisher for helpful comments and discussions and to Dr. G. Lu and Dr. K. Levin for the refractive index measurements.

References

1. Mitachi, S., Miyashita, T., and Kanamuri, T., Electron. Lett. 17, 591 (1981).

2. Tran, D. C., Fisher, C. F., and Sigel, G. H., Electron. Lett., 18, 657 (1982).

3. Maze, G., Cardin, V., and Poulain, M., Proceedings of SPIE, Geneva (1983).

4. Tran, D. C., Levin, K. H., Fisher, C. F., Burk, M. J., and Sigel, G. H., Electron. Lett. 19, 165 (1983).

Figure Captions

Figure 1 Cross-section of a fluoride glass tube preform.

Figure 2 Index profile of a fluoride glass tube preform

[$\Delta n = n_i - n(b)$, where $n_i = n(0\ \mu m) = 1.5090$]

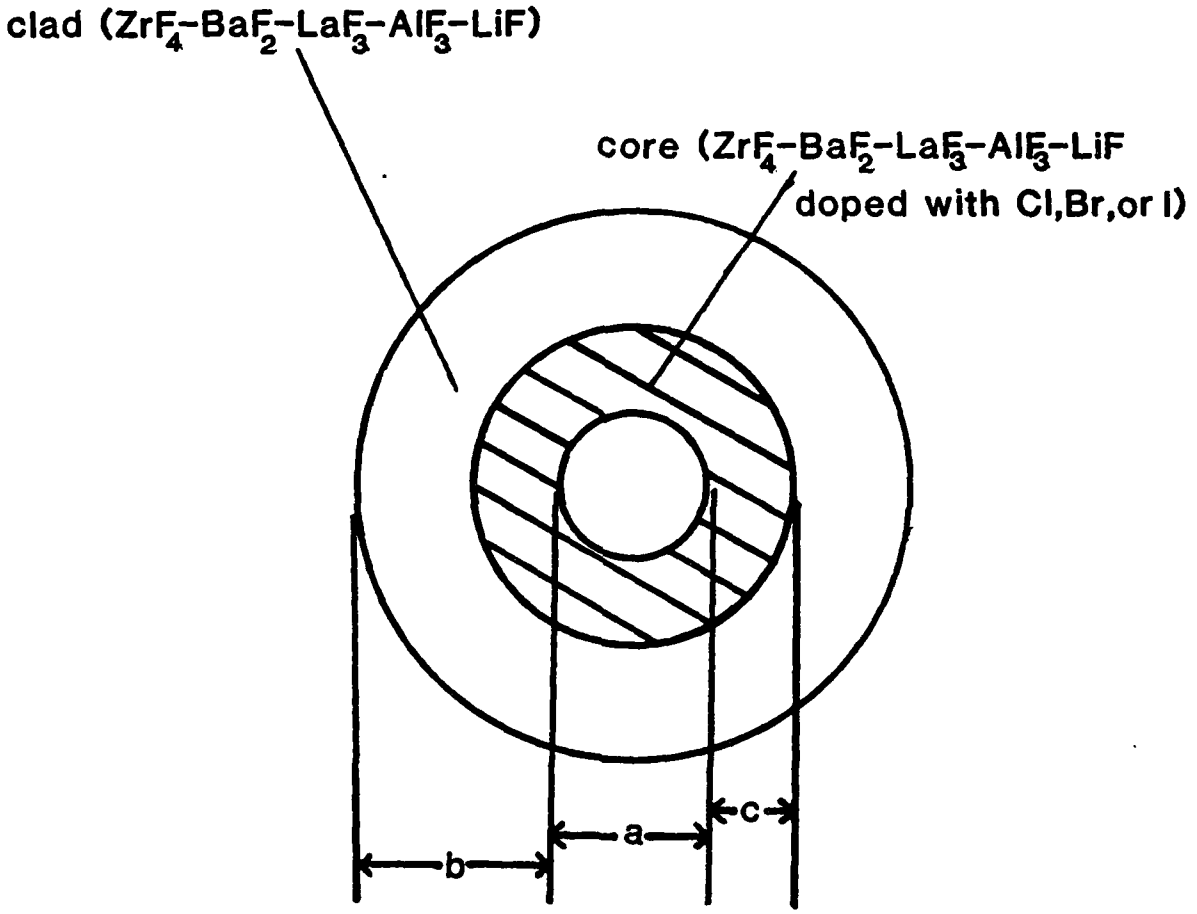
clad (ZrF_4-BaF_2-LaF_3-AlF_3-LiF)
core (ZrF_4-BaF_2-LaF_3-AlF_3-LiF
doped with Cl,Br,or I)
b
a
c

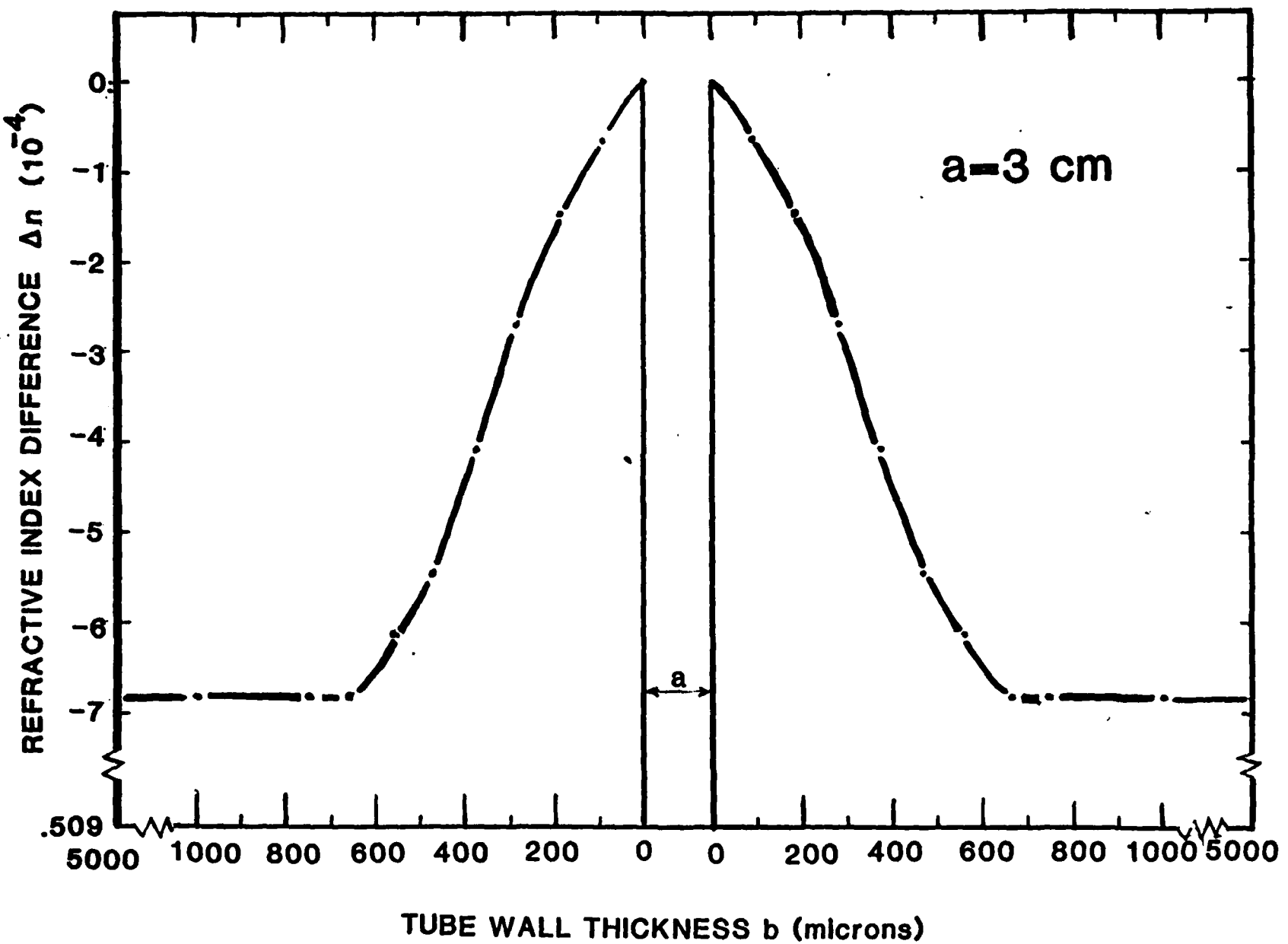
a=3 cm
REFRACTIVE INDEX DIFFERENCE Δn (10⁻⁴)
0
-1
-2
-3
-4
-5
-6
-7
.509
a
5000 1000 800 600 400 200 0 0 200 400 600 800 1000 5000
TUBE WALL THICKNESS b (microns)

OPTICAL AND LASING PROPERTIES OF Nd^{3+}-DOPED BERYLLIUM FLUORIDE GLASSES*

M. J. Weber, C. F. Cline, G. J. Linford, M. Milam,
S. E. Stokowski, and S. M. Yarema

Lawrence Livermore National Laboratory
University of California
Livermore, California 94550

Beryllium fluoride glasses are of interest for optical elements and amplifying media in lasers operating at short wavelengths and high powers because they have (1) the largest band gaps of any known glass,[1] and hence are transparent to a wide range of optical pumping and lasing wavelengths,[2] and (2) the smallest measured refractive index nonlinearities,[3] which reduces distortions due to self-focusing of intense beams. Beryllium fluoride glasses can be doped with a variety of rare earth and transition metal ions. Lasing of Nd^{3+} in fluoroberyllate glasses was reported in the 1960's.[4-6] To investigate these glasses further, we have studied the effects of glass composition on the optical and lasing properties.

Changes in the absorption spectra of Nd^{3+} with composition are shown in Fig. 1 for simple BeF_2 glass and a ternary fluoride glass. Both the width and cross sections of the transitions change. The $^4F_{3/2} \rightarrow {}^4I_{11/2}$ fluorescence spectra also changes as shown in Fig. 2. Table I

*This work was performed under the auspices of the Division of Materials Sciences, Office of Basic Energy Sciences, U. S. Department of Energy and the Lawrence Livermore National Laboratory under Contract W-7405-Eng-48.

gives examples of observed differences in the peak wavelength λ_p, stimulated emission cross section σ, effective bandwidth $\Delta\lambda_{eff}$, and calculated radiative lifetime τ_R associated with the $^4F_{3/2} \rightarrow {}^4I_{11/2}$ fluorescence for three different glass compositions. These spectroscopic properties have been used to predict Xe-flashlamp-pumped laser action.[7]

We have measured the small-signal gain coefficients for Nd^{3+}-doped BeF_2 and $KF\text{-}CaF_2\text{-}AlF_3\text{-}BeF_2$ glass amplifiers. The peak gain coefficients agree with predictions within experimental uncertainties and are included in Table I. Although there is a range of lasing parameters within a given glass former, in general the gain of beryllium fluoride glasses is higner than that for silicate glasses but not as high as for phosphate glasses.

We also measured large-signal gain saturation. The saturation parameter derived from the Frantz-Nodvik equation is plotted as a function of input fluence in Fig. 3. The variation of saturation fluence is similar to that observed for silicate, phosphate, and fluorophosphate glasses[8] and is a consequence of hole burning arising from spectroscopic inhomogeneities.[9] The small differences in the data for 1-ns and 20-ns pulses indicated that the relaxation time of the $^4I_{11/2}$ terminal laser level is $\lesssim$ 1 ns.

Beryllium fluoride glasses can be cast in large sizes; disks 20-cm diameter by 5-cm thick have been prepared.[10] The toxicity of beryllium, however, necessitates special handling requirements for the melting and finishing of these glasses. The hygroscopicity of BeF_2 is well known, but by the addition of suitable modifier cations the chemical durability can be greatly improved.[11]

References

1. R. T. Williams, D. J. Nagel, P. H. Klein, and M. J. Weber, "Vacuum Ultraviolet Properties of Beryllium Fluoride Glass," J. Appl. Phys. 52, 6279 (1981).
2. W. H. Dumbaugh and D. W. Morgan, "Preliminary Ultraviolet Transmission Data for Beryllium Fluoride Glasses", J. Non-Cryst. Solids 38/39, 211 (1980).
3. M. J. Weber, C. F. Cline, W. L. Smith, D. Milam, D. Heiman, and R. W. Hellwarth, "Measurements of the Electronic and Nuclear Contributions to the Nonlinar Refractive Index of Beryllium Fluoride Glasses", Appl. Phys. Lett. 32, 403 (1978).
4. G. T. Petrovskii, M. N. Tolstoi, P. P. Feofilov, G. A. Tsurikova, and V. N. Shapovalov, "Luminescence and Stimulated Emission of Neodymium in Beryllium Fluoride Glass", Opt. Spectrosc. USSR 21, 72 (1966).
5. O. K. Deutschbein, C. C. Pautrat, and M. Svirchovsky, "Etude de verres lasers aux fluorures", Centre Nat. D'Etudes Telecommun., Rept. 873 PEC (1968).
6. O. K. Deutschbein and C. C. Pautrat, "CW Laser at Room Temperature Using Vitreous Substances", IEEE J. Quant. Electron. QE-4, 48 (1968).
7. G. J. Linford, R. A. Saroyan, J. B. Trenholme, and M. J. Weber, "Measurements and Modeling of Gain Coefficients for Neodymium Laser Glasses," IEEE J. Quant. Electron. QE-15, 510 (1979).
8. W. E. Martin and D. Milam, "Gain Saturation in Nd:Doped Laser Materials", IEEE J. Quant. Electron. QE-18, 1155 (1982).
9. M. J. Weber, "Fluorescence and Glass Lasers", J. Non-Cryst. Solids 47, 117 (1982).
10. W. H. Dumbaugh and D. W. Morgan, Corning Glass Works (private communication).
11. C. F. Cline, D. D. Kingman, and M. J. Weber, "Durability of Beryllium Fluoride Glasses in Water: Comparison with Other Glasses and Crystals", J. Non-Cryst. Solids 33, 417 (1979).

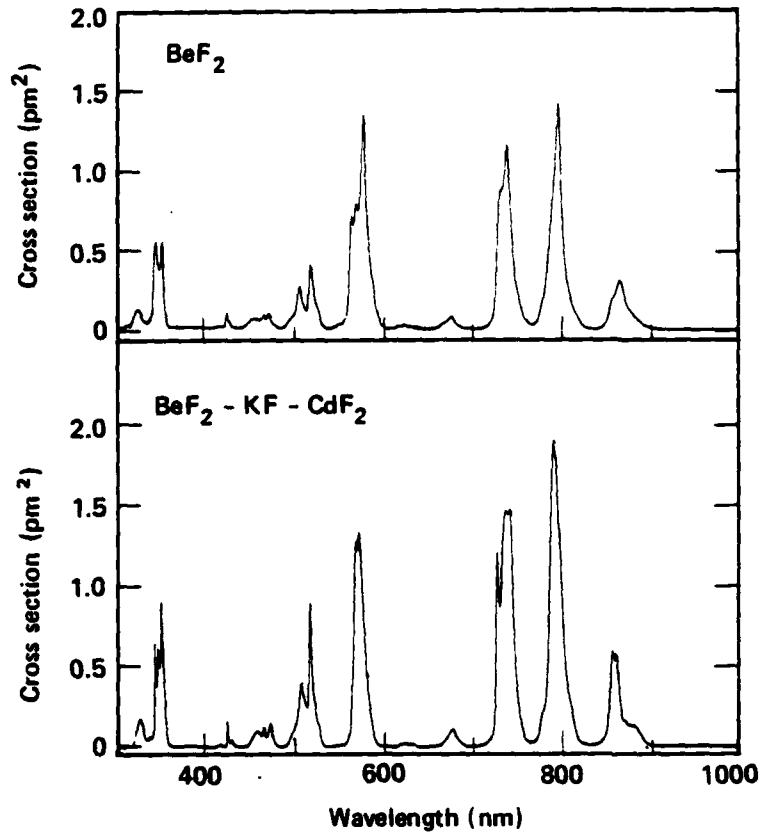

Figure 1: Absorption spectra and cross sections of Nd^{3+} in two beryllium fluoride glasses recorded at 293K.

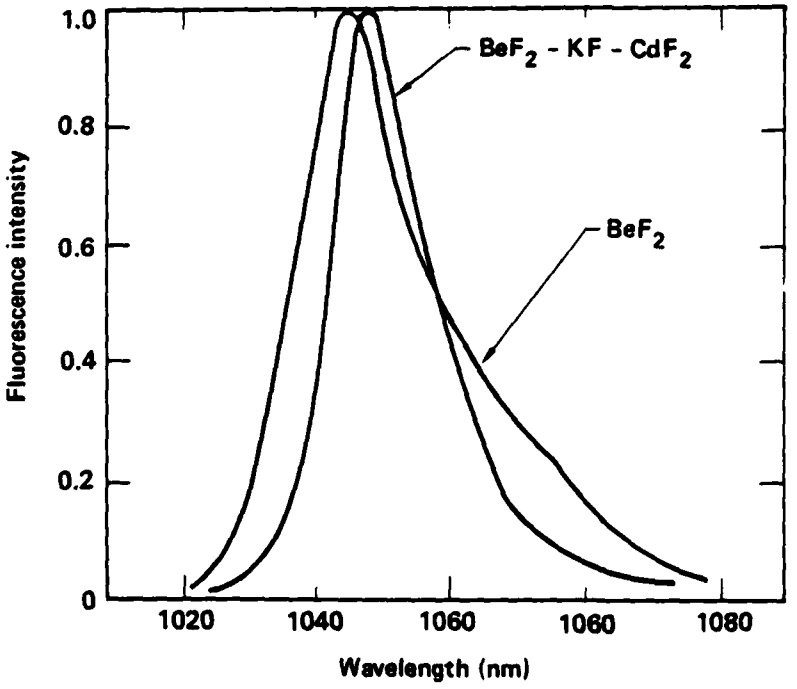

Figure 2: Comparison of the $^4F_{3/2} \rightarrow {}^4I_{11/2}$ fluorescence spectra of Nd^{3+} in two beryllium fluoride glasses at 293 K.

Table I. Spectroscopic and Lasing Parameters of Nd^{3+}-doped Beryllium Fluoride Glasses:

Composition (mol.%)	$98BeF_2$-$2NdF_3$	$60BeF_2$-$32KF$-$6CdF_2$-$2NdF_3$	$47BeF_2$-$27KF$-$14CaF_2$-$10AlF_3$-$2NdF_3$
$^4F_{3/2} \rightarrow {}^4I_{11/2}$ fluorescence:			
λ_p(nm)	1046	1048	1047
$\sigma(pm^2)$	2.0	3.8	3.2
$\Delta\lambda_{eff}$(nm)	27.7	20.1	23.2
$\tau_R(\mu s)$	920	600	610
Relative small-signal gain coefficient:			
$g(m^{-1})$	7.8	17(estimate)	14.8

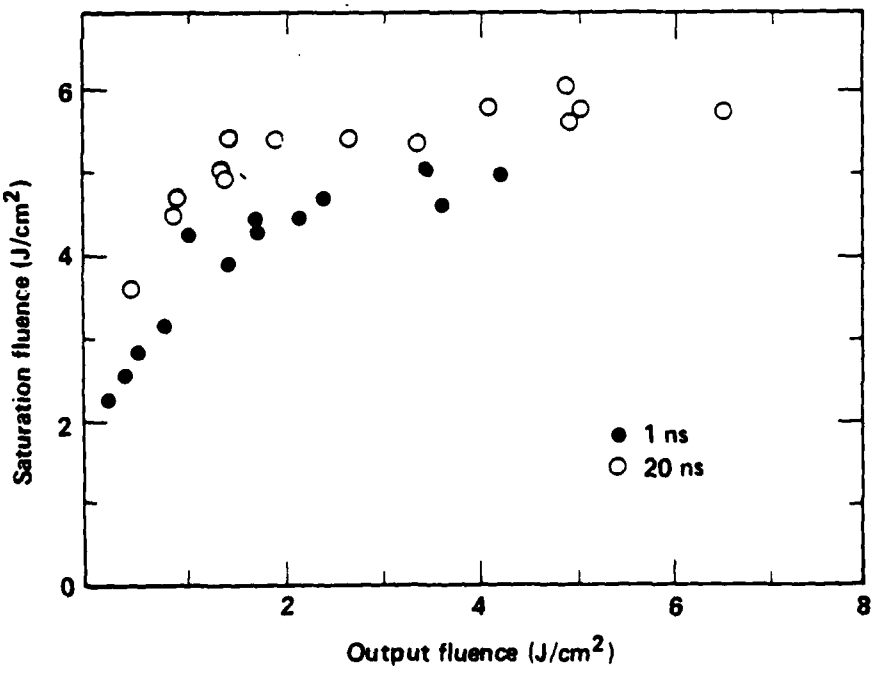

Figure 3: Saturation fluence versus input fluence at 1.053μm determined from gain measurements of a BeF_2-KF-CaF_2-AlF_3-NdF_3 glass amplifier for two pulse durations.

NEUTRON DIFFRACTION AND MOLECULAR DYNAMICS STUDIES OF VITREOUS $NaF-DyF_3-BeF_2$

Adrian C. Wright and George Etherington†

J.J. Thomson Physical Laboratory, Whiteknights, Reading, RG6 2AF, U.K.

Steven A. Brawer* and Marvin J. Weber

Lawrence Livermore National Laboratory, P.O. Box 808, Livermore, CA 94550, U.S.A.

and

Roger N. Sinclair

Materials Physics Division, A.E.R.E., Harwell, Didcot, OX11 ORA, U.K.

Rare earth containing fluoroberyllate glasses are of considerable interest in view of their possible application in the high powered lasers being developed for the laser fusion programme. At present, however, the details of the local environment of the rare earth ions, in such glasses, which determines their spectral properties, has not been established.

Neutron diffraction and Molecular Dynamics techniques have, therefore, been used to investigate the structure of vitreous $NaF-BeF_2$ containing DyF_3. Dy is a particularly favourable element for neutron diffraction in that it can be obtained as a mixture of isotopes such that the coherent neutron scattering length $\bar{b}$ is zero. Thus by studying the difference between the diffraction patterns for samples containing natural and zero scattering length Dy, it is possible to experimentally isolate the Dy-X + Dy-Dy and X-X (X = Na, Be or F) contributions to the real space correlation function and hence probe the Dy environment directly. Additional measurements have also been made on undoped $NaF-BeF_2$ and pure vitreous BeF_2.

The neutron diffraction data show that in all the glasses studied Be is tetrahedrally co-ordinated by F. Peak fits in the Gaussian approximation yield a mean Be-F bond length of between 1.548 and 1.555 Å and an r.m.s.

bond length variation of 0.063 to 0.093 Å. A similar fit to the first Dy-F peak in the Dy-X + Dy-Dy difference correlation function gives a first Dy-F distance of 2.301 Å.

The Molecular Dynamics simulations also predict tetrahedral co-ordination but fail to account for the relative packing of the BeF_4 structural units. In particular the Be-$\hat{F}$-Be angle is too great and appears to have too narrow a distribution. This is almost certainly due to the omission of angularly dependent forces - a similar increased bond angle (Zn - $\hat{Cl}$ - Zn) is also observed in analagous simulations of vitreous $ZnCl_2$. The Molecular Dynamics simulations do, however, predict the changes in the correlation function which occur on adding first NaF and then DyF_3. In particular the main features of the Dy-X + Dy-Dy difference correlation function are reproduced although the peaks are somewhat broader than observed experimentally.

In order to examine peak widths in more detail a further neutron diffraction experiment is to be performed which will yield greatly improved real space resolution. Further work on the potentials used in the Molecular Dynamics simulations is also required.

* Now at Bell Telephone Laboratories

† Now at U.C.L.A.

VISCOSITY OF SOME GLASS-FORMING BROMIDE MELTS*

by

D. Wynne, F.D. Ma, J. Lau and J.D. MacKenzie

Department of Materials Science and Engineering

University of California, Los Angeles

Extended Abstract

for

Second International Symposium on Halide Glasses

August 2-5, 1983

Rensselaer Polytechnic Institute

Troy, New York

* This work is being supported by the Directorate of Chemical and Atmospheric Sciences, Air Force Office of Scientific Research.

Extended Abstract

It has been found that glass formation can take place in $ZnBr_2$, binary systems such as $ZnBr_2$-KBr and $ZnBr_2$-TlCl, and ternary systems such as $ZnBr_2$-KBr-TlBr and $ZnBr_2$-TlBr-TlI. Because viscous flow is governed by melt structure and has a direct bearing on glass forming tendency, the viscosities of a number of bromide melts have been measured with a concentric cylinder method.

The viscosities of the melts measured are shown in Figures 1 to 3. Addition of monovalent halides results in the reduction of the viscosity of $ZnBr_2$. Viscosity-temperature relations do not obey the common Arrhenius equation but appear to follow the Fulcher equation. A comparison of the viscosity-temperature behavior of a number of molten halides is shown in Figure 4. $ZnBr_2$ resembles $ZnCl_2$ in that the viscosities of both are much higher than those of the other halides. A comparison of viscosity at the melting temperature and activation energy for viscous flow is shown in Table 1. It is seen that although the parameters for $ZnBr_2$ and $ZnCl_2$ are much less than those for the glass forming oxides and BeF_2, they are nevertheless much higher than those for other ionic salts such as $PbBr_2$ and $CdBr_2$.

The present interpretation of the viscosity data is that $ZnBr_2$ melt, similar to molten $ZnCl_2$, is somewhat polymerized with linking of $ZnBr_4$ tetrahedra. Addition of halides such as TlI and KBr, etc. results in a break-up of these linked $ZnBr_4$ tetrahedra. In a sense, then, $ZnBr_2$ can be regarded as a glass-former. Perhaps the unique feature of these glass-forming halide melts containing $ZnBr_2$ is the probability of the dominance of the $ZnBr_4$ groups whereas other divalent cations such as Hg, Cd and Pb have higher coordination numbers.

Comparison of $ZnBr_2$ melts with other glass-forming liquids and molten salts at their liquidus temperature

System	Structural type	T_m(C)	Viscosity(p)	Activation Energy (kcal/mole)
B_2O_3	polymeric	450	10^5	40
BeF_2	polymeric	540	10^6	100
$ZnCl_2$	polymeric	283	146	24.8
Li_2SiO_3	chains & rings	1200	4	24
$NaPO_3$	chains & rings	615	17	16.5
KBr	ionic	734	0.012	5.2
KI	ionic	681	0.016	5.3
TlBr	ionic	480	0.02	3.4
TlI	ionic	440	0.026	3.6
$CdBr_2$	ionic	567	0.029	4.6
$PbBr_2$	ionic	373	0.079	5.9
$HgBr_2$	ionic	236	0.026	5.0
$ZnBr_2$	polymeric(?)	394	1.65	16.7
$ZnBr_2$-KBr(55-45)	polymeric(?)	187	0.5	8.8
$ZnBr_2$-KI(55-45)	polymeric(?)	187	1.1	10.1
$ZnBr_2$-KBr-TlI (55-35-10)	polymeric(?)	177	0.58	7.8

TABLE 1

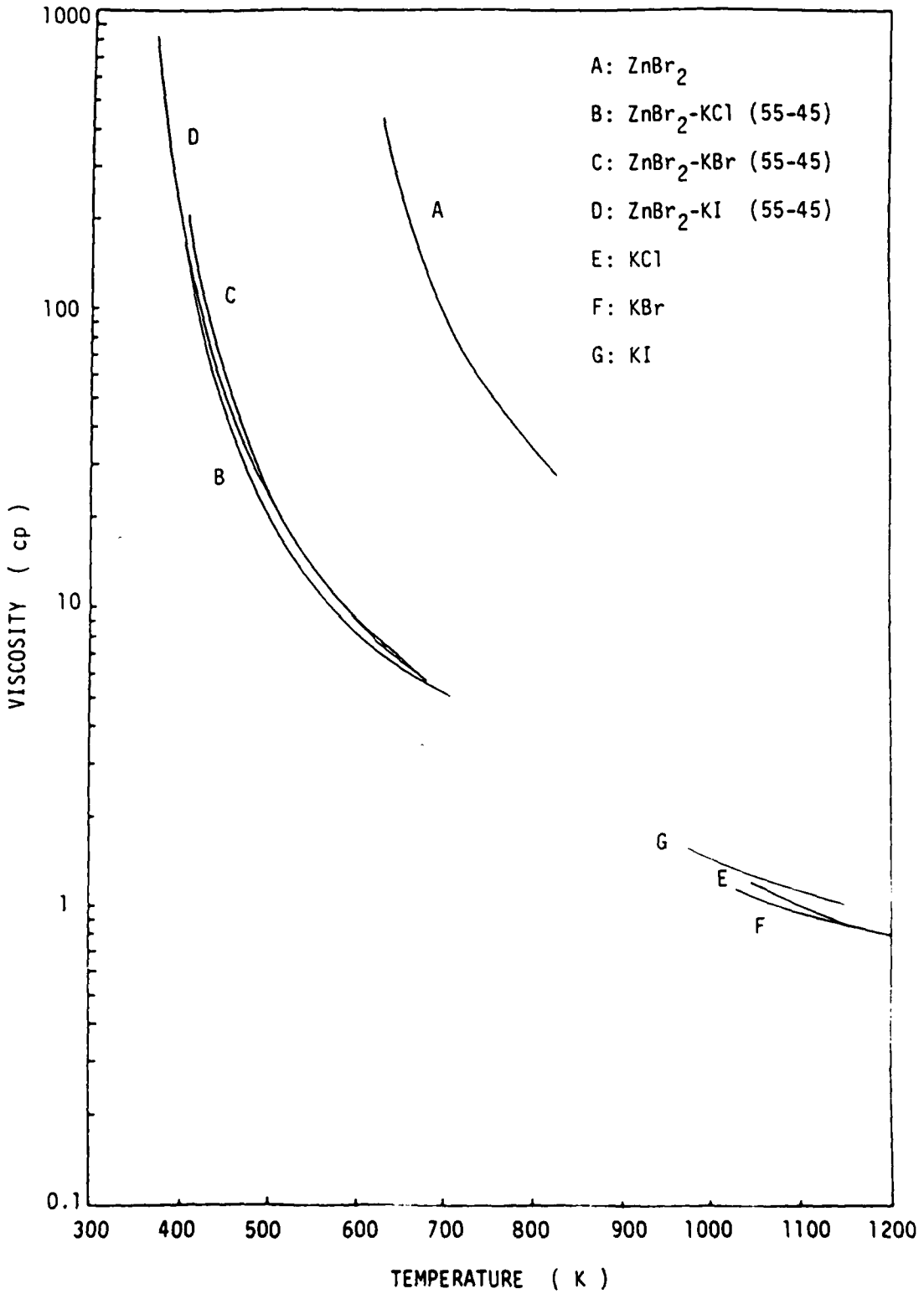
1000
100
10
1
0.1
VISCOSITY (cp)
300
400
500
600
700
800
900
1000
1100
1200
TEMPERATURE (K)
A: ZnBr2
B: ZnBr2-KCl (55-45)
C: ZnBr2-KBr (55-45)
D: ZnBr2-KI (55-45)
E: KCl
F: KBr
G: KI
A
B
C
D
E
F
G

FIGURE 1

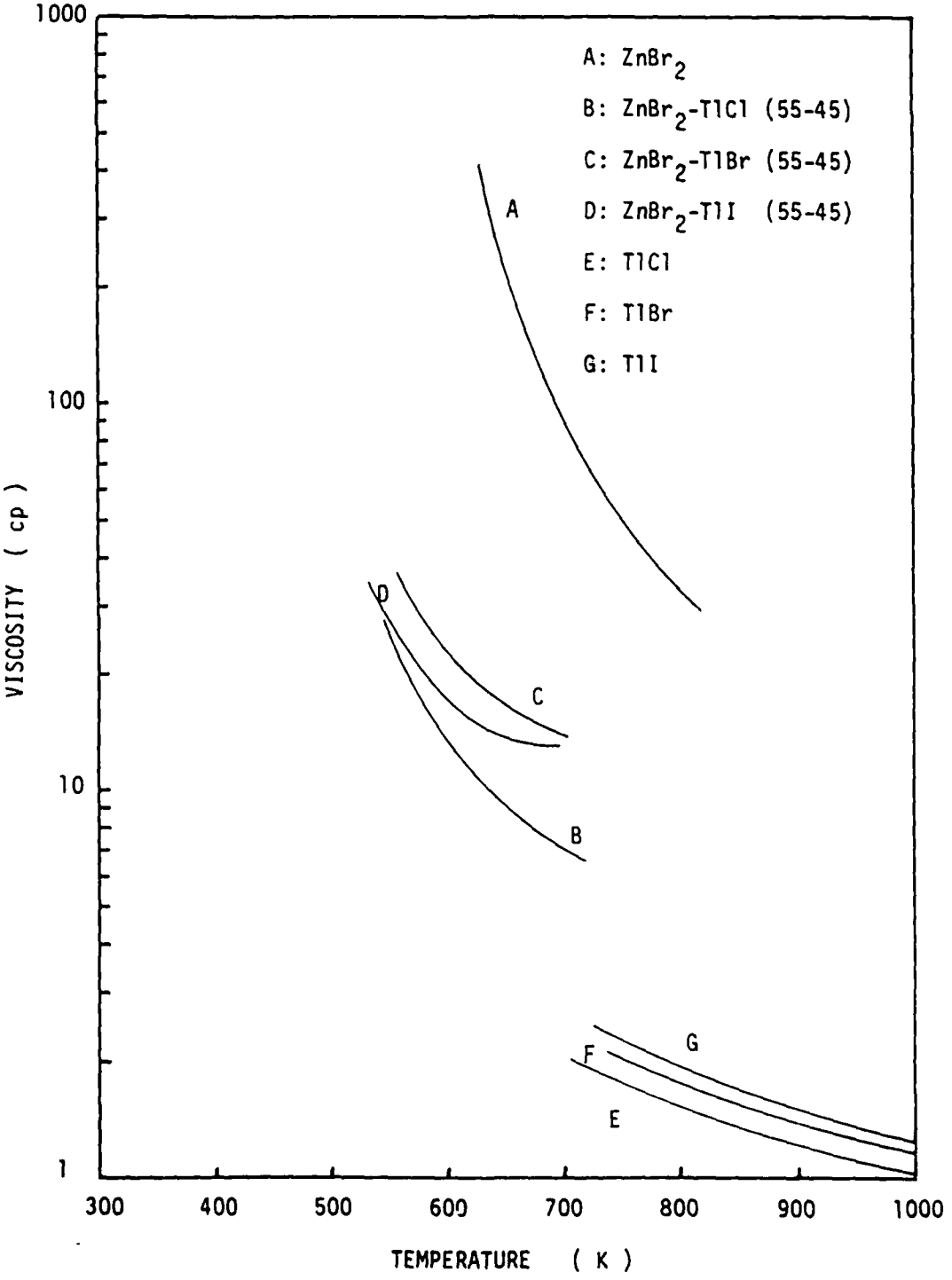
1000
100
10
1
VISCOSITY (cp)
300
400
500
600
700
800
900
1000
TEMPERATURE (K)
A: $ZnBr_2$
B: $ZnBr_2$-TlCl (55-45)
C: $ZnBr_2$-TlBr (55-45)
D: $ZnBr_2$-TlI (55-45)
E: TlCl
F: TlBr
G: TlI
A
B
C
D
E
F
G

FIGURE 2

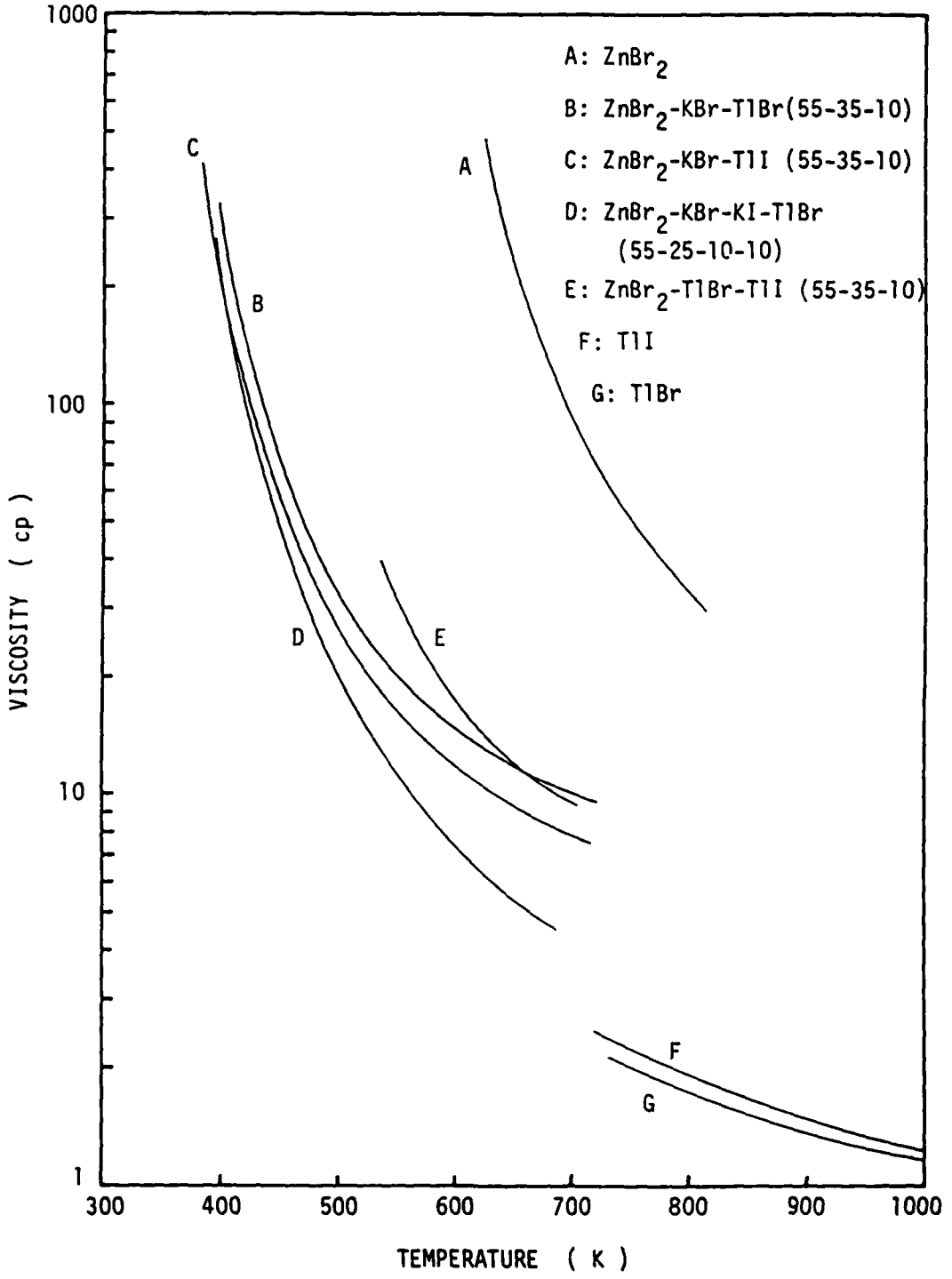
1000
100
10
1
VISCOSITY (cp)
300
400
500
600
700
800
900
1000
TEMPERATURE (K)
A: ZnBr2
B: ZnBr2-KBr-TlBr(55-35-10)
C: ZnBr2-KBr-TlI (55-35-10)
D: ZnBr2-KBr-KI-TlBr
(55-25-10-10)
E: ZnBr2-TlBr-TlI (55-35-10)
F: TlI
G: TlBr
A
B
C
D
E
F
G

FIGURE 3

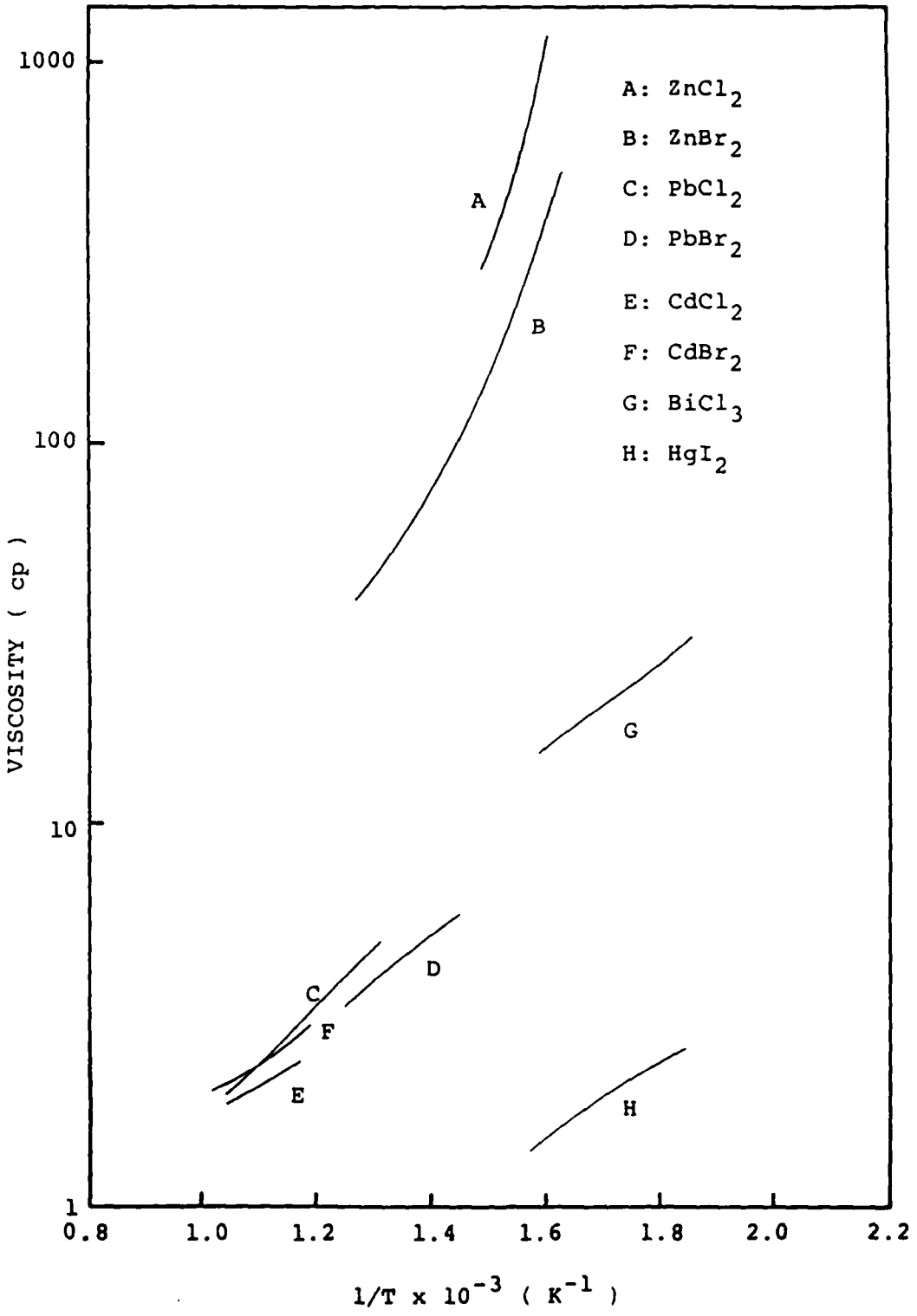
1000
100
10
1
VISCOSITY (cp)
0.8
1.0
1.2
1.4
1.6
1.8
2.0
2.2
1/T x 10^-3 (K^-1)
A: ZnCl2
B: ZnBr2
C: PbCl2
D: PbBr2
E: CdCl2
F: CdBr2
G: BiCl3
H: HgI2
A
B
C
D
E
F
G
H

FIGURE 4

NEW HALIDE GLASSES IN THE CuCl-CsBr-$PbBr_2$ SYSTEM

T. Yamagishi, J. Nishii and Y. Kaite

Research Laboratory, Nippon Sheet Glass Co., Ltd.
Konoike, Itami City, 664 Japan

Introduction

Recently there has been considerable interest in the fiber optic materials which operate at the infrared region. These fibers may be used as the flexible waveguides of CO_2 laser power (wavelength 10.6μm).
Halide materials are thought to be useful for these applications and many studies have been carried on the crystalline fibers made from halides such as silver halides or thallium halides.1),2)
Glass materials are also attractive candidates for these uses, and some glass systems based on $ZnCl_2$, $BiCl_3$, etc. have been proposed.3),4) However, these glasses are hygroscopic and rather unstable, and these properties prevent them from practical uses so far. Therefore, at present the development of new stable glasses has been expected in halide systems.
In this communication, the glass forming regions and some properties of new halide glasses based on $PbBr_2$ are reported.

Experiment

Reagent grade chemicals were dried at 110°C and mixed in a mortar. Batches of 1-5g were melted in a Pyrex tube at 450-500°C for 15-60min. in an air or a nitrogen atmosphere. Then the melts were poured onto a copper plate and promptly pressed by another copper plate (Hand press quenching). To examine the glass forming tendency at a higher cooling rate, the melts were sucked up by a syringe and droped between two rollers of a twin roller quenching apparatus (Twin roller quenching).
The degree of glass formation were evaluated by the proportion of transparent parts in the quenched samples. The glassy character of samples was confirmed by X-ray diffraction.
The glass transition temperatures(Tg) and the crystallization temperatures(Tc) of glassy samples were measured by DTA with a heating rate of 10°C/min. and the infrared absorption spectra were measured in the region of 2.5-25μm.

Results and discussion

$PbBr_2$ has been reported to have the glass forming tendency 5) and has low water solubility. Therefore $PbBr_2$ is supposed to be a potentially useful material for IR applications.
CuCl has a tetrahedrally coordinated structure and shows relatively high covalent character among monovalent metal halide compounds, therefore CuCl is expected to improve the glass forming tendency of $PbBr_2$.
The glass forming regions of the CuCl-$PbBr_2$ binary system investigated at two different cooling rates are illustrated in Fig.1(a). Though the eutectic composition of this system is not known for lack of phase diagram, the most vitrified composition is supposed to be in the vicinity of the binary eutectic composition inferred from the eutectic composition in CuCl-$PbCl_2$ (about 58CuCl-42$PbCl_2$). The glass forming tendency was examined in the 90$PbBr_2$-10RX systems (R=Li,Na,K,Cs,Cu,Ag,Tl; X=F,Cl,Br,I). In these systems, only CsCl, CsBr gave the glassy samples by the hand press quenching. The glass forming regions of the CsBr-$PbBr_2$ binary system are shown in Fig.1(b).
The center of this region corresponds to the eutectic composition of this system (about 18CsBr-82$PbBr_2$). Glass formation in the CuCl-CsBr system was not observed by the twin roller quenching.

Fig.2 shows the glass forming region in the CuCl-CsBr-$PbBr_2$ ternary system. The region a and b represent the regions in which the proportion of glassy parts in the plate samples was more than 50% and 90% respectively. The samples (30-40mm in diameter, 0.3-0.5mm in thickness) were obtained by the hand press quenching.

The X-ray diffraction patterns of some samples are shown in Fig.3. The sample (C) in the region a (in Fig.2) including crystalline parts gave some peaks mainly of crystalline $PbBr_2$. The glassy samples (A) and (B) in the region b gave only halo patterns which are typical for glasses.
Fig.4 represents the IR transmission spectra of the $37CuCl-15CsBr-48PbBr_2$ glassy samples. The glass sample(A) melted in an air atmosphere showed several absorption bands; the bands at 2.9μm and 6.3μm are probably due to OH^-, and the bands at longer wavelength are due to other impurities (ex.BrO_3^-). These absorption bands were substantially reduced in the sample(B) which was melted in a nitrogen atmosphere.

The effect of X replacement (X=Cl,Br,I) in the $37CuX-15CsX-48PbX_2$ system on the glass forming tendency was investigated. The result is shown in Fig.5, in which the numbers represent the glass forming tendency evaluated by the proportion of transparent parts in the samples obtained by the hand press quenching.
In this system, the most glassy sample was obtained when X=0.25Cl + 0.75Br, and the introduction of iodine reduced the glass forming tendency.
The glass transition temperatures(Tg) and the crystallization temperatures(Tc) for some glass compositions are listed in Table 1.
The increase of $PbBr_2$ content in the $CuCl-CsBr-PbBr_2$ system raised the glass transition temperature and lowered the value of (Tc-Tg). The introduction of iodide as CsI to this system raised the glass transition temperature.

Conclusion

The brownish-yellow glassy plates of 0.5mm in thickness were obtained by quenching between two copper plates (cooling rate $\sim 10^2$K/sec) in the new glass system of $CuCl-CsBr-PbBr_2$.
These glasses showed high infrared transparency in the wide range of wavelength, up to at least 15μm. The glasses do not seem to be attacked by moisture in the air after standing many days in a humid atmosphere.
The low glass transition temperatures may require special devices to cool the fiber materials for applications as the flexible waveguides of CO_2 laser power.

References

1) Pinnow, D. A., Gentile, A. L., Standlee, A. G. and Timper, A. J., Appl. Phys. Lett., 33(1), 28 - 29 (1978).

2) Bridges, T. J., Hasiak, J. S. and Strnad, A. R., Opt. Lett., 5(3), 85 - 86 (1980).

3) Van Uitert, L. G. and Wemple, S. H., Appl. Phys. Lett., 33(1), 57 - 59 (1978).

4) Angell, C. A. and Ziegler, D. C., Mat. Res. Bull., 16(3), 279 - 283 (1981).

5) Sun, K. H., Glass Ind., 27, 552 - 554, 580 - 581 (1946).

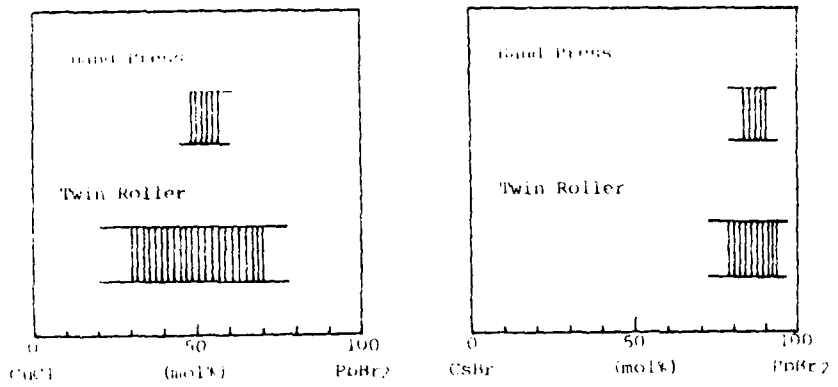

(a) $CuCl-PbBr_2$ (b) $CsBr-PbBr_2$

Fig.1 Glass forming regions in binary systems

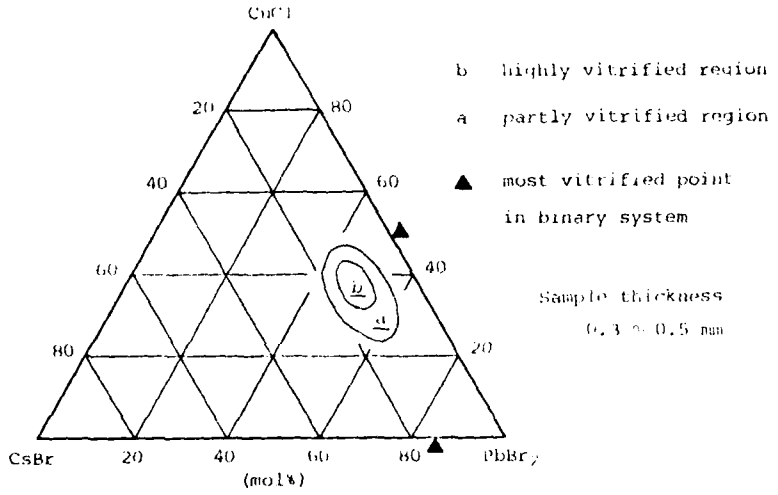

Fig.2 Glass forming region in the $CuCl-CsBr-PbBr_2$ system

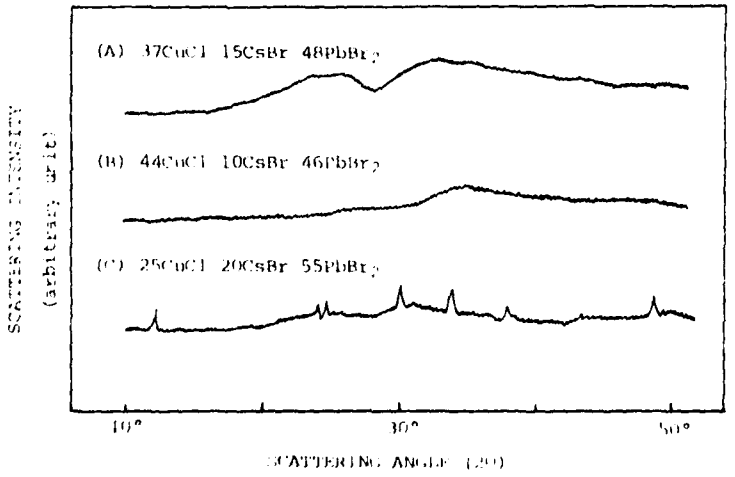

Fig.3 X-ray diffraction patterns for $CuCl-CsBr-PbBr_2$ system

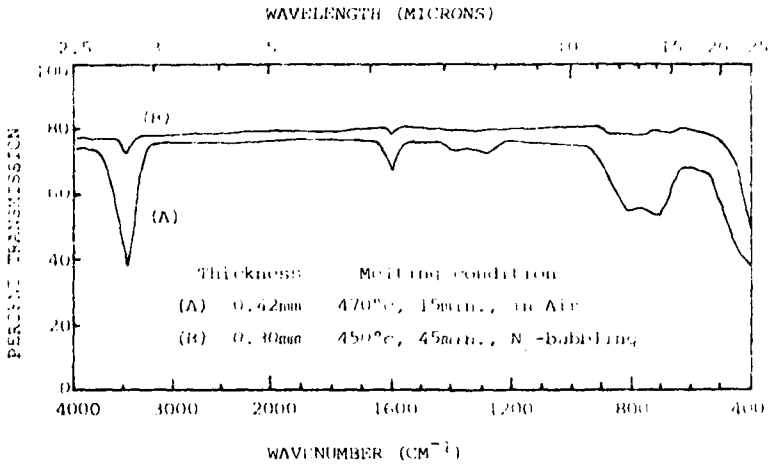

Fig.4 IR transmission spectra of $37CuCl\text{-}15CsBr\text{-}48PbBr_2$ glasses

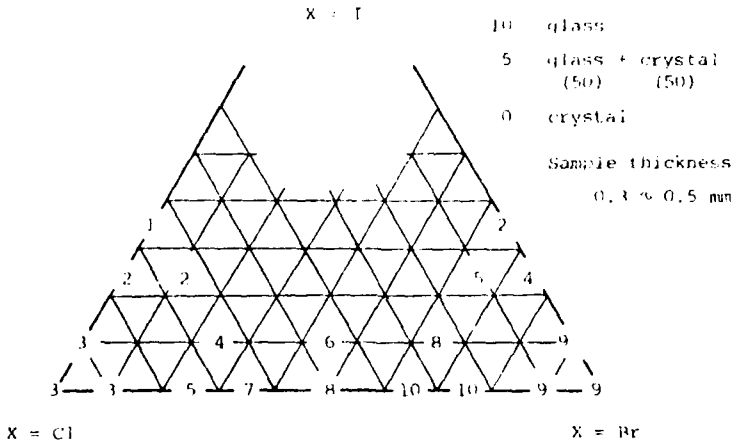

Fig.5 Glass forming tendency in the $37CuX\text{-}15CsX\text{-}48PbX_2$ system

Table 1 Glass transition temperatures (Tg) and crystallization temperatures (Tc) for some glasses

GLASS COMPOSITION (mol%)	Tg(°c)	Tc(°c)	Tc - Tg (°c)
$40CuCl\ 18CsBr\ 42PbBr_2$	21	68	47
$37CuCl\ 15CsBr\ 48PbBr_2$	26	74	48
$37CuCl\ 9CsBr\ 54PbBr_2$	30	68	38
$28CuCl\ 18CsBr\ 54PbBr_2$	34	75	41
$29CuCl\ 11CsBr\ 60PbBr_2$	36	70	34
$27CuCl\ 15CsBr\ 48PbBr_2$	25	72	47
$37CuCl\ 15CsI\ 48PbBr_2$	28	72	44

A POTENTIAL SUITABLE FOR CALCULATING ABSORPTION IN HALIDE GLASSES

Herbert B. Rosenstock*
Naval Research Laboratory
Washington, DC 20375

An "ideal" solid whose atoms interact by a purely harmonic potential $V_{ho} = (1/2)\ k\ x^2$ (Figure 1) would produce 1-phonon absorption only. Real solids, by contrast, are subject to anharmonic potentials that are responsible for the irreducible "intrinsic" multiphonon absorption observed in the infrared. One potential that has provided a useful model for multiphonon absorption calculations (1) (2) (3) is the Morse potential (4) $V_m = D\ \{1 - \exp\ [-a(x-x_0)]\ \}^2$ shown in Figure 2. Originally developed for diatomic molecules, it has two virtues that made it useful in solids as well: it is mathematically tractable (a rare feature in quantum mechanics), and it "looks reasonable". The last statement means that it behaves harmonically at low energies, then goes through an anharmonic region responsible for IR absorption before finally breaking up at a "dissociation energy" D. The details of the crucial anharmonic region can often be related to measured (elastic, optical or thermal) properties of the solid in question.

However, the dissociation energy in the Morse potential provides difficulties, both mathematical and conceptual. Mathematically, only the energy levels below D are known explicitly; hence the calculations become unreliable when either the photon energy or the equivalent temperature becomes comparable to D. The problem has been noted (3) but was not serious in crystals or high-melting glasses; but in soft, low-melting materials such as halide glasses, the energy levels above the dissociation limit are accessible and cannot be ingored (5). In addition to being not quantitatively understood, the behavior of the Morse potential near or above D is also

*Sachs Freeman Associates, Inc., Bowie, MD.

conceptually unrealistic: though bonds can conceivably be broken by an incoming photon, the result in a solid (in contrast to a molecule) is not the disappearance of an atom towards infinity; other atoms in the vicinity will keep it nearby.

We have therefore sought a potential that would be suitable in shape for halide glasses while still being mathematically tractable. The Pöschl-Teller potential (6) $V_{pt} = (p/\sin ax)^2 + (q/\cos ax)^2$ meets these criteria reasonably (Figure 3): the moving particle is harmonically bound at low energies, but at higher energies it remains confined to a finite region. Again, the detailed shape can be related to the physical properties of the glass on the one hand and to the parameters in the potential on the other. The energy levels and wave functions are known (6), (7) and the transition probabilities from and to arbitrary levels have now been calculated. According to our established formalism, the intrinsic multiphonon absorption can be inferred from them.

1. D. L. Mills and A. A. Maradudin, Phys. Rev. B10, 1713 (1974).
2. H. B. Rosenstock, Phys. Rev. B9, 1963 (1974).
3. Boyer, Harrington, Hass, & Rosenstock, Phys. Rev. B11, 1665 (1975).
4. P. M. Morse, Phys. Rev. 34, 57 (1929).
5. H. B. Rosenstock, Glass Technology (1983, in print).
6. G. Pöschl and E. Teller, Z. Physik 83, 143 (1933).
7. S. Flügge, "Practical Quantum Mechanics" (Springer, Berlin 1971), page 89.

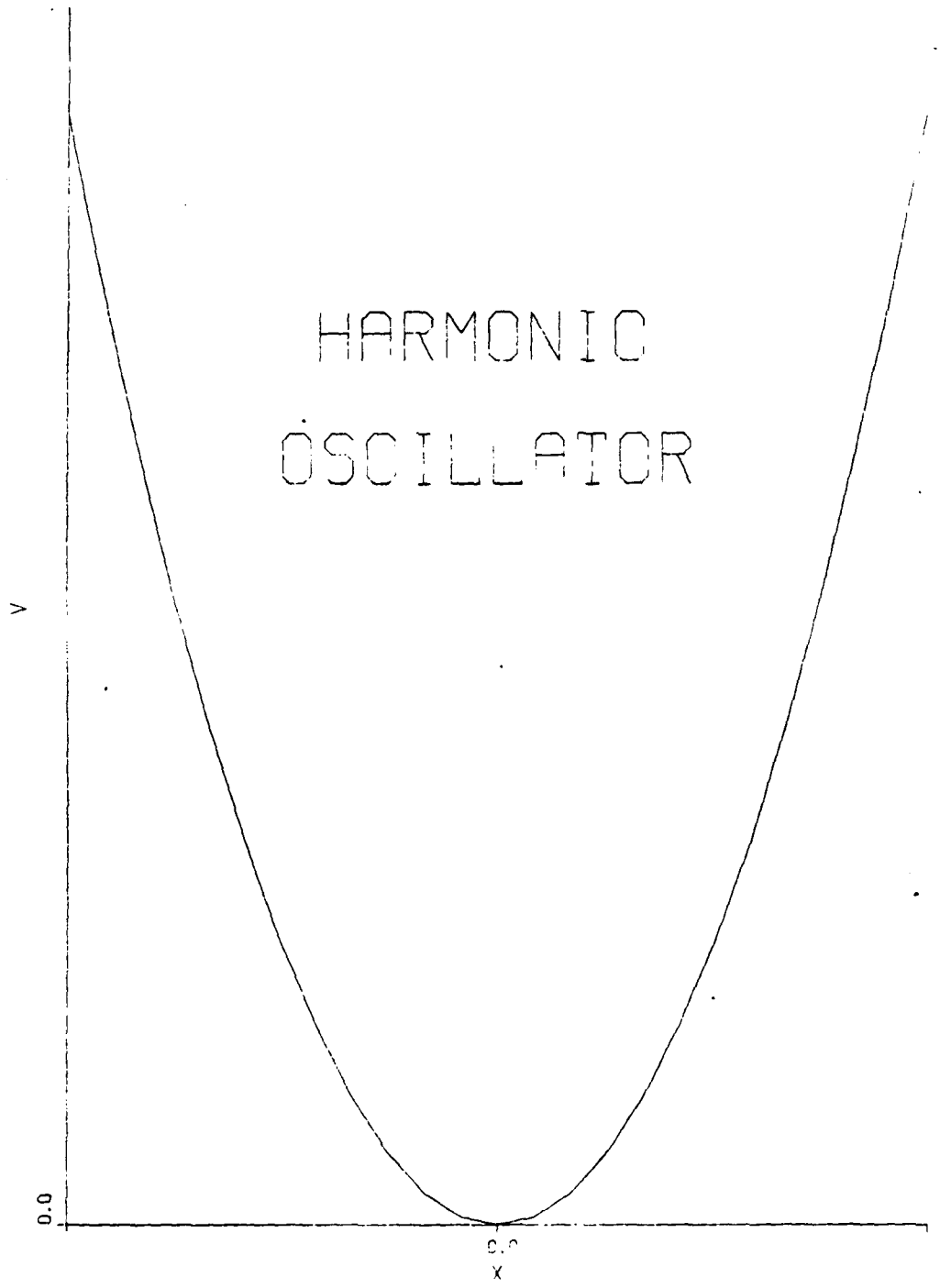
HARMONIC
OSCILLATOR
V
0.0
0.0
X

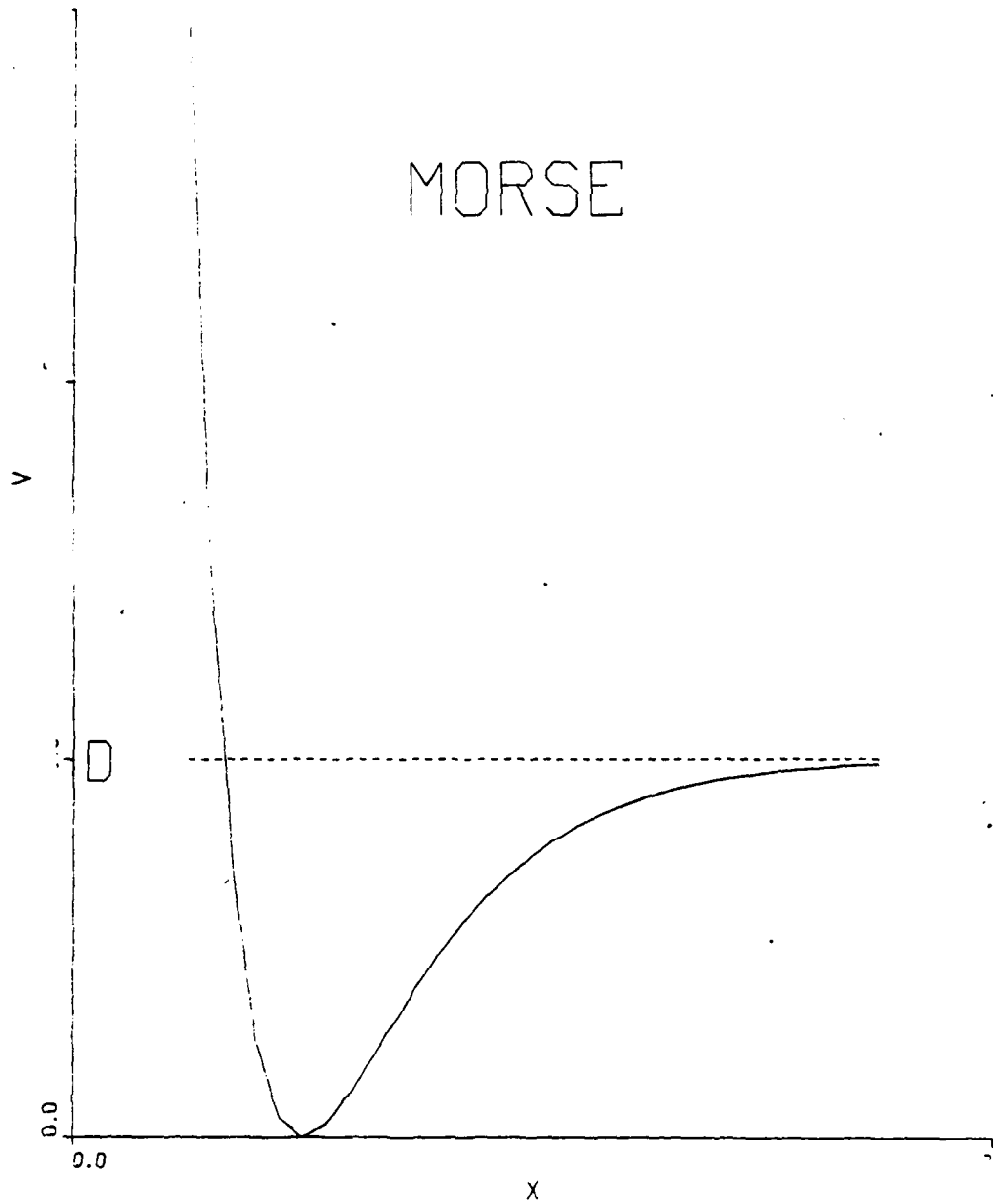
MORSE
V
D
0.0
0.0
X

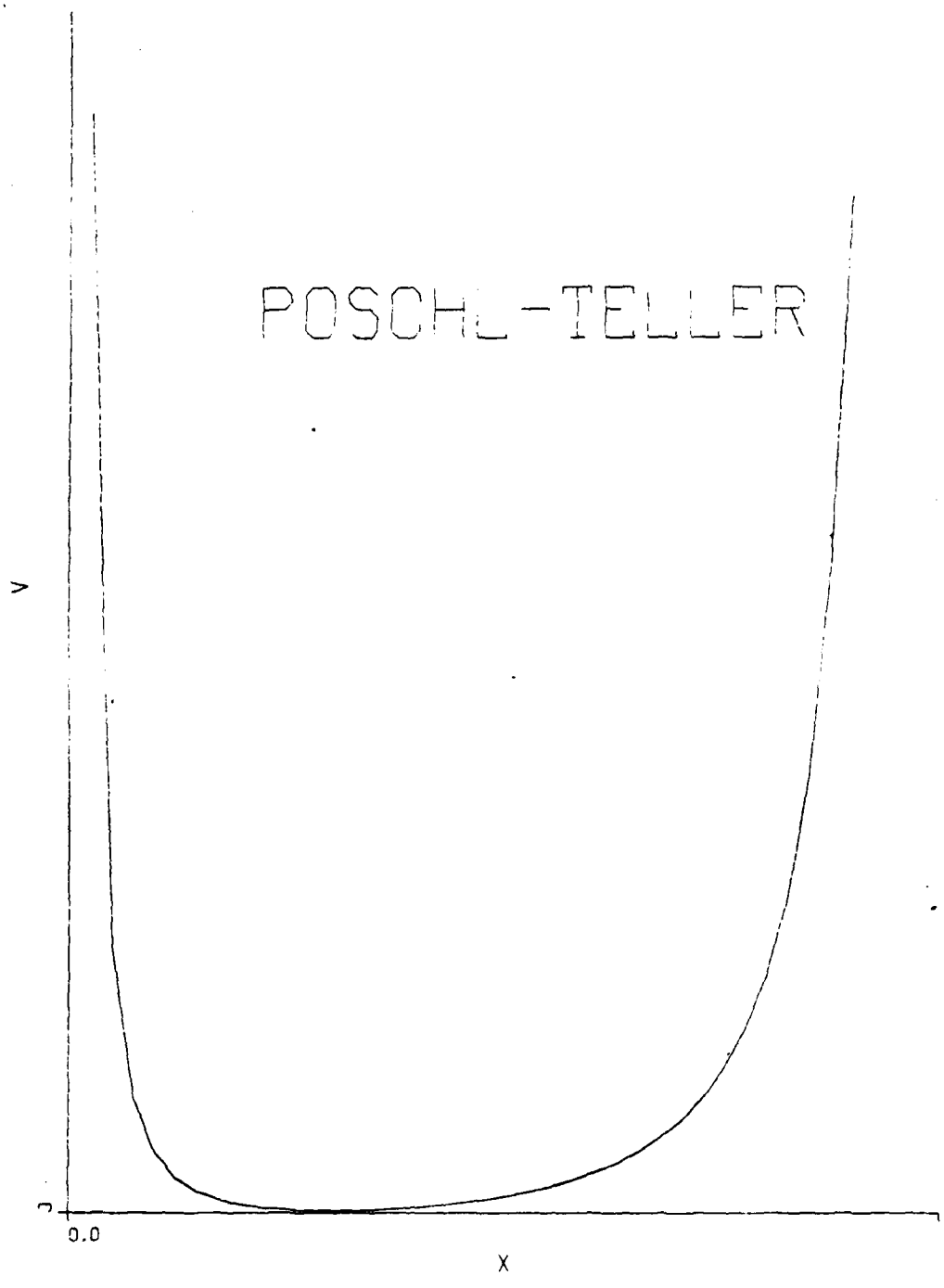
POSCHL-TELLER
V
0.0
X

VIBRATIONAL SPECTROSCOPY OF Pb/Mn/Ga FLUORIDE GLASSES

Bernard Bendow
The BDM Corporation
Albuquerque, NM 87106

Pranab K. Banerjee and Shashanka S. Mitra
University of Rhode Island
Kingston, RI 02881

C. Jacoboni and R. DePape
Universite Du Maine
72017 Le Mans Cedex, France

The vibrational characteristics of Pb/Mn/Ga fluoride glasses have been investigated using polarized Raman scattering, fundamental IR reflectivity and IR transmission measurements. The glass compositions used for this study are indicated in Table 1. As revealed by the absorbance spectra in Figure 1, they possess IR edges in the vicinity of 6 μm similar to fluorozirconates. Fundamental reflectivity spectra (see Figure 2) display two broad bands, one in the vicinity of 525 cm^{-1}, and a second with considerable structure centered in the 250-300 cm^{-1} region. The Raman scattering and depolarization spectra (as illustrated in Figures 3 and 4, for example) reveal one strong polarized band near 545 cm^{-1}, and a second broad and weakly polarized band centered near 245 cm^{-1}. The features of these spectra are quite similar to those of fluorozirconates, which display two-mode behavior in both Raman and IR reflectivity, and possess a single dominant, highly polarized peak in Raman at high frequency. The low reflectivity at frequencies above 400 cm^{-1} is closer to that of Ba/Th fluoride glasses. Based on the present observations, it appears that Pb/Mn/Ga fluoride glasses consist of well-defined structural units (of metal ions with fluorine) which give

rise to the highly polarized bands observed in Raman. It is not clear from the data whether the glass contains several different units with similar vibrational frequencies, or complex units containing several metal ions. In either case, it appears likely that the high frequency bands are associated with stretching modes, and the low frequency bands with bending modes, of the three principal cations with fluorine. The similarity to fluorozirconates suggests that Pb/Mn/Ga fluoride glasses are relatively ionic and the coordination numbers of the cations with fluorine is high.

TABLE 1. GLASS COMPOSITIONS AND SELECTED PROPERTIES (mol %)

Sample #	PbF_2	MnF_2	GaF_3	AlF_3	InF_3	ZnF_2	Density (g/cm^3)	n_D
1	38	25	37	--	--	--	5.6	1.575
2	38	25	27	--	10	--	5.7	1.584
3	38	20	30	7	--	5	5.6	1.576

In addition to the constituents stated above, all glasses contain an extra $5YF_3 + 2AlF_3$.

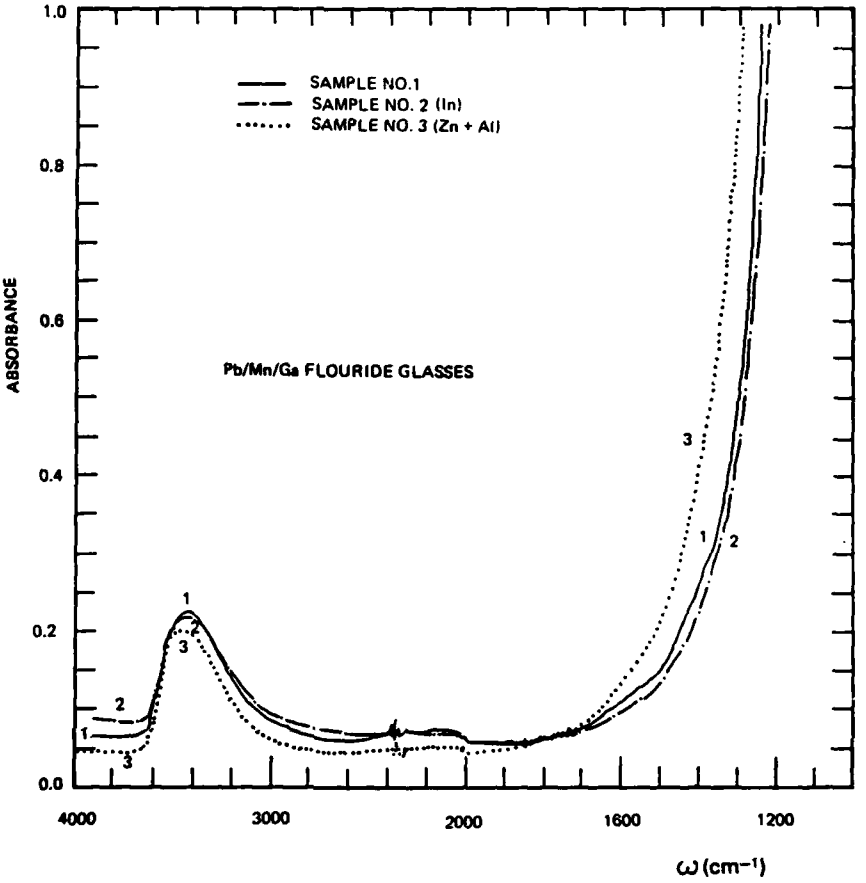
SAMPLE NO.1
SAMPLE NO. 2 (In)
SAMPLE NO. 3 (Zn + Al)
Pb/Mn/Ga FLOURIDE GLASSES
ABSORBANCE
1.0
0.8
0.6
0.4
0.2
0.0
4000
3000
2000
1600
1200
ω (cm⁻¹)

FIGURE 1

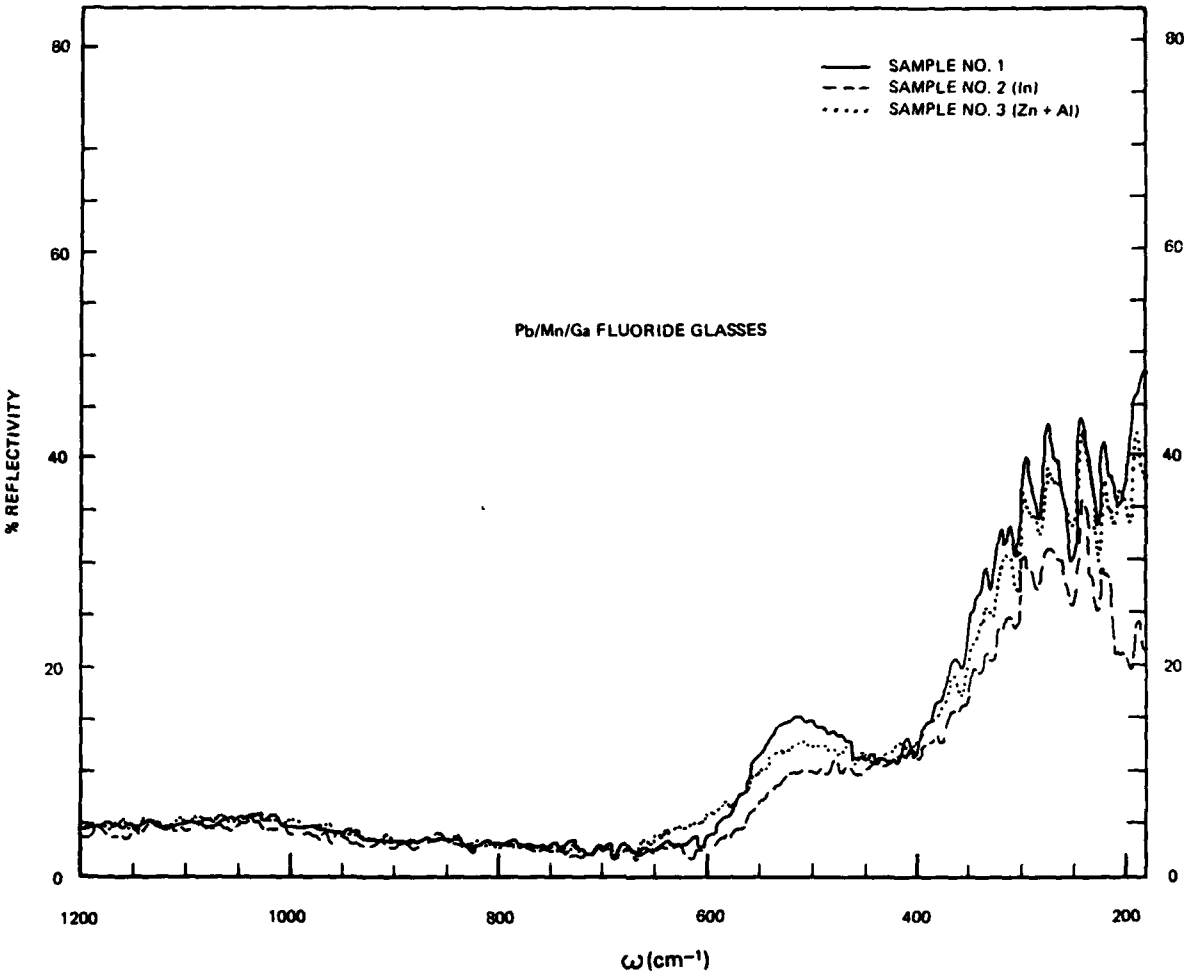
SAMPLE NO. 1
SAMPLE NO. 2 (In)
SAMPLE NO. 3 (Zn + Al)
Pb/Mn/Ga FLUORIDE GLASSES
% REFLECTIVITY
80
60
40
20
0
1200
1000
800
600
400
200
ω(cm⁻¹)

Figure 2

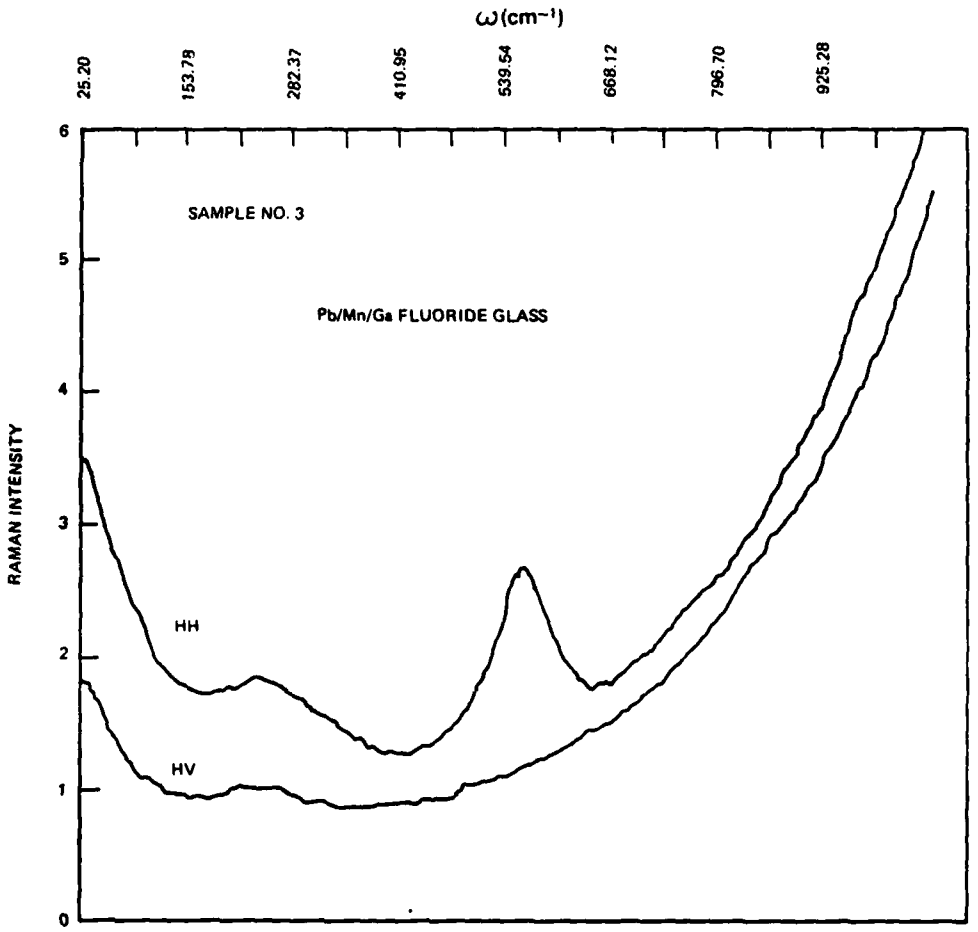
ω(cm⁻¹)
25.20
153.79
282.37
410.95
539.54
668.12
796.70
925.28
SAMPLE NO. 3
Pb/Mn/Ga FLUORIDE GLASS
RAMAN INTENSITY
HH
HV
0
1
2
3
4
5
6

Figure 3

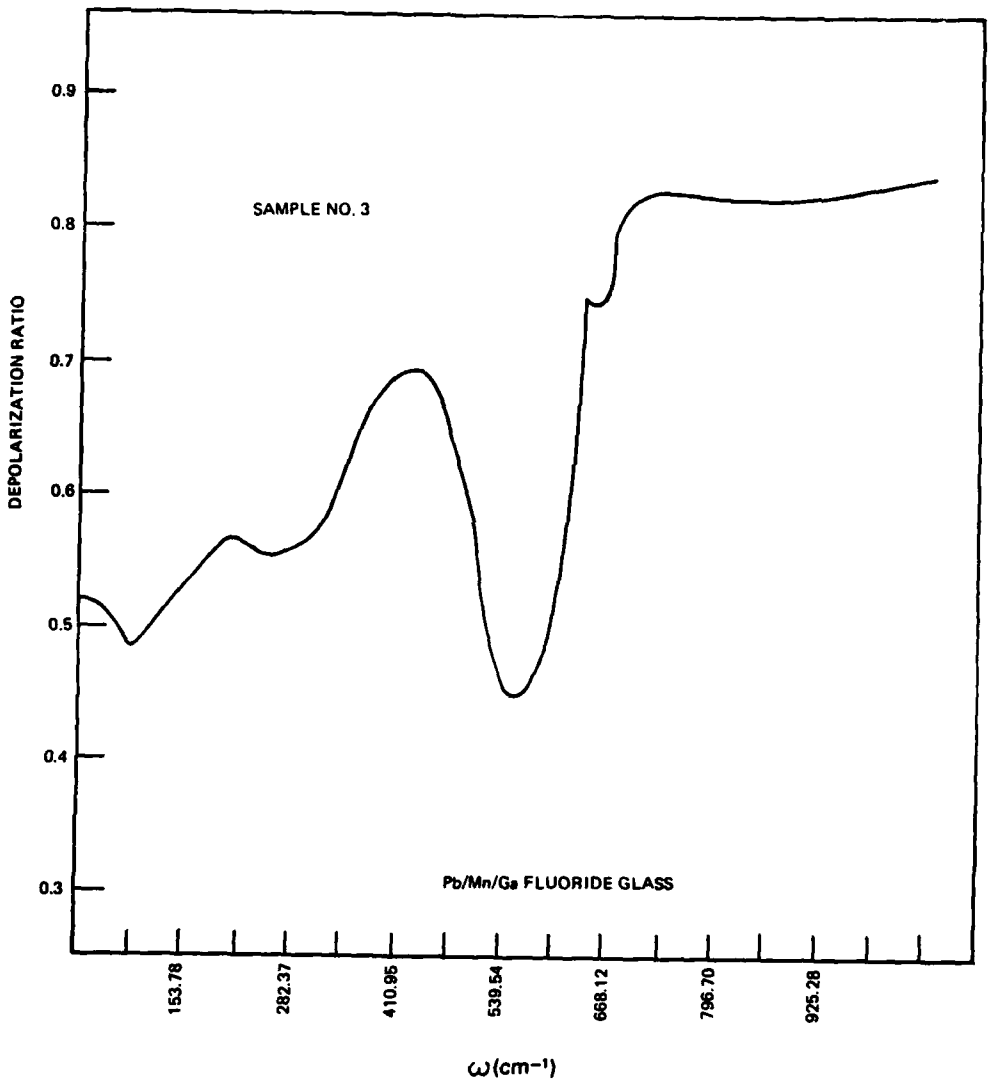
SAMPLE NO. 3
DEPOLARIZATION RATIO
0.9
0.8
0.7
0.6
0.5
0.4
0.3
Pb/Mn/Ga FLUORIDE GLASS
153.78
282.37
410.95
539.54
668.12
796.70
925.28
ω(cm⁻¹)

Figure 4

EXAFS DETERMINATION OF THE COORDINATION OF DIVALENT LEAD IN $PbO-PbCl_2$ GLASSES

K.J. Rao* and J. Wong

General Electric Corporate Research and Development

Schenectady, NY 12301 USA

and

B.G. Rao

Solid State and Structural Chemistry Unit, Indian Institute of Science

BANGALORE - 560012 INDIA

ABSTRACT

Room temperature EXAFS above the Pb L_{III} absorption edge in a series of novel $PbO-PbCl_2$ glasses containing 80-40 mol% PbO have been measured with synchrotron x-rays from CHESS at Cornell. PbO and $PbCl_2$ were used as model compounds to extract empirical phase shifts for the Pb-O and Pb-Cl pairs. A multi-shell simulation procedure was used to deduce the local structure of lead in these glasses from the experimental EXAFS signal. It is found that the coordination sphere around Pb in the glasses correspond to approximately $[PbO_2Cl_4]$ configurations confirming the earlier model predictions of the structure of these glasses.

*Visiting Research Fellow from Indian Institute of Science, BANGALORE, 560012, INDIA

P4

Bonding and Structure of Nd^{3+} in BeF_2 Glass by XANES and EXAFS Spectroscopy

K. J. Rao* and J. Wong

General Electric Corporate Research and Development
1 River Road, P.O. Box 8, Schenectady, NY 12301

and

M. J. Weber

Lawrence Livermore National Laboratory, University of California
Livermore, CA 94550

ABSTRACT

The L_{III}, L_{II} and L_I XANES and EXAFS of Nd^{3+} have been measured using synchrotron radiation from SPEAR at Stanford Synchrotron Radiation Laboratory to probe the bonding and structure of Nd^{3+} in a BeF_2 glass containing 4 mol % NdF_3. Crystalline NdF_3 and Nd_2O_3 were used as reference compounds to model the chemical environment of Nd^{3+} in the glass. It is found that in the glass there is a substantial increase in the intensity of the Nd L_{III} and L_{II} white lines compared with those of crystalline NdF_3. EXAFS analysis showed that there is a shrinkage of the innermost Nd-F bond distance and a reduction of nearest neighbor fluorine coordination to ~ 7 in the glass compared with 9 in pure NdF_3. The 7-fold coordination is in agreement with recent molecular dynamics calculations. Using Slater's atomic shielding constants, the observed increase in white line intensities in the glass was attributed to a covalency effect due to back donation of valence electron from the ligand to the partially filled 4f orbitals of the Nd^{3+} ions. This study illustrates ability of the combined XANES and EXAFS technique in elucidating the chemical bonding and local structure of a given atomic constituent in glassy solids.

* Visiting Research Fellow, Indian Institute of Science, Bangalore, India

I.R. MEASUREMENT OF THE RATE OF SURFACE LAYER DEVELOPMENT ON ZrF_4-BaF_2-LaF_3 GLASS IN AQUEOUS SOLUTION

A. J. Bruce, S. R. Loehr, N. P. Bansal
D. M. Murphy, C. T. Moynihan and R. H. Doremus
Rensselaer Polytechnic Institute
Troy, New York 12181
USA

I.R. spectra have been measured versus time for a 62 ZrF_4-33 BaF_2-5 LaF_3 glass immersed in water at room temperature. After an induction period of less than 15 minutes, the IR peaks at 3440 cm^{-1} and 1640 cm^{-1} (probably due to the OH stretching and H_2O bending modes of molecular water) (cf. Fig. 1) increase with immersion time. Plots of absorbance versus (a) total immersion time, and (b) the square root of the total immersion time, are shown in Figure 2. The linear dependence of the absorbance on $\sqrt{t}$ is consistent with a diffusion controlled process and it is believed that the development of the absorption peaks follows that of a surface layer on the glass.

This result may therefore form a basis for a quick comparative measurement of the resistance to water attack of heavy metal fluoride glasses. For example, the IR spectra of glasses would be measured versus immersion time for a period up to an hour say at three different temperatures and the rates of development of the molecular water peaks compared.

The sample studied had previously been polished first with silicon carbide paper and lapping oil and then with alumina and water. The presence of a surface layer after polishing may therefore cause the observed induction period. Prior to each spectral measurement the sample was dipped twice in acetone and once in n-hexane to remove any unbound water from the sample surface.

Attempts to dehydrate the surface of the sample after 5 hours immersion indicate that substantial reductions in the IR absorption peaks assigned

to molecular water only occur when the sample is baked at temperatures above 150°C (cf. Figure 3). This indicates that any water present is quite firmly bound. This result is consistent with a DSC measurement made on a sample of the "powdery" material which was shaken off from the surface of a ZBL sample after 4 days immersion in water at room temperature (cf. Figure 4). This shows dehydration occurring above 165°C. It is also interesting to note that a glass transition and crystallization exotherm are detected for the surface material at temperatures close to those for the bulk glass. The presence of amorphous material is consistent with preliminary X-ray diffraction measurements made on the surface material developed during room temperature immersion.

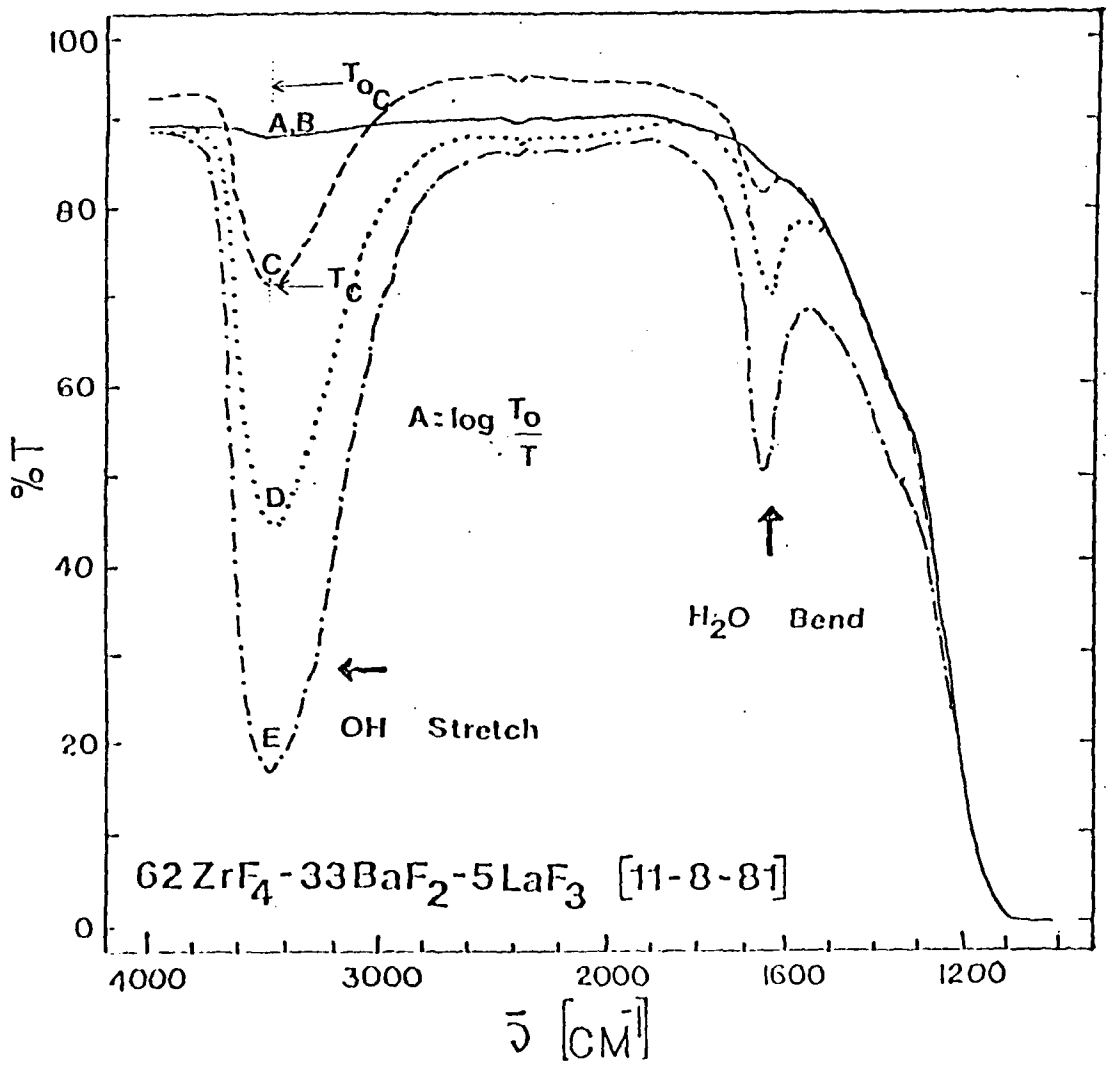

SCAN	IMMERSION TIME (min) [Ambient Temperature]
A,B	0,5
C	30
D	60
E	150

Sample thickness 2.38 mm

Surface area 1.57 cm^2

Figure 1. Growth of OH stretch and H_2O bend peaks with H_2O immersion

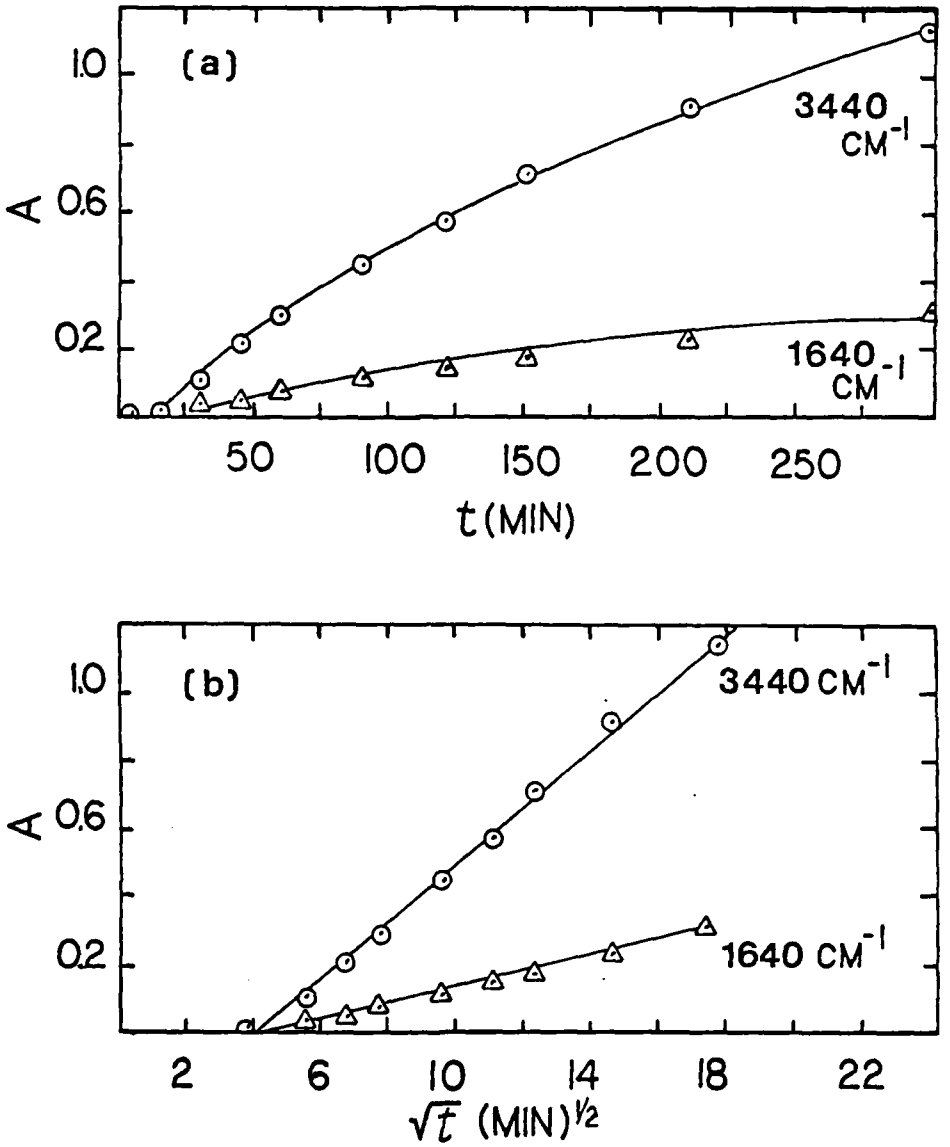

Figure 2. Absorbance vs. Immersion (a) t and (b) $\sqrt{t}$ for 3440 cm^{-1} OH stretch and 1640 cm^{-1} H_2O peaks.

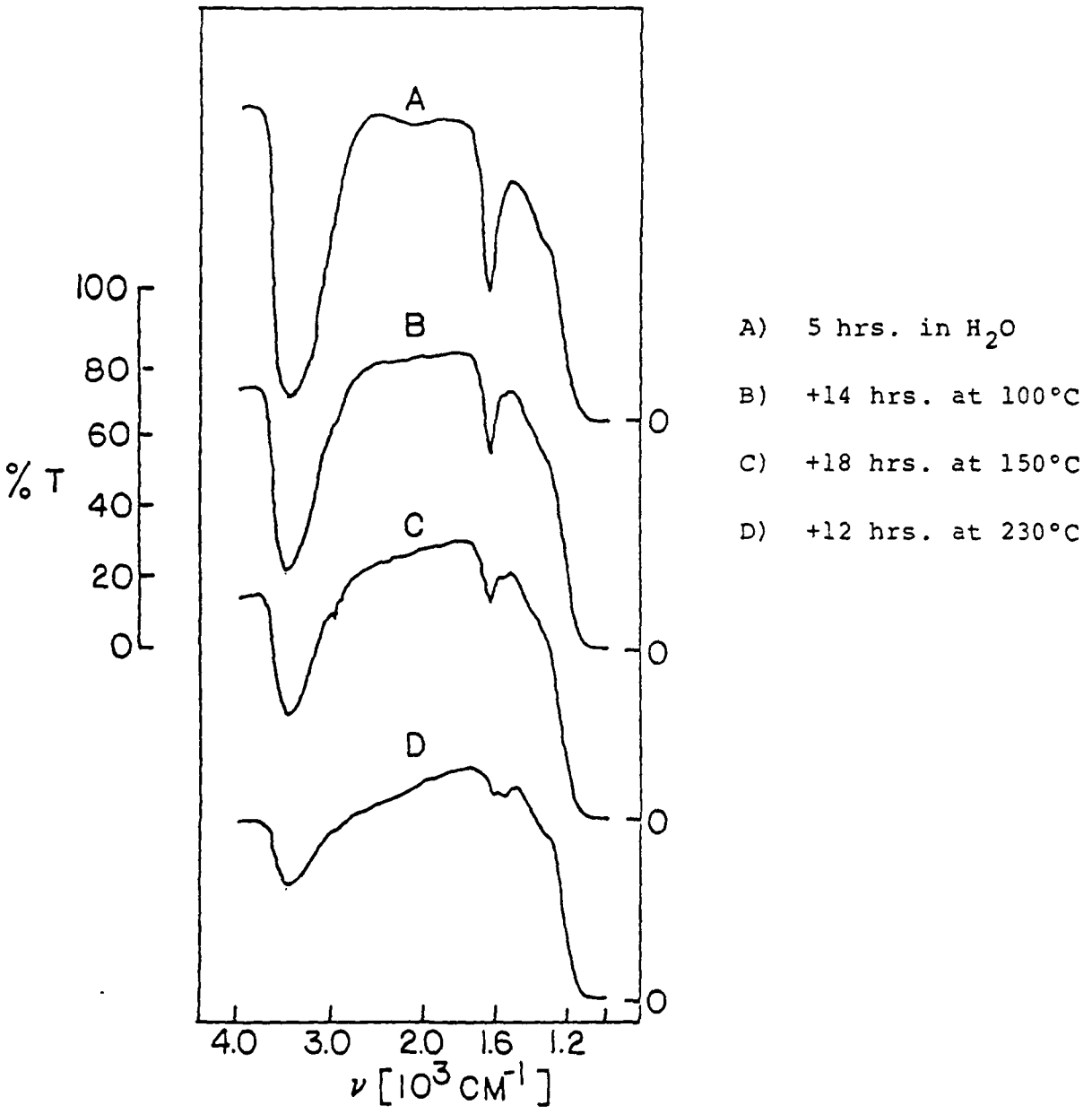

Figure 3. Effect of baking on the IR spectrum of ZBL glass previously immersed previously for 5 hrs. at room temperature.

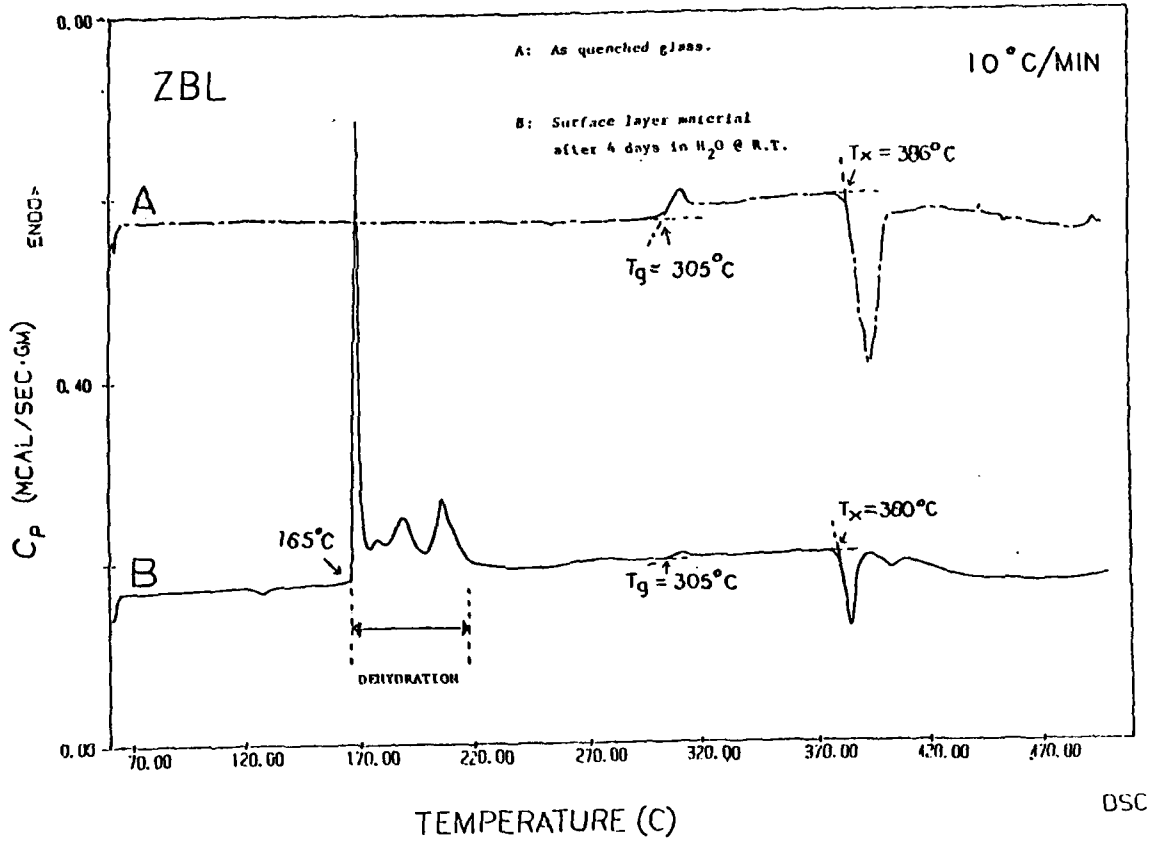

Figure 4. DSC trace of bulk (A) and hydrated (B) surface layer of 62 ZrF_4-33 BaF_2-5 LaF_3 glass at 10°C/min.

ELECTRICAL CONDUCTIVITY AND RELAXATION IN ZrF_4-BaF_2-LaF_3 GLASSES

N. L. Perazzo, D. L. Gavin, A. J. Bruce, S. R. Loehr
and C. T. Moynihan
Rensselaer Polytechnic Institute
Troy, New York 12181
USA

Electrical conductivity and relaxation measurements have been carried out on three ZrF_4-BaF_2-LaF_3 glasses whose batch compositions are given in Table I. Note that one of the glasses has been intentionally doped with oxide. Ravaine and coworkers[1-3] have shown that these materials are fluoride ion conductors.

The conductivity specimens were polished rectangular plates (2-3 mm thick, $\sim$ 10 mm on a side) with sputtered gold electrodes applied to opposite faces. The real part of the electrical conductivity σ' and the dielectric constant ε' were measured over the frequency range 0.025 to 100,000 Hz using an operational amplifier admittance bridge.

Typical results for the frequency dependence of ε' and σ' are shown at three temperature for one of the glasses in Figs. 1 and 2. These plots are similar in appearance to those observed for other ionically conducting glasses.[4,5] The high frequency dispersion in the ε' vs. f plots of Fig. 1 is due to bulk glass electrical (or dielectric) relaxation, while the low frequency dispersion (shown most clearly in the 103.4°C isotherm) is due to surface layer polarization. The low frequency plateau in the σ vs. f plots of Fig. 2 corresponds to the bulk glass d.c. conductivity σ, while the high frequency dispersion is again due to bulk glass electrical relaxation.

Our data were also analyzed using the formalisms of complex resistivity ρ^*[4,6] and electric modulus M^*[5], where

$$\rho^* = \rho' - i\rho'' = 1/i\omega\varepsilon_o[\varepsilon' - i(\sigma'/\omega\varepsilon_o)]$$

$$M^* = M' + iM'' = 1/[\varepsilon' - i(\sigma'/\omega\varepsilon_o)]$$

where ω is angular frequency and ε_o the permittivity of free space. Typical complex plane plots of M* and ρ* are shown in Figs. 3 and 4.

Extrapolation of the low temperature M* plots to intersect the M' axis yields the high frequency bulk dielectric constant ε_∞, as shown in Fig. 3. Values of ε_∞ are listed in Table I and are nearly identical within experimental error for all three glasses.

Neither the M* nor the ρ* plots are arcs of a circle with its center on the real axis, indicating that the relaxation of the electric field due to F^- ion migration in the bulk glass must be described by a spectrum of relaxation times or a non-exponential relaxation function.[5,6] In addition, the ρ* arc is not exactly symmetric and does not have the shape of a circle with its center below the real axis, as has also been found with alkali silicate glasses.[7]

The bulk glass d.c. conductivity σ was obtained from the low frequency intercept of the ρ* arc with the real axis[1,4,6,7], as shown in Fig. 4. The temperature dependence of σ of all three glasses followed the Arrhenius equation:

$$\sigma = \sigma_o \exp(-\Delta H^*/RT)$$

where ΔH^* is the activation enthalpy and R the gas constant. Arrhenius equation parameters are given in Table I. Arrhenius plots of σ vs. $10^3/T$ are shown in Fig. 5, where our conductivity results are compared with those for other alkali-free fluorozirconate glasses reported by other laboratories.[1-3,8] Our data for the 62 ZrF_4-30 BaF_2-8 LaF_3 glass are gratifying close to those reported by Ravaine et al.[1,2] for a glass of the same nominal composition.

One interesting result of the present study is that replacement of 2 mol% of BaF_2 by BaO in the 62 ZrF_4-33 BaF_2-5 LaF_3 glass appears to increase substantially the conductivity — by a factor of more than 2 at low temperatures.

It is tempting to suggest that this may be due to introduction of F^- ion vacancies along with the oxide. However, the difference in σ between the oxide-containing and oxide-free glasses could as well be due to inadvertant differences between the batch and actual glass compositions or to differences in the thermal histories in the annealing region of the two glasses. Further investigations are needed here.

It has been found[9] that exposure of fresh fluorozirconate glass surfaces to atmospheric water vapor results in the rapid formation of a thin hydrated surface layer which then shows no further increase in thickness with time. (This layer should not be confused with the thick, continually growing layers that form on these glasses when they are exposed to liquid water[10].) The present glasses were exposed to the laboratory atmosphere before depositing the gold electrodes and placing them in the dielectric cell, and they should possess the thin surface layers. We were curious to see whether these layers could be detected in our electrical measurements, since in a previous study[4] of alkali silicate glasses it was found that hydrated surface layers, which are in series electrically with the bulk glass, give rise to a second, low frequency arc in the complex resistivity plots. The presence of surface layer contributions to the low frequency ρ^* plots was detectable for the fluorozirconate glasses, but they were very small and perceptible only in enlarged plots of the low frequency part of the ρ^* data. Such an enlarged plot is shown in the inset to Fig. 4; the surface layer contribution corresponds to the minimum in the "hook" on the low frequency tail of the ρ^* plot. Using the methods outlined in Ref. 4, one can estimate from this low frequency "hook" that the thickness of the hydrated surface layer resulting from reaction of atmospheric water with fluorozirconate glasses is no more than about 0.01 μm.

Acknowledgement. Research supported by Contract No. F19628-83-C-0016 from Rome Air Development Center.

References

1. D. Leroy, J. Lucas, M. Poulain and D. Ravaine, Mat. Res. Bull., 13, 1125 (1978).

2. D. Ravaine and D. Leroy, J. Non-Cryst. Solids, 38 & 39, 575 (1980).

3. D. Ravaine, W. G. Perera and M. Minier, J. de Physique, 43, Suppl. C9, 407 (1982).

4. E. N. Boulos, A. V. Lesikar and C. T. Moynihan, J. Non-Cryst. Solids, 45, 419 (1981).

5. P. B. Macedo, C. T. Moynihan and R. Bose, Phys. Chem. Glasses, 13, 171 (1972).

6. D. Ravaine and J.-L. Souquet, J. Chim.Phys., 71, 693 (1971).

7. R. Syed, D. L. Gavin, C. T. Moynihan and A. V. Lesikar, J. Am. Ceram. Soc., 64, C118 (1981).

8. R. M. Almeida and J. D. Mackenzie, Extended Abstracts, 1st International Symposium on Halide and Other Non-Oxide Glasses, Cambridge, UK, March, 1982.

9. E. O. Gbogi, K.-H. Chung, C. T. Moynihan and M. G. Drexhage, J. Am. Ceram. Soc., 64, C51 (1981).

10. Papers 15, 19, 47 and P5, Extended Abstracts, 2nd International Symposium on Halide Glasses.

Table I. Compositions, electrical conductivity Arrhenius equation parameters and high frequency dielectric constants of ZrF_4-based glasses.

Batch Composition (mol%)	σ_o ($ohm^{-1}cm^{-1}$)	ΔH^* (kJ/mol)	ε_∞
62 ZrF_4-30 BaF_2-8 LaF_3	2.93×10^2	73.45	11.5
62 ZrF_4-33 BaF_2-5 LaF_3	2.73×10^2	73.45	11.8
62 ZrF_4-31 BaF_2-5 LaF_3-2 BaO	1.92×10^2	69.81	12.0

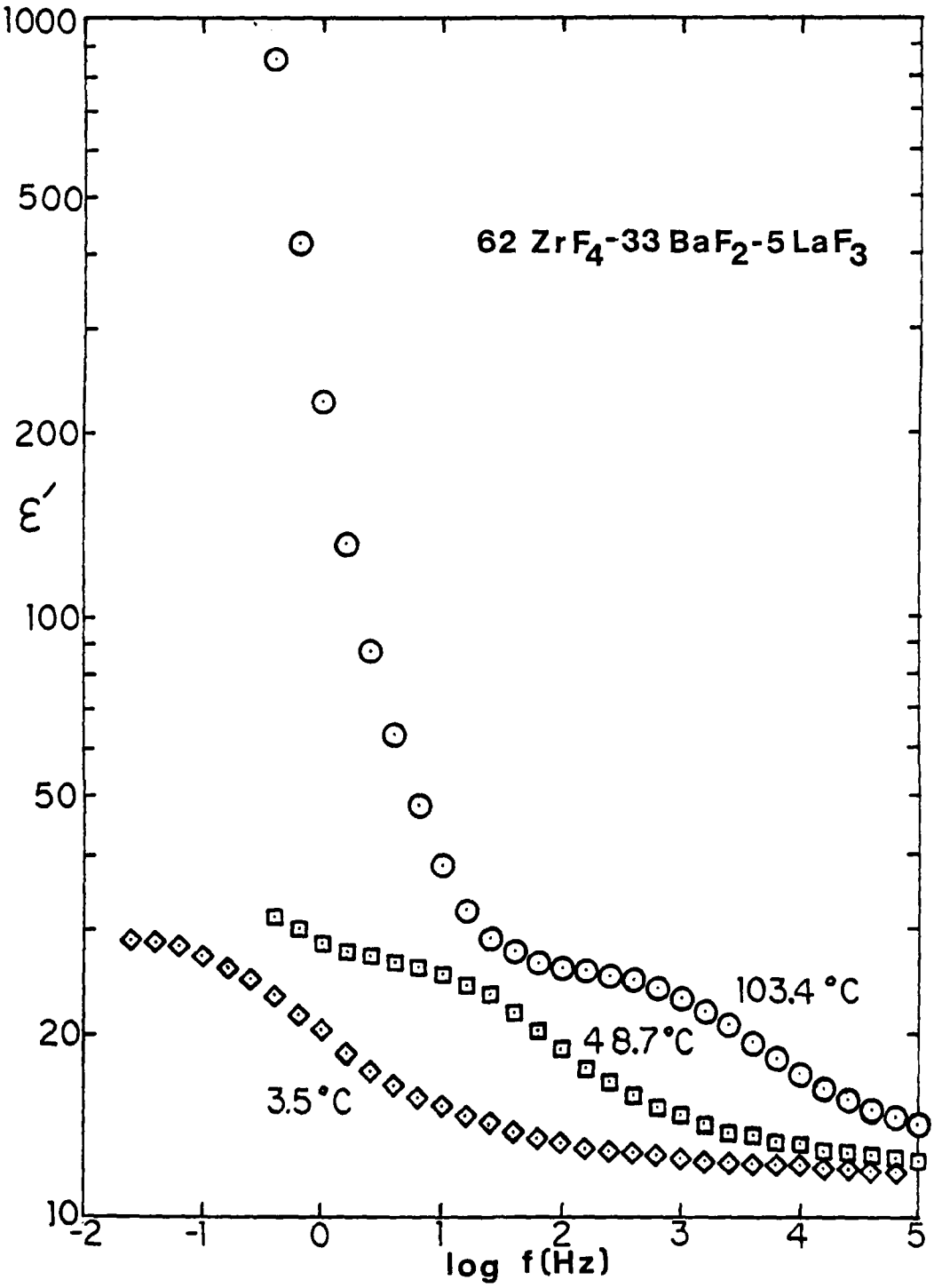

Figure 1. Frequency dependence of dielectric constant at three temperatures for 62 ZrF_4-33 BaF_2-5 LaF_3 glass.

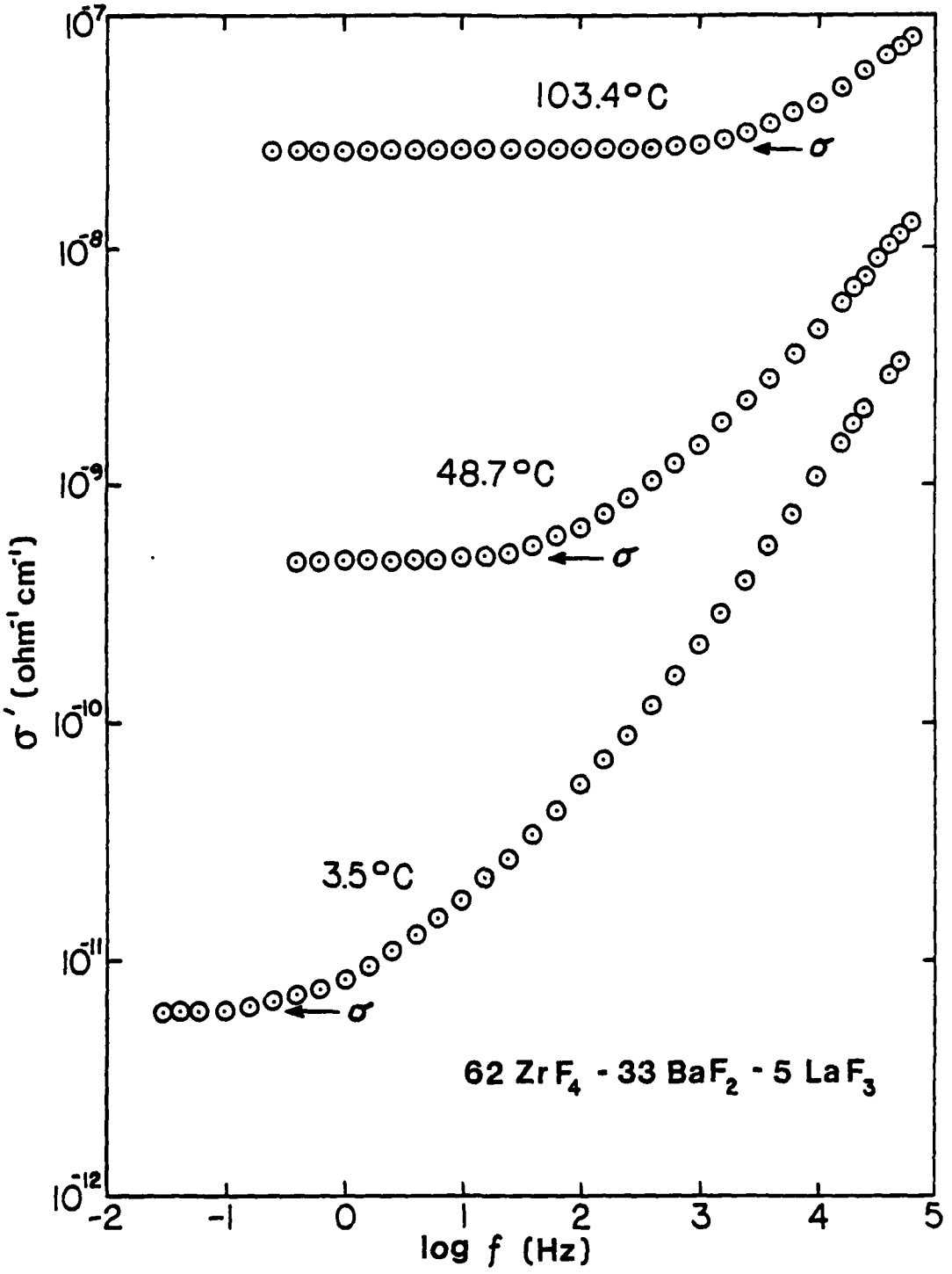

Figure 2. Frequency dependence of electrical conductivity at three temperatures for 62 ZrF_4-33 BaF_2-5 LaF_3 glass.

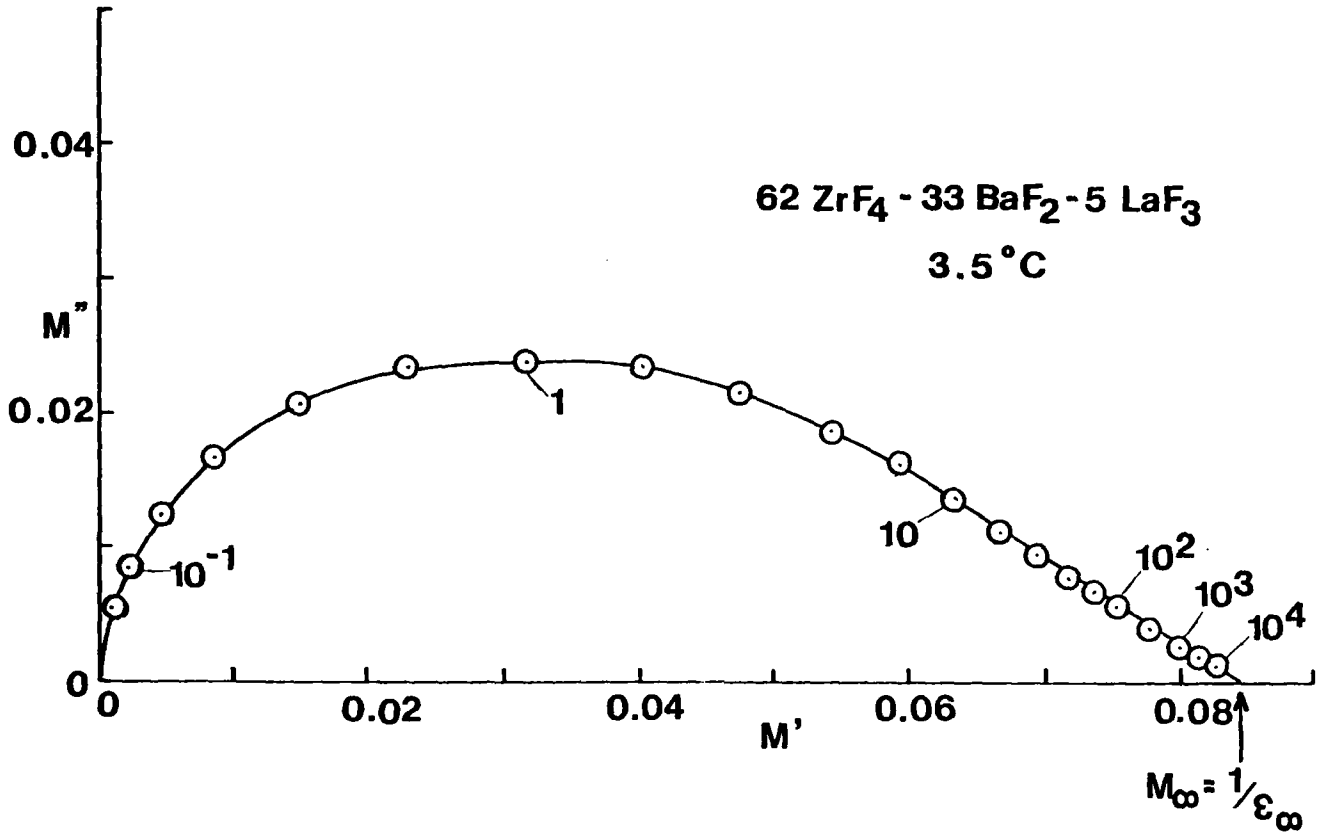

Figure 3. Complex plane plot of imaginary vs. real parts of electric modulus of 62 ZrF_4-33 BaF_2-5 LaF_3 glass 3.5°C. Numbers next to data points are measurement frequencies in Hz.

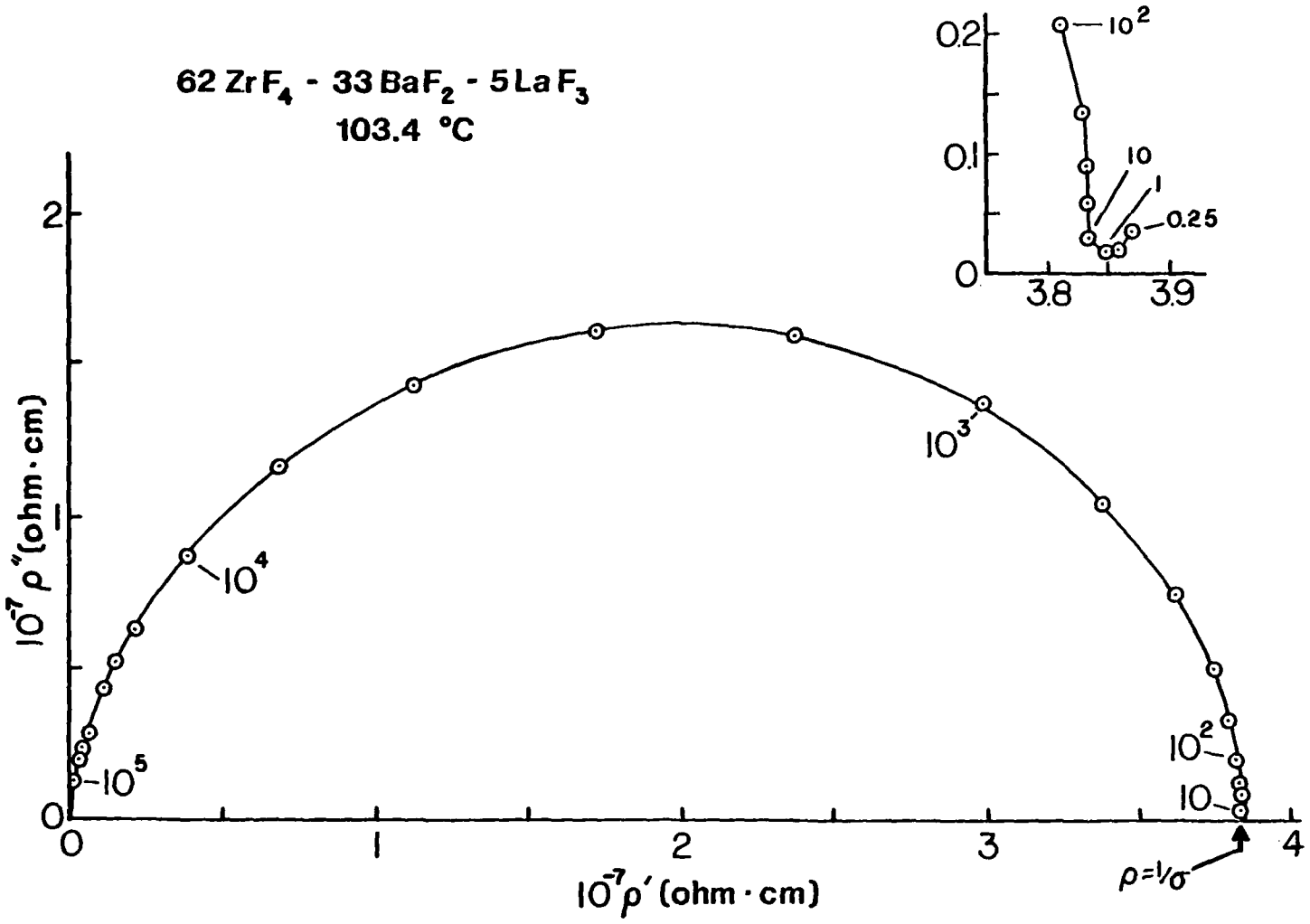

Figure 4. Complex plane plot of imaginary vs. real parts of complex resistivity of 62 ZrF_4-33 BaF_2-5 LaF_3 glass at 103.4°C. Numbers next to data points are measurement frequencies in Hz. Inset is enlargement of low frequency part of plot.

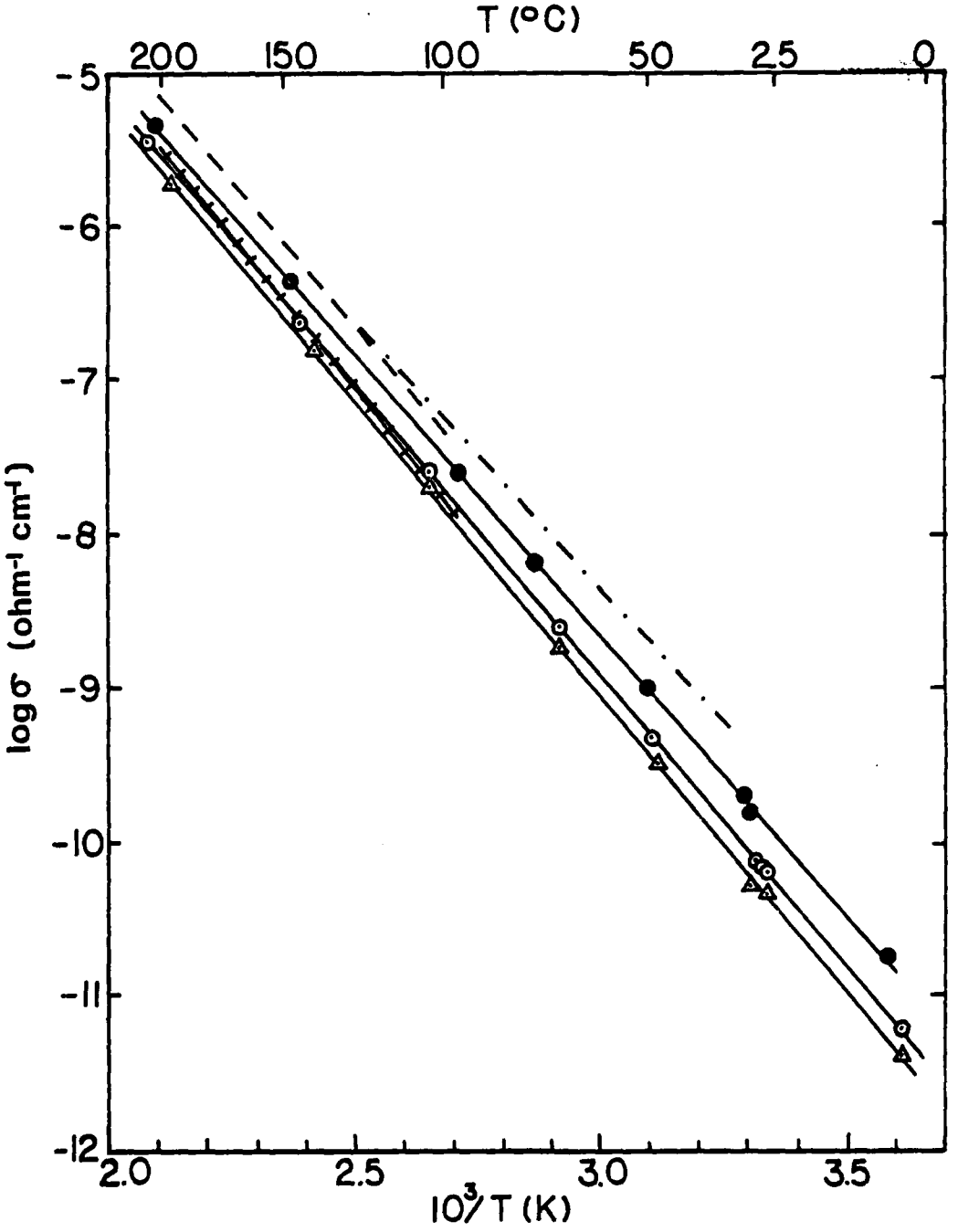

Figure 5. Arrhenius plots of fluorizirconate glass electrical conductivities.

	Compositions (mol%)					
	ZrF_4	BaF_2	LaF_3	ThF_4	BaO	
△	62	30	8	-	-	present study
+	62	30	8	-	-	Refs. 1,2
⊙	62	33	5	-	-	present study
●	62	31	5	-	2	present study
– – –	58.7	31.3	-	10	-	Refs. 1-3
•–•–•	64	36	-	-	-	Ref. 8

Unclassified

SECURITY CLASSIFICATION OF THIS PAGE (When Data Entered)

REPORT DOCUMENTATION PAGE

READ INSTRUCTIONS BEFORE COMPLETING FORM

1. REPORT NUMBER: NA	2. GOVT ACCESSION NO.: AD-A144 269
3. RECIPIENT'S CATALOG NUMBER:	
4. TITLE (and Subtitle): Extended Abstracts - Second International Symposium on Halide Glasses	5. TYPE OF REPORT & PERIOD COVERED: Final, 1 June 83 - 31 Dec 83
	6. PERFORMING ORG. REPORT NUMBER:
7. AUTHOR(s): C. T. Moynihan - Principal Investigator	8. CONTRACT OR GRANT NUMBER(s): N00014-83-G-0091
9. PERFORMING ORGANIZATION NAME AND ADDRESS: Materials Engineering Department, Rensselaer Polytechnic Institute, Troy, NY 12181	10. PROGRAM ELEMENT, PROJECT, TASK AREA & WORK UNIT NUMBERS:
11. CONTROLLING OFFICE NAME AND ADDRESS: Leader, Information Sciences Division; Associate Director for Engineering Sciences Research Programs	12. REPORT DATE: August 2-5, 1983
	13. NUMBER OF PAGES: 60 abstracts
14. MONITORING AGENCY NAME & ADDRESS (if different from Controlling Office): Office of Naval Research, 800 No. Quincy Street, Arlington, VA 22217	15. SECURITY CLASS. (of this report): Unclassified
	15a. DECLASSIFICATION/DOWNGRADING SCHEDULE:

16. DISTRIBUTION STATEMENT (of this Report)

Approved for public release; distribution unlimited. Reproduction in whole or in part is permitted for any purpose of the United States government.

17. DISTRIBUTION STATEMENT (of the abstract entered in Block 20, if different from Report)

DTIC ELECTE JUL 27 1984 S A

18. SUPPLEMENTARY NOTES

19. KEY WORDS (Continue on reverse side if necessary and identify by block number)

fluoride glass, halide glass, optical fibers

20. ABSTRACT (Continue on reverse side if necessary and identify by block number)

This document is the Extended Abstracts of the 2nd International Symposium on Halide Glasses held at Rensselaer Polytechnic Institute, August 2-5, 1983. It contains extended abstracts of 60 papers on optical, thermal, electrical and mechanical properties of halide glasses and on their potential applications.

DD FORM 1 JAN 73 1473 EDITION OF 1 NOV 65 IS OBSOLETE

Unclassified

SECURITY CLASSIFICATION OF THIS PAGE (When Data Entered)

ATE
LME